

UC Riverside

UC Riverside Electronic Theses and Dissertations

Title

Advancing Methods to Synthesize Nitrogen-Containing Small Molecules for Catalysis and as Potential Therapeutics

Permalink

<https://escholarship.org/uc/item/3f14t4f6>

Author

Palchak, Zachary

Publication Date

2018

Peer reviewed|Thesis/dissertation

UNIVERSITY OF CALIFORNIA
RIVERSIDE

Advancing Methods to Synthesize Nitrogen-Containing Small Molecules for
Catalysis and as Potential Therapeutics

A Dissertation submitted in partial satisfaction
of the requirements for the degree of

Doctor of Philosophy

in

Chemistry

by

Zachary Lawrence Palchak

June 2018

Dissertation Committee:

Dr. Catharine H. Larsen, Chairperson

Dr. Christopher Switzer

Dr. Richard J. Hooley

Copyright by
Zachary Lawrence Palchak
2018

The Dissertation of Zachary Lawrence Palchak is approved:

Committee Chairperson

University of California, Riverside

ACKNOWLEDGEMENTS

The text and results discussed in the following chapters of this dissertation are, in part or in full, a reprint of the material as they appear in the following publications:

Chapter 2:

Palchak, Z. L.; Lussier, D. J.; Pierce, C. J.; Larsen, C. H. *Green Chem.* **2015**, 17, 1802. DOI: 10.1039/c4gc02318h

Chapter 3:

Palchak, Z. L.; Lussier, D. J.; Pierce, C. J.; Yoo, H.; Larsen, C. H. *Adv. Synth. Catal.* **2015**, 357, 539. DOI: 10.1002/adsc.201401037

Chapter 4:

Palchak, Z. L.; Nguyen, P. T.; Larsen, C. H. *Beilstein J. Org. Chem.* **2015**, 11, 1425. DOI: 10.3762/bjoc.11.154

Larsen, C. H.; Palchak, Z. L. *U.S. Provisional Patent Application No. 62/201,424*, **2015**.

I acknowledge the National Science Foundation (CHE-1352665) and the American Chemical Society Petroleum Research Fund for partial support of this research.

ABSTRACT OF THE DISSERTATION

Advancing Methods to Synthesize Nitrogen-Containing Small Molecules for
Catalysis and as Potential Therapeutics

by

Zachary Lawrence Palchak

Doctor of Philosophy, Graduate Program in Chemistry
University of California, Riverside, June 2018
Dr. Catharine H. Larsen, Chairperson

Analysis of the current top grossing pharmaceuticals finds that a vast number of them contain amines. As a result, the development of methodologies for the formation of amine-containing compounds is of high value and great importance. With the ability to treat: cancer, HIV, malaria, diabetes, and depression, as well as other ailments, increased efforts have been made to optimize the production of these compounds to increase yield while decreasing the environmental impact. This work is ongoing, and is a culmination of the fields of organic synthesis, catalysis, green chemistry, and biochemistry. The work in the Larsen group revolves largely around the use of copper-based catalysis to access hindered amine scaffolds through single-step, multicomponent reactions. Further functionalization of these compounds allows for the synthesis of previously unknown, biologically active, α -amino triazoles. Preparation and analysis of electronically diverse pyridyl triazoles allows for the development of new

complexes with platinum and palladium. These pyridyl triazole palladium complexes are highly reactive under mild aerobic conditions when used in Suzuki-Miyaura cross-coupling reactions. Pyridyl pyrazoles are another class of compounds that show promise in the field of catalysis. Utilization of electronically diverse ligands allows for fine-tuning of the resulting complex for both classes of ligands. With further investigation, this may allow for the discovery of new reactivity in organic transformations.

Table of Contents

Abstract	v
List of Schemes	x
List of Figures	xii
List of Tables	xiv
Chapter One: Nitrogen Containing Small Molecules	
1.1 Introduction	1
1.2 Definition of “Small Molecules”	1
1.3 Lipinski’s Rule of Five for Biologically Active Molecules	3
1.4 Examples of Biologically Active Nitrogen Containing Small Molecules	4
1.5 References	7
Chapter Two: Kinetic Analysis of Propargylamine Formation Through Condensation-Alkynylation	
2.1 Introduction	9
2.2 Background on Propargylamine Formation via Copper(II) catalyzed Condensation-Alkynylation	10
2.3 Determining Conditions for Kinetic Analysis of Propargylamine Formation	13
2.4 Kinetic Analysis of the Condensation-Alkynylation Pathway to Form Propargylamines	19
2.5 Synthetically Useful Silyl-Protected Propargylamines Through Utilization of TIPS-Acetylene	28
2.6 References	31
2.7 Supporting Information	35
Chapter Three: Kinetic Analysis of Propargylamine Formation Through Hydroamination-Alkynylation	
3.1 Introduction	46
3.2 Propargylamine Formation via Hydroamination-Alkynylation	48

3.3 Kinetic Analysis of the Copper(II) Catalyzed Hydroamination-Alkynylation Pathway to Form Propargylamines	56
3.4 Synthesis of 1-Amino-dienes Through Hydroamination-Hydrovinylation ..	64
3.5 References	67
3.6 Supporting Information	71
Chapter Four: α-Tetrasubstituted Triazoles for Biological Testing	
4.1 Introduction	76
4.2 Background on Biologically Active α -Tetrasubstituted Triazoles	77
4.3 Formation of Structurally Diverse α -Tetrasubstituted Triazoles	79
4.4 New Found Biological Activity of Some α -Tetrasubstituted Triazoles	88
4.5 References	94
4.6 Supporting Information	96
Chapter Five: Pyridine Triazoles as Ligands and Biologically Active Compounds	
5.1 Introduction	144
5.2 Background on Pyridyl Triazoles as Biologically Active Compounds	144
5.3 Formation of Structurally Diverse Aryl Substituted Pyridyl Triazoles	147
5.4 Functionalization of Pyridyl Triazoles Through Halogenation	154
5.5 Derivatization of Iodo-Pyridyl Triazoles	164
5.6 References	167
5.7 Supporting Information	169
Chapter Six: Pyridyl Triazole Complexes with Palladium and Platinum	
6.1 Introduction	227
6.2 Background on Pyridyl Triazoles as Ligands for Metal Complexes	227
6.3 Palladium Complexes with Diverse Pyridyl Triazole Ligands	229
6.4 Activity of Pyridyl Triazole Pd(II) Complexes in Suzuki Cross-Coupling ..	236
6.5 Platinum Complexes with Diverse Pyridyl Triazole Ligands	241
6.6 References	260
6.7 Supporting Information	266

Chapter Seven: Pyridine Pyrazoles as Ligands and Complexation with Palladium

7.1	Introduction	345
7.2	Synthesis of Electronically Diverse Pyridine Pyrazoles	346
7.3	Pyridine Pyrazoles as Ligands for Metal Complexes	350
7.4	Palladium Complexes with Diverse Pyridine Pyrazole Ligands	351
7.5	References	357
7.6	Supporting Information	361

List of Schemes

Scheme 2.1: Comparison of conditions for three-component coupling with aldehydes and cyclohexanone	10
Scheme 2.2: First methods specifically designed for three component coupling with cyclohexanone	11
Scheme 2.3: Basis for developing a green method for ketone-amine-alkyne coupling	12
Scheme 2.4: Solvent free conditions results in a faster reaction with higher yield for ketone-amine-alkyne coupling	15
Scheme 2.5: Mechanism for the reaction of cyclohexanone with amines and alkynes	19
Scheme 3.1: Trisubstituted vs. tetrasubstituted products resulting from hydroamination-nucleophile addition reactions	46
Scheme 3.2: Selectivity of tandem hydroamination-alkynylation under solvent free conditions	50
Scheme 3.3: Markovnikov hydroamination with secondary amines and bulky alkynes can lead to increased allylic strain between substituents	52
Scheme 3.4: Explanation for increased reaction rates of secondary amines in hydroamination-alkynylation reactions	56
Scheme 3.5: Proposed mechanism for the dual catalytic cycle of tandem hydroamination-alkynylation	59
Scheme 3.6: Unprecedented tandem hydroamination-hydrovinylation to form 1-aminodiene	65
Scheme 4.1: Proposed method for ketone-amine-alkyne coupling followed by tandem silyl deprotection, triazole formation	79
Scheme 4.2: Initial conditions for the formation of α -tetrasubstituted triazoles.	81
Scheme 4.3: Conditions for the silyl deprotection/CuAAC reaction applied to tert-butylacetylene	87

Scheme 4.4: High overall yield is obtained for 1,2,3-triazoles after a two step reaction sequence from commercially available starting materials	88
Scheme 5.1: Initial conditions for the synthesis of pyridyl triazoles	150
Scheme 5.2: Method for in situ iodination to form iodo-triazole yields dimerized pyridyl triazole	155
Scheme 5.3: Two mechanistic pathways for the preparation of iodo-triazoles from preformed iodo-alkynes	156
Scheme 5.4: Proposed mechanism for the formation of iodo-alkynes	158
Scheme 5.5: Decreased reaction temperature prevents dimerization of trifluoromethylated iodo-pyridyl triazole	161
Scheme 5.6: Synthesis of highly reactive <i>tert</i> -butyl azide	162
Scheme 5.7: Preparation of tris-triazole (TTTA) ligand	163
Scheme 5.8: Use of TTTA ligand in iodo-triazole formation completely prevents dimerization reaction	163
Scheme 5.9: Catalytic cycle for palladium catalyzed Suzuki-Miyaura cross-coupling reaction	165
Scheme 5.10: Result of Suzuki cross-coupling with iodo-pyridyl triazole and 4-methoxyboronic acid	165
Scheme 6.1: One step synthesis of bis-PyTriPd(BF ₄) ₂ complex	240
Scheme 6.2: Two step method for preparing of bis-PyTriPd(BF ₄) ₂ complex ..	240
Scheme 6.3: Catalytic cycle for Suzuki-Miyaura cross-coupling with PyTriPdCl ₂ complexes	242
Scheme 6.4: Initial conditions for Suzuki cross-coupling with PyTriPdCl ₂	244
Scheme 7.1: Synthesis of pyridyl pyrazoles from 1,3-diketones with hydrazine hydrate	347
Scheme 7.2: Synthesis of pyridyl pyrazoles from amino-enones with hydrazine hydrate	348

List of Figures

Figure 1.1: Examples of biologically active α -tetrasubstituted amines	5
Figure 1.2: Preparation of an anti-HIV drug via acetylide addition to premade ketimine	5
Figure 2.1: Formation of propargylamine over time at varying loadings of the CuCl_2 catalyst in condensation-alkynylation reactions	21
Figure 2.2: Plot of reaction rate at CuCl_2 loadings to determine the reaction dependence of the catalyst in condensation-alkynylation reactions	22
Figure 2.3: Formation of propargylamine over time at variable equivalents of ketone, amine, and alkyne	23
Figure 2.4: Plot of reaction rate at varying concentrations of cyclohexanone...	24
Figure 2.5: Plot of reaction rate at varying concentrations of benzylamine	25
Figure 2.6: Plot of reaction rate at varying concentrations of 1-octyne	25
Figure 2.7: Formation of propargylamine over time with electronically diverse benzylamines in condensation-alkynylation reactions	27
Figure 3.1: Formation over time of benzylamine-derived propargylamines from tandem hydroamination-alkynylation	58
Figure 3.2: Reaction rate of tandem hydroamination-alkynylation reaction with secondary amines at varying catalyst loadings of $\text{Cu}(\text{OTf})_2$	62
Figure 3.3: Plot of reaction rate at varying concentrations of 1-hexyne in tandem hydroamination-alkynylation	63
Figure 3.4: Plot of reaction rate at varying concentrations of morpholine in tandem hydroamination-alkynylation	64
Figure 4.1: Propargylamine-derived triazoles with therapeutic effects	76
Figure 4.2: Comparison of the biological activity of tetrasubstituted vs. tri-substituted carbons bearing amines	78
Figure 4.3: Biological activity of α -tetrasubstituted triazoles against the A549 lung cancer cell line	89
Figure 5.1: Pyridyl triazoles as inhibitors of NMPRTase	145

Figure 5.2: Biological activity of pyridyl triazoles as inhibitors of MIF	147
Figure 5.3: ^1H NMR analysis of electronically diverse pyridyl triazoles	153
Figure 6.1: ^1H NMR analysis of the electronic diversity of bis-PyTriPt(BF ₄) ₂ complexes	232
Figure 6.2: ^1H NMR analysis of diverse of PyTriPdCl ₂ complexes	239
Figure 7.1: ^1H NMR analysis of diverse of PyPyrPdCl ₂ complexes	354

List of Tables

Table 2.1: Screen of copper salts as catalysts in ketone-amine-alkyne coupling reaction	14
Table 2.2: Range of amines that cleanly convert to propargylamine in ketone-amine-alkyne reaction	17
Table 2.3: Mild copper catalysis produces propargylamines with a wide range of substituted alkynes	18
Table 2.4: Synthesis of readily deprotectable propargylamines through ketone-amine-alkyne coupling with TIPS-acetylene	29
Table 3.1: Screen of copper salts as catalysts in tandem hydroamination-alkynylation reactions	51
Table 3.2: Analysis of the steric effects of alkyne substitution in the hydroamination-alkynylation reaction with secondary amines	53
Table 3.3: Range of amines and alkynes that cleanly convert to propargylamines in via tandem hydroamination-alkynylation	55
Table 4.1: Solvent screen for optimization of tandem deprotection-CuAAC reaction	82
Table 4.2: Screen of copper catalysts for silyl deprotection-triazole formation..	82
Table 4.3: Optimization of additional reaction conditions to form α -tetrasubstituted triazoles	83
Table 4.4: Scope of silyl-protected propargylamines that are cleanly converted into hindered triazoles through tandem deprotection-cyclization	85
Table 4.5: Assorted azides for the formation of α -tetrasubstituted triazoles	86
Table 4.6: Additional α -tetrasubstituted triazoles prepared for the Eli Lilly OIDD program	90
Table 5.1: Synthesis of electronically diverse aryl azides	150
Table 5.2: Preparation of electronically diverse pyridyl triazoles	151
Table 5.3: Synthesis of halogenated 2-ethynylpyridines	159
Table 5.4: Preparation of iodo-pyridyl triazoles for substitution reactions	160

Table 5.5: Synthesis of hydroxylated and alkoxyated pyridyl triazoles	166
Table 6.1: Bis-PyTriPt(II) complexes with stabilizing BF ₄ anions	231
Table 6.2: X-ray crystal structure of bis-CF ₃ PyTriPt(BF ₄) ₂	233
Table 6.3: Diverse PyTriPtCl ₂ complexes as cis-platin analogues	234
Table 6.4: X-ray crystal structure of PyTriPtCl ₂	236
Table 6.5: PyTriPdCl ₂ complexes as potential catalysts for cross-coupling reactions	237
Table 6.6: X-ray crystal structure of MePyTriPdCl ₂	240
Table 6.7: Catalyst loading screen of PyTriPdCl ₂ for Suzuki cross-coupling	245
Table 6.8: Determining optimal temperature for PyTriPdCl ₂ catalyzed cross-coupling reaction	246
Table 6.9: Base screen in Suzuki cross-coupling shows that carbonate bases are superior with PyTriPdCl ₂ catalyst	247
Table 6.10: Determining optimal ratio of DMF:H ₂ O in PyTriPdCl ₂ catalyzed cross-coupling reaction	248
Table 6.11: Screen of additional organic solvents for the Suzuki cross-coupling reaction with PyTriPdCl ₂	249
Table 6.12: Assessing the effect of decreased concentration of H ₂ O with alcohol and ether based solvents in PyTriPdCl ₂ catalyzed cross-coupling	250
Table 6.13: Use of EtOH as the solvent system allows for the complete removal of H ₂ O	251
Table 6.14: Determining optimal solvent concentration in the Suzuki cross-coupling reaction with PyTriPdCl ₂	251
Table 6.15: Screen of electronically diverse PyTriPdCl ₂ to determine optimal catalyst for Suzuki cross-coupling	252
Table 6.16: Base equivalents screen to obtain full conversion in Suzuki cross-coupling reaction	253

Table 6.17: Aryl halide substrate scope in cross-coupling reaction with $\text{CF}_3\text{PyTriPdCl}_2$	255
Table 6.18: Assessing steric effects on the active site of catalysis with $\text{CF}_3\text{PyTriPdCl}_2$	256
Table 6.19: $\text{CF}_3\text{PyTriPdCl}_2$ catalyst remains highly active in Suzuki cross-coupling with heteroaryl bromides	257
Table 6.20: Assessing the substrate scope of aryl boronic acids in cross-coupling reactions catalyzed by $\text{CF}_3\text{PyTriPdCl}_2$	259
Table 7.1: Synthesis of electronically diverse pyridyl pyrazoles via a one-pot 1,3 cyclization reaction with ethynyl pyridine	349
Table 7.2: X-ray crystal structure of the PyPyr Ligand	350
Table 7.3: Unique PyPyrPdCl ₂ complexes as potential catalysts	353
Table 7.4: X-ray crystal structure of the PyPyrPdCl ₂ complex	355
Table 7.5: Low catalytic activity of diverse PyPyrPdCl ₂ complexes in Suzuki cross-coupling reactions	356

Chapter One: Nitrogen Containing Small Molecules

1.1 Introduction:

The ability to readily access therapeutic targets and their intermediates has kept the field of small-molecule methodology at the forefront of academic and industrial research. The vast number of amine containing compounds that are currently top grossing pharmaceuticals demonstrates their inherent bioactivity and importance as synthetic targets. The development of methodologies for the formation of amine-containing compounds is of high value. With the ability to treat cancer,¹ HIV,² malaria,³ diabetes,⁴ and depression,⁵ as well as other ailments, increased efforts have been made to optimize the production of these compounds to increase yield while decreasing the environmental impact.

The prime focus of the research discussed herein has been the development and analysis of novel routes to access complex amine scaffolds, and development of new heteroaromatic based catalysts for organic transformations. An important factor that must be considered when determining research targets is the bioavailability of the desired compounds. Many of the compounds generated during the development and assessment of small-molecule methodologies possess high bioavailability. The rules and limitations that govern this field are discussed in the following sections of this chapter.

1.2 Definition of “Small Molecules”:

A number of factors contribute to the bioavailability of small molecules. One factor that is dominant is the ability of the target compound to engage in the

critical process of protein-protein interactions.⁶ These processes are responsible on the fundamental level for many ailments in the human body. In some cases, it is desirable for a target compound to encourage this interaction, while in others the disruption of the protein-protein interface is important. As a result of diversity, the shape of the typical protein interface varies, this adds to the difficulty of identifying drug targets.

On average, there is approximately 750-1500 Å² of surface area inside a protein cluster, and X-ray structures of proteins do not always show the small, deep, cavities that are the small molecule binding sites.⁷ It is however, often not necessary for a small molecule to cover the entire surface of the binding site. Rather, by binding to a much smaller portion of the protein, the interaction necessary to achieve the desired activation/deactivation can occur.⁸⁻¹¹ Further, for many protein-protein interactions the two surfaces involved often have a significant degree of flexibility.^{12,13} Thus, there might be conformations of the active site that are preferable for small molecule binding that are not visible in the solid state single crystal structure.¹⁴⁻¹⁶

In order for the target compound to enter the pocket created in a protein-protein cluster and make it to the active site, the molecule must be of an appropriate size. In general, the definition of what can be considered a small molecule is given in relation to its molecular weight. Through experimental observation, coupled with chemical computation, the optimal range for the

molecular weight of drug targets has been determined to be around 160 to 500 AMU with a polar surface area no greater than 140 \AA^2 .^{17,18}

1.3 Lipinski's Rule of Five for Biologically Active Molecules:

In addition to the limitation with regards to the molecular weight of a target drug, other attributes of drug-like compounds have been studied.¹⁹⁻²¹ From this a general rule of thumb has been determined to evaluate the "drug likeness" of a particular compound with regards to its pharmacological activity. Many of these attributes are based on the chemical or physical properties that come into play when determining whether a compound will be an orally active drug in humans. These rules were first formulated and compiled by Christopher Lipinski in 1997, based on an observation that many orally administered drugs are small lipophilic molecules.¹⁹

In his report, Lipinski states that in order for a candidate drug to have the best chance to reach the market, and have the lowest possible rates of attrition during clinical trials it should not violate more than one of the following criteria: (1) there should be no more than 5 hydrogen bond donors present in the molecule, (2) there should be no more than 10 hydrogen bond acceptors, (3) the compound should have a molecular weight less than 500 Daltons, and (4) that the compound is sufficiently lipophilic enough to pass through the cell wall. The lipophilicity is measured using an octanol-water mixture and the partition coefficient ($\log P$) for an optimal compound should not be greater than 5.^{19,20}

While a drug target must be lipophilic enough to enter a cell, it must first be administered. The most common method for administering pharmaceuticals is through oral or intravenous pathways, which require that the compound be soluble in an aqueous environment. The best way to insure this solubility is met is through the utilization of hydrogen donating (NH or OH) and hydrogen accepting (N or O) groups. These motifs can interact with water through hydrogen bonding which allows for solvation of the compound in aqueous media. While this interaction is critical to allow the compound to enter the biological environment, if an excess of polar groups are present, the ability to enter and interact with the largely non-polar protein active site will be decreased. Thus, while their inclusion is necessary, a limitation to the polarity of a particular drug target is critical to its success as a biologically active compound.

1.4 Examples of Biologically Active Nitrogen Containing Small Molecules:

There exists a wide range of natural products and biologically active compounds that contain tetrasubstituted carbons bearing amines. A few examples of which are shown in figure 1.1.^{1,22-24} Compounds such as the antitumor agent, salinosporamide A, the anesthetic, carfentanil, the lycopodium alkaloid, (-)-lycodine, and the enzyme inhibitor, (R)- α -methylphenylalanine, all contain the important tetrasubstituted α -amino core highlighted in red.

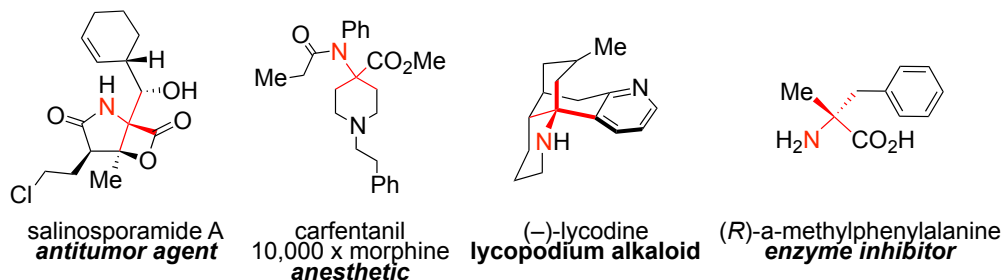


Figure 1.1: Examples of biologically active α -tetrasubstituted amines

An example of a highly important tetrasubstituted propargylamine is the HIV reverse transcriptase inhibitor shown in figure 1.2. This compound and additional derivatives are formed through the stoichiometric addition of a premade metal acetylide to an isolated ketimine intermediate.² While this is an effective method for the preparation of these compounds, the need to synthesize and isolate the intermediates, as well as the caution that must be used when generating metal acetylides, creates a need for the development of further methodology that allows for the bypassing of these wasteful and potentially hazardous steps.

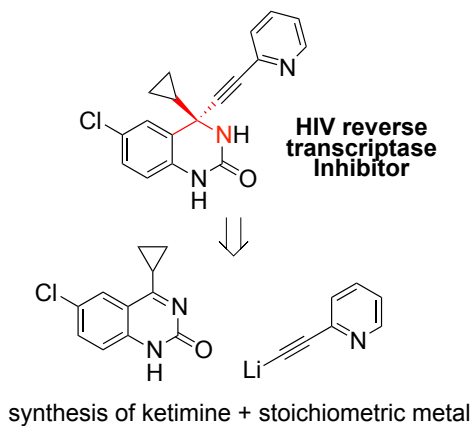


Figure 1.2: Preparation of an anti-HIV transcription drug through stoichiometric addition of nucleophile to premade ketimine.

Such strategies have been developed,²⁵⁻²⁷ and the analysis of these methods is discussed in the following chapters. Additionally, the preparation and use of highly active, heteroaromatic-based catalysts are disclosed. These compounds have demonstrated significant promise in the fields of catalysis and organometallics. Further work with these compounds will show whether their development will allow for the discovery of new organic transformations.

1.5 References:

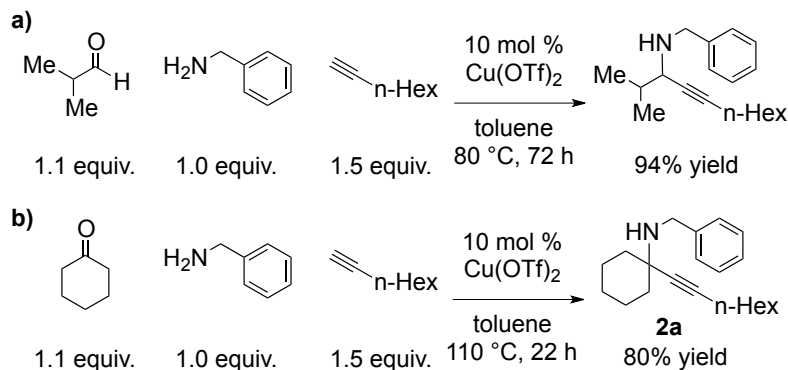
- 1) Feling, R. H.; Buchanan, G. O.; Mincer, T. J.; Kauffman, C. A.; Jensen, P. R.; Fenical, W. *Angew. Chem. Int. Ed.* **2003**, *42*, 355.
- 2) Huffman, M. A.; Yasuda, N.; DeCamp, A. E.; Grabowski, E. J. J. *J. Org. Chem.* **1995**, *60*, 1590.
- 3) Stephens, J. W. W.; Yorke, W.; Blacklock, B.; Macfie, J. W. S.; Cooper, C. F. *Ann. Trop. Med.* **1917**, *11*, 113.
- 4) Ahrén, B. *Expert Opin. Emerg. Drugs* **2008**, *13*, 593.
- 5) Oshiro, Y.; Sato, S.; Kurahashi, N.; Tanaka, T.; Kikuchi, T.; Tottori, K.; Uwahodo, Y.; Nishi, T. *J. Med. Chem.* **1998**, *41*, 658.
- 6) Arkin, M. R.; Wells, J. A. *Nat. Rev. Drug Discov.* **2004**, *3*, 301.
- 7) Lo Conte, L.; Chothia, C.; Janin, J. *J. Mol. Biol.* **1999**, *285*, 2177.
- 8) Bogan, A. A.; Thorn, K. S. *J. Mol. Biol.* **1998**, *280*, 1.
- 9) Clackson, T.; Wells, J. A. *Science* **1995**, *267*, 383.
- 10) DeLano, W. L. *Curr. Opin. Struct. Biol.* **2002**, *12*, 14.
- 11) Ma, B.; Elkayam, T.; Wolfson, H.; Nussinov, R. *Proc. Natl Acad. Sci. USA* **2003**, *100*, 5772.
- 12) Sundberg, E. J.; Mariuzza, R. A. *Structure Fold. Des.* **2000**, *8*, R137.
- 13) DeLano, W. L.; Ultsch, M. H.; de Vos, A. M.; Wells, J. A.; *Science* **2000**, *287*, 1279.
- 14) Teague, S. J. *Nature Rev. Drug Discov.* **2003**, *2*, 527.
- 15) Luque, I.; Freire, E. *Proteins* **2000**, *S4*, 63.
- 16) Ma, B.; Shatsky, M.; Wolfson, H. J.; Nussinov, R. *Protein Sci.* **2002**, *11*, 184.
- 17) Ghose, A. K.; Viswanadhan, V. N.; Wendoloski, J. J. *J. Comb. Chem.* **1999**, *1*, 55.

- 18) Veber, D. F.; Johnson, S. R.; Cheng, H. Y.; Smith, B. R.; Ward, K. W.; Kopple, K. D. *J. Med. Chem.* **2002**, *45*, 2615.
- 19) Lipinski, C. A.; Lombardo, F.; Dominy, B. W.; Feeney, P. J. *Adv. Drug. Deliv. Rev.* **1997**, *46*, 3.
- 20) Lipinski, C. A. *J. Pharmacol. Toxicol. Methods* **2000**, *44*, 235.
- 21) Lipinski, C. A. *Drug Discovery Today* **2004**, *1*, 337.
- 22) Vardanyan, R. S.; Hrubby, V. J. *Future Med. Chem.* **2014**, *6*, 385.
- 23) Ma, X.; Gang, D. R. *Nat. Prod. Rep.* **2004**, *21*, 752.
- 24) Clayden, J.; Donnard, M.; Lefranc, J.; Tetlow, D. J. *Chem. Commun.* **2011**, *47*, 4624.
- 25) Palchak, Z. L.; Lussier, D. J.; Pierce, C. J.; Larsen, C. H. *Green Chem.* **2015**, *17*, 1802.
- 26) Palchak, Z. L.; Lussier, D. J.; Pierce, C. J.; Yoo, H.; Larsen, C. H. *Adv. Synth. Catal.* **2015**, *357*, 539.
- 27) Palchak, Z. L.; Nguyen, P. T.; Larsen, C. H. *Beilstein J. Org. Chem.* **2015**, *11*, 1425.

Chapter Two: Kinetic Analysis of Propargylamine Formation Through Condensation-Alkynylation

2.1 Introduction:

The multi-component¹⁻⁵ reaction of aldehydes, amines, and alkynes is the most efficient method for the synthesis of trisubstituted propargylamines. These building blocks allow for rapid access to valuable, biologically active targets.⁶⁻³⁷ This one-pot method avoids the labor intensive synthesis and isolation of imine intermediates for subsequent alkynylation.¹⁸⁻²⁴ These multi-component reactions are of further value, as they decrease chemical waste.³⁸⁻⁴¹ However, much of the precedent for these reactions has been optimized for the conversion of aldehydes to trisubstituted propargylamines. When a ketone is exchanged for the aldehyde, the reaction fails to proceed and the corresponding tetrasubstituted propargylamine is not observed.⁶⁻¹⁰ This results because the ketimine, which is formed in situ, is a significantly less reactive electrophile for the nucleophilic attack than its aldimine counterpart.^{42,43} A ketone that has especially high reactivity is cyclohexanone, due to the strain released upon attack and conversion of the sp^2 carbon to sp^3 .⁴⁴⁻⁴⁷ As such, there is precedent for the reaction of cyclohexanones under catalytic conditions that were developed for aldehydes (Scheme 2.1).⁴⁸



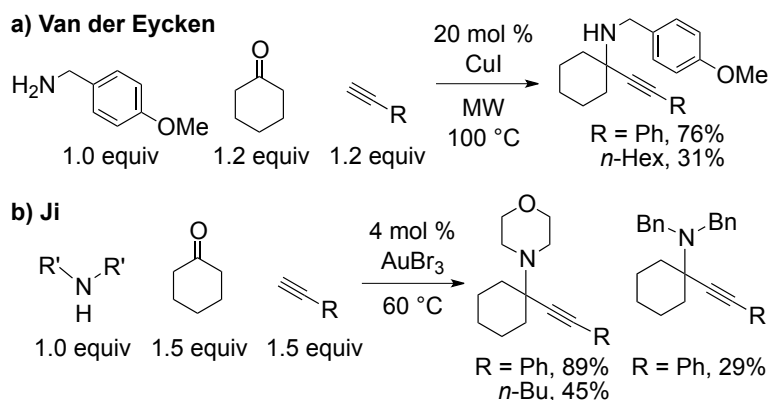
Scheme 2.1: Similar conditions allow for the three-component coupling of an aldehyde or of cyclohexanone.

2.2 Background on Propargylamine Formation via Copper(II) Catalyzed Condensation-Alkynylation:

Use of copper(II) triflate ($\text{Cu}(\text{OTf})_2$) as a catalyst for the three-component coupling of an aldehyde, amine, and alkyl alkyne, furnishes the trisubstituted propargylamine in high yield (Scheme 2.1b). By replacing the aldehyde with cyclohexanone, the tetrasubstituted propargylamine may be prepared in high yield under the same conditions. The first method developed specifically for the formation of propargylamines from cyclohexanone was reported by Van der Eycken (Scheme 2.2a).⁴⁹ In this report, the reaction is activated using microwave irradiation, for the coupling of primary benzylamines with cyclohexanone and phenyl acetylene with catalytic amounts of copper iodide (CuI) (20 mol%) at 100 °C.

A subsequent report by Ji *et al.* published a year later, showed that using a gold(III) bromide (AuBr_3) catalyst at decreased loading (4 mol%) allowed for a

similar reaction to proceed using cyclic secondary amines at 60°C (Scheme 2.2b).⁵⁰



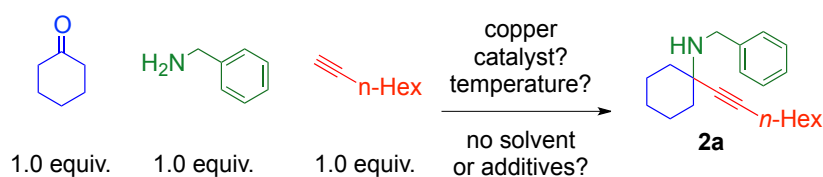
Scheme 2.2: The first three-component couplings designed for cyclohexanones.

As both of these reported methods were solvent free, they produced significantly less waste than the previous methods using toluene for the formation of trisubstituted propargylamines.⁴⁸⁻⁵⁰ When discussing the atom economy of a reaction, the solvent, almost always, represents the largest amount of “auxiliary waste”.⁵¹ While many reports highlight their use of “greener solvents”,⁵² solvent-free reactions leave a smaller environmental impact and thus should be pursued more frequently when developing methodology.⁵²⁻⁵⁵

While methods for the use of cyclohexanone have been developed, the substrate scope of these reactions have been largely limited to either primary or secondary cyclic amines with aryl terminal alkynes. When alkyl alkynes were used, significant drop in reactivity and subsequent yield was observed.^{49,50} The reaction of an electron-rich benzylamines with cyclohexanone and phenylacetylene affords the product in 76% yield, whereas the comparable

reaction using 1-octyne proceeds to give the product in 31% yield (Scheme 2.2a).⁴⁹ Further, when a secondary acyclic amine is used with phenylacetylene under the conditions reported by Ji, a three-fold decrease in reactivity is observed (Scheme 2.2b).⁵⁰ Additionally, while some secondary amines can be utilized under AuBr₃ catalysis, this catalyst is 100-times more expensive than CuI.⁵⁶

The analysis of methods for the purpose of decreasing catalyst loadings is a major focus in the development of green chemistry.³⁸⁻⁴¹ However, reducing waste from the use of excess starting materials receives little attention.⁵² If a developed method is to be applied in total synthesis, the waste of precious starting materials, derived from multiple synthetic steps, must be considered. All of the methods discussed previously waste between 0.4-1.0 equivalents of the starting materials.⁴⁸⁻⁵⁰ Therefore, in addition to developing methods that allow for solvent free reactions, another condition must be to discover ways to use only one equivalent of each reactant and avoid wasteful use of starting materials. This would allow for the formation of water to be the sole by-product of the reaction of cyclohexanone with an amine and an alkyne.



Scheme 2.3: The basis for developing a green ketone-amine-alkyne reaction with broader substrate scope.

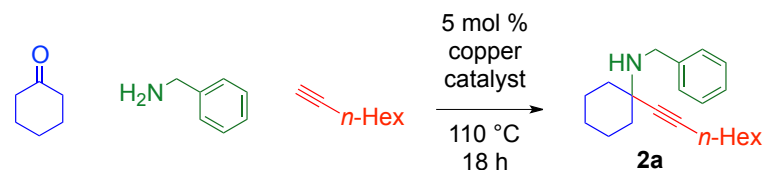
Thus, work was undertaken to combine the different advantages of each of the previously discussed methods⁴⁸⁻⁵⁰ to develop one synthetic protocol that

allowed for no solvent, decreased loadings of an inexpensive catalyst, no additional additives, high reactivity of both primary and secondary amines with both aryl and non-aryl alkynes, and use of equimolar amounts of all three starting materials (Scheme 2.3). All of these objectives were met when the first copper(II) chloride (CuCl_2) catalyzed reaction to produce tetrasubstituted propargylic amines was reported by members of the Larsen research group.⁵⁷ The objective of developing this reaction using a green chemistry platform was likely a key to its discovery.

2.3 Determining Conditions for Kinetic Analysis of Propargylamine Formation:

The first step to developing this “green” methodology was the removal of the solvent, toluene. When solvent is used, the high reactivity of $\text{Cu}(\text{OTf})_2$ as a catalyst for the reaction of cyclohexanone with a primary benzylamine and alkyl alkyne affords the desired product. However, when the solvent is removed from this reaction, large amounts of side products are observed. Thus, it was necessary to screen a wide range of copper catalysts to determine which would best be suited to operate under the desired solvent free conditions with equimolar amounts of the ketone, amine, and alkyne starting materials (Table 2.1).⁵⁷ Copper(I) and copper(II) sources were tested at 5 mol% loading and compared to a control reaction, which was performed in the absence of copper. Unsurprisingly, with the control, no propargylamine was observed after stirring for over 3 days therefore confirming the need for a copper catalyst. Also, when

solvent free conditions are used, the catalytic activity does not relate to the oxidation state of the copper source.

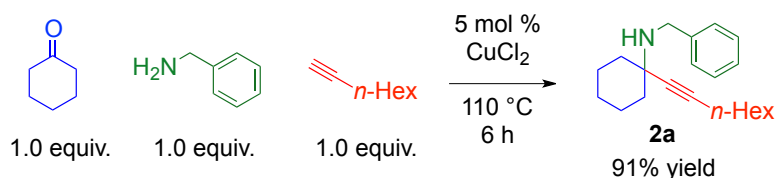


Entry	Copper Source	GC Yield (%)
1	Cu(II) triflate	59
2	Cu(II) acetate	72
3	Cu(II) bromide	72
4	Cu(II) chloride	99
5	Cu(II) perchlorate hexahydrate	50
6	Cu(II) sulfate	38
7	Cu(II) ethoxide	52
8	Cu(II) bis(hexafluoroacetoacetonato) hydrate	27
9	Cu(II) hydroxide	32
10	Cu(I) triflate tetrakisacetonitrile	45
11	Cu(I) acetate	56
12	Cu(I) bromide	72
13	Cu(I) chloride	89
14	Cu(I) bromide dimethylsulfide	94
15	Cu(I) thiophene-2-carboxylate	70
16	Cu(I) iodide	81
17	Cu(I) hexafluorophosphate tetrakisacetonitrile	46

Table 2.1: Copper screen shows that copper halides are superior to triflates under solvent free conditions.

Both Cu(II) bromide and Cu(I) bromide give identical conversion when the reaction is analyzed by gas chromatography (GC), with 72% conversion observed in both cases. However when Cu(II) chloride is used, the catalyst demonstrates superior reactivity compared to Cu(I) chloride as nearly quantitative conversion is observed. Additionally, it is observed that both

copper(I) and copper(II) halides demonstrate higher reactivity for the production of propargylamine (**2a**) than any of the other copper sources that were tested. While both CuCl_2 and $\text{CuBr}\cdot\text{Me}_2\text{S}$ demonstrate exceptional reactivity, CuCl_2 was observed to provide a faster initial rate of product formation.⁵⁷ Comparison of entries 1 vs. 4 shows the superior catalytic activity of CuCl_2 compared to the previously reported $\text{Cu}(\text{OTf})_2$, towards the formation of propargylamine (**2a**). Here, CuCl_2 provides 99% GC yield of the fully-substituted propargylamine whereas $\text{Cu}(\text{OTf})_2$ only produces 59% of the product during the 18 h time frame. When the reaction of cyclohexanone, benzylamines, and 1-octyne is performed with 5 mol% CuCl_2 under solvent free conditions at 110 °C, the tetrasubstituted propargylamine (**2a**) is isolated in 91% yield after only 6 h (Scheme 2.4). Additionally, no preference was observed for the reactivity of the copper catalyst under an inert atmosphere of either argon or nitrogen. However, while the reaction proceeds cleanly under air, an 18% decrease in conversion to propargylamine (**2a**) was observed.



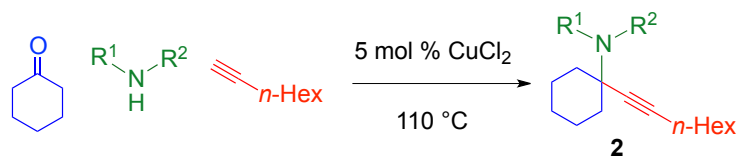
Scheme 2.4: No solvent and less catalyst produce a faster reaction with higher yield.

While the previous examples of propargylamine formation with cyclohexanone were limited to either primary⁴⁹ or secondary⁵⁰ amines with predominately phenylacetylene as the alkyne, determination of the amine

substrate scope began by assessing amines that were reactive with 1-octyne under these solvent-free, CuCl₂ catalyzed conditions (Table 2.2).⁵⁷ It was observed that primary amines were reactive and able to produce the corresponding propargylamines in good yield.

The coupling of 4-methoxybenzyl amine with cyclohexanone and 1-octyne proceeded efficiently and the product was isolated in 87% yield, an almost three-fold increase compared to the previous report which utilized quadruple the catalyst loading.⁴⁹ Additionally, acyclic secondary amines could be utilized and the product with *N*-methylbenzylamine could be isolated in comparable yields to those obtained when cyclic secondary amines were used. Under identical conditions, 2 equivalents of 1-octyne with 2 equivalents of cyclohexanone afforded a bis-propargylamine when piperazine was used.

A survey of alkynes showed that this methodology had a broad tolerance with regards to this component (Table 2.3).⁵⁷ Whereas previous reports demonstrated that use of alkyl alkynes resulted in nearly half the yield compared to the use of phenylacetylene, under solvent free conditions, these products could be isolated in nearly identical yields (entries 1-2). Propargylamines from other alkyl alkynes also form in good yield (entries 3-5). Further, silyl-protect alkynes and those bearing silyl-protected alcohols also react and the products can be isolated in 91% and 84% yield respectively. This is the first report where silyl and silyloxy tetrasubstituted propargylamines were obtained from a direct, catalytic, reaction with cyclohexanone.^{18, 57}



Entry	Amine	time (h)	Product	Yield (%)
1		6		91
2		5		87
3		5		74
4		4		88
5		3		92
6		2		88
7		16		68 ^b

^b (2.0 mmol) cyclohexanone and (2.0 mmol) 1-octyne were used.

Table 2.2: Range of amines for the ketone-amine-alkyne reaction with cyclohexanone and 1-octyne.

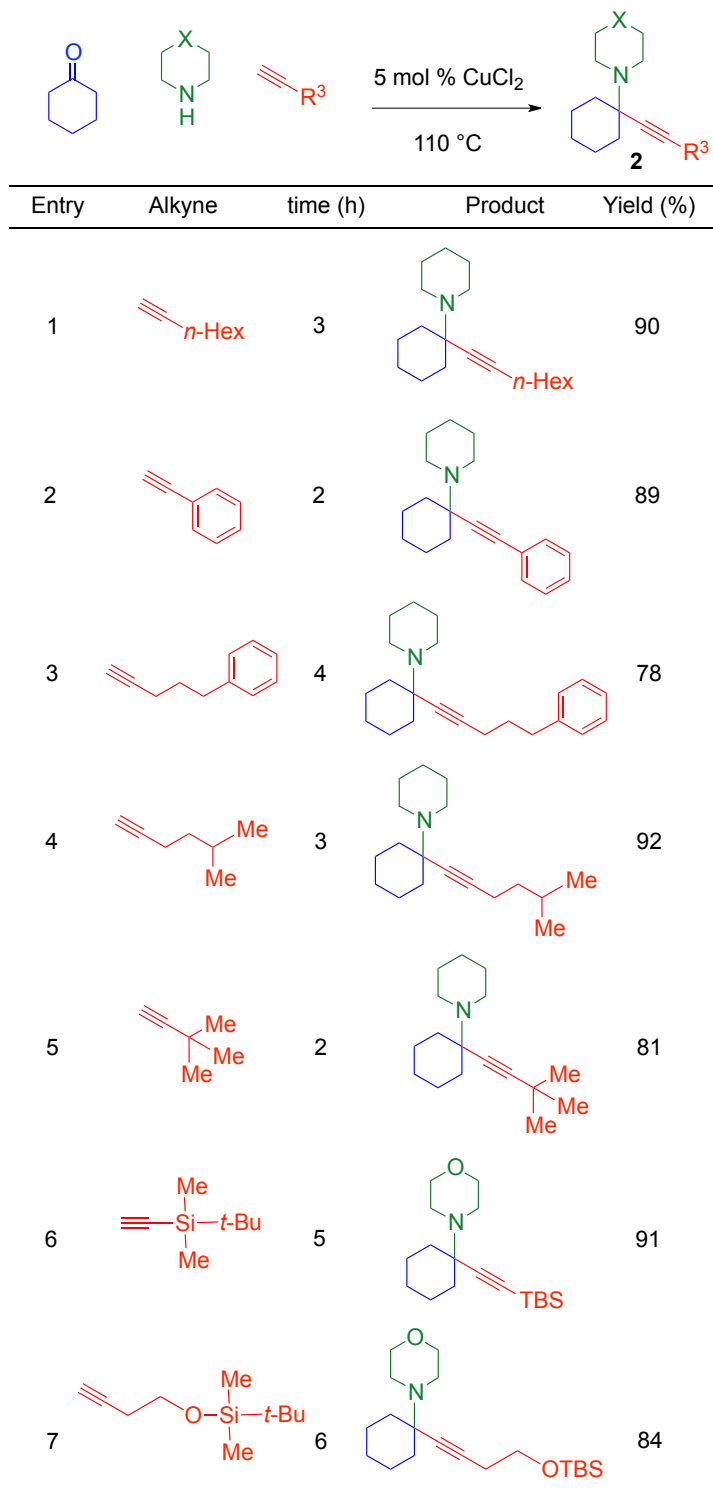
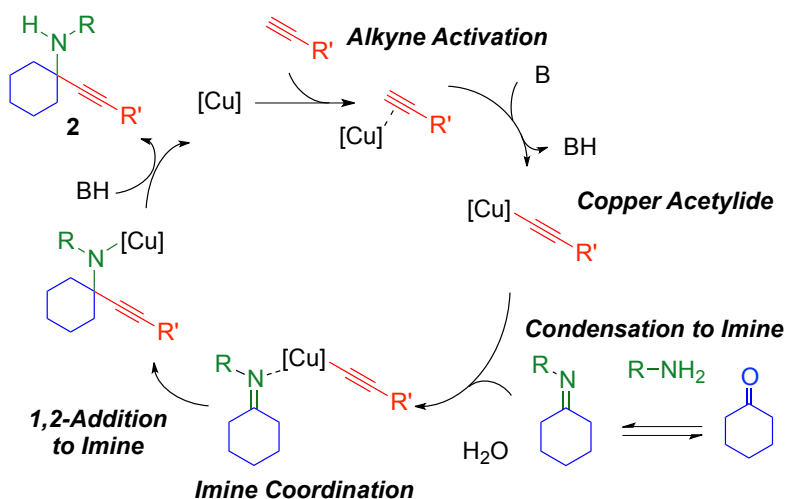


Table 2.3: Mild copper catalysis cleanly converts alkyl, aryl, silyl, and siloxyl alkynes.

2.4 Kinetic Analysis of the Condensation-Alkynylation Pathway to Form Propargylamines:

The mechanism for the CuCl_2 catalyzed reaction of cyclohexanone, an amine, and a terminal alkyne, begins with the activation of the alkyne (Scheme 2.5). Here the terminal alkyne proton is acidified through the binding of the π -system to copper and subsequent deprotonation by base (B) forms the nucleophilic copper acetylide. The electrophilic ketimine is formed through the condensation of the amine with cyclohexanone. Coordination of the ketimine to the copper acetylide precedes the nucleophilic attack on the imine.^{8,18-24} Addition of the acetylide to the ketimine forms the tetrasubstituted propargylamine. The copper is released and re-enters the catalytic cycle for further reaction.



Scheme 2.5: Catalytic cycle for the cyclohexanone-amine-alkyne coupling reaction.

Ketimine formation through condensation of the amine on cyclohexanone is reversible, and a steady-state concentration of the ketimine is observed when

benzylamines is used. The formation of ketimine from primary amines is detectible by GC analysis and correlates to samples of ketimine that were synthesized separately and confirmed by proton NMR.⁵⁸⁻⁶⁰ The addition of one to three equivalents of water is observed to have little effect of the reaction. However, when five to ten equivalents of water are added, product formation is reduced. The additional water is believed to shift the equilibrium from favoring ketimine formation to favoring the hydrolysis of the ketimine back to starting materials. While primary amines form ketimine intermediates, secondary amines form ketiminium when condensation with cyclohexanone occurs. This cationic intermediate is not observable by GC analysis. Attempts were made to detect the positively-charged ketiminium in the crude reaction mixture by NMR but this was hampered by the paramagnetic nature of the copper(II) catalyst.

As cyclohexanone and the amine are incorporated into the ketimine, which is attacked by the copper acetylide, if addition of the acetylide to the ketimine is the rate-determining step, the overall reaction should be first order in copper catalyst, cyclohexanone, amine, and alkyne.

To confirm the order of reaction for each component, the rate of formation of propargylamine product (**2a**) is measured while the concentration of each reagent or reactant is varied. The catalyst operates best under solvent-free conditions; it was shown that CuCl_2 becomes inactive when significant dilution with solvent is used. However, it was necessary to decrease the reaction rate slightly for reasonable sampling intervals during the first 10% of product

formation. While diluting the system with 0.1 M or 1.0 M acetonitrile shuts down the catalyst, using toluene was ideal as the reaction rate was observed to be cut in half at 1.0 M concentration.

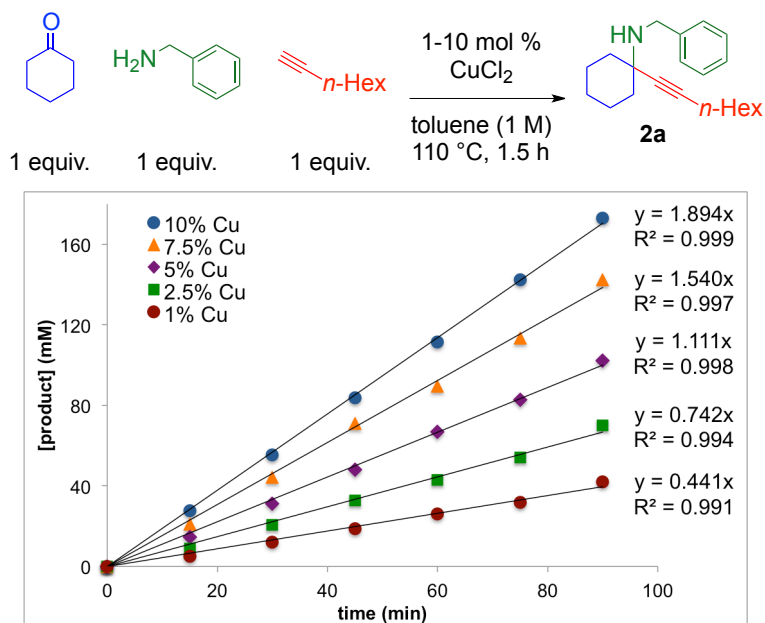


Figure 2.1: The formation of product over time at catalyst loadings from 1-10 mol% CuCl₂ each provide a linear plot with R² > 0.99.

The initial rate of reaction (i.e. the rate of product formation) is measured during the first 10% of product formation, and can be measured using GC analysis for each set of reaction parameters. By comparing to a dodecane internal standard, the concentration of propargylamine can be calculated for a given reaction time. The product formation over time for 1, 2.5, 5, 7.5, and 10 mol% CuCl₂ was measured and plotted in Figure 2.1. To measure the order of each reaction component, a set of identical reactions is started at the same time such that each data point represents the sole sample taken from one reaction. The plot of the data with a linear R² value > 0.99 at each catalyst loading

demonstrates that the data is reliable and that reactions run in parallel are uniform and reproducible. When the initial rate of reaction (V_0) is plotted against the corresponding concentration of CuCl_2 , a straight line with $R^2 = 0.998$ is observed and demonstrates that the reaction is first order with respect to the copper catalyst (Figure 2.2).

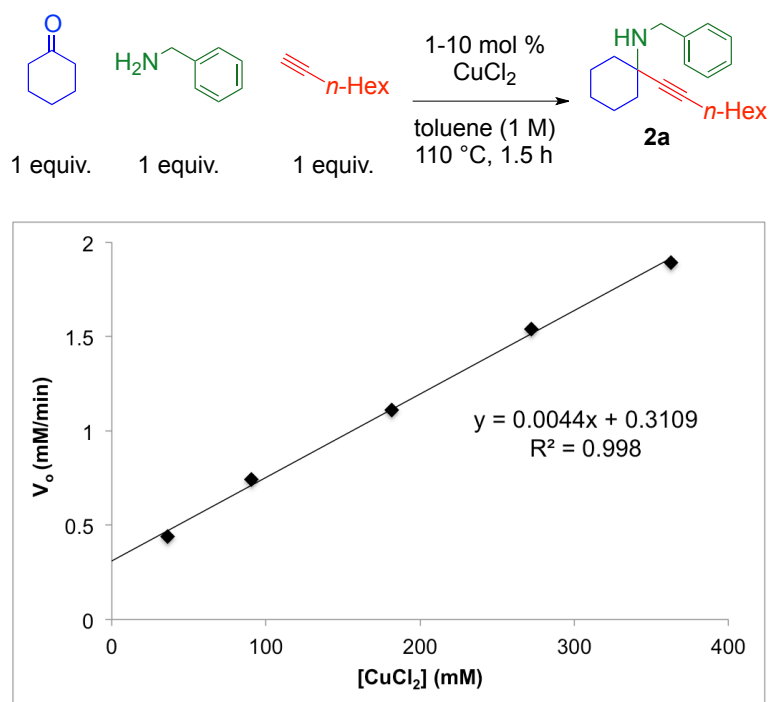
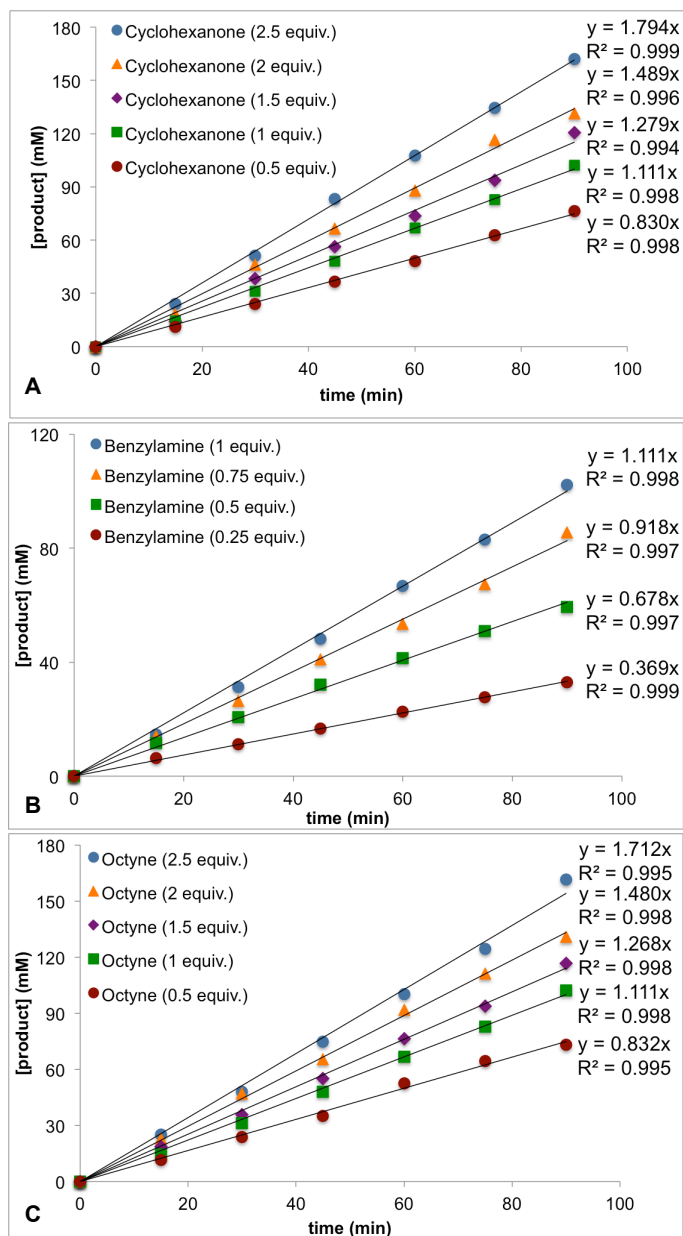
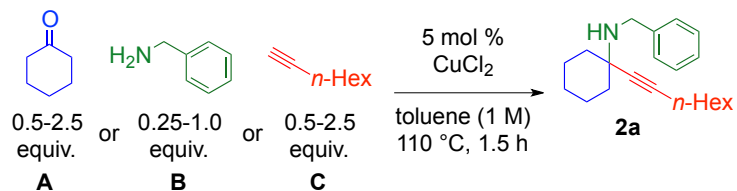


Figure 2.2: A linear plot of reaction rate indicates a first order dependence on copper(II) chloride.

The same procedure was used to determine the order of reaction for each of the remaining three reaction components. The formation of product over time is plotted with respect to varying concentrations of cyclohexanone (Figure 2.3a), benzylamine (Figure 2.3b) and 1-octyne (Figure 2.3c).



Each component is varied one at a time while the others are held at 1 equivalent.

Figure 2.3: The formation of product over time at variable equivalents of ketone/amine/alkyne, each provide a linear plot with $R^2 > 0.99$.

A graph of the initial rate of product formation (V_0) at each concentration of cyclohexanone shows a linear plot, with an $R^2 = 0.991$. This confirms that the reaction is first order with respect to the ketone starting material (Figure 2.4).

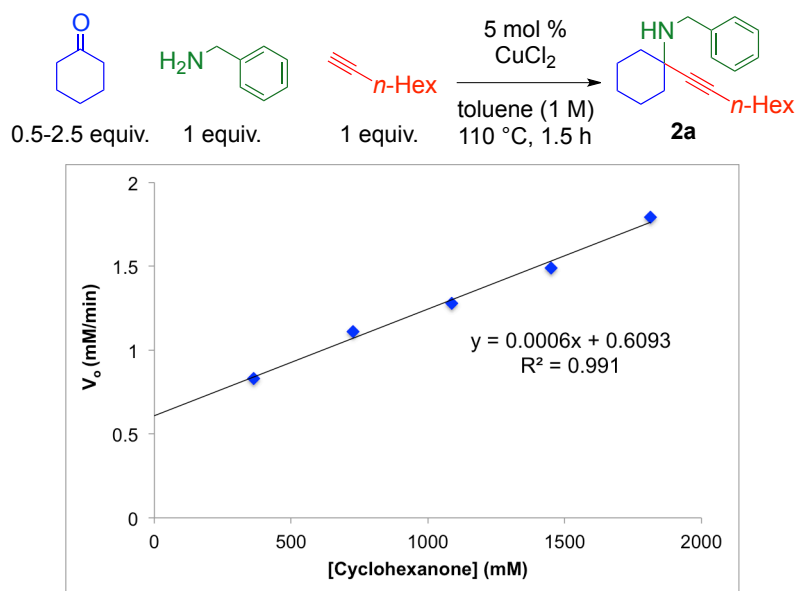


Figure 2.4: A linear plot of reaction rate indicates a first order dependence on cyclohexanone.

When the rate of product formation at varying concentrations of benzylamine is graphed, a linear plot is observed with an $R^2 = 0.996$, indicating that the reaction is first order with respect to the primary amine (Figure 2.5).

Finally, when the initial rate of product formation is graphed for each concentration of 1-octyne, a linear plot with $R^2 = 0.994$ indicates that this three-component reaction is indeed first order with respect to the terminal alkyne (Figure 2.6).

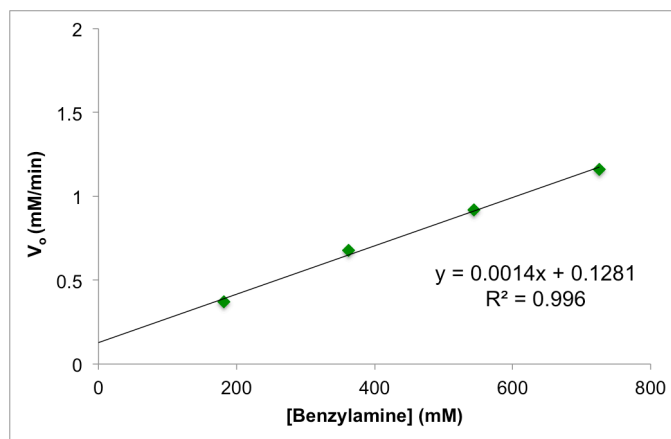
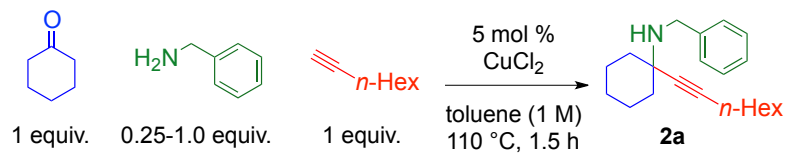


Figure 2.5: A linear plot of reaction rate indicates a first order dependence on amine.

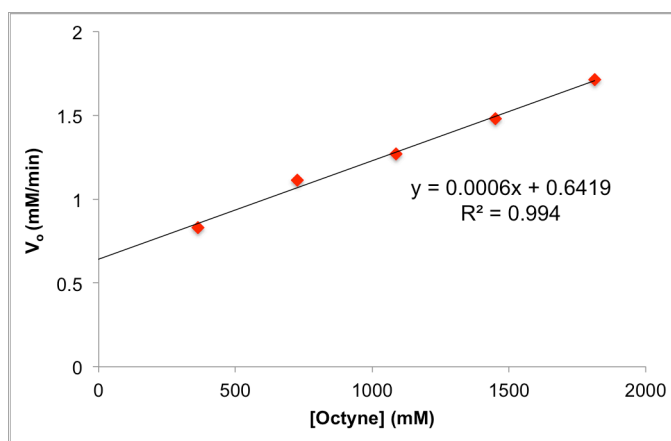
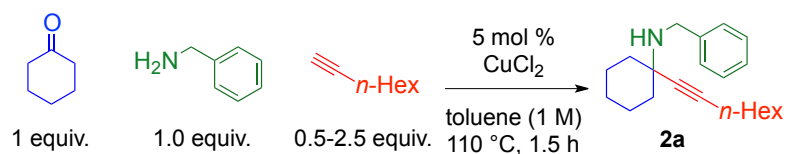


Figure 2.6: A linear plot of reaction rate indicates a first order dependence on alkyne.

The rate-determining step of the multicomponent reaction of ketones, amines, and alkynes is generally believed to be the nucleophilic attack of the

metal acetylide on the imine electrophile.¹⁸⁻³⁷ For this to be true, the nucleophilicity of the acetylide should be most important. It is reasonable to expect that some difference in rate would be observed between an alkyl acetylide and one bearing aryl substitution. For terminal alkynes, a stronger base should accelerate the formation of the copper acetylide. In the case of the reaction to form tetrasubstituted propargylamine, it would be expected that electron-donating substituents on the benzylamine would increase the rate of reaction and a decrease in reaction rate would be observed with electron-withdrawn benzylamines are used.

To experimentally determine the rate-limiting step, the formation of propargylamine over time for the CuCl₂ catalyzed reaction of cyclohexanone and 1-octyne with electronically diverse *para*-substituted benzylamines was analyzed. Analysis of aliquots by GC, taken over the first 90 min of the reaction run in toluene, provides the relative rates of product formation when 4-methoxybenzylamine, 4-methylbenzylamine, 4-chlorobenzylamine, and 4-(trifluoromethyl)benzylamine are used. Contrary to what was expected, a reaction rate that was an order of magnitude faster was observed for the most electron-poor 4-CF₃-benzylamine compared to the most electron-rich 4-MeO-benzylamine. Further, 4-Cl-benzylamine reacts nearly four times faster and 4-Me-benzylamine over twice as fast as 4-MeO-benzylamine (Figure 2.7).

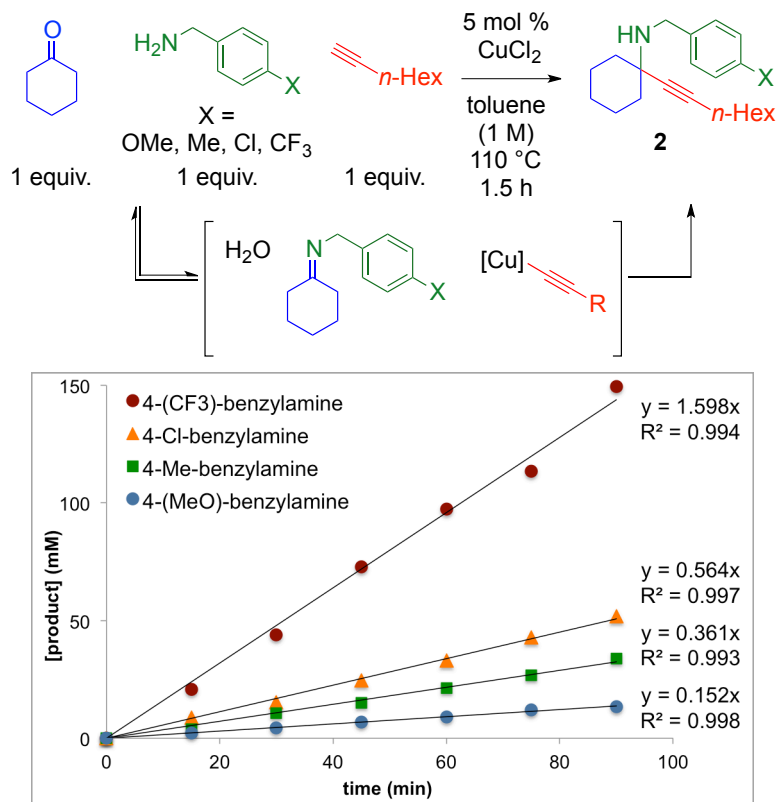


Figure 2.7: Electron-poor 4-CF₃-benzylamine reacts 10.5-times faster than electron-rich 4-MeO-benzylamine, this confirms that alkylation is the rate-limiting step.

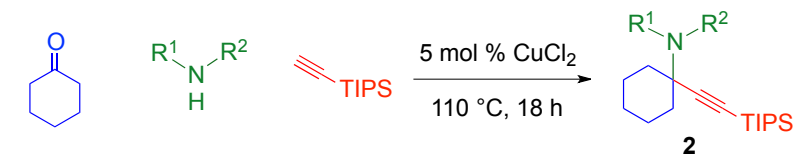
Closer examination of the GC data showed that a greater steady-state concentration of the cyclohexyl-derived ketimine was observed using 4-MeO-benzylamine compared to 4-CF₃-benzylamine. This can be explained as during the course of the reaction, the ketimine intermediate is stabilized by the electron-donating methoxy group. This is observed as a 30% increase in the concentration of this intermediate compared to the destabilized ketimine resulting from the electron-withdrawn 4-CF₃-benzylamine. The more stable, electron-rich ketimine (X = OMe) forms in a higher concentration but is less electrophilic and thus less susceptible to nucleophilic attack by the copper acetylide. In contrast,

the less stable, electron-poor ketimine ($X = CF_3$) forms in a lower concentration but is much more electrophilic and thus reacts with the copper acetylide much more rapidly.

2.5 Synthetically Useful Silyl-Protected Propargylamines Though

Utilization of TIPS-Acetylene:

The utility of tetrasubstituted propargylamines can be increased through the use of silyl alkynes. The resulting product is readily deprotectable and a terminal alkyne can be obtained. Treatment of the silyl-protected propargylamine with a nucleophilic fluoride source allows for the unmasking of the alkyne which can allow for further use in alkyne based chemistry.⁶¹ A wide range of reactions beyond the addition of a terminal alkyne to an imine or other electrophile are possible.¹⁸ One of the best known reactions with terminal alkynes is the 1,3-dipolar reaction known as the Huisgen cycloaddition. Here, the terminal alkyne can react with an organic azide to form an aromatic triazole ring via “click” chemistry.⁶²⁻⁶⁴ Previously reported conditions for the formation of trisubstituted propargylamines using $Cu(OTf)_2$ as a catalyst required equimolar amounts of base, compared to catalyst, to prevent protodesilylation when trialkylsilyl alkynes were used.⁴⁸ However, when the aforementioned, solvent-free $CuCl_2$ conditions are used,⁵⁷ a variety of TIPS-protected tetrasubstituted propargylamines can be prepared without the need for additional additives or base (Table 2.4).



Entry	Amine	Product	Yield (%)
1			80
2			75
3			76
4			73 ^b
5			98
6			70

^b Reaction was complete in 6 hours.

Table 2.4: Silyl alkynes react readily with cyclohexanone and a range of amines.

The reaction of cyclohexanone, (triisopropylsilyl)-acetylene, and a primary or secondary benzylamine cleanly affords the protected propargylamines **2c-2e** in high yield (75-80%). Secondary cyclic amines are also reactive and the resulting tetrasubstituted products **2f-2h** can be formed in high to near quantitative yield. Thus, in addition to the ability to manipulate the amines and alkynes used in this solvent-free, copper catalyzed system, these new silyl-protected alkynes allow for even further functionalization of the tetrasubstituted propargylamines.

2.6 References:

- 1) Posner, G. H. *Chem. Rev.* **1986**, *86*, 831.
- 2) Weber, L.; Illgen, K.; Almstetter, M. *Synlett*, **1999**, 366.
- 3) Dömling, A. *Chem. Rev.* **2006**, *106*, 17.
- 4) Touré, B. B.; Hall, D. G. *Chem. Rev.* **2009**, *109*, 4439.
- 5) Biggs-Houck, J. E.; Younai A.; Shaw, J. T. *Curr. Opin. Chem. Biol.* **2010**, *14*, 371.
- 6) Yamada, K.; Tomoika, K. *Chem. Rev.* **2008**, *108*, 2874.
- 7) Trost, B. M.; Weiss, A. H. *Adv. Synth. Catal.* **2009**, *351*, 963.
- 8) Blay, G.; Monleón, A.; Pedro, J. R. *Curr. Org. Chem.* **2009**, *13*, 1498.
- 9) Yoo, W. J.; Zhao, L.; Li, C. J. *Aldrichimica Acta*, **2011**, *44*, 43.
- 10) Peshkov, V. A.; Pereshivko, O. P.; Van der Eycken. E. V. *Chem. Soc. Rev.* **2012**, *41*, 3790.
- 11) Ryan, C. W.; Ainsworth, C. *J. Org. Chem.* **1961**, *26*, 1547.
- 12) Konishi, M.; Ohkuma, H.; Tsuno, T.; Oki, T. *J. Am. Chem. Soc.* **1990**, *112*, 3715.
- 13) Nilsson, B.; Vargas, H. M.; Ringdahl, B.; Hacksell, U. *J. Med. Chem.* **1992**, *35*, 285.
- 14) Hattoi, K.; Miyata, M.; Yamamoto, H. *J. Am. Chem. Soc.* **1993**, *115*, 1151.
- 15) Huffman, M. A.; Yasuda, N.; DeCamp, A. E.; Grabowski, E. J. *J. Org. Chem.* **1995**, *60*, 1590.
- 16) Kauffman, G. S.; Harris, G. D.; Dorow, R. L.; Stone, B. R. P.; Parsons, R. L.; Pesti, J. A.; Magnus, N. A.; Fortunak, J. M.; Confalone, P. N.; Nugent, W. A. *Org. Lett.* **2000**, *2*, 3119.
- 17) Kihara, K.; Aoki, T.; Moriguchi, A.; Yamamoto, H.; Maeda, M.; Tojo, N.; Yamanaka, T.; Ohkubo, M.; Matsuoka, N.; Seki, J.; Mutoh, S. *Drug Dev. Res.* **2004**, *61*, 233.

- 18) Fischer, C.; Carreira, E. M. *Org. Lett.* **2001**, *3*, 4319.
- 19) Koradin, C.; Polborn, K.; Knochel, P. *Angew. Chem. Int. Ed.* **2002**, *41*, 2535.
- 20) Wei, C.; Li, C. J. *J. Am. Chem. Soc.* **2002**, *124*, 5638.
- 21) Jiang, B.; Si, Y. G. *Tetrahedron Lett.* **2003**, *44*, 6767.
- 22) Fischer, C.; Carreira, E. M. *Synthesis*, **2004**, 1497.
- 23) Benaglia, M.; Negri, D.; Dell'Anna, G. *Tetrahedron Lett.* **2004**, *45*, 8705.
- 24) Colombo, F.; Benaglia, M.; Orlandi, S.; Usuelli, F.; Celentano, G. *J. Org. Chem.* **2006**, *71*, 2064.
- 25) Dyatkin, A. B.; Rivero, R. A. *Tetrahedron Lett.* **1998**, *39*, 3647.
- 26) Sakaguchi, S.; Kubo, T.; Ishii, Y. *Angew. Chem. Int. Ed.* **2001**, *40*, 2534.
- 27) Li, C. J.; Wei, C. *Chem. Commun.* **2002**, 268.
- 28) Wei, C.; Li, C.-J. *Green Chem.* **2002**, *4*, 39.
- 29) Li, C.-J. *Acc. Chem. Res.*, **2002**, *35*, 533.
- 30) Koradin, C.; Polborn, K.; Knochel, P. *Angew. Chem. Int. Ed.* **2002**, *41*, 2535.
- 31) Fassler, R.; Frantz, D. E.; Oetiker, J.; Carreira, E. M. *Angew. Chem. Int. Ed.* **2002**, *41*, 3054.
- 32) Zhang, J. H.; Wei, C.; Li, C.-J. *Tetrahedron Lett.* **2002**, *43*, 5731.
- 33) Gommermann, N.; Koradin, C.; Polborn, K.; Knochel, P. *Angew. Chem. Int. Ed.* **2003**, *42*, 5763.
- 34) Koradin, C.; Gommermann, N.; Polborn, K.; Knochel, P. *Chem. Eur. J.* **2003**, *9*, 2797.
- 35) Wei, C. M.; Li, C. J. *J. Am. Chem. Soc.* **2003**, *125*, 9584.
- 36) Leadbeater, N. E.; Torenus, H. M.; Tye, H. *Mol. Diversity*, **2003**, *7*, 135.
- 37) Wei, C.; Li, Z.; Li, C. J. *Org. Lett.* **2003**, *23*, 4473.

- 38) Noyori, R. *Green Chem.* **2003**, *5*, G37.
- 39) Sheldon, R. A. *Green Chem.* **2005**, *7*, 267.
- 40) Noyori, R. *Chem. Commun.* **2005**, 1807;
- 41) Sheldon, R. A. *Chem. Commun.* **2008**, 3352.
- 42) Zhuang, W.; Saaby, S.; Jørgensen, K. A. *Angew. Chem. Int. Ed.* **2004**, *43*, 4476.
- 43) Ma, Y.; Lobkovsky, E.; Collum, D. B. *J. Org. Chem.* **2005**, *70*, 2335.
- 44) Anslyn, E.V.; Dougherty, D. A. *Modern Physical Organic Chemistry*, University Science Books, Sausalito, CA, **2006**, p 562.
- 45) Wheeler, O. H. *J. Am. Chem. Soc.* **1957**, *79*, 4191.
- 46) Cherest, M.; Felkin, H.; Prudent, N. *Tetrahedron Lett.* **1968**, 2199.
- 47) Cherest, M.; Felkin, H. *Tetrahedron Lett.* **1968**, 2205.
- 48) Meyet, C. E.; Pierce, C. J.; Larsen, C. H. *Org. Lett.* **2012**, *14*, 964.
- 49) Pereshivko, O. P.; Peshkov, V. A.; Van der Eycken, E. V. *Org. Lett.* **2010**, *12*, 2638.
- 50) Cheng, M.; Zhang, Q.; Hu, X. Y.; Li, B. G.; Ji, J. X.; Chan, A. S. C. *Adv. Synth. Catal.* **2011**, *353*, 1274.
- 51) Li, C.-J.; Trost, B. M. *Proc. Natl. Acad. Sci. USA*, **2008**, *105*, 702.
- 52) Jessop, P. G. *Green Chem.* **2011**, *13*, 1391.
- 53) Lippard, S. J. *Chem. Eng. News* **2000**, *78*, 64.
- 54) Thomas, J. M.; Raja, R.; Sankar, G.; Johnson, B. F. G.; Lewis, D. W. *Chem. Eur. J.* **2001**, *7*, 2972.
- 55) Walsh, P. J.; Li, H.; Anaya de Parrodi, C. *Chem. Rev.* **2007**, *107*, 2503.
- 56) CuI costs 57 USD for 100g at Sigma-Aldrich. Cost of 1g of AuBr₃ (99.9+%) ranges from 86 USD at Strem Chemicals, Inc., to 125 USD at Sigma-Aldrich.

- 57) Pierce, C. J.; Larsen, C. H. *Green Chem.* **2012**, *14*, 2672.
- 58) Weingarten, H.; Chupp, J. P.; White, W. A. *J. Org. Chem.* **1967**, *92*, 3246.
- 59) Chupp, J. P.; White, W. A. *J. Org. Chem.* **1968**, *92*, 2357.
- 60) Liu, G.; Cogan, D. A.; Owens, T. D.; Tang, T. P.; Ellman, J. A. *J. Org. Chem.* **1999**, *64*, 1278.
- 61) Gommermann, N.; Gehrig, A.; Knochel, P. *Synlett* **2005**, 2976.
- 62) Huisgen, R. *Pure Appl. Chem.* **1989**, *61*, 613.
- 63) Rostovtsev, V. V.; Green, L. G.; Fokin, V. V.; Sharpless, B. K. *Angew. Chem. Int. Ed.* **2002**, *41*, 2596.
- 64) Meldal, M.; Tomøe, C. W. *Chem. Rev.* **2008**, *108*, 2952.

2.7 Supporting Information:

General reagent information

All reactions were set up in the air and carried out in oven-dried screw-cap test-tubes with Teflon seals under an atmosphere of nitrogen. Flash column chromatography was performed using silica gel purchased from Silicycle. CuCl_2 was purchased from Acros and used as supplied. Amines were purchased from Acros Organics, Alfa Aesar, or Aldrich and distilled before use. All ketones and alkynes were purchased from Acros Organics, Alfa Aesar or TCI America and were purified by distillation before use.

General analytical information

^1H and ^{13}C NMR spectra were measured on a Varian Inova 400 (400 MHz) spectrometer using CDCl_3 as a solvent and trimethylsilane as an internal standard. The following abbreviations are used singularly or in combination to indicate the multiplicity of signals: s - singlet, d - doublet, t - triplet, q - quartet, m - multiplet and br - broad. NMR spectra were acquired at 300 K. Gas chromatography (GC) was carried out on an Agilent Technologies 6850 Network GC System, and dodecane was used as the internal standard. IR spectra were recorded on Perkin Elmer Spectrum One FT-IR Spectrometer. Attenuated total reflection infrared (ATR-IR) was used for analysis with selected absorption maxima reported in wavenumbers (cm^{-1}). Mass spectrometric data was collected on a HP 5989A GC/MS quadrupole instrument. Exact masses were recorded on

a Waters GCT Premier ToF instrument using direct injection of samples in acetonitrile into the electrospray source.

General procedure for the synthesis of tetrasubstituted propargylamines:

An oven-dried test tube equipped with a magnetic stir bar was charged with 5 mol % CuCl₂, capped with a septum, and purged with argon for 5 min. Cyclohexanone (1.0 equiv), alkyne (1.0 equiv.), and amine (1.0 equiv) were added, and the septum under Argon pressure was then quickly replaced with a Teflon-seal screw cap. The reaction was stirred at 110 °C for the indicated time. Upon reaction completion as confirmed by GC analysis, the mixture was cooled to room temperature and loaded directly atop a silica gel column. Chromatography with the solvent system indicated as the eluent afforded the desired product.

N-benzyl-1-(oct-1-yn-1-yl)cyclohexanamine (2a):

Prepared according to the general procedure: Benzylamine (110 μL, 1.0 mmol), cyclohexanone (104 μL, 1.0 mmol), 1-octyne (148 μL, 1.0 mmol), CuCl₂ (6.7 mg, 0.05 mmol) afford the title compound as a clear light yellow oil in 90% yield (0.268 g, 0.90 mmol) after chromatography on silica gel (20% EtOAc/hexanes). Characterization of this propargylamine matches that published in: Pierce, C. J.; Larsen, C. H. *Green Chem.* **2012**, 14, 2627.

1-(oct-1-yn-1-yl)-N-(4-(trifluoromethyl)benzyl)cyclohexanamine (2b):

Prepared according to the general procedure: 4-(trifluoromethyl)benzylamine (142 μL, 1.0 mmol), cyclohexanone (103 μL, 1.0 mmol), octyne (147 μL, 1.2

mmol), and CuCl_2 (6.7 mg, 0.05 mmol) afford the title compound as a yellow oil in 74% yield (0.270 g, 0.74 mmol) after chromatography on silica gel (20% EtOAc in hexanes). IR (film) 2946, 2853, 2155, 1460, 1325, 1174 cm^{-1} . ^1H NMR (400 MHz, CDCl_3) δ 7.47 (d, J = 8 Hz, 2H), 7.40 (d, J = 8 Hz, 2H), 3.86 (s, 2H), 2.17 (t, J = 6.8 Hz, 2H), 1.75 (d, J = 12 Hz, 2H), 1.60-1.12 (m, 17H), 0.81 (t, J = 6.8 Hz, 3H). ^{13}C NMR (100 MHz, CDCl_3) δ 145.8, 128.8, 128.7 (2 overlapping carbons), 125.3 (J = 4.0 Hz), 123.15, 84.9, 83.81, 55.0, 47.6, 38.7, 31.5, 29.3, 28.7, 26.1, 23.1, 22.8, 18.9, 14.2. HRMS (ESI) m/z calcd for $[\text{M}+\text{H}]^+$ requires 366.2403, found 366.2420.

4-*N*-(4-(trifluoromethyl)benzyl)-1-((triisopropylsilyl)ethynyl)

cyclohexanamine (2c):

Prepared according to the general procedure: 4-(trifluoromethyl)-benzylamine (142 μL , 1.0 mmol), cyclohexanone (103 μL , 1.0 mmol), (triisopropylsilyl) acetylene (269 μL , 1.2 mmol), and CuCl_2 (6.7 mg, 0.05 mmol) afford the title compound as a yellow oil in 80% yield (0.350 g, 0.80 mmol) after chromatography on silica gel (20% EtOAc in hexanes). IR (film) 2936, 2863, 2155, 1462, 1323, 1163 cm^{-1} . ^1H NMR (400 MHz, CDCl_3 , 25 $^\circ\text{C}$) δ 7.46 (d, J = 8 Hz, 2H), 7.39 (d, J = 8 Hz, 2H), 3.90 (s, 2H), 1.78 (d, J = 12 Hz, 3H), 1.58 (m, 6H), 1.33 (m, 2H), 1.13 (m, 2H) 1.02 (d, J = 4 Hz, 18H). ^{13}C NMR (100 MHz, CDCl_3 , 25 $^\circ\text{C}$) δ 145.5, 128.8 (2 overlapping carbons), 125.3 (J = 4.0 Hz) (2 carbons overlapped), 112.1, 84.4, 55.8, 47.8, 38.4, 26.0, 23.1, 18.8, 11.4. HRMS (ESI) m/z calcd for $[\text{M}+\text{H}]^+$ requires 438.2798, found 438.2775.

***N*-benzyl-1-((triisopropylsilyl)ethynyl)cyclohexanamine (2d):**

Prepared according to the general procedure: benzylamine (109 μL , 1.0 mmol), cyclohexanone (103 μL , 1.0 mmol), (triisopropylsilyl) acetylene (269 μL , 1.2 mmol), and CuCl_2 (6.7 mg, 0.05 mmol) afford the title compound as a yellow oil in 75% yield (0.277 g, 0.75 mmol) after chromatography on silica gel (10% EtOAc in hexanes). IR (film) 2931, 2862, 2154, 1461, 1279 cm^{-1} . ^1H NMR (400 MHz, CDCl_3 , 25 $^\circ\text{C}$) δ 7.27 (d, J = 7.2 Hz, 2H), 7.21 (t, J = 7.2 Hz, 2H), 7.13 (t, J = 7.2 Hz, 1H), 3.84 (s, 2H), 1.80 (d, J = 16 Hz, 3H), 1.59 (m, 6H), 1.34 (m, 2H), 1.17 (m, 2H) 1.03 (d, J = 4 Hz, 18H). ^{13}C NMR (100 MHz, CDCl_3 , 25 $^\circ\text{C}$) δ 141.2, 128.8, 128.6, 127.0, 112.5, 84.2, 55.9, 48.4, 38.4, 26.1, 23.3, 18.9, 11.5. HRMS (ESI) m/z calcd for $[\text{M}+\text{H}]^+$ requires 370.2925, found 370.2936.

***N*-benzyl-*N*-methyl-1-((triisopropylsilyl)ethynyl) cyclohexanamine (2e):**

Prepared according to the general procedure: *N*-methyl-benzylamine (129 μL , 1.0 mmol), cyclohexanone (103 μL , 1.0 mmol), (triisopropylsilyl) acetylene (269 μL , 1.2 mmol), and CuCl_2 (6.7 mg, 0.05 mmol) afford the title compound as a yellow oil in 76% yield (0.291 g, 0.76 mmol) after chromatography on silica gel (10% EtOAc in hexanes). IR (film) 2932, 2863, 2153, 1462, 1058 cm^{-1} . ^1H NMR (400 MHz, CDCl_3 , 25 $^\circ\text{C}$) δ 7.24 (d, J = 8 Hz, 2H), 7.20 (t, J = 8 Hz, 2H), 7.11 (t, J = 8 Hz, 1H), 3.53 (s, 2H), 2.06 (s, 3H), 1.96 (d, J = 12 Hz, 3H), 1.64 (m, 2H), 1.54 (t, J = 9.6 Hz, 2H), 1.45 (t, J = 12 Hz, 2H), 1.18 (m, 4H) 1.03 (d, J = 4 Hz, 18H). ^{13}C NMR (100 MHz, CDCl_3 , 25 $^\circ\text{C}$) δ 141.2, 128.9, 128.2, 126.6, 109.0,

84.7, 59.6, 56.0, 36.98, 35.3, 25.9, 23.1, 18.9, 11.4. HRMS (ESI) m/z calcd for $[M+H]^+$ requires 384.3081, found 384.3089.

4-methyl-1-(1-((triisopropylsilyl)ethynyl)cyclohexyl) piperidine (2f):

Prepared according to the general procedure: 4-methyl-piperidine (117 μ L, 1.0 mmol), cyclohexanone (103 μ L, 1.0 mmol), (triisopropylsilyl) acetylene (269 μ L, 1.2 mmol), and CuCl_2 (6.7 mg, 0.05 mmol) afford the title compound as a yellow oil in 98% yield (0.354 g, 0.98 mmol) after chromatography on silica gel (20% EtOAc in hexanes). IR (film) 2926, 2863, 2154, 1462, 1258 cm^{-1} . ^1H NMR (400 MHz, CDCl_3 , 25 $^\circ\text{C}$) δ 2.96 (d, J = 16 Hz, 2H), 2.14 (t, J = 12 Hz, 2H), 1.96 (d, J = 16 Hz, 3H), 1.58 (m, 7H), 1.30 (t, J = 12.4 Hz, 3H), 1.13 (m, 5H), 1.01 (d, J = 4 Hz, 18H). ^{13}C NMR (100 MHz, CDCl_3 , 25 $^\circ\text{C}$) δ 108.9, 85.19, 59.4, 46.4, 36.3, 35.0, 31.1, 25.8, 23.2, 21.8, 18.8, 11.4. HRMS (ESI) m/z calcd for $[M+H]^+$ requires 362.3238, found 362.3226.

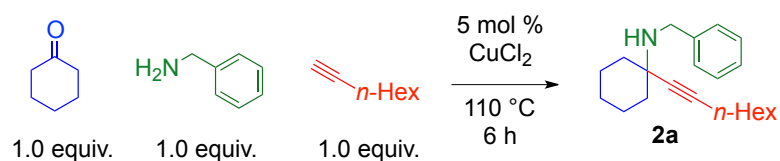
1-methyl-4-(1-((triisopropylsilyl)ethynyl)cyclohexyl) piperazine (2g):

Prepared according to the general procedure: 1-methyl-piperazine (110 μ L, 1.0 mmol), cyclohexanone (103 μ L, 1.0 mmol), (triisopropylsilyl) acetylene (269 μ L, 1.2 mmol), and CuCl_2 (6.7 mg, 0.05 mmol) afford the title compound as a yellow oil in 70% yield (0.253 g, 0.70 mmol) after column chromatography on silica gel (25% methanol in CH_2Cl_2). IR (film) 2932, 2863, 2155, 1456, 1283 cm^{-1} . ^1H NMR (400 MHz, CDCl_3 , 25 $^\circ\text{C}$) δ 2.65 (bs, 4H), 2.46 (bs, 4H), 2.22 (s, 3H), 1.91 (d, J = 16 Hz, 3H), 1.56 (m, 6H), 1.32 (t, J = 12 Hz, 2H), 1.12 (m, 2H), 1.00 (d, J = 4 Hz, 18H). ^{13}C NMR (100 MHz, CDCl_3 , 25 $^\circ\text{C}$) δ 108.0, 86.2, 58.9, 55.6, 45.8, 45.7,

35.9, 25.6, 22.9, 18.7, 11.3. HRMS (ESI) m/z calcd for $[M+H]^+$ requires 363.3190, found 363.3203.

Concentrated solvent screen study:

Carried out under the general procedure except with an added 1 mL solvent as indicated in entries 2-4: benzylamine (110 μ L, 1.0 mmol), cyclohexanone (104 μ L, 1.0 mmol), 1-octyne (148 μ L, 1.0 mmol), CuCl₂ (6.8 mg, 0.05 mmol), and dodecane internal standard (20 μ L). GC aliquots were flushed through a silica gel pipette plug with diethyl ether.

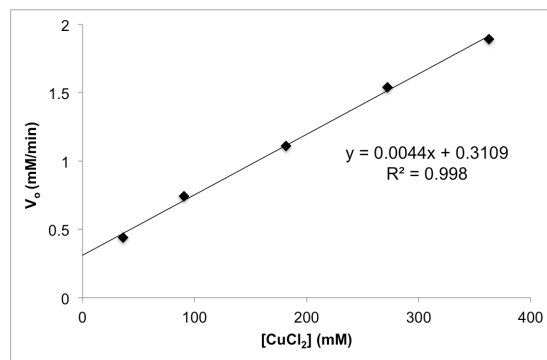
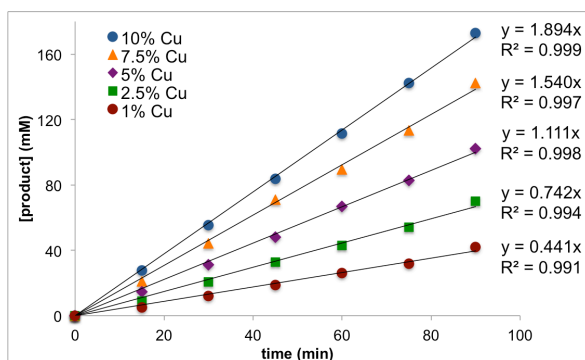
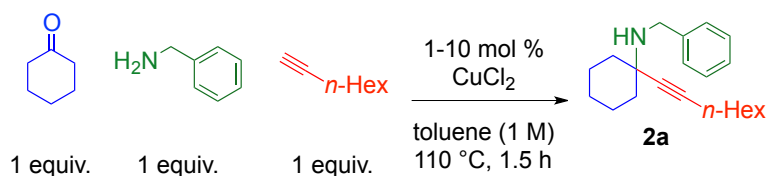


Entry	Solvent	GC yield (%)
1	none	90
2	hexanes	5
3	toluene	52
4	acetonitrile	18

Catalyst (CuCl₂) loading study:

At each catalyst loading, a set of identical reactions was set up; each data point represents the sole sample taken from a reaction. An oven-dried test tube equipped with a magnetic stir bar was charged with CuCl₂ (1–10 mol %, 1.3 mg–13.4 mg), capped with a septum, and purged with argon for 5 min. Cyclohexanone (103 μ L, 1.0 mmol), octyne (147 μ L, 1.0 mmol), benzylamine (109 μ L, 1.0 mmol), dodecane internal standard (20 ml), and toluene (1 mL) were added via syringe. Under argon pressure, the septum was then quickly replaced

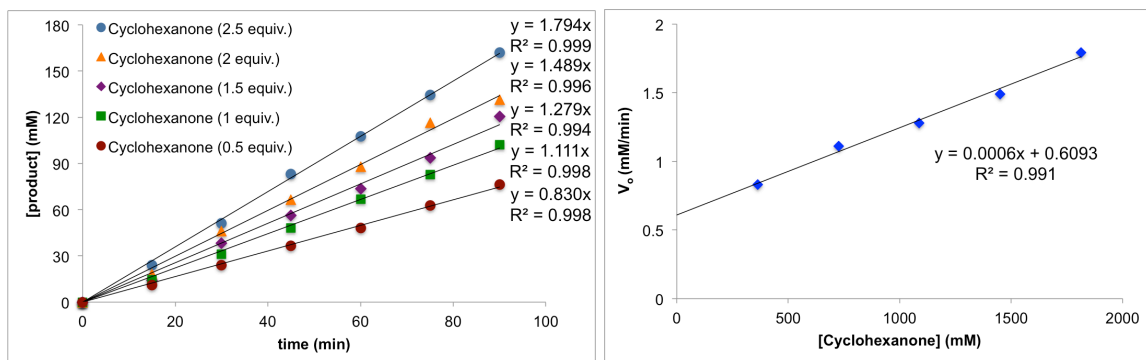
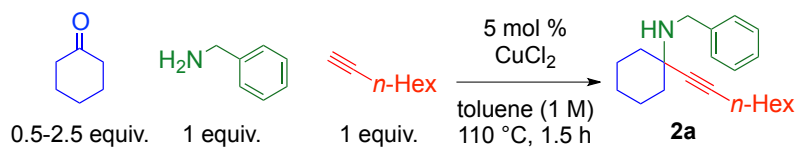
with a Teflon-seal screw cap. The reaction was stirred at 110 °C for 90 min. GC aliquots at each time point were flushed through a silica gel pipette plug with diethyl ether.



Cyclohexanone Concentration Study:

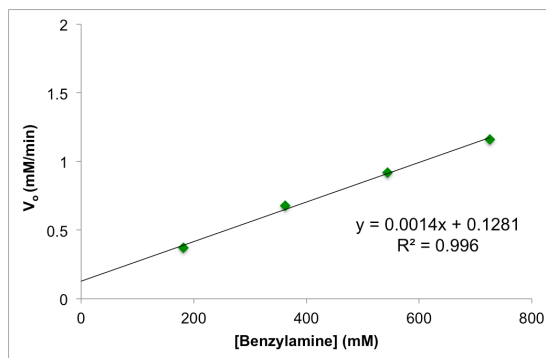
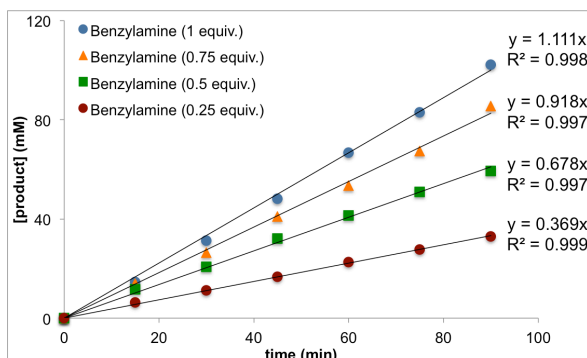
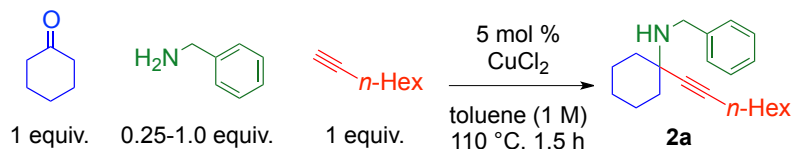
At each concentration of cyclohexanone, a set of identical reactions was set up; each data point represents the sole sample taken from a reaction. An oven-dried test tube equipped with a magnetic stir bar was charged with CuCl₂ (5 mol %, 6.7 mg), capped with a septum, and purged with argon for 5 min. Toluene (1051 μL - 846 μL) was added such that the total reaction volume remained constant. The dodecane internal standard (20 μL) was added, followed by cyclohexanone (51 μL - 257 μL, 0.5 - 2.5 mmol), benzylamine (109 μL, 1.0 mmol) and octyne (147 μL, 1.0 mmol). Under argon pressure, the septum was then quickly replaced with a Teflon-seal screw cap. The reaction was stirred at 110 °C for 90 min. GC

aliquots at each time point were flushed through a silica gel pipette plug with diethyl ether.



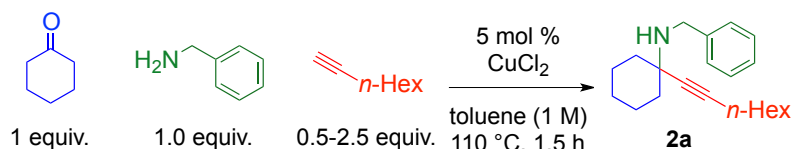
Benzylamine Concentration Study:

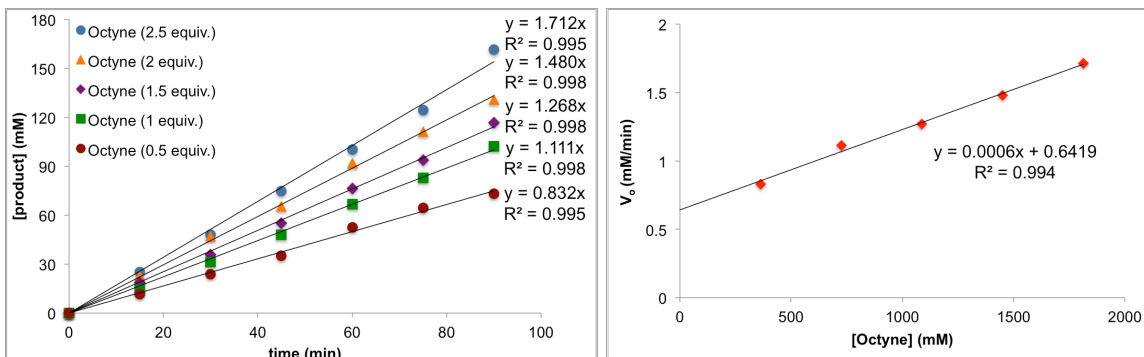
At each concentration of benzylamine, a set of identical reactions was set up; each data point represents the sole sample taken from a reaction. An oven-dried test tube equipped with a magnetic stir bar was charged with CuCl₂ (5 mol %, 6.7 mg), capped with a septum, and purged with argon for 5 min. Toluene (1081 μL - 837 μL) was added such that the overall concentration was kept constant. The dodecane internal standard (20 μL) was added, followed by cyclohexanone (103 μL, 1.0 mmol), benzylamine (27 μL - 272 μL, 0.25 - 2.5 mmol), and octyne (147 μL, 1.0 mmol). Under argon pressure, the septum was then quickly replaced with a Teflon-seal screw cap. The reaction was stirred at 110 °C for 90 min. GC aliquots at each time point were flushed through a silica gel pipette plug with diethyl ether.



1-Octyne Concentration Study:

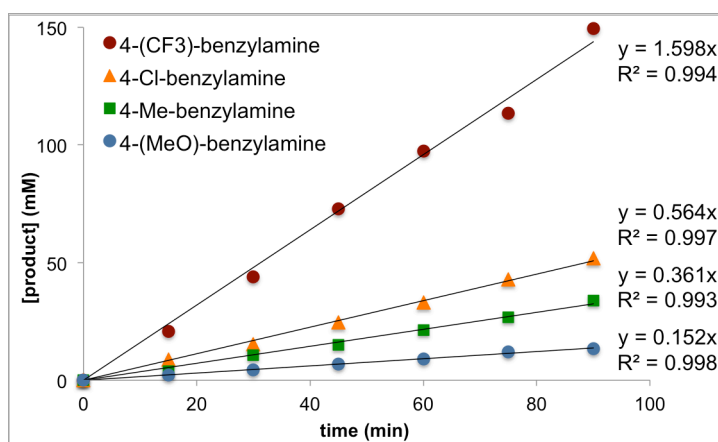
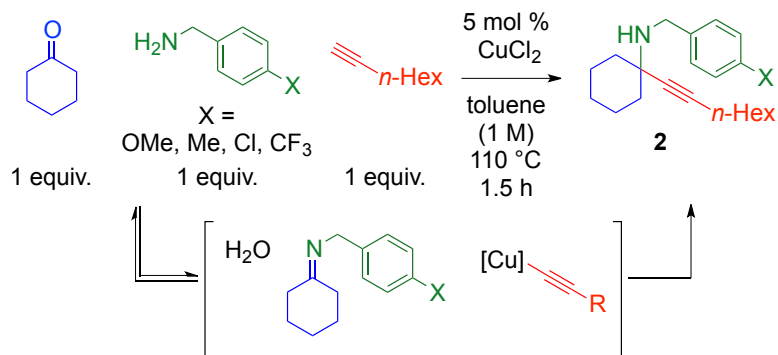
At each concentration of 1-octyne, a set of identical reactions was set up; each data point represents the sole sample taken from a reaction. An oven-dried test tube equipped with a magnetic stir bar was charged with CuCl₂ (5 mol %, 6.7 mg), capped with a septum, and purged with argon for 5 min. Toluene (1073 μL - 780 μL) was added such that the total volume was kept constant. The dodecane internal standard (20 μL) was added, followed by cyclohexanone (103 μL, 1.0 mmol), benzylamine (109 μL, 1.0 mmol), and octyne (73 μL - 367 μL, 0.5 - 2.5 mmol). Under argon pressure, the septum was then quickly replaced with a Teflon-seal screw cap. The reaction was stirred at 110 °C for 90 min. GC aliquots at each time point were flushed through a silica gel pipette plug with diethyl ether.





Relative rates of *para*-substituted benzylamines (X = OMe, Me, Cl, or CF₃):

For each substituted benzylamine, a set of identical reactions was set up; each data point represents the sole sample taken from a reaction. An oven-dried test tube equipped with a magnetic stir bar was charged with CuCl₂ (5 mol %, 6.7 mg), capped with a septum, and purged with argon for 5 min. Toluene (A: 979 μ L, B: 982 μ L, C: 987 μ L D: 967 μ L) was added such that the overall concentration was kept constant. The dodecane internal standard (20 μ L) was added, followed by cyclohexanone (103 μ L, 1.0 mmol), then either 4-methoxybenzylamine (A, 130 μ L, 1.0 mmol), 4-methylbenzylamine (B, 127 μ L, 1.0 mmol), 4-chlorobenzylamine (C, 122 μ L, 1.0 mmol), or 4-(trifluoromethyl)benzylamine (D, 142 μ L, 1.0 mmol) was added followed by octyne (147 μ L, 1.0 mmol). Under argon pressure the septum was then quickly replaced with a Teflon-seal screw cap. The reaction was stirred at 110 °C for 90 min. GC aliquots at each time point were flushed through a silica gel pipette plug with diethyl ether.



Characterization of additional tetrasubstituted propargylamines including ¹H and ¹³C NMR Spectra is available at:

<http://dx.doi.org/10.1039/C2GC35713E>

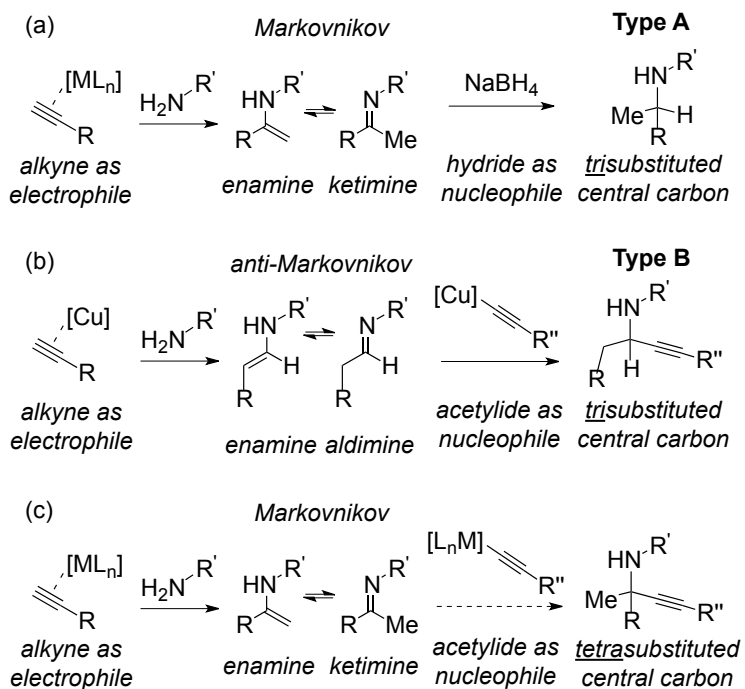
and

<http://dx.doi.org/10.1039/C4GC02318H>

Chapter Three: Kinetic Analysis of Propargylamine Formation Through Hydroamination-Alkynylation

3.1 Introduction:

One method for incorporating amines into organic compounds that is attractive in its atom economy¹ is hydroamination.²⁻⁶ Compared to the condensation of an amine on a ketone to form a ketimine, the splitting of an N-H bond across the pi-system of an alkyne results in the conversion of all atoms in the starting material into the product.⁷⁻⁹ If the hydroamination on the alkyne generates an enamine with Markovnikov regioselectivity, the subsequent tautomerization to ketimine and reduction with a hydride source yields an α -amino trisubstituted carbon as shown in scheme 3.1a.^{8,9}



Scheme 3.1: Comparing trisubstituted products **A** & **B** with tetrasubstituted propargylic amine **C**.

This was first accomplished with the use of Cd/Zn based catalysis,¹⁰ then Zr,¹¹ Ti,¹² and lanthanides¹³ were found to be active in imine formation from the intermolecular hydroamination of terminal alkynes. The highest degree of regioselectivity is observed when organometallic catalysts containing bridging or bulky ligands are used.^{8,9} Utilization of carbon-based nucleophiles in tandem with hydroamination allows for broadened synthetic utility of the ketimine intermediates.^{14,15}

In contrast to other catalyst systems, when copper catalysis has been used in tandem hydroamination reactions, the formation of product has proceeded through an anti-Markovnikov mechanism and formation of aldimine is observed. Subsequent reaction of the aldimine with *in situ* generated copper acetylide forms the less-hindered trisubstituted propargylamine product (Scheme 3.1b).¹⁶⁻¹⁹ To produce the tetrasubstituted product, Markovnikov hydroamination to form the ketimine must be directly followed by the addition of an acetylide nucleophile (Scheme 3.1c).²⁰ Prior to work towards this objective, no such reaction had been reported in the 50 years since the discovery of intermolecular hydroamination of an alkyne.⁷⁻¹⁹ In fact, dual Cu/Ti catalysis was required for the first example of direct synthesis of the tetrasubstituted propargylamine shown in 3.1c using an unactivated ketone, and amine followed by alkynylation.²¹

As a result of the high-energy barrier to ketimine formation and subsequent attack, compared to aldimines,²² examples of the multicomponent reaction of an amine, ketone and carbon based nucleophile are quite rare.^{21,23}

However, these tetrasubstituted amines derivatives have a wide range of medicinal applications. With use ranging from radiological imaging to therapeutic treatments for HIV, cancer, and malaria, as well as activity as potent antivirals, development of methods for the formation of hindered amines and addition of nucleophiles to ketimines is of high importance.²⁴⁻²⁷

3.2 Propargylamine Formation via Hydroamination-Alkynylation:

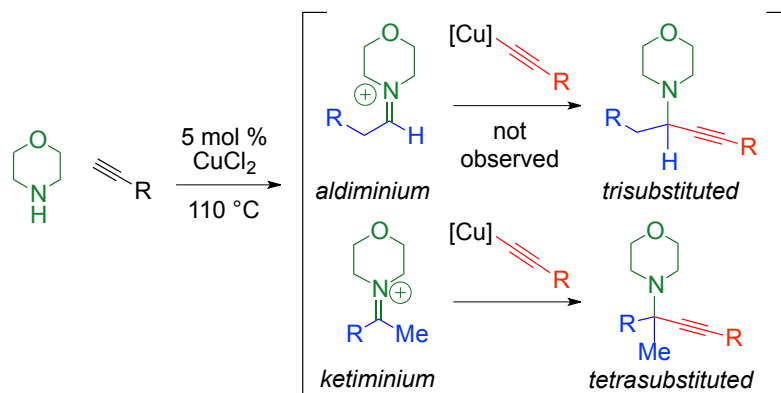
Use of hydroamination is an attractive alternative to circumvent the large barrier to *in situ* ketimine formation.²¹ Additionally, hydroamination in combination with ketimine alkynylation would provide a one-step method for the preparation of tetrasubstituted propargylamines. However, there are difficulties associated with this methodology, 1) an alkyne must be activated as the electrophile in order for hydroamination with the amine to occur, and 2) a subsequent equivalent of the alkyne must be able to be activated to form the nucleophilic acetylide to attack the resultant ketimine. Further, achieving this tandem reaction is complicated as the catalyst that best activates the alkyne for hydroamination is unlikely to be optimal for the formation of the necessary acetylide nucleophile.

While use of gold catalysis is well-precedented for the alkynylation of imines,²⁸⁻³⁰ the ketimine that results from gold-catalyzed intermolecular hydroamination of alkynes is not alkynylated.³¹⁻³⁹ An example of such, is the (SPhos)Au(NTf)₂ catalyzed hydroamination reaction with both terminal alkynes and the less-reactive, internal alkynes.³⁹ Heating the reaction to 100°C does not

result in alkylation, rather, two sequential hydroaminations occur and produce the *N,N*-divinyl derivative with *p*-toluidine.

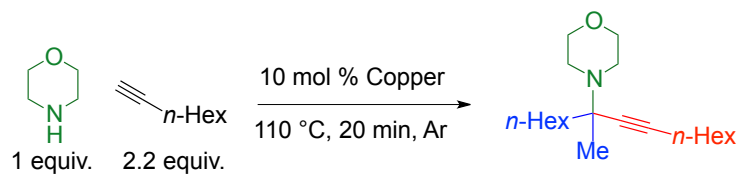
Additionally, while examples of copper catalysts are widespread for the alkylation of imines,²⁴ use in Markovnikov hydroamination is restricted to a few solid-supported compounds.⁴⁰⁻⁴³ The anti-Markovnikov hydroamination with ethyl propiolate, catalyzed by CuBr₂, in toluene, produces an aldimine that is attacked by the acetylide to give a trisubstituted propargylamine.¹⁶⁻¹⁸ Similarly, a reaction catalyzed by CuBr, in the solvent dioxane, occurs with diethylamine and octyne.¹⁹

Previous reports discussed in chapter 2 have demonstrated that the use of green, solvent-free conditions⁴⁴ can be critical for the catalytic formation of ketimine intermediates.^{21,45} As such, removal of solvent should allow for development of a copper-catalyzed method for a tandem hydroamination-alkylation that does not produce aldiminium and rather, produces ketiminium to give the tetrasubstituted product. Satisfyingly, the solvent-free reaction of morpholine and 1-octyne with 5 mol% copper(II) chloride produces the tetrasubstituted propargylamine as the sole product after a 24 h reaction time (Scheme 3.2).⁴⁶



Scheme 3.2: Tandem hydroamination–alkynylation under solvent-free conditions produces solely the tetrasubstituted product shown in the bottom right.

The first step to optimize the tandem hydroamination-alkynylation reaction was to screen a variety of copper(I) and copper(II) salts for their catalytic activity under solvent-free conditions (Table 3.1).⁴⁶ It was observed that while copper(I) and copper(II) acetate, along with copper(I) iodide were inactive, many of the other copper sources were able to catalyze the formation of tetrasubstituted propargylamine. Further, while copper(II) bromide is known to produce trisubstituted propargylamine,¹⁶⁻¹⁹ small amounts of tetrasubstituted product are observed when solvent-free conditions are used. When copper salts containing triflate (OTf) counter anions were used, both $\text{Cu}(\text{OTf})_2$ and $\text{Cu}(\text{OTf}) \cdot (\text{MeCN})_4$ provided high reactivity and the formation of product was observed as a 94% corrected GC yield (Table 3.1, entries 3 and 7).⁴⁶ Additionally, when 1-octyne is used the tetrasubstituted propargylamine is the observed as the dominant product under these solvent-free conditions.



Entry	Copper source	GC yield [%] ^[b]
1	CuCl ₂	15
2	CuBr ₂	12
3	Cu(OTf) ₂	94
4	CuCl	53
5	CuBr	53
6	CuBr•SMe ₂	43
7	CuOTf•(MeCN) ₄	94

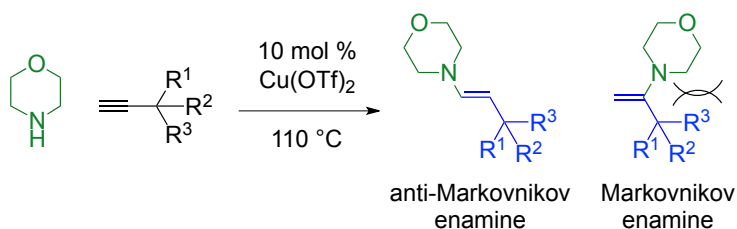
^[b] GC yield of product by comparison to dodecane internal standard and correction for GC burn ratio.

Table 3.1: Copper triflates are superior catalysts for tandem hydroamination-alkynylation.

Use of an inert argon atmosphere allowed the reaction to proceed cleanly. When an atmosphere of nitrogen or air was used it was observed that the conversion to product decreased by 15%. While alkyne hydration can occur when exposed to water, adding up to 10 mol% is tolerated when alkyl alkynes are used. When additional water is added at amounts greater than 50 mol% the rate of propargylamine formation decreases dramatically.

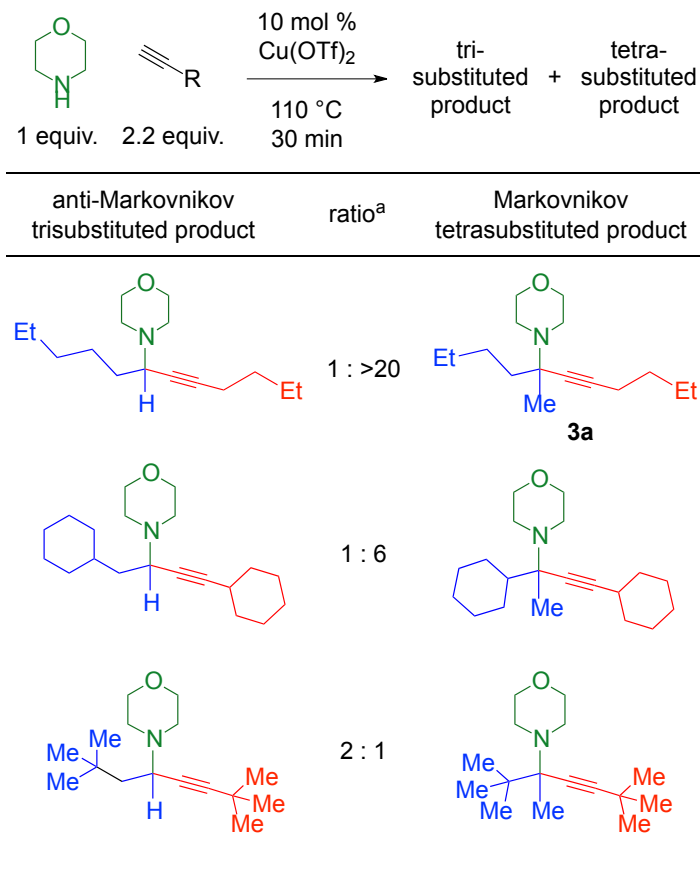
When terminal alkynes carrying bulky substituents are used, one would predict that the high selectivity for the Markovnikov product would decrease.⁴⁷ This should be particularly evident when secondary amines are used, as there should be a limit to the steric demand of the alkyne as this leads to greater allylic strain between the amine and alkyne substituents on the initially formed enamine.^{8,9} Comparably, as anti-Markovnikov hydroamination proceeds through a

1,2-*trans*-disubstituted enamine, Markovnikov hydroamination proceeds via a 1,1-disubstituted enamine (Scheme 3.3). As the substituents (R^1 , R^2 , and R^3) adjacent to the triple bond change from hydrogen atoms to alkyl groups, a decrease in the number of lower energy conformations, in which an H atom can sit in the plane of the enamine, will occur.



Scheme 3.3: Markovnikov hydroamination with bulky alkynes leads to greater allylic strain between the secondary amine and alkyne substituents.

Analysis of product distribution between tetrasubstituted propargylamine and the trisubstituted product was performed using GC (Table 3.2).⁴⁶ When the steric bulk of the alkyne is increased from 1-hexyne to cyclohexylacetylene and further to *tert*-butyl acetylene, the ratio of tetrasubstituted product to trisubstituted product decreases substantially. With *tert*-butyl acetylene, the reaction actually formed twice as much of the undesired trisubstituted propargylamine compared to the desired product. This was confirmed using ¹H NMR analysis as a diagnostic α -amino peak at ~3.3 ppm could be measured and correlated with GC retention times.



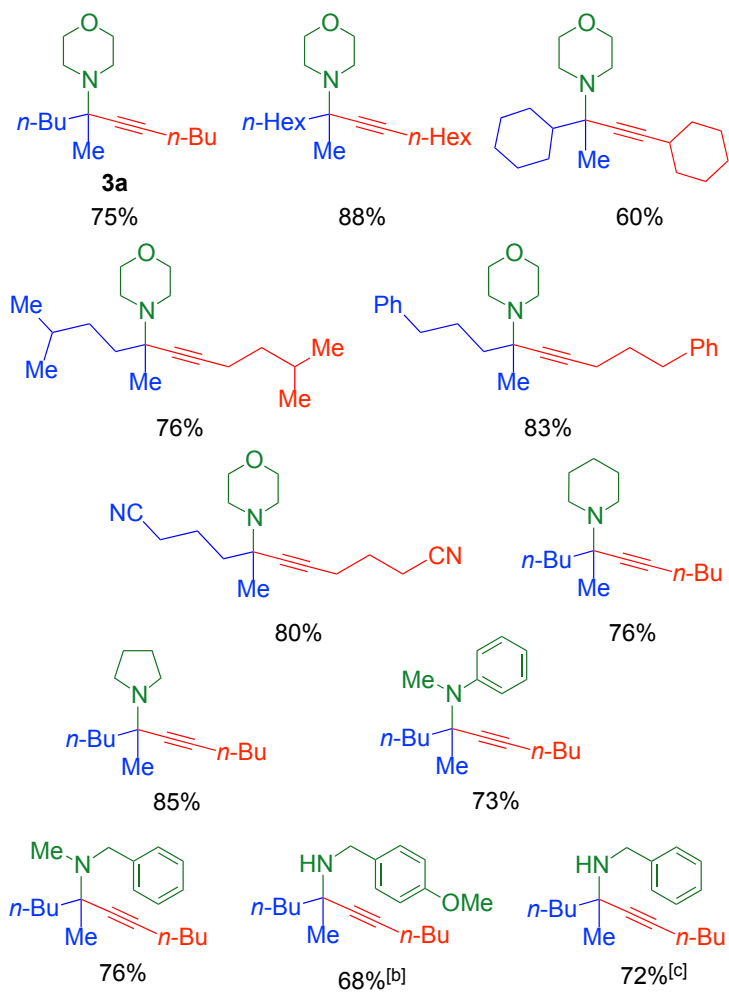
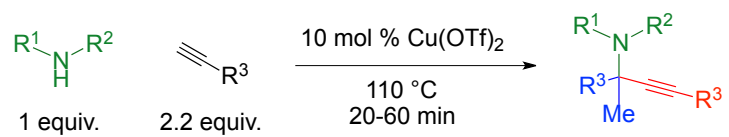
^a Ratio determined by GC analysis.

Table 3.2: Increasing steric bulk of alkyne partitions tandem reaction away from favoring ketimine-derived tetrasubstituted products towards aldimine-derived trisubstituted products.

The sole product of the tandem reaction with 1-hexyne is the tetrasubstituted propargylamine (**3a**). Increasing the size of the steric bulk to the tertiary carbon of cyclohexylacetylene results in a 6:1 ratio of tetrasubstituted to trisubstituted product. The quaternary carbon on *tert*-butylacetylene is of sufficient size to override the selectivity for the Markovnikov product, from the solvent-free Cu(OTf)₂ catalysis, and favor the formation the trisubstituted propargylamine. When the copper catalysis is applied in the presence of solvent,

formation of the trisubstituted products is favored even when less bulky alkynes are used.¹⁶⁻¹⁹

The range of amines and alkynes that can be incorporated into the tetrasubstituted propargylamine is demonstrated in table 3.3. A variety of alkynes can be used bearing alkyl, aryl, or nitrile groups, and all react efficiently with morpholine.⁴⁶ In 25-45 min this method produces compounds where the alkyl (R) group can be linear, cyclic, branched, or aryl. Even a dinitrile-containing product can be formed selectively in 1 h in 80% yield. In addition to morpholine, piperidine and pyrrolidine also react with 1-hexyne in 20 min to form product in 76% and 85% yield respectively. While various other groups have commented on the limited success of alkyl amines in hydroamination using coinage metal catalysts,^{8,9,39,47} the ability of this methodology to efficiently form product with reaction of non-aniline substrates is highly advantageous. N-methylaniline reacts efficiently as does N-methylbenzylamine. However, while secondary N-methylbenzylamine proceeds in 30 min in a 76% yield, primary benzylamine requires a 10 h reaction time to obtain the product in 72% yield. Additionally, para-methoxybenzylamine provides product in good yield but also requires a substantially increased reaction time as complete consumption of amine requires 12 h.⁴⁶

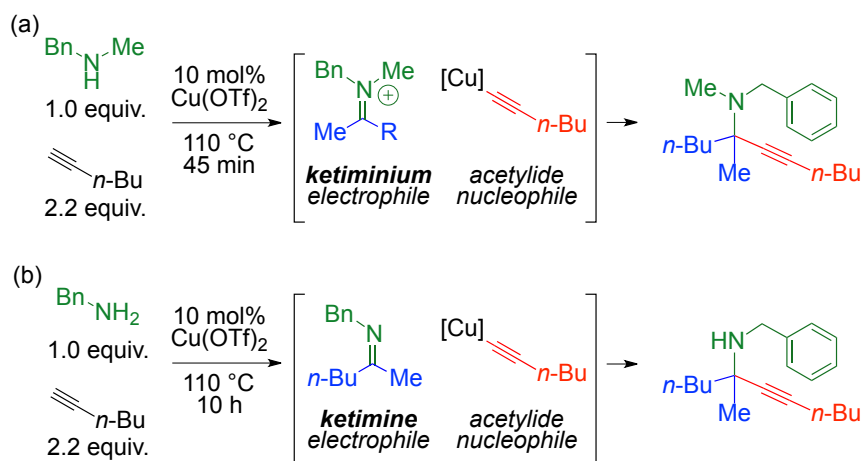


^b 12 hours. ^c 10 hours

Table 3.3: Range of amines and alkynes in the copper(II)-catalyzed tandem hydroamination–alkynylation reaction.

Thus, in contrast with secondary amines, which proceed to completion in 20–60 min, the reaction with primary amines converts at a rate 20-times more slowly. An explanation can be obtained by looking at the key intermediate. A secondary amine must react via formation of a ketiminium (Scheme 3.4a), and as

this is a charged intermediate, it cannot be observed by GC during the course of the reaction. In contrast, the reaction with primary amines such as benzylamine with 1-hexyne, a 1:3 ratio of ketimine to benzylamine is observed by GC when an aliquot of the reaction is taken after 1 h (Scheme 3.4b).⁴⁶



Scheme 3.4: Increased rate of reaction for secondary amines compared to primary amines could be explained as a result of differing imine intermediates.

3.3 Kinetic Analysis of the Copper(II) Catalyzed Hydroamination-Alkynylation Pathway to Form Propargylamines:

In an attempt to increase the reaction rate of the hydroamination-alkynylation reaction with benzylamine, various reaction conditions were assessed. Diluting the reaction with the addition of solvent slowed or arrested the formation of propargylamine. This was not unexpected as previous attempts to form propargylamine with morpholine in acetonitrile, dichloroethane, 1,4-dioxane, DMF, DMSO, ethyl acetate, THF, or toluene provided the product in half the yield as is formed in one h under solvent-free conditions.

Increasing the reaction temperature was also observed to not increase the reaction rate or the yield of the product with benzylamine. The addition of 10 mol% acetic acid or triflic acid did not result in an increase in product formation, and the addition of 10 mol% of hydrochloric or sulfuric acid prevented the reaction from proceeding entirely. Similarly, the addition of 20 mol% of base including potassium *tert*-butoxide, pyridine, triethylamine, or cesium carbonate did not result in an increased reaction rate. Thus the analysis of the rate of reaction with benzylamines was performed without any additives. While the reaction rate was slow compared to that observed when secondary amines are used, reliable data could be obtained by analyzing reaction aliquots taken every 60 min over the course of 4 h.

When determining the rate-limiting step of the hydroamination-alkylation reaction with benzylamines, it is reasonable to expect that if hydroamination is the limiting step that a more electron-rich nucleophilic amine should react faster than one that is electron-poor. If the reverse is observed and use of a more electron-poor amine results in an increased rate, then that suggests that the alkynylation of the resulting ketimine is rate-determining. This can be explained as a result of the fact that a more electron-poor ketimine intermediate is more electrophilic and will undergo the reaction with a common nucleophile more rapidly.

To observe this experimentally, the initial rate of product formation was analyzed for different primary benzylamines (Figure 3.1). A plot showing the

increase in concentration of the product over time for the tandem reaction of 1-hexyne with either 4-methoxybenzylamine, benzylamine or 4-(trifluoromethyl)benzylamine is shown. It is observed the initial rate of reaction when 4-CF₃-benzylamine is used is 1.5 times faster than that with benzylamine and more than an order of magnitude faster than the observed rate with 4-MeO-benzylamine. Detection of the ketimine intermediate also suggests that the rate-determining step for primary benzylamines must be the alkynylation of the ketimine.

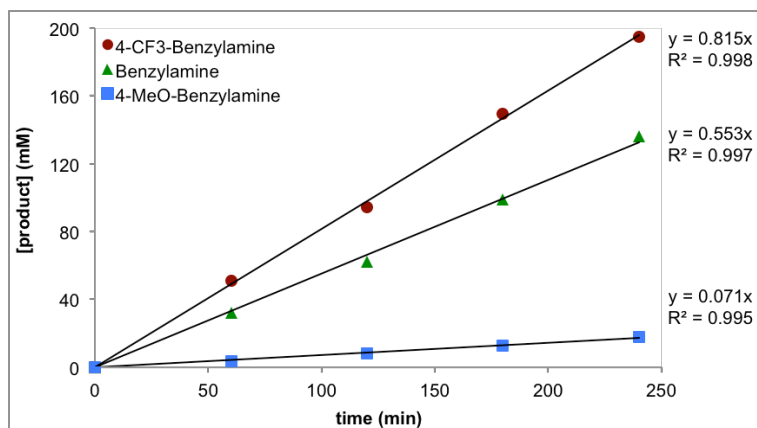
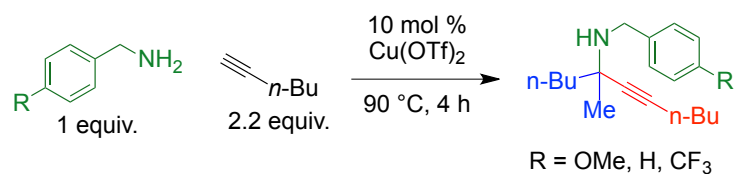
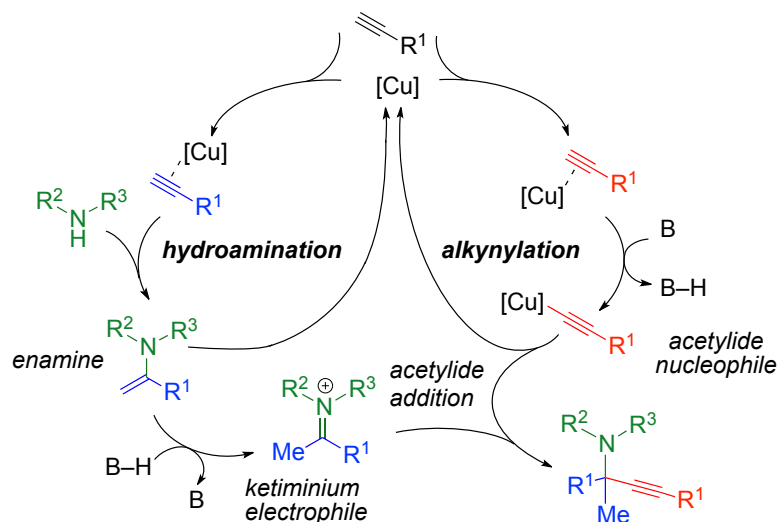


Figure 3.1: Plot of concentration of benzylamine-derived product (mM) versus time, shows that 4-(trifluoromethyl) benzylamine reacts fastest.

In order for this hydroamination-alkynylation reaction to form propargylamine, two separate catalytic cycles involving alkyne activation must merge into one symbiotic process (Scheme 3.5). The hydroamination cycle begins with the activation of the alkyne through π -coordination with copper to

form an electrophile and then subsequent attack by the secondary amine.^{8,9,40-43} Markovnikov hydroamination then frees the catalyst to re-enter the cycle and forms the 1,1-disubstituted enamine. This initial intermediate then undergoes reversible tautomerization to form the desired ketiminium. At the same time, the alkylation cycle begins in a similar fashion with the activation of the alkyne through π -coordination with copper. However, here the alkyne is deprotonated and forms the copper acetylide nucleophile.²⁴ These two cycles intersect when the copper acetylide attacks the alkyne-derived ketiminium and produces the tetrasubstituted propargylamine and the copper catalyst is regenerated.



Scheme 3.5: Proposed dual catalytic cycle for tandem Markovnikov hydroamination-alkynylation.

Previous work published in the literature has demonstrated that enamines are capable bases for the formation of copper acetylides from terminal alkynes.⁴⁸ If the enamine formed through hydroamination of the alkyne by a secondary

amine, deprotonates another equivalent of terminal alkyne, then the resulting ketiminium electrophile and required copper acetylide nucleophile are formed concurrently. These two species would be in proximity to each other and the rapid formation of propargylamine would occur. When primary amines are used, tautomerization to form ketimine occurs. However, the neutral ketimine is not as electrophilic as the ketiminium generated with secondary amines and thus a slower reaction rate is expected and observed.

Deuteration of the starting alkyne allows for analysis of the mechanism for product formation. By observing where the deuterium results in the final product a more precise picture of the proceeding reaction can be obtained.^{35,48} Markovnikov hydroamination of deuterium-labeled 5-hexynenitrile with morpholine results in the incorporation of deuterium at the methyl group of the propargylamine.⁴⁹ Analysis of the ¹H NMR of the deuterated product shows dideuteration of the methyl group attached to the fully substituted center.⁴⁶ The first deuterium present in the alkyne must be located at the enamine terminus upon Markovnikov hydroamination.³⁵ The second deuterium is obtained if the mono-deuterated enamine deprotonates the deuterated 5-hexynenitrile during tautomerization and formation of the copper acetylide.⁴⁸

To aid in the determination of the roles each reactant plays during the course of the tandem hydroamination alkynylation reaction, the order in copper catalyst, alkyne, and secondary amine were assessed. The concentration of product vs. time was measured during the first tenth of the reaction to obtain the

initial rate of reaction (V_0) under each set of conditions. Due to the fact that the reaction of morpholine with 1-hexyne to product propargylamine (**3a**) is rapid and reaches completion in 45 min, the reaction temperature was lowered by 20 °C to a temperature of 90 °C so that GC samples could be taken at reasonably spaced time points.

To further decrease the reaction rate while ensuring the reliability of the acquired data the effect of dilution with solvent was analyzed. The use of acetonitrile as solvent at 110 °C slows the reaction substantially and at 90°C only trace product is observed. When toluene is used, and the reaction is heated to 90 °C the formation of product is cut in half compared to when the reaction is performed using solvent-free conditions at the same temperature.⁵⁰ Thus, to adequately monitor the production of the tetrasubstituted propargylamine (**3a**) the method of combining morpholine, 1-hexyne, and $\text{Cu}(\text{OTf})_2$ at 90 °C in toluene (1.0M) under argon atmosphere, was utilized.

The catalytic cycle shown in scheme 3.5 demonstrates that copper(II) triflate should activate the alkyne for both hydroamination and for deprotonation to form the copper acetylide. If either the hydroamination to form the ketiminium electrophile or the deprotonation to form the acetylide nucleophile is rate-limiting, then a first order dependence on the copper catalyst would be observed. A plot of the initial reaction rate (V_0) for the tandem reaction of morpholine with 1-hexyne to form product (**3a**) at varying concentration of copper(II) triflate (2.5-20 mol%) resulted in a straight line with $R^2 = 0.9989$ (Figure 3.2).⁵⁰ This indicates a

first order dependence on catalyst. This does not imply that the copper catalyst is not involved in more than step, as both the hydroamination and formation of the acetylide require the participation of the copper catalyst. However, it does justify the notion that these steps are not of equal rate and that the first of them must be rate-determining.

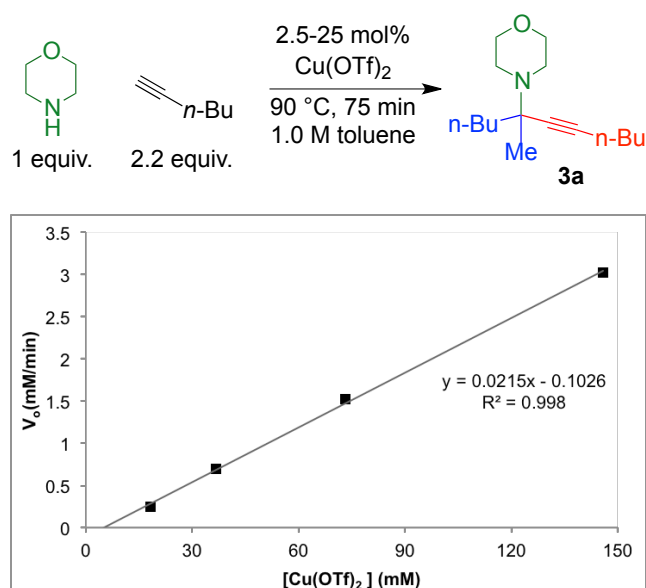


Figure 3.2: The initial rate of product formation (V_0 , mM/min) versus the concentration of copper(II) triflate catalyst (mM).

If hydroamination is the rate-limiting step, then the overall reaction would be first order in catalyst, amine, and alkyne as only one equivalent of each is required to form the product of this individual step. If alkynylation is rate-limiting, then the reaction should be first order in catalyst and amine but second order in alkyne. This is further explained from the fact that enamine has been demonstrated to be the active base in the deprotonation to form acetylide. Thus in order to form the product of this step, the propargylamine (**3a**), one equivalent

of amine and two equivalents of alkyne must be consumed during the copper catalysis. The order, with respect to the alkyne, was determined by measuring the initial rate of product formation at 1.1-5.5 equivalents of 1-hexyne in the reaction with morpholine (Figure 3.3). A straight line with $R^2 = 0.9975$ was obtained, and indicates a first order dependence on the concentration of 1-hexyne.⁵⁰ This suggests that there is one critical role for the alkyne in the rate-limiting step and that this step must be the hydroamination by the amine to form the ketiminium intermediate.

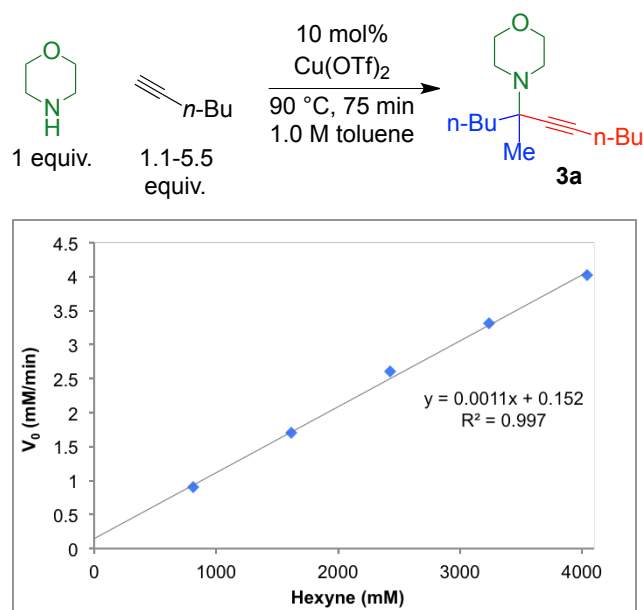


Figure 3.3: The initial reaction rate V_0 (mM/min) versus the concentration of 1-hexyne (mM).

When the equivalents of the amine, morpholine, were varied, it was observed that the reaction becomes saturated above 1.5 equivalents.⁴⁸ The initial rate of reaction at 1.5, 2, and 2.5 equivalents of the amine with 1-hexyne are nearly identical and thus, a limit to the effect of this component towards reaction

rate exists. A plot of the initial reaction rate from 0.5 to 1.5 equivalents of morpholine result in a straight line with $R^2 = 0.9996$ (Figure 3.4).⁵⁰ This confirms that the tandem Markovnikov hydroamination-alkynylation to form tetrasubstituted propargylamine is also first order in amine.

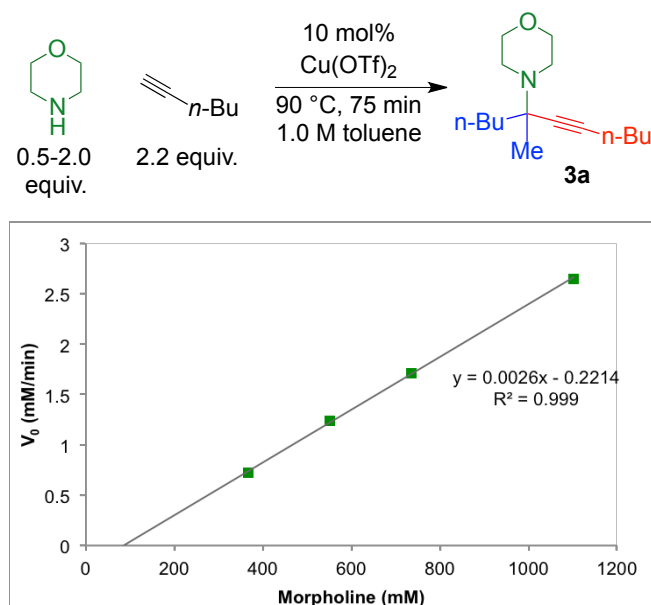
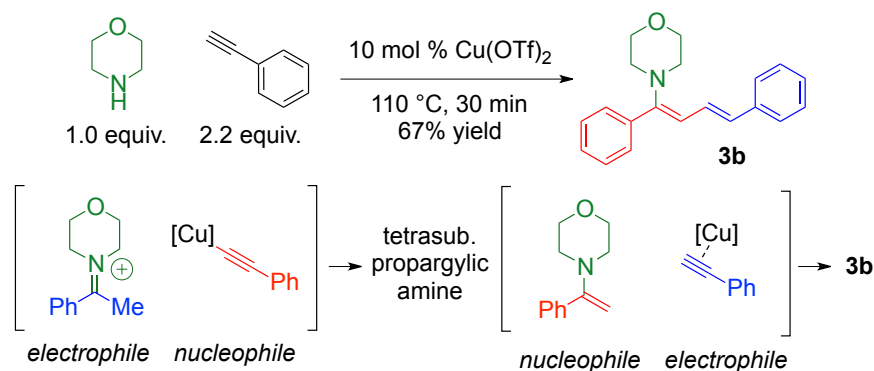


Figure 3.4: The initial reaction rate V_0 (mM/min) versus the concentration of morpholine (mM).

3.4 Synthesis of 1-Aminodienes Through Hydroamination-Hydrovinylation:

While a variety of steps and divergent reaction pathways are possible with amines and alkynes upon activation,^{8,9,31,32} a single, hindered, propargylamine is produced in a matter of min with alkyl alkynes. Aryl alkynes, can be converted into a wide range of compounds due to the propensity for hydroarylation and other types of arene-based mechanisms.³⁵⁻³⁸ In the reaction of phenylacetylene with morpholine under the standard conditions for propargylamine formation, 1-

aminodiene (**3b**) is formed rather than the expected tetrasubstituted product. Instead of the enamine tautomerization to give the ketiminium electrophile, attack of the nucleophilic enamine^{51,52} on the copper activated phenylacetylene electrophile is postulated to lead to the observed formation of 1-amino-1,3-butadiene (**3b**) (Scheme 3.6). The proposed mechanism is analogous to the hydrovinylation reactions that have been used to prepare other various dienes.⁵³⁻
⁶² Such as, the ruthenium-catalyzed codimerization of alkynes with electron-poor alkenes to produce substituted 1,3-butadienes as was reported in 1999.⁵⁴ Catalysts such as rhodium, cobalt, nickel, and ruthenium remain the most popular catalyst for the formation of these product through what has been commonly termed alkyne hydrovinylation.⁵³⁻⁶² Previous to our report, copper had not been reported as a catalyst for this alkyne transformation.



Scheme 3.6: Phenylacetylene undergoes unprecedented tandem hydroamination–hydrovinylation to 1-aminodiene.

The critical difference in this methodology, is that the enamine supplies the reactive vinyl species rather than previously used electron-poor acrylates or styrene derivatives. 1-Amino-1,3-butadienes are difficult to prepare in high

yield⁶³⁻⁶⁵ and the most successful methods go about synthesizing these compounds through cross coupling reactions. Further, it was surprising that the product (**3b**) is stable under conditions adequate for hydroamination as dienes are well-precedented to undergo this type of chemistry.⁶⁶⁻⁷² Through a review of the literature, this represents the first synthesis of a 1-aminodiene via hydroamination.⁷³ Despite the fact that simple dienes are common substrates for amine addition,⁶³⁻⁶⁵ this unique hydroamination-hydrovinylation sequence cleanly prepares 1-amino-1,3-butadiene in one step from simple commercially available starting materials. This reaction to form 1-morpholinyl-1,4-diphenyl-1,3-butadiene (**3b**) is unprecedented as it represents: 1) a previously unknown copper catalyzed alkyne hydrovinylation, 2) a tandem process of hydroamination-hydrovinylation, and 3) a one-step method for the synthesis of 1-amino-1,3-butadiene with no byproducts.

3.5 References:

- 1) Trost, B. M. *Science* **1991**, *254*, 1471.
- 2) Müller, T. E.; Beller, M. *Chem. Rev.* **1998**, *98*, 675.
- 3) Doye, S. *Synlett* **2004**, 1653.
- 4) Marks, T. J.; Hong, S. *Acc. Chem. Res.* **2004**, *37*, 673.
- 5) Hultsch, K. C. *Adv. Synth. & Catal.* **2005**, *347*, 367.
- 6) Müller, T. E.; Hultsch, K. C.; Yus, M.; Foubelo, F.; Tada, M. *Chem. Rev.* **2008**, *108*, 3795.
- 7) Alonso, F.; Beletskaya, I. P.; Yus, M. *Chem. Rev.* **2004**, *104*, 3079.
- 8) Pohlki, F.; Doye, S. *Chem. Soc. Rev.* **2003**, *32*, 104.
- 9) Severin, R.; Doye, S. *Chem. Soc. Rev.* **2007**, *36*, 1407.
- 10) Kruse, C. W.; Kleinschmidt, R. F. *J. Am. Chem. Soc.* **1961**, *83*, 213.
- 11) Walsh, P. J.; Baranger, A. M.; Bergman, R. G. *J. Am. Chem. Soc.* **1992**, *114*, 1708.
- 12) Li, Y.; Marks, T. J. *Organometallics* **1996**, *15*, 3770.
- 13) Haak, E.; Bytschkov, I.; Doye, S. *Angew. Chem., Int. Ed.* **1999**, *38*, 3389.
- 14) Lee, A. V.; Schafer, L. L. *Synlett* **2006**, 2973.
- 15) Lee, A. V.; Sajitz, M.; Schafer, L. L. *Synthesis* **2009**, 97.
- 16) Zhou, L.; Jiang, H.-F.; Li, C.-J. *Adv. Synth. Catal.* **2008**, *350*, 2226.
- 17) Li, C.-J.; Jiang, H.-F.; Zhou, L.; Bohle, D. *Synlett* **2009**, 2009, 937.
- 18) Zhou, L.; Shuai, Q.; Jiang, H.-F.; Li, C.-J. *Chem. Eur. J.* **2009**, *15*, 11668.
- 19) Han, J.-B.; Xu, B.; Hammond, G. B. *J. Am. Chem. Soc.* **2010**, *132*, 916.
- 20) Liu, X. Y.; Ding, P.; Huang, J.-S.; Che, C. M. *Org. Lett.* **2007**, *9*, 2645.

- 21) Pierce, C. J.; Nguyen, M.; Larsen, C. H. *Angew. Chem. Int. Ed.* **2012**, *51*, 12289.
- 22) Guthrie, J. P. *Can. J. Chem.* **1975**, *53*, 898.
- 23) Prakash, G. K. S.; Mathew, T.; Panja, C.; Alconcel, S.; Vaghoo, H.; Do, C.; Olah, G. A. *Proc. Natl. Acad. Sci. USA* **2007**, *104*, 3703.
- 24) Blay, G.; Monleon, A.; Pedro, J. R. *Curr. Org. Chem.* **2009**, *13*, 1498.
- 25) Clayden, J.; Donnard, M.; Lefranc, J.; Tetlow, D. J. *Chem. Commun.* **2011**, *47*, 4624.
- 26) Huffman, M. A.; Yasuda, N.; DeCamp, A. E.; Grabowski, E. J. J. *J. Org. Chem.* **1995**, *60*, 1590.
- 27) Kauffman, G. S.; Harris, G. D.; Dorow, R. L.; Stone, B. R. P.; R. Parsons, L. Jr.; Pesti, J. A.; Magnus, N. A.; Fortunak, J. M.; Confalone, P. N.; Nugent, W. A. *Org. Lett.* **2000**, *2*, 3119.
- 28) Wei, C.; Li, C.-J. *J. Am. Chem. Soc.* **2003**, *125*, 9584.
- 29) Lo, V. K.-R.; Liu, Y.; Wong, M.-K.; Che, C. M. *Org. Lett.* **2006**, *8*, 1529.
- 30) Yoo, W.-J.; Zhao, L.; Li, C.-J. *Aldrichimica Acta* **2011**, *44*, 43.
- 31) Widenhoefer, R. A.; Han, X. *Eur. J. Org. Chem.* **2006**, *2006*, 4555.
- 32) Corma, A.; Leyva-Perez, A.; Sabater, M. J. *Chem. Rev.* **2011**, *111*, 1657.
- 33) Lavallo, V.; Frey, G. D.; Donnadieu, B.; Soleilhavoup, M.; Bertrand, G. *Angew. Chem., Int. Ed.* **2008**, *47*, 5224.
- 34) Lavallo, V.; Wright, J. H. II.; Tham, F. S.; Quinlivan, S. *Angew. Chem., Int. Ed.* **2013**, *52*, 3172.
- 35) Luo, Y.; Li, Z.; Li, C.-J. *Org. Lett.* **2005**, *7*, 2675.
- 36) Yi, C. S.; Yun, S. Y. *J. Am. Chem. Soc.* **2005**, *127*, 17000.
- 37) Yi, C. S.; Yun, S. Y.; Guzei, I. A.; *J. Am. Chem. Soc.* **2005**, *127*, 5782.
- 38) Lavallo, V.; Frey, G. D.; Kousar, S.; Donnadieu, B.; Bertrand, G. *Proc. Natl. Acad. Sci. U. S. A.* **2007**, *104*, 13569.

- 39) Leyva, A.; Corma, A. *Adv. Synth. Catal.* **2009**, *351*, 2876.
- 40) Penzien, J.; Haeßner, C.; Jentys, A.; Köhler, K.; Müller, T. E.; Lercher, J. A. *J. Catal.* **2004**, *221*, 302.
- 41) Joseph, T.; Shanbhag, G. V.; Halligudi, S. B. *J. Mol. Catal. A: Chemical* **2005**, *236*, 139.
- 42) Shanbhag, G. V.; Kumbar, S. M.; Joseph, T.; Halligudi, S. B. *Tetrahedron Lett.* **2006**, *47*, 141.
- 43) Shanbhag, G.; Joseph, T.; Halligudi, S.; *J. Catal.* **2007**, *250*, 274.
- 44) Walsh, P. J.; Li, H.; de Parrodi, C. A. *Chem. Rev.* **2007**, *107*, 2503.
- 45) Pierce, C. J.; Larsen, C. H. *Green Chem.* **2012**, *14*, 2672.
- 46) Pierce, C. J.; Yoo, H.; Larsen, C. H. *Adv. Synth. Catal.* **2013**, *355*, 3586.
- 47) Zeng, X.; Frey, G. D.; Kousar, S.; Bertrand, G. *Chem. Eur. J.* **2009**, *15*, 3056.
- 48) Koradin, C.; Gommermann, N.; Polborn, K.; Knochel, P. *Chem. Eur. J.* **2003**, *9*, 2797.
- 49) Bew, S. P.; Hiatt-Gipson, G. D.; Lovell, J. A.; Poullain, C. *Org. Lett.* **2012**, *14*, 456.
- 50) See Supporting Information for additional details.
- 51) Nakamura, M.; Fujimoto, T.; Endo, K.; Nakamura, E. *Org. Lett.* **2004**, *6*, 4837.
- 52) Fujimoto, T.; Endo, K.; Tsuji, H.; Nakamura, M.; Nakamura, E. *J. Am. Chem. Soc.* **2007**, *130*, 4492.
- 53) Mitsudo, T.; Zhang, S. W.; Watanabe, Y. *J. Chem. Soc., Chem. Commun.* **1991**, 598.
- 54) Yi, C. S.; Lee, D. W.; Chen, Y. *Organometallics*, **1999**, *18*, 2043.
- 55) Shibata, Y.; Hirano, M.; Tanaka, K. *Org. Lett.* **2008**, *10*, 2829.
- 56) Trost, B. M.; Martos-Redruejo, A. *Org. Lett.* **2009**, *11*, 1071.

- 57) Neisius, N. M.; Plietker, B. *Angew. Chem., Int. Ed. Engl.* **2009**, *48*, 5752.
- 58) Mannathan S.; Cheng, C.-H. *Chem. Commun.* **2010**, *46*, 1923.
- 59) Yang, C.-M.; Jeganmohan, M.; Parthasarathy, K. Cheng, C.-H. *Org. Lett.* **2010**, *12*, 3610.
- 60) Horie, H.; Kurahashi, T.; Matsubara S. *Chem. Commun.* **2010**, *46*, 7229.
- 61) Horie, H.; Koyama, I.; Kurahashi, T.; Matsubara, S. *Chem. Commun.* **2011**, *47*, 2658.
- 62) Schabel, T.; Plietker, B. *Chem. Eur. J.* **2013**, *19*, 6938.
- 63) Barluenga, J.; Aznar, F.; Moriel, P.; Valdés, C. *Adv. Synth. Catal.* **2004**, *346*, 1697.
- 64) Barluenga, J.; Valdes, C. *Chem. Commun.* **2005**, 4891.
- 65) Maas, G.; Rahm, R. *Z. Naturforsch., B: Chem. Sci.* **2005**, *60b*, 673.
- 66) Takahashi, S.; Shibano, T.; Hagihara, N. *Bull. Chem. Soc. Japan* **1968**, *41*, 454.
- 67) Löber, O.; Kawatsura, M.; Hartwig, J. F. *J. Am. Chem. Soc.* **2001**, *123*, 4366.
- 68) Pawlas, J.; Nakao, Y.; Kawatsura, M.; Hartwig, J. F. *J. Am. Chem. Soc.* **2002**, *124*, 3669.
- 69) Qin, H.; Yamagiwa, N.; Matsunaga, S.; Shibasaki, M. *J. Am. Chem. Soc.* **2006**, *128*, 1611.
- 70) Brouwer, C.; He, C. *Angew. Chem. Int. Ed.* **2006**, *45*, 1744.
- 71) Stubbert, B. D.; Marks, T. J. *J. Am. Chem. Soc.* **2007**, *129*, 4253.
- 72) Kovacs, G.; Ujaque, G.; Lledos, A. *J. Am. Chem. Soc.* **2008**, *130*, 853-864.
- 73) Sarma, R.; Prajapati, D. *Chem. Commun.* **2011**, *47*, 9525.

3.6 Supporting Information:

4-(5-methylundec-6-yn-5-yl)morpholine (3a):

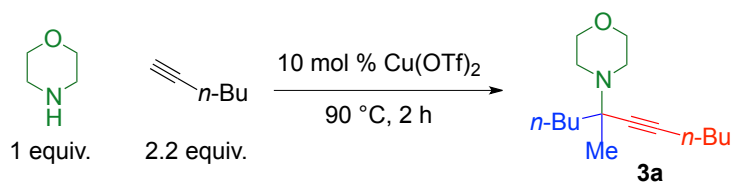
Morpholine (88 μ L, 1.0 mmol), 1-hexyne (256 μ L, 2.2 mmol), Cu(OTf)₂ (36.2 mg, 0.1 mmol), was stirred at 110 °C for 45 min to afford the title compound as an orange liquid in 72% yield (0.181 g, 0.72 mmol) after column chromatography on silica gel (10% EtOAc/hexanes). Characterization of this propargylamine matches that published in: Pierce, C. J.; Yoo, H.; Larsen, C. H. *Adv. Synth. Catal.* **2013**, 355, 3586.

4-[(1Z,3E)-1,4-Diphenylbuta-1,3-dien-1-yl]morpholine (3b): Morpholine (88 μ L, 1.0 mmol), phenylacetylene (242 μ L, 2.2 mmol), and Cu(OTf)₂ (36.2 mg, 0.1 mmol) were stirred at 110 °C for 30 min to afford the title compound as an orange oil after column chromatography on silica gel (10% EtOAc/hexanes); yield: 67% as an average of two runs (0.230 g, 0.79 mmol) and (0.160 g, 0.55 mmol). ¹H NMR (400 MHz, CDCl₃): δ 7.50–7.32 (m, 5 H), 7.26–7.16 (m, 4 H), 7.15–7.03 (m, 1 H), 6.70 (dd, *J*=15.5, 10.8 Hz, 1 H), 6.42 (d, *J*=15.5 Hz, 1 H), 5.64 (d, *J*=10.7 Hz, 1 H), 3.85–3.63 (m, 4 H), 3.00–2.84 (m, 4 H); ¹³C NMR (100 MHz, CDCl₃): δ =152.7, 143.4, 138.9, 137.0, 130.5, 128.7, 128.6, 128.0, 126.6, 126.2, 125.8, 106.8, 67.2, 49.7; HRMS: *m/z*=292.1705, calculated for [M+H]⁺: 292.1696.

General Procedure for Rate Studies

Each time point was run as a separate side-by-side experiment under one set of conditions (varying catalyst, amine, or alkyne) such that earlier sampling would not alter the data collected at later time points. After the tests below showed that

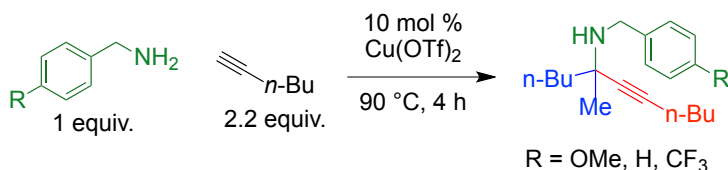
conversion of morpholine and 1-hexyne into product **3a** after 2h without solvent (entry 1) is double that in toluene (entry 3), kinetic experiments were carried out in toluene (1.0 M). As with most other solvents, the reaction in acetonitrile (entry 2, MeCN) at 90 °C results in trace product formation.

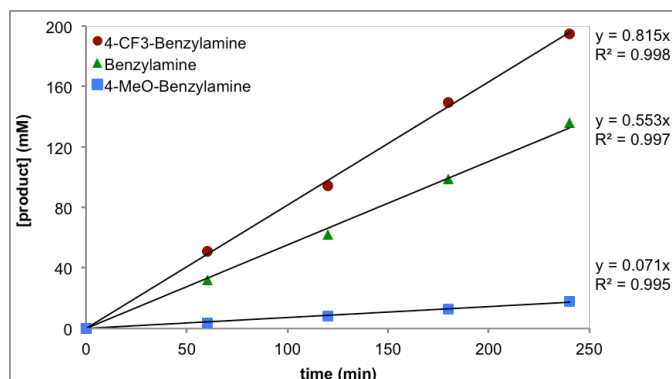


Entry	Solvent	GC yield [%]
1	none	76
2	MeCN (1.0 M)	<1
3	toluene (1.0 M)	32

Relative rates of *para*-substituted benzylamines (R = OMe, H, or CF₃):

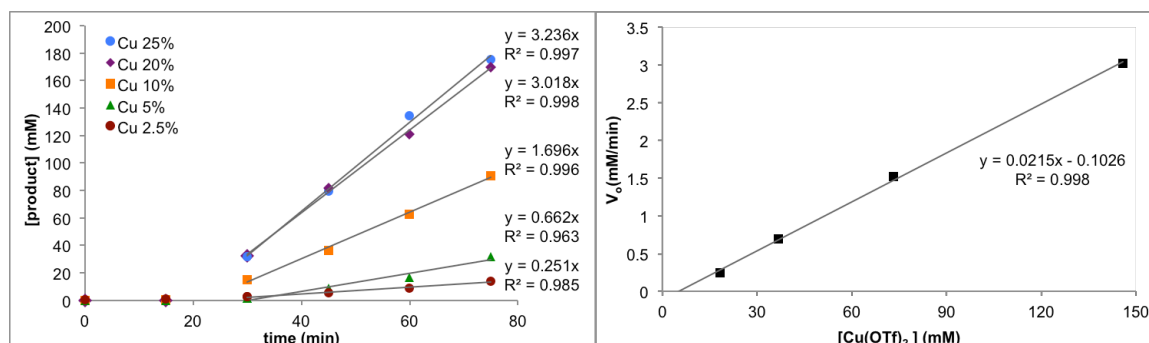
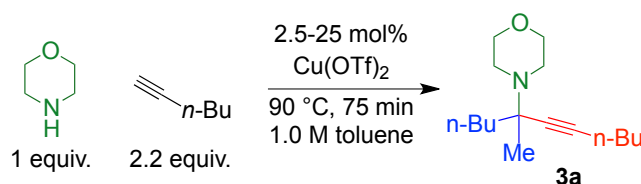
For each substituted benzylamine, to an oven-dried test tube equipped with magnetic stir bar and Teflon-seal screw cap 10 mol% Cu(OTf)₂ was added. The tube is purged with argon for 5 min. 1-Hexyne (2.2 mmol), 4-substituted benzylamine (1.0 mmol), toluene (1 mL), and dodecane internal standard (20 μL) are added, and the reaction is stirred at 90 °C for the indicated time. Aliquots are flushed through a silica gel pipette plug with diethyl ether for GC analysis.





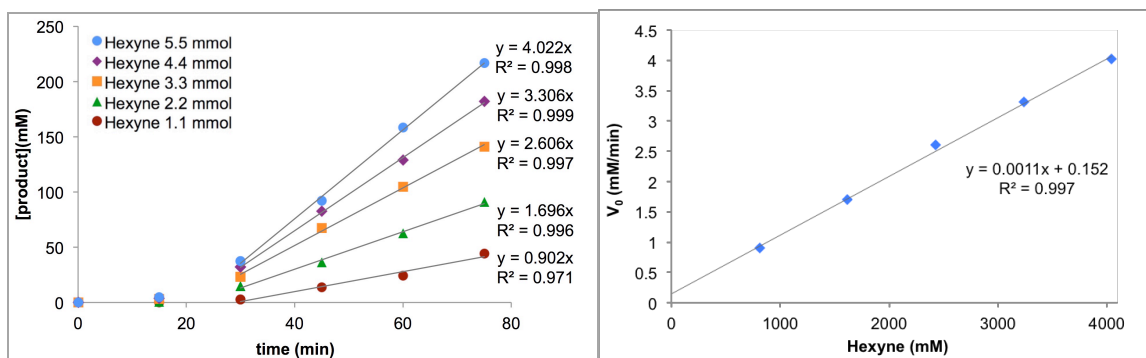
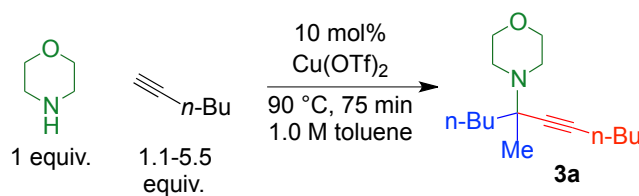
Catalyst ($\text{Cu}(\text{OTf})_2$) loading study:

For each time point in the catalyst loading study, to an oven-dried test tube equipped with magnetic stir bar and Teflon-seal screw cap 2.5, 5, 10, or 20 mol% $\text{Cu}(\text{OTf})_2$ was added. The tube is purged with argon for 5 min. 1-Hexyne (2.2 mmol), morpholine (1.0 mmol), toluene (1 mL), and dodecane internal standard (20 μL) are added, and the reaction is stirred at 90 °C for the indicated time. Aliquots are flushed through a silica gel pipette plug with diethyl ether for GC analysis.



1-Hexyne Concentration Study:

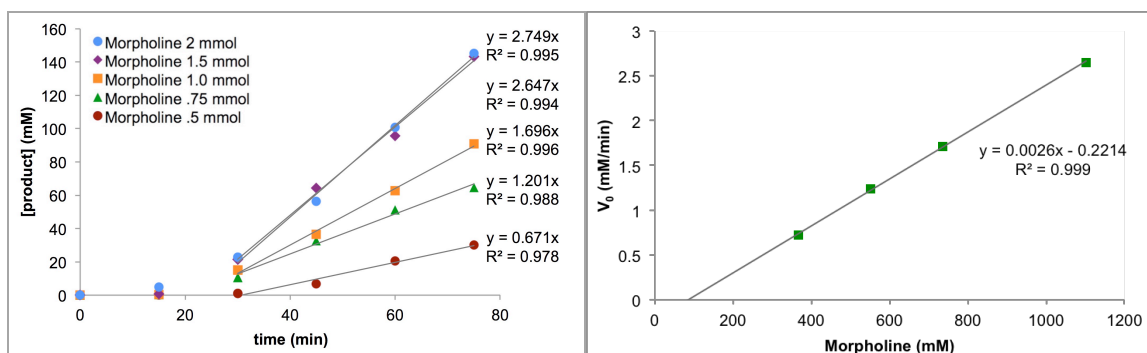
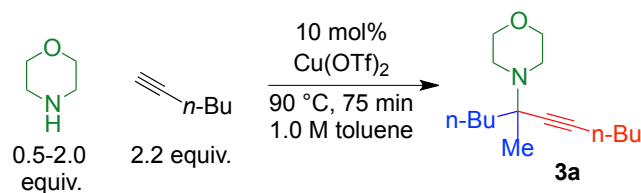
For each time point in the alkyne loading study, to an oven-dried test tube equipped with magnetic stir bar and Teflon-seal screw cap 10 mol% Cu(OTf)₂ was added. The tube is purged with argon for 5 min. 1-Hexyne (1.1, 2.2, 3.3, 4.4, 5.5 mmol), morpholine (1.0 mmol), and dodecane internal standard (20 μL) are added, and the reaction is stirred at 90 °C for the indicated time. Aliquots are flushed through a silica gel pipette plug with diethyl ether for GC analysis.



Morpholine Concentration Study:

For each time point in the amine loading study, to an oven-dried test tube equipped with magnetic stir bar and Teflon-seal screw cap 10 mol% Cu(OTf)₂ was added. The tube is purged with argon for 5 min. 1-Hexyne (2.2 mmol), morpholine (0.5, 0.75, 1.0, or 1.5 mmol), toluene (1 mL), and dodecane internal standard (20 μL) are added, and the reaction is stirred at 90 °C for the indicated

time. Aliquots are flushed through a silica gel pipette plug with diethyl ether for GC analysis.



Characterization of tetrasubstituted propargylamines including

¹H and ¹³C NMR spectra is available at:

<http://dx.doi.org/10.1002/adsc.201300937>

¹H and ¹³C NMR spectra for 1-aminodiene (3b) is available at:

<https://doi.org/10.1002/adsc.201401037>

Chapter Four: α -Tetrasubstituted Triazoles for Biological Testing

4.1 Introduction:

The utility of 1,2,3-triazoles is widespread with applications in biological systems and drug development.¹⁻¹² The ability of the copper-catalyzed azide-alkyne cycloaddition reaction (CuAAC) to regioselectively introduce a wide variety of substituents on 1,4-disubstituted 1,2,3-triazoles makes this system an excellent method to facilitate rapid drug screening and exploration of structure-activity relationships.^{10,13-18} These Huisgen reactions¹⁹ of organic azides with terminal alkynes^{1,2} allow for tracking in biological systems and development of lead compounds by identifying key motifs.

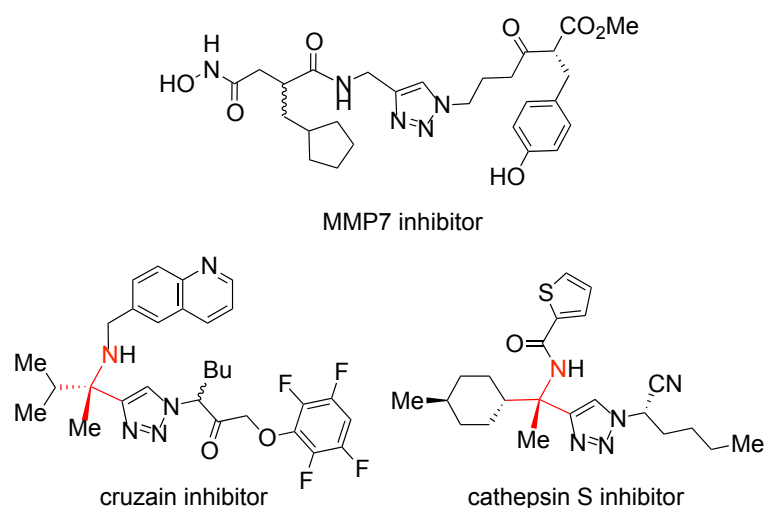


Figure 4.1: A sampling of propargylamine-derived triazoles with therapeutic effects includes α -tetrasubstituted triazoles as cruzain and cathepsin inhibitors.

The use of propargylamines as the terminal alkyne component has precedent in the synthesis of highly selective inhibitors (Figure 4.1).² With the difficulty in forming tetrasubstituted propargylamines, examples of the

incorporation of deprotectable variants for the formation of triazoles is extremely rare.²⁰ Thus, development of reliable methods for the preparation of these deprotectable propargylamines and subsequent reactions to directly convert them into 1,2,3-triazoles is of high value. These methods should be robust and allow for utilization of a wide range of substrates. From here, a library of compounds could be generated using high throughput screening to determine their inherent biological activity.

4.2 Background on Biologically Active α -Tetrasubstituted Triazoles:

The Ellman group has demonstrated the ability of their chiral sulfinylimine protocol to synthesize propargylamine-derived α -tetrasubstituted triazoles (Figure 4.1). Of the compounds they prepared, one triazole showed activity as a cruzain inhibitor with activity against the parasite *Trypanosoma cruzi*, which is known to cause Chagas' disease.⁶ Additionally, another of the α -tetrasubstituted triazoles they prepared demonstrated the ability to inhibit cathepsin S. Inhibition of this protein has been shown to potentially treat ailments ranging from inflammation, to autoimmune disorders such as rheumatoid arthritis.^{7,8} The relevant core of the cathepsin S inhibitor is highlighted in red and was synthesized in six steps. Formation of isolation of the N-sulfinyl ketimine is followed by the stoichiometric addition of a trimethylsilyl-protected alkynyllithium reagent. Removal of the silyl and sulfinyl protecting groups then permits the CuAAC reaction with a resin-bound azide. Acylation of the amine and subsequent dehydration yields the final active α -tetrasubstituted triazole.⁷

The often-lengthy synthesis of tetrasubstituted propargylamine precursors limits their use in the preparation of compounds like α -tetrasubstituted triazoles. The majority of three-component couplings produce trisubstituted propargylamines. In these reactions, copper remains as the most popular catalyst for the multicomponent coupling of an aldehyde, an amine, and an alkyne.^{21,22} Methods for the corresponding reaction with ketones rather than aldehydes are rare due to the lower electrophilicity and greater steric hindrance.^{20,23-26} As a release of torsional strain occurs when the sp^2 center in the six-membered ring is attacked, cyclohexanone has been shown to be a special case of cyclic ketone that is nearly as reactive as an aldehyde.²⁵ When this ketone is used in amination reactions the resulting tetrasubstituted (red) cyclohexylamine can be found in natural alkaloids such as (-)-lycodine²⁷ (Figure 4.2), as well as highly active drugs like ketamine and phencyclidine (1-(1-phenylcyclohexyl)piperidine, PCP).²⁸

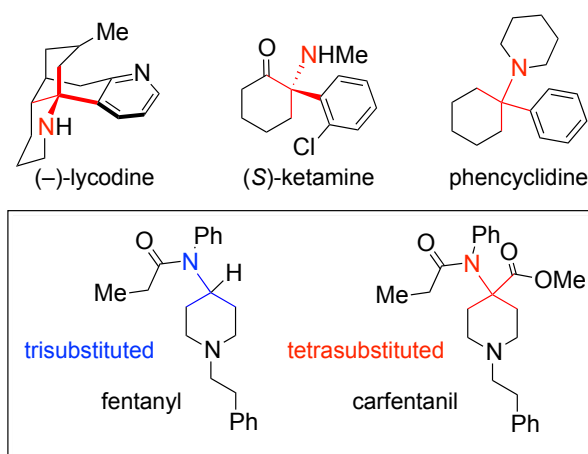
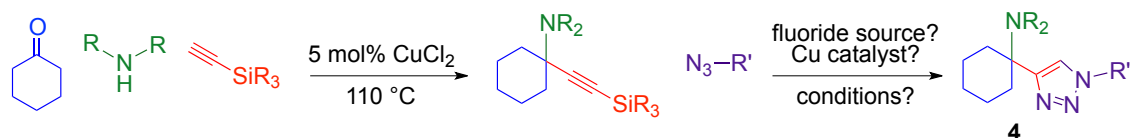


Figure 4.2: A tetrasubstituted carbon bearing an amine (red) can provide increased in activity compared to the trisubstituted carbon bearing an amine (blue).

Compared to the corresponding trisubstituted variants, tetrasubstituted carbons bearing amines can provide much higher levels of biological activity. As an example, fentanyl (blue, Figure 4.2), an anesthetic that is 100 times the strength of morphine.²⁹ Comparison to the tetrasubstituted variant carfentanil (red, Figure 4.2), shows that for the tetrasubstituted variant, the activity is increased two orders of magnitude as carfentanil is over 10,000 times as active as morphine.

4.3 Formation of Structurally Diverse α -Tetrasubstituted Triazoles:

A method to streamline the synthesis of alpha-tetrasubstituted triazoles would be a two-step/three reaction sequence as shown in scheme 4.1. The first step utilizes the solvent-free copper-catalyzed three-component coupling of cyclohexanone with an amine and silyl-protected alkynes to produce protected propargylamines.^{20, 25}



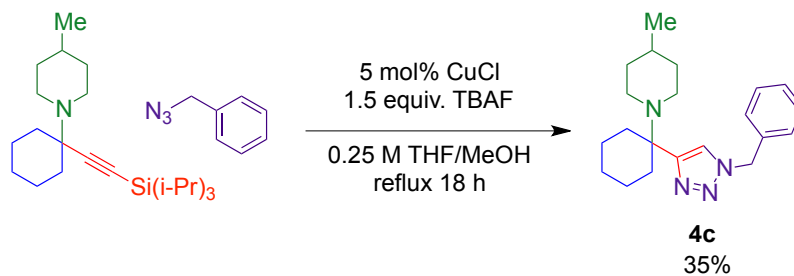
Scheme 4.1: Ketone-amine-alkyne coupling followed by tandem silyl deprotection and triazole formation.

Trimethylsilyl (TMS) acetylene was found to be unstable in the presence of the copper(II) chloride catalyst. Triethylsilyl (TES) acetylene also did not convert efficiently to product and multiple side products were observed. Triisopropylsilyl (TIPS) acetylene was found to be superior as higher conversion to product was observed compared to *tert*-butyldimethylsilyl (TBDMS) acetylene

and was chosen as the alkyne source for the formation of the silylated tetra-substituted propargylamines.

While there is precedent for the use of TMS-protected alkynes in the conversion to triazoles via the one-pot silyl deprotection CuAAC reaction,³⁰⁻³³ there are no previous reports for this conversion with TIPS-protected alkynes. As the removal of the triisopropylsilyl protecting group is more difficult compared to the less hindered trimethylsilyl, conditions for the removal of TIPS include 1.5 equivalents of AgF or Cu(OAc)₂ combined with the addition of tetrabutylammonium fluoride (TBAF).^{34,35} Additionally, the α -tetrasubstituted triazoles synthesized by the Ellman group using the CuAAC reaction were prepared with desilylated, purified tetrasubstituted propargylamine.⁶⁻⁸ Therefore, the goal in developing the second portion of the reaction sequence was to design a method that enables a tandem deprotection-cycloaddition with tetrasubstituted, TIPS-protected, propargylamines that would allow for a reaction in situ with various azides to give the hindered triazole products.

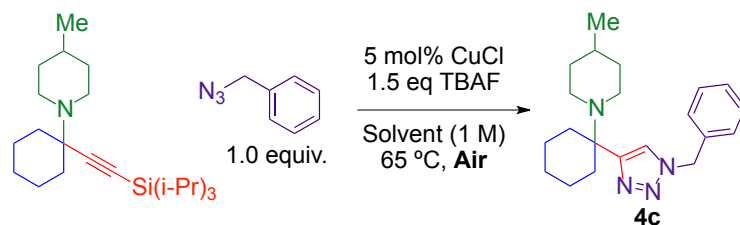
As a copper(I) catalyst is needed for the azide-alkyne cycloaddition reaction the development of the methodology for the one-pot deprotection-cyclization began with use of 5 mol% Cu(I) chloride with 1.5 equivalents of TBAF in THF/MeOH at reflux with benzyl azide and a 4-methylpiperidine derived propargylamine (**2f**) (Scheme 4.2). This procedure was able to produce the desired α -tetrasubstituted triazole (**4c**) in 35% yield with minimal side products.



Scheme 4.2: Initial conditions for the tandem deprotection-CuAAC to form alpha tetrasubstituted triazole.

In order to optimize the reaction, an analysis of solvents reported for triazole formation² was performed (Table 4.1). Aqueous solvent mixtures produce only trace amounts of product at 1 h and no increase in product formation was observed after 18 h. Methanol and *tert*-butanol both provide around two-thirds conversion to triazole (**4c**) after allowing the reaction to proceed for 18 h. While tetrahydrofuran also provides similar conversion to product in 18 h a significant amount of side products were observed and alcohol based solvents were chosen for further optimization studies. Use of an inert atmosphere of argon resulted in a significant increase in conversion to product (**4c**) to 85% in MeOH, EtOH, or *i*-PrOH (Table 4.1).

To increase the rate of reaction and obtain complete conversion of propargylamine to triazole, copper(I) and copper(II) sources with an equal amount of sodium ascorbate as a reducing agent were tested with MeOH as solvent (Table 4.2). All of the combinations of Cu(II) salts with the reductant, gave higher GC yields compared to any of the Cu(I) salts tested. This is inline with other reports that CuAACs often perform better with copper(I) salts that are generated in situ from reduction of the corresponding copper(II) source.²



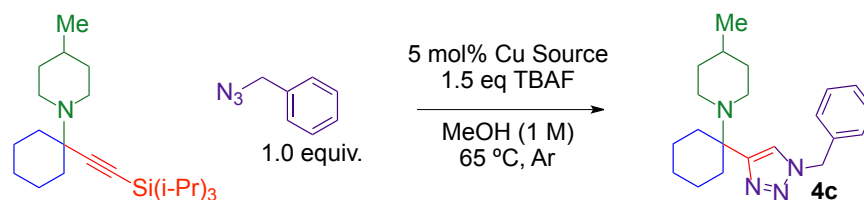
Entry	Solvent	GC yield (%): at 1h	at 18 h
1	MeOH	13	65
2	<i>t</i> -BuOH	6	62
3	THF	5	68 ^a
4	<i>t</i> -BuOH/H ₂ O 1:1	21	2
5	DMSO/H ₂ O 2:1	0	0
6	DMF/H ₂ O 1:2	0	0
7	THF/MeOH 1:1	4	34 ^a

Under Argon			
Entry	Solvent	GC yield (%): at 1h	at 18 h
1	MeOH	32	86 ^b
2	EtOH	51	87 ^b
3	<i>i</i>-PrOH	66	85^b

^a Significant side product was observed

^b GC Yield at 5h is the same as 18 h with 84, 83, and 85% respectively.

Table 4.1: Solvent screen for optimization of triazole formation shows that alcohols are superior and result in no unreacted deprotected propargylamine.

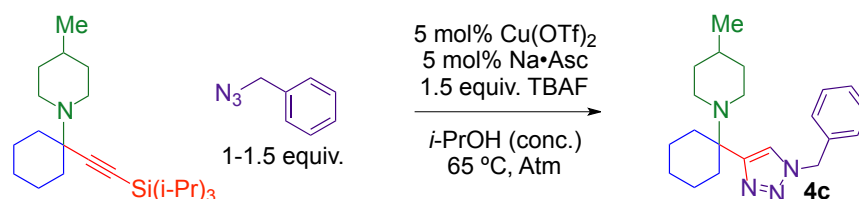


Entry	Cu Source	GC yield (%) at 1 h	GC yield (%) at 5 h	GC yield (%) at 18 h
1	Cu(II) triflate	39	99	99
2	Cu(II) acetate monohydrate	46	60	82
3	Cu(II) bromide	65	73	86
4	Cu(II) chloride	72	89	90
5	Cu(II) fluoride dihydrate	69	83	88
6	Cu(II) sulfate pentahydrate	49	64	79
7	Cu Powder	24	38	24
8	Cu(I) bromide	62	75	63
9	Cu(I) chloride	46	60	76

^a All Cu(II) sources required 5 mol% Na-Ascorbate as an additive

Table 4.2: Catalyst screen shows that copper(II) triflate is a superior catalyst, giving full conversion after 5 h.

After an 18 h reaction time copper(II) chloride produces triazole (**4c**) in 90% GC yield. However, copper(II) triflate demonstrated superior reactivity with the ability to produce triazole (**4c**) in quantitative GC yield. This catalyst is rare in CuAAC reactions, copper(II) triflate is known to product protic acid in solution. While formation of acid could result in proto-desilation of the protected propargylamine,³⁶ this is not observed. A range of alcohol solvents³⁷ were tested with the most active catalyst, in situ reduced Cu(OTf)₂. Isopropanol was observed to provide better conversion compared to methanol, ethanol, and *tert*-butanol after 1 h. A control reaction showed that in isopropanol with copper(II) triflate the reaction reached full conversion in 6 h.



Entry	Atmosphere	Azide equiv.	Concentration	GC yield (%) at 1 h	GC yield (%) at 18 h
1	Air	1.0	1.0 M	17	41
2	Argon	1.0	1.0 M	25	55
3	Nitrogen	1.0	1.0 M	28	65
4	Nitrogen	1.5	1.0 M	42	49
5	Nitrogen	1.5	0.5 M	53	43
6	Nitrogen	1.5	2.0 M	65	87

Table 4.3: Tandem reaction proceeds best under nitrogen atmosphere with 1.5 equivalents of azide at a concentration of 2.0 M.

The effect of ambient atmosphere was compared to inert atmosphere with isopropanol as solvent. Argon was found to be not necessary, and an atmosphere of nitrogen provided 24% higher GC yield than air (Table 4.3). Tests of the effect of reactant concentration found no significant difference between 0.5

M and 1.0 M but increasing the concentration to 2.0 M nearly doubled the GC yield after 18 h (Table 4.3). To finish reaction optimization, the loading of the copper(II) catalyst was varied from 2.5 mol% to 25 mol% copper(II) triflate with an equimolar amount of sodium ascorbate. The highest isolated yields were obtained with 10 mol% of Cu(OTf)₂ with 10 mol% of Na•Asc as the in situ reductant.

With the optimized reaction conditions determined, selected triisopropylsilyl protected propargylamines from chapter 2, as well as two additional propargylamines (**4a**) and (**4b**) were cleanly converted to triazoles (**4c-4h**) through CuAAC with benzyl azide (Table 4.4). The substrate used during optimization (**4c**) is isolated in 66% yield after 6 h under these standard conditions: 10 mol% Cu(OTf)₂, 10 mol% Na•Asc, and 1.5 equivalents of TBAF in isopropanol (2.0 M) at 65 °C. The readily deprotectable,³⁸ *N,N*-diallyl variant (**4d**) was obtained in 67% yield after recrystallization in hexanes. This allows for further functionalization in a similar fashion to the synthesis of the cathepsin S inhibitor in figure 4.1. Deprotection of the nitrogen followed by acylation would allow for the formation of the triazole amide.⁶⁻⁸ The morpholinyl triazole (**4e**) and *N*-4-(trifluoromethyl)benzyl triazole (**4f**) are isolated in 72% and 76% yield respectively. The triazole (**4g**) derived from cyclopentylamine and *N*-methylpiperazine-derived (**4h**) were obtained in 65% and 73%.

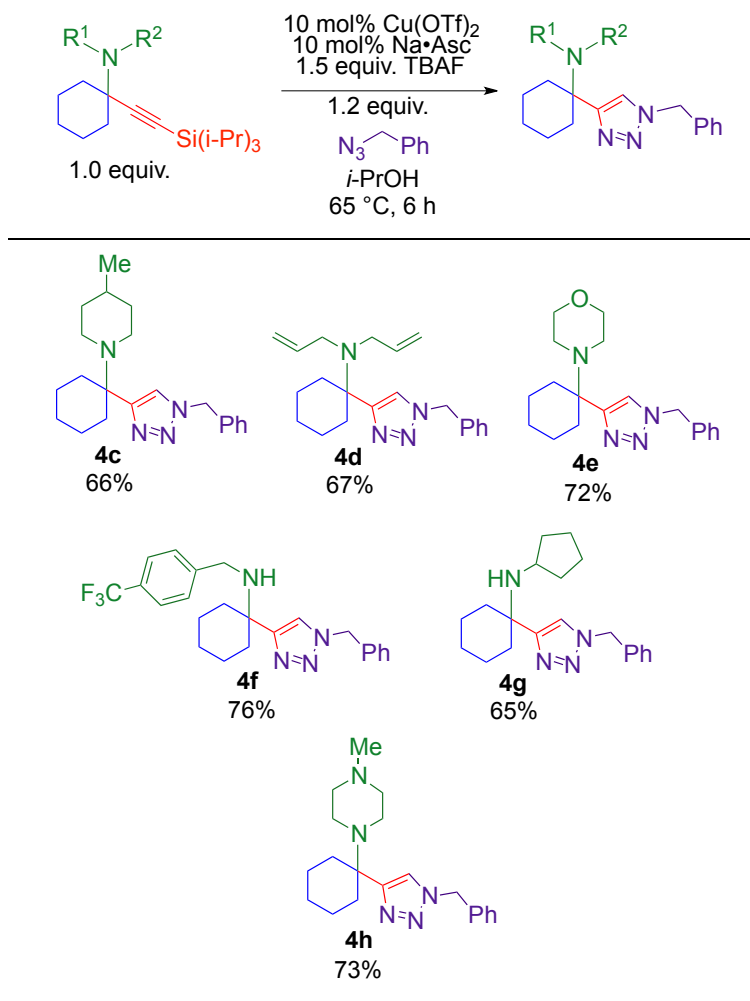


Table 4.4: Tetrasubstituted silyl protected propargylamines form hindered triazole products in good yield through tandem deprotection-cyclization.

Additional organic azides were synthesized according to known procedures.³⁹⁻⁴¹ 4-Methylbenzyl azide forms triazole (**4i**) in a comparable yield to (**4c**), but electron-poor 4-(trifluoromethyl)benzyl azide forms triazole (**4j**) in decreased yield (Table 4.5). Aryl and alkyl azides display similar reactivity in the formation of triazoles (**4k**) and (**4l**), and the HCl salt of lipophilic triazole (**4l**) is isolated in 56% yield. As the 4-methylpiperidine derived TIPS-protected

propargylamine is utilized throughout table 4.5, the lower yields observed in some cases can be attributed to the intrinsic efficiency of the reacting azide.

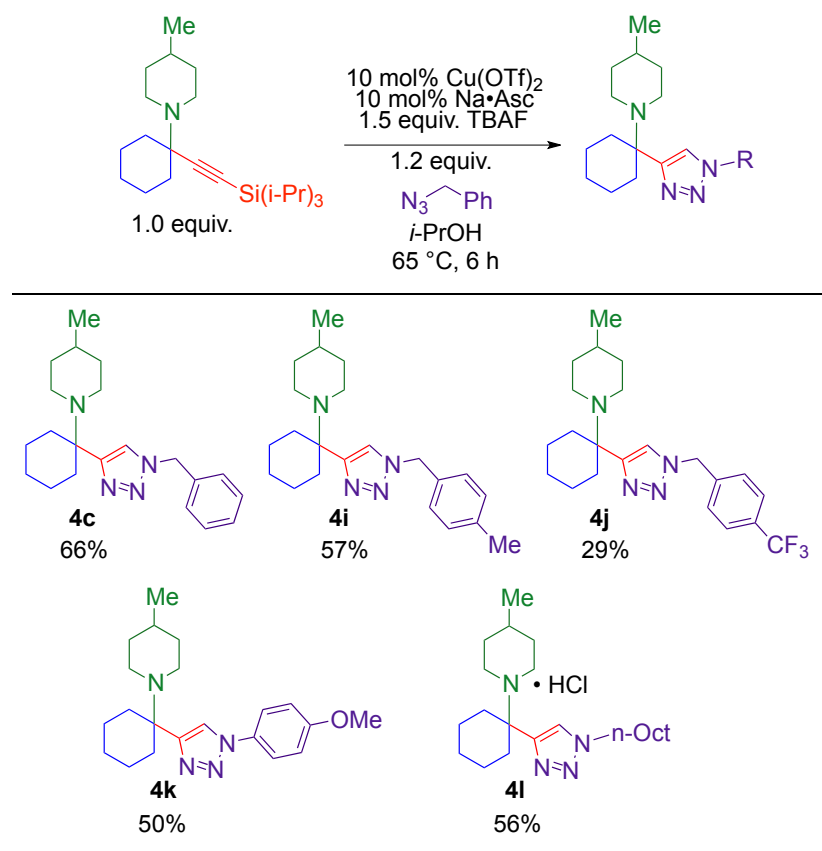
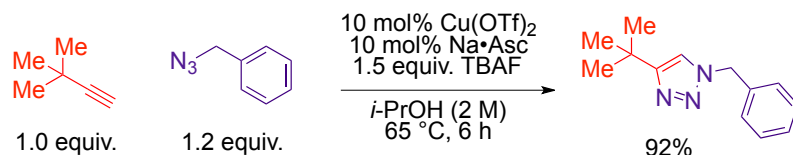


Table 4.5: Assorted azides for formation of alpha-tetrasubstituted triazoles.

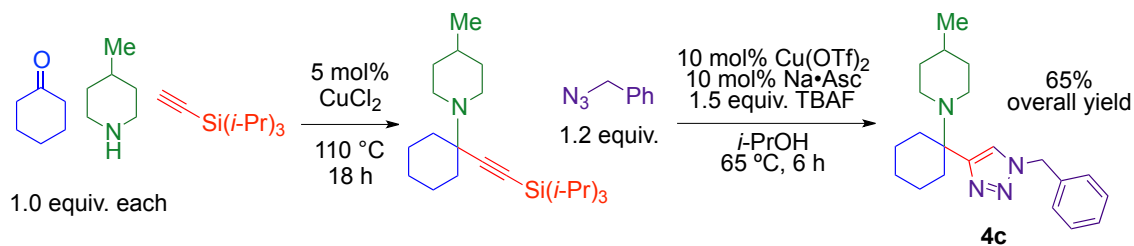
Control reactions were performed to determine whether these conditions developed for the *in situ* silyl deprotection would otherwise affect the reaction when an azide was combined with a simpler non-silyl protected alkyne. The CuAAC reaction of benzyl azide and *tert*-butylacetylene proceeds in 92% yield, thus, decomposition of the benzyl azide or the non-silyl alkyne is unlikely (Scheme 4.3). Further, this reaction proceeds to give 92% isolated yield with or without TBAF in the presence of Cu(OTf)₂ under standard conditions. This

indicates that the sensitivity of the silyl-protected propargylamine is likely behind the lower yields of the propargylamine-derived triazoles as these react with benzyl azide under identical conditions.



Scheme 4.3: Silyl deprotection/click conditions applied to *tert*-butylacetylene. An identical yield is observed without TBAF.

This two-step sequence is able to convert commercially available starting materials into valuable, complex, α -tetrasubstituted triazoles in only three reactions. Triazole (**4c**) is isolated in 65% overall yield across these two steps (Scheme 4.4). The first step requires heating 5 mol% CuCl₂ with equimolar amounts of cyclohexanone, 4-methylpiperidine, and TIPS-acetylene. This reaction uses no added ligands, solvents, additives or excess starting materials, the sole byproduct for the formation of the silyl-protected propargylamines is one equivalent of water.²⁰ The second step to form the α -tetrasubstituted triazole, combines the silyl-deprotection with an azide-alkyne cycloaddition to produce the complex product in only 6 h. This tandem reaction is optimal with copper(II) triflate and sodium ascorbate as a mild reductant. The ability of copper(II) triflate to act as a highly functioning catalyst for this reaction was unexpected, as there are no reports for its use as a catalyst in the CuAAC reaction.^{1,2}



Scheme 4.4: High overall yield of 1,2,3-triazoles fully-substituted at the alpha position after a two step reaction sequence.

4.4 New Found Biological Activity of Some α -Tetrasubstituted Triazoles:

With a library of α -tetrasubstituted triazoles prepared, it was desirable to determine if any of these compounds possessed biological activity. Through collaboration with the UCR School of Medicine a select number of substrates with varying amines and azide components were tested against the A549 lung cancer cell line (Figure 4.3). Of those tested, the cyclopentylamine substrate, coupled with benzyl azide, demonstrated activity with an IC_{50} at 35 μ M. Additionally, the 4-methylpiperidine substrate that was coupled with 4-(trifluoromethyl)benzyl azide had even greater activity at suppressing the growth of this type of cancer cells with an IC_{50} at 25 μ M.

As these α -tetrasubstituted triazoles derived from propargylamines were unknown to have anticancer activity, this discovery was exciting and called for the synthesis of additional compounds for testing. As the most active compound (**4j**) bearing the 4-(trifluoromethyl)benzyl substituted triazole could be compared to other triazoles derived from the same 4-methylpiperidine substituted propargylamine it was clear that the inherent biological activity lay in the azide component. Similarly, as the cyclopentylamine derived triazole (**4g**) was the only

other active compound of those tested, and it shared the same triazole substitution derived from benzyl azide as other inactive substrates, the activity of this compound was likely inherent to the amine.

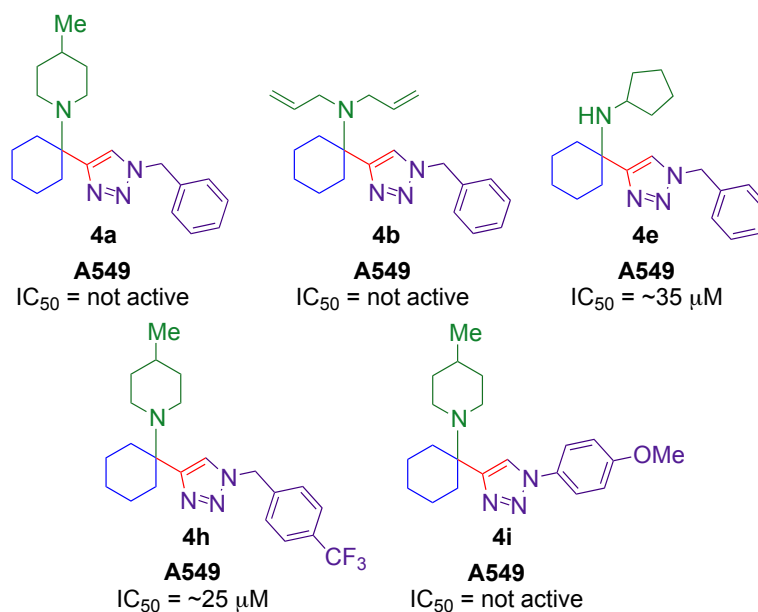


Figure 4.3: Biological activity of some alpha tetrasubstituted triazoles against the A549 lung cancer cell line.

These two factors were used to develop additional α -tetrasubstituted triazoles for further biological testing. In addition to cyclopentylamine, a motif that is commonly seen in pharmaceuticals and biological agents is the cyclopropylmethyl group. Thus, cyclopropylmethyl amine was also a desirable substrate to incorporate into the α -tetrasubstituted triazoles being used for additional testing. Since the most active compound was derived from a 4-(trifluoromethyl)benzyl azide, the use of a further fluorinated amine was also of interest.

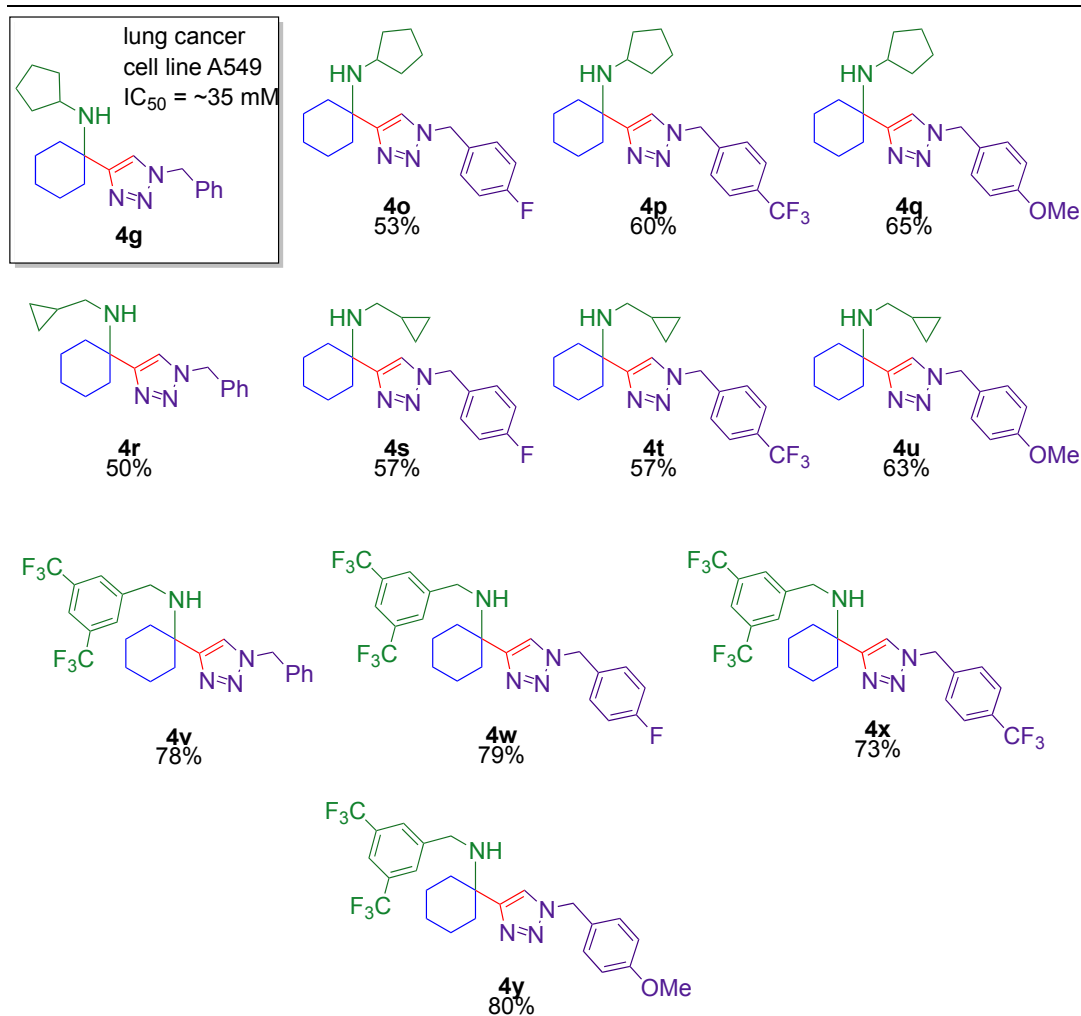
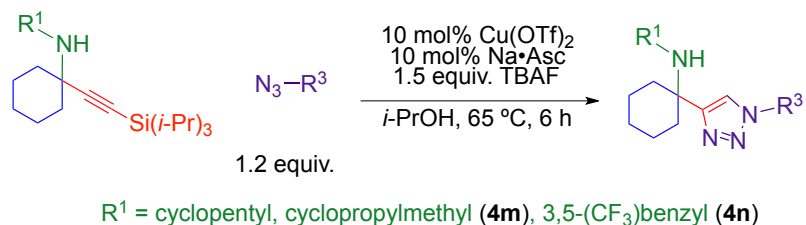


Table 4.6: Additional alpha-tetrasubstituted triazole for biological testing through the Eli Lilly OIDD program.

The three propargylamines that were used for the preparation of additional substrates for testing were the prepared using either: cyclopentylamine, cyclopropylmethylamine (**4m**), or 3,5-(trifluoromethyl)benzylamine (**4n**). These

three were each reacted with four different azides to produce: benzyl, 4-fluorobenzyl, 4-(trifluoromethyl)benzyl and 4-(methoxy)benzyl substituted triazoles (**4o-4y**) (Table 4.6). These along with the originally prepared triazoles were then submitted to the Eli Lilly *Open Innovation Drug Discovery* (OIDD) program, where they were tested for activity against a wide range of proprietary assays. Two of these compounds (**4p**) and (**4w**) demonstrated significant biological activity. The cyclopentylamine derived, 4-(trifluoromethyl)benzylated triazole (**4p**), which was a result of the combination of the two previously active components from the lung cancer cell line test, possessed an IC₅₀ of 2.2 μM against hNav1.7 and an IC₅₀ of 1.1 μM against hNav 1.5. Inhibition of the hNav1 receptor protein is known to decrease the activity of the associated voltage-gated sodium ion channels. hNav1.7 is expressed in both pain and sympathetic neurons in the spine and its inhibition is being looked at as a potential chronic pain treatment for ailments such as neurodegenerative diseases.⁴²⁻⁴⁴ The counterpart, hNav1.5 is found primarily in cardiac muscle and plays a major role in impulse propagation. Inhibition of hNav1.5 is being investigated as a possible treatment for irregular heart beat or other irregular heart events.^{45,46} While it is promising that triazole (**4p**) demonstrates a high activity towards hNav1-type proteins, in order for a drug to be viable as a candidate it should also be selective. As this α-tetrasubstituted triazole is highly active towards both hNav1.5 and hNav1.7 it is an unlikely candidate for future trials but is a good model for the development of additional compounds.

The triazole (**4w**) also possessed notable activity in the OIDD study. The combination of the 3,5-(trifluoromethyl)benzylamine derived propargylamine with 4-fluorobenzyl azide produced a triazole with an EC₅₀ of 4.1 μM towards glucagon-like peptide 1 (GLP-1). This peptide is produced via the proglucagon gene located in ileal L-cells and is a response to nutrient intake in the small intestine.⁴⁷ GLP-1 is known to stimulate glucose-dependent insulin release from the pancreas.⁴⁸ As such, secretion of GLP-1 has been shown to be decreased in patients with type-2 diabetes. In clinical trials, upregulating secretion of GLP-1 is effective regardless of the duration or severity of the diabetes. Thus, increasing the secretion of GLP-1 in the body and controlling its activity, has become a major focus of investigation for developing treatments of type-2 diabetes over the past decade.⁴⁹

Development of methodology to streamline the process of preparing α -tetrasubstituted triazoles, it has become possible to obtain large libraries of these compounds from low-cost starting materials. This in turn allows for the study of the inherent activity of these compounds through structure-activity-relationship analysis. Rather than needing to prepare and isolate all of the intermediates for the synthesis of these compounds this method allows for preparation in only two steps with minimal column chromatography. The final triazoles are isolated via recrystallization, are prepared in good yield, with minimal side products. The first step of this procedure is solvent free and the second final step uses a “green” alcohol based solvent in small amounts. This procedure is largely atom efficient,

as such, this method is scalable, and large quantities of product could be produced in a single run. This method was developed for the preparation of compounds for biological testing, the typical synthesis of the discussed α -tetrasubstituted triazoles prepared enough material for thousands of biological assays. Further work on this research is ongoing, and additional compounds with unprecedented biological activity are likely to be discovered as a result of this work.

4.5 References:

- 1) Meldal, M.; Tornøe, C. W. *Chem. Rev.* **2008**, *108*, 2952.
- 2) Hein, J. E.; Fokin, V. V. *Chem. Soc. Rev.* **2010**, *39*, 1302.
- 3) Tornøe, C. W.; Christensen, C.; Meldal, M. *J. Org. Chem.* **2002**, *67*, 3057.
- 4) Rostovtsev, V. V.; Green, L. G.; Fokin, V. V.; Sharpless, K. B. *Angew. Chem., Int. Ed.* **2002**, *41*, 2596.
- 5) Brik, A.; Muldoon, J.; Lin, Y.-C.; Elder, J. H.; Goodsell, D. S.; Olson, A. J.; Fokin, V. V.; Sharpless, K. B.; Wong, C.-H. *ChemBioChem* **2003**, *4*, 1246.
- 6) Brak, K.; Doyle, P. S.; McKerrow, J. H.; Ellman, J. A. *J. Am. Chem. Soc.* **2008**, *130*, 6404.
- 7) Patterson, A. W.; Wood, W. J. L.; Hornsby, M.; Lesley, S.; Spraggon, G.; Ellman, J. A. *J. Med. Chem.* **2006**, *49*, 6298.
- 8) Wood, W. J. L.; Patterson, A. W.; Tsuruoka, H.; Jain, R. K.; Ellman, J. A. *J. Am. Chem. Soc.* **2005**, *127*, 15521.
- 9) Zhang, L.; Chen, X.; Xue, P.; Sun, H. H. Y.; Williams, I. D.; Sharpless, K. B.; Fokin, V. V.; Jia, G. *J. Am. Chem. Soc.* **2005**, *127*, 15998.
- 10) Pagliai, F.; Pirali, T.; Del Grosso, E.; Di Brisco, R.; Tron, G. C.; Sorba, G.; Genazzani, A. A. *J. Med. Chem.* **2006**, *49*, 467.
- 11) Srinivasan, R.; Uttamchandani, M.; Yao, S. Q. *Org. Lett.* **2006**, *8*, 713.
- 12) Tron, G. C.; Pirali, T.; Billington, R. A.; Canonico, P. L.; Sorba, G.; Genazzani, A. A. *Med. Res. Rev.* **2008**, *28*, 278.
- 13) Gupte, A.; Boshoff, H. I.; Wilson, D. J.; Neres, J.; Labello, N. P.; Somu, R. V.; Xing, C.; Barry, C. E., III; Aldrich, C. C. *J. Med. Chem.* **2008**, *51*, 7495.
- 14) Ferreira, S. B.; Soderro, A. C. R.; Cardoso, M. F. C.; Lima, E. S.; Kaiser, C. R.; Silva, F. P., Jr.; Ferreira, V. F. *J. Med. Chem.* **2010**, *53*, 2364.
- 15) Van Poecke, S.; Negri, A.; Gago, F.; Van Daele, I.; Solaroli, N.; Karlsson, A.; Balzarini, J.; Van Calenbergh, S. *J. Med. Chem.* **2010**, *53*, 2902.
- 16) Li, Y.; Shen, M.; Zhang, Z.; Luo, J.; Pan, X.; Lu, X.; Long, H.; Wen, D.;

- Zhang, F.; Leng, F.; Li, Y.; Tu, Z.; Ren, X.; Ding, K. *J. Med. Chem.* **2012**, *55*, 10033.
- 17) Testa, C.; Scrima, M.; Grimaldi, M.; D'Ursi, A. M.; Dirain, M. L.; Lubin-Germain, N.; Singh, A.; Haskell-Luevano, C.; Chorev, M.; Rovero, P.; Papini, A. *M. J. Med. Chem.* **2014**, *57*, 9424.
- 18) Brik, A.; Muldoon, J.; Lin, Y.-C.; Elder, J. H.; Goodsell, D. S.; Olson, A. J.; Fokin, V. V.; Sharpless, K. B.; Wong, C.-H. *ChemBioChem* **2003**, *4*, 1246.
- 19) Huisgen, R. *Pure Appl. Chem.* **1989**, *61*, 613.
- 20) Palchak, Z. L.; Lussier, D. J.; Pierce, C. J.; Larsen, C. H. *Green Chem.* **2015**, *17*, 1802.
- 21) Blay, G.; Monleon, A.; Pedro, J. R. *Curr. Org. Chem.* **2009**, *13*, 1498.
- 22) Yoo, W. J.; Zhao, L.; Li, C.-J. *Aldrichimica Acta* **2011**, *44*, 43.
- 23) Pereshivko, O. P.; Peshkov, V. A.; Van der Eycken, E. V. *Org. Lett.* **2010**, *12*, 2638.
- 24) Cheng, M.; Zhang, Q.; Hu, X.-Y.; Li, B.-G.; Ji, J.-X.; Chan, A. S. C. *Adv. Synth. Catal.* **2011**, *353*, 1274.
- 25) Pierce, C. J.; Larsen, C. H. *Green Chem.* **2012**, *14*, 2672.
- 26) Pierce, C. J.; Nguyen, M.; Larsen, C. H. *Angew. Chem., Int. Ed.* **2012**, *51*, 12289.
- 27) Ma, X.; Gang, D. R. *Nat. Prod. Rep.* **2004**, *21*, 752.
- 28) Clayden, J.; Donnard, M.; Lefranc, J.; Tetlow, D. J. *Chem. Commun.* **2011**, *47*, 4624.
- 29) Vardanyan, R. S.; Hruby, V. J. *Future Med. Chem.* **2014**, *6*, 385.
- 30) Aucagne, V.; Leigh, D. A. *Org. Lett.* **2006**, *8*, 4505.
- 31) Fletcher, J. T.; Bumgarner, B. J.; Engels, N. D.; Skoglund, D. A. *Organometallics* **2008**, *27*, 5430.
- 32) Fletcher, J. T.; Walz, S. E.; Keeney, M. E. *Tetrahedron Lett.* **2008**, *49*, 7030.

- 33) Beltrán, E.; Serrano, J. L.; Sierra, T.; Giménez, R. *Org. Lett.* **2010**, *12*, 1404.
- 34) Escamilla, I. V.; Ramos, L. F. R.; Escalera, J. S.; Hernandez, A. A. *J. Mex. Chem. Soc.* **2011**, *55*, 133.
- 35) Heuft, M. A.; Collins, S. K.; Yap, G. P. A.; Fallis, A. G. *Org. Lett.* **2001**, *3*, 2883.
- 36) Meyet, C. E.; Pierce, C. J.; Larsen, C. H. *Org. Lett.* **2012**, *14*, 964.
- 37) Jessop, P. G. *Green Chem.* **2011**, *13*, 1391.
- 38) Koradin, C.; Polborn, K.; Knochel, P. *Angew. Chem., Int. Ed.* **2002**, *41*, 2535.
- 39) Shinde, S. S.; Chi, H. M.; Lee, B. S.; Chi, D. Y. *Tetrahedron Lett.* **2009**, *50*, 6654.
- 40) Asano, K.; Matsubara, S. *Org. Lett.* **2010**, *12*, 4988.
- 41) Rossy, C.; Majimel, J.; Delapierre, M. T.; Fouquet, E.; Felpin, F.-X. *J. Organomet. Chem.* **2014**, *755*, 78.
- 42) Emery, E. C.; Luiz, A. P.; Wood, J. N. *Expert Opin. Ther. Targets* **2016**, *20*, 975.
- 43) Nassar, M. A.; Stirling, L. C.; Forlani, G.; Baker, M. D.; Matthews, E. A.; Dickenson, A. H.; Wood, J. N. *Proc. Natl. Acad. Sci. U. S. A.* **2004**, *101*, 12706.
- 44) Abrahamsen, B.; Zhao, J.; Asante, C. O.; Cendan, C. M.; Marsh, S.; Martinez-Barbera, J. P.; Nassar, M. A.; Dickenson, A. H.; Wood, J. N. *Science* **2008**, *321*, 702.
- 45) Milne, J. R.; Hellestrand, K. J.; Bexton, R. S.; Burnett, P. J.; Debbas, N. M. G.; Camm, A. J. *Eur. Heart J.* **1984**, *5*, 99.
- 46) Balsler, J. R. *J. Mol. Cell Cardiol.* **2001**, *33*, 599.
- 47) Lim, G. E.; Brubaker, P. L. *Diabetes*, **2006**, *55*, S70.
- 48) Dungan, K.; Buse, J. B. *Clin. Diabetes* **2005**, *23*, 56.
- 49) Holst, J. J. *Physiol. Rev.* **2007**, *87*, 1409.

4.6 Supporting Information:

General reagent information:

All reactions were set up under ambient atmosphere and carried out in oven-dried screw-cap test-tubes with Teflon seals under an atmosphere of nitrogen. Flash column chromatography was performed using silica gel purchased from Silicycle. $\text{Cu}(\text{OTf})_2$ and CuCl_2 was purchased from Strem and Acros respectively and used as supplied. Amines were purchased from Acros Organics, Alfa Aesar, or Aldrich and distilled before use. All ketones and alkynes were purchased from Acros Organics, Alfa Aesar or TCI America and were purified by distillation before use. Silyl-protected propargylamines were prepared according to the published literature (Palchak, Z. L.; Lussier, D. J.; Pierce, C. J.; Larsen, C. H. *Green Chem.* **2015**, 17, 1802). Azides were purchased from Alfa Aesar, or Enamine and used as supplied. Additional azides were prepared in accordance with the published literature (Asano, K.; Matsubara, S. *Org. Lett.* **2010**, 12, 4988).

General analytical information:

^1H and ^{13}C NMR spectra were measured on a Varian Inova (400 MHz or 500 MHz) or a Bruker (600 MHz) spectrometer using CDCl_3 or $\text{DMSO}-d_6$ as solvent and trimethylsilane as an internal standard. The following abbreviations are used singularly or in combination to indicate the multiplicity of signals: s - singlet, d - doublet, t - triplet, q - quartet, qn - quintet, m - multiplet and br - broad. NMR spectra were acquired at 300 K. Gas chromatography (GC) was carried out on an Agilent Technologies 6850 Network GC System, and dodecane was used as

the internal standard. ATR-IR spectra were taken on a Bruker:ALPHA FTIR Spectrometer. Attenuated total reflection infrared (ATR-IR) was used and the spectra was analyzed using the OPUS software with selected absorption maxima reported in wavenumbers (cm^{-1}). Mass spectrometric data was collected on a HP 5989A GC/MS quadrupole instrument. Exact masses were recorded on a Waters GCT Premier TOF instrument using direct injection of samples in acetonitrile into the electrospray source.

General procedure for the synthesis of α -tetrasubstituted triazoles:

An oven-dried test tube equipped with a magnetic stir bar was charged with 10 mol% $\text{Cu}(\text{OTf})_2$ and 10 mol % sodium ascorbate ($\text{Na}\cdot\text{Asc}$), capped with a septum, and vacuum purged with nitrogen. Isopropanol was added followed by the silyl-protected propargylamine (1.0 equiv), azide (1.2 equiv), tetrabutylammonium fluoride (TBAF), 1 M in THF (1.5 equiv), and the internal standard dodecane (20 μL). The septum was then replaced under nitrogen pressure with a Teflon-seal screw cap. The reaction was stirred at 65 $^\circ\text{C}$ for the indicated time. Upon reaction completion as confirmed by GC analysis, the mixture was cooled to room temperature and the reaction was quenched with ~5 mL H_2O . The reaction was then extracted into diethyl ether, dried over sodium sulfate and concentrated. The resulting oil was placed under high vacuum to remove trace solvent and the resulting product was a brown crude solid. The crude solid was then recrystallized in hexanes to obtain pure triazole product as an off-white solid.

***N,N*-diallyl-1-((triisopropylsilyl)ethynyl)cyclohexanamine (4a):**

Prepared according to the general procedure outline in chapter 2: diallylamine (309 μL , 2.5 mmol), cyclohexanone (258 μL , 2.5 mmol), (triisopropylsilyl) acetylene (673 μL , 3 mmol), and CuCl_2 (16.75 mg, 0.13 mmol) afford the title compound as a yellow oil in 61% yield (0.548 g, 1.52 mmol) after gradient chromatography on silica gel (100% hexanes \rightarrow 5% EtOAc in hexanes). ATR-IR (film) 2934, 2863, 2152, 1462, 915 cm^{-1} . ^1H NMR (500 MHz, CDCl_3 , 25 $^\circ\text{C}$) δ 5.95 (m, 2H), 5.12 (dd, $J = 15.5$ Hz, $J = 2$ Hz, 2H), 5.03 (dd, $J = 9$ Hz, $J = 1$ Hz, 2H), 3.31 (d, $J = 6$ Hz, 4H), 2.01 (d, $J = 12$ Hz, 2H), 1.63 (m, 5H), 1.40 (td, $J = 8$ Hz, $J = 3.5$ Hz, 2H), 1.15 (m, 18H), 1.08 (d, $J = 5$ Hz, 21H). ^{13}C NMR (125 MHz, CDCl_3 , 25 $^\circ\text{C}$) δ 138.0, 115.9, 110.8, 85.2, 59.5, 52.0, 37.6, 25.8, 23.3, 18.9, 11.5. HRMS (ESI) m/z calcd for $[\text{M}+\text{H}]^+$ requires 360.3081, found 360.3033.

***N*-cyclopentyl-1-((triisopropylsilyl)ethynyl)cyclohexanamine (4b):**

Prepared according to the general procedure outline in chapter 2: cyclopentylamine (248 μL , 2.5 mmol), cyclohexanone (258 μL , 2.5 mmol), (triisopropylsilyl) acetylene (673 μL , 3 mmol), and CuCl_2 (16.75 mg, 0.13 mmol) afford the title compound as a yellow oil in 67% yield (0.580 g, 1.68 mmol) after gradient chromatography on silica gel (100% hexanes \rightarrow 20% EtOAc in hexanes). ATR-IR (film) 2932, 2862, 2153, 1449, 882 cm^{-1} . ^1H NMR (400 MHz, CDCl_3 , 25 $^\circ\text{C}$) δ 3.45 (qn, $J = 7.6$ Hz, 1H), 1.82 (m, 4H), 1.62 (m, 7H), 1.48 (m, 2H), 1.30 (m, 5H), 1.05 (m, 21H). ^{13}C NMR (100 MHz, CDCl_3 , 25 $^\circ\text{C}$) δ 113.3,

83.7, 55.9, 55.6, 39.4, 35.8, 26.0, 24.3, 23.4, 18.9, 11.5. HRMS (ESI) m/z calcd for $[M+H]^+$ requires 348.3081, found 348.3045.

1-(1-(1-benzyl-1H-1,2,3-triazol-4-yl)cyclohexyl)-4-methylpiperidine (4c):

Prepared according to the general procedure: The corresponding silyl-protected propargylamine (360 mg, 1.0 mmol), benzyl azide (158 μ L, 1.2 mmol), TBAF 1M in THF (1500 μ L, 1.5 mmol), $\text{Cu}(\text{OTf})_2$ (35 mg, 0.1 mmol), and Na•Asc (21 mg, 0.1 mmol) afford the title compound as an off white solid in 66% yield (0.224 g, 0.66 mmol) after two recrystallizations from hexanes. ATR-IR: 3122, 2913, 1455 cm^{-1} . ^1H NMR (400 MHz, CDCl_3 , 25 $^\circ\text{C}$) δ 7.34 (m, 3H), 7.18 (d, J = 7.6 Hz, 2H), 7.15 (s, 1H), 5.51 (s, 2H), 2.99 (d, J = 10.8 Hz, 2H), 2.11 (m, 2H), 1.88 (t, J = 10 Hz, 2H), 1.67 (t, J = 4 Hz, 2H) 1.53 (m, 4H), 1.37 (p, J = 5.2 Hz, 2H) 1.15 (m, 5H), 0.81 (d, J = 4.8 Hz, 3H) ^{13}C NMR (100 MHz, CDCl_3 , 25 $^\circ\text{C}$) δ 149.0, 135.4, 129.2, 128.7, 127.8, 121.3, 57.7, 54.0, 45.9, 35.3, 34.5, 31.3, 26.2, 22.4, 22.0. HRMS (ESI) m/z calcd for $[M+H]^+$ requires 339.2548, found 339.2571.

***N,N*-diallyl-1-(1-benzyl-1H-1,2,3-triazol-4-yl)cyclohexanamine (4d):**

Prepared according to the general procedure: The corresponding silyl-protected propargylamine (360 mg, 1.0 mmol), benzyl azide (158 μ L, 1.2 mmol), TBAF 1M in THF (1500 μ L, 1.5 mmol), $\text{Cu}(\text{OTf})_2$ (35 mg, 0.1 mmol), and Na•Asc (21 mg, 0.1 mmol) afford the title compound as a yellow waxy solid in 67% yield (0.225 g, 0.67 mmol) after chromatography on silica gel (Solvent gradient: 100% hexanes, 10%, 20%, 50% EtOAc in hexanes). ATR-IR: 3132, 2932, 1453 cm^{-1} . ^1H NMR (400 MHz, CDCl_3 , 25 $^\circ\text{C}$) δ 7.29 (m, 3H), 7.14 (m, 3H), 5.66 (m, 2H), 5.46 (s,

2H), 4.93 (d, $J = 17.2$ Hz, 2H), 4.82 (d, $J = 10.4$ Hz, 2H), 3.06 (d, $J = 6.0$ Hz, 4H), 2.06 (m, 2H) 1.83 (t, $J = 10$ Hz, 2H), 1.62 (m, 2H), 1.32 (m, 2H), 1.17 (m, 2H). ^{13}C NMR (100 MHz, CDCl_3 , 25 °C) δ 151.4, 139.1, 135.3, 129.2, 128.7, 127.9, 121.4, 114.9, 58.7, 54.1, 51.9, 45.4, 26.1, 22.6. HRMS (ESI) m/z calcd for $[\text{M}+\text{H}]^+$ requires 337.2387, found 337.2370.

4-(1-(1-benzyl-1*H*-1,2,3-triazol-4-yl)cyclohexyl)morpholine (4e):

Prepared according to the general procedure: The corresponding silyl-protected propargylamine (349 mg, 1.0 mmol), benzyl azide (158 μL , 1.2 mmol), TBAF 1M in THF (1500 μL , 1.5 mmol), $\text{Cu}(\text{OTf})_2$ (35 mg, 0.1 mmol), and Na•Asc (21 mg, 0.1 mmol) afford the title compound as a white solid in 72% yield (0.234 g, 0.72 mmol) after two recrystallizations from hexanes. ATR-IR: 3125, 2928, 1449 cm^{-1} . ^1H NMR (400 MHz, CDCl_3 , 25 °C) δ 7.34 (m, 3H), 7.20 (dd, $J = 7.6$ Hz, 2 Hz, 2H), 7.16 (s, 1H), 5.51 (s, 2H), 3.62 (t, $J = 4.4$ Hz, 4H), 2.34 (m, 4H), 2.04 (m, 2H), 1.90 (t, $J = 10$ Hz, 2H) 1.68 (m, 2H), 1.40 (t, $J = 5.6$ Hz, 2H) 1.23 (m, 2H). ^{13}C NMR (100 MHz, CDCl_3 , 25 °C) δ 148.5, 135.1, 129.3, 128.8, 127.9, 121.3, 67.8, 57.4, 54.1, 46.1, 33.7, 26.1, 22.1. HRMS (ESI) m/z calcd for $[\text{M}+\text{H}]^+$ requires 327.2179, found 327.2187.

1-(1-(1-benzyl-1*H*-1,2,3-triazol-4-yl)-*N*-(4-(trifluoromethyl)benzyl)cyclohexanamine (4f):

Prepared according to the general procedure: The corresponding silyl-protected propargylamine (437 mg, 1.0 mmol), benzyl azide (158 μL , 1.2 mmol), TBAF 1M in THF (1500 μL , 1.5 mmol), $\text{Cu}(\text{OTf})_2$ (35 mg, 0.1 mmol), and Na•Asc (21 mg,

0.1 mmol) afford the title compound as an off white solid in 76% yield (0.316 g, 0.76 mmol) after two recrystallizations from hexanes. ATR-IR: 3149, 2938, 1456 cm^{-1} . ^1H NMR (400 MHz, CDCl_3 , 25 °C) δ 7.48 (d, J = 8 Hz, 2H), 7.35 (d, J = 6.4 Hz, 2H), 7.31 (d, J = 8 Hz, 2H), 7.21 (s, 1H), 7.18 (d, J = 6.4 Hz, 2H), 5.46 (s, 2H), 3.39 (s, 2H), 1.91 (t, J = 9.6 Hz, 2H), 1.79 (m, 2H), 1.64 (m, 2H), 1.45 (m, 1H) 1.33 (m, 3H), 1.20 (m, 1H). ^{13}C NMR (100 MHz, CDCl_3 , 25 °C) δ 154.6, 145.6, 135.1, 129.3(2 overlapped peaks), 128.8, 128.5, 128.0, 125.3(2 overlapped peaks), 120.8, 54.7, 54.2, 46.5, 36.3, 26.0, 22.1. HRMS (ESI) m/z calcd for $[\text{M}+\text{H}]^+$ requires 415.2104, found 415.2115.

1-(1-benzyl-1*H*-1,2,3-triazol-4-yl)-*N*-cyclopentylcyclohexanamine (4g):

Prepared according to the general procedure: The corresponding silyl-protected propargylamine (348 mg, 1.0 mmol), benzyl azide (158 μL , 1.2 mmol), TBAF 1M in THF (1500 μL , 1.5 mmol), $\text{Cu}(\text{OTf})_2$ (35 mg, 0.1 mmol), and Na•Asc (21 mg, 0.1 mmol) afford the title compound as an off white solid in 65% yield (0.316 g, 0.76 mmol) after chromatography on silica gel (Solvent gradient: 100% hexanes, 10%, 20%, 50% EtOAc in hexanes) and finally recrystallized out of hexanes. ATR-IR: 3124, 2940, 1445 cm^{-1} . ^1H NMR (400 MHz, CDCl_3 , 25 °C) δ 7.34 (m, 3H), 7.25 (s, 1H), 7.20 (dd, J = 7.6 Hz, 2 Hz, 2H), 5.51 (s, 2H), 2.72 (p, J = 8.4 Hz, 2H), 2.07 (m, 2H), 1.67 (m, 4H), 1.51 (m, 4H) 1.38 (m, 2H), 1.30 (m, 4H) 1.05 (m, 2H). ^{13}C NMR (100 MHz, CDCl_3 , 25 °C) δ 154.8, 135.3, 129.2, 128.7, 127.9, 121.2, 54.9, 54.5, 54.1, 37.1, 35.4, 26.1, 23.9, 22.6. HRMS (ESI) m/z calcd for $[\text{M}+\text{H}]^+$ requires 325.2387, found 325.2400.

1-(1-(1-benzyl-1*H*-1,2,3-triazol-4-yl)cyclohexyl)-4-methylpiperazine (4h):

Prepared according to the general procedure: The corresponding silyl-protected propargylamine (362 mg, 1.0 mmol), benzyl azide (158 μ L, 1.2 mmol), TBAF 1M in THF (1500 μ L, 1.5 mmol), Cu(OTf)₂ (35 mg, 0.1 mmol), and Na•Asc (21 mg, 0.1 mmol) afford the title compound as an off white solid in 73% yield (0.250 g, 0.73 mmol) after two recrystallizations from hexanes. ATR-IR: 3124, 2929, 1452 cm^{-1} . ¹H NMR (500 MHz, CDCl₃, 25 °C) δ 7.37 (m, 3H), 7.24 (d, *J* = 7.0 Hz, 2H), 7.18 (s, 1H), 5.50 (s, 2H), 2.4 (m, 4H), 2.21 (s, 3H), 2.11 (m, 2H), 1.93 (t, *J* = 10 Hz, 2H) 1.70 (m, 2H), 1.42 (p, *J* = 5.5 Hz, 2H) 1.25 (m, 2H). ¹³C NMR (125 MHz, CDCl₃, 25 °C) δ 148.1, 134.8, 129.0, 128.5, 127.9, 121.0, 57.1, 55.8, 53.9, 45.9, 45.1, 33.9, 26.0, 22.0. HRMS (ESI) *m/z* calcd for [M+H]⁺ requires 340.2496, found 340.2493.

4-methyl-1-(1-(1-(4-methylbenzyl)-1*H*-1,2,3-triazol-4-yl)cyclohexyl)

piperidine (4i):

Prepared according to the general procedure: The corresponding silyl-protected propargylamine (360 mg, 1.0 mmol), 4-methyl benzyl azide (176 mg, 1.2 mmol), TBAF 1M in THF (1500 μ L, 1.5 mmol), Cu(OTf)₂ (35 mg, 0.1 mmol), and Na•Asc (21 mg, 0.1 mmol) afford the title compound as an off white solid in 57% yield (0.201 g, 0.57 mmol) after two recrystallizations from hexanes. ATR-IR: 3119, 2915, 1458 cm^{-1} . ¹H NMR (400 MHz, CDCl₃, 25 °C) δ 7.15 (d, *J* = 8 Hz, 2H), 7.13 (s, 1H), 7.09 (d, *J* = 8 Hz, 2H), 5.47 (s, 2H), 2.99 (d, *J* = 10.8 Hz, 2H), 2.33 (s, 3H), 2.11 (m, 2H), 1.88 (t, *J* = 12.4 Hz, 2H) 1.69 (m, 2H), 1.54 (m, 2H), 1.37 (p, *J*

= 5.6 Hz, 2H), 1.20 (m, 2H), 1.19 (m, 3H), 0.81 (d, $J = 5.2$ Hz, 3H). ^{13}C NMR (100 MHz, CDCl_3 , 25 °C) δ 148.9, 138.5, 132.3, 129.9, 127.9, 121.2, 57.7, 53.9, 46.0, 35.4, 34.5, 31.2, 26.2, 22.4, 22.0, 21.3. HRMS (ESI) m/z calcd for $[\text{M}+\text{H}]^+$ requires 353.2700, found 353.2689.

4-methyl-1-(1-(1-(4-(trifluoromethyl)benzyl)-1*H*-1,2,3-triazol-4-yl)cyclohexyl) piperidine (4j):

Prepared according to the general procedure: The corresponding silyl-protected propargylamine (360 mg, 1.0 mmol), 4-(trifluoromethyl)benzyl azide (210 mg, 1.2 mmol), TBAF 1M in THF (1500 μL , 1.5 mmol), $\text{Cu}(\text{OTf})_2$ (35 mg, 0.1 mmol), and $\text{Na}\cdot\text{Asc}$ (21 mg, 0.1 mmol) afford the title compound as an off white solid in 29% yield (0.117 g, 0.29 mmol) after two recrystallizations from hexanes. ATR-IR: 3118, 2939, 1456 cm^{-1} . ^1H NMR (500 MHz, CDCl_3 , 25 °C) δ 7.64 (d, $J = 8$ Hz, 2H), 7.32 (d, $J = 8$ Hz, 2H), 7.24 (s, 1H), 5.61 (s, 2H), 3.04 (d, $J = 10$ Hz, 2H), 2.14 (m, 2H), 1.95 (t, $J = 11$ Hz, 2H), 1.72 (m, 2H) 1.58 (t, $J = 9.5$ Hz, 4H), 1.42 (t, $J = 6$ Hz, 2H) 1.24 (m, 2H), 1.15 (m, 2H), 0.85 (d, $J = 4.5$ Hz, 3H). ^{13}C NMR (125 MHz, CDCl_3 , 25 °C) δ 149.2, 139.1, 130.6, 127.7, 126.0, 121.2, 57.5, 53.2, 45.8, 35.1, 34.2, 31.1, 26.0, 22.1, 21.8. HRMS (ESI) m/z calcd for $[\text{M}+\text{H}]^+$ requires 407.2417, found 407.2391.

1-(1-(1-(4-methoxyphenyl)-1*H*-1,2,3-triazol-4-yl)cyclohexyl)-4-methyl piperidine (4k):

Prepared according to the general procedure: The corresponding silyl-protected propargylamine (360 mg, 1.0 mmol), 1-azido-4-methoxy benzene (179 mg, 1.2

mmol), TBAF 1M in THF (1500 μ L, 1.5 mmol), Cu(OTf)₂ (35 mg, 0.1 mmol), and Na•Asc (21 mg, 0.1 mmol) afford the title compound as an off white beige solid in 50% yield (0.177 g, 0.50 mmol) after two recrystallizations from hexanes. ATR-IR: 3132, 2922, 1513 cm^{-1} . ¹H NMR (400 MHz, CDCl₃, 25 °C) δ 7.64 (d, *J*= 78.8 Hz, 2H), 7.62 (s, 1H), 6.99 (d, *J*= 9.2 Hz, 2H), 3.85 (s, 3H), 3.08 (d, *J* = 10.4 Hz, 2H), 2.24 (m, 2H), 1.96 (t, *J* = 10.8 Hz, 2H), 1.70 (m, 4H) 1.57 (m, 2H), 1.43 (m, 2H) 1.28 (m, 3H), 1.16 (m, 2H), 0.82 (d, *J* = 5.6 Hz, 3H). ¹³C NMR (100 MHz, CDCl₃, 25 °C) δ 159.7, 149.0, 131.0, 122.1, 119.5, 114.8, 57.7, 55.8, 46.0, 35.4, 34.5, 31.2, 26.2, 22.4, 22.1. HRMS (ESI) *m/z* calcd for [M+H]⁺ requires 355.2492, found 355.2505.

4-methyl-1-(1-(1-octyl-1*H*-1,2,3-triazol-4-yl)cyclohexyl)piperidin-1-ium chloride (4l):

Prepared according to the general procedure: The corresponding silyl-protected propargylamine (360 mg, 1.0 mmol), 1-azido-octane (186 mg, 1.2 mmol), TBAF 1M in THF (1500 μ L, 1.5 mmol), Cu(OTf)₂ (35 mg, 0.1 mmol), and Na•Asc (21 mg, 0.1 mmol) afford the title compound as an off white solid in 56% yield (0.201 g, 0.56 mmol) after chromatography on silica gel (solvent gradient: 100% hexanes, 10%, 20%, 50%, 100% EtOAc in hexanes) and finally precipitated out of diethyl ether as the HCl salt. ATR-IR: 3152, 2925, 2465, 1450 cm^{-1} . ¹H NMR (500 MHz, CDCl₃, 25 °C) δ 11.48 (s, 1H), 8.01 (s, 1H), 4.41 (t, *J*= 7 Hz, 2H), 3.60 (d, *J*= 11 Hz, 2H), 2.84 (d, *J* = 12 Hz, 2H), 2.50 (d, *J* = 10.5 Hz, 2H), 2.34 (t, *J* = 11.5 Hz, 2H), 2.13 (q, *J* = 12.5 Hz, 2H), 1.95 (m, 2H), 1.83 (d, *J* = 13 Hz, 2H),

1.72 (d, $J = 14$ Hz, 2H), 1.57 (d, $J = 11$ Hz, 1H), 1.29 (m, 14H), 1.17 (d, $J = 11$ Hz, 1H), 0.96 (d, $J = 6$ Hz, 3H) 0.87 (t, $J = 6.5$ Hz, 3H). ^{13}C NMR (125 MHz, CDCl_3 , 25 °C) δ 142.2, 125.6, 67.0, 50.8, 47.2, 31.6, 30.9, 30.5, 30.1, 29.8, 29.0, 28.8, 26.5, 24.4, 22.9, 22.5, 20.8, 14.0. HRMS (ESI) m/z calcd for $[\text{M}+\text{H}]^+$ requires 361.3326, found 361.3316.

***N*-(cyclopropylmethyl)-1-((triisopropylsilyl)ethynyl)cyclohexanamine (4m):**

Prepared according to the general procedure outline in chapter 2: cyclopropylmethylamine (215 μL , 2.5 mmol), cyclohexanone (258 μL , 2.5 mmol), (triisopropylsilyl) acetylene (673 μL , 3 mmol), and CuCl_2 (16.75 mg, 0.13 mmol) afford the title compound as a yellow oil in 60% yield (0.500 g, 1.50 mmol) after gradient chromatography on silica gel (100% hexanes \rightarrow 50% EtOAc in hexanes). ATR-IR (film) 2932, 2863, 2154, 1461, 882 cm^{-1} . ^1H NMR (500 MHz, CDCl_3 , 25 °C) δ 2.60 (d, $J = 7$ Hz, 2H), 1.83 (d, $J = 12$ Hz, 2H), 1.63 (m, 5H), 1.35 (m, 2H), 1.20 (m, 2H), 1.05 (m, 21H), 0.95 (qn, $J = 7$ Hz, 1H), 0.47 (d, $J = 7.5$ Hz, 2H), 0.12 (d, $J = 4.5$ Hz, 2H). ^{13}C NMR (125 MHz, CDCl_3 , 25 °C) δ 112.2, 83.7, 55.3, 48.7, 38.3, 25.9, 23.1, 18.7, 11.5, 11.3, 3.5. HRMS (ESI) m/z calcd for $[\text{M}+\text{H}]^+$ requires 334.2925, found 334.2943.

***N*-(3,5-bis(trifluoromethyl)benzyl)-1-((triisopropylsilyl)ethynyl)cyclohexanamine (4n):**

Prepared according to the general procedure outline in chapter 2: 3,5-bis(trifluoromethyl)benzylamine (608 mg, 2.5 mmol), cyclohexanone (258 μL , 2.5 mmol), (triisopropylsilyl) acetylene (673 μL , 3 mmol), and CuCl_2 (16.75 mg, 0.13

mmol) afford the title compound as a yellow oil in 57% yield (0.723 g, 1.43 mmol) after gradient chromatography on silica gel (100% hexanes -> 20% EtOAc in hexanes). ATR-IR (film) 2938, 2864, 2154, 1462, 1275 cm^{-1} . ^1H NMR (400 MHz, CDCl_3 , 25 $^\circ\text{C}$) δ 7.83 (s, 2H), 7.75 (s, 1H), 4.06 (s, 2H), 1.87 (d, J = 12 Hz, 2H), 1.67 (m, 5H), 1.41 (m, 3H), 1.22 (m, 1H), 1.10 (m, 21H). ^{13}C NMR (125 MHz, CDCl_3 , 25 $^\circ\text{C}$) δ 144.0, 131.4, 128.5, 123.5, 120.8, 111.5, 84.6, 55.9, 47.3, 38.3, 25.8, 23.0, 18.7, 11.2. HRMS (ESI) m/z calcd for $[\text{M}+\text{H}]^+$ requires 506.2672, found 506.2699.

**N-cyclopentyl-1-(1-(4-fluorobenzyl)-1H-1,2,3-triazol-4-yl)cyclohexanamine
(4o):**

Prepared according to the general procedure: The corresponding silyl-protected propargylamine (348 mg, 1.0 mmol), 4-fluorobenzyl azide (181 mg, 1.2 mmol), TBAF 1M in THF (1500 μL , 1.5 mmol), $\text{Cu}(\text{OTf})_2$ (35 mg, 0.1 mmol), and $\text{Na}\cdot\text{Asc}$ (21 mg, 0.1 mmol) afford the title compound as an off white solid in 53% yield (0.180 g, 0.53 mmol) after two recrystallizations from hexanes. ATR-IR: 3130, 2941, 1447 cm^{-1} . ^1H NMR (500 MHz, $\text{DMSO}-d_6$) δ 7.95 (s, 1H), 7.31 (t, J = 8.0 Hz, 2H), 7.19 (t, J = 9.0 Hz, 2H), 5.55 (s, 2H), 2.66 (qn, J = 8.0 Hz, 1H), 1.93 (m, 2H), 1.63 (m, 4H), 1.45 (m, 2H), 1.36 (m, 4H), 1.24 (m, 4H), 1.01 (q, J = 9.0 Hz, 2H). ^{13}C NMR (150 MHz, CDCl_3) δ 163.7, 162.1, 131.1, 129.8, 121.0, 116.3, 54.8, 54.4, 53.4, 37.0, 35.4, 26.0, 23.8, 22.5. HRMS (ESI) m/z calcd for $[\text{M}+\text{H}]^+$ requires 343.2253, found 343.2236.

N-cyclopentyl-1-(1-(4-(trifluoromethyl)benzyl)-1H-1,2,3-triazol-4-

yl)cyclohexanamine (4p):

Prepared according to the general procedure: The corresponding silyl-protected propargylamine (348 mg, 1.0 mmol), 4-(trifluoromethyl)benzyl azide (210 mg, 1.2 mmol), TBAF 1M in THF (1500 μ L, 1.5 mmol), Cu(OTf)₂ (35 mg, 0.1 mmol), and Na•Asc (21 mg, 0.1 mmol) afford the title compound as an off white solid in 60% yield (0.236 g, 0.60 mmol) after two recrystallizations from hexanes. ATR-IR: 3115, 2200, 1423 cm^{-1} . ¹H NMR (600 MHz, CDCl₃) δ 7.56 (d, *J* = 8.0 Hz, 2H), 7.26 (d, *J* = 8.0 Hz, 2H), 7.19 (s, 1H), 5.53 (s, 2H), 2.70 (m, 1H), 2.04 (s, 2H), 1.68 (m, 2H), 1.59 (m, 3H), 1.49 (m, 4H), 1.35 (m, 2H), 1.25 (m, 4H), 1.02 (m, 2H). ¹³C NMR (125 MHz, DMSO-*d*₆) δ 160.6, 141.2, 128.6, 128.4, 128.3, 125.6, 122.4, 54.0, 53.8, 52.0, 36.4, 34.7, 25.6, 23.2, 21.8. HRMS (ESI) *m/z* calcd for [M+H]⁺ requires 393.2221, found 393.2228.

N-cyclopentyl-1-(1-(4-methoxybenzyl)-1H-1,2,3-triazol-4-yl)cyclohexanamine (4q):

Prepared according to the general procedure: The corresponding silyl-protected propargylamine (348 mg, 1.0 mmol), 1-(azidomethyl)-4-methoxy benzene (196 mg, 1.2 mmol), TBAF 1M in THF (1500 μ L, 1.5 mmol), Cu(OTf)₂ (35 mg, 0.1 mmol), and Na•Asc (21 mg, 0.1 mmol) afford the title compound as an off white solid in 65% yield (0.232 g, 0.65 mmol) after two recrystallizations from hexanes ATR-IR: 3125, 2192, 1442 cm^{-1} . ¹H NMR (600 MHz, CDCl₃) δ 7.22 (s, 1H), 7.18 (dd, *J* = 7.0, 5.0 Hz, 2H), 6.88 (dd, *J* = 7.0, 5.0 Hz, 2H), 5.45 (s, 2H), 3.80 (s, 3H),

2.72 (p, $J = 8.0$ Hz, 1H), 2.07 (s, 2H), 1.70 (m, 2H), 1.62 (m, 3H), 1.52 (m, 4H), 1.42 (m, 2H), 1.29 (m, 4H), 1.05 (m, 2H). ^{13}C NMR (150 MHz, CDCl_3) δ 159.9, 154.7, 129.5, 127.3, 120.9, 114.5, 55.5, 54.9, 54.4, 53.7, 37.1, 35.5, 26.1, 23.9, 22.5. HRMS (ESI) m/z calcd for $[\text{M}+\text{H}]^+$ requires 355.2453, found 355.2449.

1-(1-benzyl-1H-1,2,3-triazol-4-yl)-N-(cyclopropylmethyl)cyclohexanamine

(4r):

Prepared according to the general procedure: The corresponding silyl-protected propargylamine (333 mg, 1.0 mmol), benzyl azide (158 μL , 1.2 mmol), TBAF 1M in THF (1500 μL , 1.5 mmol), $\text{Cu}(\text{OTf})_2$ (35.0 mg, 0.1 mmol), and $\text{Na}\cdot\text{Asc}$ (21.0 mg, 0.1 mmol) afford the title compound as an off white solid in 50 % yield (0.154 g, 0.5 mmol) after two recrystallizations from hexanes. ATR-IR: 3119, 2191, 1436 cm^{-1} . ^1H NMR (500 MHz, $\text{DMSO}-d_6$) δ 7.94 (s, 1H), 7.36 (t, $J = 7.5$ Hz, 2H), 7.31 (t, $J = 7.0$ Hz, 1H), 7.22 (d, $J = 7.0$ Hz, 2H), 5.56 (s, 2H), 1.99 (d, $J = 7.0$ Hz, 2H), 1.87 (m, 2H), 1.64 (m, 4H), 1.57 (m, 1H), 1.41 (m, 1H), 1.28 (m, 4H), 0.29 (q, $J = 6.5$ Hz, 2H), -0.14 (q, $J = 4.5$ Hz, 2H). ^{13}C NMR (125 MHz, $\text{DMSO}-d_6$) δ 153.3, 136.5, 128.7, 127.9, 127.5, 121.9, 53.5, 52.6, 46.7, 35.6, 25.6, 21.5, 11.5, 3.2. HRMS (ESI) m/z calcd for $[\text{M}+\text{H}]^+$ requires 311.2191, found 311.2157.

N-(cyclopropylmethyl)-1-(1-(4-fluorobenzyl)-1H-1,2,3-triazol-4-yl)

cyclohexanamine (4s):

Prepared according to the general procedure: The corresponding silyl-protected propargylamine (333 mg, 1.0 mmol), 4-fluorobenzyl azide (181 mg, 1.2 mmol), TBAF 1M in THF (1500 μL , 1.5 mmol), $\text{Cu}(\text{OTf})_2$ (35 mg, 0.1 mmol), and $\text{Na}\cdot\text{Asc}$

(21 mg, 0.1 mmol) afford the title compound as an off white solid in 57% yield (0.188 g, 0.57 mmol) after two recrystallizations from hexanes. ATR-IR: 3106, 2191, 1513 cm^{-1} . ^1H NMR (500 MHz, $\text{DMSO-}d_6$) δ 7.93 (s, 1H), 7.31 (dd, $J = 9.0$, 3.0 Hz, 2H), 7.19 (t, $J = 9.0$ Hz, 2H), 5.54 (s, 2H), 1.98 (d, $J = 7.0$ Hz, 2H), 1.85 (m, 2H), 1.64 (m, 4H), 1.51 (m, 1H), 1.41 (m, 1H), 1.28 (m, 3H), 0.71 (m, 1H), 0.29 (q, $J = 5.5$ Hz, 2H), -0.15 (q, $J = 4.5$ Hz, 2H). ^{13}C NMR (125 MHz, $\text{DMSO-}d_6$) δ 162.2, 153.9, 133.1, 130.3, 122.3, 115.9, 53.9, 52.3, 47.1, 36.1, 26.1, 22.0, 12.0, 3.7. HRMS (ESI) m/z calcd for $[\text{M}+\text{H}]^+$ requires 329.2097, found 329.1984.

N-(cyclopropylmethyl)-1-(1-(4-(trifluoromethyl)benzyl)-1H-1,2,3-triazol-4-yl) cyclohexanamine (4t):

Prepared according to the general procedure: The corresponding silyl-protected propargylamine (333 mg, 1.0 mmol), 4-(trifluoromethyl)benzyl azide (210 mg, 1.2 mmol), TBAF 1M in THF (1500 μL , 1.5 mmol), $\text{Cu}(\text{OTf})_2$ (35 mg, 0.1 mmol), and $\text{Na}\cdot\text{Asc}$ (21 mg, 0.1 mmol) afford the title compound as an off white solid in 57% yield (0.217 g, 0.57 mmol) after two recrystallizations from hexanes. ATR-IR: 3125, 2942, 1428 cm^{-1} . ^1H NMR (500 MHz, $\text{DMSO-}d_6$) δ 7.98 (s, 2H), 7.74 (d, $J = 8.0$ Hz, 2H), 7.42 (d, $J = 8.0$ Hz, 2H), 5.68 (s, 2H), 1.99 (d, $J = 7.0$ Hz, 2H), 1.87 (m, 2H), 1.65 (m, 4H), 1.53 (m, 1H), 1.42 (m, 1H), 1.29 (m, 3H), 0.72 (qn, $J = 7$ Hz, 1H), 0.29 (d, $J = 7.5$ Hz, 2H), -0.14 (d, $J = 5$ Hz, 2H). ^{13}C NMR (125 MHz, $\text{DMSO-}d_6$) δ 160.6, 153.5, 141.1, 128.4, 128.3, 125.6, 122.2, 53.5, 52.0, 46.7, 35.6, 25.6, 21.5, 11.5, 3.2. HRMS (ESI) m/z calcd for $[\text{M}+\text{H}]^+$ requires 379.2065, found 379.2030.

N-(cyclopropylmethyl)-1-(1-(4-methoxybenzyl)-1H-1,2,3-triazol-4-

yl)cyclohexanamine (4u):

Prepared according to the general procedure: The corresponding silyl-protected propargylamine (333 mg, 1.0 mmol), 1-(azidomethyl)-4-methoxybenzene (196 mg, 1.2 mmol), TBAF 1M in THF (1500 μ L, 1.5 mmol), Cu(OTf)₂ (35 mg, 0.1 mmol), and Na•Asc (21 mg, 0.1 mmol) afford the title compound as an off white solid in 63% yield (0.214 g, 0.63 mmol) after two recrystallizations from hexanes. ATR-IR: 3119, 2214, 1457 cm^{-1} . ¹H NMR (400 MHz, CDCl₃) δ 7.20 (s, 1H), 7.18 (d, *J* = 9.0 Hz, 2H), 6.89 (d, *J* = 9.0 Hz, 2H), 5.44 (s, 2H), 3.81 (s, 3H), 2.07 (d, *J* = 7.0 Hz, 2H), 2.01 (m, 2H), 1.73 (m, 2H), 1.62 (m, 4H), 1.42 (m, 2H), 1.33 (m, 2H), 0.79 (m, 1H), 0.37 (q, *J* = 8.5 Hz, 2H), -0.10 (q, *J* = 6.0 Hz, 2H). ¹³C NMR (100 MHz, CDCl₃) δ 160.0, 154.1, 129.5, 127.1, 120.7, 114.6, 55.5, 54.3, 53.7, 47.5, 36.1, 26.0, 22.3, 11.7, 3.5. HRMS (ESI) *m/z* calcd for [M+H]⁺ requires 341.2297, found 341.2262.

1-(1-benzyl-1H-1,2,3-triazol-4-yl)-N-(3,5-bis(trifluoromethyl)benzyl)

cyclohexanamine (4v):

Prepared according to the general procedure: The corresponding silyl-protected propargylamine (505 mg, 1.0 mmol), benzyl azide (158 μ L, 1.2 mmol), TBAF 1M in THF (1500 μ L, 1.5 mmol), Cu(OTf)₂ (35 mg, 0.1 mmol), and Na•Asc (21 mg, 0.1 mmol) afford the title compound as an off white solid in 78% yield (0.378 g, 0.78 mmol) after two recrystallizations from hexanes. ATR-IR: 3112, 2191, 1385 cm^{-1} . ¹H NMR (600 MHz, CDCl₃) δ 7.65 (s, 2H), 7.64 (s, 1H), 7.32 (m, 3H), 7.20

(m, 3H), 5.46 (s, 2H), 3.47 (s, 2H), 1.92 (m, 2H), 1.79 (m, 2H), 1.63 (m, 4H), 1.46 (m, 1H), 1.34 (m, 3H). ^{13}C NMR (150 MHz, CDCl_3) δ 154.3, 144.2, 135.0, 131.6, 129.3, 128.9, 128.3, 128.1, 124.9, 122.2, 120.7, 54.7, 54.2, 46.2, 36.3, 26.0, 22.1. HRMS (ESI) m/z calcd for $[\text{M}+\text{H}]^+$ requires 483.1939, found 483.1943.

N-(3,5-bis(trifluoromethyl)benzyl)-1-(1-(4-fluorobenzyl)-1H-1,2,3-triazol-4-yl)cyclohexanamine (4w):

Prepared according to the general procedure: The corresponding silyl-protected propargylamine (505 mg, 1.0 mmol), 4-fluorobenzyl azide (181 mg, 1.2 mmol), TBAF 1M in THF (1500 μL , 1.5 mmol), $\text{Cu}(\text{OTf})_2$ (35 mg, 0.1 mmol), and $\text{Na}\cdot\text{Asc}$ (21 mg, 0.1 mmol) afford the title compound as an off white solid in 79% yield (0.393 g, 0.79 mmol) after two recrystallizations from hexanes. ATR-IR: 3095, 2191, 1513 cm^{-1} . ^1H NMR (500 MHz, $\text{DMSO}-d_6$) δ 7.99 (s, 1H), 7.91 (s, 2H), 7.88 (s, 1H), 7.31 (t, $J = 9.0$ Hz, 2H), 7.17 (t, $J = 9.0$ Hz, 2H), 5.54 (s, 2H), 3.56 (s, 2H), 1.99 (m, 2H), 1.75 (m, 2H), 1.65 (m, 2H), 1.43 (m, 1H), 1.31 (m, 3H). ^{13}C NMR (125 MHz, CDCl_3) δ 163.0, 154.4, 144.2, 131.3, 130.8, 130.0, 128.3, 123.5, 120.8, 120.5, 116.3, 54.7, 53.5, 46.1, 36.3, 26.0, 22.1. HRMS (ESI) m/z calcd for $[\text{M}+\text{H}]^+$ requires 501.1844, found 501.1777.

N-(3,5-bis(trifluoromethyl)benzyl)-1-(1-(4-(trifluoromethyl)benzyl)-1H-1,2,3-triazol-4-yl)cyclohexanamine (4x):

Prepared according to the general procedure: The corresponding silyl-protected propargylamine (505 mg, 1.0 mmol), 4-(trifluoromethyl)benzyl azide (210 mg, 1.2 mmol), TBAF 1M in THF (1500 μL , 1.5 mmol), $\text{Cu}(\text{OTf})_2$ (35 mg, 0.1 mmol), and

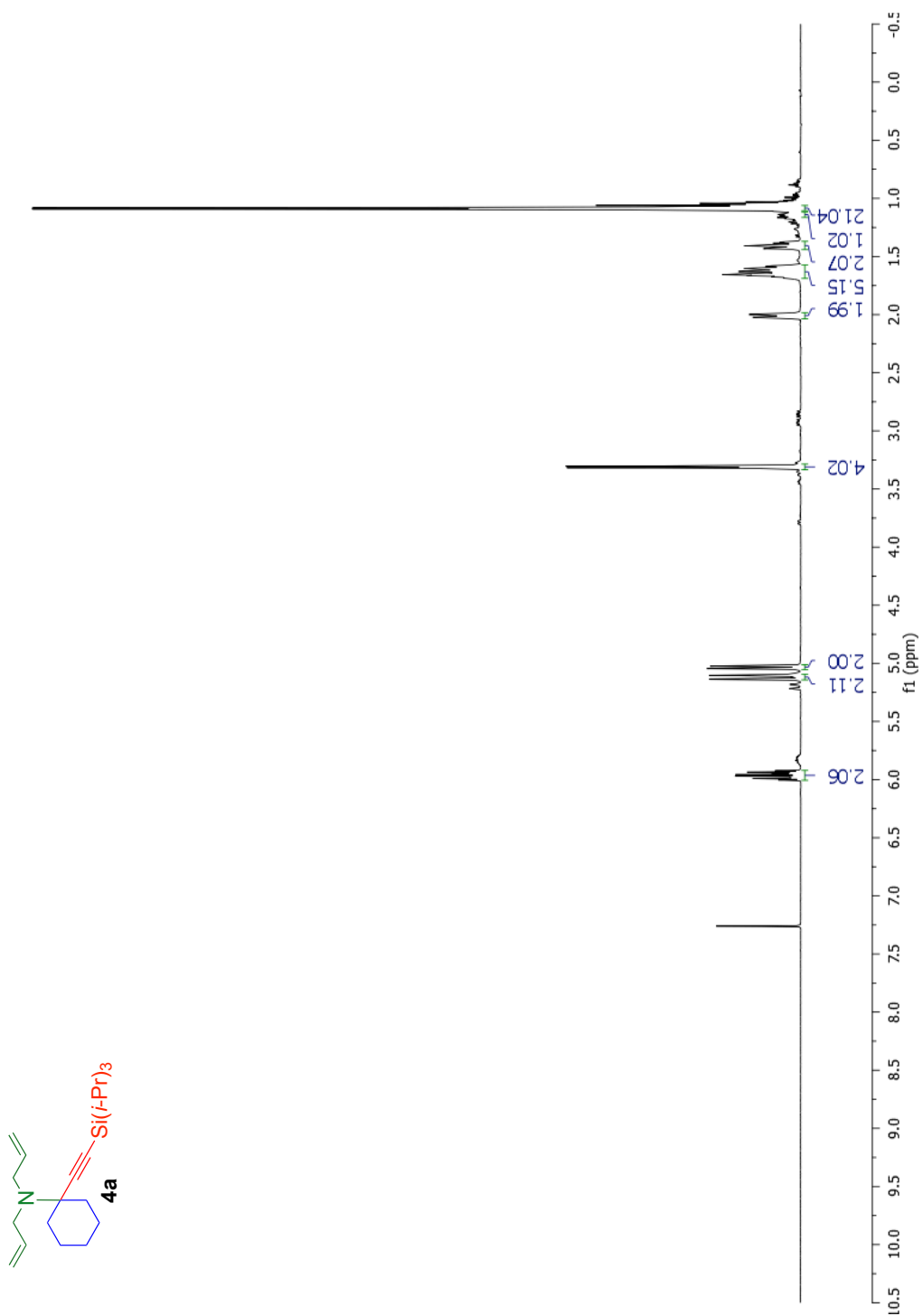
Na•Asc (21 mg, 0.1 mmol) afford the title compound as an off white solid in 73% yield (0.401 g, 0.73 mmol) after two recrystallizations from hexanes ATR-IR: 3113, 2942, 1385 cm^{-1} . ^1H NMR (500 MHz, $\text{DMSO-}d_6$) δ 8.05 (s, 1H), 7.91 (s, 2H), 7.85 (s, 1H), 7.70 (d, $J = 8.0$ Hz, 2H), 7.41 (d, $J = 8.0$ Hz, 2H), 5.69 (s, 2H), 3.57 (s, 2H), 2.63 (s, 1H), 2.01 (m, 2H), 1.77 (m, 2H), 1.65 (m, 2H), 1.42 (m, 1H), 1.32 (m, 3H). ^{13}C NMR (100 MHz, $\text{DMSO-}d_6$) δ 153.1, 145.9, 141.0, 129.6, 128.3, 128.2, 125.6, 125.1, 124.5, 122.5, 122.4, 119.8, 54.1, 52.0, 44.9, 35.8, 25.6, 21.7. HRMS (ESI) m/z calcd for $[\text{M}+\text{H}]^+$ requires 551.1813 found 551.1700.

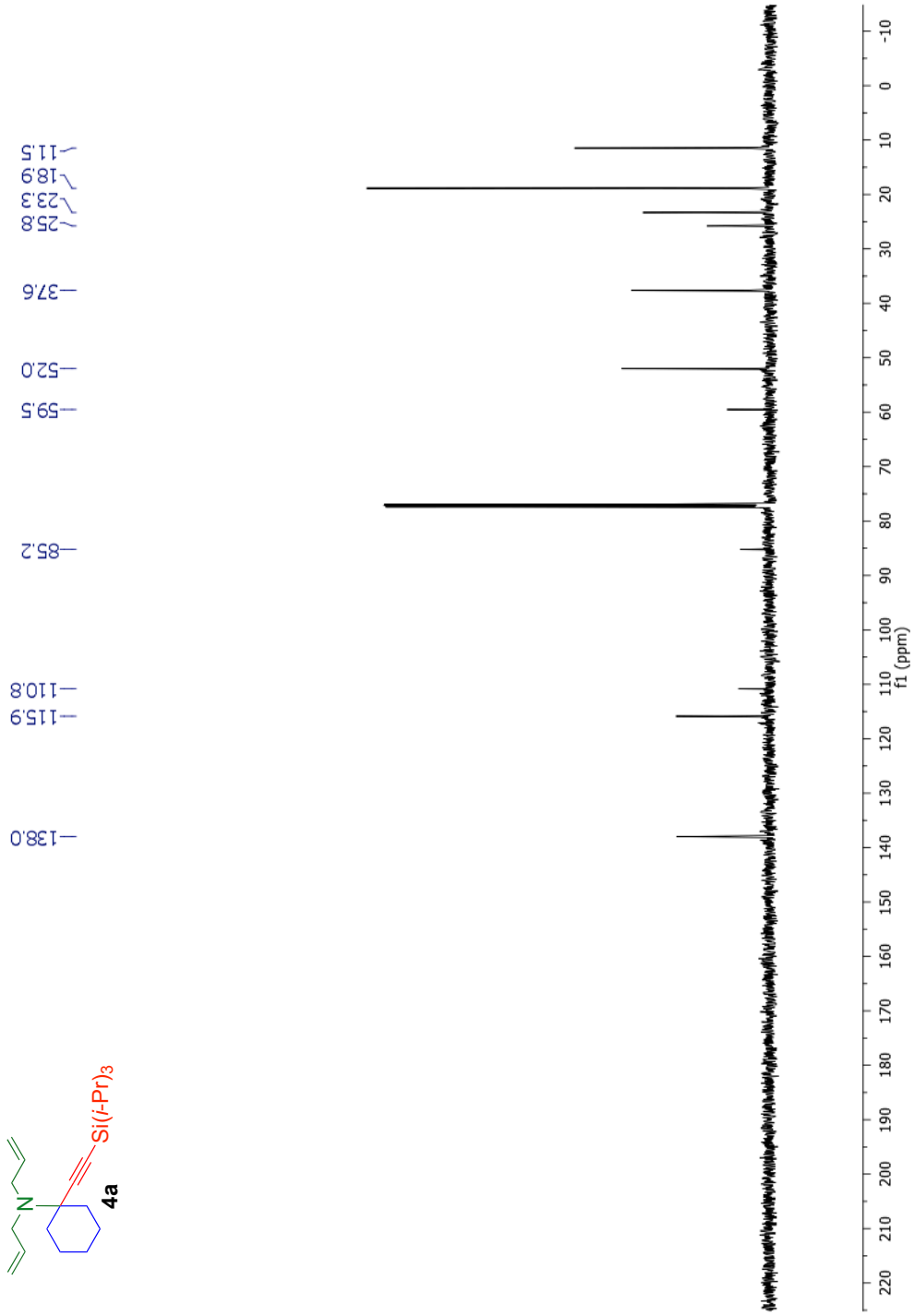
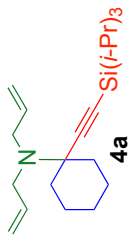
N-(3,5-bis(trifluoromethyl)benzyl)-1-(1-(4-methoxybenzyl)-1H-1,2,3-triazol-4-yl)cyclohexanamine (4y):

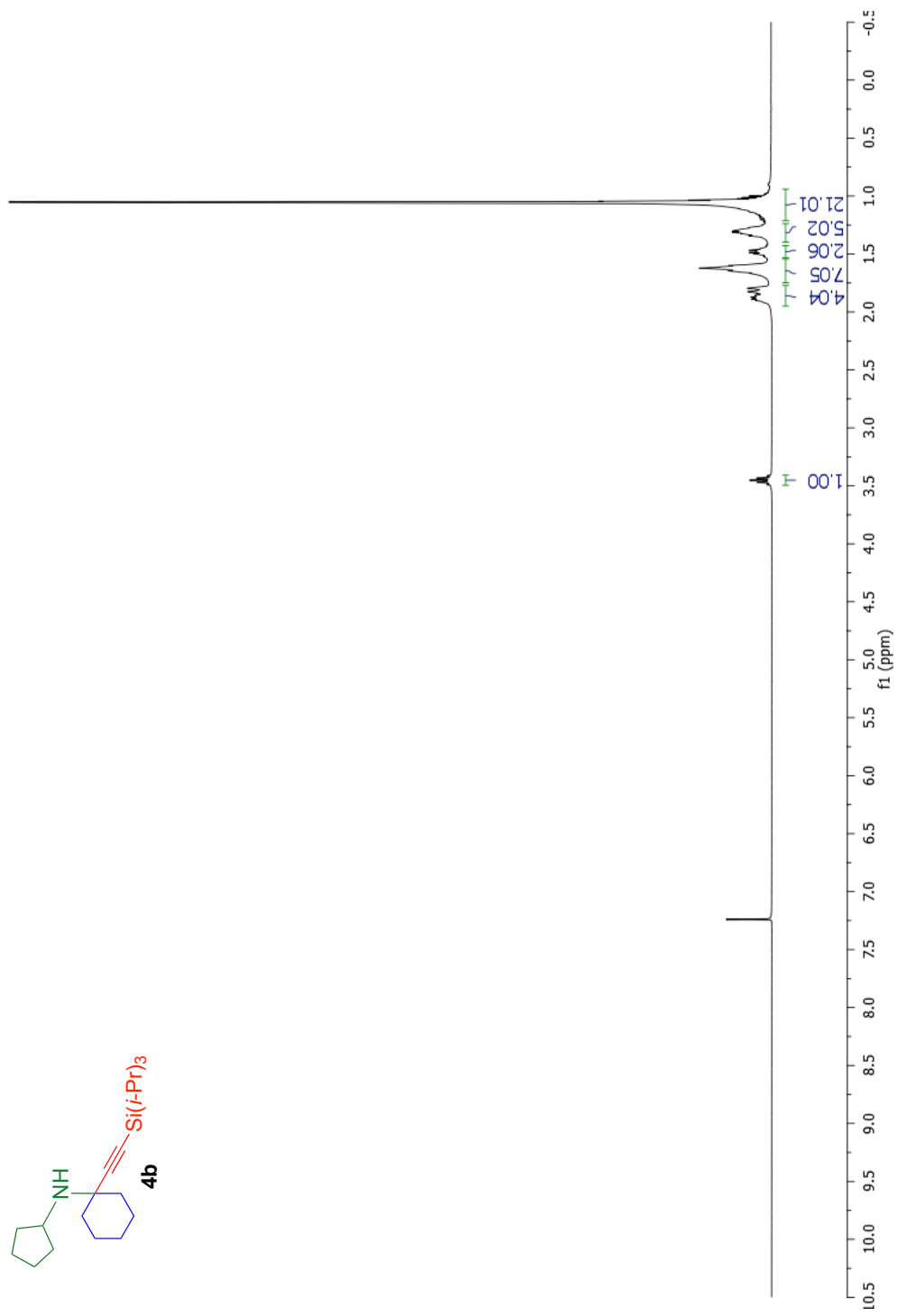
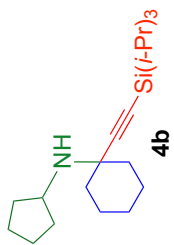
Prepared according to the general procedure: The corresponding silyl-protected propargylamine (505 mg, 1.0 mmol), 1-(azidomethyl)-4-methoxybenzene (196 mg, 1.2 mmol), TBAF 1M in THF (1500 μL , 1.5 mmol), $\text{Cu}(\text{OTf})_2$ (35 mg, 0.1 mmol), and Na•Asc (21 mg, 0.1 mmol) afford the title compound as an off white solid in 80% yield (0.413 g, 0.80 mmol) after two recrystallizations from hexanes. ATR-IR: 3110, 2294, 1445 cm^{-1} . ^1H NMR (600 MHz, CDCl_3) δ 7.72 (s, 2H), 7.70 (s, 1H), 7.24 (s, 1H), 7.22 (d, $J = 9.0$ Hz, 2H), 6.90 (d, $J = 9.0$ Hz, 2H), 5.46 (s, 2H), 3.81 (s, 3H), 3.54 (s, 2H), 1.98 (m, 2H), 1.85 (m, 2H), 1.71 (m, 2H), 1.65 (b, 1H), 1.53 (m, 1H), 1.40 (m, 3H). ^{13}C NMR (150 MHz, CDCl_3) δ 160.0, 154.1, 144.2, 131.5, 129.7, 128.3, 126.8, 123.5, 120.8, 120.4, 114.6, 55.4, 54.7, 53.8, 46.1, 36.3, 26.0, 22.1. HRMS (ESI) m/z calcd for $[\text{M}+\text{H}]^+$ requires 513.2044, found 513.201.

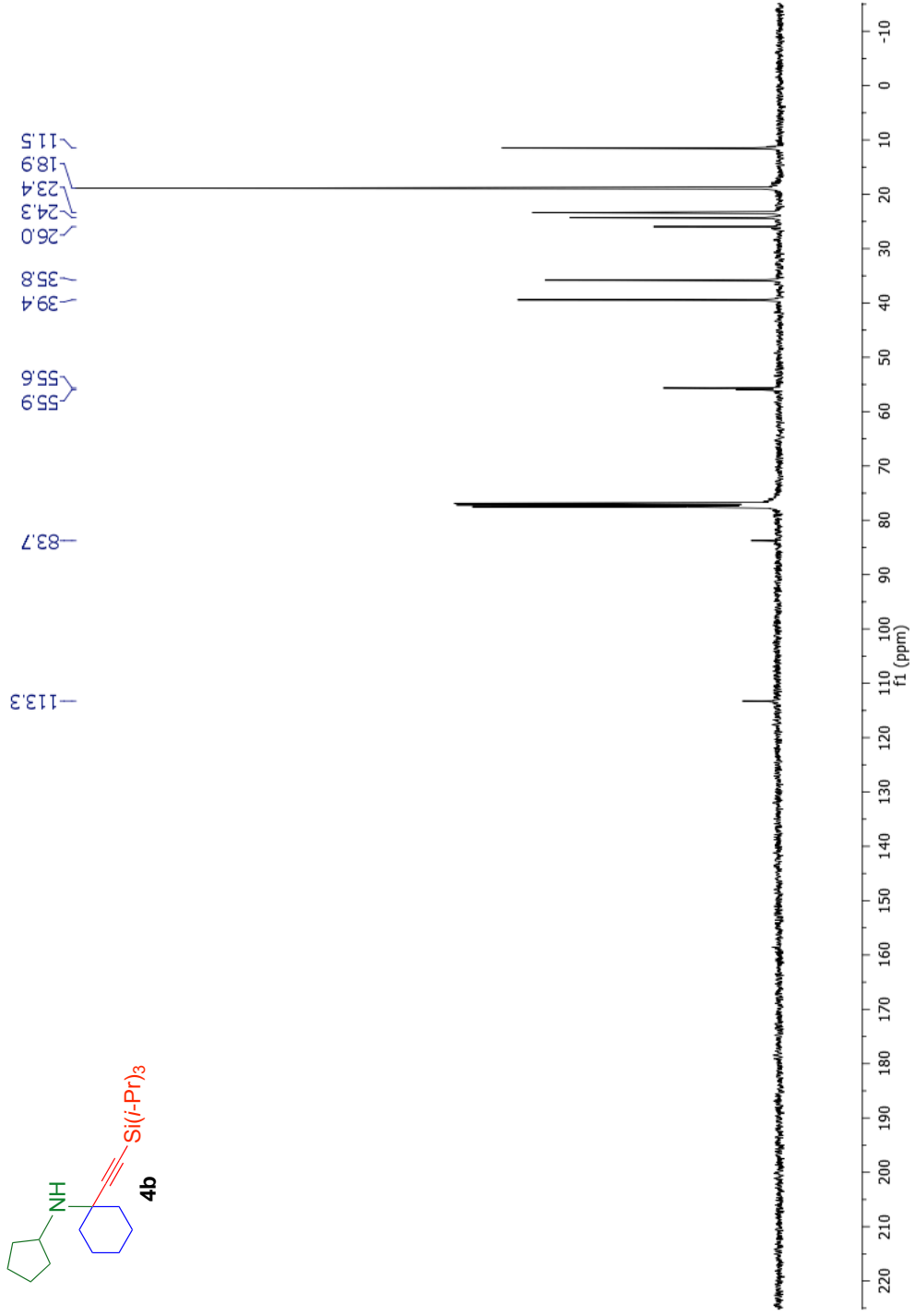
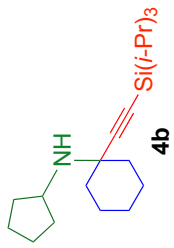
^1H and ^{13}C NMR Spectra for compounds 4c – 4l is available at:

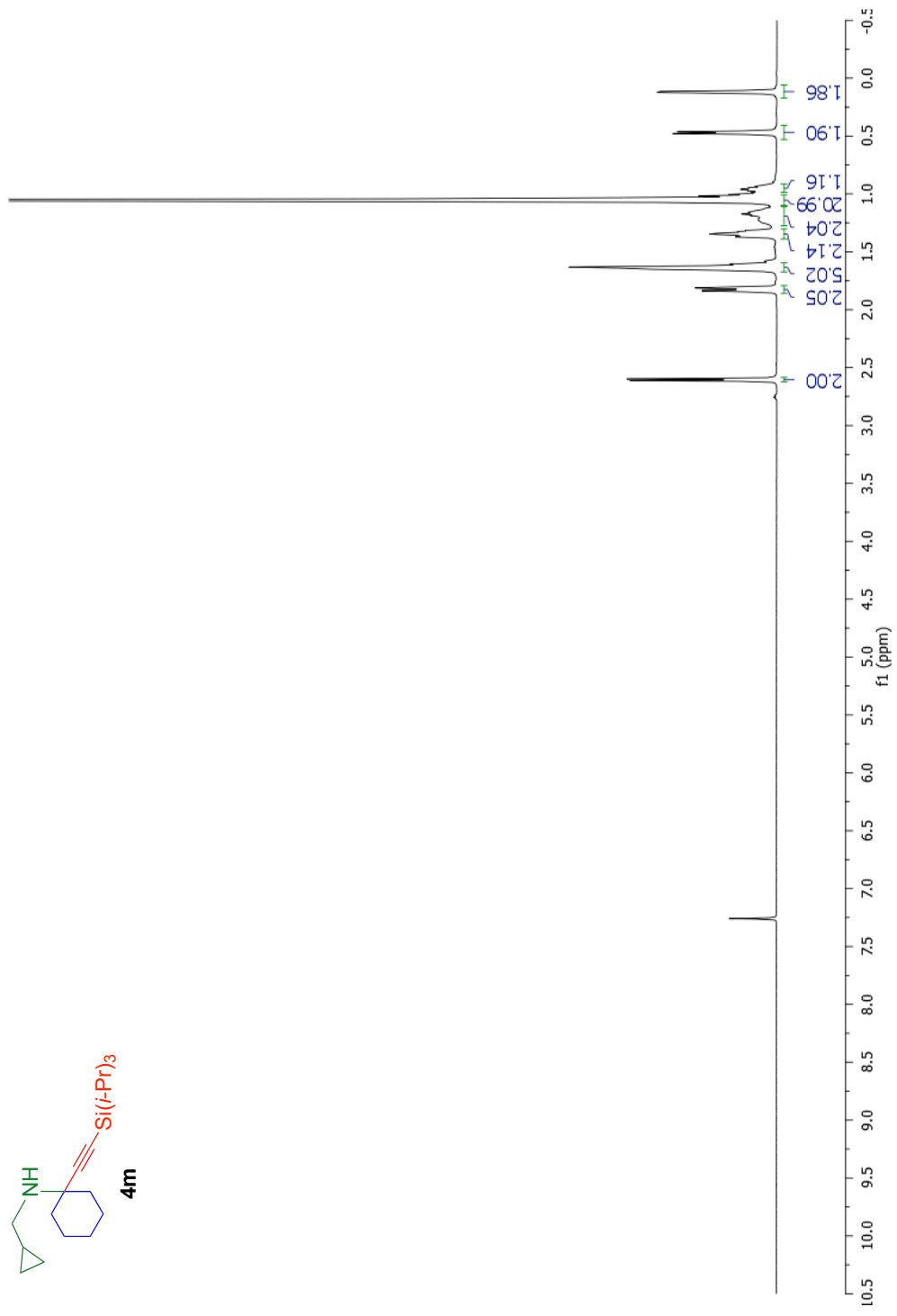
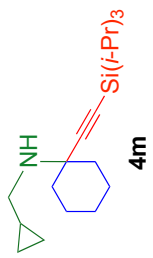
<http://dx.doi.org/10.3762/bjoc.11.154>

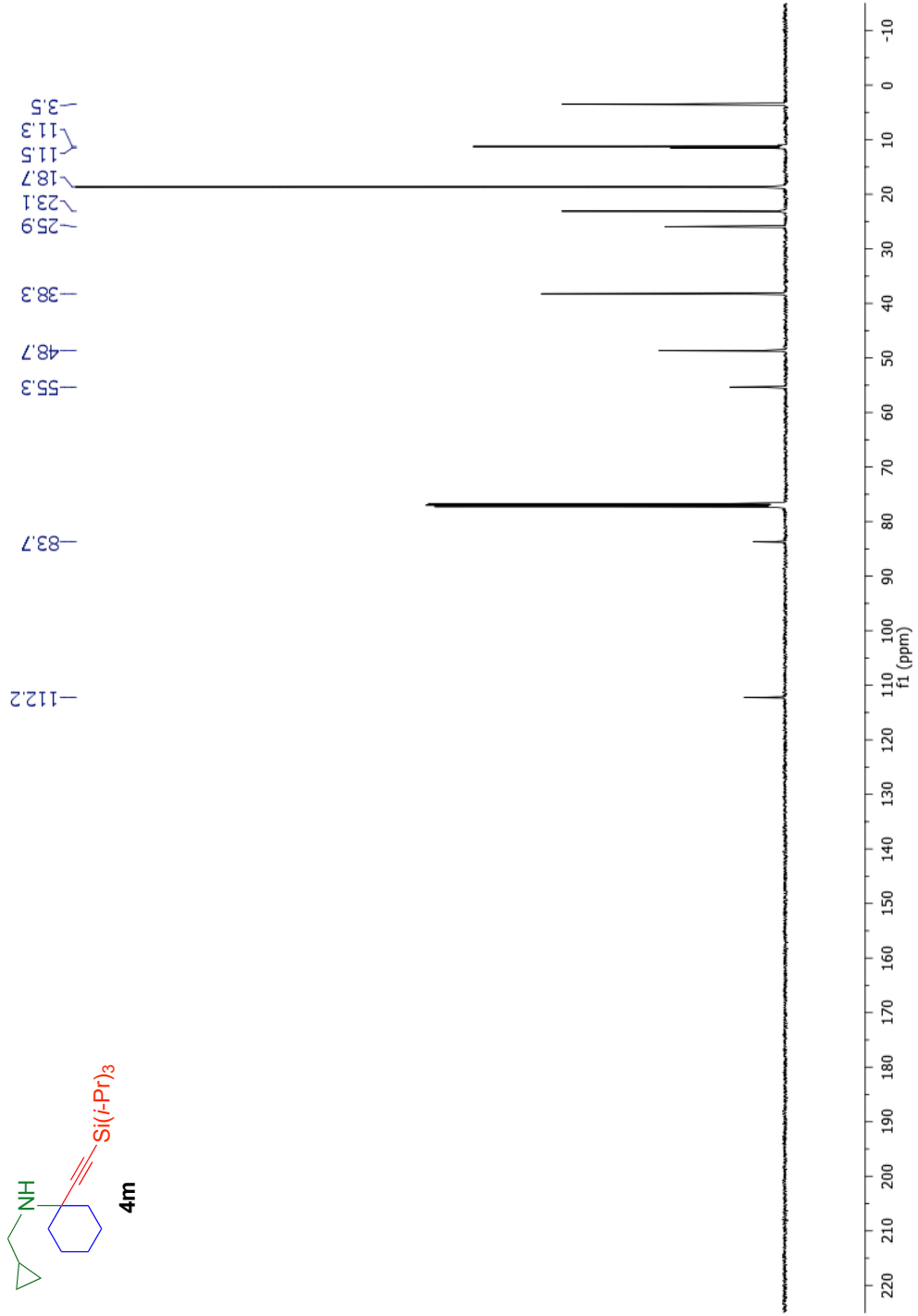
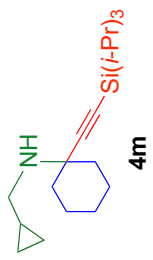


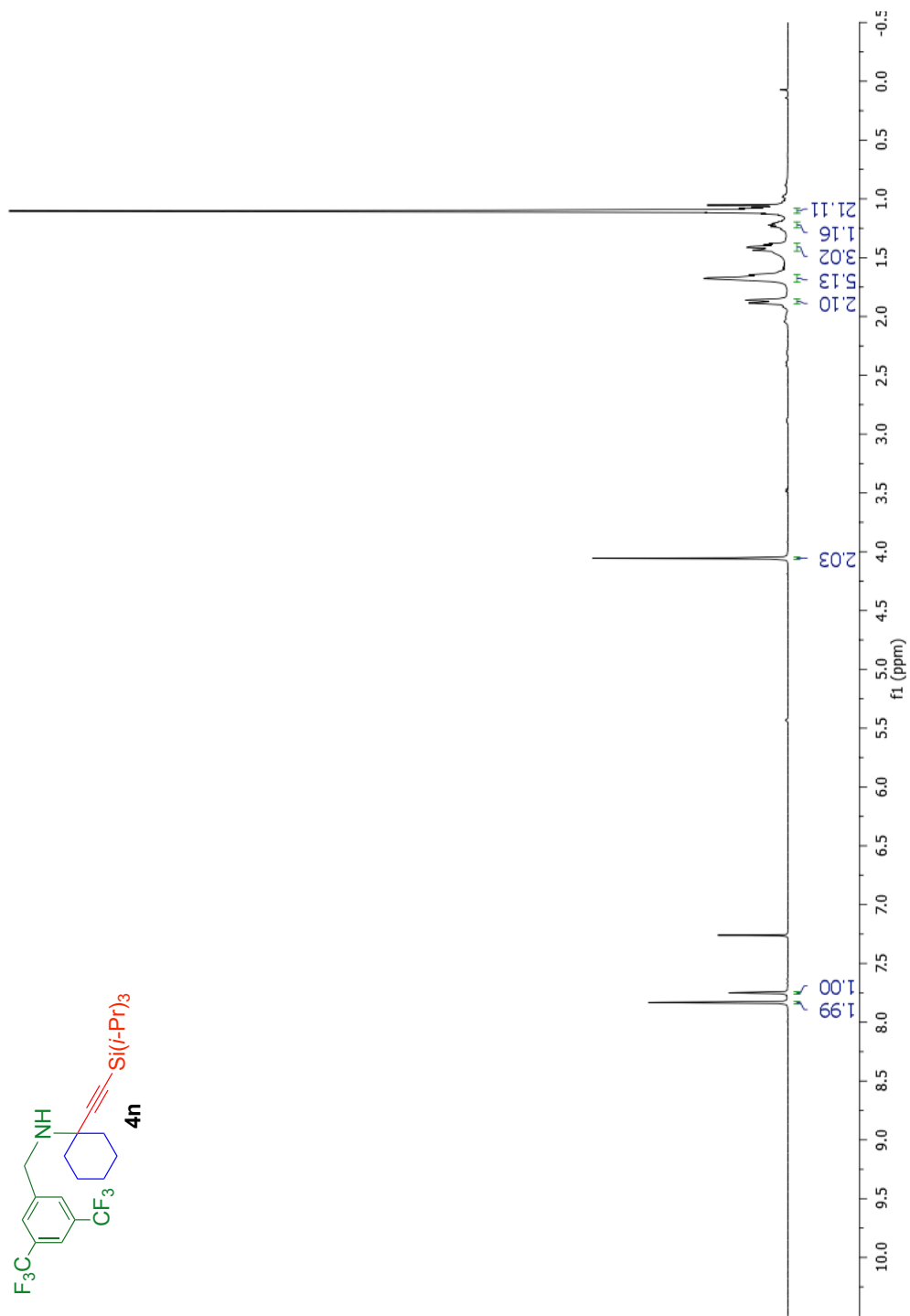
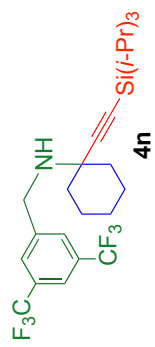


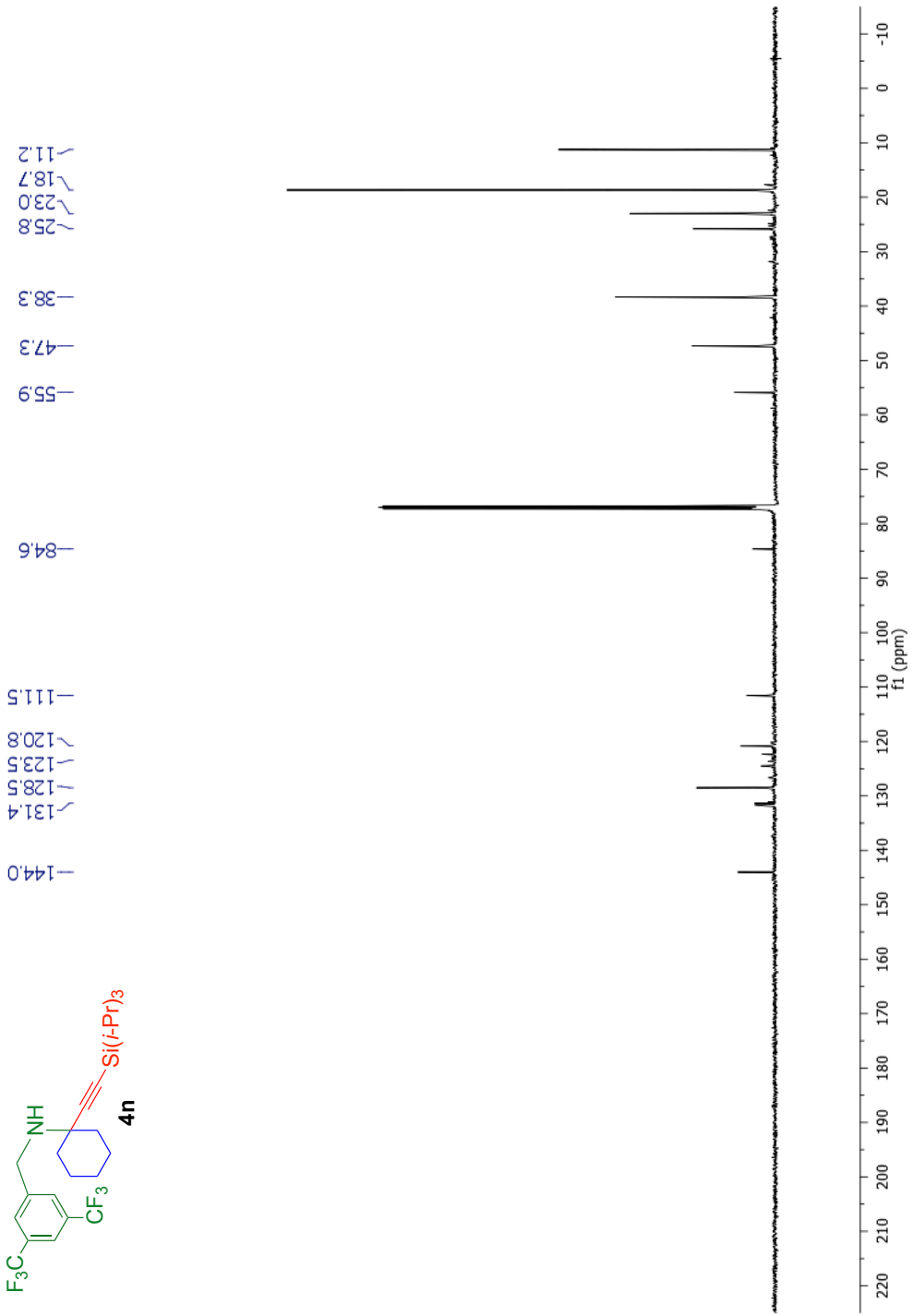
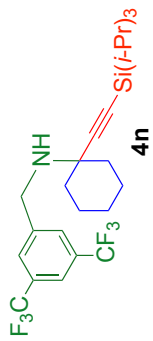


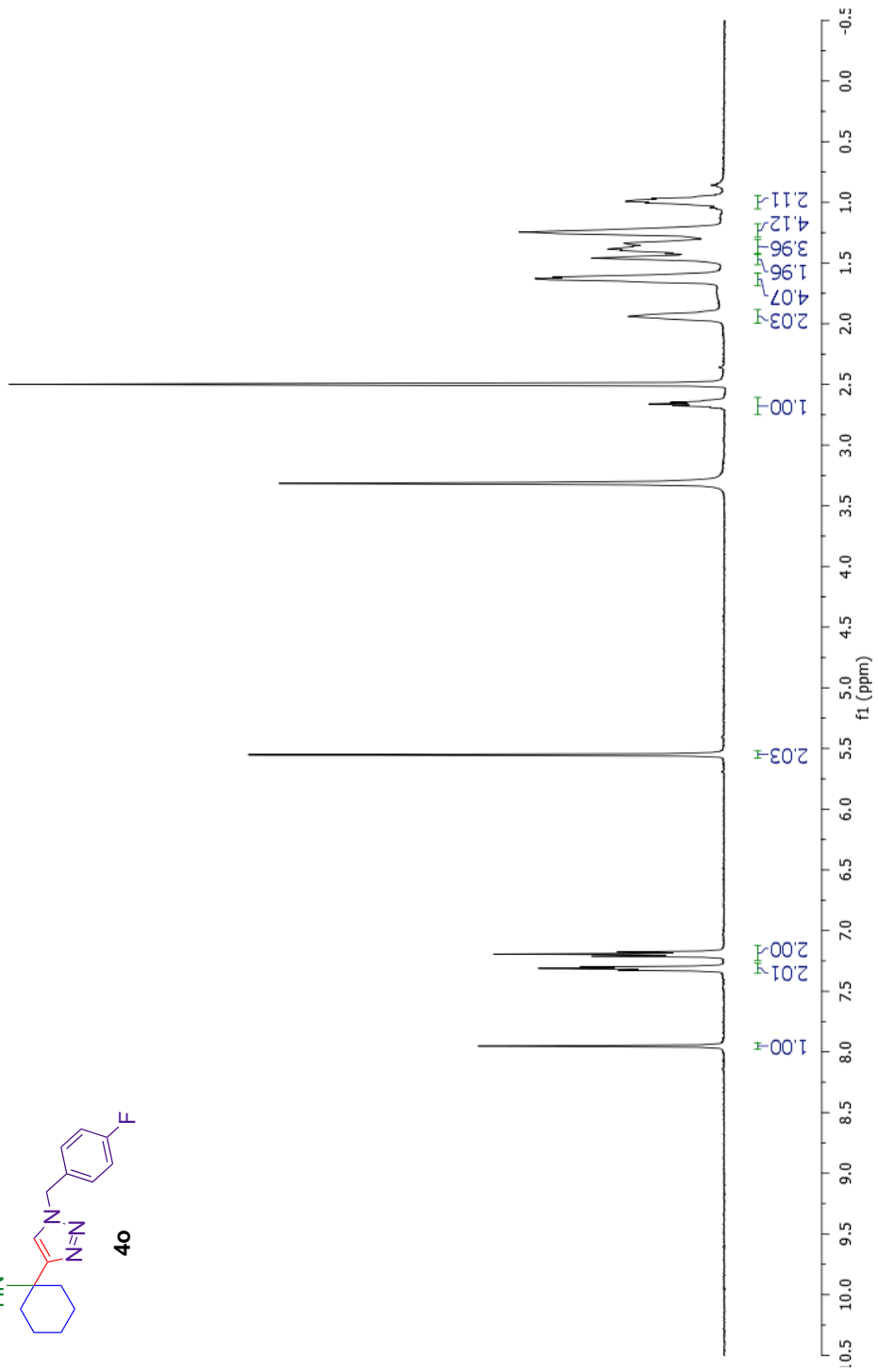
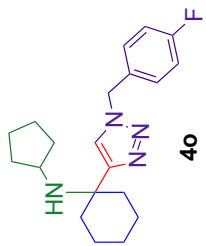


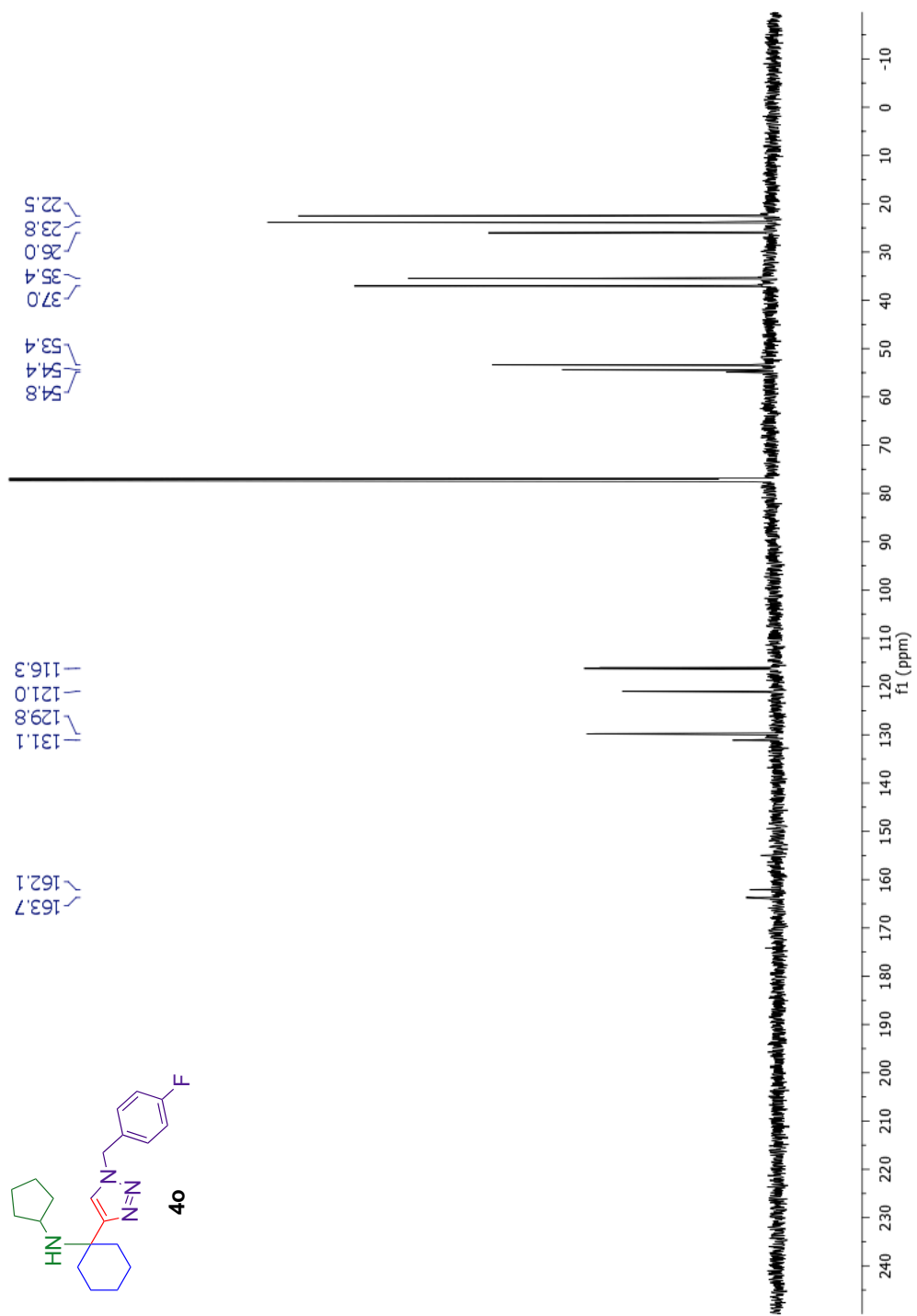


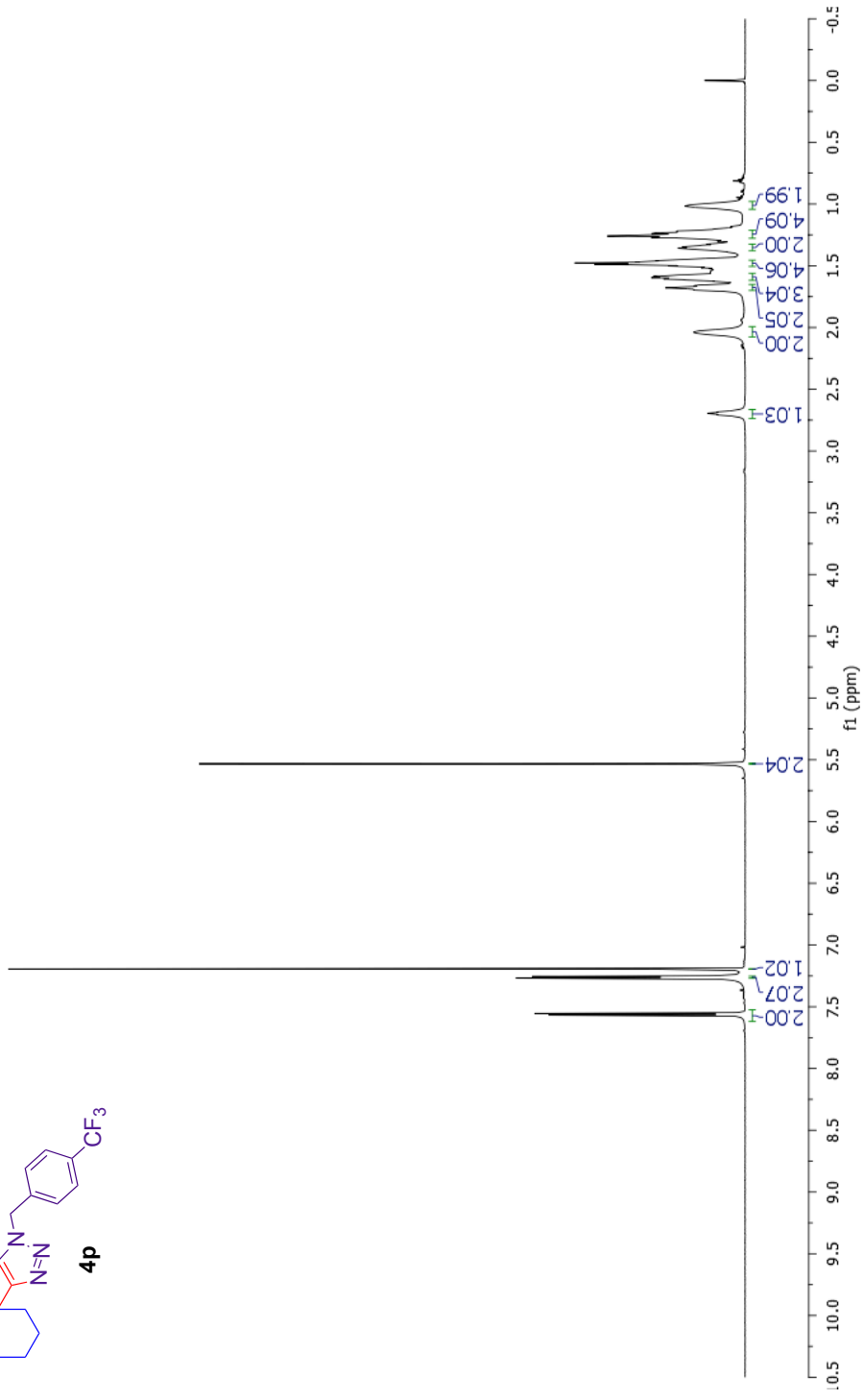
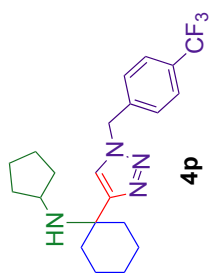


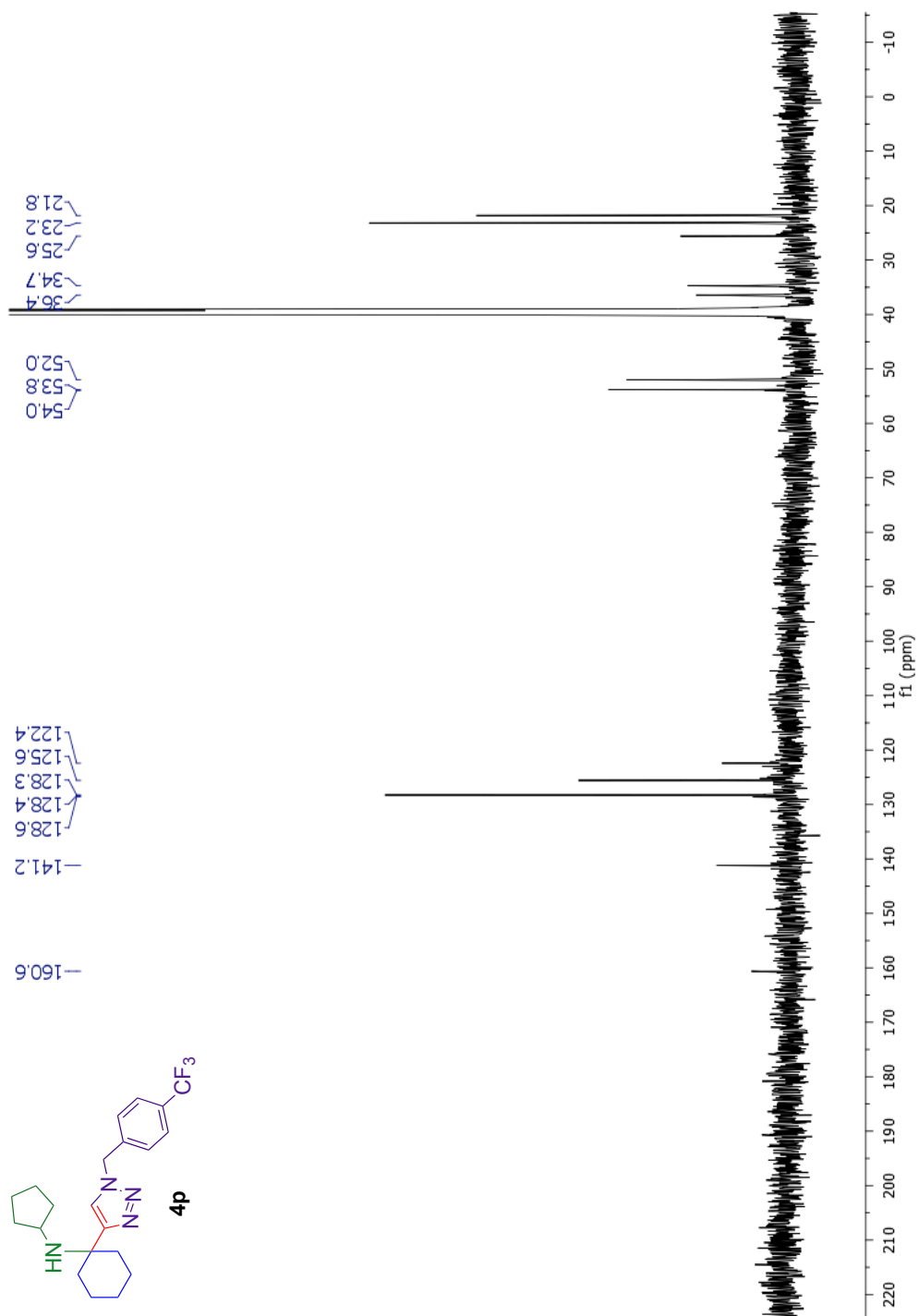


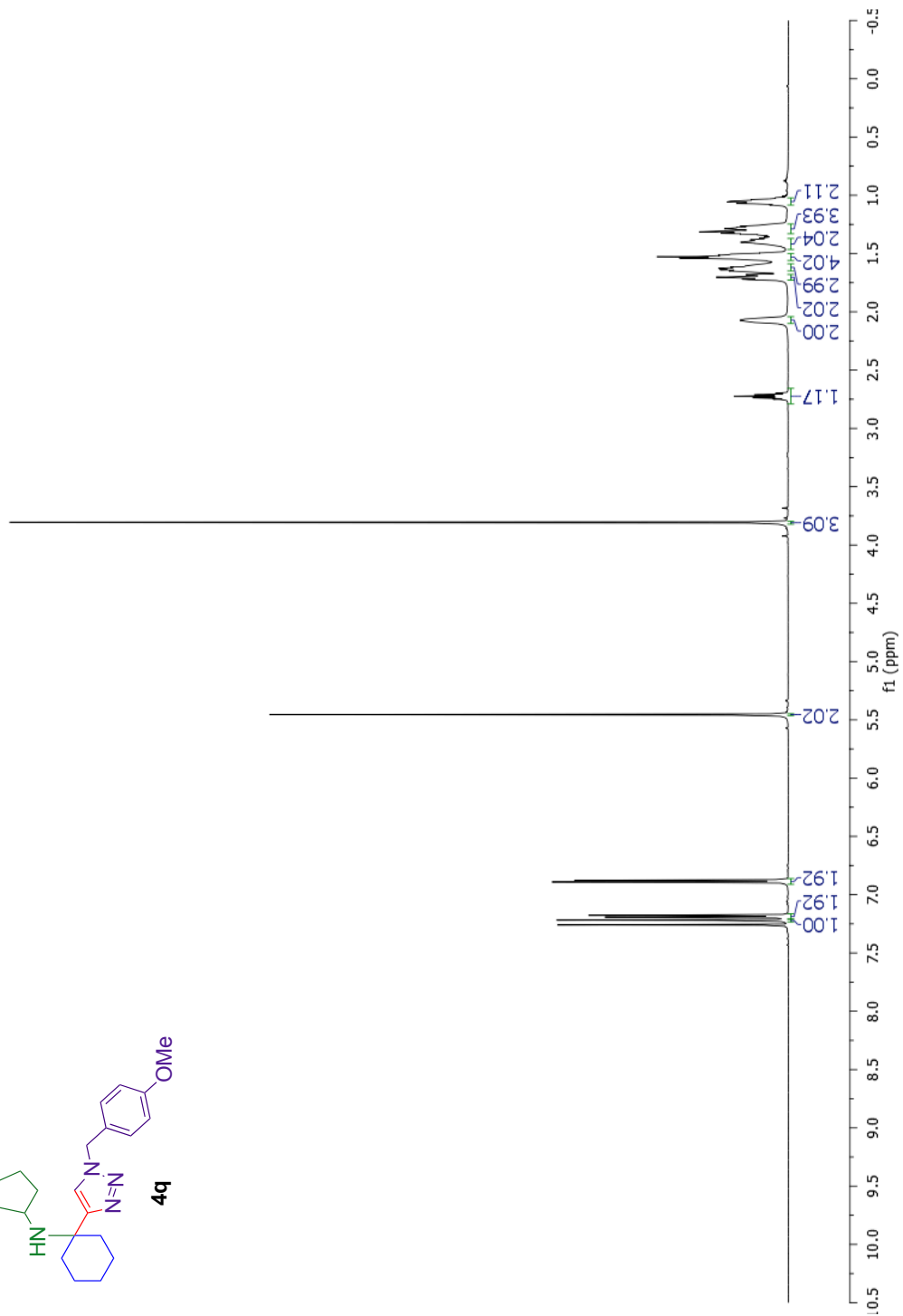
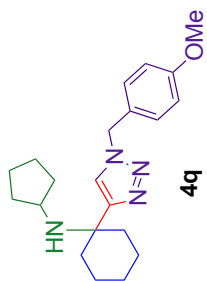


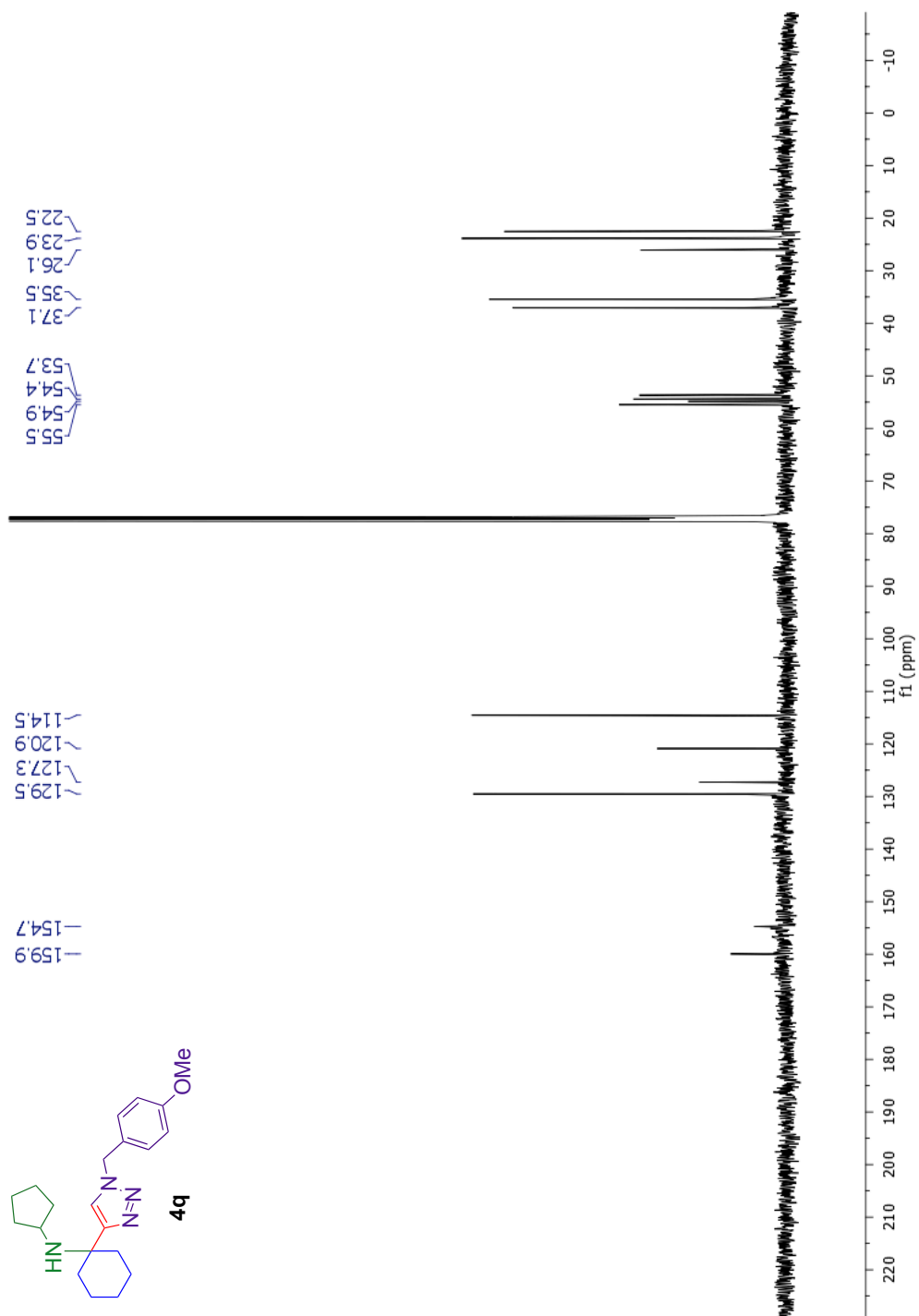


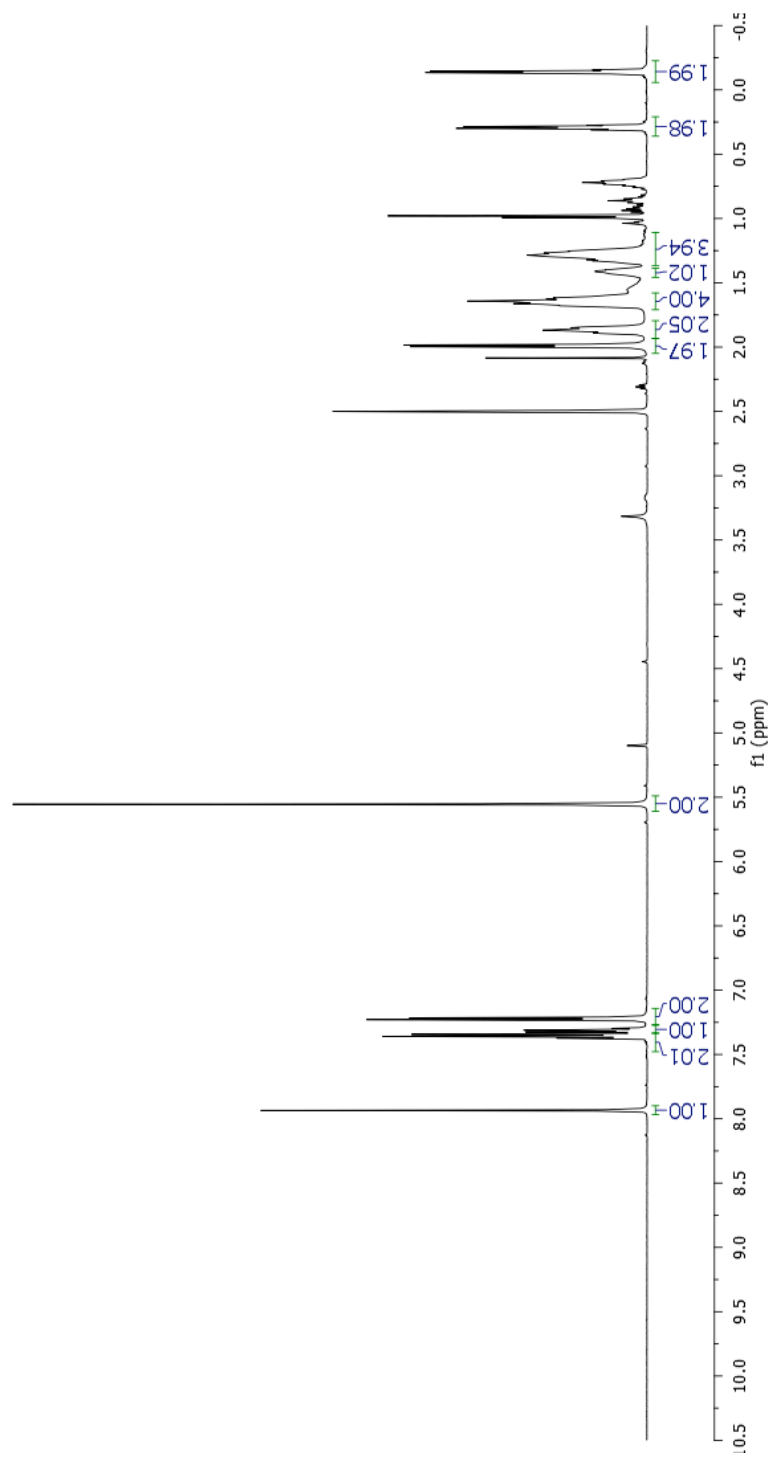
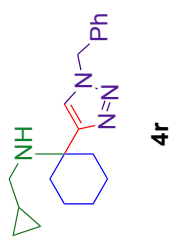


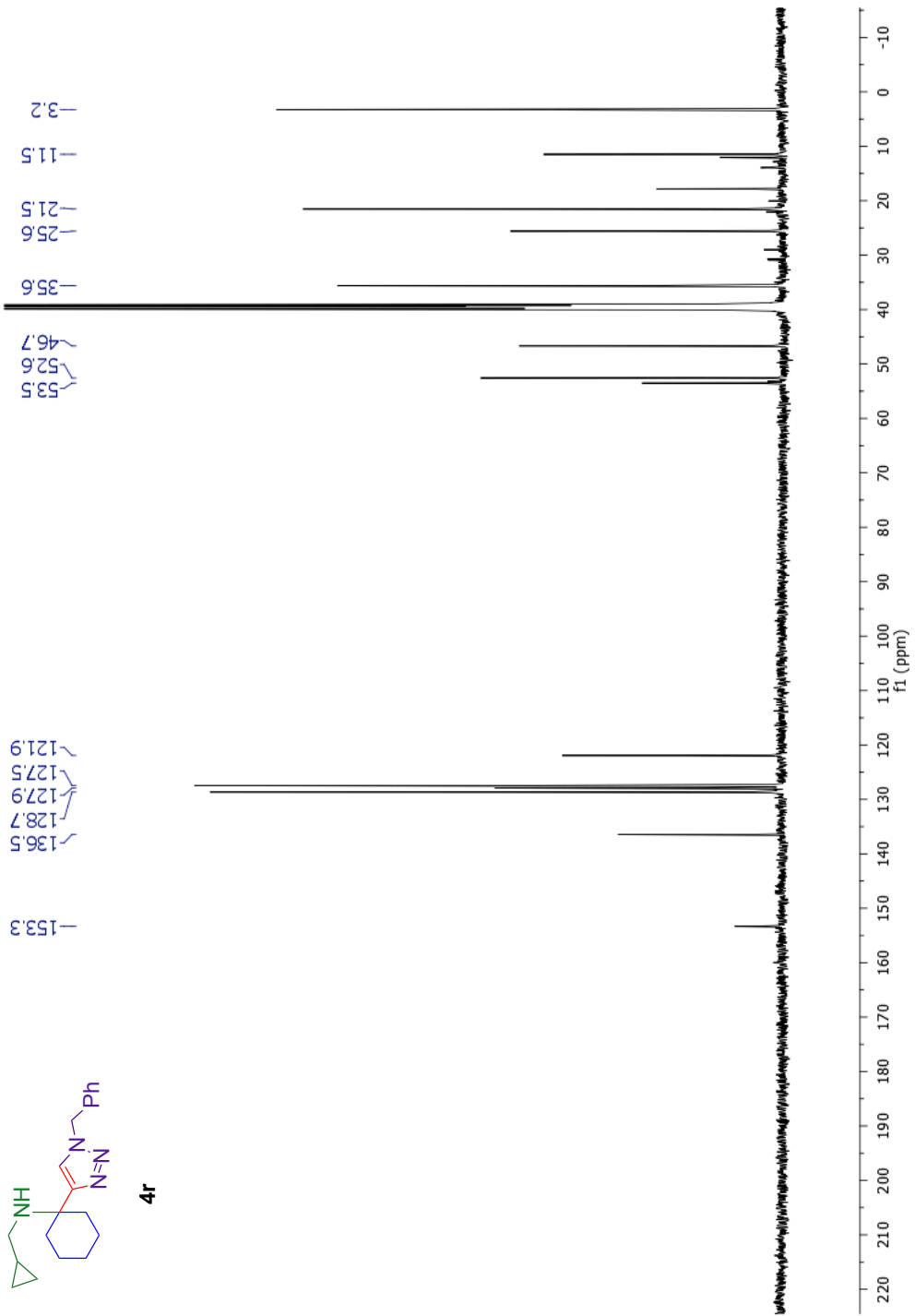
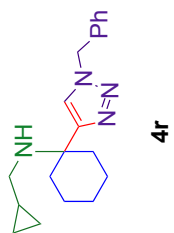


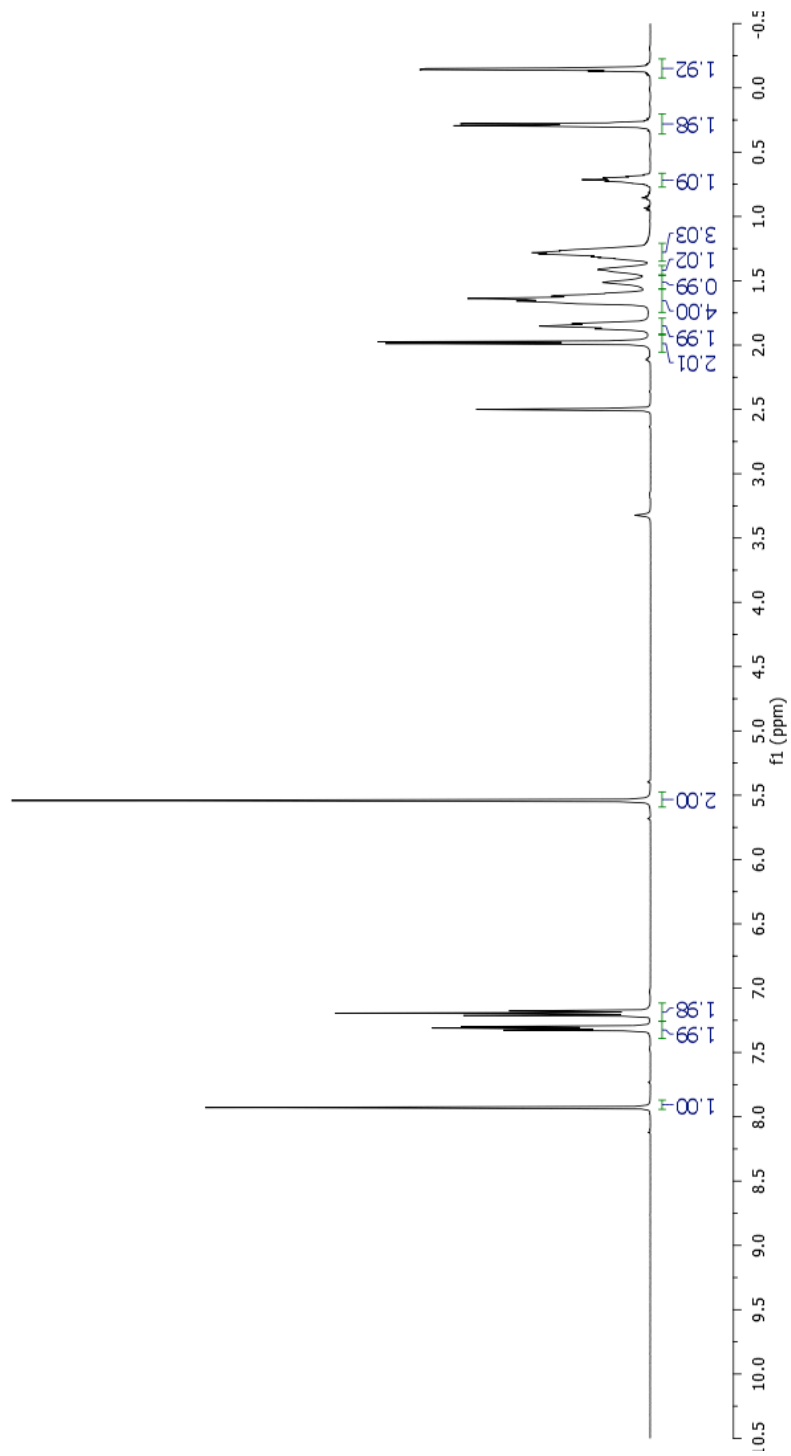
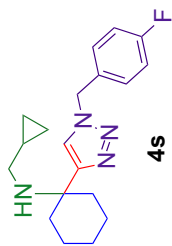


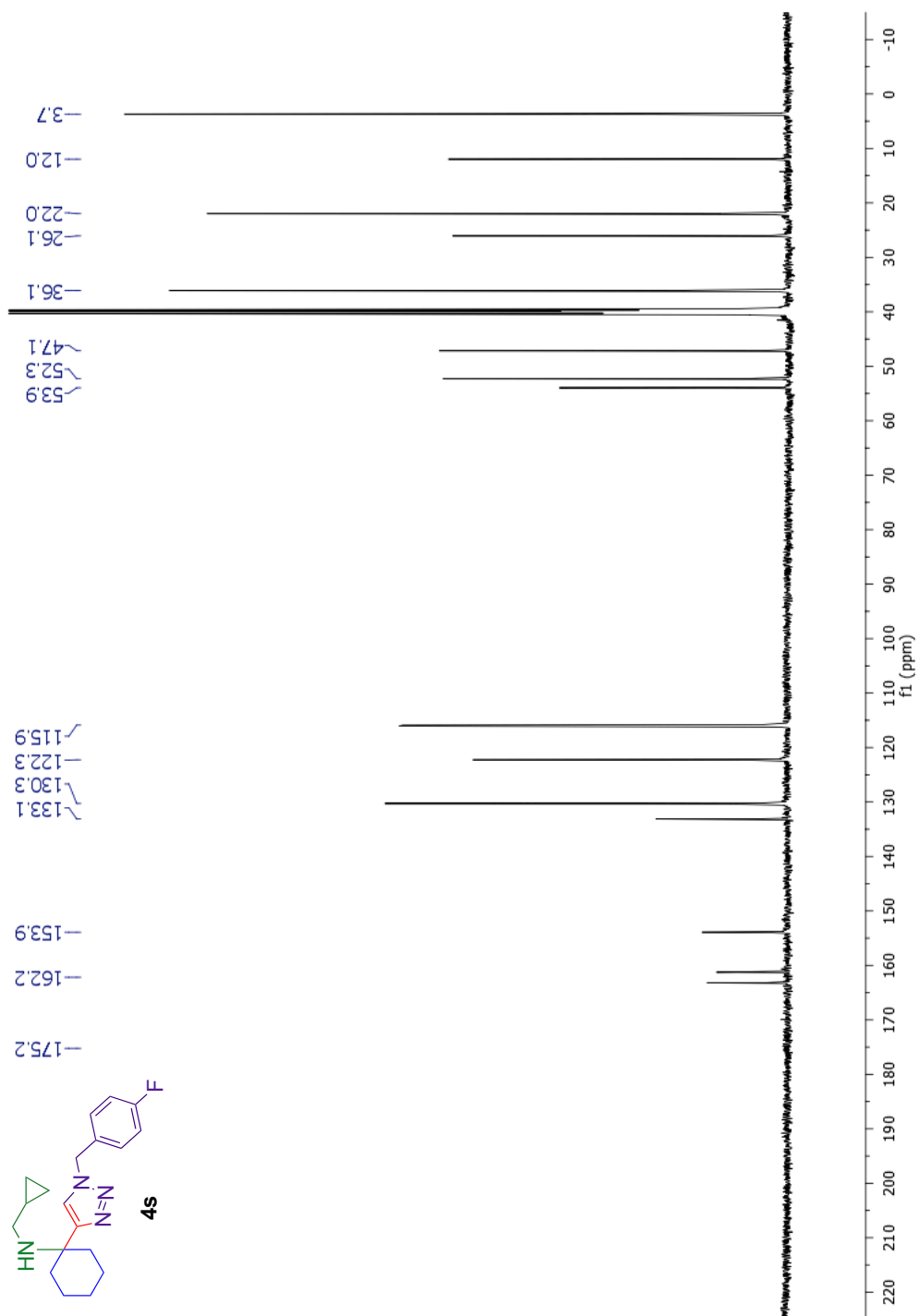


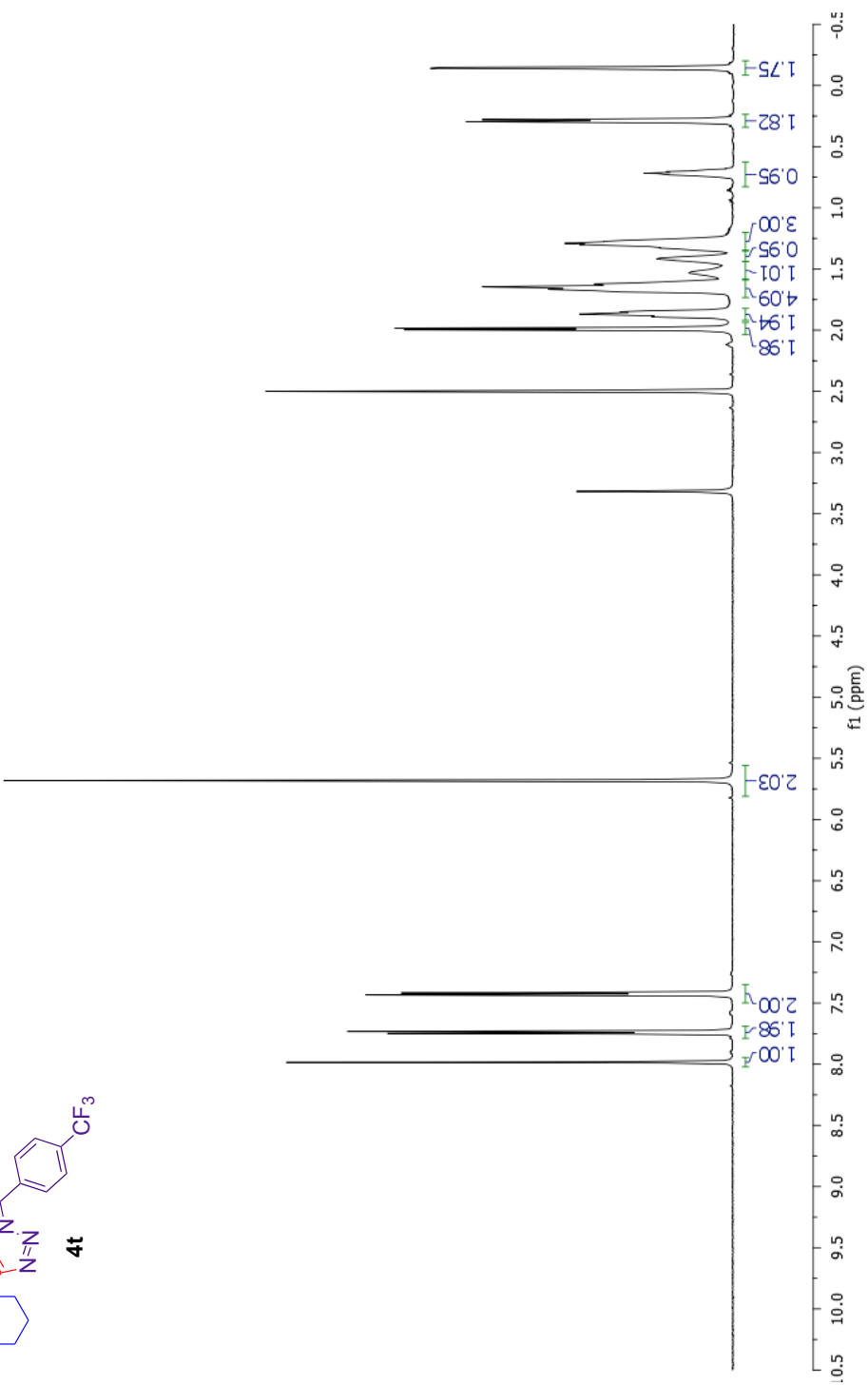
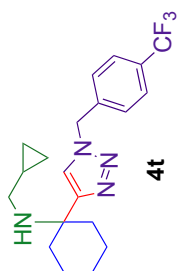


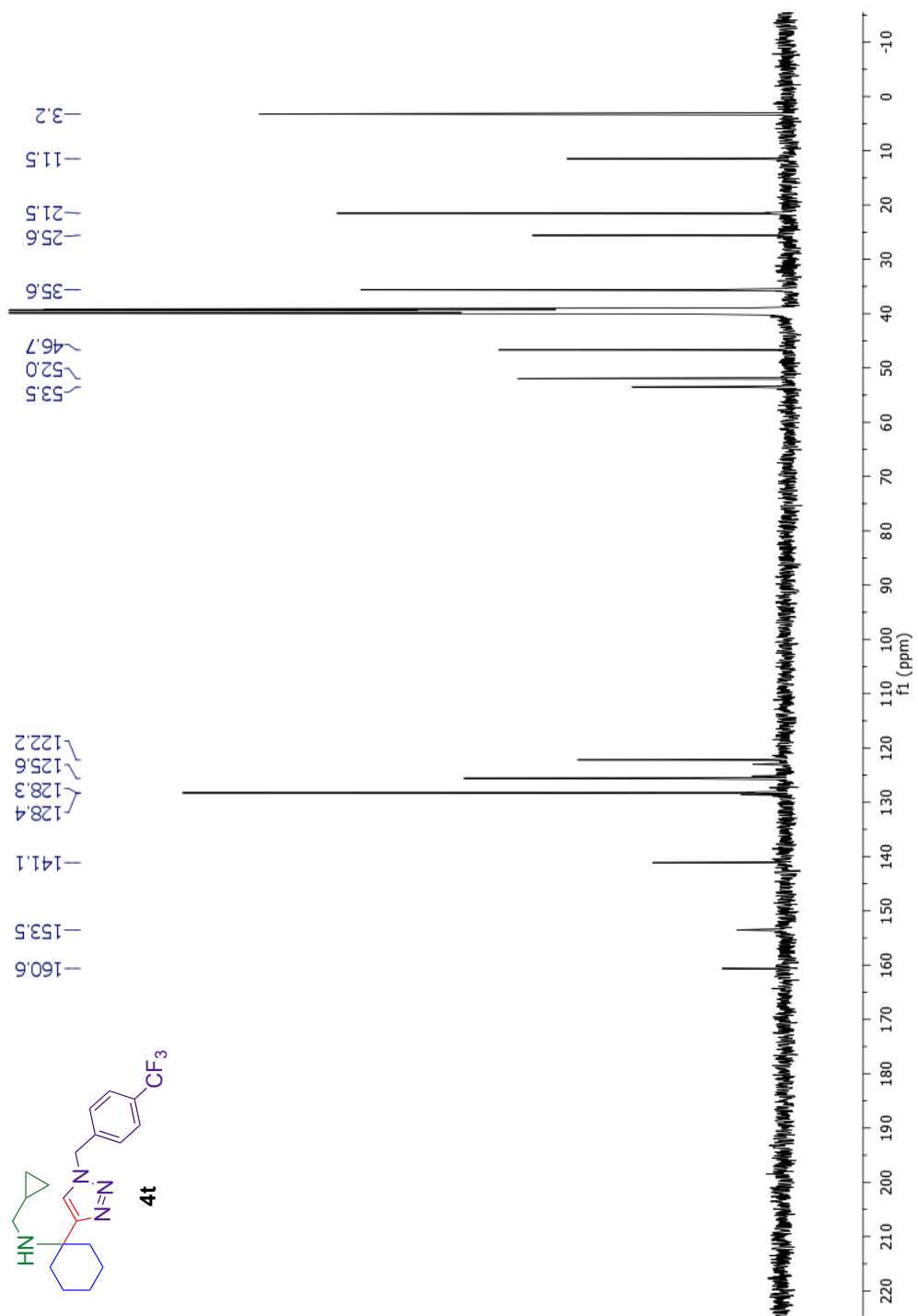
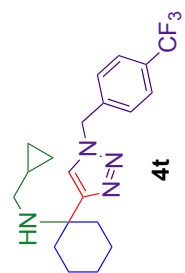


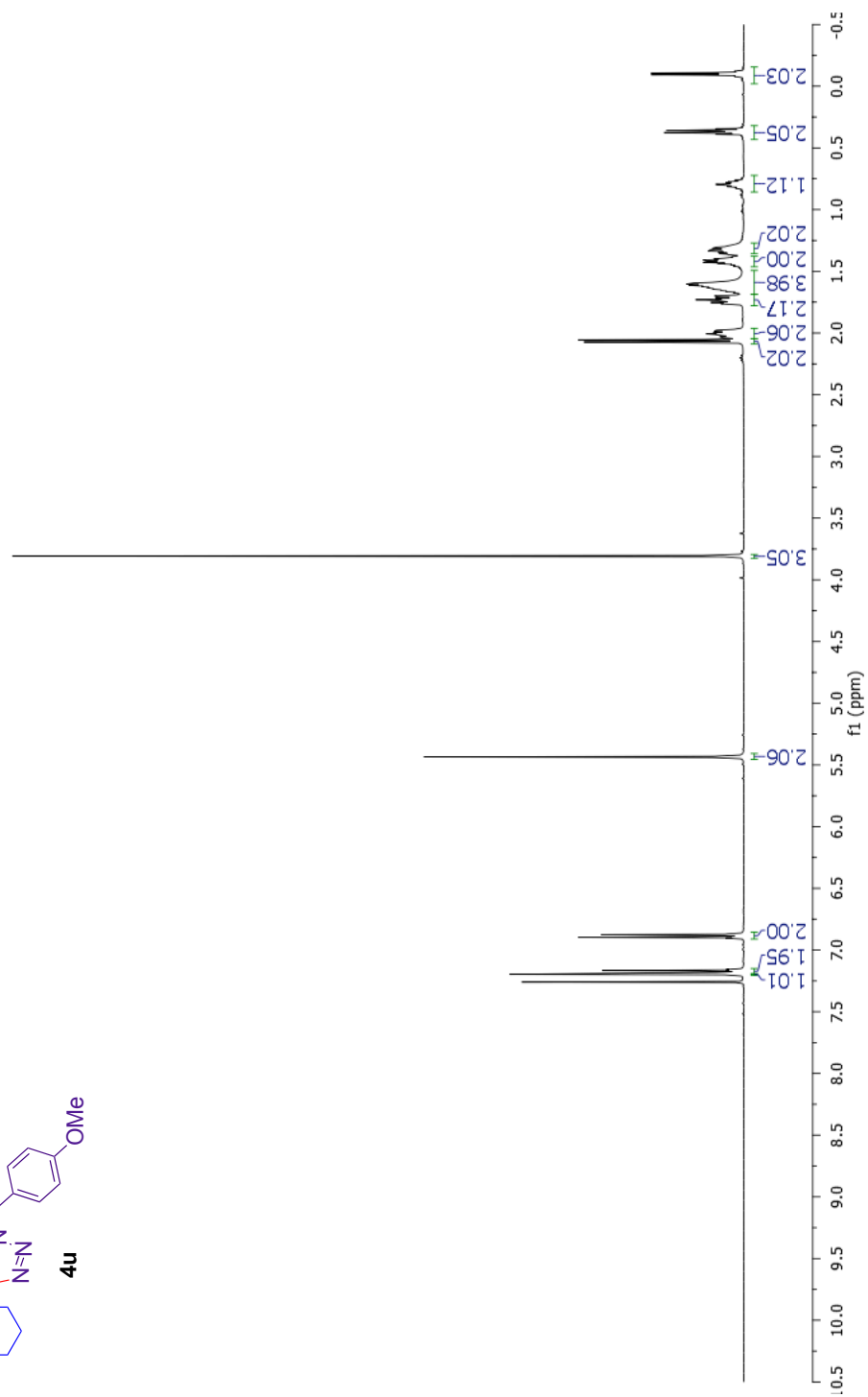
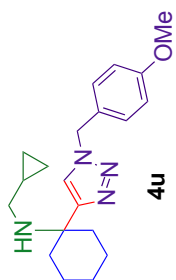


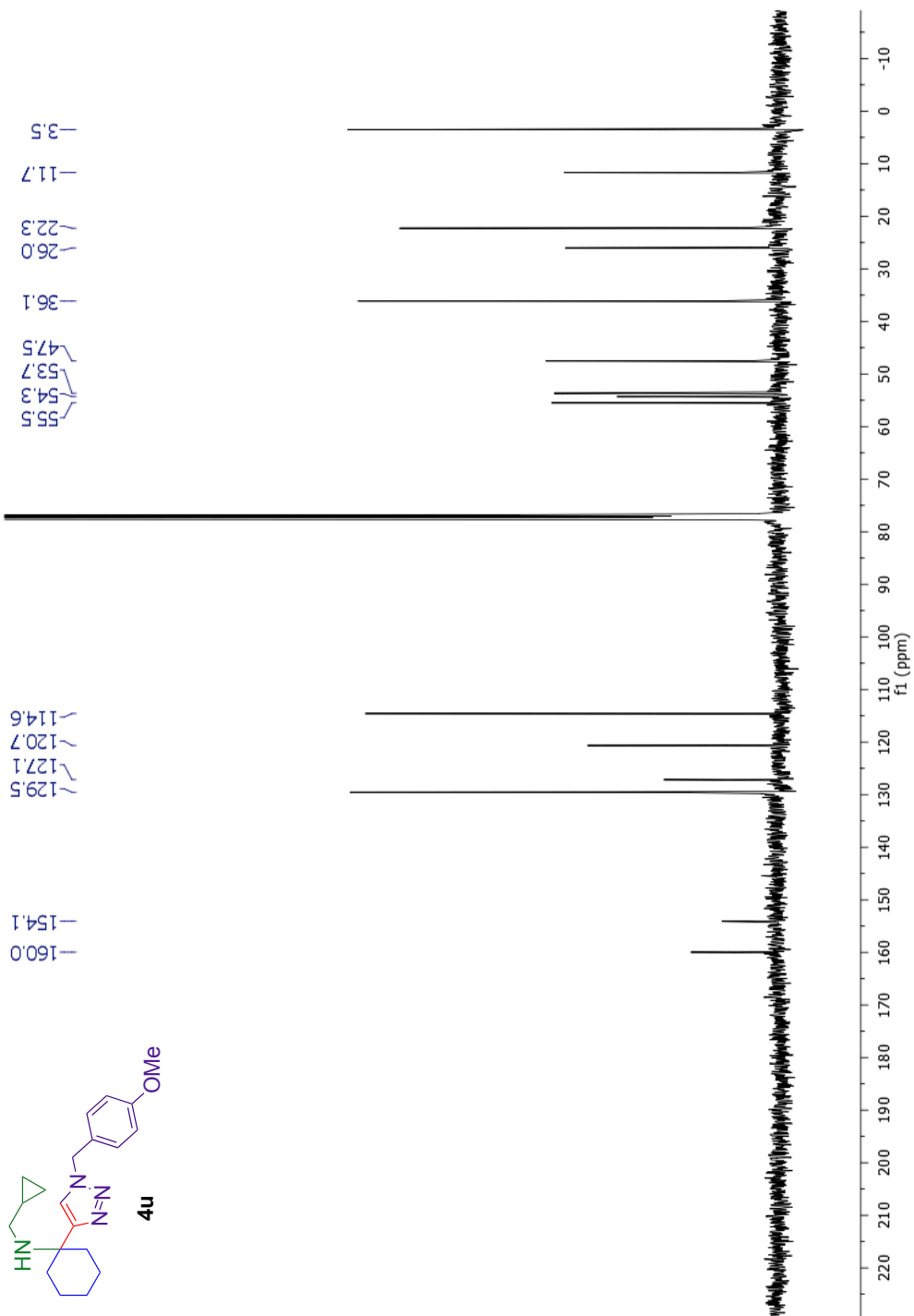
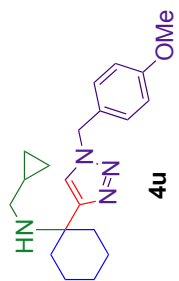


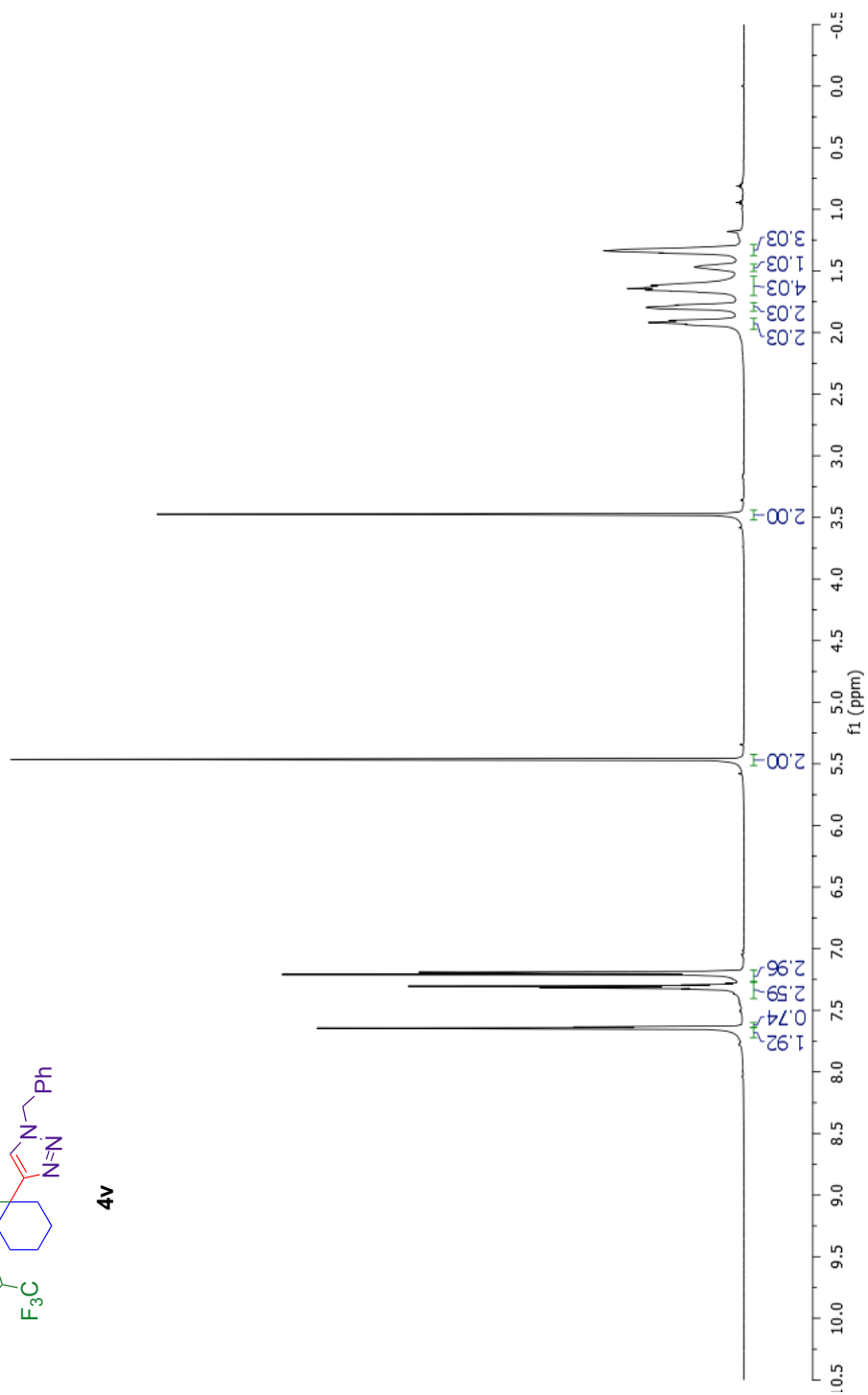
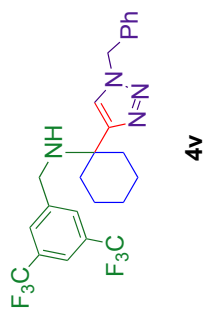


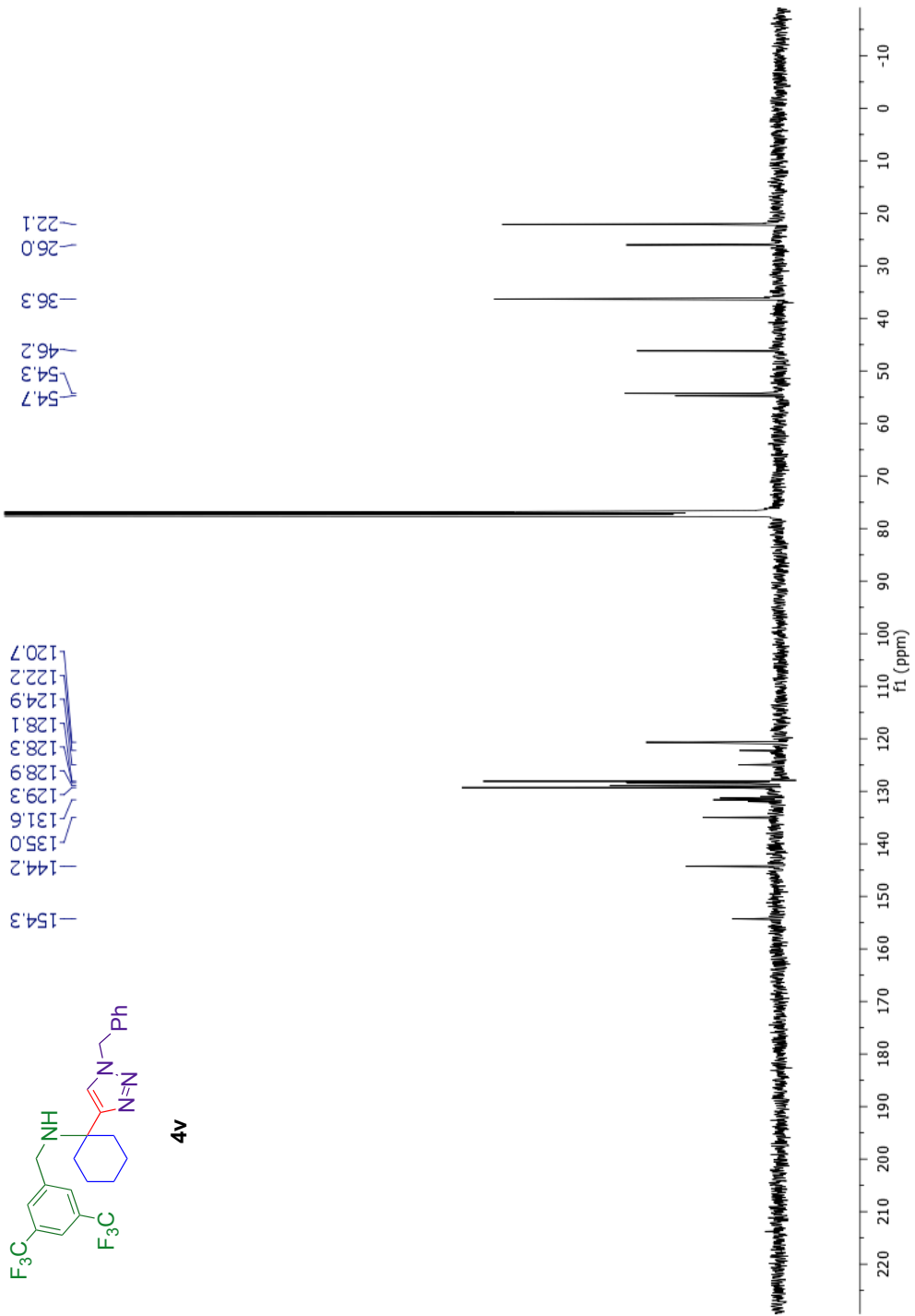


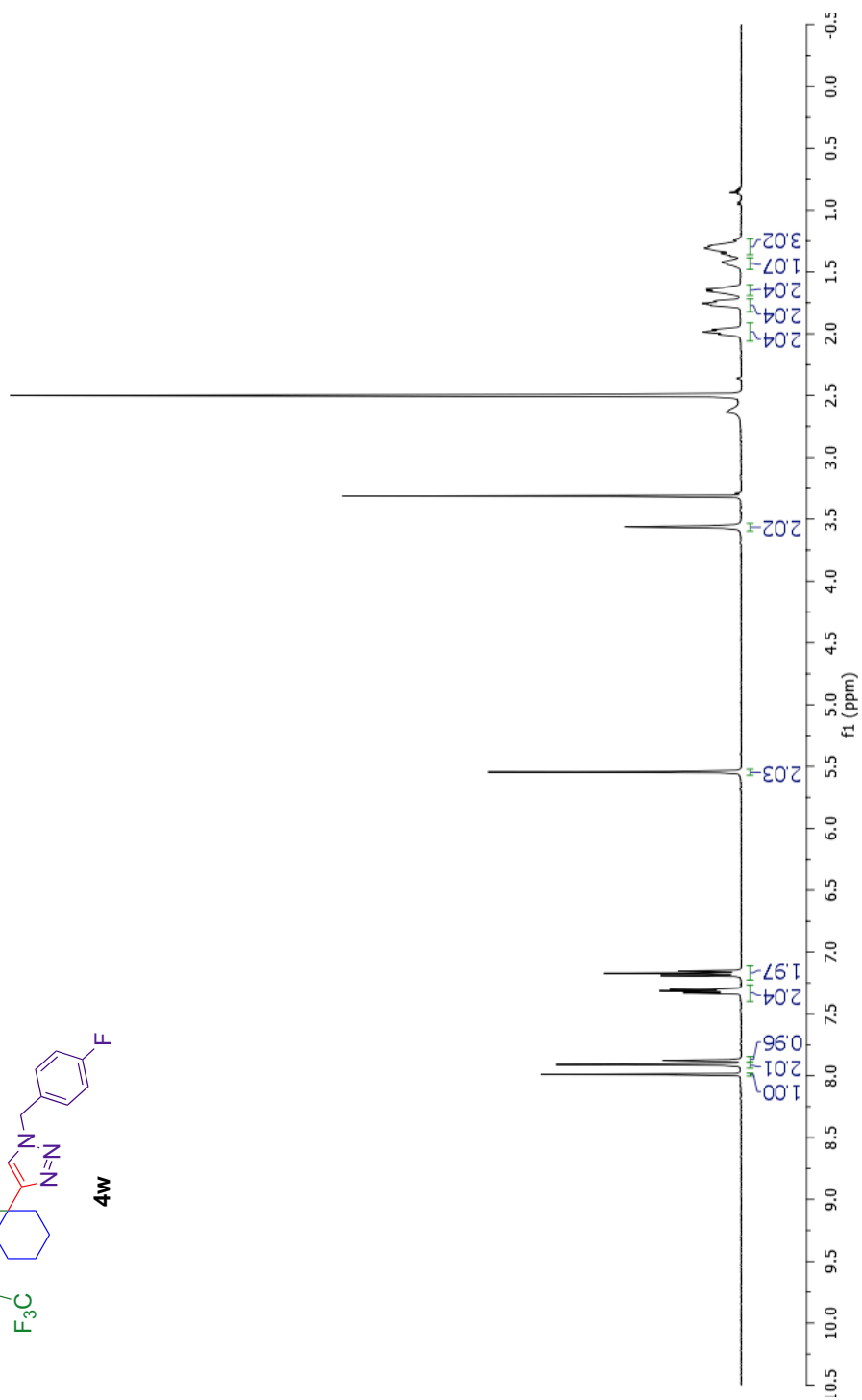
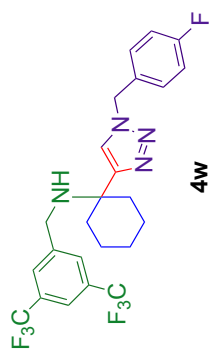


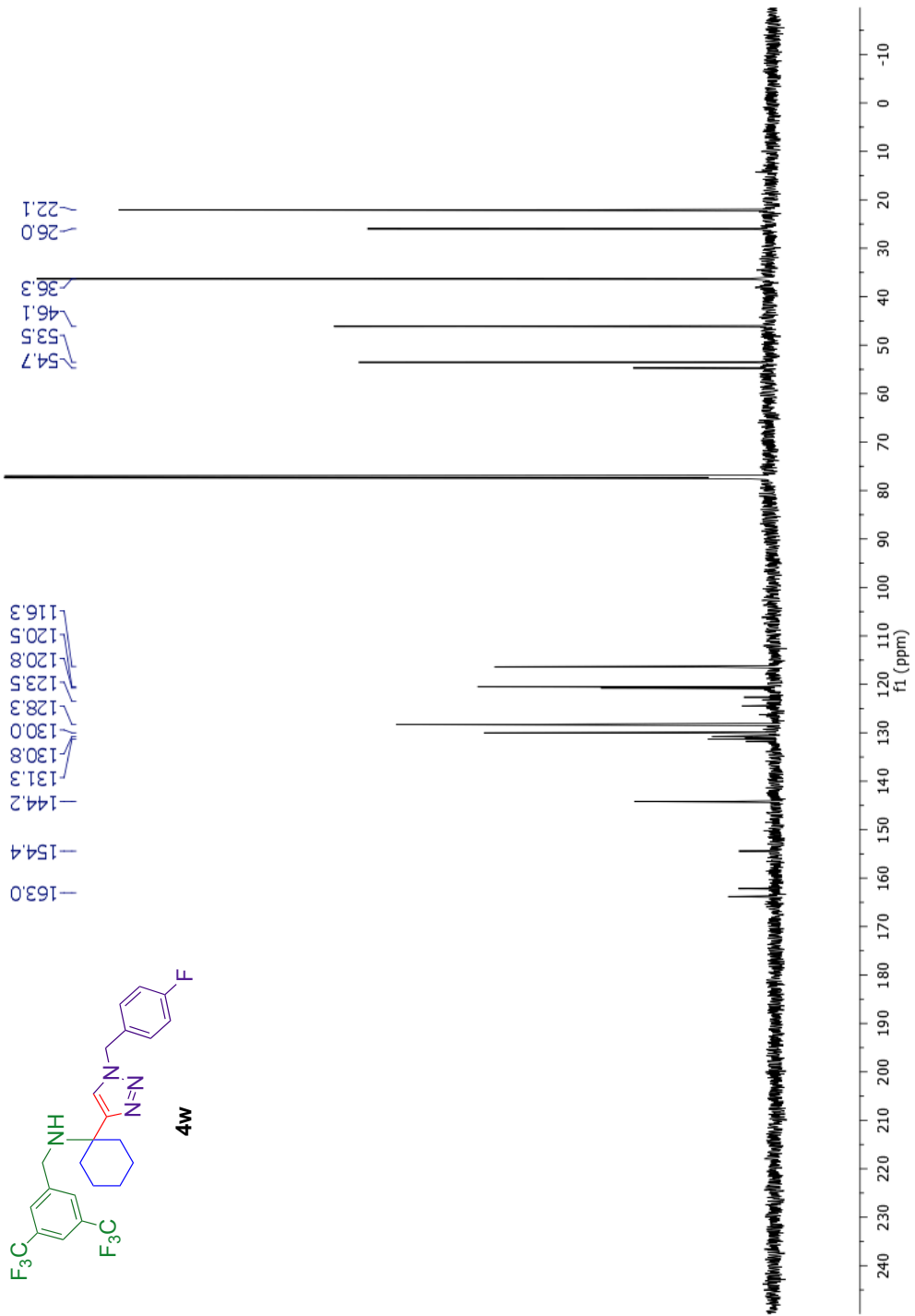
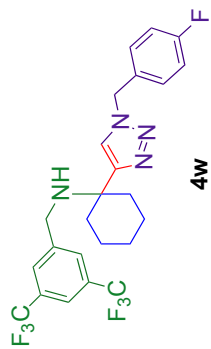


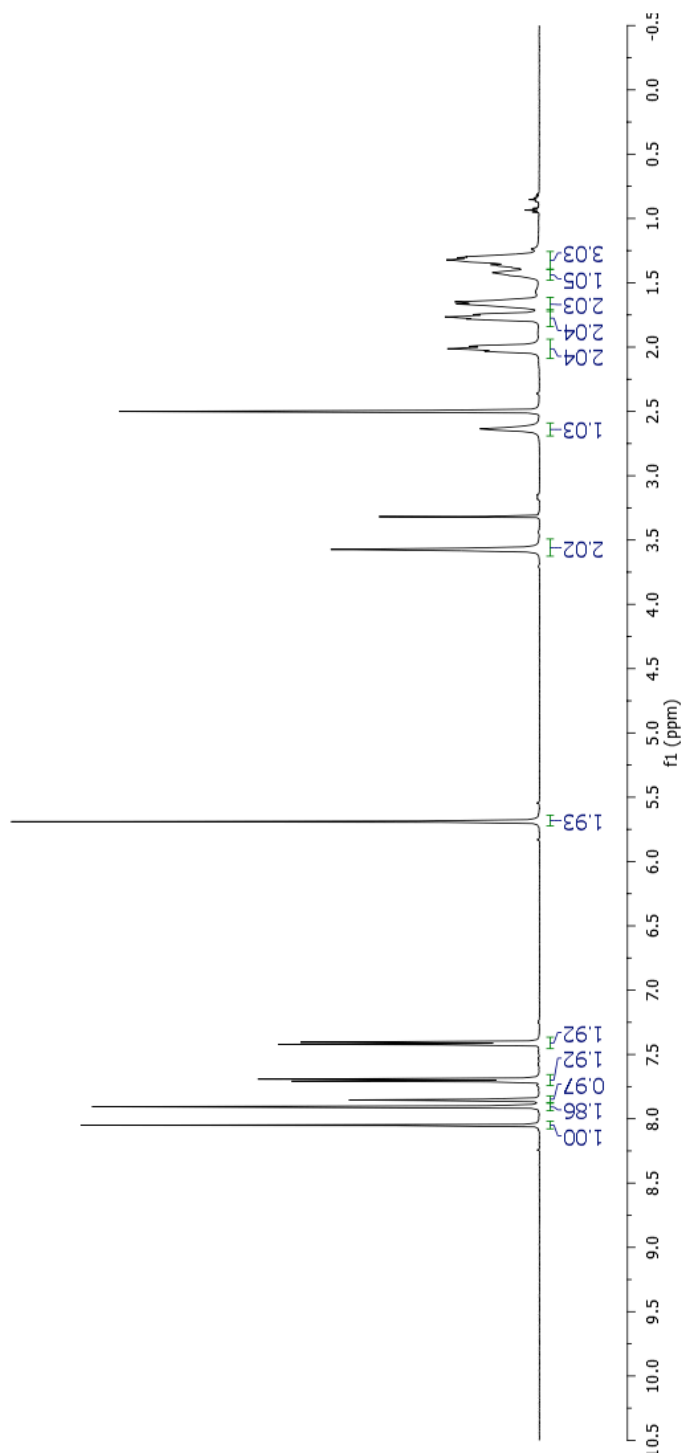
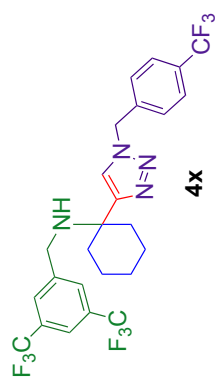


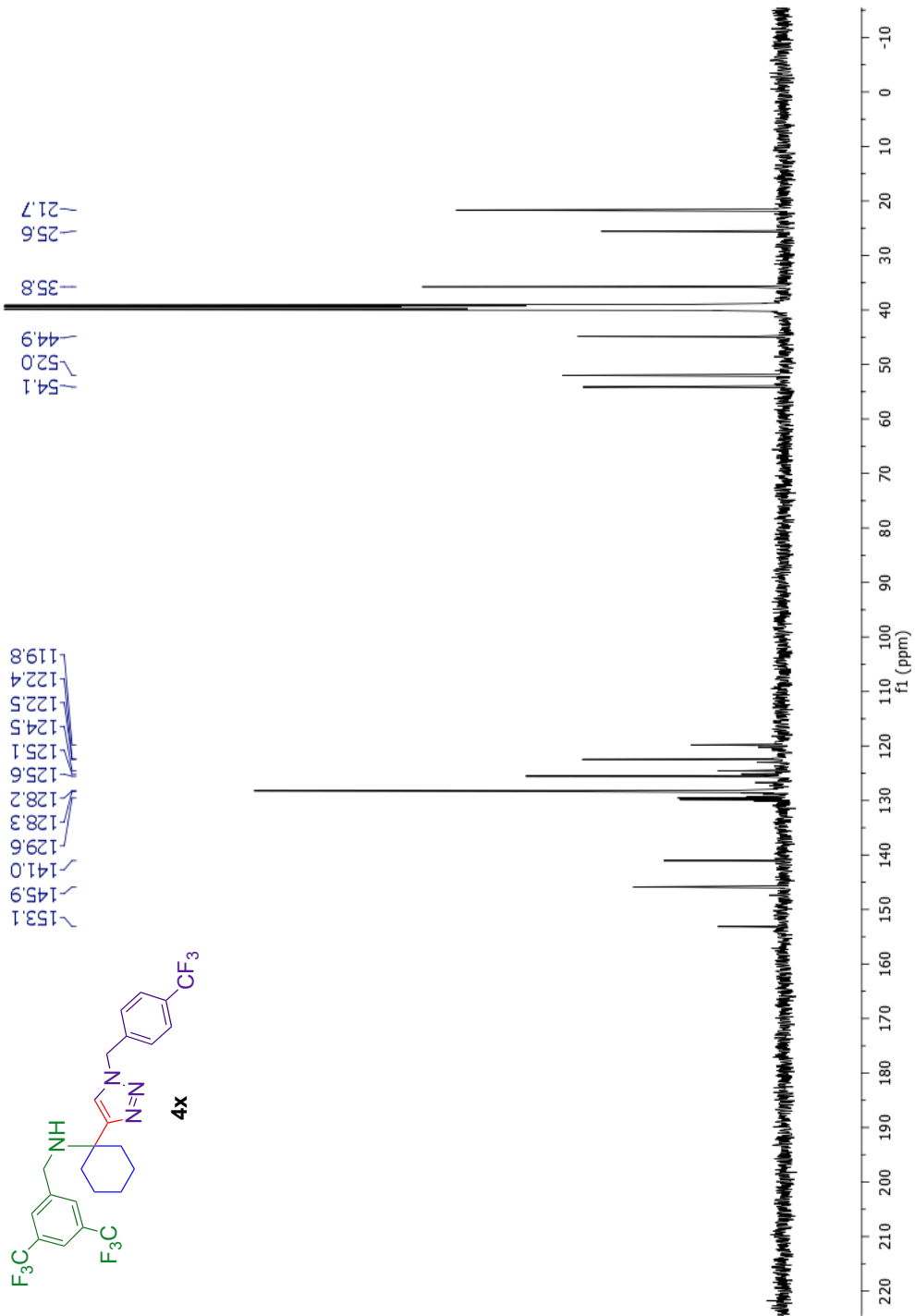
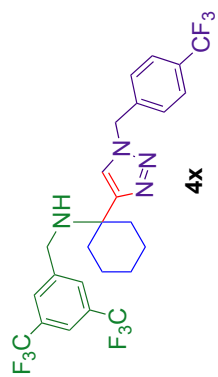


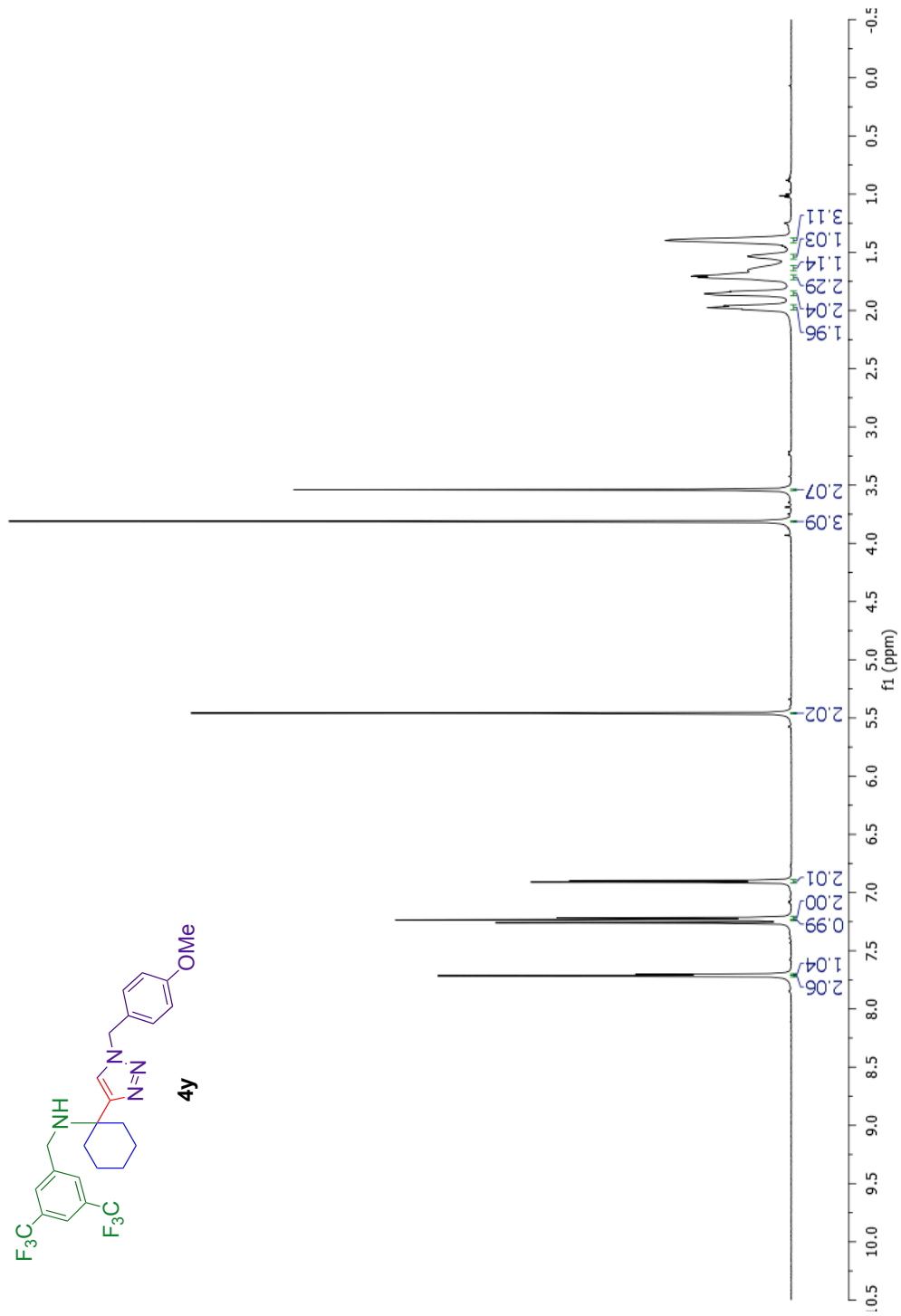
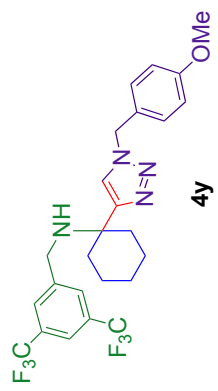


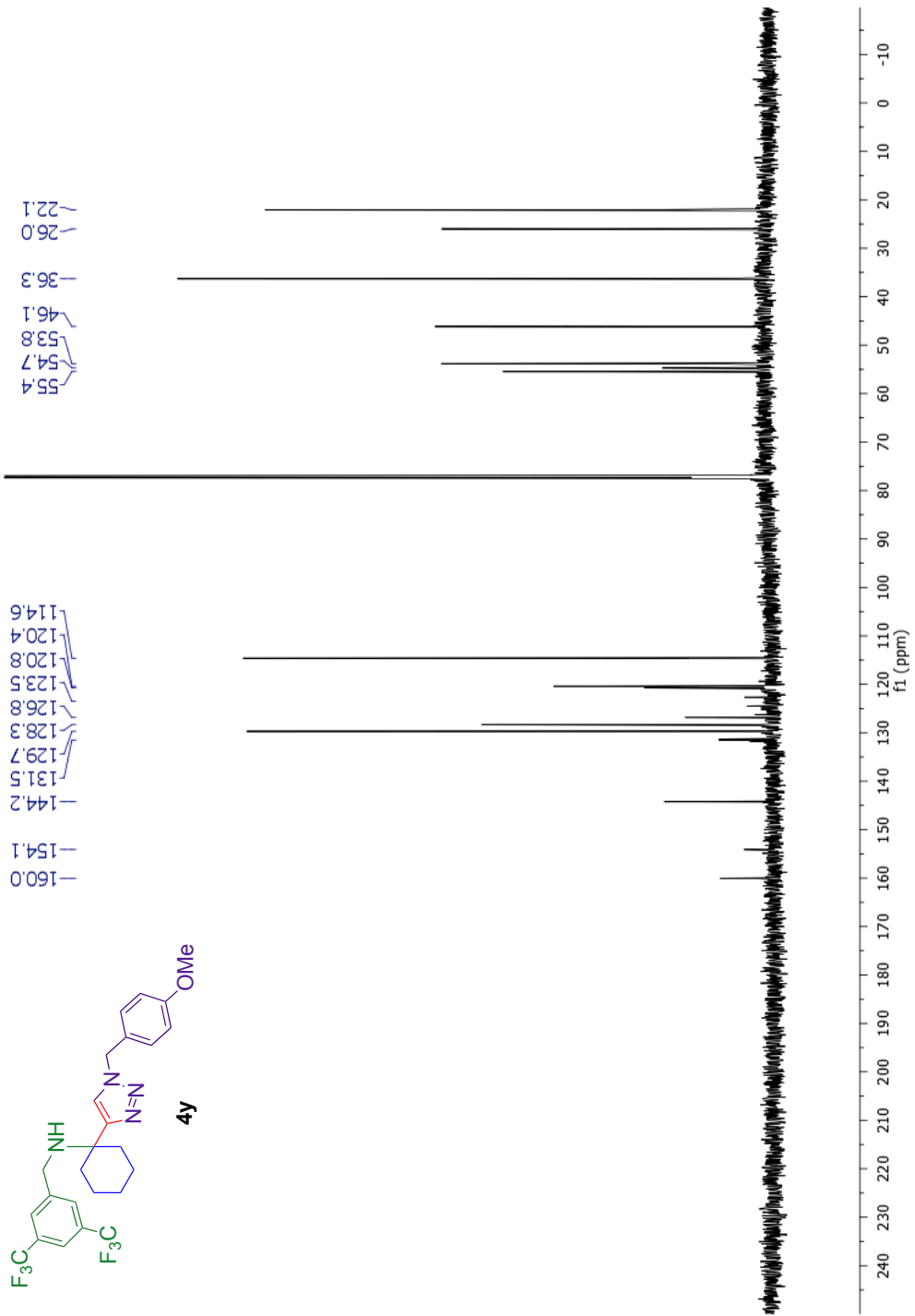












Chapter Five: Pyridine Triazoles as Biologically Active Compounds

5.1 Introduction:

The robustness of the copper-catalyzed azide-alkyne cycloaddition (CuAAC) or “click” reaction to provide 1,2,3-disubstituted triazoles makes it an excellent method for the preparation of compound libraries for biological analysis. Through simple derivatization of the azide, synthesis of triazoles with minute differences can be achieved. This, in combination with the terminal alkyne, 2-ethynyl pyridine, allows this method to afford pyridyl triazoles that can be tuned electronically and sterically to meet a particular demand.

5.2 Background on Pyridyl Triazoles as Biologically Active Compounds:

Generation of libraries of substituted pyridyl triazoles for analysis of biological activity has resulted in discoveries of activity as a potent nicotinamide phosphoribosyltransferase (NMPRTase) inhibitor,¹ and as an inhibitor of the tautomerase activity of human macrophage migration inhibitory factor (MIF).²

In the first report it was investigated whether inhibition of NAD synthesis or salvage pathways could be a viable combatant to the growth and spread of cancerous cells. It was proposed that interfering with NAD(P) levels might lead to cell death in cells that have a high usage rate of this pyridine nucleotide, mainly, tumoral cells.³ Eukaryotic cells have several mechanisms for replenishing NAD levels.⁴⁻⁵ The most dominant pathway relies on the enzyme NMPRTase, which converts nicotinamide into nicotinamide mononucleotide which is then converted to NAD.¹ This has prompted investigation in NMPRTase as a target for potential

antitumor drugs. Based on initial results,⁶ 185 pyridyl triazole derivatives were prepared and tested as NMPRTase inhibitors. Of those tested, five compounds demonstrated an IC_{50} at nanomolar concentrations (Figure 5.1). The most active compound, a 3-pyridyl triazole bearing a 2-aminobiphenyl aromatic group was found to be an excellent inhibitor of NMPRTase with an IC_{50} of 3.0 nM. While this did not out compete the parent compound that prompted the study with regards to the IC_{50} , the pyridyl-triazole did demonstrate increased metabolic stability which is believed to be one of the main problems with the inhibitors of NMPRTase that are currently in clinical trials.⁷

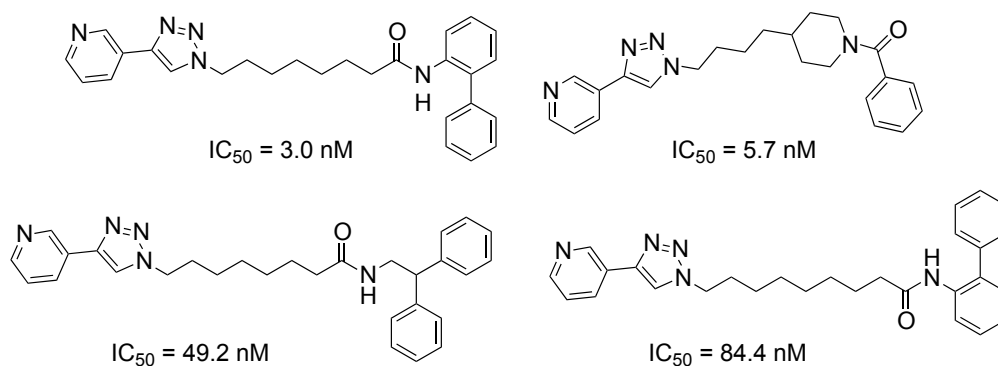


Figure 5.1: Pyridyl triazoles as inhibitors of nicotinamide phosphoribosyltransferase (NMPRTase).

The second example of the utility of the CuAAC reaction for analysis of pyridyl triazoles for biological activity comes from a report on the inhibition of tautomerase activity of human macrophage migration inhibitory factor (MIF).² This proinflammatory cytokine associated with numerous inflammatory diseases as well as cancer and is an obvious target for inhibition studies. MIF is widely expressed in many types of cells including macrophages, endothelial cells, and

T-cells.⁸⁻¹⁰ When activated, the cells release MIF, which promotes the release of other inflammatory cytokines. Excessive inflammatory response has been associated with tissue damage and autoimmune diseases such as rheumatoid arthritis, lupus erythematosus, and Crohn's disease. The connection between inflammatory disease and cancer is also well established,¹¹ and MIF has been shown to enhance cell growth by inhibiting the tumor suppressor gene p53. MIF is overexpressed in many cancer cells and can serve as a marker for disease progression.

A combined approach of synthesis and molecular modeling was employed to develop compounds with inhibitory activity towards MIF. Of the 34 compounds that were prepared in the report those bearing the 2-pyridyl or 2-quinolinyly moiety were found to demonstrate the highest levels of activity towards inhibition of MIF (Figure 5.2). The IC₅₀ of the 2-pyridyl triazole is reported at 8.8 micromolar and 2-quinolinyly at 0.6 micromolar. Additional substitution on the pyridyl/quinolinyly ring as well as the pendant phenyl ring on the triazole was investigated. However, a systematic approach to this substitution by varying only the electronic density on the corresponding ring system though subtle changes in substitution was not performed. This vacancy in the understanding of these compounds warrants further inquiry and a systematic approach to substitution should be adopted.

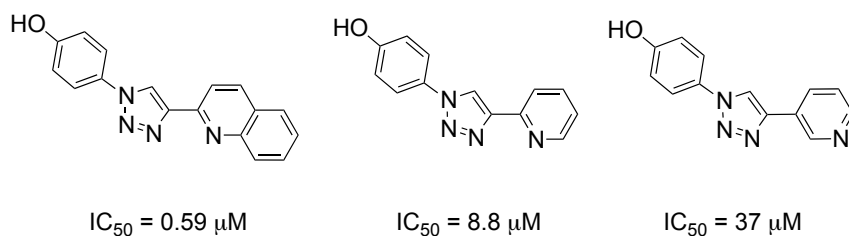


Figure 5.2: Pyridyl triazoles as inhibitors of human macrophage migration inhibitory factor (MIF).

5.3 Formation of Structurally Diverse Aryl Substituted Pyridyl Triazoles:

The facile synthesis of 1,4-triazoles through utilization of the CuAAC reaction allows for systematic substitution of a desired system through derivatization of the azide or alkyne components. For the study of 2-pyridyl triazoles (PyTri), substitution of the utilized azide allows for preparation of compounds with differences in the electronic nature of the aromatic system. The systematic design of these compounds with specific structural and physical properties is crucial for the development and analysis of new functional materials such as pharmaceuticals, and catalysts.¹² Utilization of aryl substituted azides in combination with aryl alkyne results in a system that is fully conjugated. This is highly desirable as the electronic nature of the compounds can be tuned via substitution on the azide or alkyne and this modification will be felt by the entire conjugated system. As such, it was important to prepare a series of aryl azides that ranged in substitution from electron rich compounds bearing electron donating groups such as methoxy and methyl, to those with electron poor character, incorporating electron withdrawing substituents such as halogens and trifluoromethyl groups.

Synthesis of the desired azides was relatively straight forward starting from anilines with the desired substitution.^{13,14} In order to convert the aniline moiety to the necessary azide the original amine must be first converted to a diazonium intermediate. This can be done by first preparing a cold acidic aqueous solution of 6 molar hydrochloric acid and sodium nitrite in an ice/brine bath. It is important to note that significantly higher conversion to the diazonium intermediate was obtained when the nitrite salt was added dropwise in an aqueous medium rather than neat addition of the solid. If done correctly the acidic solution should take on a dark blue/green color and minimal production of gaseous nitric acid as an orange gas is observed. After the aqueous acidic solution is prepared, the aniline, bearing the desired substitution, is added dropwise with vigorous stirring. Upon addition of the aniline, the reaction solution will turn orange to dark red depending on the substitution with the electron rich compounds being darker in color. Post addition of aniline, the reaction is allowed to proceed for a period of 30 min for the formation of the diazonium to take place.

In order to obtain azide clean of other impurities, it is important to isolate the diazonium away from unreacted aniline. This can be achieved through formation of a diazonium salt that is largely insoluble in acidic aqueous media. The addition of sodium tetrafluoroborate to the reaction mixture cleanly forms the tetrafluoroborate diazonium salt in 30 min with vigorous stirring. This salt precipitates from the acidic solution and can be isolated via filtration as a cream colored solid. It should be noted that diazonium salts, when dried, can become

dangerously unstable through spontaneous fissure of the carbon-N₂ bond. With this in mind, the filtration of the diazonium salt should be done with care and the solid should not be taken to complete dryness and should be immediately used to generate the desired azide. This can be accomplished by preparing an aqueous solution of sodium azide and cooling this solution down to near 0 °C via an ice/brine bath. Once this cold azide solution is prepared, slow addition of the diazonium salt can take place by adding the solid directly using a plastic spatula. Preparation of the azide solution and addition of the diazonium salt should be done using non-metal utensils, as formation of only small amounts of metal azides and diazoniums can be dangerous and potentially explosive. After addition of the diazonium salt to the azide solution the reaction is allowed to warm to ambient temperature over the course of 18 h. After which the desired azide may be isolated via extraction with diethyl ether and slow concentration in an ambient water bath without further purification. As organic azides are known to be unstable when concentrated, the isolated compounds should be used quickly, or, if long-term storage is desired, the azides should be diluted in an organic solvent that is compatible with triazole formation such as tetrahydrofuran or alcoholic solvents such as ethanol or isopropanol.

Preparation of a wide range of aryl azides (**5a-5e**) bearing electronically diverse substitution was achieved using the method described above (Table 5.1). These compounds were obtained in relatively high yield with a high degree of purity as evident by thin layer chromatography. Further characterization of these

organic azides was not performed as they were immediately used for triazole formation.

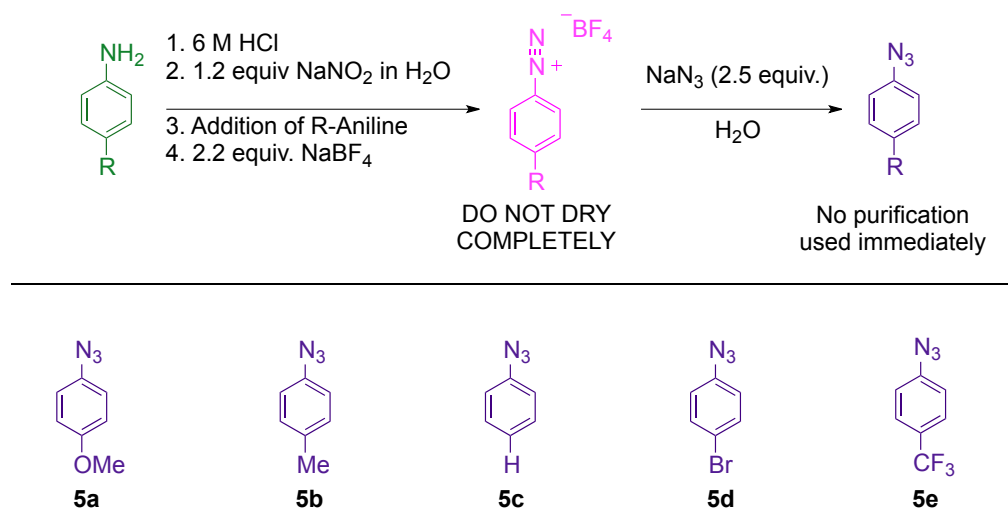
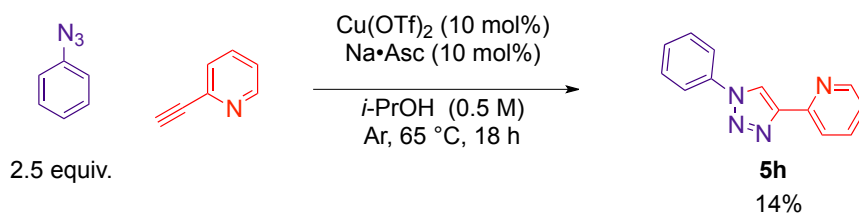


Table 5.1: Synthesis of electronically diverse aryl azides as precursors to pyridyl triazoles.

Synthesis of the electronically diverse 2-pyridyl triazoles was initially attempted under conditions that were optimized for triazole formation from silyl-protected propargylamines.¹⁵ Utilization of catalytic copper(II) triflate (Cu(OTf)₂) in the presence of sodium ascorbate in dry isopropanol proved to be an inadequate system for preparation of phenyl pyridyl triazole (**5h**) as low yields were observed (Scheme 5.1).



Scheme 5.1: Initial conditions for the synthesis of pyridyl triazoles are successful but low yielding.

When a more traditional system was used, consisting of copper(II) sulfate pentahydrate with sodium ascorbate in aqueous ethanol, conversion to the desired compounds greatly improved. Thus preparation of 2-pyridyl triazoles (**5f-5j**) bearing electronically diverse phenyl substitution was achieved (Table 5.2).

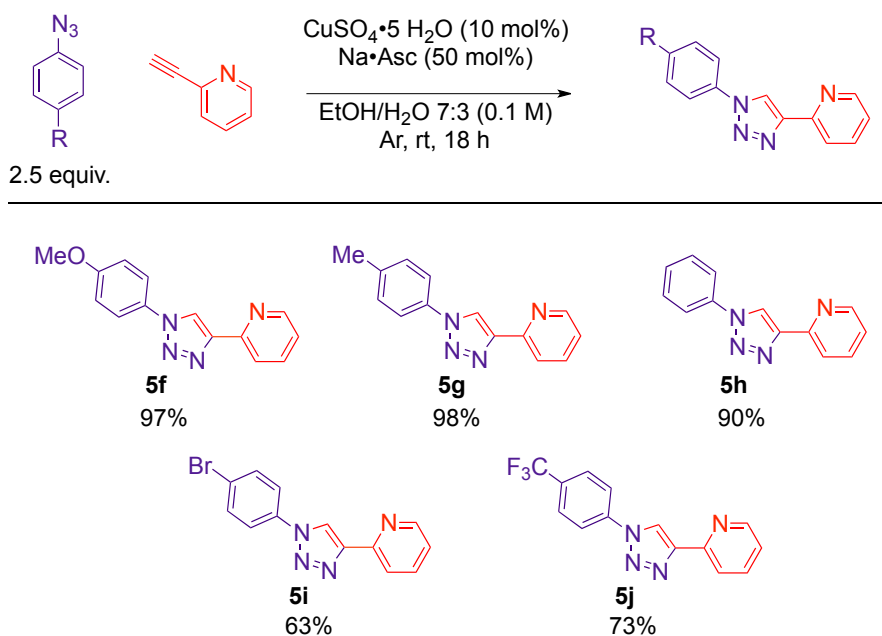


Table 5.2: Synthesis of electronically diverse pyridyl triazoles.

These compounds could be isolated in good to high yields via the CuAAC reaction of substituted phenyl azides and 2-ethynyl pyridine. The compounds were obtained with a high degree of purity, which allowed for facile characterization. Additionally this system was scalable, and gram quantities could be prepared in a single run.

With the objective of preparing 2-pyridyl triazoles with systematic electronically diverse substitution accomplished, analysis of this class of compounds was undertaken through comparison of the corresponding ^1H NMR

spectra. Satisfyingly, the diagnostic proton on the triazole ring could be tracked as the electronic character of the system changed. As the substitution on the phenyl ring varied from electron donating (**5f**) to the electron withdrawn (**5j**) the diagnostic singlet, representative of the electronic nature of the system, was observed to move stepwise downfield (Figure 5.3).

One characteristic that was notable was the relative solubility of the compounds in organic solvents. As the substitution on the phenyl ring became more electron withdrawn, the relative solubility of the compounds decreased. To further investigate whether this trend could be countered, further functionalization of these pyridyl triazoles was necessary.

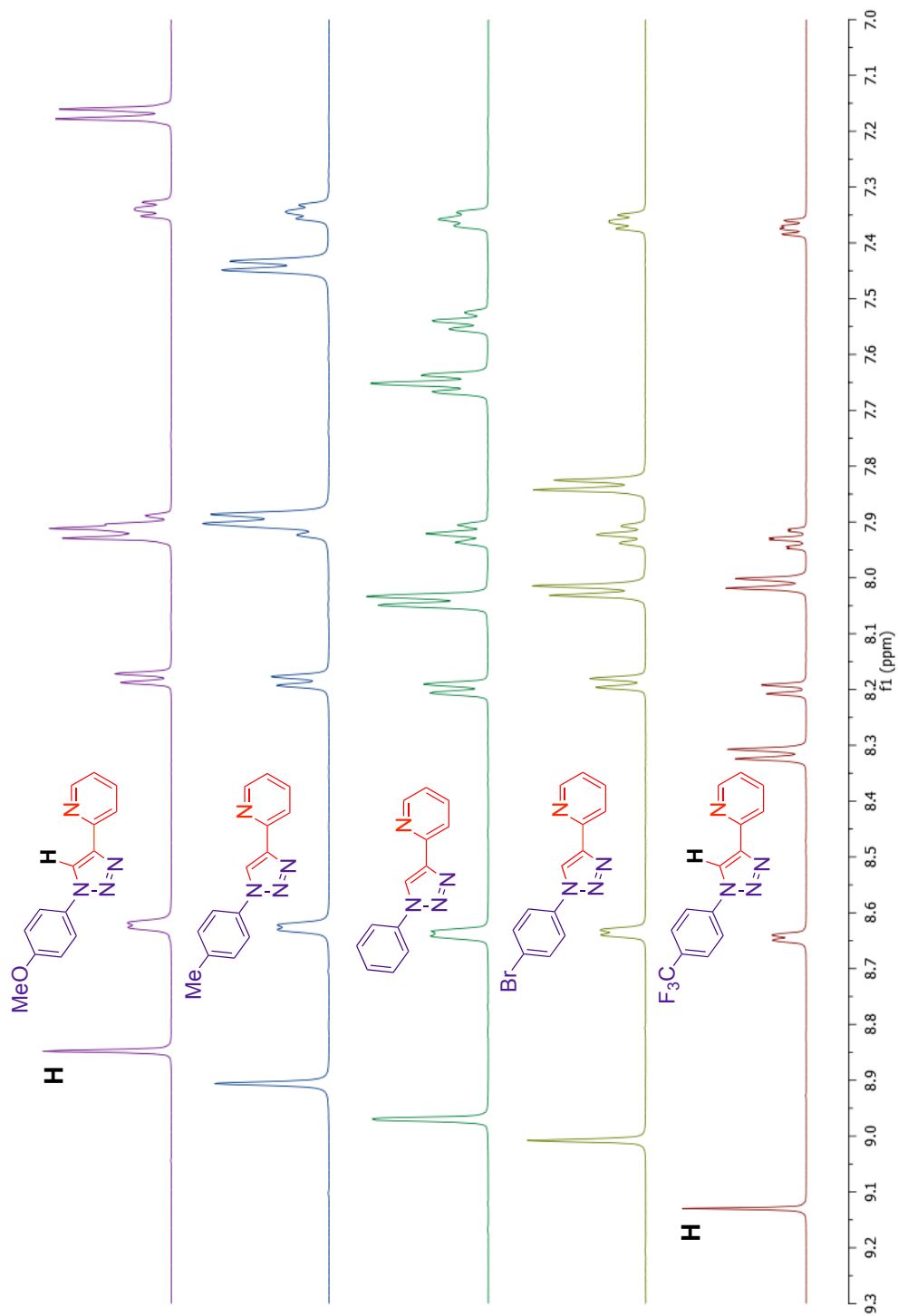
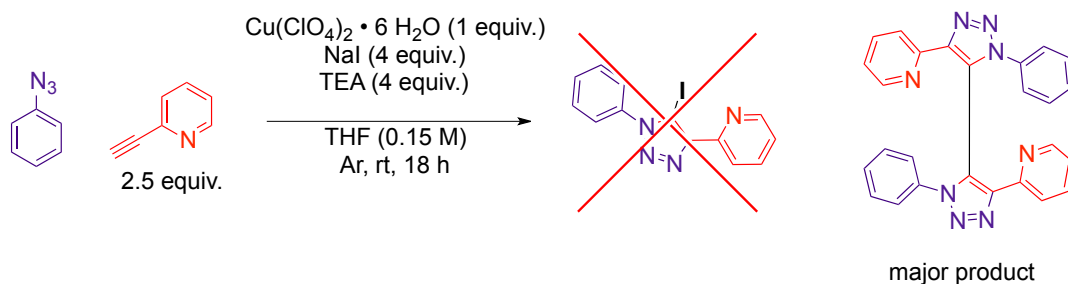


Figure 5.3: ¹H NMR analysis of the electronic diversity of pyridyl triazoles 5f - 5j.

5.4 Functionalization of Pyridyl Triazoles Through Halogenation:

In order to further functionalize the desired electronically diverse pyridyl triazoles, it was necessary to install a reactive group on the triazole ring. This approach should have little impact on the electronic nature of the system and allow the variability of the compounds to remain intact. Halogenation of the system should be a straightforward method to install the reactive group at the desired location on the triazole ring while allowing the formation of the pyridyl triazole to proceed. Literature on the synthesis of 5-halo-triazoles focuses largely on the formation of substituted iodo-triazoles and further functionalization of these compounds is reported to be facile.¹⁶⁻¹⁸ It should be noted however, that previous reports on the synthesis of iodo-pyridyl triazoles were scarce and only examples where comparable compounds were formed on minute scale could be located.¹⁹ Following the available literature,¹⁹ methods for preparing iodo-pyridyl triazoles in one step from aryl azides and terminal alkynes were attempted. This method utilized stoichiometric amounts of copper(II) perchlorate in combination with four equivalents of sodium iodide in order to generate the active copper(I) species as well as the iodinating reagent I_3 in situ. In order to encourage deprotonation and subsequent formation of the copper acetylide, triethylamine was included as a base. While the report claims this system is tolerant and able to afford the desired 5-iodo-pyridyl triazoles in high yields, utilization of this procedure with phenyl azide and 2-ethynylpyridine provided only trace amounts

of the desired product. Rather, what was observed was formation of large amounts of a pyridyl triazole dimer (Scheme 5.2).



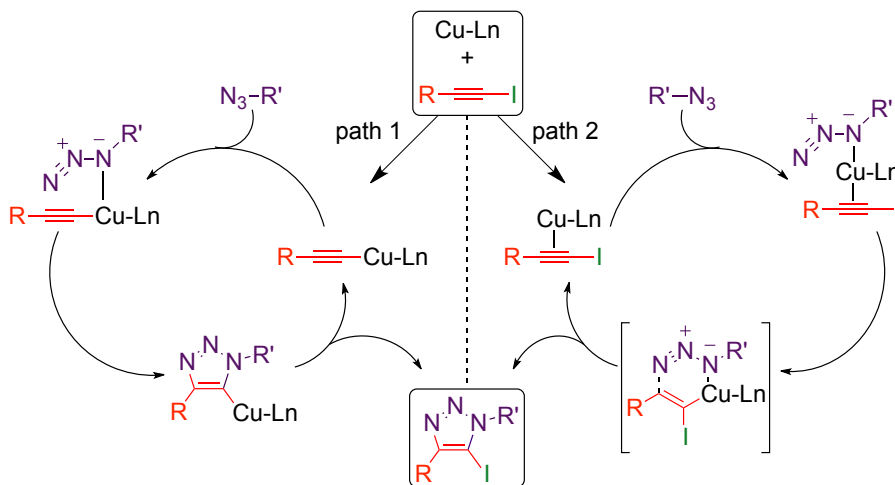
Scheme 5.2: Attempt at preparation of iodo-triazole through in situ iodination results in formation of pyridyl triazole dimer.

While it is unfortunate that the desired compounds could not be obtained via this one pot method, it is interesting that formation of these products is not discussed in the corresponding literature. Additionally, if 3-ethynylpyridine were utilized in this method, the dimerized product would have high potential as an interesting ligand class.

Further review of the literature showed that a different approach may be capable of furnishing the desired 5-iodo-pyridyl triazoles. If the iodo-ethynyl pyridine (**5k**) was prepared and isolated this could be used in the CuAAC with copper(I) iodide in the presence of an amine ligand to obtain the desired compounds.²⁰ The mechanism for this reaction has the potential to differ slightly from that of the standard CuAAC (Scheme 5.3). One possible route that is similar to that of the standard CuAAC proceeds through the formation of the standard copper acetylide complex after oxidative addition into the C-I bond of the iodoalkyne. Subsequent coordination of the azide to the copper center through

the nitrogen adjacent to the substitution allows for cyclization to occur and the product is a cupric triazolide. Exchange of the copper through reaction with a subsequent equivalent of the iodoalkyne completes the cycle and produces the desired iodo-triazole.

Alternatively, the process may begin through activation of the iodoalkyne through the formation of a π -complex intermediate. This intermediate can then react with the azide as before through coordination of the substituted nitrogen bearing the negative charge. This brings the azide and alkyne into proximity and allows for the cyclization to proceed via a vinylidene-type transition state to furnish the desired compound 5-iodo-pyridyl triazole. The distinctive feature of this reaction pathway is that the C-I bond in the alkyne is not severed during the catalysis.

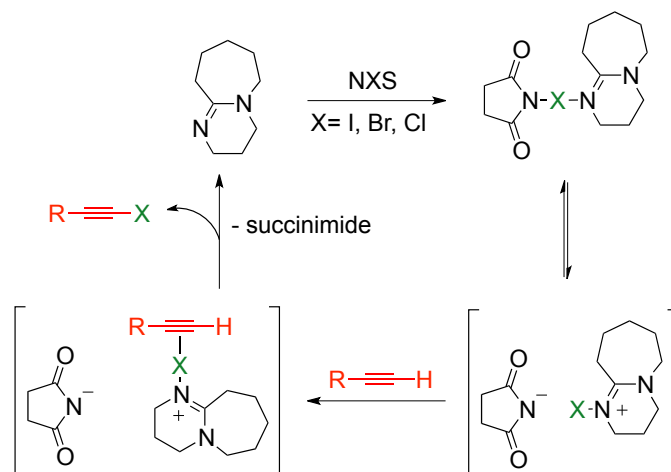


Scheme 5.3: Two pathways for the catalytic cycle to form iodo pyridyl triazoles.

Current literature reports have deemed the second pathway as more likely based on a number of observations. First the main support comes from the fact

that the iodo-triazole is reported as the exclusive product from this reaction even when the reaction is carried out in protic solvents. If this cupric triazole intermediate is formed, as it would be in pathway 1 then protonation of the intermediate should occur rapidly and proto-triazole should be observed. The complete absence of this product determines that pathway 1 cannot be the dominant route for this reaction.

With this strategy in mind the halogenated ethynylpyridines were prepared. These compounds could be synthesized rapidly through the reaction of electrophilic halogenating reagents with the terminal alkyne when exposed to sufficient base.²¹ By combining the alkyne with N-halosuccinimides bearing the desired halogen in tetrahydrofuran and activating the system with the base 1,8-diazabicyclo[5.4.0]undec-7-ene (DBU) the desired haloalkyne could be obtained. A possible mechanism for this reaction is shown in scheme 5.4 and involves the generation of a highly electrophilic halogen species through the reaction of the halogenated succinimide with DBU to generate a halogen bond adduct.²²⁻²⁵ This species then reacts with the terminal alkyne to form a π -complex that subsequently undergoes deprotonation by DBU to generate the haloalkyne.



Scheme 5.4: Proposed mechanism for the formation of iodo-alkynes using N-halosuccinimides and DBU.

While this reaction is reported to work well at room temperature, initial results were low yielding and the reaction appeared significantly more sluggish than reported. However, it was observed that upon addition of the DBU a large exotherm occurred. Thus, it was practical to try to counteract this by running the reaction in an ice bath as a heat sink. This modification allowed the reaction to proceed rapidly and high yields were obtained when N-iodosuccinimide and N-bromosuccinimide were used. It is reported that use of N-chlorosuccinimide is incapable of furnishing chlorinated alkynes via this process.²¹ However, when the reaction was performed in combination with an ice bath, the desired chlorinated ethynylpyridines were obtained in low yields (Table 5.3).

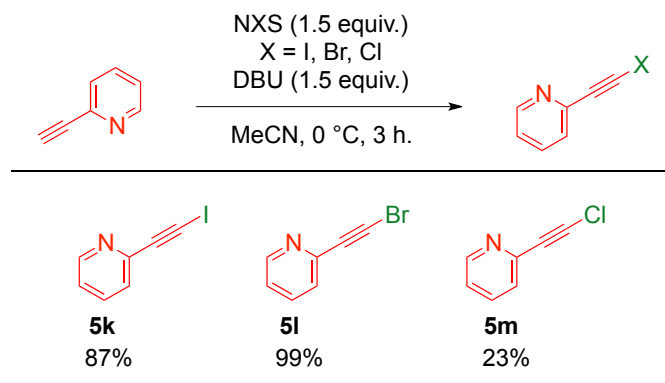


Table 5.3: Synthesis of halogenated 2-ethynylpyridines.

With the halogenated alkynes (**5k-5m**) in hand, work began on the synthesis of halogenated pyridyl triazoles. As there was literature precedent for the preparation of the iodo-triazoles it was logical to begin with the utilization of the iodoalkyne. Initial results using the alkyne as the limiting reagent with a slight excess of azide in tetrahydrofuran with a 10 mol% loading of copper(I) iodide and two equivalents of the amine ligand, triethylamine, the reaction was run at ambient temperature and the desired 5-iodotriazoles (**5n-5q**) could be isolated in low yields (Table 5.4). The exception to this was when the azide, 4-trifluoromethyl phenyl azide was used. Here no desired product was formed after 24 h when the reaction was run at room temperature. Additionally, what was observed was formation of the trifluoromethylated dimer compound.

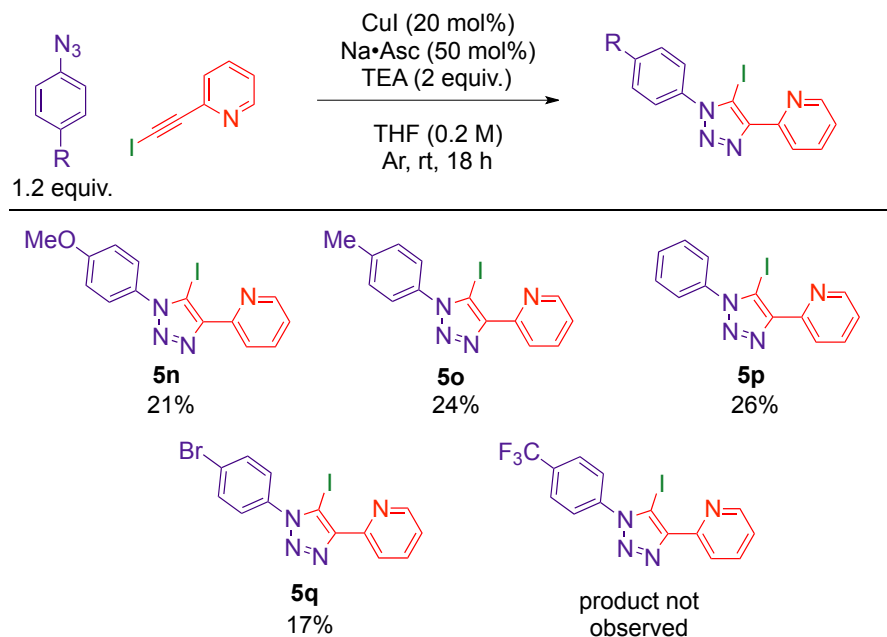
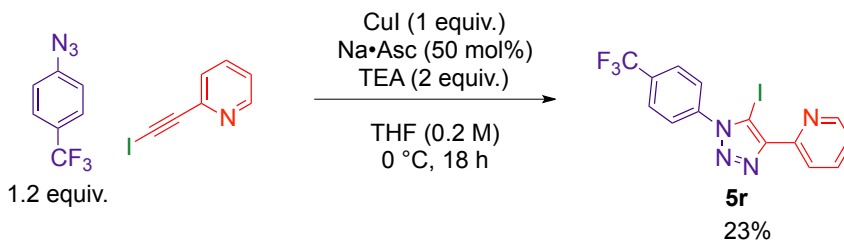


Table 5.4: Synthesis of iodo pyridyl triazoles.

In an attempt to prevent the dimerization, which was rationalized to occur from the reaction of the cupric triazolide with an equivalent of the desired iodo-triazole, the reaction was run in an ice/brine bath and the reaction was not allowed to warm to ambient temperature. In addition to the decreased reaction temperature, the amount of copper catalyst was increased in order to achieve full consumption of the iodo-alkyne. Satisfyingly, under these conditions, the dimerization of the product did not occur and the desired compound (**5r**) could be isolated in low yields (Scheme 5.5). While the desired products could only be isolated in small quantities, the consumption of the starting material did occur. The loss of product was then attributed to decomposition during purification. Unfortunately, this has occurred regardless of the solid phase used during the purification.



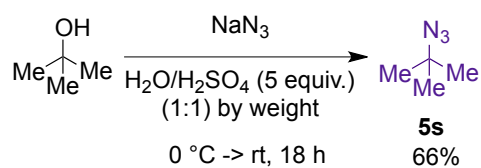
Scheme 5.5: Decreased reaction temperature and increased catalyst loading prevents dimerization of trifluoromethylated iodo pyridyl triazole.

While decreased temperatures allowed for increased yields of the trifluoromethylated iodo-triazole, the same approach when utilizing other aryl azides prevented the reaction from progressing altogether. Additionally, as the dimerized product was observed in all cases, it is proposed that when aryl azides are used in combination with 2-ethynylpyridine the mechanism for product formation cannot solely be that involving the vinylidene-type transition state and likely both pathways are occurring simultaneously.

Further analysis was performed in an attempt to prevent dimerization and to increase isolated yields. A search in the literature resulted in determining that if a more bulky amine type ligand was utilized, perhaps the nucleophilic attack of the cupric triazolide on the iodo-triazole could be prevented. It was reported that utilization of a tris-triazoleamine ligand such as tris((1-*tert*-butyl-1H-1,2,3-triazolyl)methyl)amine (TTTA) resulted in significantly increased reaction rates for the formation of iodo-triazoles as well as prevention of unwanted side products including the dimerized triazole.²⁶

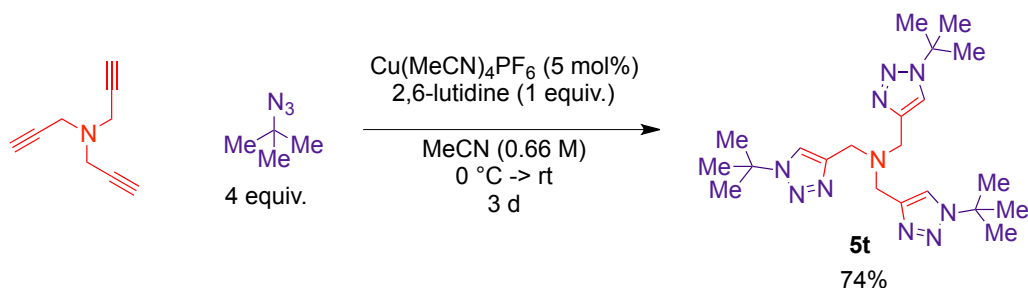
Preparation of the tris-triazoleamine is relatively straightforward and occurs through the CuAAC reaction of tripropargylamine with *tert*-butyl azide.²⁷

As *tert*-butyl azide is highly reactive due to its low molecular weight and high nitrogen to carbon ratio its synthesis should be undertaken with caution and any azide formed should be used immediately or properly disposed of. *Tert*-butyl azide (**5s**) was successfully prepared though the reaction of *tert*-butanol in highly acidic media with sodium azide (Scheme 5.6). This reaction proceeds through the formation of a tertiary carbocation from the loss of water from *tert*-butanol and subsequent attack of the azide anion. Fortunately the desired azide is highly hydrophobic and when the reaction is poured into a separatory funnel and allowed to settle, the desired product forms as a distinct layer on top of the aqueous acidic solution. This can then be easily separated and the azide was dried over sodium sulphate for immediate use.²⁸



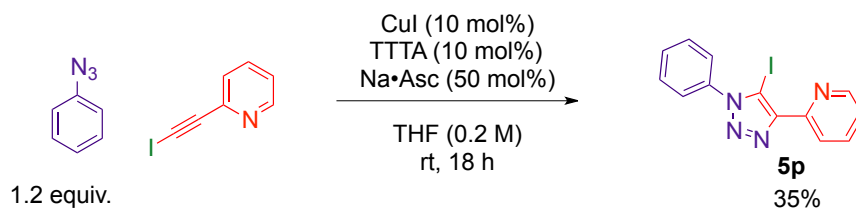
Scheme 5.6: Synthesis of highly reactive *tert*-butyl azide.

The synthesis of the ligand, TTTA (**5t**), from *tert*-butyl azide and tripropargylamine proceeds efficiently, albeit with long reaction times. When the reaction is catalyzed with 5 mol% copper(I) tetrakis(acetonitrile) hexafluorophosphate in acetonitrile at ambient temperature and allowed to run for 3 d the tris-triazole product can be isolated via filtration and is obtained as a white solid (Scheme 5.7).



Scheme 5.7: Synthesis of the TTTA ligand from *tert*-butyl azide and tripropargylamine.

Satisfyingly, utilization of an equimolar amount of TTTA compared to the copper catalyst for the CuAAC reaction to form iodo-pyridyl triazoles, allowed the reaction to proceed without the formation of the undesired dimer and with increased yield of (**5p**) compared to the previous method using TEA (Scheme 5.8).



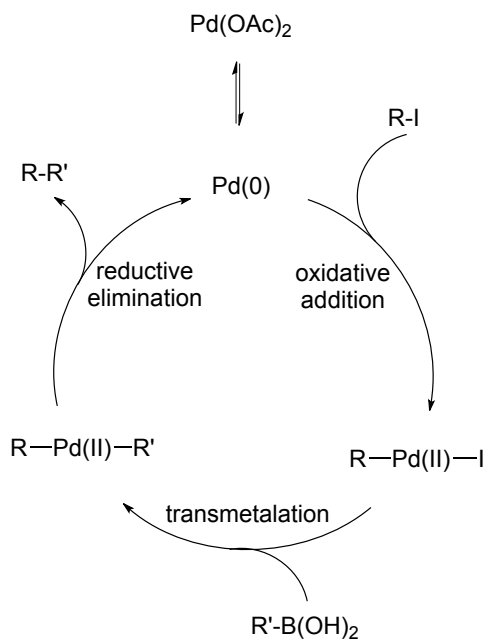
Scheme 5.8: Utilization of TTTA instead of TEA prevents dimerization and increases yield of iodo pyridyl triazole.

With the iodo-triazoles prepared, investigation began into whether the corresponding brominated and chlorinated compounds could be prepared using the same method from the brominated and chlorinated alkynes. Unfortunately, when these reaction were run using the corresponding halogenated copper(I) salts the reaction did not progress and only the starting azides and alkynes were observed. When the reactions were run utilizing copper(I) iodide only trace

amounts of the iodo-triazole were formed as evident by mass spectrometry and none of the desired bromo- or chloro-triazoles were formed. Future work on the synthesis of these compounds will be performed, when and if their preparation is deemed necessary. For now, focus remains on the synthesis of iodo-triazoles and their further functionalization.

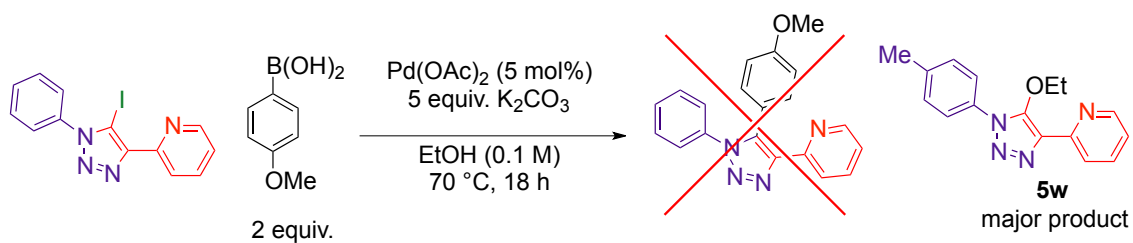
5.5 Derivatization of Iodo-Pyridyl Triazoles:

When considering methods for the functionalization of iodo-triazoles one reaction that has precedent, and is ubiquitous with aryl iodides, is the Suzuki-Miyaura cross-coupling reaction.¹⁶ This method utilizes a catalytic amount of a palladium(II) source which forms the active palladium(0) catalyst in situ. The functionalization comes as a result of the coupling of the aryl iodide with an aryl boronic acid and the resulting product is one that contains a covalent bond between the two aryl groups. The mechanism for this reaction is shown in scheme 5.9. The reaction proceeds by the reduction of the palladium(II) source to the active palladium(0) through loss of the anionic ligands. Oxidative addition of the palladium occurs through the insertion of the metal into the C-I bond of the aryl iodide. Following this, transmetalation occurs with the boronic acid via the exchange the iodide on palladium with the aryl group of the boronic acid. Once both aryl groups are coordinated to the metal center, reductive elimination can occur. This generates the desired product and regenerates the active palladium(0) to restart the catalytic cycle.



Scheme 5.9: Catalytic cycle for the palladium catalyzed cross coupling of aryl iodides with aryl boronic acids.

Unfortunately, when the iodo-pyridyl triazoles were utilized in this process with phenyl boronic acid and palladium(II) acetate in dry THF with the base potassium carbonate the production of the desired aryl substituted pyridyl triazole did not take place and only starting materials were observed. When ethanol was used as the solvent, production of the ethoxylated pyridyl triazole (**5w**) occurred (Scheme 5.10).



Scheme 5.10: Attempt at Suzuki cross coupling with iodo pyridyl triazole and 4-methoxyboronic acid furnishes alkyoxylated triazole as the major product.

Further experimentation showed that this resulted from a simple substitution mechanism and not through palladium-catalyzed cross-coupling. Simply dissolving the iodo-triazole in ethanol and exposing the system to base while heating produces the ethoxy substituted compound (**5w**) in good yield. To determine if there are limitations to this method, alcoholic solvents of increasing steric bulk were utilized. Satisfyingly, alkoxyated pyridyl triazoles bearing methoxy (**5v**), ethoxy (**5w**), isopropoxy (**5x**) substitution could be prepared using this method (Table 5.5). When *tert*-butanol was used as solvent the reaction failed to proceed and the starting iodo-triazole was obtained and the steric limitation of the system was determined. Additionally, hydroxylated pyridyl triazole (**5u**) was prepared by using DI-H₂O dissolved in *tert*-butanol as solvent. These substituted compounds demonstrated a significant increase in solubility in organic solvents compared to proto-triazoles. Further work is being done to optimize this system and to determine if the method allows for incorporation of other types of nucleophiles including alkylated thiols and amines.

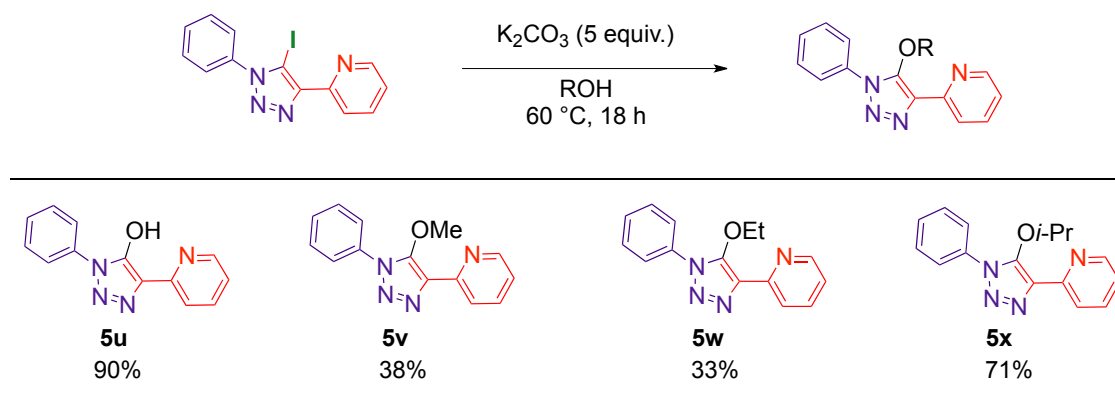


Table 5.5: Synthesis of hydroxylated and alkoxyated pyridyl triazoles from iodo pyridyl triazoles.

5.6 References:

- 1) Colombano, G.; Travelli, C.; Galli, U.; Caldarelli, A.; Chini, M. G.; Canonico, P. L.; Sorba, G.; Bifulco, G.; Tron, G. C.; Genazzi, A. A. *J. Med. Chem.* **2010**, *52*, 616.
- 2) Dziedzic, P.; Cisneros, J. A.; Robertson, M. J.; Hare, A. A.; Danford, N. E.; Baxter, R. H. G.; Jorgensen, W. L. *J. Am. Chem. Soc.* **2015**, *137*, 2996.
- 3) Khan, J. A.; Forouhar, F.; Tao, X.; Tong, L. *Expert Opin. Ther. Targets.* **2007**, *11*, 695.
- 4) Magni, G.; Amici, A.; Emanuelli, M.; Orsomando, G.; Raffaelli, N.; Ruggieri, S. *Cell. Mol. Life Sci.* **2004**, *61*, 19.
- 5) Bieganowski, P.; Brenner, C. *Cell.* **2004**, *117*, 495.
- 6) Galli, U.; Ercolano, E.; Carraro, L.; Blasi Roman, C. R.; Sorba, G.; Canonico, P. L.; Genazzani, A. A.; Tron, G. C.; Billington, R. A. *ChemMedChem.* **2008**, *5*, 771.
- 7) Beauparlant, P.; Bedard, D.; Bernier, C.; Chan, H.; Gilbert, K.; Goulet, D.; Gratton, M. O.; Lavoie, M.; Roulston, A.; Turcotte, E.; Watson, M. *Anti-Cancer Drugs.* **2009**, *5*, 346.
- 8) Morand, E. F.; Leech, M.; Bernhagen, J. *Nat. Rev. Drug. Discovery.* **2006**, *5*, 399.
- 9) Greven, D.; Leng, L.; Bucala, R. *Expert Opin. Ther. Targets.* **2010**, *14*, 253.
- 10) Asare, Y.; Schmitt, M.; Bernhagen, J. *Thromb. Haemost.* **2013**, *109*, 391.
- 11) Conroy, H.; Mawhinney, L.; Donnelly, S. C. Q. *J. Med.* **2010**, *103*, 831.
- 12) Tawfig, K. M.; Miller, G. J.; Al-Jeboori, M. J.; Fennell, P. S.; Coles, S. J.; Tizzard, G. J.; Wilson, C.; Potgieter, H. *Acta. Cryst. B* **2014**, *70*, 379.
- 13) Lucas, H. J.; Kennedy, E. R. *Org. Synth.* **1939**, *19*, 55.
- 14) Lindsay, R. O.; Allen, C. F. H. *Org. Synth.* **1942**, *22*, 96.
- 15) Palchak, Z. L.; Nguyen, P. T.; Larsen, C. H. *Beilstein J. Org. Chem.* **2015**, *11*, 1425.

- 16) Deng, J.; Wu, Y M.; Chen, Q-Y. *Synthesis*. **2005**, *16*, 2730.
- 17) Li, L.; Zhang, G.; Zhu, A.; Zhang, L. *J. Org. Chem.* **2008**, *73*, 3630.
- 18) Hein, J. E.; Fokin, V. V. *Chem. Soc. Rev.* **2010**, *39*, 1302.
- 19) Brotherton, W. S.; Clark, R. J.; Zhu, L. *J. Org. Chem.* **2012**, *77*, 6443.
- 20) Hein, J. E.; Tripp, J. C.; Krasnova, L. B. Sharpless, K. B.; Fokin, V. V. *Angew. Chem. Int. Ed.* **2009**, *48*, 8018.
- 21) Li, M.; Li, Y.; Zhao, B.; Liang, F.; Jin, L Y. *RSC Adv.* **2014**, *4*, 30046.
- 22) Castellote, I.; Moron, M.; Burgos, C.; Alvarez-Builla, J.; Martin, A.; Gomez-Sal, P.; Vaquero, J. J. *Chem. Commun.* **2007**, 1281.
- 23) Crowston, E. H.; Lobo, A. M.; Prabhakar, S.; Rzepa, H. S.; Williams, D. J. *J. Chem. Soc., Chem. Commun.* **1984**, 276.
- 24) Raatikainen, K.; Rissanen, K. *Chem. Sci.* **2012**, *3*, 1235.
- 25) Wang, Y. M.; Wu, J.; Hoong, C.; Rauniyar, V.; Toste, F. D. *J. Am. Chem. Soc.* **2012**, *134*, 12928.
- 26) Michaels, H. A.; Zhu, L. *e-EROS*. **2011**, DOI: 10.1002/047084289X.m01357.
- 27) Chan, T. R.; Hilgraf, R.; Sharpless, K. B.; Fokin, V. V. *Org. Lett.* **2004**, *6*, 2853.
- 28) Bottaro, J. C.; Penwell, P. E.; Schmitt, R. *Synth. Commun.* **1997**, *27*, 1465.

5.7 Supporting Information:

General Reagent Information

All reactions were set up on the benchtop in oven-dried glassware or dried scintillation vials. Flash column chromatography was performed using silica purchased from Silicycle. Solvents for chromatography were purchased from Fisher Chemicals and used as obtained. HPLC grade Tetrahydrofuran and Acetonitrile was purchased from Fisher Chemicals and dried via passage through activated alumina in a commercial solvent purification system (Pure Process Technologies, Inc.). NMR solvents were purchased from Acros Organics or Cambridge Isotope Laboratories and used as obtained. Anilines were purchased from Oakwood Chemicals, Chem-Impex International, and Acros Organics and distilled before use. 2-ethynylpyridine was purchased from Ark Pharm Inc. and distilled before use. Sodium azide was purchased from Fisher Chemicals and used as obtained. Sodium nitrite was purchased from Wards Science and used as obtained. Sodium tetrafluoroborate was purchased from Strem Chemicals and used as obtained. Copper(I) iodide was purchased from Sigma Aldrich, stored in a glove box under Nitrogen and used as obtained. N-iodosuccinimide was purchased from Oakwood Chemicals and used as obtained. N-bromosuccinimide and N-chlorosuccinimide was purchased from Acros Organics and used as obtained. Triethylamine was purchased from Fisher Chemicals and distilled before use. Tert-butanol was purchased from Acros Organics and used as obtained.

General analytical information

^1H and ^{13}C NMR spectra were measured on a Varian Inova 500 (500 MHz) spectrometer using acetone- d_6 or CDCl_3 as solvents and tetramethylsilane as an internal standard. The following abbreviations are used singularly or in combination to indicate the multiplicity of signals: s - singlet, d - doublet, t - triplet, q - quartet, qn - quintet, sx - sextet, sp - septet, m - multiplet and br - broad. NMR spectra were acquired at 300 K. Gas chromatography (GC) was carried out on an Agilent Technologies 6850 Network GC System, and dodecane was used as the internal standard. ATR-IR spectra were taken on a Bruker:ALPHA FTIR Spectrometer. Attenuated total reflection infrared (ATR-IR) was used and the spectra was analyzed using the OPUS software with selected absorption maxima reported in wavenumbers (cm^{-1}). Mass spectrometric data was collected on a HP 5989A GC/MS quadrupole instrument. Exact masses were recorded on a Waters GCT Premier TOF instrument using direct injection of samples in methanol/acetonitrile into the electrospray source.

General procedure for the production of aryl azides:

To a 100 mL round-bottom flask equipped with a magnetic stir bar was added an equal portion of concentrated hydrochloric acid (HCl) and deionized water (DI- H_2O). This solution was then cooled in an ice/brine bath and allowed to stir for 10-15 min. Sodium nitrite was dissolved in minimal DI- H_2O and this solution was added dropwise to the surface of the aqueous acidic solution. The solution should gradually change in color until it reaches greenish-blue. The aniline

bearing the desired substitution was then added dropwise and the solution becomes red-orange in color. This solution was allowed to stir for 30 min to allow the formation of the diazonium to take place. Sodium tetrafluoroborate was then added slowly so that mixing of the system was not disrupted. Precipitation of a cream colored solid occurred after 30 min and was isolated by filtration. An aqueous solution of sodium azide was prepared in a separate round-bottom flask equipped with a magnetic stir bar and was placed in an ice/brine bath to cool. The isolated diazonium salt was then added slowly and evolution of nitrogen gas was observed. Formation of the aryl azide occurred and was observed as a yellow oil dispersed in the aqueous solution. The azide was extracted from the solution in diethyl ether and the organic extract was washed with brine and dried over sodium sulfate. The extract was then concentrated to obtain the desired azide. The azide was either used immediately without further purification or characterization or was dissolved in an appropriate organic solvent for long-term storage.

Synthesis of 1-azido-4-methoxybenzene (5a):

Concentrated HCl (20 mL, 240 mmol), and deionized H₂O (20 mL) were combined in a round-bottom flask and cooled on an ice/brine bath. Sodium nitrite (1.65 g, 24 mmol) was dissolved in minimal DI-H₂O (< 5mL) and added dropwise to the aqueous acidic solution. *p*-Anisidine (2.46 g, 20 mmol) was added and stirred for 30 min. Sodium tetrafluoroborate (4.8 g, 44 mmol) was added and precipitation of 4-methoxybenzenediazonium tetrafluoroborate occurred. This salt

was isolated by filtration and not taken to complete dryness. Sodium azide (4.2 g, 64 mmol) was added to DI-H₂O (50 mL) in a separate round-bottom flask and stirred in an ice/brine bath. The diazonium salt was then added to the azide solution and the reaction was allowed to occur and warm to ambient temperature over the course of 18 h. The title compound was isolated via extraction in diethyl ether from the aqueous azide solution and after drying was concentrated to yield 1.65 g, 55% yield of the crude azide.

Synthesis of 1-azido-4-methylbenzene (5b):

Concentrated HCl (20 mL, 240 mmol), and deionized H₂O (20 mL) were combined in a round-bottom flask and cooled on an ice/brine bath. Sodium nitrite (1.65 g, 24 mmol) was dissolved in minimal DI-H₂O (< 5mL) and added dropwise to the aqueous acidic solution. *p*-Toluidine (2.14 g, 20 mmol) was added and stirred for 30 min. Sodium tetrafluoroborate (4.8 g, 44 mmol) was added and precipitation of 4-methylbenzenediazonium tetrafluoroborate occurs. This salt was isolated by filtration and not taken to complete dryness. Sodium azide (4.2 g, 64 mmol) was added to DI-H₂O (50 mL) in a separate round-bottom flask and stirred in an ice/brine bath. The diazonium salt was then added to the azide solution and the reaction was allowed to occur and warm to ambient temperature over the course of 18 h. The title compound was isolated via extraction in diethyl ether from the aqueous azide solution and after drying was concentrated to yield 1.86 g, 70% yield of the crude azide.

Synthesis of 1-azidobenzene (5c):

Concentrated HCl (20 mL, 240 mmol), and deionized H₂O (20 mL) were combined in a round-bottom flask and cooled on an ice/brine bath. Sodium nitrite (1.65 g, 24 mmol) was dissolved in minimal DI-H₂O (< 5mL) and added dropwise to the aqueous acidic solution. Aniline (1.8 mL, 20 mmol) was added and stirred for 30 min. Sodium tetrafluoroborate (4.8 g, 44 mmol) was added and precipitation of benzenediazonium tetrafluoroborate occurs. This salt was isolated by filtration and not taken to complete dryness. Sodium azide (4.2 g, 64 mmol) was added to DI-H₂O (50 mL) in a separate round-bottom flask and stirred in an ice/brine bath. The diazonium salt was then added to the azide solution and the reaction was allowed to occur and warm to ambient temperature over the course of 18 h. The title compound was isolated via extraction in diethyl ether from the aqueous azide solution and after drying was concentrated to yield 1.55 g, 65% yield of the crude azide.

Synthesis of 1-azido-4-bromobenzene (5d):

Concentrated HCl (20 mL, 240 mmol), and deionized H₂O (20 mL) were combined in a round-bottom flask and cooled on an ice/brine bath. Sodium nitrite (1.65 g, 24 mmol) was dissolved in minimal DI-H₂O (< 5mL) and added dropwise to the aqueous acidic solution. 4-Bromoaniline (3.45 g, 20 mmol) was added and stirred for 30 min. Sodium tetrafluoroborate (4.8 g, 44 mmol) was added and precipitation of 4-bromobenzenediazonium tetrafluoroborate occurs. This salt was isolated by filtration and not taken to complete dryness. Sodium azide (4.2 g,

64 mmol) was added to DI-H₂O (50 mL) in a separate round-bottom flask and stirred in an ice/brine bath. The diazonium salt was then added to the azide solution and the reaction was allowed to occur and warm to ambient temperature over the course of 18 h. The title compound was isolated via extraction in diethyl ether from the aqueous azide solution and after drying was concentrated to yield 2.60 g, 65% yield of the crude azide.

1-azido-4-(trifluoromethyl)benzene (5e):

Concentrated HCl (20 mL, 240 mmol), and deionized H₂O (20 mL) were combined in a round-bottom flask and cooled on an ice/brine bath. Sodium nitrite (1.65 g, 24 mmol) was dissolved in minimal DI-H₂O (< 5mL) and added dropwise to the aqueous acidic solution. 4-trifluoromethylaniline (2.51 mL, 20 mmol) was added and stirred for 30 min. Sodium tetrafluoroborate (4.8 g, 44 mmol) was added and precipitation of 4-(trifluoromethyl)benzenediazonium tetrafluoroborate occurs. This salt was isolated by filtration and not taken to complete dryness. Sodium azide (4.2 g, 64 mmol) was added to DI-H₂O (50 mL) in a separate round-bottom flask and stirred in an ice/brine bath. The diazonium salt was then added to the azide solution and the reaction was allowed to occur and warm to ambient temperature over the course of 18 h. The title compound was isolated via extraction in diethyl ether from the aqueous azide solution and after drying was concentrated to yield 2.84 g, 75% yield of the crude azide.

General procedure for the production of pyridyl triazoles (PyTri):

To a 20 mL scintillation vial equipped with a magnetic stir bar and PTFE coated screw cap was added copper(II) sulfate pentahydrate ($\text{CuSO}_4 \cdot 5 \text{H}_2\text{O}$) and the vial was purged with argon for 5 min. Ethanol (EtOH) was added followed by DI- H_2O in a ratio 2/3 EtOH and 1/3 DI- H_2O . Sodium ascorbate ($\text{Na}\cdot\text{Asc}$) was added and the solution turns a dark brown color. Phenyl azide bearing the desired substitution was added dropwise followed by dropwise addition of 2-ethynyl pyridine. The reaction was allowed to run at ambient temperature for 18 h. Upon completion the reaction was diluted with H_2O and the product was extracted with ethyl acetate (EtOAc). The organic extracts were combined, washed with brine, and dried over sodium sulfate. Column chromatography was performed on silica using EtOAc/Hexanes as an eluent. The desired pyridyl triazoles were obtained as solids.

2-(1-(4-methoxyphenyl)-1H-1,2,3-triazol-4-yl)pyridine (MeOPyTri) (5f):

$\text{CuSO}_4 \cdot 5 \text{H}_2\text{O}$ (50 mg, 0.2 mmol) was added to a scintillation vial and purged with argon for 5 min. EtOH (14 mL) and DI- H_2O (7 mL) were added followed by $\text{Na}\cdot\text{Asc}$ (198 mg, 1 mmol). 1-azido-4-methoxybenzene (745 mg, 5 mmol) was added dropwise, followed by dropwise addition of 2-ethynylpyridine (222 μL , 2.2 mmol). The reaction was run at ambient temperature for 18 h to afford the title compound as a white solid in 97% yield (536 mg, 2.1 mmol) after a gradient column chromatography on silica gel (20% EtOAc/Hexanes up to 50% EtOAc/Hexanes). ATR-IR: 3142, 3004, 2924, 2841, 1591, 1514, 1258, 1023,

824, 777, 716, 515 cm^{-1} . ^1H NMR (500 MHz, acetone- d_6) δ 8.85 (s, 1H), 8.62 (d, $J = 4$ Hz, 1H), 8.18 (d, $J = 8$ Hz, 1H), 7.92 (d, $J = 8.5$ Hz, 2H), 7.90 (t, $J = 6$ Hz, 1H), 7.34 (t, $J = 6$ Hz, 1H), 7.17 (d, $J = 9$ Hz, 2H), 3.90 (s, 3H). ^{13}C NMR (125 MHz, acetone- d_6) δ 160.9, 151.4, 150.6, 149.6, 137.7, 131.5, 123.8, 122.8, 121.4, 120.5, 115.7, 56.0. HRMS calculated requires $[\text{M}+\text{H}]^+$: 253.1084. Found m/z : 253.0975.

2-(1-(4-methylphenyl)-1H-1,2,3-triazol-4-yl)pyridine (MePyTri) (5g):

$\text{CuSO}_4 \cdot 5 \text{H}_2\text{O}$ (50 mg, 0.2 mmol) was added to a scintillation vial and purged with argon for 5 min. EtOH (14 mL) and DI- H_2O (7 mL) were added followed by Na•Asc (198 mg, 1 mmol). 1-azido-4-methylbenzene (665 mg, 5 mmol) was added dropwise, followed by dropwise addition of 2-ethynylpyridine (222 μL , 2.2 mmol). The reaction was run at ambient temperature for 18 h to afford the title compound as a white solid in 98% yield (509 mg, 2.2 mmol) after column chromatography on silica gel (30% EtOAc/Hexanes). ATR-IR: 3118, 2999, 2921, 1591, 1517, 1400, 1232, 1035, 814, 792, 533, 471 cm^{-1} . ^1H NMR (500 MHz, acetone- d_6) δ 8.91 (s, 1H), 8.62 (d, $J = 4$ Hz, 1H), 8.19 (d, $J = 8$ Hz, 1H), 7.90 (m, 3H), 7.44 (d, $J = 8$ Hz, 2H), 7.35 (t, $J = 6$ Hz, 1H), 2.34 (s, 3H). ^{13}C NMR (125 MHz, acetone- d_6) δ 151.3, 150.6, 149.7, 139.7, 137.7, 135.9, 131.1, 123.8, 121.3, 121.1, 120.6, 21.0. HRMS calculated requires $[\text{M}+\text{H}]^+$: 237.1135. Found m/z : 237.1055.

2-(1-phenyl)-1H-1,2,3-triazol-4-yl)pyridine (PyTri) (5h):

$\text{CuSO}_4 \cdot 5 \text{H}_2\text{O}$ (175 mg, 0.5 mmol) was added to a scintillation vial and purged

with argon for 5 min. EtOH (40 mL) and DI-H₂O (20 mL) were added followed by Na•Asc (693 mg, 3.5 mmol). 1-azido-benzene (1.55 g, 13 mmol) was added dropwise, followed by dropwise addition of 2-ethynylpyridine (707 μ L, 7 mmol). The reaction was run at ambient temperature for 18 h to afford the title compound as an orange solid in 90% yield (1.4 g, 6.3 mmol) after column chromatography on silica gel (30% EtOAc/Hexanes). ATR-IR: 3118, 3051, 1592, 1502, 1403, 1236, 1035, 756, 684, 533 cm^{-1} . ¹H NMR (500 MHz, acetone-*d*₆) δ 8.97 (s, 1H), 8.63 (d, J = 4.5 Hz, 1H), 8.20 (d, J = 7.5 Hz, 1H), 8.04 (d, J = 8 Hz, 2H), 7.92 (t, J = 7.5, 1H), 7.66 (t, J = 7 Hz, 2H), 7.54 (t, J = 7 Hz, 1H), 7.36 (t, J = 6.5 Hz, 1H). ¹³C NMR (125 MHz, acetone-*d*₆) δ 151.2, 150.6, 149.8, 138.1, 137.7, 130.7, 129.6, 123.9, 121.4, 121.2, 120.6. HRMS calculated requires [M+H]⁺: 223.0978. Found *m/z*: 223.0895.

2-(1-(4-bromophenyl)-1H-1,2,3-triazol-4-yl)pyridine (BrPyTri) (5i):

CuSO₄ • 5 H₂O (50 mg, 0.2 mmol) was added to a scintillation vial and purged with argon for 5 min. EtOH (14 mL) and DI-H₂O (7 mL) were added followed by Na•Asc (198 mg, 1 mmol). 1-azido-4-bromobenzene (990 mg, 5 mmol) was added dropwise, followed by dropwise addition of 2-ethynylpyridine (202 μ L, 2.0 mmol). The reaction was run at ambient temperature for 18 h to afford the title compound as a off white solid in 63% yield (377 mg, 1.3 mmol) after column chromatography on silica gel (30% EtOAc/Hexanes). ATR-IR: 3128, 3097, 3054, 2919, 1600, 1495, 1396, 1235, 1009, 817, 779, 494 cm^{-1} . ¹H NMR (500 MHz, acetone-*d*₆) δ 9.01 (s, 1H), 8.64 (d, J = 4 Hz, 1H), 8.18 (d, J = 8 Hz, 1H), 8.02 (d,

J = 9 Hz, 2H), 7.92 (t, J = 8 Hz, 1H), 7.83 (d, J = 8.5 Hz, 2H), 7.36 (t, J = 5.5 Hz, 1H). ¹³C NMR (125 MHz, acetone-*d*₆) δ 151.0, 150.6, 150.0, 137.8, 137.3, 133.8, 124.0, 123.0, 122.6, 121.5, 120.6. HRMS calculated requires [M+H]⁺: 301.0083. Found *m/z*: 300.9958.

2-(1-(4-(trifluoromethyl)phenyl)-1H-1,2,3-triazol-4-yl)pyridine (CF₃PyTri) (5j):

CuSO₄ • 5 H₂O (200 mg, 0.8 mmol) was added to a scintillation vial and purged with argon for 5 min. EtOH (40 mL) and DI-H₂O (20 mL) were added followed by Na•Asc (792 mg, 4 mmol). 1-azido-4-(trifluoromethyl)benzene (2.84 g, 15 mmol) was added dropwise, followed by dropwise addition of 2-ethynylpyridine (808 μL, 8 mmol). The reaction was run at ambient temperature for 18 h to afford the title compound as a white solid in 73% yield (1.69 g, 5.8 mmol) after column chromatography on silica gel (30% EtOAc/Hexanes). ATR-IR: 3121, 3092, 3060, 1570, 1409, 1322, 1159, 1105, 1066, 846, 785, 596, 496 cm⁻¹. ¹H NMR (500 MHz, acetone-*d*₆) δ 9.13 (s, 1H), 8.65 (d, J = 4.5 Hz, 1H), 8.32 (d, J = 8.5 Hz, 2H), 8.20 (d, J = 8 Hz, 1H), 8.01 (d, J = 8.5 Hz, 2H), 7.93 (td, J = 1.5 Hz, J = 8 Hz, 1H), 7.37 (td, J = 1.5 Hz, J = 4.5 Hz, 1H). ¹³C NMR (125 MHz, acetone-*d*₆) δ 150.8, 150.7, 150.1, 140.8, 137.8, 130.7, 128.0, 126.0, 124.1, 123.8, 121.6, 120.7. HRMS calculated requires [M+H]⁺: 291.0852. Found *m/z*: 291.0768.

General procedure for the production of halogenated 2-ethynylpyridines:

To a 50 mL roundbottom flask equipped with a magnetic stir bar was added N-halogenated succinimide. Dry acetonitrile was added and the reaction was placed in an ice/brine bath and allowed to cool. 2-Ethynylpyridine was added

dropwise. Lastly, 1,8-diazabicyclo[5.4.0]undec-7-ene (DBU) was added and the reaction was stirred for the indicated amount of time. Once the reaction has reached its end point as determined by TLC the reaction was diluted with DI-H₂O and extracted with EtOAc. The organic extracts were combined, washed with brine, and dried over sodium sulfate. The halogenated alkynes were purified over silica using EtOAc/Hexanes as the eluent.

2-(iodoethynyl)pyridine (5k):

N-iodosuccinimide (3.35 g, 15 mmol) was added to a 50 mL roundbottom flask followed by dry acetonitrile (20 mL). The reaction was cooled while stirring in an ice/brine bath. 2-Ethynylpyridine (1.1 mL, 10 mmol) was added dropwise. DBU (2.24 mL, 15 mmol) was added dropwise and the reaction was allowed to run for 3 h. The title compound was obtained as a gray solid in 87% yield (1.98 g, 8.6 mmol) after gradient column chromatography on silica gel (5% EtOAc/Hexanes up to 20% EtOAc/Hexanes). ATR-IR: 2161, 1581, 1460, 1423, 996, 768, 735 cm⁻¹. ¹H NMR (500 MHz, acetone-*d*₆) δ 8.55 (dt, J = 0.5 Hz, J = 4 Hz, 1H), 7.80 (td, J = 1.5 Hz, J = 6 Hz, 1H), 7.49 (dt, J = 1 Hz, J = 7.5 Hz, 1H), 7.37 (td, J = 1 Hz, J = 3.5 Hz, 1H). ¹³C NMR (125 MHz, acetone-*d*₆) δ 150.8, 144.0, 137.2, 128.5, 124.4, 94.6, 13.6. HRMS calculated requires [M+H]⁺: 229.9461. Found *m/z*: 229.9452.

2-(bromoethynyl)pyridine (5l):

N-bromosuccinimide (2.7 g, 15 mmol) was added to a 50 mL roundbottom flask followed by dry acetonitrile (20 mL). The reaction was cooled while stirring in an

ice/brine bath. 2-Ethynylpyridine (1.1 mL, 10 mmol) was added dropwise. DBU (2.24 mL, 15 mmol) was added dropwise and the reaction was allowed to run for 3 h. The title compound was obtained as a black solid in 99% yield (1.78 g, 9.9 mmol) after gradient column chromatography on silica gel (5% EtOAc/Hexanes up to 20% EtOAc/Hexanes). ATR-IR: 2193, 1580, 1460, 1425, 993, 769, 735 cm^{-1} . ^1H NMR (500 MHz, acetone- d_6) δ 8.56 (d, $J = 5$ Hz, 1H), 7.80 (td, $J = 2$ Hz, $J = 5.5$ Hz, 1H), 7.53 (d, $J = 8$ Hz, 1H), 7.39 (td, $J = 1$ Hz, $J = 4$ Hz, 1H). ^{13}C NMR (125 MHz, acetone- d_6) δ 151.0, 143.4, 137.3, 128.3, 124.5, 80.8, 51.9. HRMS calculated requires $[\text{M}+\text{H}]^+$: 181.9600. Found m/z : 181.9544.

2-(chloroethynyl)pyridine (5m):

N-chlorosuccinimide (2.0 g, 15 mmol) was added to a 50 mL roundbottom flask followed by dry acetonitrile (20 mL). The reaction was cooled while stirring in an ice/brine bath. 2-Ethynylpyridine (1.1 mL, 10 mmol) was added dropwise. DBU (2.24 mL, 15 mmol) was added dropwise and the reaction was allowed to run for 3 h. The title compound was obtained as a brown oil in 23% yield (320 mg, 2.3 mmol) after gradient column chromatography on silica gel (5% EtOAc/Hexanes up to 20% EtOAc/Hexanes). ATR-IR: 3052, 2226, 1580, 1462, 1427, 990, 773, 677, 625, 528 cm^{-1} . ^1H NMR (500 MHz, acetone- d_6) δ 8.55 (dt, $J = 0.5$ Hz, $J = 4$ Hz, 1H), 7.81 (td, $J = 1.5$ Hz, $J = 6$ Hz, 1H), 7.50 (dt, $J = 1$ Hz, $J = 6$ Hz, 1H), 7.40 (td, $J = 1$ Hz, $J = 4$ Hz, 1H). ^{13}C NMR (125 MHz, acetone- d_6) δ 151.0, 142.8, 137.4, 128.4, 124.6, 70.1, 68.2. HRMS calculated requires $[\text{M}+\text{H}]^+$: 138.0105. Found m/z : 138.0080.

General procedure for the production of pyridyl iodo-triazoles:

To a 20 mL scintillation vial equipped with a magnetic stir bar and PTFE coated screw cap was added copper(I) iodide (CuI) and the vial was purged with argon for 5 min. THF was added followed by sodium ascorbate (Na•Asc). Triethylamine (TEA) was added dropwise and if necessary the reaction was cooled on an ice/brine bath. Phenyl azide bearing the desired substitution was added dropwise. 2-iodoethynylpyridine was dissolved in minimal THF and this solution was added dropwise to the reaction. The reaction was allowed to run at ambient temperature for 18 h. Upon completion the reaction was diluted with H₂O and the product was extracted with ethyl acetate (EtOAc). The organic extracts were combined, washed with brine, and dried over sodium sulfate. Column chromatography was performed on silica using EtOAc/Hexanes as an eluent. The desired pyridyl iodo-triazoles were obtained as solids.

2-(5-iodo-1-(4-methoxyphenyl)-1H-1,2,3-triazol-4-yl)pyridine (I-(MeOPyTri)) (5n):

CuI (38 mg, 0.2 mmol) was added to a scintillation vial and purged with argon for 5 min. THF (5 mL) was added followed by Na•Asc (99 mg, 0.5 mmol). TEA (280 μ L, 2 mmol) was added dropwise and the solution was stirred for 5 min. 1-azido-4-(methoxy)benzene (179 mg, 1.2 mmol) was added dropwise. 2-iodoethynylpyridine (229 mg, 1 mmol) was dissolved in THF (1 mL) and this solution was added dropwise. The reaction was run at ambient temperature for

18 h to afford the title compound as a orange-brown solid in 21% yield (80 mg, 0.21 mmol) after gradient column chromatography on silica gel (10% EtOAc/Hexanes up to 30% EtOAc/Hexanes). ATR-IR: 2922, 2846, 1590, 1514, 1422, 1240, 1017, 992, 827, 791, 708, 566, 514 cm^{-1} . ^1H NMR (500 MHz, acetone- d_6) δ 8.70 (d, $J = 4$ Hz, 1H), 8.19 (d, $J = 8$ Hz, 1H), 7.94 (td, $J = 1.5$ Hz, $J = 6$ Hz, 1H), 7.56 (d, $J = 8.5$ Hz, 2H), 7.40 (td, $J = 1$ Hz, $J = 4$ Hz, 1H), 7.20 (d, $J = 9$ Hz, 2H), 3.94 (s, 3H). ^{13}C NMR (125 MHz, acetone- d_6) δ 161.9, 151.2, 149.9, 148.7, 137.6, 131.1, 129.2, 124.0, 122.3, 115.3, 81.5, 56.1. HRMS calculated requires $[\text{M}+\text{H}]^+$: 379.0050. Found m/z : 379.0020.

2-(5-iodo-1-(4-methylphenyl)-1H-1,2,3-triazol-4-yl)pyridine (I-(MePyTri)) (5o):

CuI (38 mg, 0.2 mmol) was added to a scintillation vial and purged with argon for 5 min. THF (5 mL) was added followed by Na•Asc (99 mg, 0.5 mmol). TEA (280 μL , 2 mmol) was added dropwise and the solution was stirred for 5 min. 1-azido-4-(methyl)benzene (160 mg, 1.2 mmol) was added dropwise. 2-iodoethynylpyridine (229 mg, 1 mmol) was dissolved in THF (1 mL) and this solution was added dropwise. The reaction was run at ambient temperature for 18 h to afford the title compound as a tan solid in 24% yield (87 mg, 0.24 mmol) after gradient column chromatography on silica gel (10% EtOAc/Hexanes up to 20% EtOAc/Hexanes). ATR-IR: 3065, 2917, 1592, 1514, 1399, 1237, 995, 821, 787, 712, 570, 525 cm^{-1} . ^1H NMR (500 MHz, acetone- d_6) δ 8.70 (ddd, $J = 4.8$, 1.7, 0.9 Hz, 1H), 8.19 (dt, $J = 7.9$, 1.0 Hz, 1H), 7.94 (td, $J = 7.8$, 1.8 Hz, 1H), 7.52 (m, 4H), 7.40 (ddd, $J = 7.6$, 4.8, 1.1 Hz, 1H), 2.49 (s, 3H). ^{13}C NMR (125 MHz,

acetone- d_6) δ 151.2, 149.9, 149.0, 141.4, 137.6, 135.9, 130.7, 127.6, 124.0, 122.3, 80.9, 21.3. HRMS calculated requires $[M+H]^+$: 363.0101. Found m/z : 363.0115.

2-(5-iodo-1-phenyl-1H-1,2,3-triazol-4-yl)pyridine (I-(PyTri)) (5p):

Cul (19 mg, 0.1 mmol) was added to a scintillation vial and purged with argon for 5 min. THF (5 mL) was added followed by Na•Asc (99 mg, 0.5 mmol). TTTA (43 mg, 0.1 mmol) was added and the solution was stirred for 5 min. 1-azido-benzene (143 mg, 1.2 mmol) was added dropwise. 2-iodoethynylpyridine (229 mg, 1 mmol) was dissolved in THF (1 mL) and this solution was added dropwise. The reaction was run at ambient temperature for 18 h to afford the title compound as a tan solid in 35% yield (122 mg, 0.35 mmol) after gradient column chromatography on silica gel (10% EtOAc/Hexanes up to 20% EtOAc/Hexanes). ATR-IR: 3051, 3018, 1591, 1499, 1418, 1245, 995, 785, 763, 734, 692, 570 cm^{-1} . ^1H NMR (500 MHz, acetone- d_6) δ 8.71 (d, J = 4.4 Hz, 1H), 8.20 (d, J = 8.0 Hz, 1H), 7.95 (td, J = 7.8, 1.7 Hz, 1H), 7.73 – 7.65 (m, 5H), 7.41 (dd, J = 7.1, 5.3 Hz, 1H). ^{13}C NMR (125 MHz, acetone- d_6) δ 151.1, 149.9, 149.0, 138.3, 137.6, 131.1, 130.3, 127.8, 124.0, 122.4, 80.8. HRMS calculated requires $[M+H]^+$: 348.9945. Found m/z : 348.9955.

2-(5-iodo-1-(4-bromophenyl)-1H-1,2,3-triazol-4-yl)pyridine (I-(BrPyTri)) (5q):

Cul (38 mg, 0.2 mmol) was added to a scintillation vial and purged with argon for 5 min. THF (5 mL) was added followed by Na•Asc (99 mg, 0.5 mmol). TEA (280 μL , 2 mmol) was added dropwise and the solution was stirred for 5 min. 1-azido-

4-(bromo)benzene (238 mg, 1.2 mmol) was added dropwise. 2-iodoethynylpyridine (229 mg, 1 mmol) was dissolved in THF (1 mL) and this solution was added dropwise. The reaction was run at ambient temperature for 18 h to afford the title compound as a dark tan solid in 24% yield (74 mg, 0.17 mmol) after gradient column chromatography on silica gel (10% EtOAc/Hexanes up to 20% EtOAc/Hexanes). ATR-IR: 3086, 3061, 2923, 2844, 1592, 1488, 1241, 1056, 985, 834, 783, 739, 623, 520 cm^{-1} . ^1H NMR (500 MHz, acetone- d_6) δ 8.71 (d, $J = 3.5$ Hz, 1H), 8.19 (d, $J = 8$ Hz, 1H), 7.95 (td, $J = 2$ Hz, $J = 6$ Hz, 1H), 7.90 (d, $J = 8.5$ Hz, 2H), 7.67 (d, $J = 8.5$ Hz, 2H), 7.41 (td, $J = 1$ Hz, $J = 3.5$ Hz, 1H). ^{13}C NMR (125 MHz, acetone- d_6) δ 150.9, 149.9, 149.1, 137.7, 137.5, 133.5, 129.8, 124.7, 124.1, 122.4, 80.9. HRMS calculated requires $[\text{M}+\text{H}]^+$: 426.9050. Found m/z : 426.9055.

2-(5-iodo-1-(4-(trifluoromethyl)phenyl)-1H-1,2,3-triazol-4-yl)pyridine

(I-(CF₃PyTri)) (5r):

CuI (190 mg, 1 mmol) was added to a scintillation vial and purged with argon for 5 min. THF (5 mL) was added followed by Na•Asc (99 mg, 0.5 mmol). TEA (280 μL , 2 mmol) was added dropwise and the solution was stirred for 5 min. 1-azido-4-(trifluoromethyl)benzene (225 mg, 1.2 mmol) was added dropwise. 2-iodoethynylpyridine (229 mg, 1 mmol) was dissolved in THF (1 mL) and this solution was added dropwise. The reaction was placed in an ice/brine bath located in a cold room at ~ 4 $^\circ\text{C}$ and run for 18 h to afford the title compound as a tan solid in 23% yield (96 mg, 0.23 mmol) after gradient column chromatography

on silica gel (5% EtOAc/Hexanes up to 20% EtOAc/Hexanes). ATR-IR: 3081, 1614, 1321, 1162, 1109, 1072, 1007, 853, 786, 742, 511 cm^{-1} . ^1H NMR (500 MHz, acetone- d_6) δ 8.72 (d, $J = 4$ Hz, 1H), 8.21 (dt, $J = 1$ Hz, $J = 8$ Hz, 1H), 8.09 (d, $J = 8.5$ Hz, 2H), 7.99 (d, $J = 8.5$ Hz, 2H), 7.96 (td, $J = 2$ Hz, $J = 6$ Hz, 1H), 7.43 (ddd, $J = 1$ Hz, $J = 1.5$ Hz, $J = 3.5$ Hz, 1H). ^{13}C NMR (125 MHz, acetone- d_6) δ 150.8, 149.9, 149.4, 141.3, 137.7, 132.5, 132.2, 128.7, 127.6, 124.2, 122.4, 80.6. HRMS calculated requires $[\text{M}+\text{H}]^+$: 416.9819. Found m/z : 426.9055.

2-azido-2-methylpropane (5s):

Sulfuric acid (9.8 g, 100 mmol) was added to a 50 mL roundbottom flask equipped with a magnetic stir bar and the flask was placed in an ice/brine bath. DI- H_2O (10 mL) was added followed by sodium azide (1.63 g, 25 mmol). Once the azide was dissolved *tert*-butanol (1.9 mL, 20 mmol) was added dropwise and the solution was stirred for 15 min and then removed from stirring and allowed to stand for 18 h. The title compound was obtained as a colorless oil in 66% yield (1.31 g, 13 mmol) after separating the neat oil away from the acidic aqueous solution using a separatory funnel and dried over sodium sulfate. ^1H NMR (500 MHz, CDCl_3) δ 1.28 (s, 9H).

tris((1-(*tert*-butyl)-1H-1,2,3-triazol-4-yl)methyl)amine (TTTA) (5t):

Copper(I) tetrakis(acetonitrile) hexafluorophosphate (56 mg, 0.15 mmol) was added to a scintillation vial and purged with argon for 5 min. MeCN (5 mL) was added followed by 2,6-lutidine (350 μL , 3 mmol) and the solution was placed in an ice/brine bath and stirred for 5 min. 1-azido-2-methylpropane (1.31 g, 13

mmol) was added dropwise. Tripropargylamine (425 μL , 3 mmol) was added to the solution dropwise. The reaction was run and allowed to warm to ambient temperature over 3 days to afford the title compound as a white solid in 74% yield (950 mg, 2.2 mmol) after filtration and washing the solid with cold MeCN. ATR-IR: 3146, 2982, 1374, 1207, 1109, 1047, 847, 819 cm^{-1} . ^1H NMR (500 MHz, CDCl_3) δ 7.88 (s, 1H), 3.77 (s, 2H), 1.68 (s, 9H). ^{13}C NMR (125 MHz, CDCl_3) δ 143.3, 121.3, 59.3, 47.1, 30.2. HRMS calculated requires $[\text{M}+\text{H}]^+$: 429.3197. Found m/z : 429.3091.

General procedure for the production of substituted pyridyl triazoles:

To an 8 mL scintillation vial equipped with a magnetic stir bar and Teflon-seal screw cap was added iodo-PhPyTri. The alkyl alcohol/water solution bearing the desired substitution was added as solvent. Potassium carbonate in excess was added as base. The reaction was placed on a hot block at 60 $^\circ\text{C}$ and allowed to run for 18 h. Upon completion the reaction was diluted with DI- H_2O and the product was extracted with EtOAc. The organic extracts were combined, washed with brine and dried over sodium sulfate. Column chromatography was performed on silica using EtOAc/Hexanes as an eluent. The desired substituted pyridyl triazoles were obtained as solids.

1-phenyl-4-(pyridin-2-yl)-1H-1,2,3-triazol-5-ol (OH-(PyTri)) (5u):

5-Iodo-PhPyTri (87 mg, 0.25 mmol), was added to a dried 8 mL scintillation vial. Tert-butanol (5 mL) and DI- H_2O (1 mL) was added followed by K_2CO_3 (173 mg, 1.25 mmol) The reaction was run at ambient temperature for 60 $^\circ\text{C}$ for 18 h to

afford the title compound as a white solid in 90% yield (54 mg, 0.23 mmol) after gradient column chromatography on silica gel (5% EtOAc/Hexanes up to 20% EtOAc/Hexanes). ATR-IR: 3310, 3089, 3039, 1661, 1598, 1530, 1498, 1435, 1311, 1061, 879, 748, 688, 656, 506 cm^{-1} . ^1H NMR (500 MHz, acetone- d_6) δ 9.64 (br, 1H), 9.08 (d, $J = 7$ Hz, 1H), 8.40 (d, $J = 9$ Hz, 1H), 8.00 (d, $J = 8$ Hz, 2H), 7.71 (td, $J = 1.5$ Hz, $J = 6.5$ Hz, 1H), 7.38 (m, 3H), 7.13 (t, $J = 7$ Hz, 1H). ^{13}C NMR (125 MHz, acetone- d_6) δ 160.0, 139.8, 135.1, 132.7, 130.0, 129.6, 127.1, 124.5, 120.7, 120.1, 117.8 HRMS calculated requires $[\text{M}+\text{H}]^+$: 239.0927. Found m/z : 239.0848.

2-(5-methoxy-1-phenyl-1H-1,2,3-triazol-4-yl)pyridine (MeO-(PyTri)) (5v):

5-Iodo-PhPyTri (87 mg, 0.25 mmol), was added to a dried 8 mL scintillation vial. Dry methanol (5 mL) was added followed by K_2CO_3 (173 mg, 1.25 mmol) The reaction was run at ambient temperature for 60 °C for 18 h to afford the title compound as a yellow solid in 38% yield (24 mg, 0.10 mmol) after gradient column chromatography on silica gel (5% EtOAc/Hexanes up to 20% EtOAc/Hexanes). ATR-IR: 2923, 1598, 1494, 1367, 1297, 973, 767, 687, 604, 512 cm^{-1} . ^1H NMR (500 MHz, acetone- d_6) δ 8.69 (d, $J = 5$ Hz, 1H), 8.16 (d, $J = 8$ Hz, 1H), 7.90 (td, $J = 2$ Hz, $J = 6$ Hz, 1H), 7.78 (d, $J = 7.5$ Hz, 2H), 7.64 (t, $J = 7.5$ Hz, 2H), 7.56 (tt, $J = 2$ Hz, $J = 7.5$ Hz, 1H), 7.33 (td, $J = 1$ Hz, $J = 3.5$ Hz, 1H), 4.21 (s, 3H). ^{13}C NMR (125 MHz, acetone- d_6) δ 151.8, 150.5, 150.1, 137.5, 136.4, 132.5, 130.3, 129.9, 124.3, 122.9, 121.8, 63.2. HRMS calculated requires $[\text{M}+\text{H}]^+$: 253.1084. Found m/z : 253.1099.

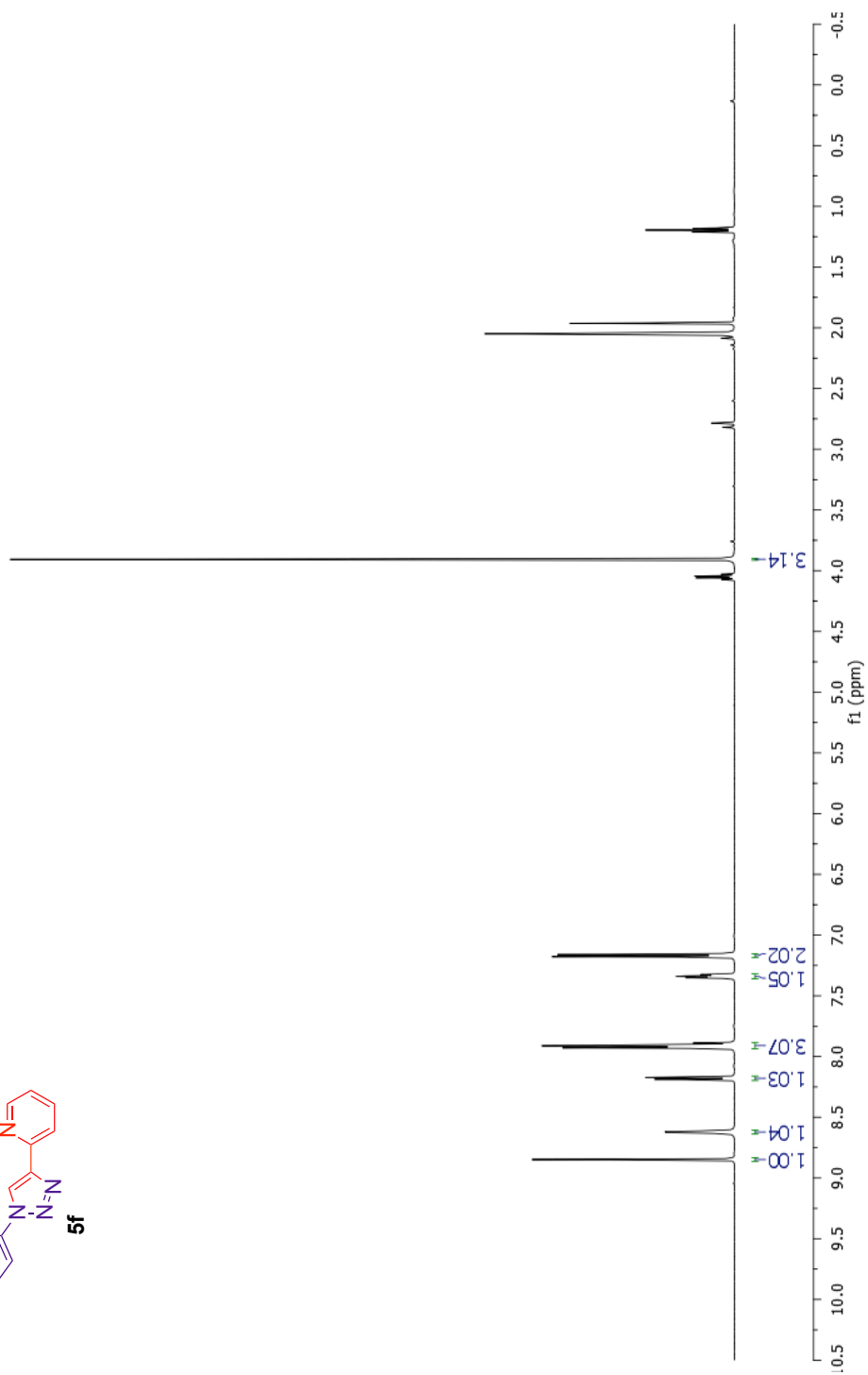
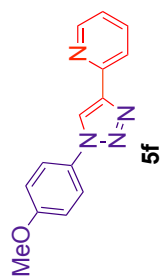
2-(5-ethoxy-1-phenyl-1H-1,2,3-triazol-4-yl)pyridine (EtO-(PyTri)) (5w):

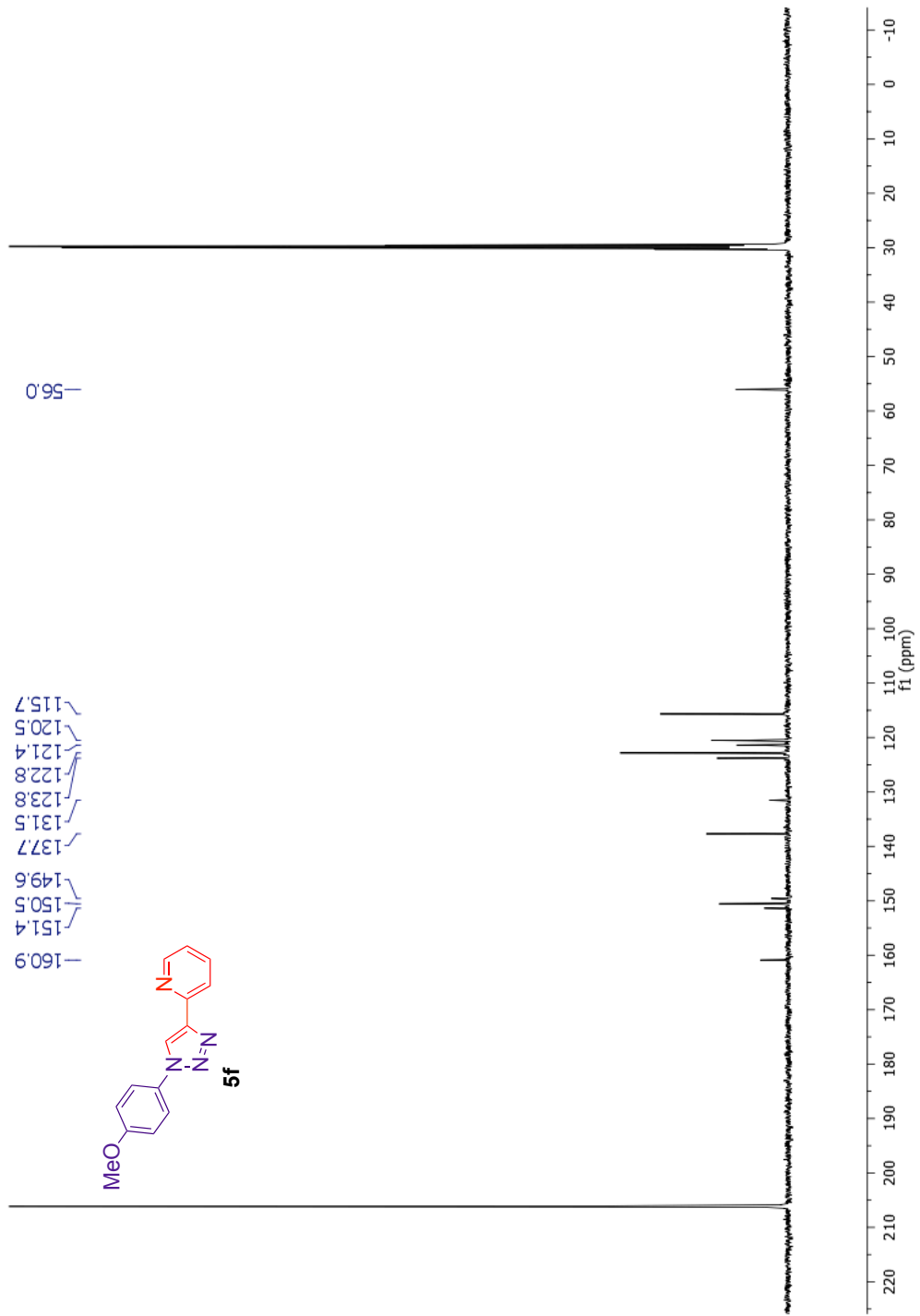
5-Iodo-PhPyTri (87 mg, 0.25 mmol), was added to a dried 8 mL scintillation vial. Dry ethanol (5 mL) was added followed by K_2CO_3 (173 mg, 1.25 mmol) The reaction was run at ambient temperature for 60 °C for 18 h to afford the title compound as a yellow solid in 33% yield (22 mg, 0.083 mmol) after gradient column chromatography on silica gel (5% EtOAc/Hexanes up to 20% EtOAc/Hexanes). ATR-IR: 3055, 2980, 1595, 1492, 1374, 1197, 1013, 981, 888, 761, 688, 602 cm^{-1} . 1H NMR (500 MHz, acetone- d_6) δ 8.67 (d, J = 4.5 Hz, 1H), 8.16 (d, J = 8 Hz, 1H), 7.89 (td, J = 1.5 Hz, J = 6 Hz, 1H), 7.78 (d, J = 7.5 Hz, 2H), 7.64 (t, J = 7.5 Hz, 2H), 7.56 (tt, J = 1.5 Hz, J = 7.5 Hz, 1H), 7.31 (td, J = 1 Hz, J = 4 Hz, 1H), 4.54 (q, J = 7 Hz, 2H), 1.28 (t, J = 7 Hz, 3H). ^{13}C NMR (125 MHz, acetone- d_6) δ 151.9, 150.1, 149.5, 137.5, 136.5, 132.6, 130.3, 129.8, 124.4, 122.9, 121.6, 72.6, 15.3. HRMS calculated requires $[M+H]^+$: 267.1240. Found m/z : 267.1709.

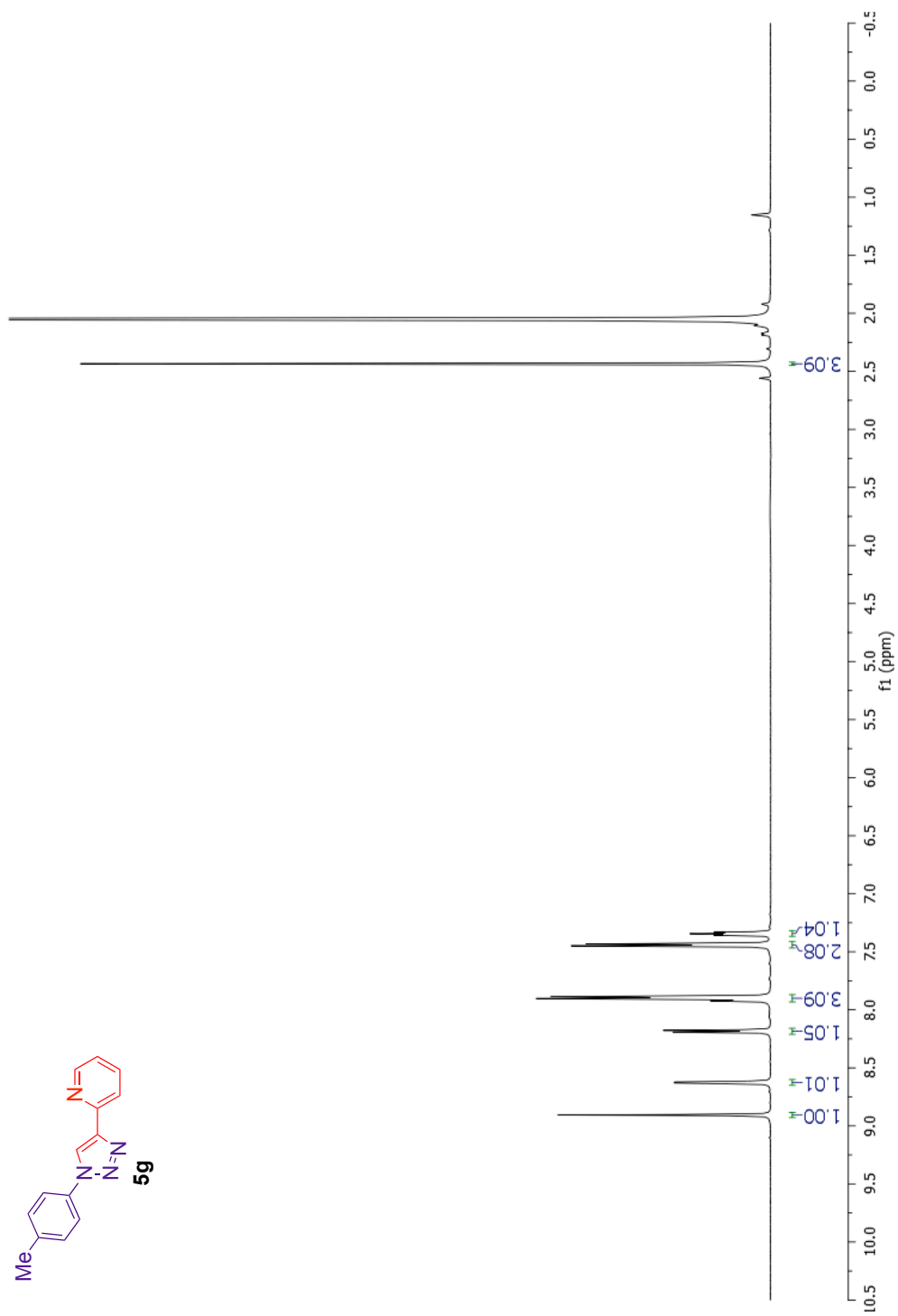
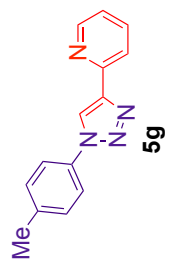
2-(5-isopropoxy-1-phenyl-1H-1,2,3-triazol-4-yl)pyridine (iPrO-(PyTri)) (5x):

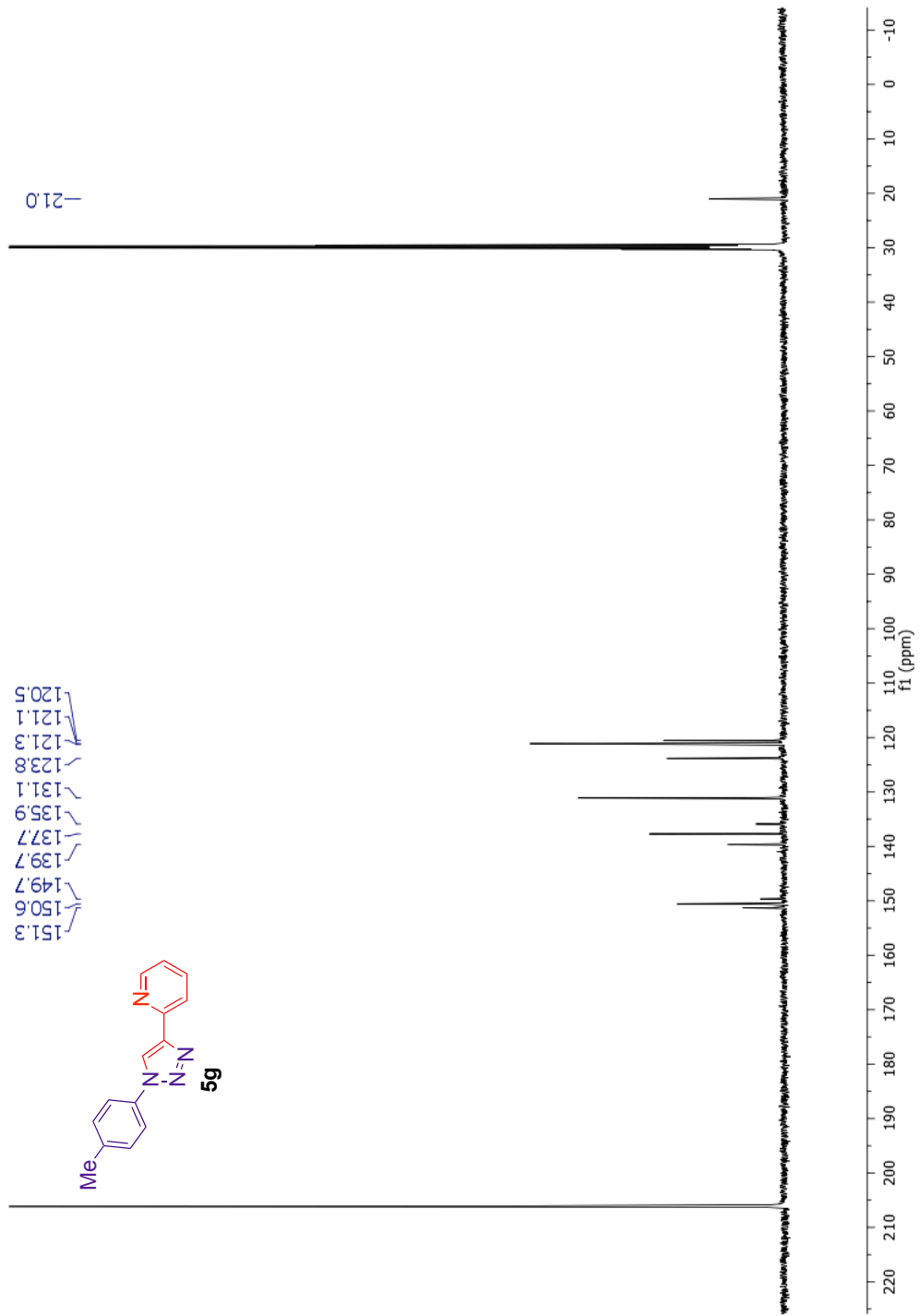
5-Iodo-PhPyTri (87 mg, 0.25 mmol), was added to a dried 8 mL scintillation vial. Dry isopropanol (5 mL) was added followed by K_2CO_3 (173 mg, 1.25 mmol) The reaction was run at ambient temperature for 60 °C for 18 h to afford the title compound as a yellow solid in 71% yield (50 mg, 0.18 mmol) after gradient column chromatography on silica gel (5% EtOAc/Hexanes up to 20% EtOAc/Hexanes). ATR-IR: 3058, 2970, 1595, 1486, 1375, 1259, 1096, 912, 765, 692, 604 cm^{-1} . 1H NMR (500 MHz, acetone- d_6) δ 8.67 (d, J = 5 Hz, 1H), 8.17 (d,

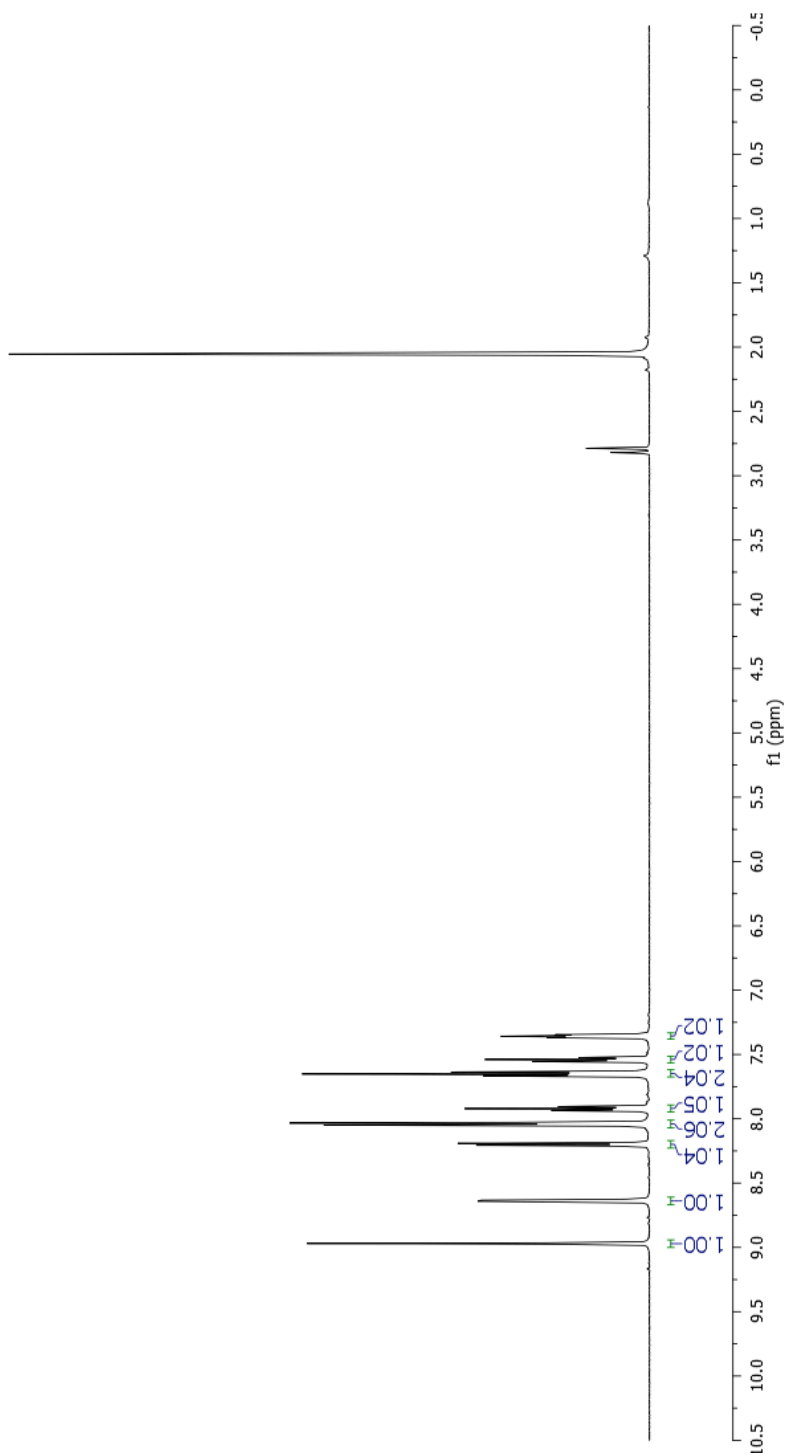
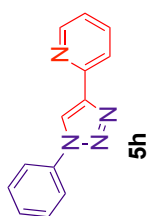
J = 8 Hz, 1H), 7.89 (td, J = 2 Hz, J = 6 Hz, 1H), 7.80 (d, J = 7.5 Hz, 2H), 7.64 (t, J = 7.5 Hz, 2H), 7.55 (t, J = 7.5 Hz, 1H), 7.31 (td, J = 1 Hz, J = 4 Hz, 1H), 5.16 (sp, J = 6 Hz, 1H), 1.18 (d, J = 6 Hz, 6H). ¹³C NMR (125 MHz, acetone-*d*₆) δ 152.1, 150.1, 148.6, 137.5, 136.7, 132.8, 130.2, 129.7, 124.6, 122.8, 121.5, 80.4, 22.3. HRMS calculated requires [M+H]⁺: 281.1397. Found *m/z*: 281.1363

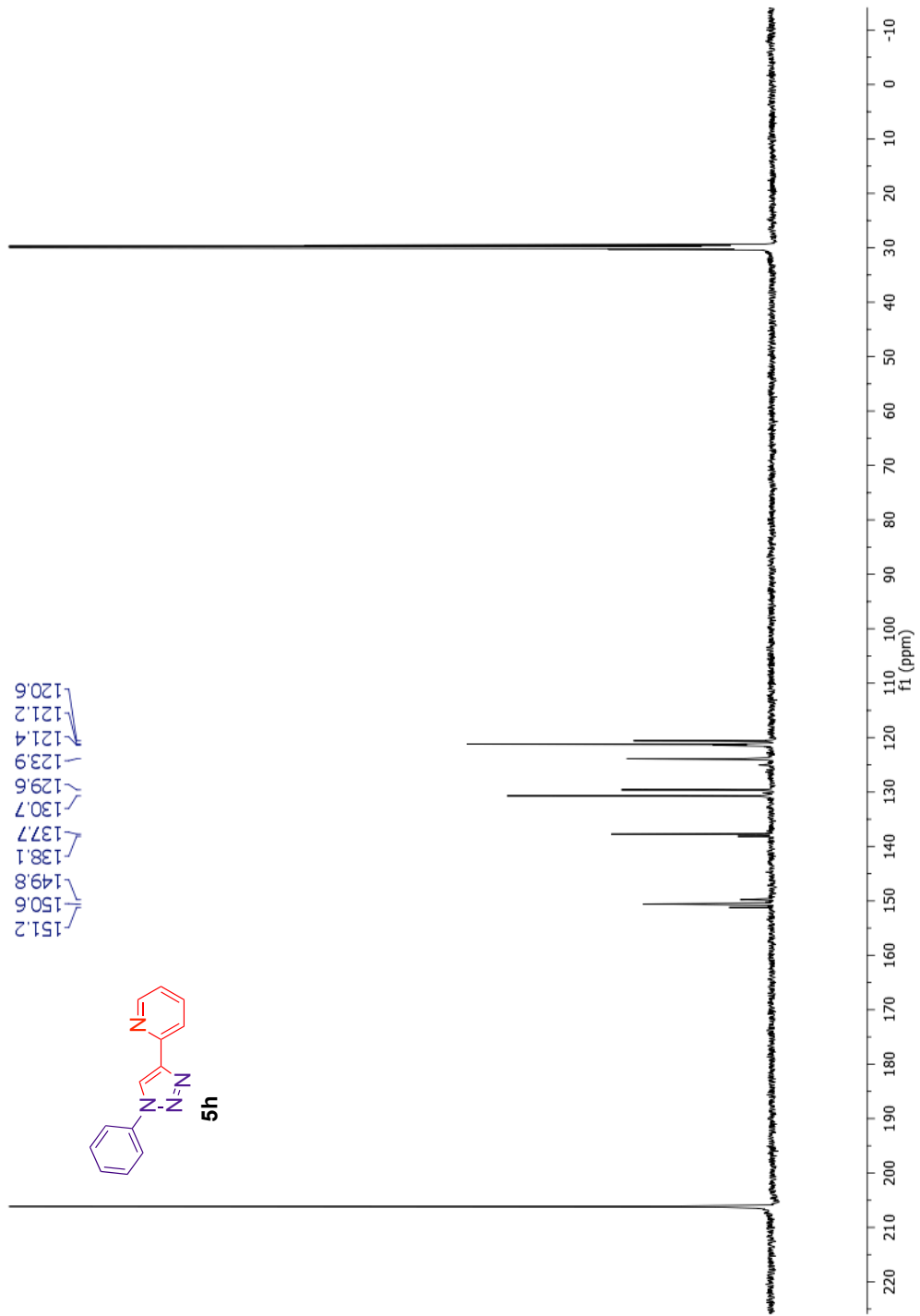


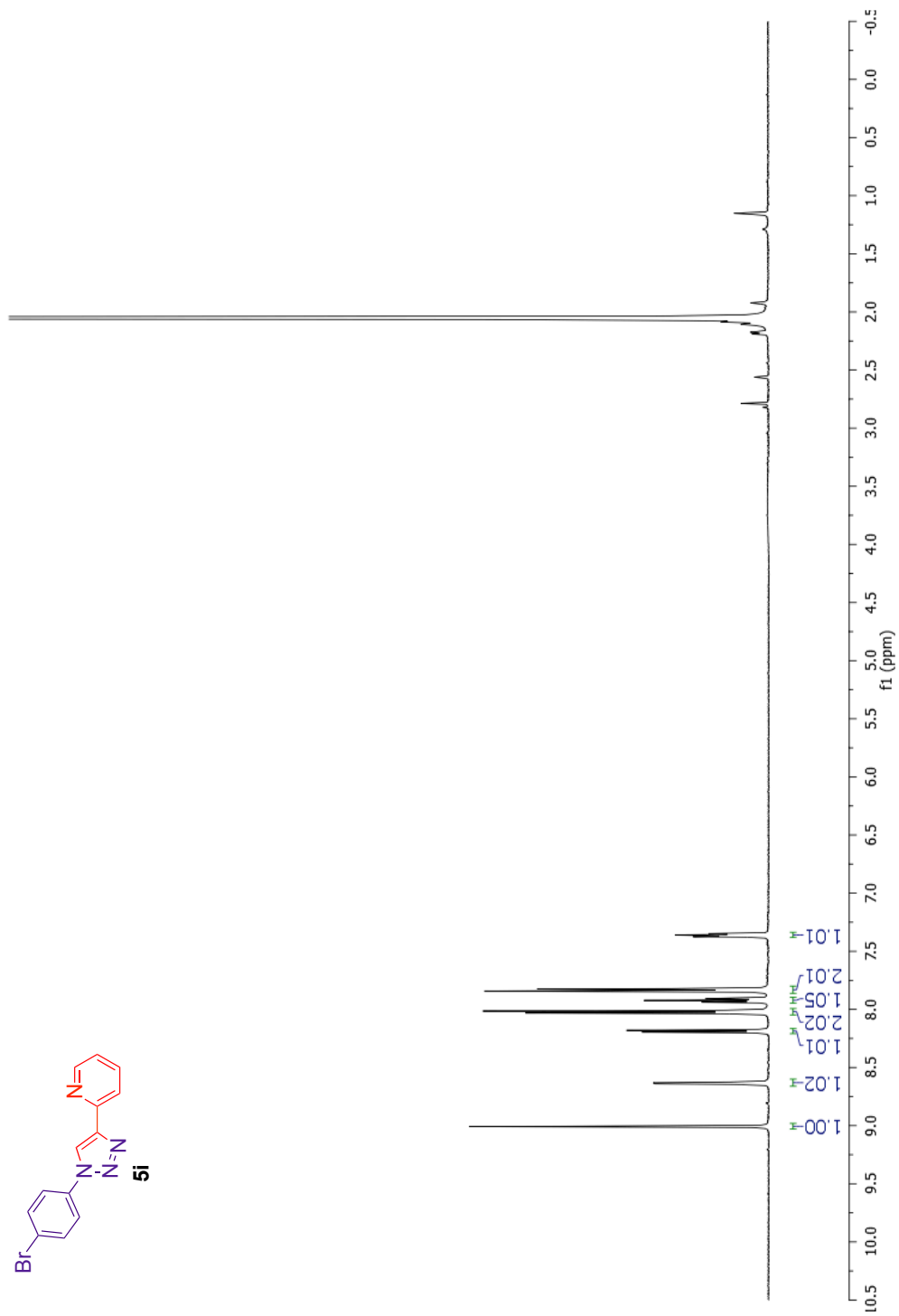
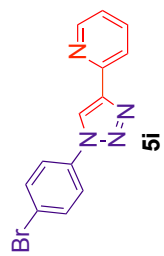


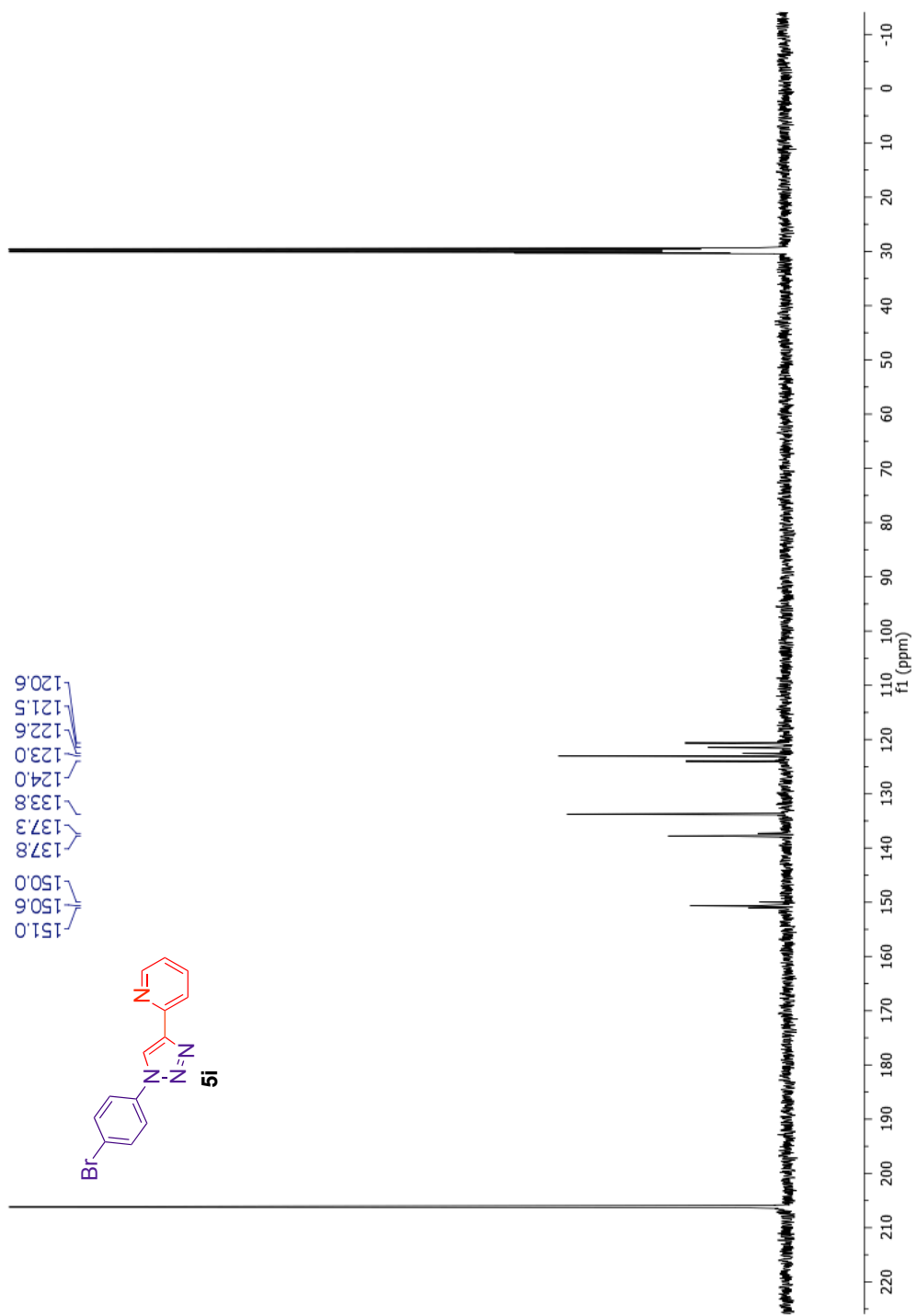


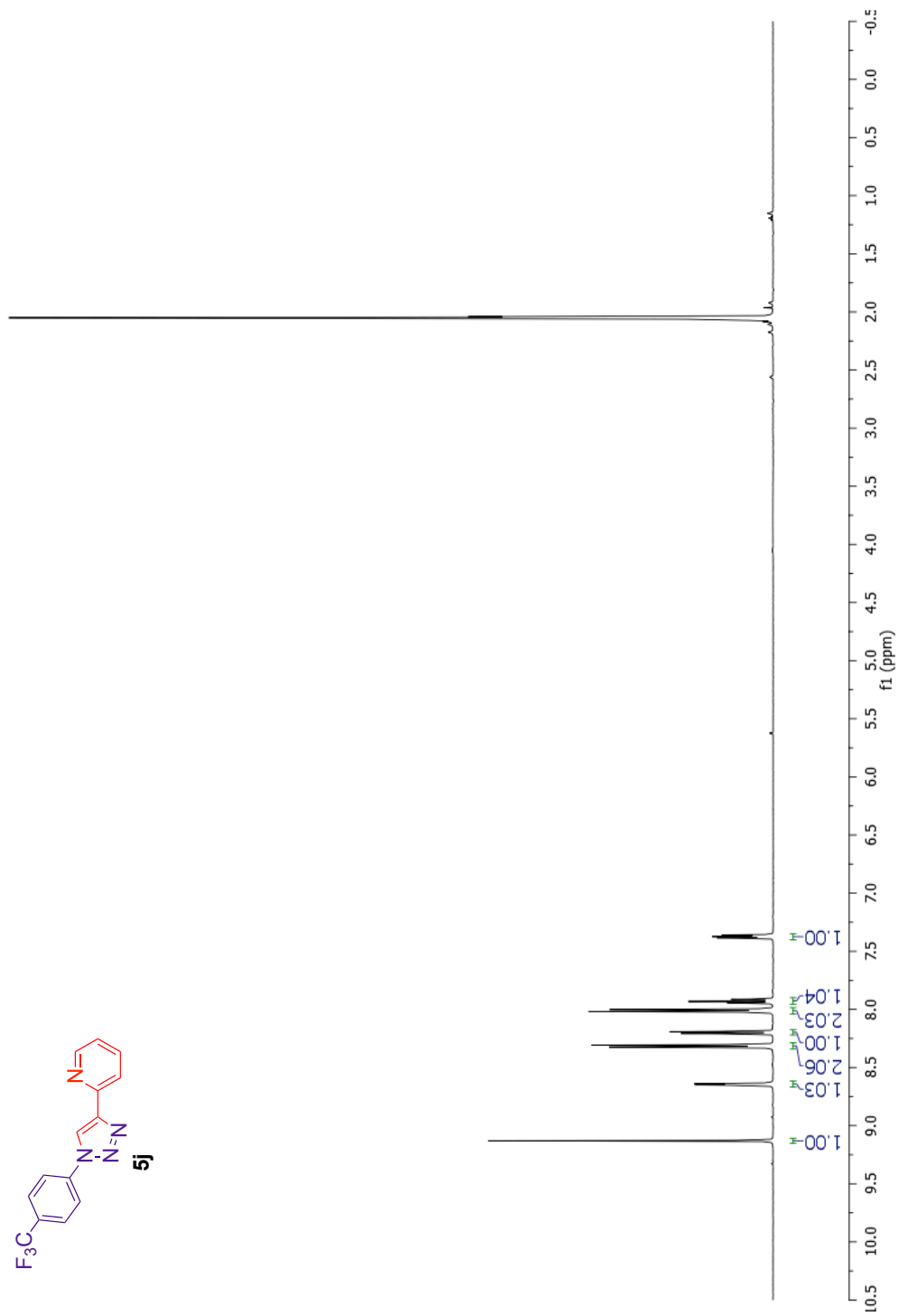
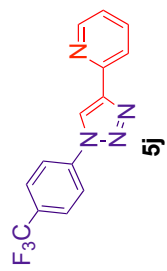


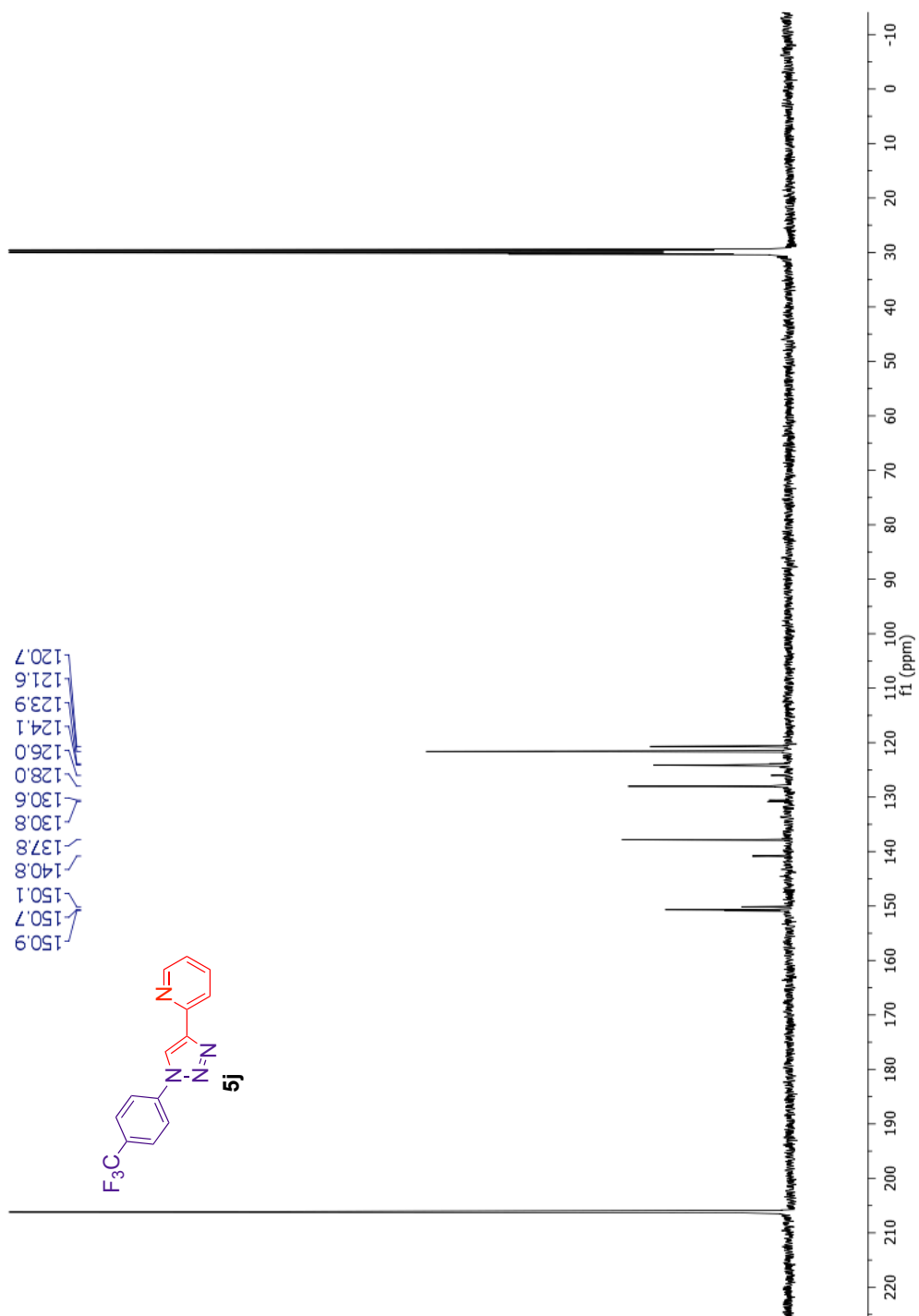


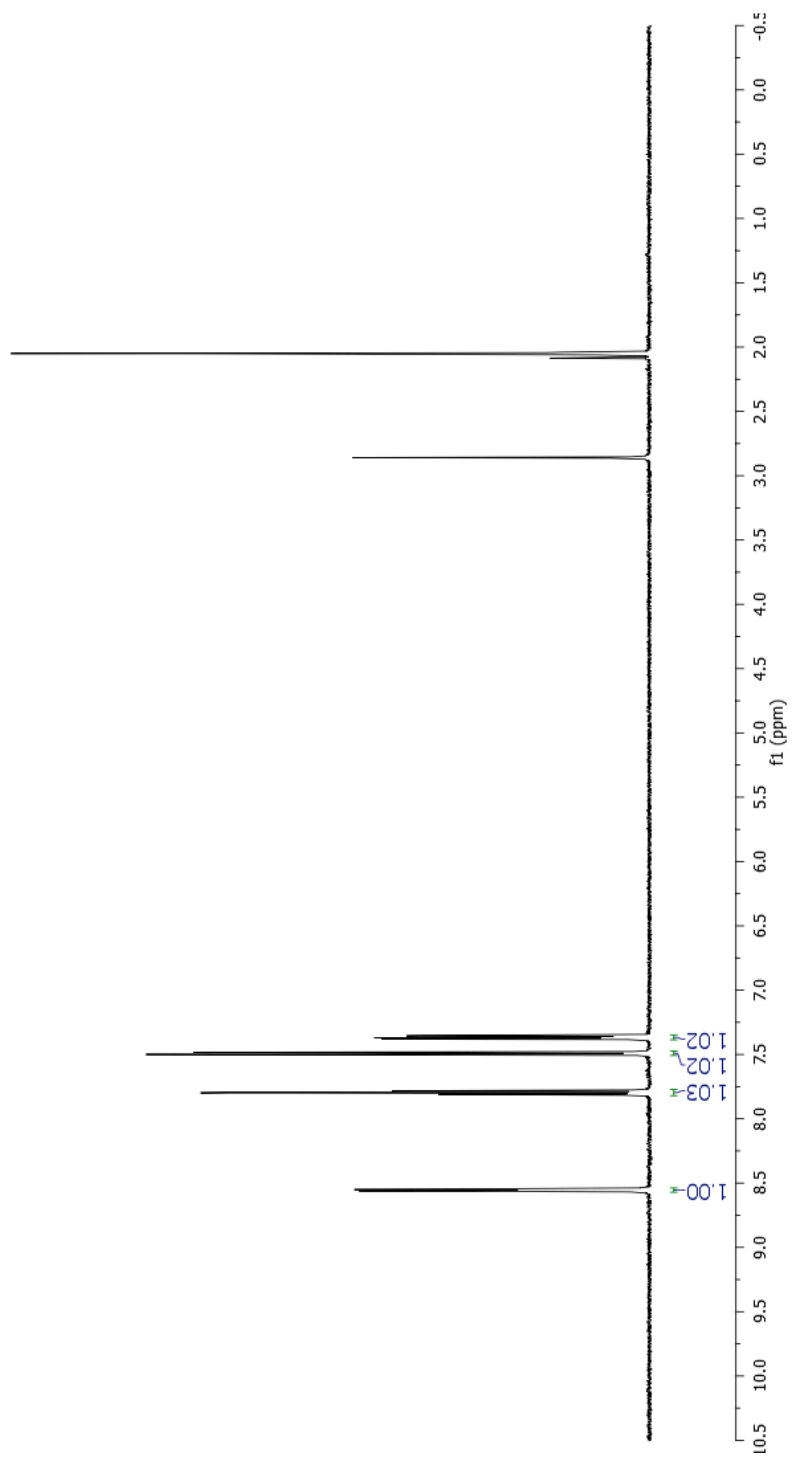
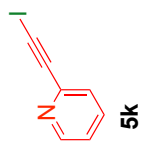


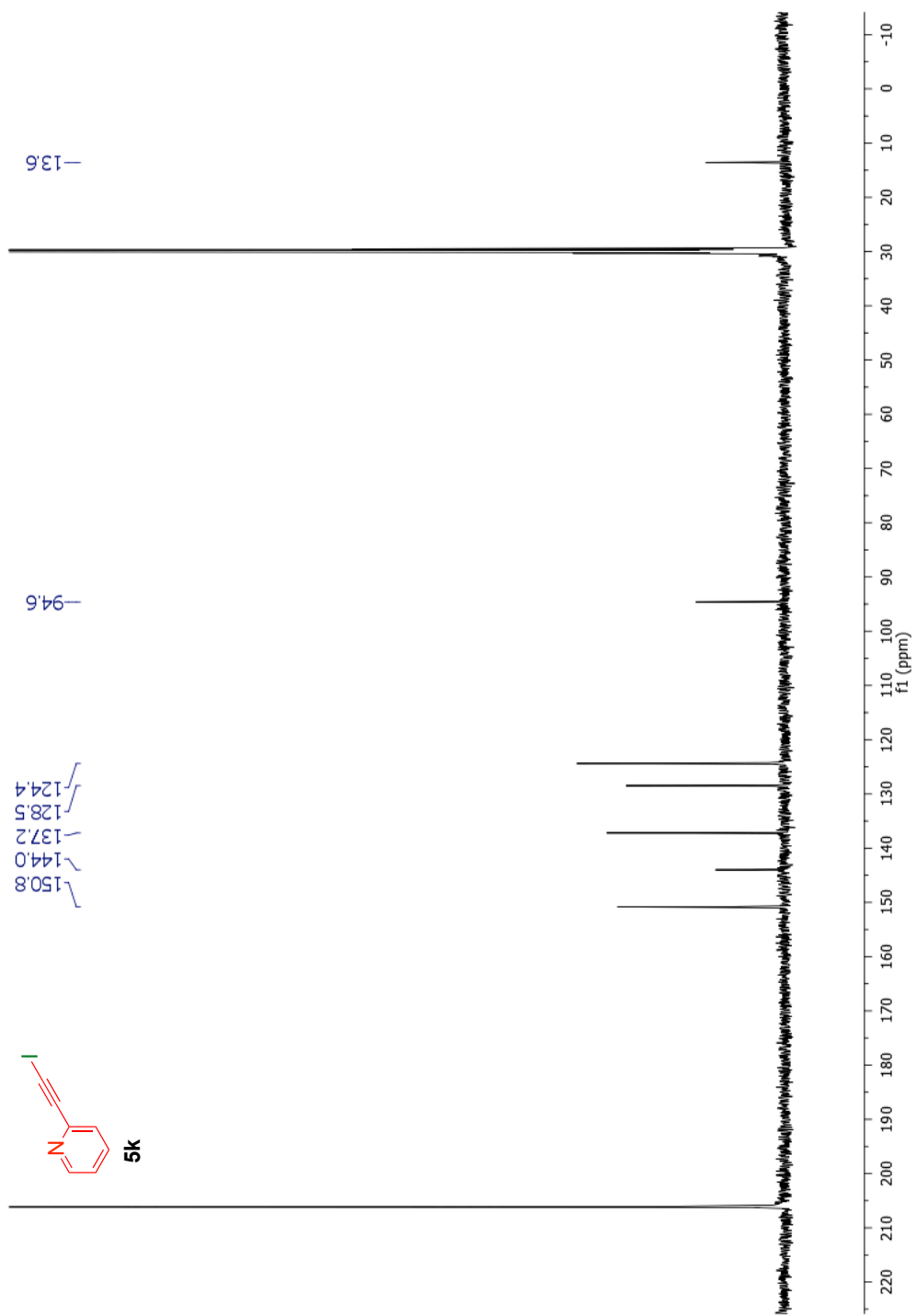


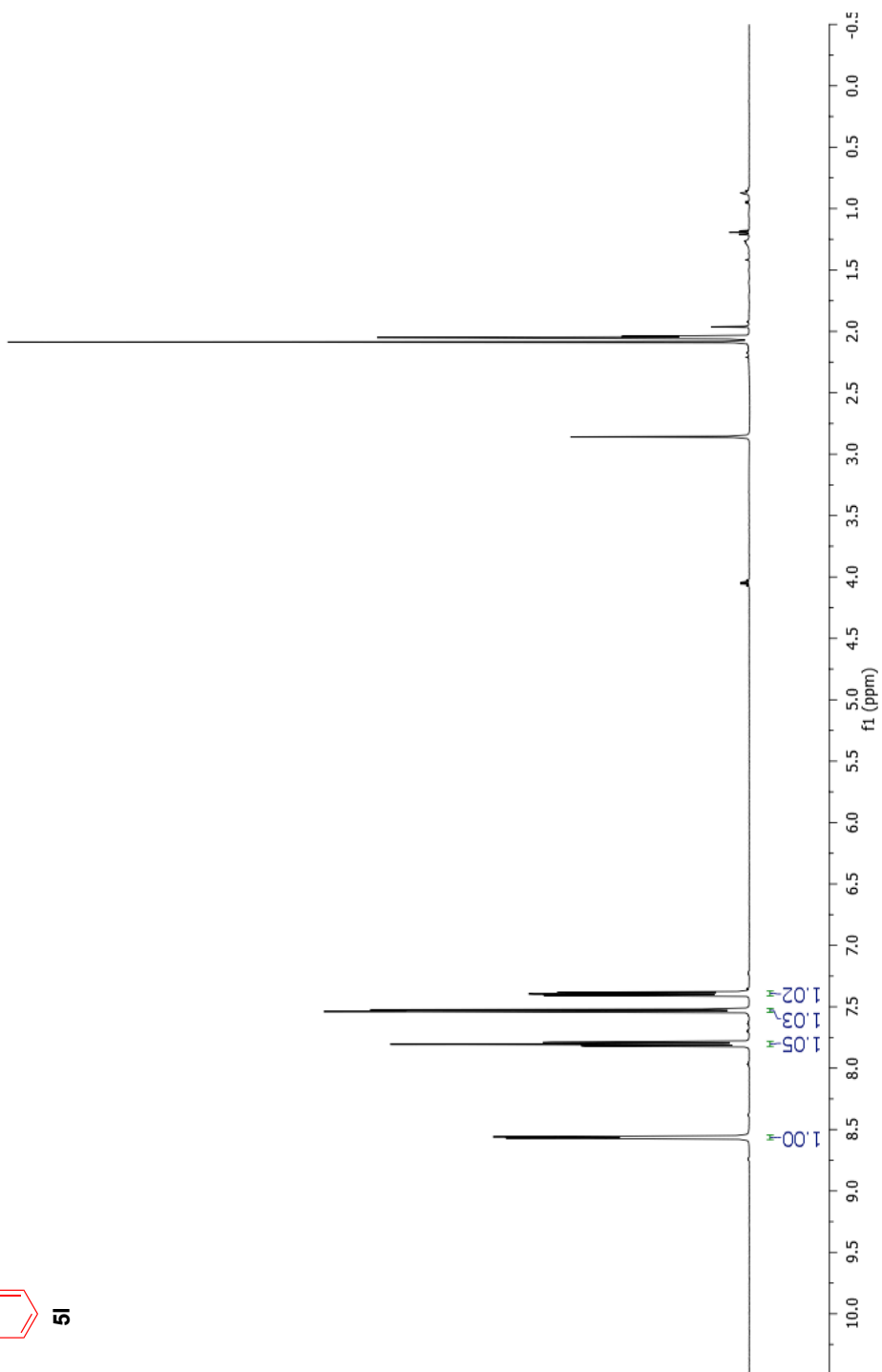
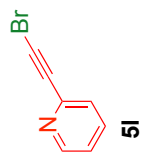


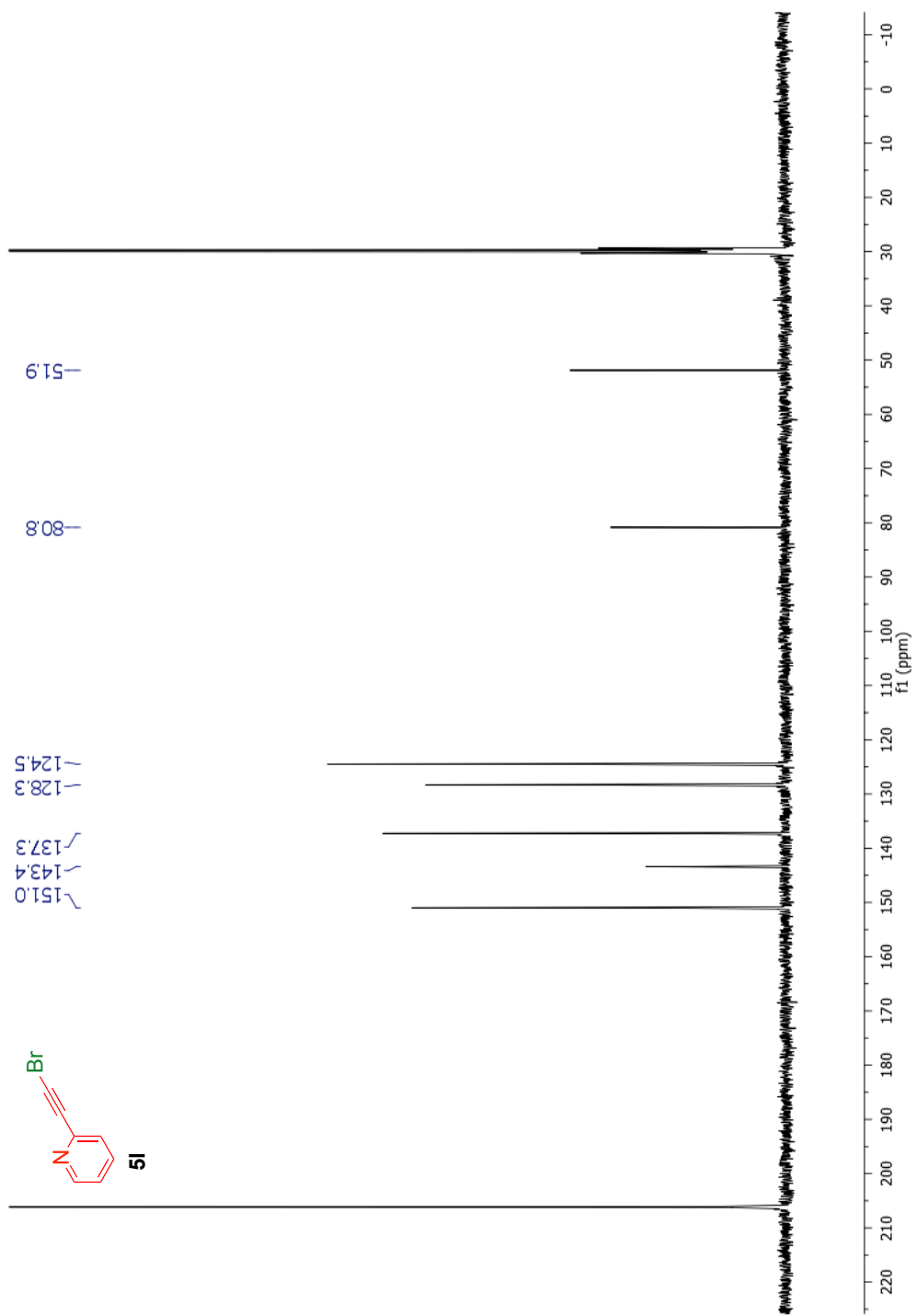


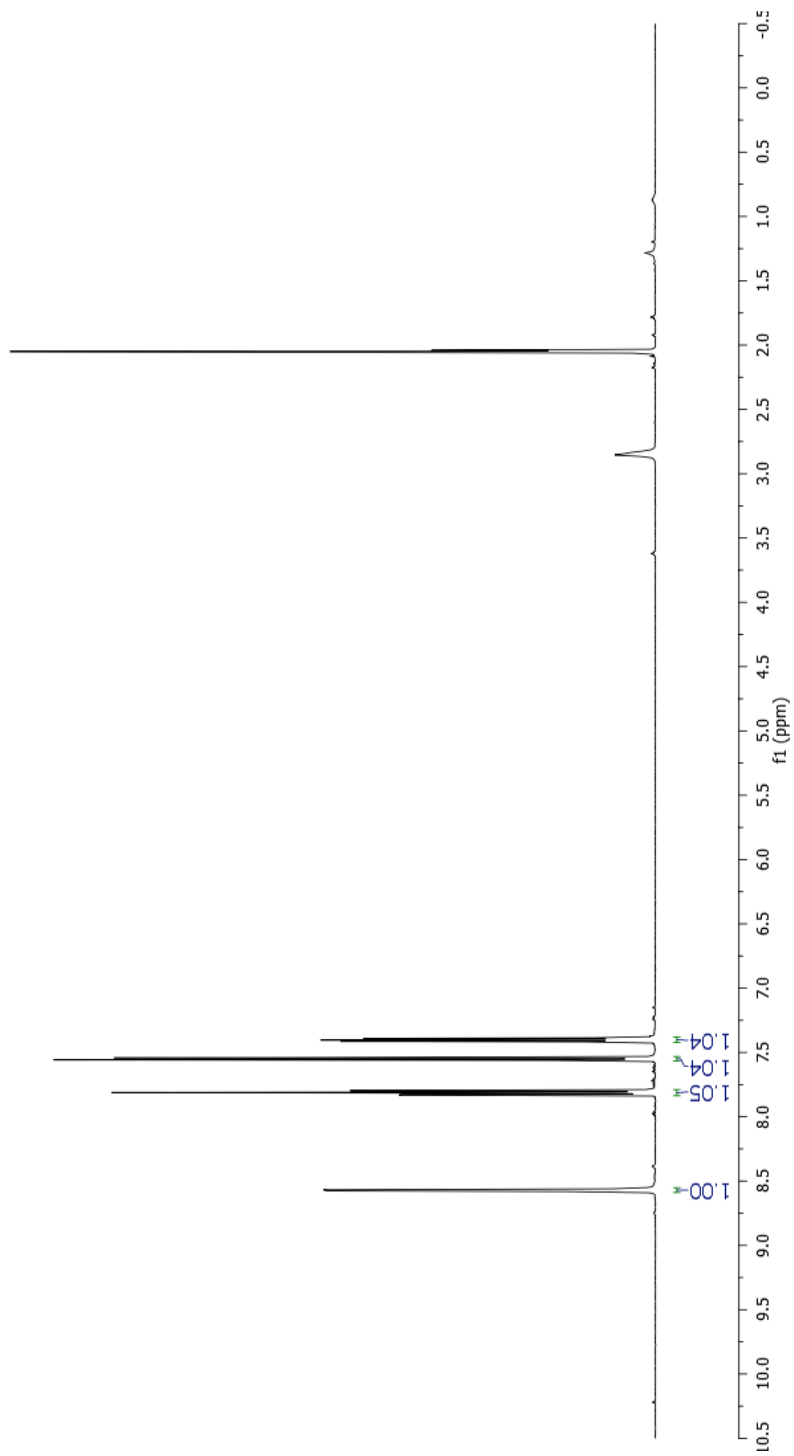
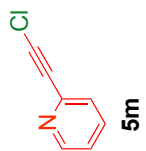


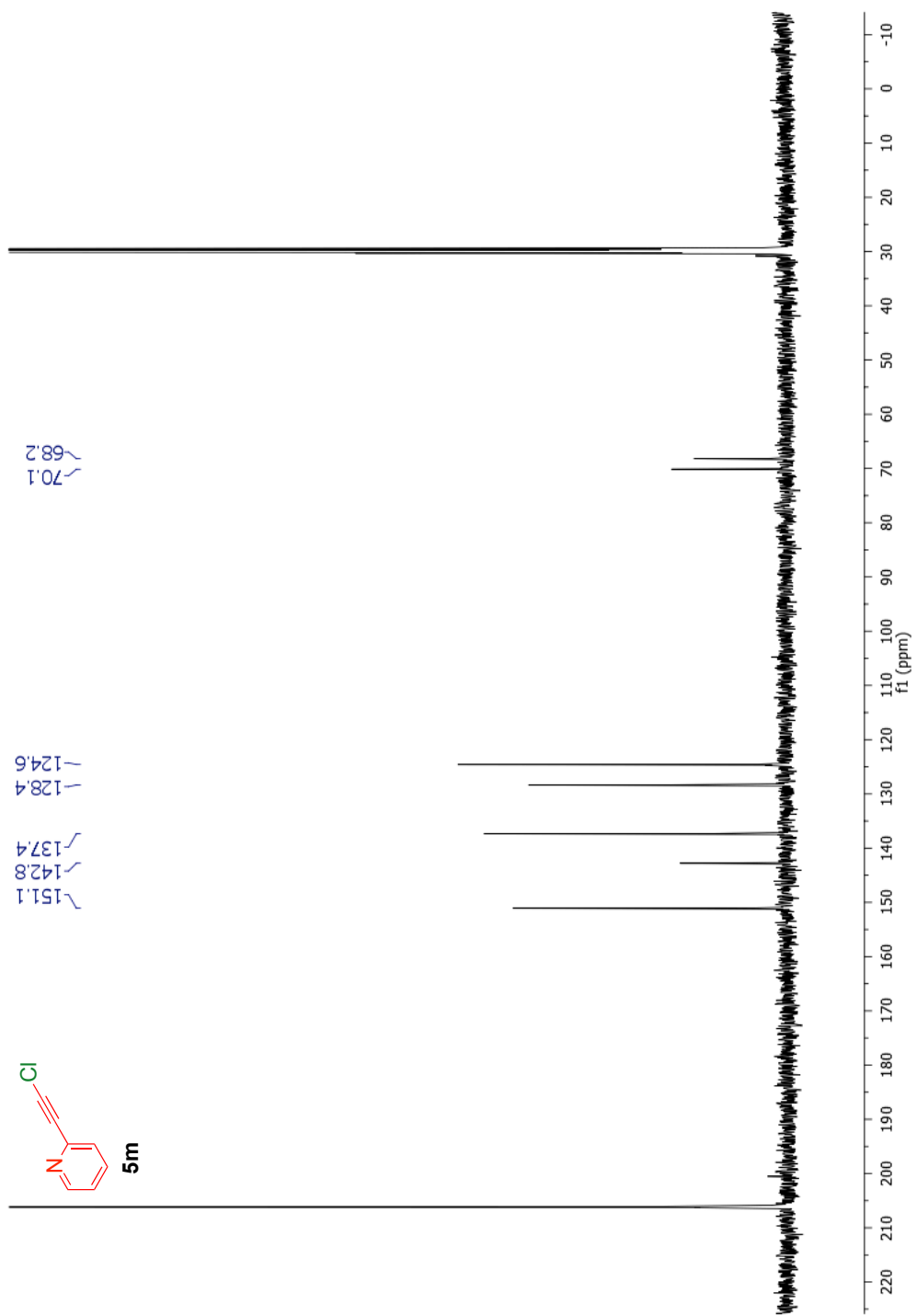


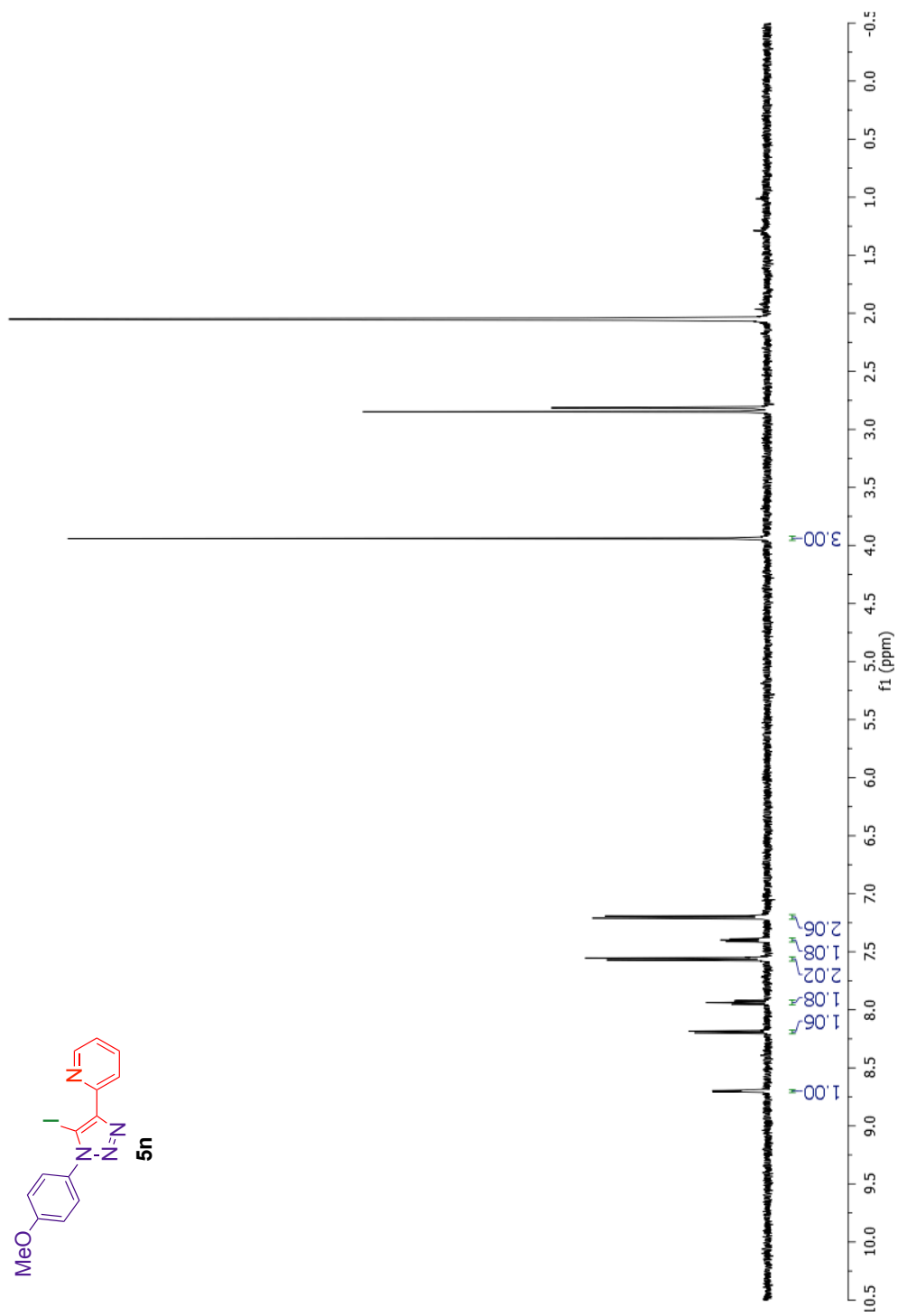
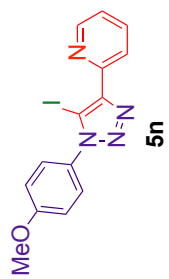


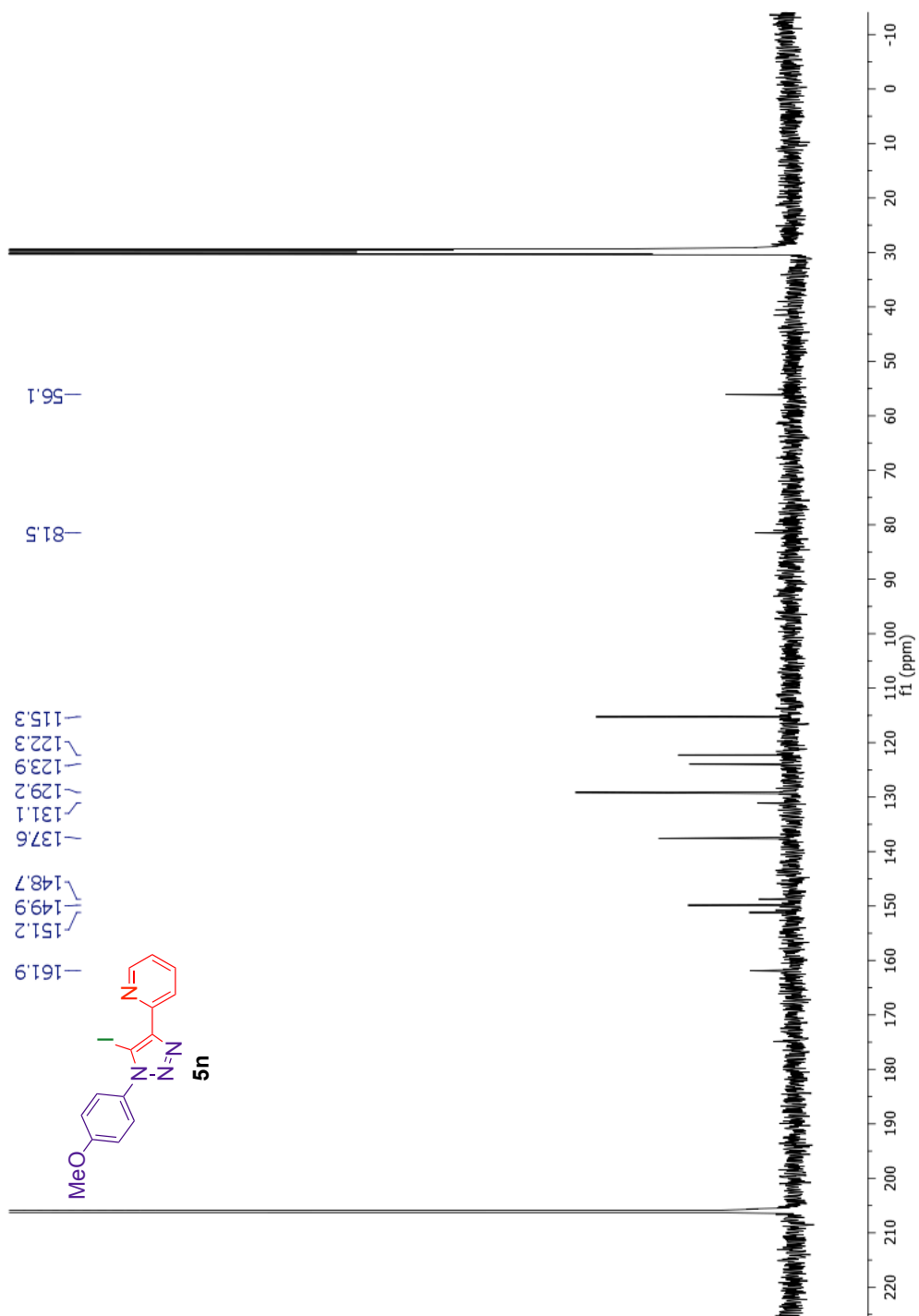


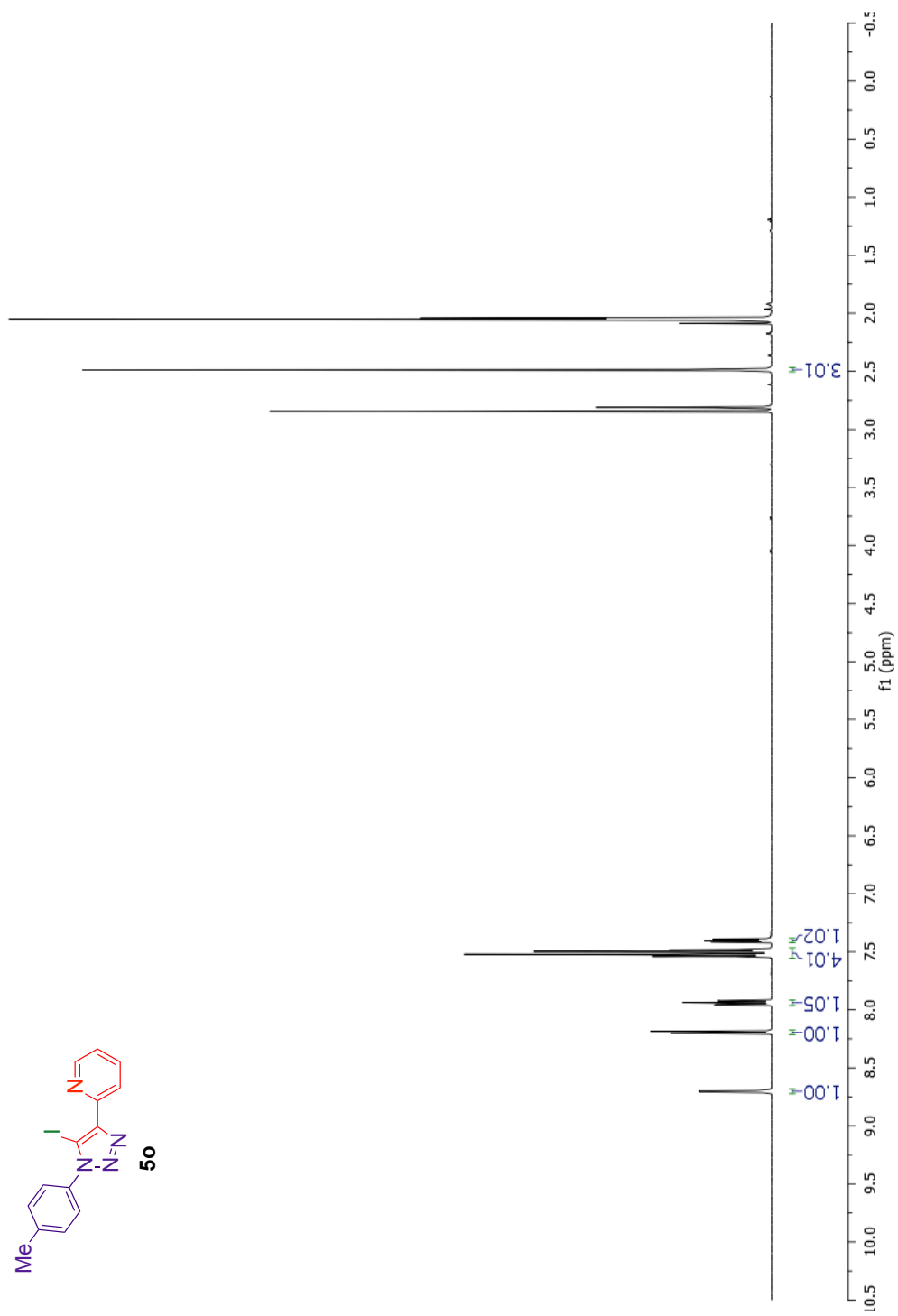
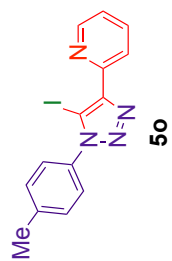


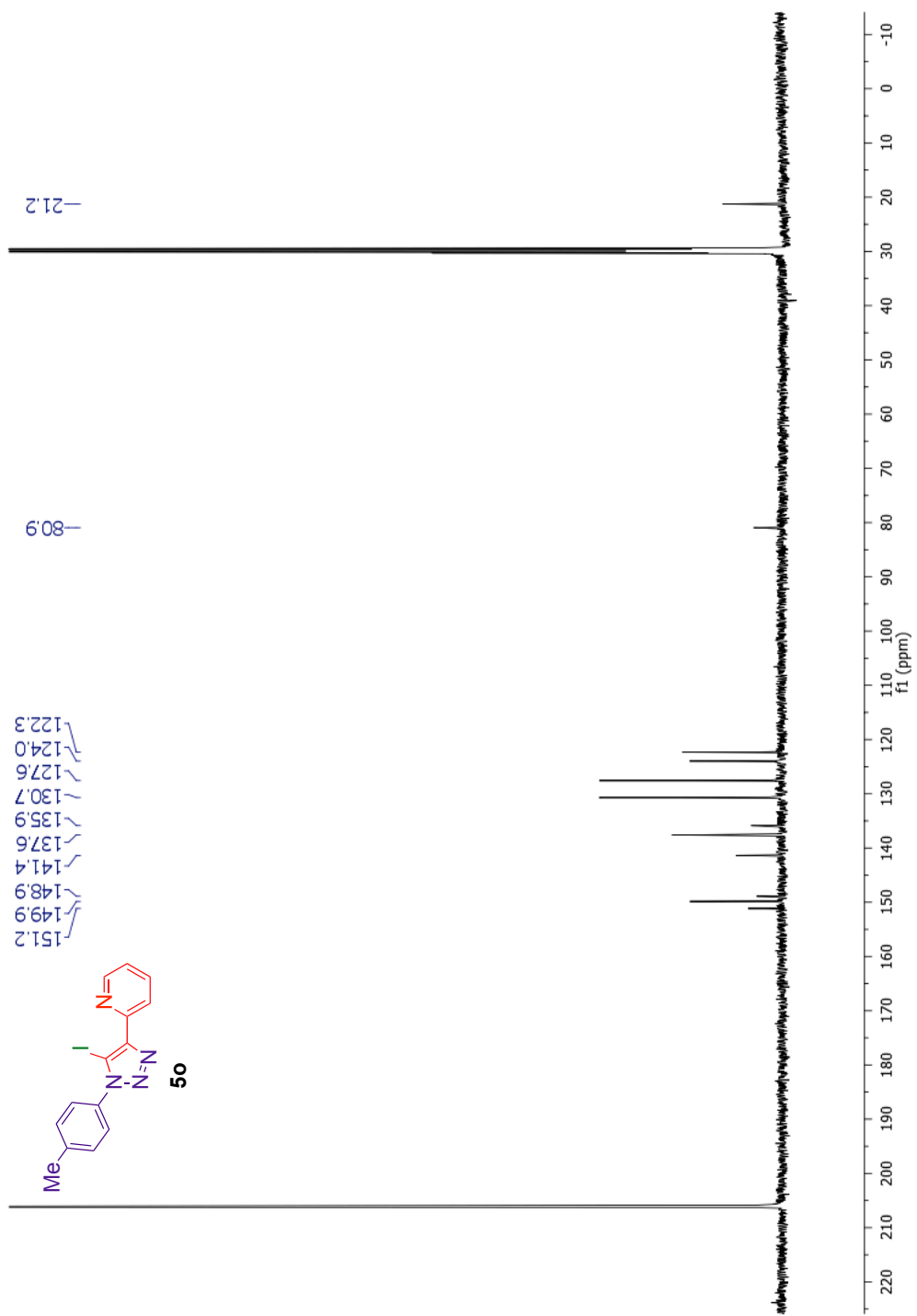


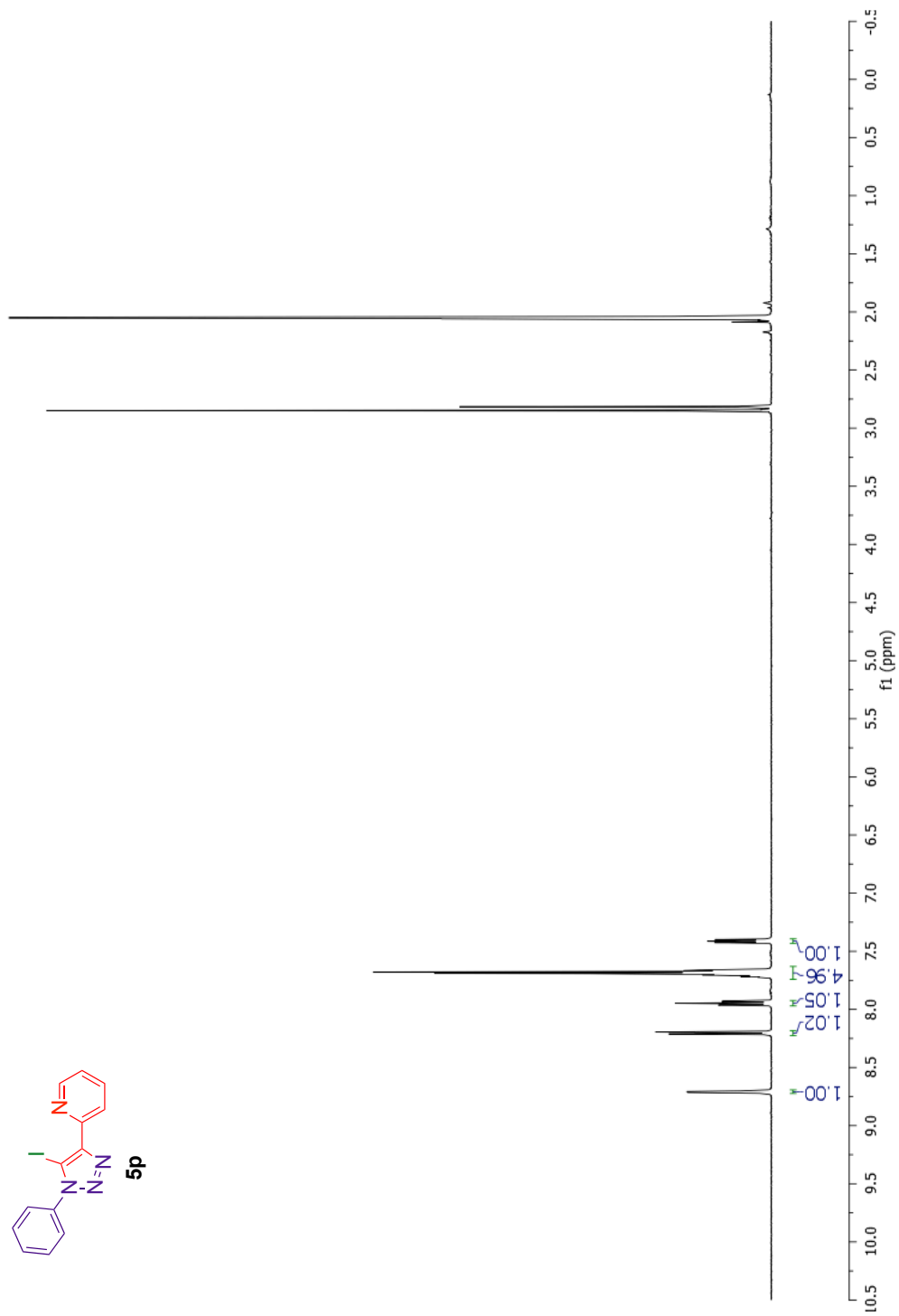
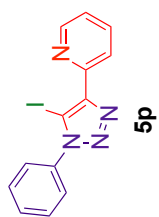


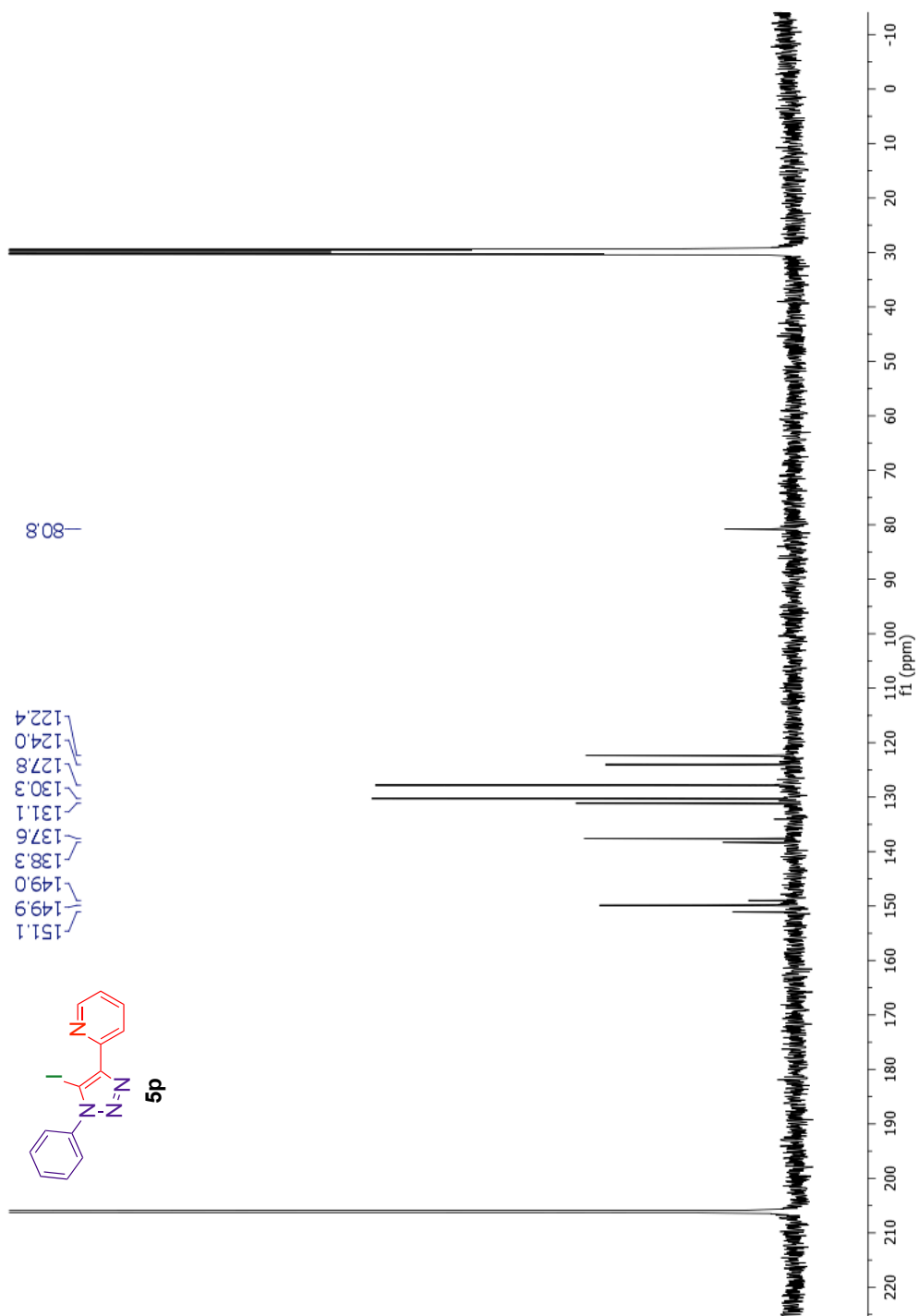


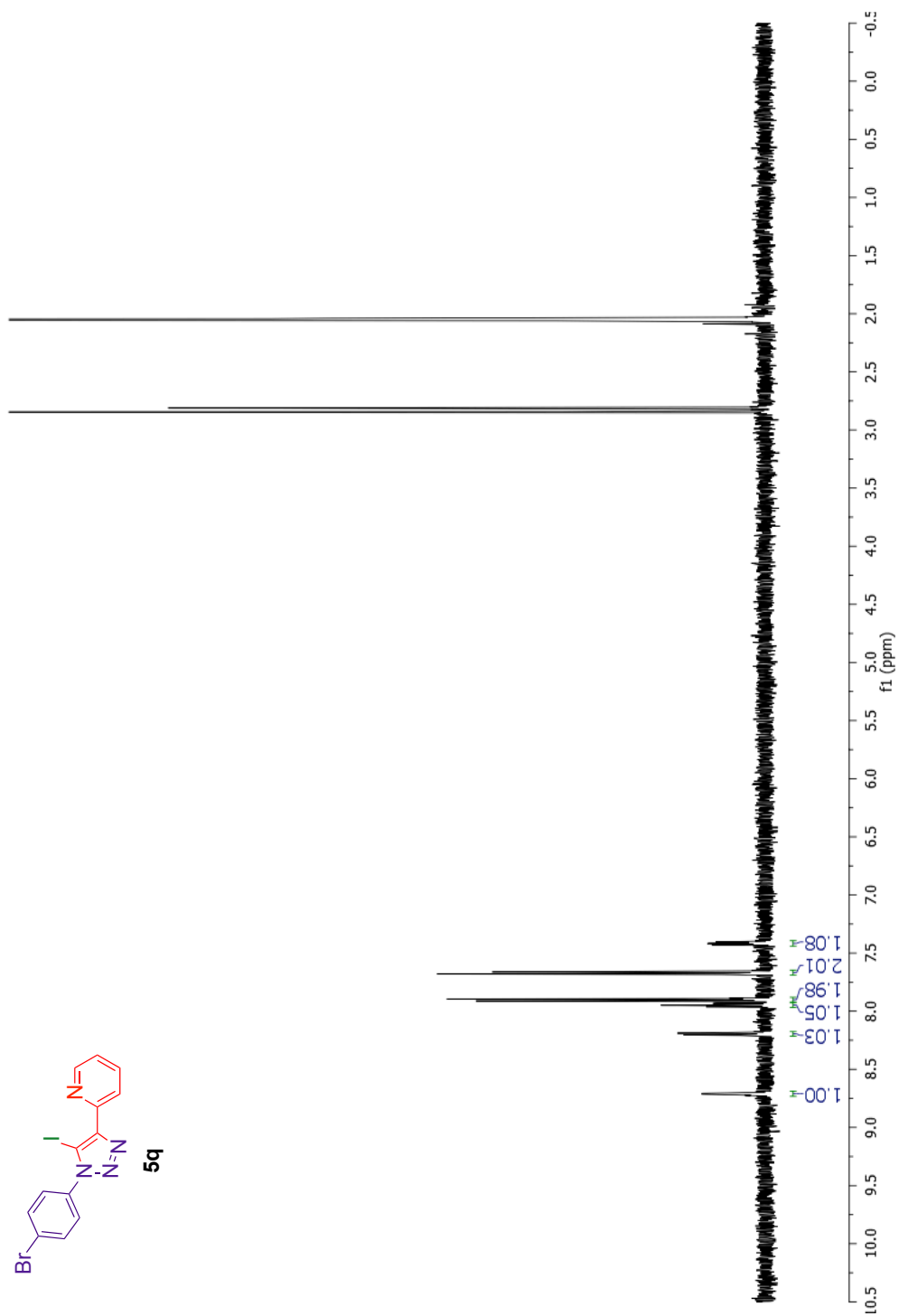
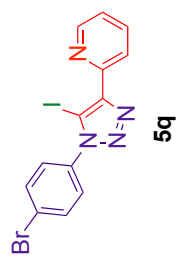


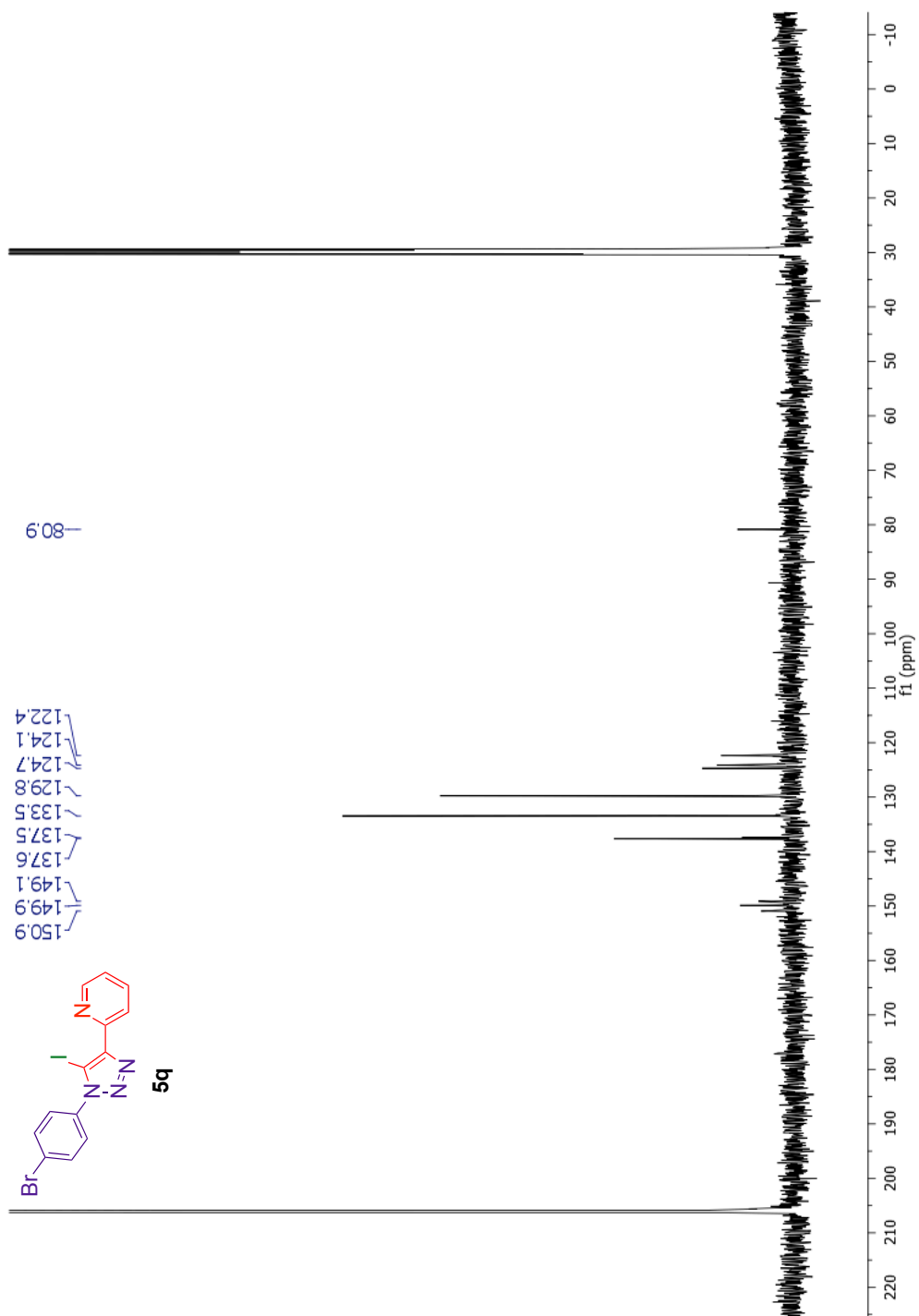


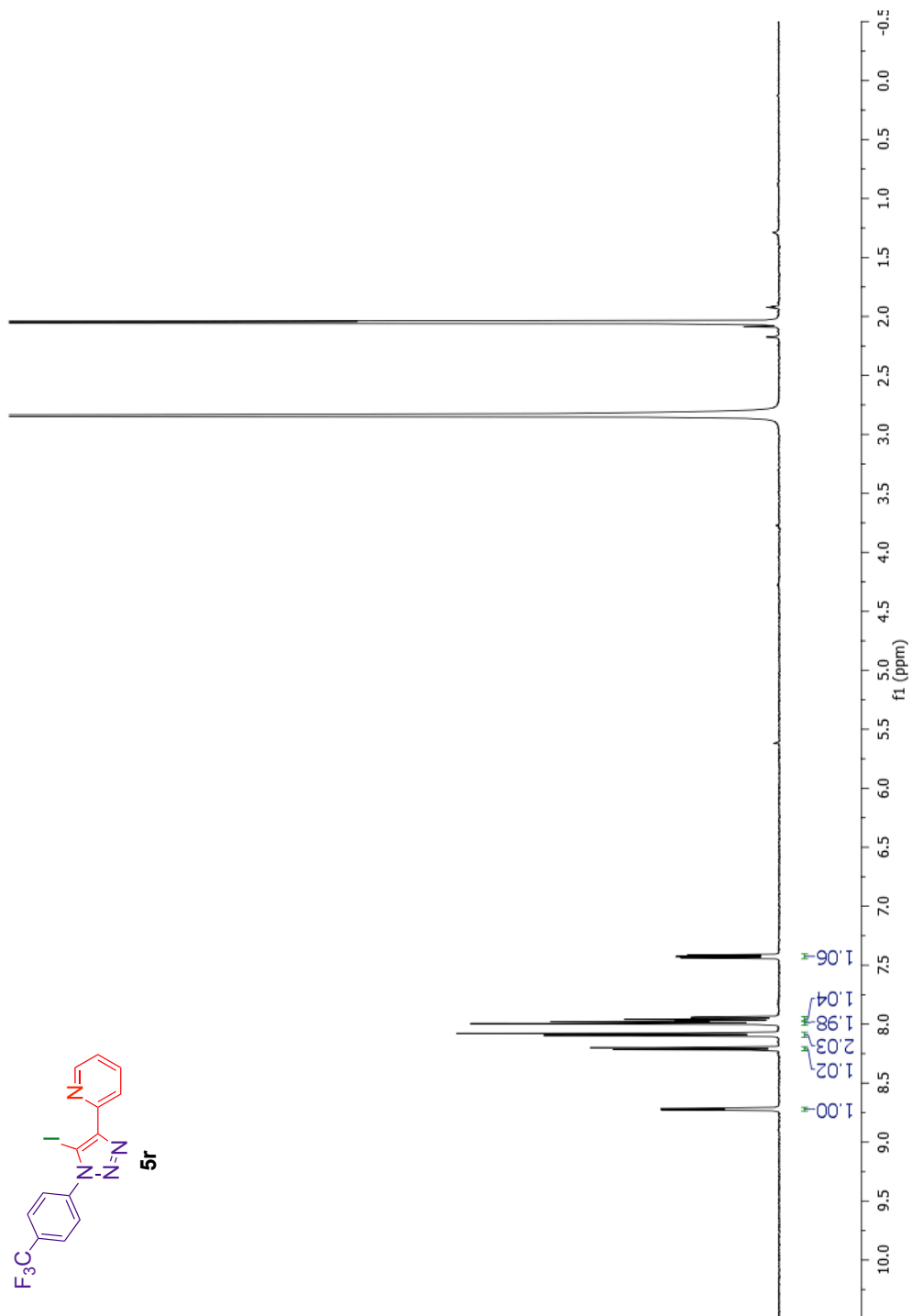
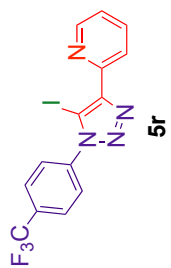


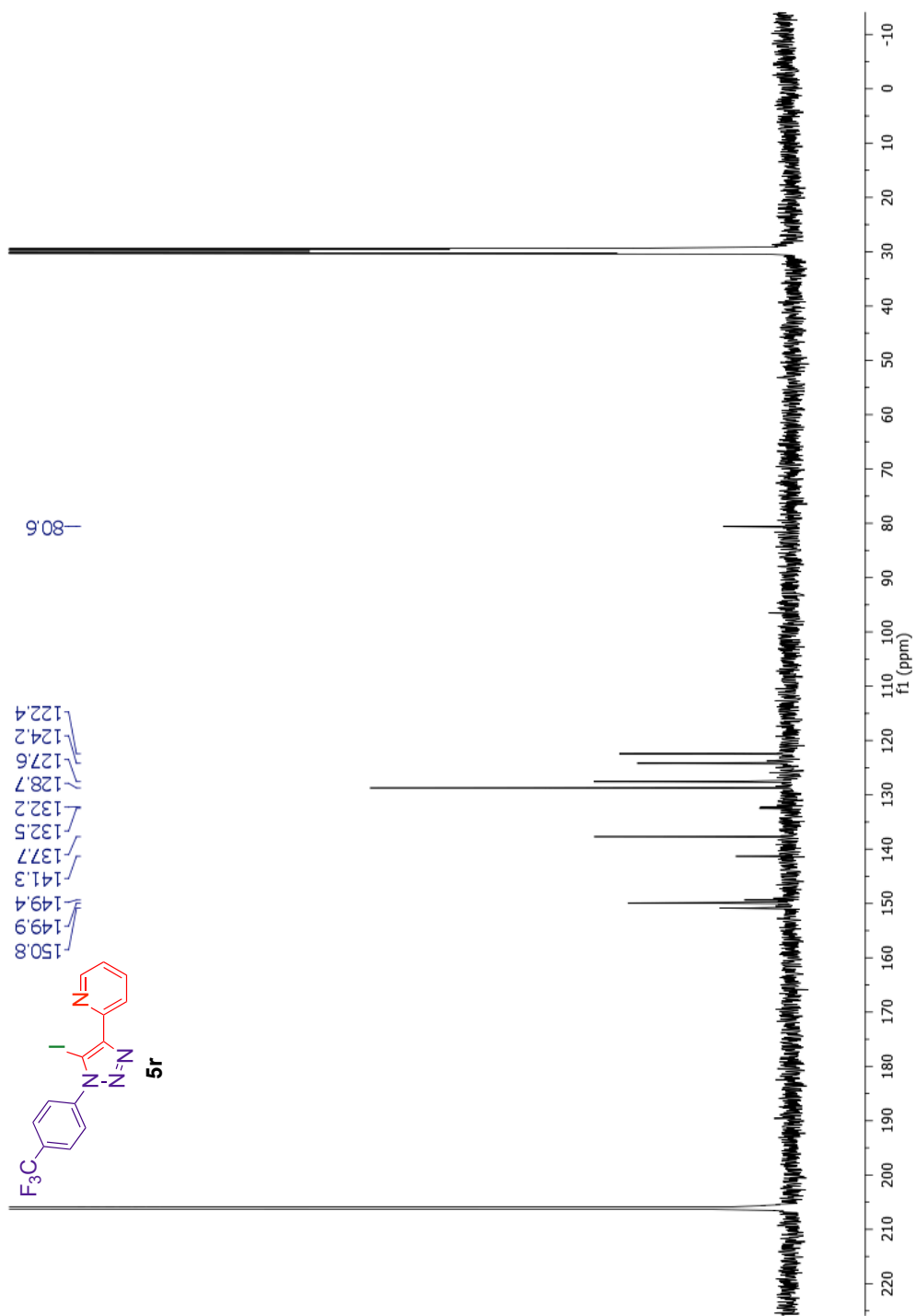


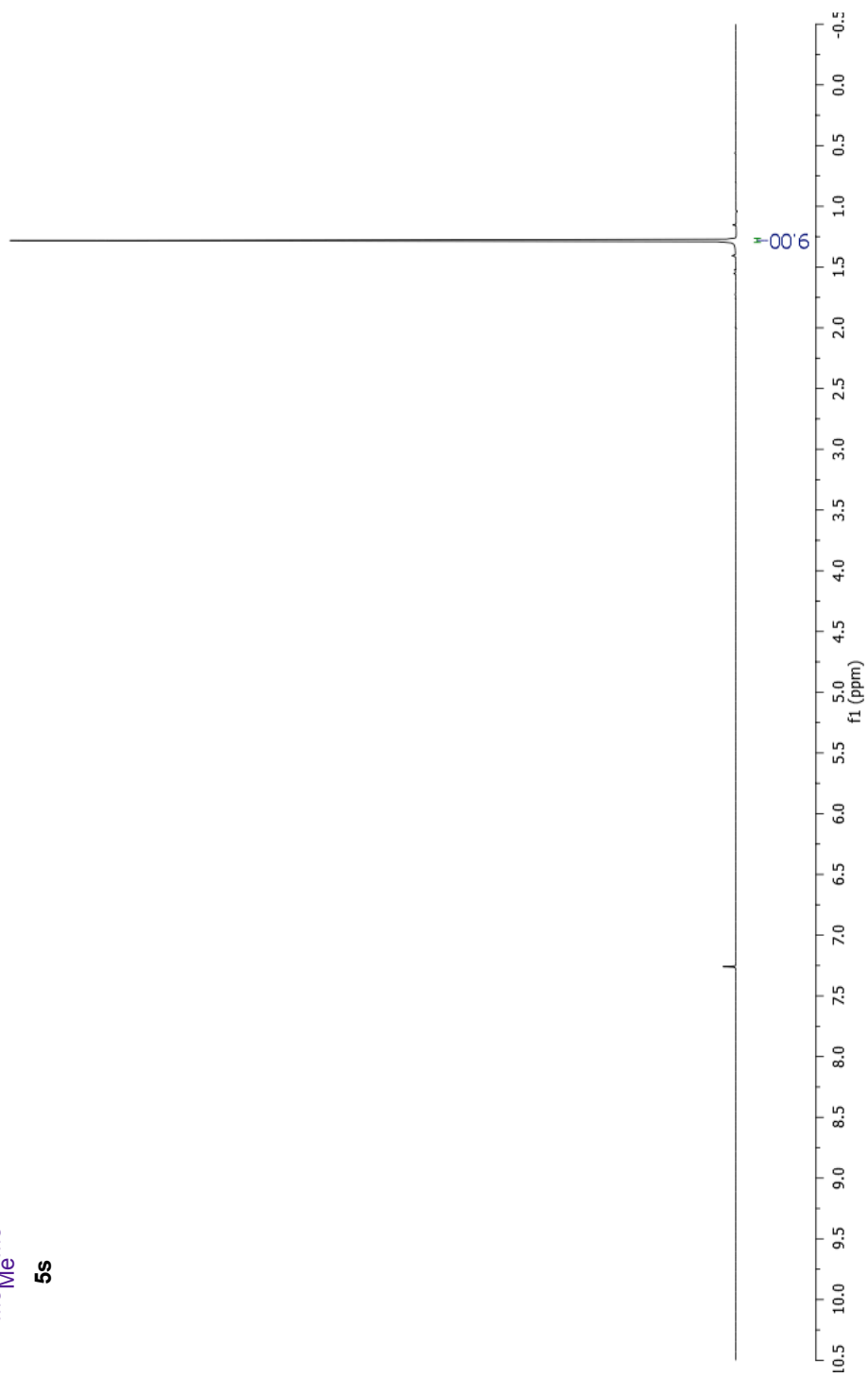
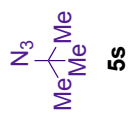


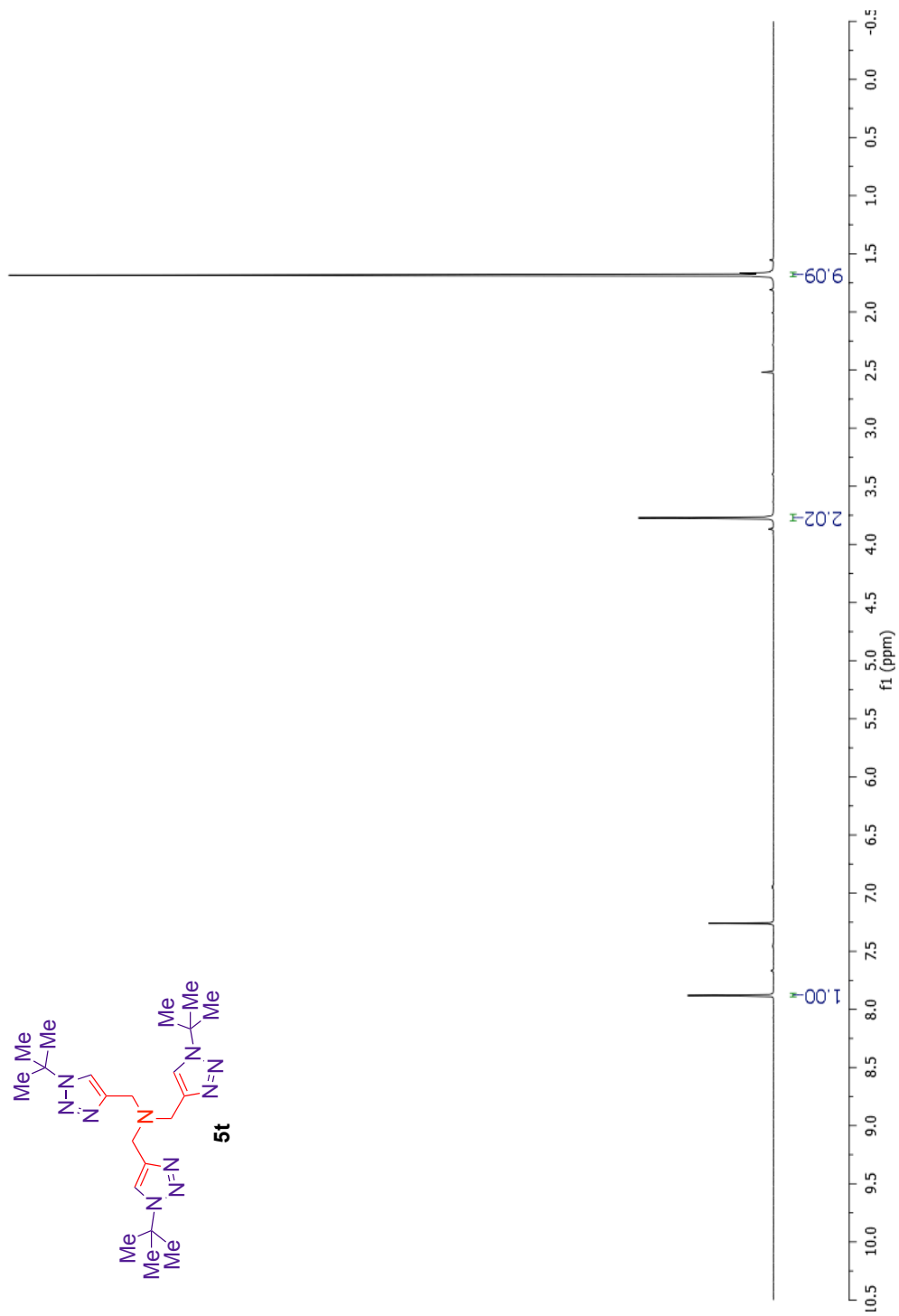
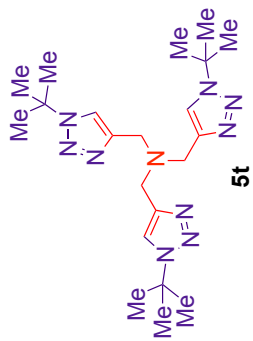


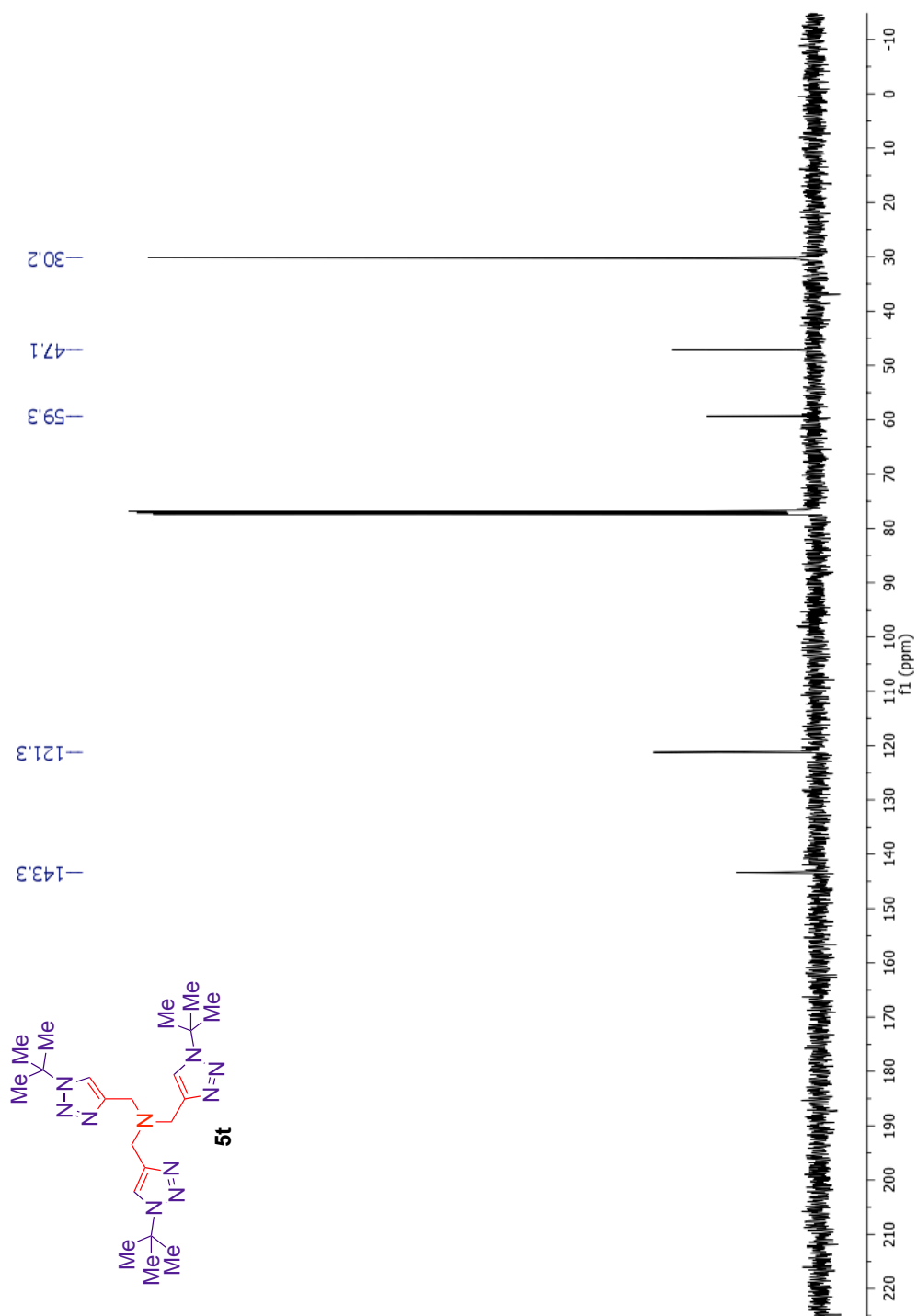


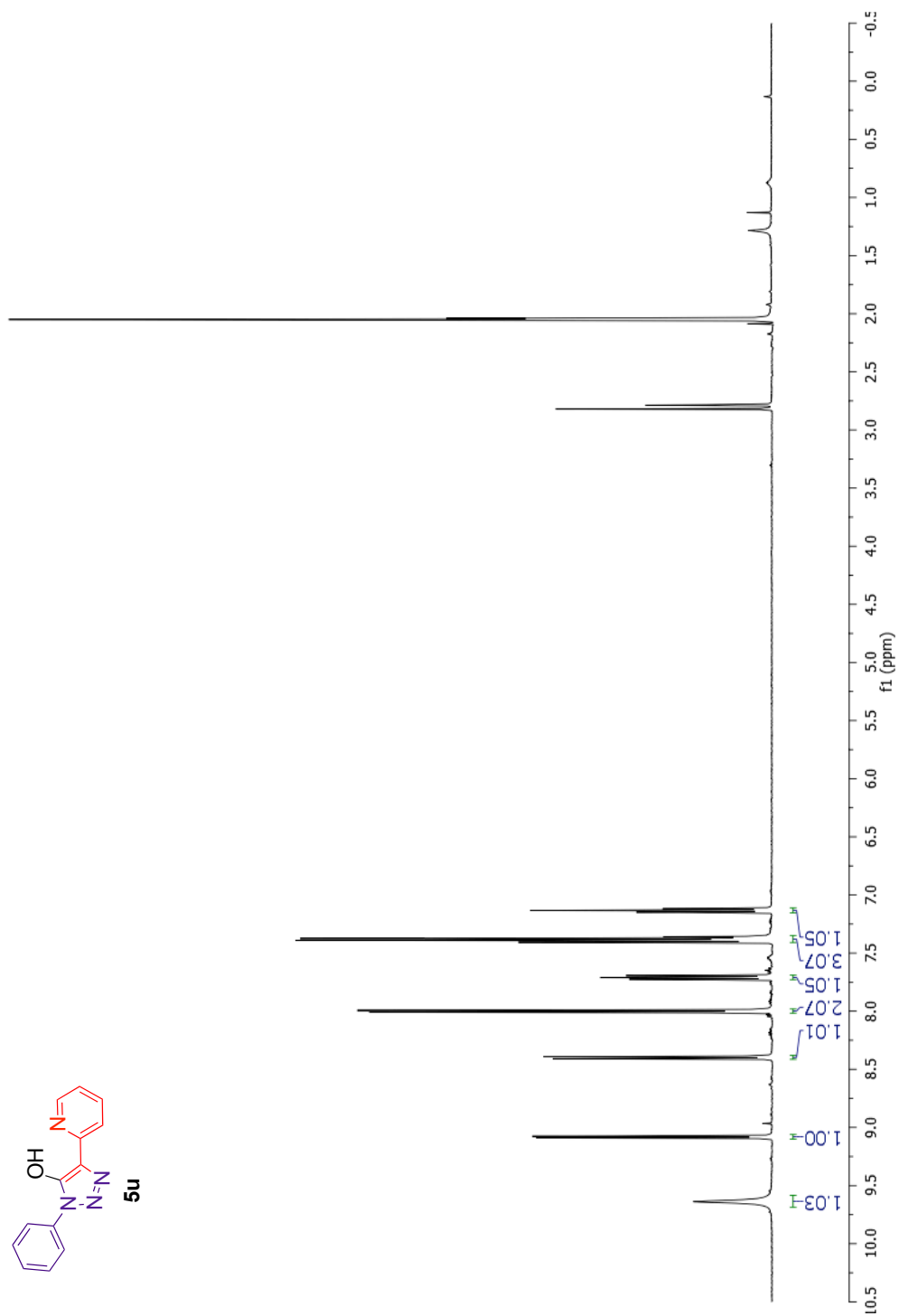
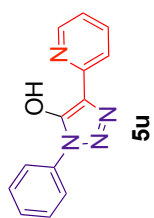


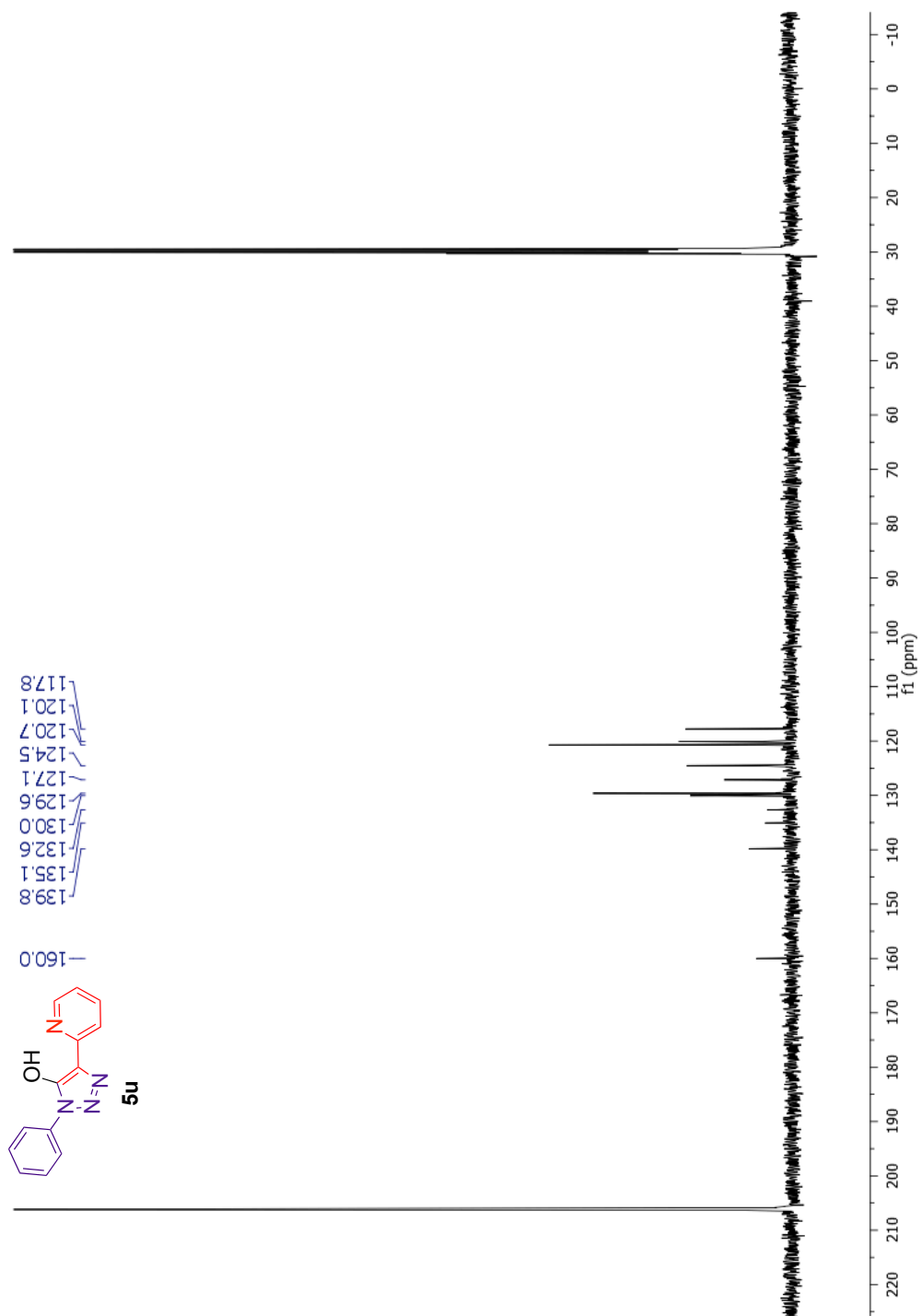


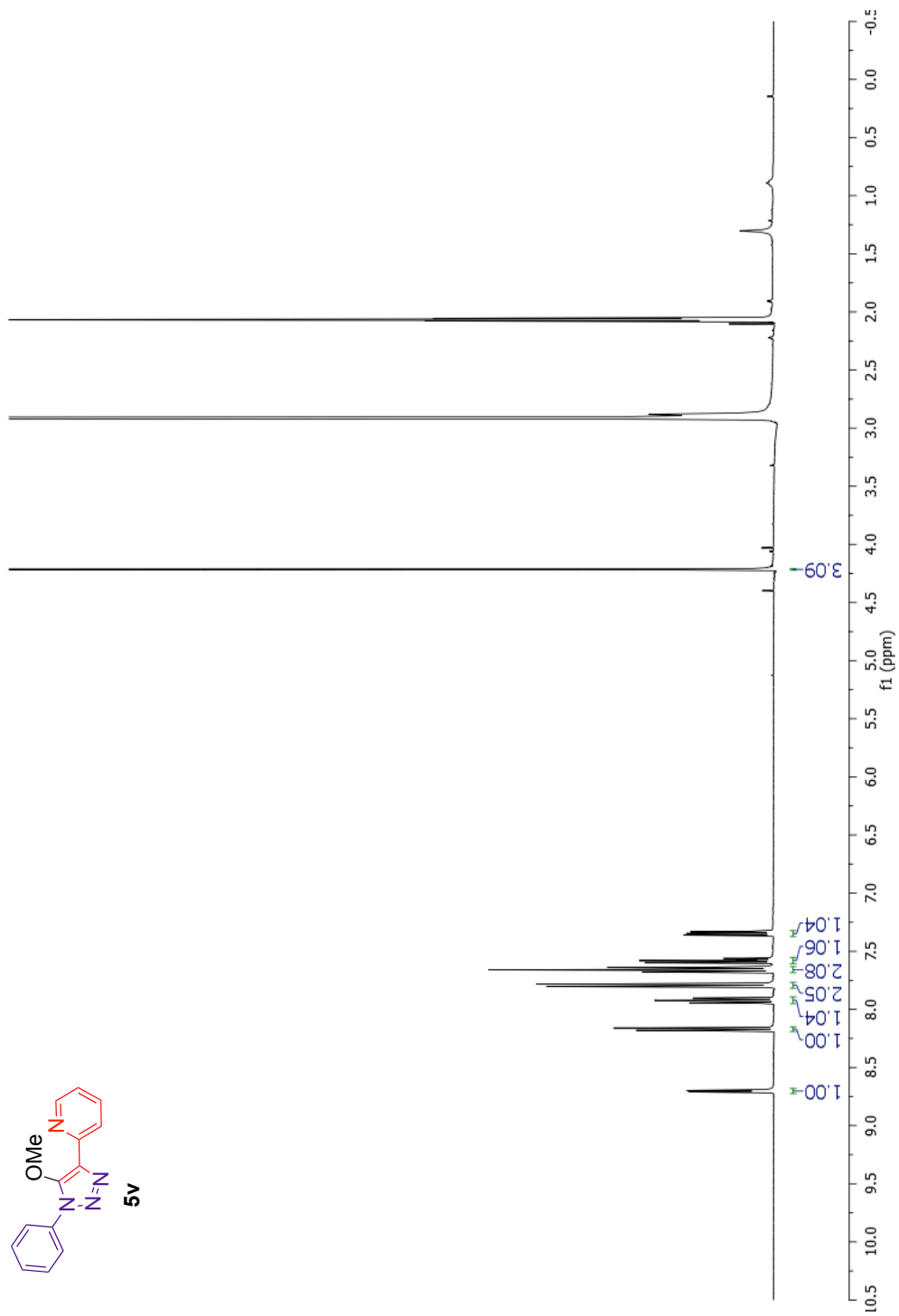
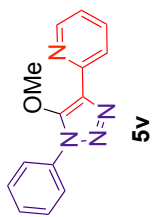


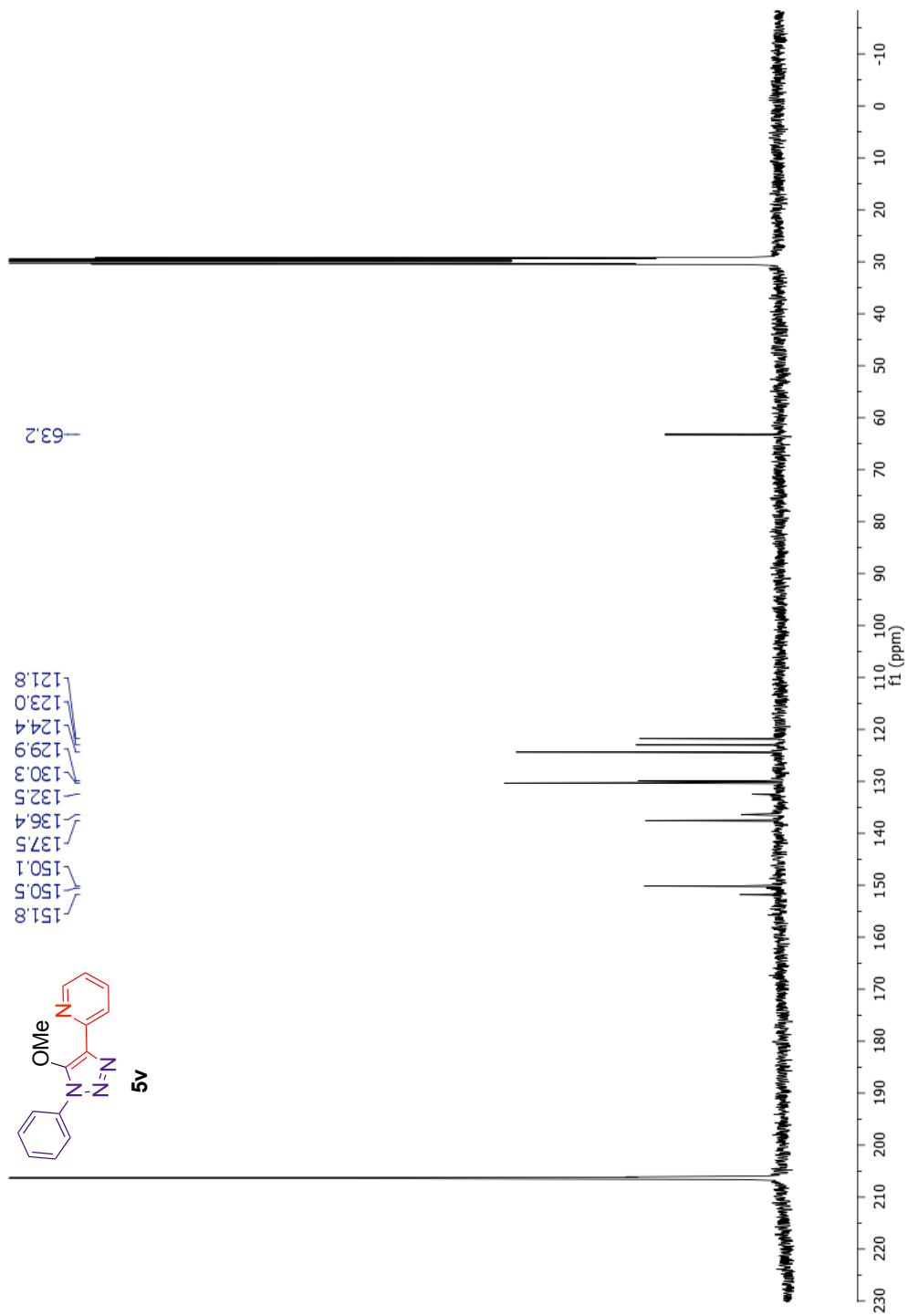


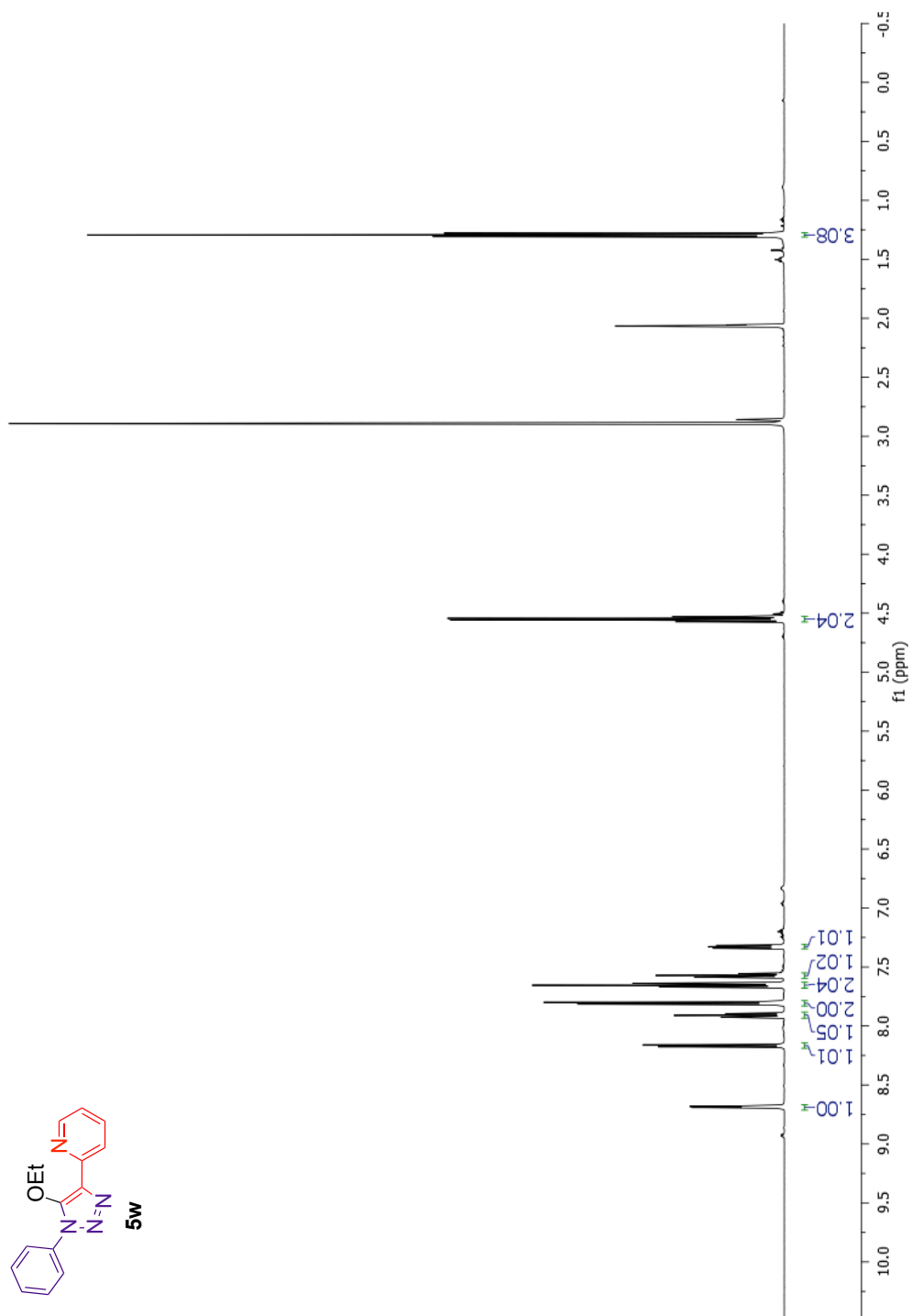
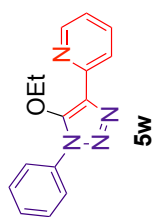


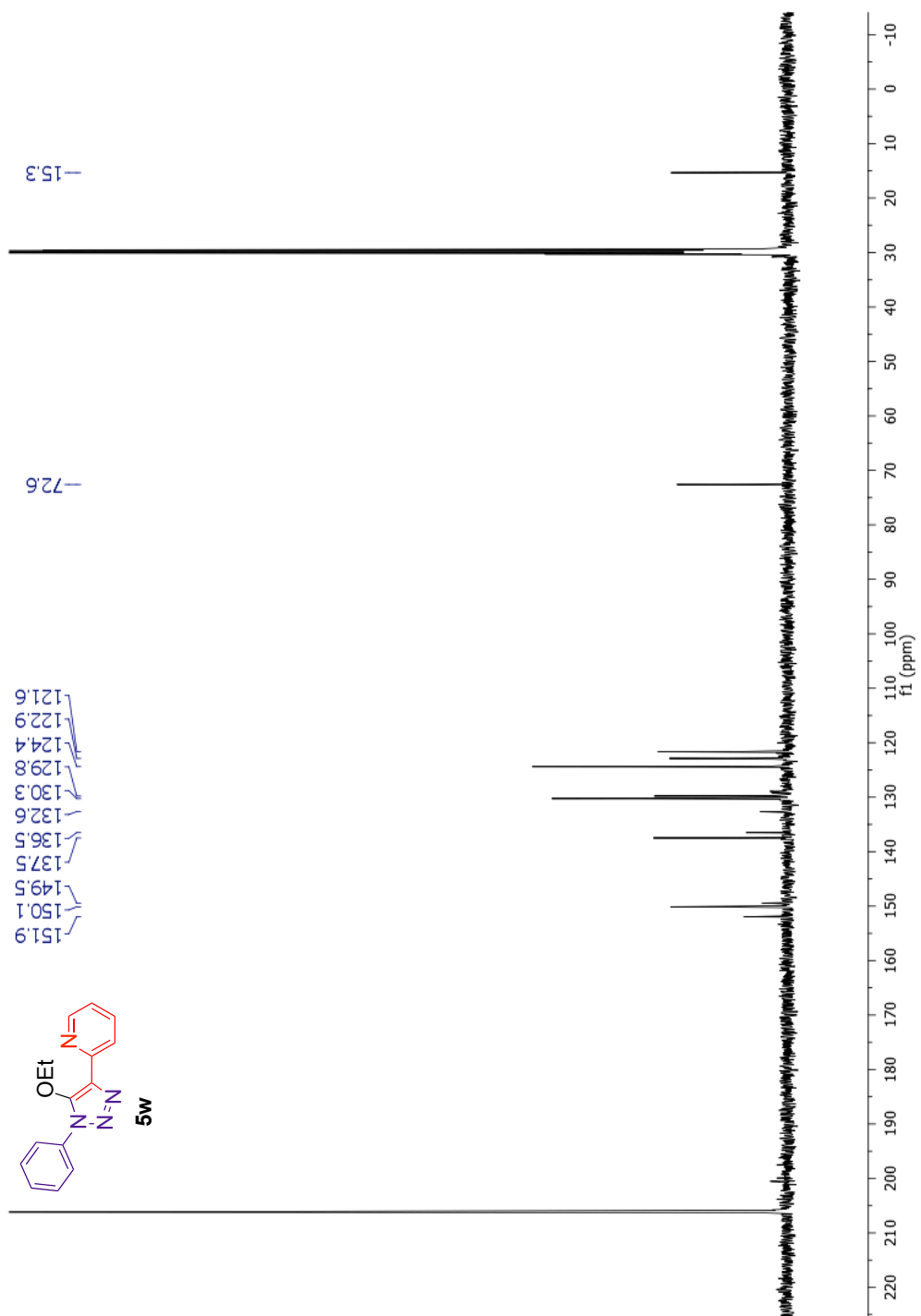


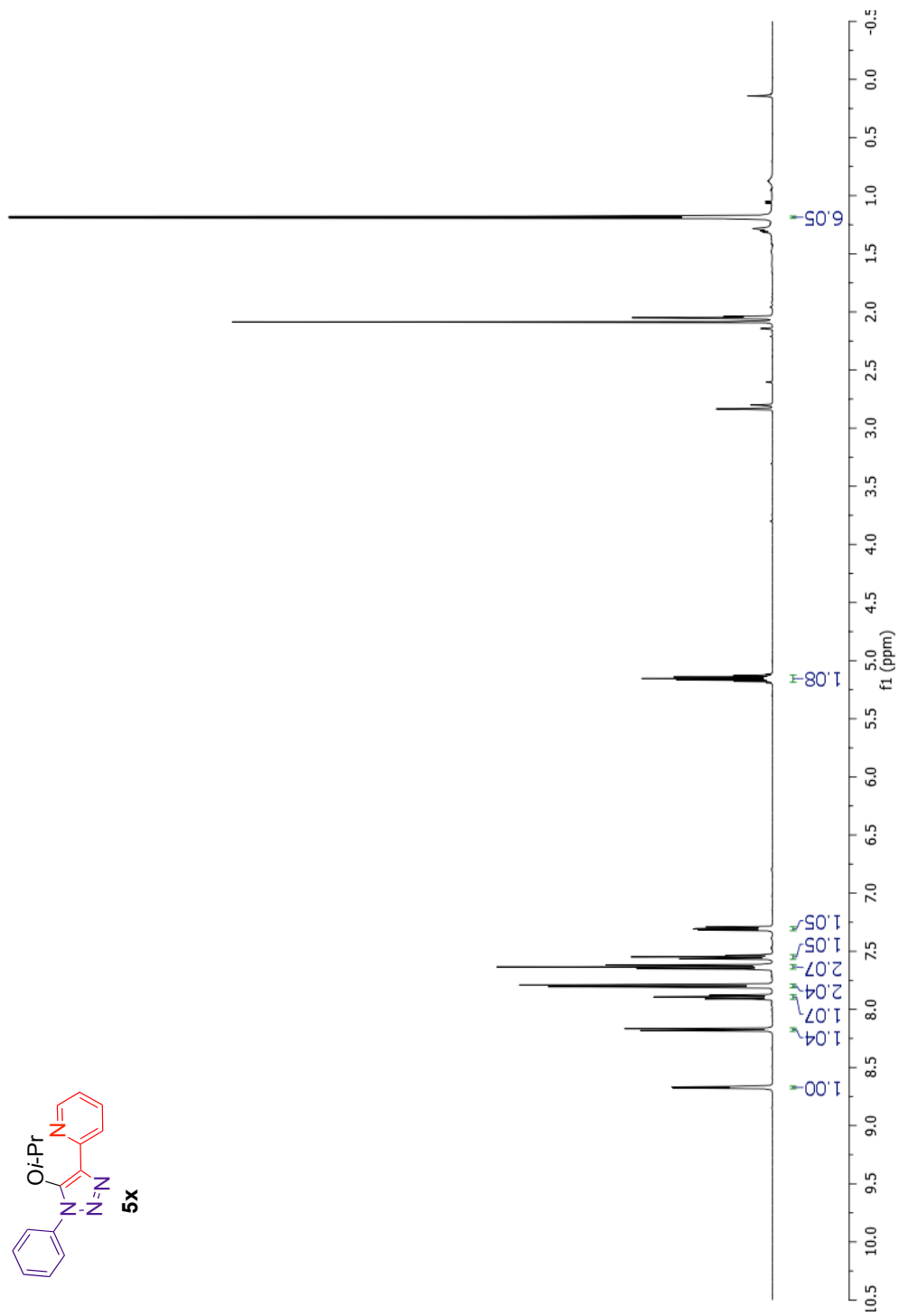
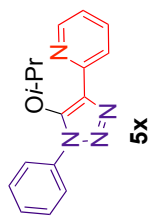


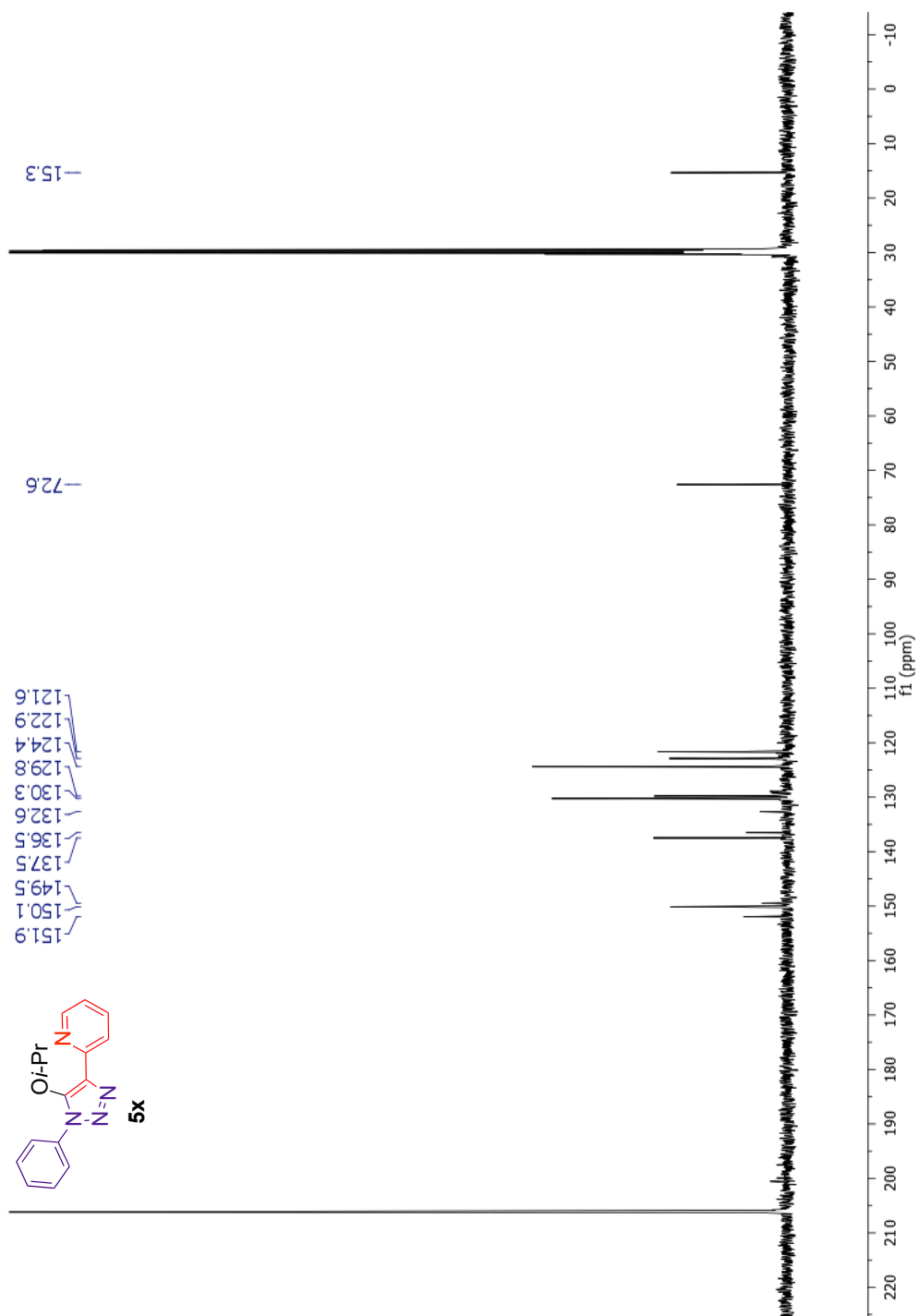












Chapter Six: Pyridyl Triazole Complexes with Platinum and Palladium

6.1 Introduction:

The synthesis and analysis of metal complexes with potential biological activity continues to be a developing field and one that has received a great deal of support in recent decades. With the resistance limitations of current therapeutics such as cisplatin, many complexes have been identified with different biological behavior and equivalent or higher potential to kill cancerous cells.¹⁻⁵ This chapter is focused on the utilization of 2-pyridyl triazoles (PyTri) to form complexes of type ML and ML₂, where M represents a metal center (Pt or Pd) and L represents PyTri ligands. In addition to their biological relevance the complexes containing palladium centers are known to have potential as active catalysts in organic transformations. The synthesis of these PyTri complexes and their activity as catalysts are discussed herein.

6.2 Background on Pyridyl Triazoles as Ligands for Metal Complexes:

The design and synthesis of heterocyclic ligands continues to be at the cutting edge of modern coordination chemistry and is of high importance in the fields of metallo-pharmaceuticals,⁶⁻¹⁵ and catalysis.¹⁶⁻²³ However, there still exists very few modular, facile, and high yielding methods for accessing these functionalized ligand scaffolds.²⁴

The CuAAC reaction of terminal alkynes with organic azides is an excellent method in this regard. As such it has become a favored methodology for the synthesis of functional ligands due to its mild reaction conditions,

substrate tolerability, and its reliability with regards to high yields of the desired triazole product.²⁵⁻²⁷ Additionally, due to the fact that the 1,4-functionalized triazoles generated via this method have the ability to act as N or C type donor ligands there has been tremendous amount of interest in their use as a ligand architecture in the past decade. This work has resulted in the utilization of these ligands to form mono-, bis-, tris-, and polydentate scaffolds with a variety of metal ions, and the resulting coordination properties have been examined.²⁸⁻⁶³

The use of the CuAAC method for the preparation of 2-pyridyl triazoles is an excellent example of the utility of this reaction. These compounds are highly desirable as their synthesis is facile, highly modifiable and the resulting compounds have been shown to be an excellent class of ligands with the N type donor ability of the pyridyl component and the N or C type donor of the triazole.

There is a plethora of examples of the use of PyTri's in metal complexes with a variety of metal centers. These include copper(II),⁶⁴ silver(I),^{64,65} ruthenium(II),⁶⁶ rhenium(I),⁶⁷ palladium(II),^{24,29,68-72} platinum(II),⁷⁰⁻⁷³ and iridium.⁷⁴ While these complexes have been extensively studied, a systematic approach to analyze electronically diverse complexes, through the simple derivatization of the PyTri ligand, could not be found.

Thus in this chapter it is reported the synthesis of electronically diverse mono- and bis-PyTri complexes with platinum(II) and palladium(II). Additionally, further analysis of the palladium(II) complexes with regards to their activity in Suzuki-Miyaura cross-coupling reactions is discussed.

6.3 Platinum Complexes with Electronically Diverse Pyridyl Triazole

Ligands:

Using the previously prepared PyTri's, as discussed in chapter 5, it was proposed that preparation of mono- and bis-platinum(II) (Pt) complexes bearing these electronically diverse ligands would be an important step towards studying the biological activity of these cisplatin analogs. While some studies have reported the preparation of these PyTriPt(II) complexes the some reports go on to further functionalize these complexes through the displacement of the initial halogen groups from the metal center.⁷³ This displacement is often involving NH-type ligands so that the resulting complexes have increased solubility and stability compared to cisplatin. While these complexes are biologically interesting and certainly worthy of study, the analysis of the initially formed PyTriPt(II) dichloride complexes where the PyTri ligand is derivatized in an systematic, electronically diverse, fashion is a notable vacancy in the literature. Thus the goal of preparing of these compounds bearing the full range of electronically diverse PyTri ligands was set, and the advancements to satisfy this objective are reported herein.

The formation of these complexes began with the analysis of suitable Pt precursors for complex formation. Of those that are commercially available, potassium tetrachloroplatinate (K_2PtCl_4), platinum dichloride ($PtCl_2$) and platinum *cis*-dichlorobis(dimethyl sulfoxide) ($PtCl_2(DMSO)_2$) was used in initial testing for complex formation. Surprisingly, K_2PtCl_4 , which is reported to be the most soluble

of the platinum precursors mentioned, was unable to form the desired complex when the complexation was run in acetonitrile (MeCN). Fully dissolving the platinum precursor in trace amounts of DI-H₂O followed by the addition of MeCN and PyTri ligand also furnished none of the desired complex, and only free ligand was observed by ¹H NMR. Utilization of a halide abstracting agent, silver tetrafluoroborate (AgBF₄) to help generate an unhindered and more electrophilic platinum source in situ was also unsuccessful and this platinum precursor was thus deemed incapable at furnishing the desired PyTriPt(II) complexes despite literature precedent suggesting otherwise.⁷⁵

Work then began on the use of PtCl₂ as the metal precursor. When the complexation was attempted in MeCN at 65 °C, formation of a species that is inconsistent with free PyTri ligand was observed. However, complete conversion did not occur and multiple species were evident by ¹H NMR. To encourage conversion to a single species, two equivalents of the halide-abstracting agent AgBF₄ was added. Under these conditions the reaction cleanly formed a single complex as evident by ¹H NMR. Further analysis of the product determined the species to be an ML₂ type complex where two PyTri ligands surround the platinum center. Additionally, the dicationic complex is stabilized by two non-coordinating BF₄ anions. This method was robust and able to furnish bis-PyTriPt(II)(BF₄)₂ complexes (**6a-6e**) across the entire series of electronically diverse PyTri ligands (Table 6.1). Analysis of this series of complexes by ¹H NMR

showed a similar trend to the free ligands where the diagnostic triazole singlet could be tracked as it moved downfield in a stepwise fashion (Figure 6.1).

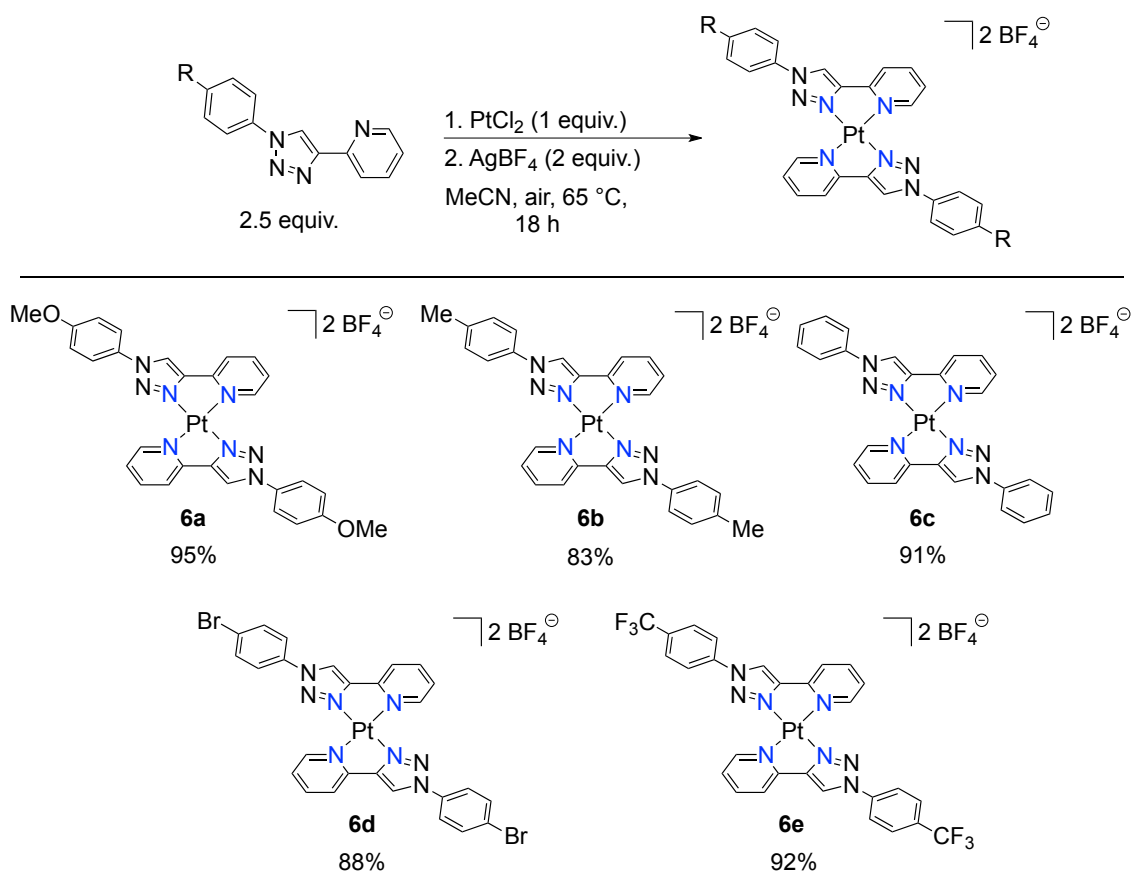


Table 6.1: Electronically diverse bis-PyTriPt(II) complexes with stabilizing BF₄[−] anions

In order to confirm the absolute configuration of these complexes, X-ray quality crystals were grown from a saturated sample of complex in MeCN. Upon standing for 7 days colorless crystals of very high quality were obtained for the trifluoromethylated complex (**6e**). X-ray crystallography was performed and the predicted structure of the complex was confirmed and was obtained as a solvated structure with MeCN (Table 6.2).

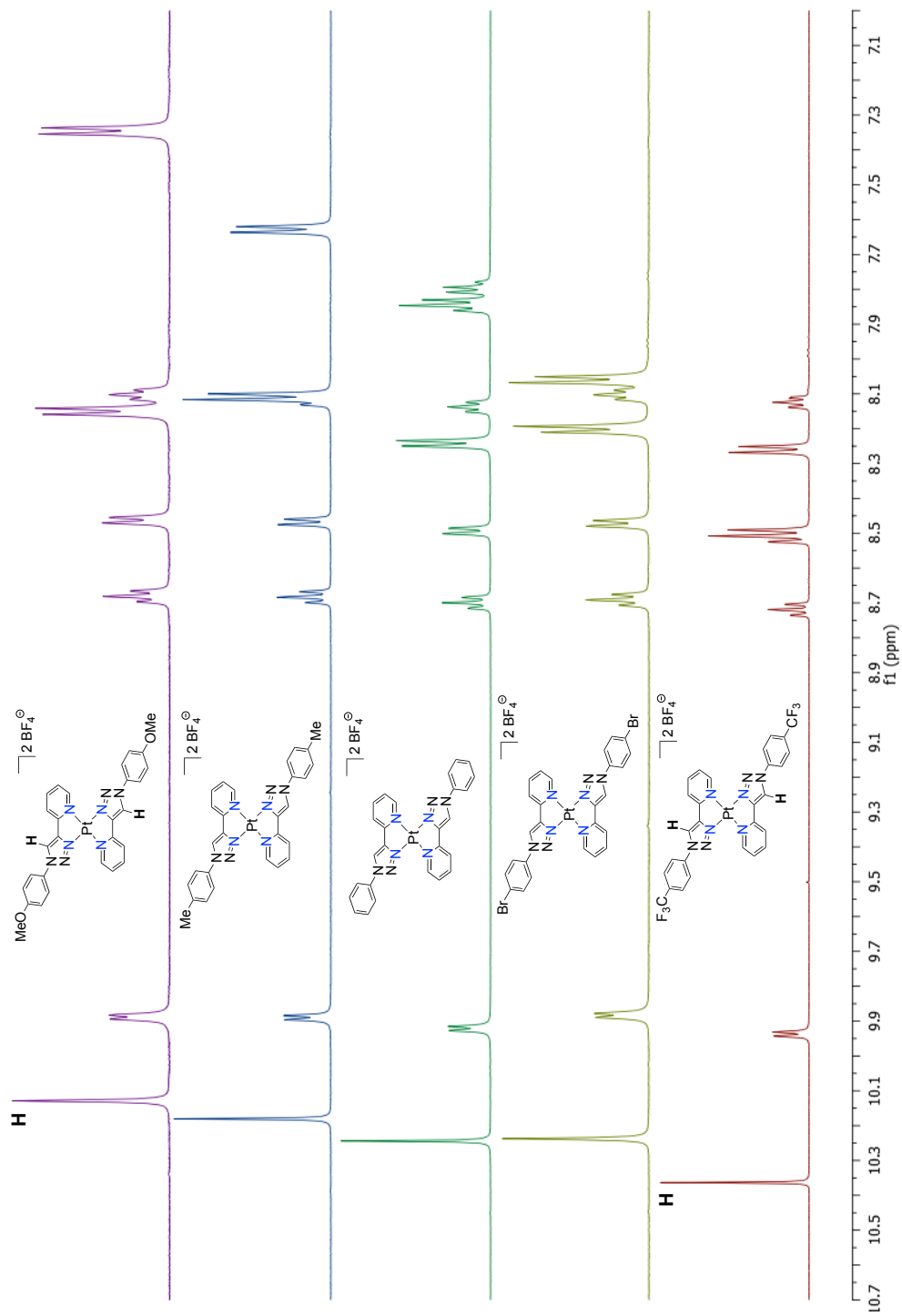


Figure 6.1: ^1H NMR analysis of the electronic diversity of bis-PyTriPt(BF₄)₂ complexes.

The (MePyTri)₂Pt(BF₄)₂ complex (**6b**) was chosen as a representative sample of this class of complexes and elemental analysis was performed. The experimental data was in agreement with the calculated values.

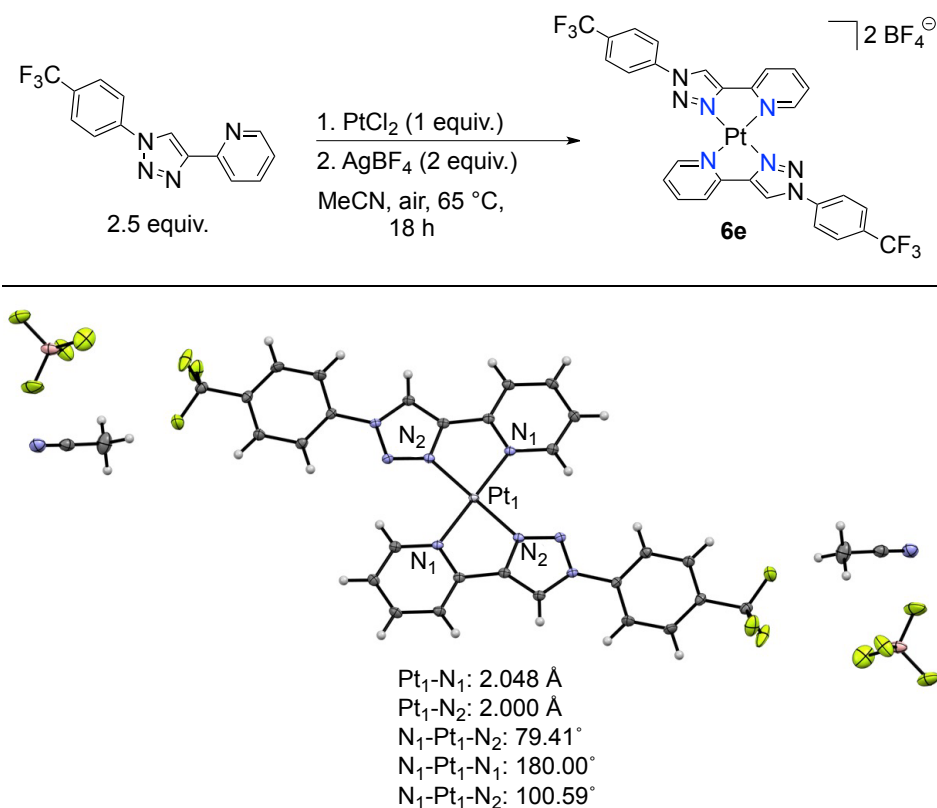


Table 6.2: X-ray crystal structure of bis-CF₃PyTriPt(BF₄)₂ as a solvated complex with MeCN.

With the success of preparing the bis-PyTriPt(II) complexes additional work to develop a method to prepare and isolate mono-ligated complexes was undertaken. As K₂PtCl₄ and PtCl₂ had demonstrated an inability to cleanly form mono-complex the platinum precursor PtCl₂(DMSO)₂ was used. This precursor also has literature precedent for the formation of mono-complexes with N,N heterocyclic ligands.⁷⁰ When this platinum source was used in slight excess with

1 equivalent of PyTri ligand, dissolved in MeCN, complexation occurred at ambient temperature. The desired mono-complex (ML) precipitated from solution over the course of 18 h and was isolated using a centrifuge.

Satisfyingly, the desired mono-PyTriPt(II)Cl₂ complexes (**6f-6j**) could be prepared using this methodology and the entire series of electronically diverse PyTri ligands could be utilized (Table 6.3).

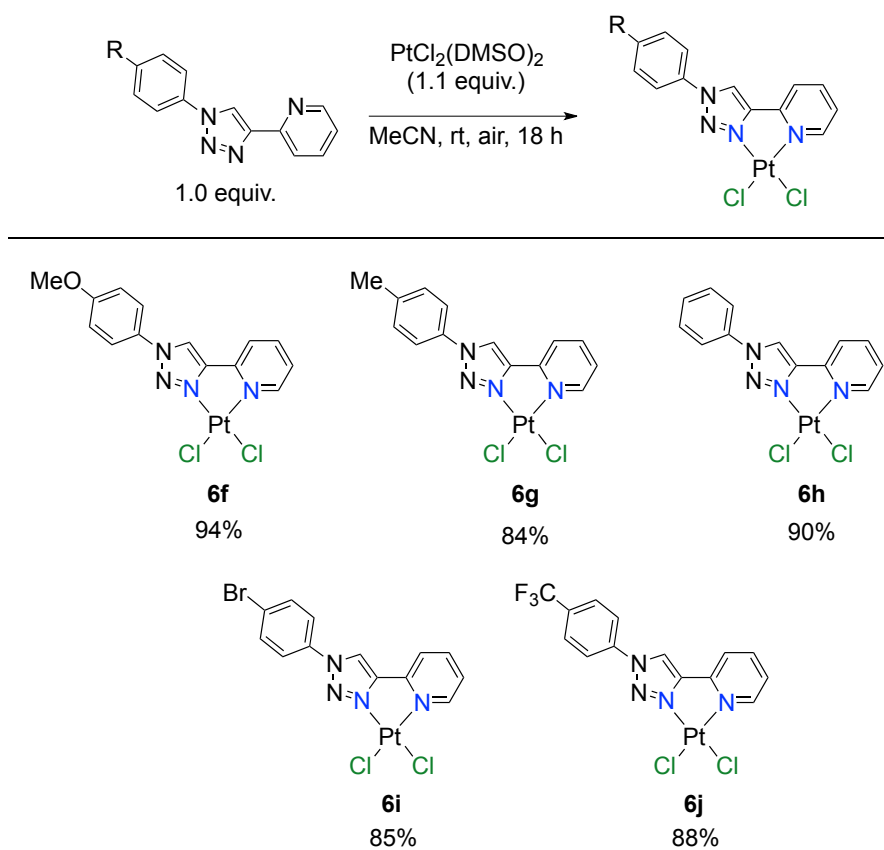


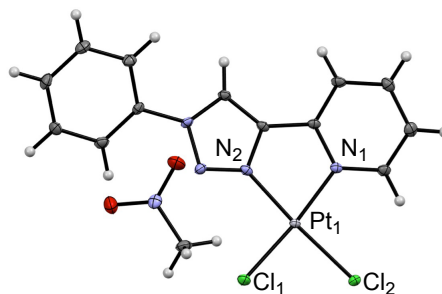
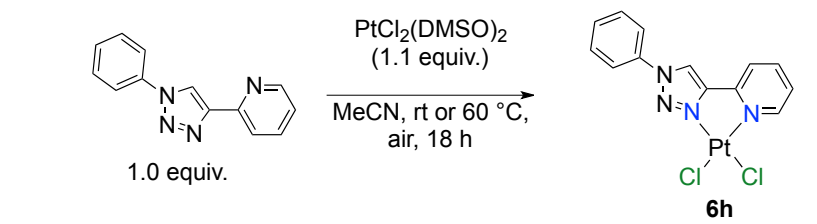
Table 6.3: Electronically diverse PyTriPtCl₂ complexes as cis-platin analogues

These complexes were found to be very soluble in DMSO-*d*₆ and this solvent was initially chosen for characterization. ¹H NMR showed that in this solution a DMSO adduct formed with the complex and small duplicate peaks were

observed. To confirm these peaks came from adduct formation and not an impurity in the sample, NMR in MeNO₂-d₃ was taken. In this solvent, no adduct formation was observed. However, the complexes were significantly less soluble in MeNO₂-d₃ and much longer acquisition times were necessary. Due to the decreased solubility in MeNO₂-d₃, NMR characterization was performed using DMSO-d₆, despite small amounts of adduct formation.

In order to confirm the absolute orientation of the complexes, X-ray quality crystals were grown of the PyTriPtCl₂ complex (**6h**). These crystals were obtained from slow evaporation of a dilute MeNO₂ solution of the complex and appeared yellow in color. X-ray crystallography confirmed the predicted structure of the complex and was obtained as a solvated structure with MeNO₂ (Table 6.4). The PyTriPtCl₂ complex (**6h**) was again chosen as a representative sample of this class of complexes and elemental analysis was performed. The experimental data was in agreement with the calculated values.

With the series of both mono- and bis-PyTriPt(II) complexes prepared, future work to assess their biological activity and utility against cisplatin resistant cancer cells will be performed at a later date.



$\text{Pt}_1\text{-Cl}_1$: 2.2900 Å
 $\text{Pt}_1\text{-N}_1$: 2.035 Å
 $\text{Pt}_1\text{-N}_2$: 1.989 Å
 $\text{N}_1\text{-Pt}_1\text{-N}_2$: 79.84°

Table 6.4: X-ray crystal structure of PyTriPtCl₂ as a solvated complex with MeNO₂.

6.4 Palladium Complexes with Diverse Pyridyl Triazole Ligands:

Synthesis of cis-dichloro- and bis-ligated PyTri-palladium(II) complexes is especially important to the fields of organo-catalysis,^{29,69} and metallo-pharmaceuticals⁷⁶ and as such, methods for the preparation of these complexes using highly tune-able ligands is of high value. With derivatized PyTri ligands on hand, work on determining a robust method for the preparation of these complexes was performed.

Utilization of bis(acetonitrile)dichloropalladium(II) (PdCl₂(MeCN)₂) was used as the palladium precursor for complexation reactions to form ML type mono-PyTriPdCl₂. The complexation reactions were set up by measuring

$\text{PdCl}_2(\text{MeCN})_2$ into the reaction vial followed by the addition of dichloromethane (DCM) as solvent. Once the palladium precursor had dissolved, addition of the PyTri ligand bearing the desired substitution, dissolved in minimal DCM, occurred. The desired substituted PyTriPdCl₂ complex precipitated from solution at ambient temperature over the course of 18 h. The solid was collected using a centrifuge and washed with additional DCM to remove remaining metal and free ligand. This method allowed for the preparation of the desired series of mono-PyTriPdCl₂ complexes (**6k-6o**) bearing substitution ranging from electron donating (OMe) to electron withdrawn (CF₃) (Table 6.5).

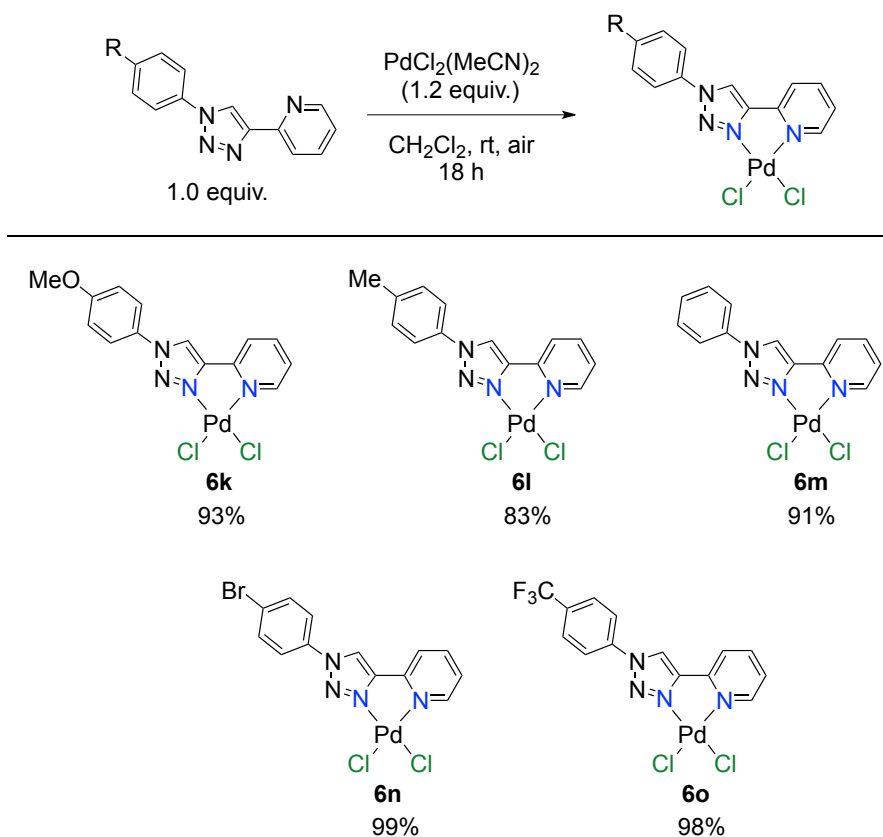


Table 6.5: Electronically diverse PyTriPdCl₂ complexes as potential catalysts for cross-coupling reactions

Analysis of this series of substituted PyTriPdCl₂ complexes by ¹H NMR showed a similar trend to the previous complexes where the diagnostic triazole singlet could be tracked as it moved downfield in a stepwise fashion (Figure 6.2). In order to confirm the absolute orientation of the complexes, X-ray quality crystals were grown of the MePyTriPdCl₂ complex (**6l**). These crystals were obtained from slow evaporation of a dilute MeNO₂ solution of the complex and appeared red in color. X-ray crystallography confirmed the predicted structure of the complex and was obtained (Table 6.6). The BrPyTriPdCl₂ complex (**6n**) was chosen as a representative sample of this class of complexes and elemental analysis was performed. The experimental data was in agreement with the calculated values.

For the synthesis of bis-PyTriPd(II) complexes two different approaches could be utilized. The bis-complex could be prepared directly if the palladium precursor tetrakis(acetonitrile)palladium(II) tetrafluoroborate (Pd(MeCN)₄(BF₄)₂) is used. This method requires dissolving the precursor in MeCN followed by addition of 2.5 equivalents of the PyTri ligand dissolved in minimal MeCN. Precipitation of the bis-PyTriPd(II)(BF₄)₂ complex (**6p**) occurred after stirring at ambient temperature for 18 h (Scheme 6.1).

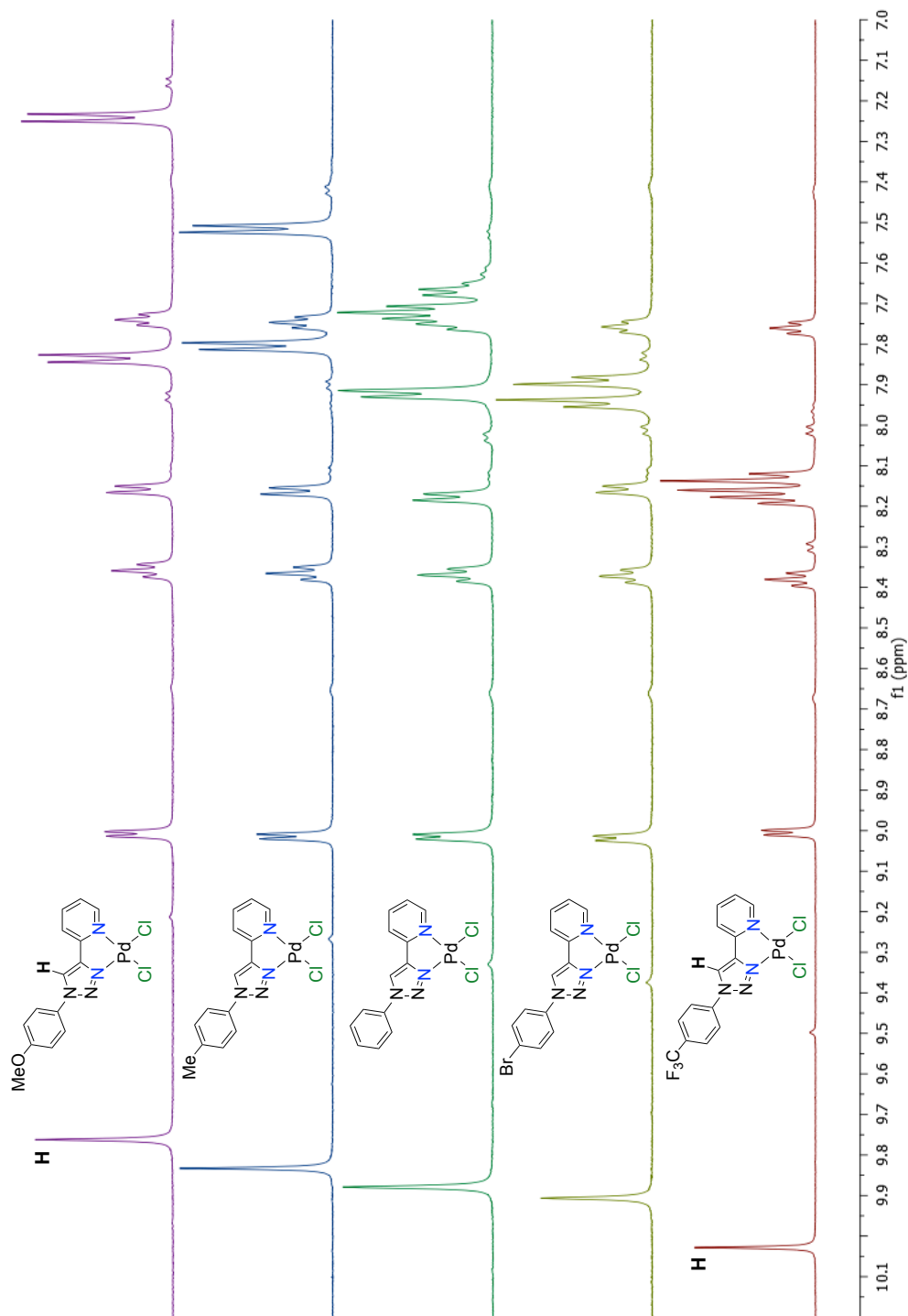
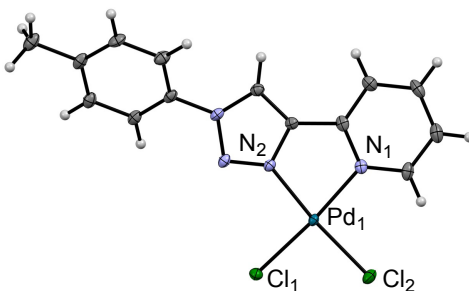
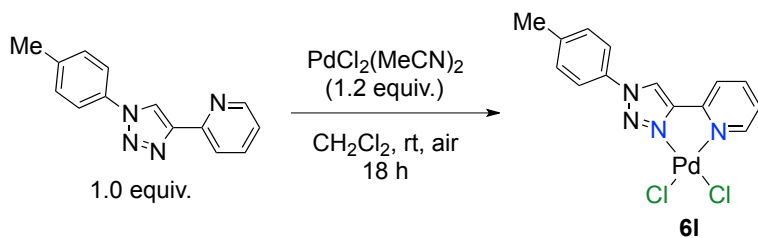
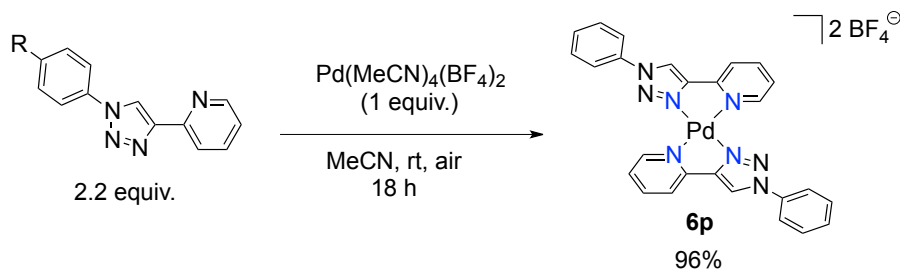


Figure 6.2: ^1H NMR analysis of the electronic diversity of PyTriPdCl₂ complexes.

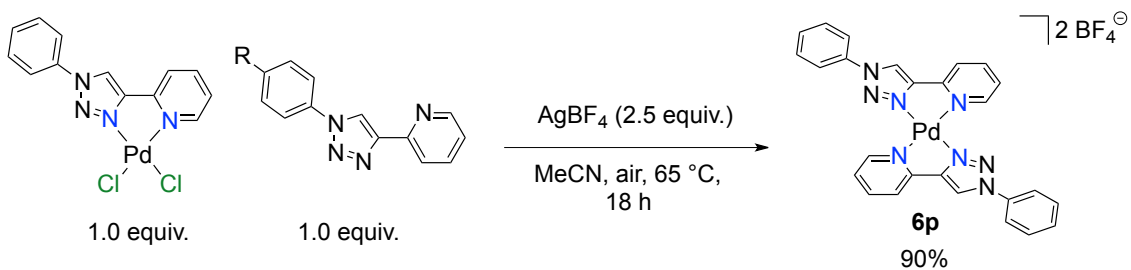


Pd₁-Cl₁: 2.2744 Å
 Pd₁-N₁: 2.055 Å
 Pd₁-N₂: 2.012 Å
 N₁-Pd₁-N₂: 80.33°

Table 6.6: X-ray crystal structure of the PyTriPdCl₂ complex.



Scheme 6.1: One step synthesis of bis-PyTriPd(BF₄)₂ complex is high yielding from Pd(BF₄)₂ precursor

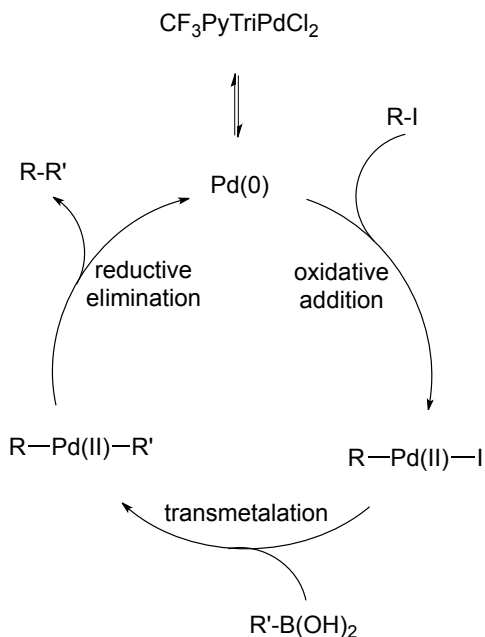


Scheme 6.2: Two step synthesis of bis-PyTriPd(BF₄)₂ complex from PyTriPdCl₂ precursor

Additionally, the bis-complex can be prepared using the PyTriPdCl₂ complex as the starting precursor. Adding an additional equivalent of PyTri ligand in acetonitrile to the precursor followed by addition of 2.5 equivalents of the halide-abstracting agent AgBF₄, furnishes the bis-complex (**6p**) in 90% yield after refluxing for 18 h (Scheme 6.2). Characterization of this complex matches that published in the literature.²⁴ If further analysis of this class of bis-PyTriPd(II) complexes is required the entire series of bis-complexes can be synthesized using this methodology.

6.5 Activity of Pyridyl Triazole Pd(II) Complexes in Suzuki Cross Coupling:

Palladium-catalyzed cross-coupling is currently considered one of the most important reactions in organic synthesis.⁷⁷ Of the many types of cross-coupling reactions, the Suzuki-Miyaura coupling of an aryl halide and aryl boronic acid is the most widely used due to its high catalytic efficiency, commercially available starting materials and the low toxicity of the catalyst. The catalytic cycle for this reaction was discussed in chapter 5 and is shown again in scheme 6.3 for clarity. Many of the most prominent catalysts for this cross coupling reaction contain ligands based on electron rich phosphane,⁷⁸⁻⁸² or N-heterocyclic carbene ligands.⁸³⁻⁸⁹ While these catalysts are highly reactive, their sensitivity to oxygen and subsequent degradation in storage requires use and storage under an inert atmosphere. As such, recent progress in the development of palladium based catalysts using nitrogen based chelates such as porphyrin,⁹⁰ diketimines,⁹¹ and pyridine based ligands⁹²⁻⁹⁵ has been made.



Scheme 6.3: Catalytic cycle for the palladium catalyzed cross coupling of aryl iodides with aryl boronic acids.

The rigidity and high stability of these nitrogen ligands in air has led to increased stability of the resulting catalysts. This allows the cross coupling reactions to be performed at higher temperatures and in some circumstances under aerobic conditions.^{96,97} While there are many examples of palladium based catalysts for the Suzuki reaction, development of highly active catalysts that allow for reduced catalysts loading, while also allowing for mild reaction conditions and large substrate scope is still an area of great importance.

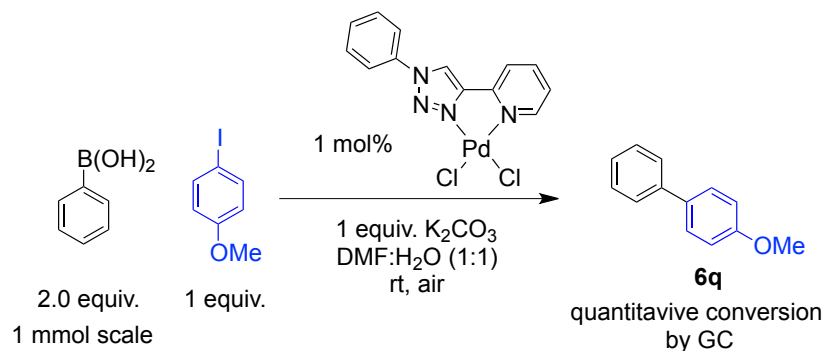
Based on this need for further investigation, 2-pyridyl triazoles have emerged as a ligand class with great potential in catalysis. With the successful synthesis of the electronically diverse PyTri compounds discussed in chapter 5 and the use of these ligands to make highly stable palladium dichloride

complexes discussed above, work to determine the reactivity of these compounds towards this highly valuable cross coupling reaction was undertaken.

Precedent in the literature⁶⁹ showed that the simple phenyl substituted PyTri complex (**6m**) was active in the Suzuki cross coupling reaction and 590 catalytic turnovers were observed for the reaction of 4-methoxy-bromo-benzene with phenylboronic acid. While this demonstrated the ability of this complex class to perform the desired cross coupling reaction, it was hypothesized that tuning the complex electronically would allow for increased catalytic turnovers and higher substrate scope. Thus work began on the study of this reaction using the electronically diverse PyTriPdCl₂ complexes discussed previously.

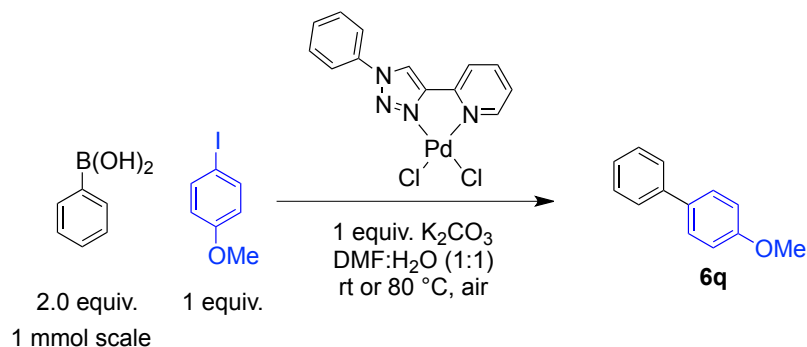
Analysis began using conditions similar to that reported in the literature precedent. When 4-iodoanisole was reacted with excess phenylboronic acid in a 1 to 1 solution of N,N-dimethylformamide (DMF) and DI-H₂O using an equivalent of potassium carbonate (K₂CO₃) as base and the system was loaded with 1 mol% of the PyTriPdCl₂ complex complete conversion to 4-methoxy-biphenyl (**6q**) occurred after 18 h and 100 catalytic turnovers were observed (Scheme 6.4).

To determine the limit for decreasing catalyst loading under these conditions the amount of catalyst added was decreased by 10-fold and 100-fold and the reaction was monitored by GC for 1 h. At ambient temperature the necessary catalyst loading matched that in the literature precedent at 0.1 mol% and the reaction containing 0.01 mol% failed to proceed.



Scheme 6.4: Initial conditions for successful Suzuki cross-coupling with PyTriPdCl₂ complex.

However when the reaction temperature was increased to 80 °C, the reaction containing the 0.01 mol% of catalyst, the catalyst was activated and 7400 catalytic turnovers were observed for the production of the methoxylated biphenyl product. Further decreases of catalyst loading at this elevated temperature were incapable at furnishing the desired product. Thus the limit to catalyst loading was determined to be 0.01 mol% (Table 6.7).

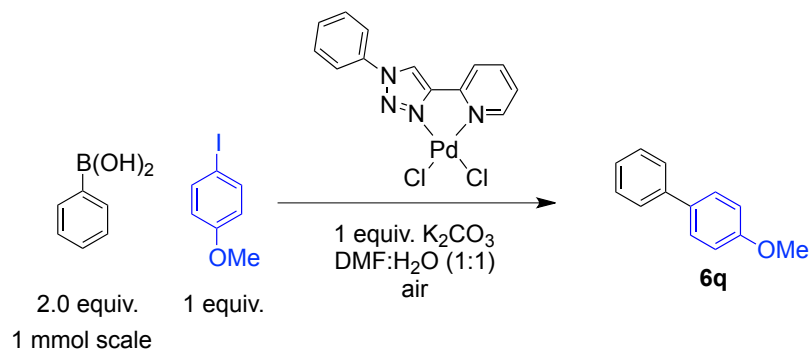


Catalyst Loading	temp (°C)	time (min)	GC Yield (%)
1 mol%	rt	60	58
0.1 mol%	rt	60	34
0.01 mol%	rt	60	<2
0.01 mol%	80	60	74
0.001 mol%	80	60	<2
0.0001 mol%	80	60	<1

^a All uncorrected GC yields.

Table 6.7: Assessing optimal catalyst loading of PyTriPdCl₂ complex for Suzuki cross-coupling.

The step in the optimization of this system was to perform a temperature screen to determine the temperature at which the catalyst becomes inactive. Side by side trials were performed at 80 °C, 60 °C, 40 °C and ambient temperature (Table 6.8). It was determined that a reaction temperature less than 40 °C rendered the catalyst largely inactive and thus this was the temperature chosen for further optimization.

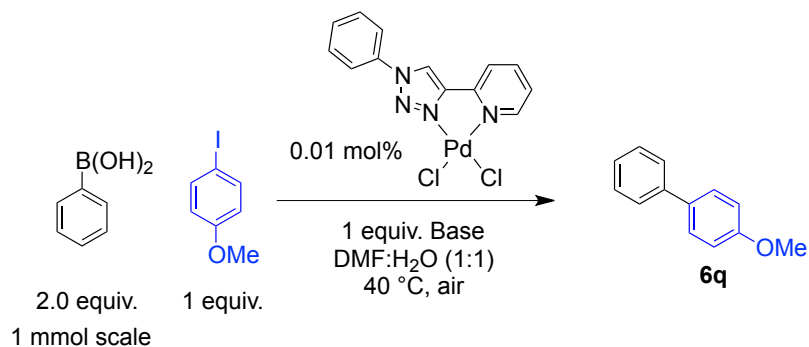


Catalyst Loading	temp (°C)	time (min)	GC Yield (%)
0.01 mol%	80	60	74
0.01 mol%	60	60	77
0.01 mol%	40	60	30
0.01 mol%	rt	60	<2

^a All uncorrected GC yields.

Table 6.8: Determining temperature limitations of the PyTriPdCl₂ catalyzed Suzuki cross-coupling.

A base screen was performed to find one that was optimal for this system. Those tested were carbonates, hydroxide, alkoxides, and amine type bases (Table 6.9). Of those tested carbonates demonstrated much higher reactivity with these catalysts and continued use of K₂CO₃ was chosen due to its decreased cost and ease of use compared to Cs₂CO₃.

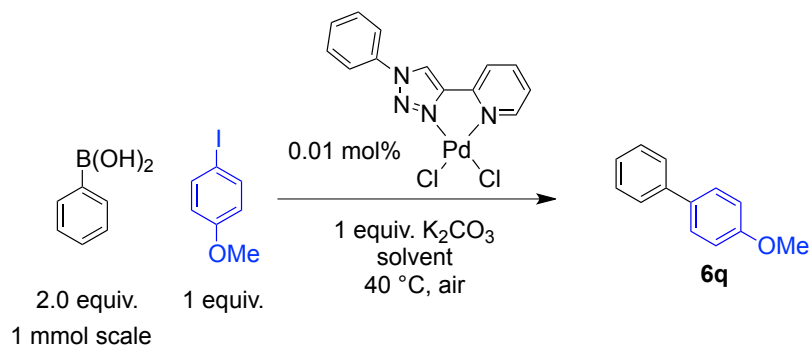


Base	temp (°C)	time (min)	GC Yield (%)
K ₂ CO ₃	40	180	25
Cs ₂ CO ₃	40	180	25
NaOH	40	180	10
NaOEt	40	180	11
Et ₃ N	40	180	19

^a All uncorrected GC yields.

Table 6.9: Base screen shows carbonate salts are optimal with PyTriPdCl₂ for Suzuki cross-coupling.

The next objective was to decrease the amount of DI-H₂O used as solvent. This was a concern as potential hydrolysis of the dichloride catalyst and subsequent loss of ligand could occur. The ratio of organic solvent to DI-H₂O was varied from 9:1 to 1:9 in a stepwise fashion and it was determined that when the organic solvent was DMF a 50/50 mixture was required to get optimal conversion to the desired product (Table 6.10). Further optimization by assessing additional organic solvents was performed.

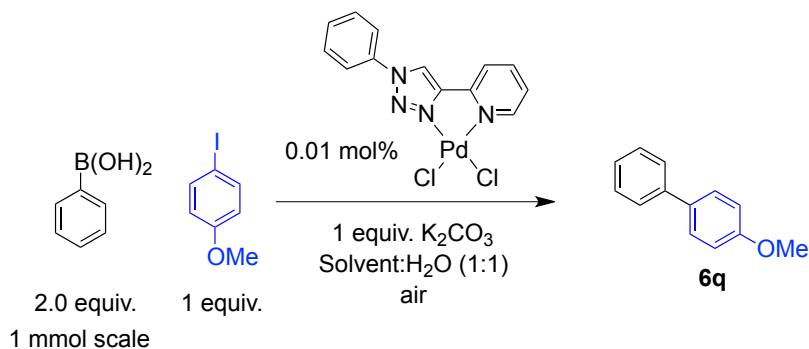


DMF:H ₂ O	temp (°C)	time (min)	GC Yield (%)
9:1	40	180	<1
8:2	40	180	3
7:3	40	180	10
6:4	40	180	19
5:5	40	180	25
4:6	40	180	19
3:7	40	180	13
2:8	40	180	2
1:9	40	180	3

^a All uncorrected GC yields.

Table 6.10: Assessing optimal ratio of solvent to H₂O shows that 50:50 gives highest conversion when DMF is solvent.

Those tested included DMF as a control, MeOH, EtOH, MeCN, and dioxane. Of those tested, EtOH and dioxane demonstrated were optimal with dioxane giving the highest conversion (Table 6.11).

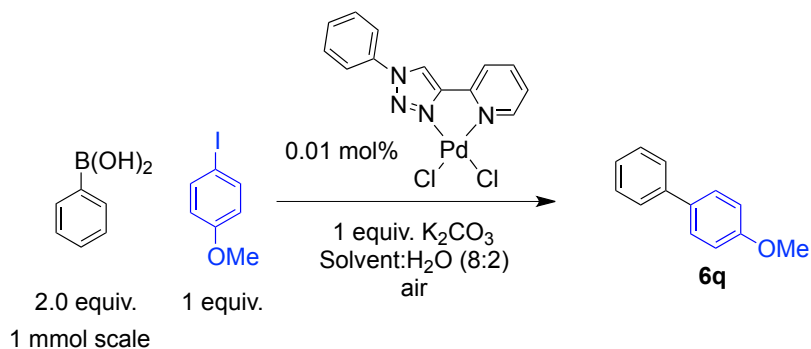


Solvent	temp (°C)	time (min)	GC Yield (%)	GC Yield @ 16 h (%)
DMF	40	180	20	42
MeOH	40	180	15	38
EtOH	40	180	25	68
MeCN	40	180	23	57
Dioxane	40	180	47	80

^a All uncorrected GC yields.

Table 6.11: Solvent screen demonstrates that EtOH and dioxane are preferred with 50:50 H₂O compared to DMF.

When EtOH and dioxane were used with decreased amounts of DI-H₂O, EtOH was observed to be the superior solvent (Table 6.12). Further, when EtOH is used as solvent, DI-H₂O can be removed completely as was initially desired, and a high percent conversion to product was observed after 16 h. (Table 6.13).

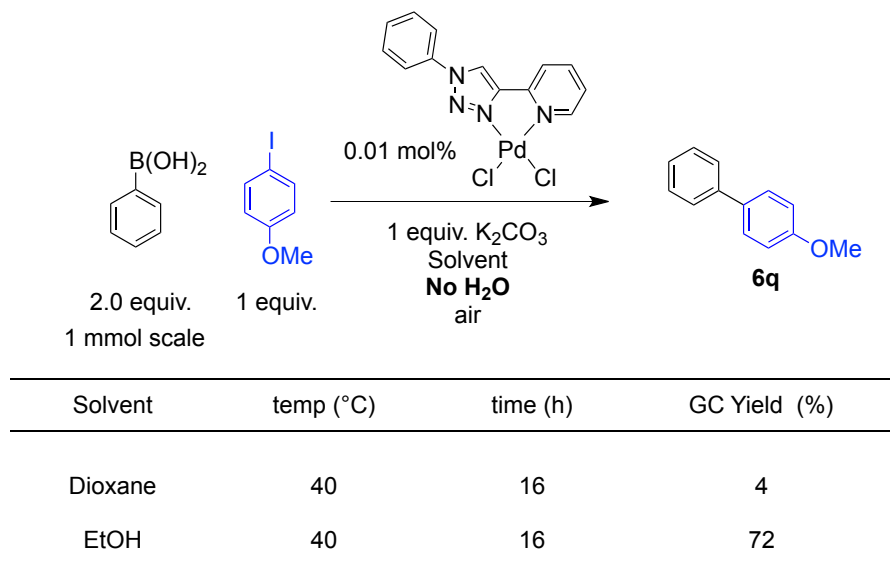


Solvent	temp ($^{\circ}C$)	time (h)	GC Yield (%)
DMF	40	18	7
Dioxane	40	18	31
EtOH	40	18	69

^a All uncorrected GC yields.

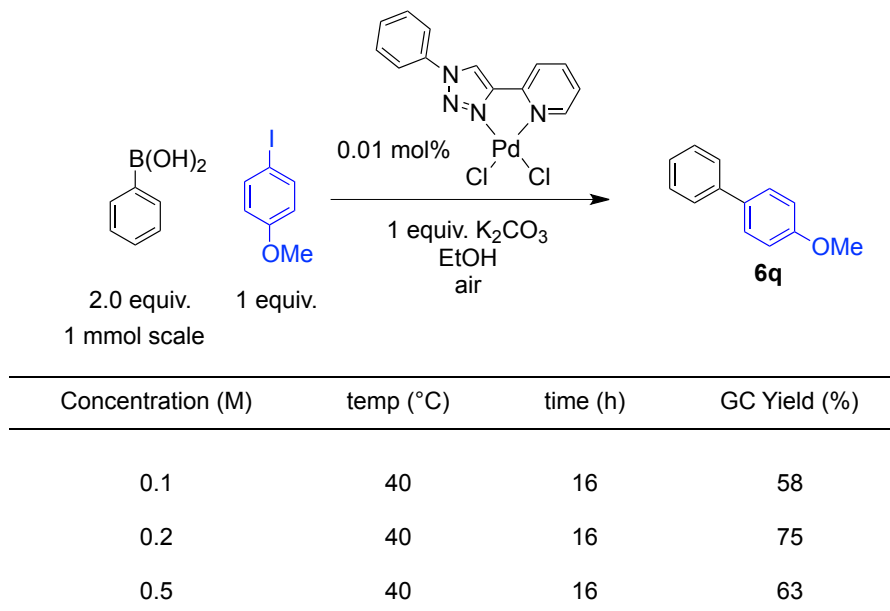
Table 6.12: When the ratio of solvent is increased to 80:20 with H_2O , EtOH stands out as optimal solvent.

With the water removed from the system the amount of organic solvent necessary to achieve optimal conversion was assessed. Increasing the concentration by decreasing the volume of solvent used was assessed at 0.1, 0.2, and 0.5 M (Table 6.14). The highest conversion was observed for the reaction run at 0.2 M concentration.



^a All uncorrected GC yields.

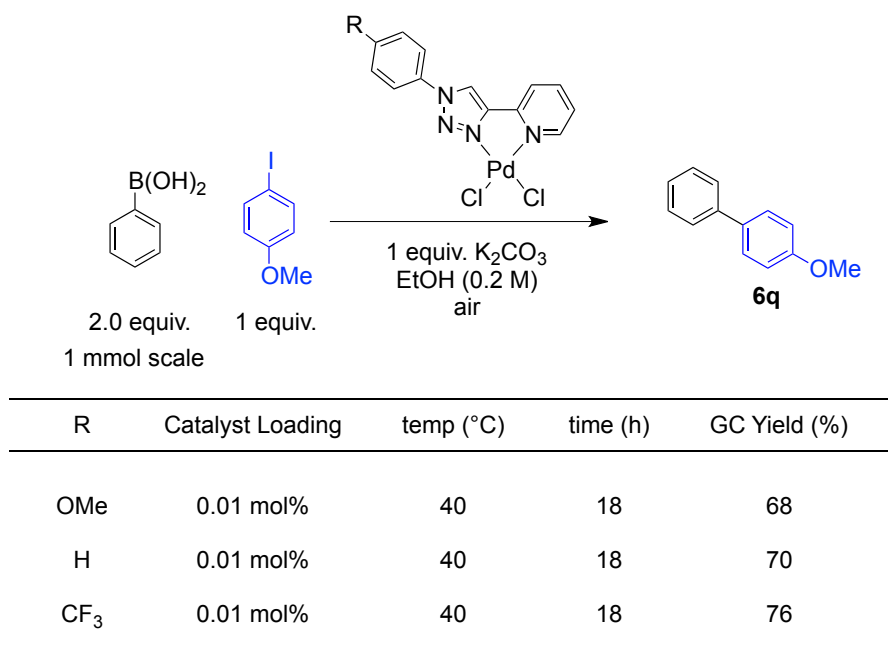
Table 6.13: When EtOH is used as solvent, removal of all H₂O leads to increased conversion to product.



^a All uncorrected GC yields.

Table 6.14: Concentration screen shows that 0.2 mmol/milliliter gives highest conversion.

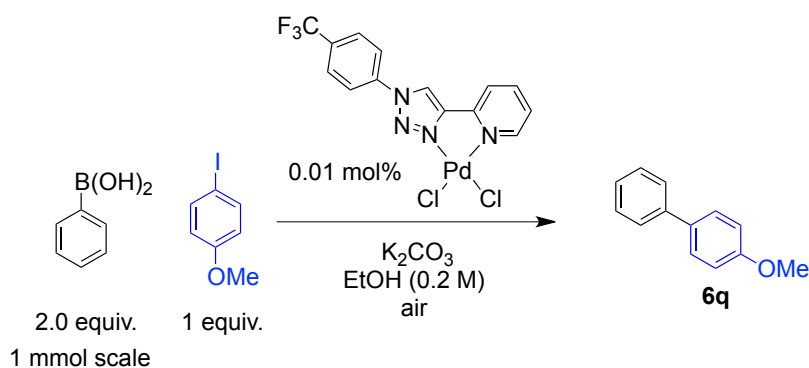
With the reaction parameters determined, the final step to optimizing the reaction was to assess which of the electronically diverse PyTriPdCl₂ complexes was most active towards Suzuki cross coupling. Analysis of the electron-rich (**6k**), neutral (**6m**), and electron-poor (**6o**) complexes at 0.01 mol% catalyst loading showed that the CF₃PyTriPdCl₂ was the most active after 18 h (Table 6.15). This led to the hypothesis that the oxidative addition step of the reaction was likely rate determining as the rate of this step would increase as the catalytic complex became more electrophilic. If reductive elimination of the di-aryl product was rate determining it is proposed that use of a more electron-rich catalyst should have the highest conversion within a set amount of time.



^a All uncorrected GC yields.

Table 6.15: Screen of diverse PyTriPdCl₂ catalysts shows that electron withdrawn CF₃PyTriPdCl₂ has increased reactivity.

Final optimization occurred with a base equivalents screen. The amount of K_2CO_3 was varied from 0.5 equivalents to 5 equivalents as shown in table 6.16. The use of 5 equivalents of base allowed the reaction to go to complete conversion in only 8 h. With the optimized conditions determined, work to assess the substrate scope of the system was performed.



Equiv. K_2CO_3	temp ($^{\circ}C$)	time (h)	GC Yield (%)
0.5	40	3	38
1	40	3	44
2	40	3	57
3	40	3	65
4	40	3	75
5	40	3	80
		8	>99

^a All uncorrected GC yields.

Table 6.16: Base equivalents screen shows 5 equivalents allows for full conversion to product in 8 h.

Through the optimization experiments it was observed that aryl iodides reacted rapidly and 10,000 catalytic turnovers occurred. To assess the reactivity of aryl bromides, electron-rich to electron-poor substrates were tested.

Satisfyingly, all substrates converted efficiently, and the products (**6q-6s**) could be isolated in good to high yields.

To assess whether aryl chlorides would react with this catalyst, an aryl halide consisting of both a bromide and chloride substitution was tested. Here when the reaction was performed in the presence of 2 equivalents of the aryl boronic acid, coupling occurred only at the site of the bromide substitution leading to compound (**6t**) where the chloride was left untouched (Table 6.17). Thus, aryl chlorides were deemed unreactive with this catalyst system. While this is an unfortunate limitation to these catalysts, it allows for further functionalization of the diaryl products using a different catalytic system if additional functionalization is desired.

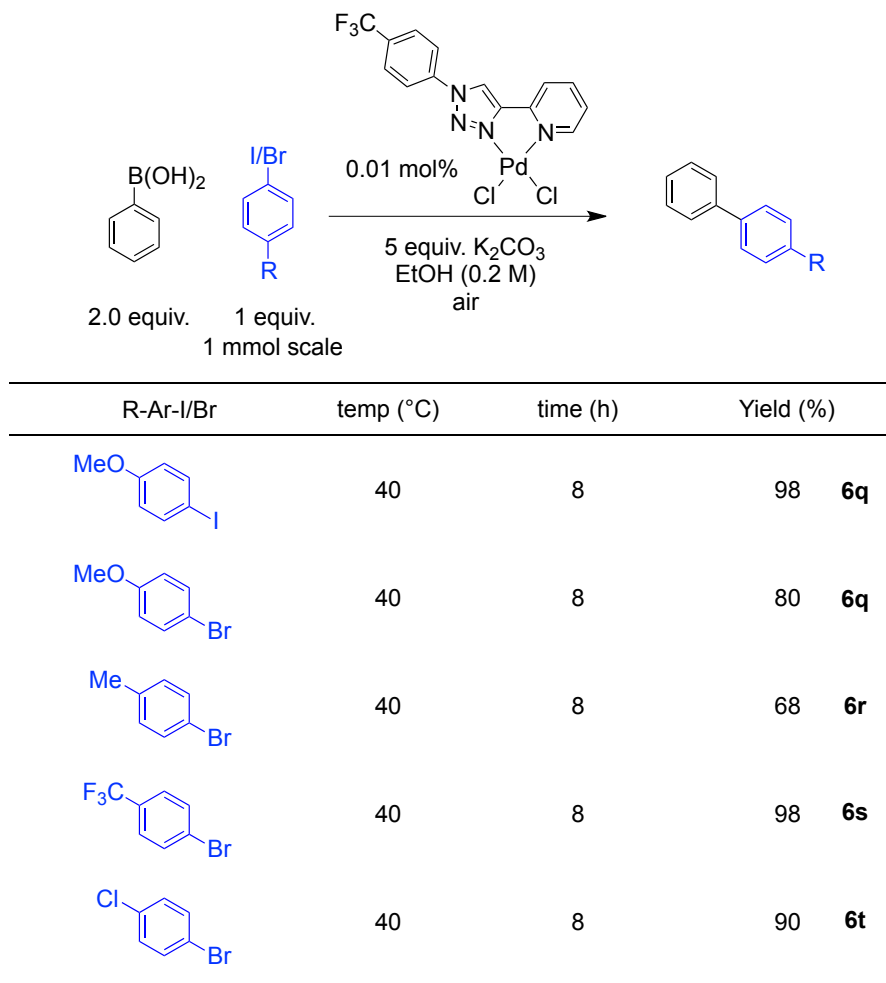
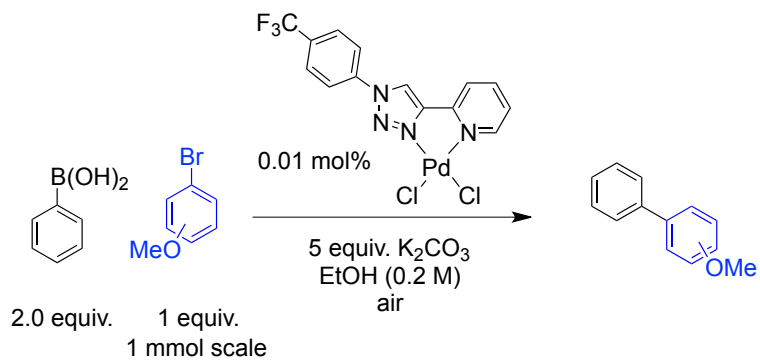


Table 6.17: Substrate scope of aryl halides shows that high yields are obtained for aryl iodides and aryl bromides, aryl chlorides are unreactive.

To determine if there were steric limitations to the system, aryl bromides with methoxy substitution at the *para*-, *meta*-, or *ortho*- position were tested. It was observed that as the substitution got closer to the active site of catalysis, (*i.e.* the position bearing the bromide substituent) the reaction became more sluggish and the yield of the desired product (**6u**) decreased (Table 6.18).

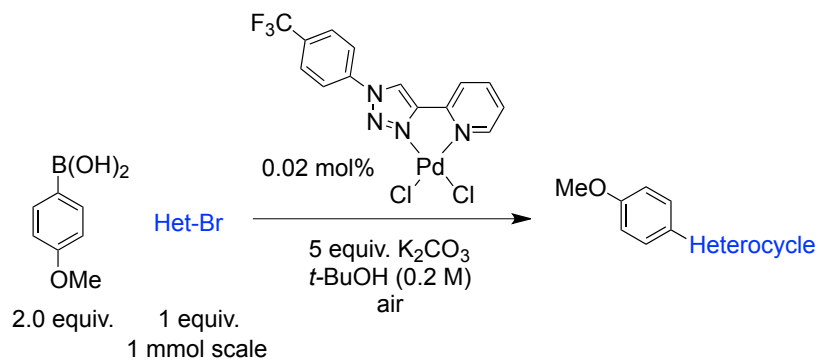


R-Ar-Br	temp (°C)	time (h)	Yield (%)	
	40	8	80	6q
	40	8	60	6u
	40	8	13 ^a	

^a Measured as an uncorrected GC yield.

Table 6.18: As the substitution approaches the active site on the aryl halide, reactivity is decreased due to steric interactions.

To determine whether heteroaromatic bromides could be utilized, a series of these compounds were tested. Initial results showed that reaction with these substrates was sluggish when the reaction was run at 40 °C. When the reaction temperature was increased to 80 °C the reaction proceeded efficiently and the coupled diaryl products (**6v-6y**) could be isolated in good to exceptional yields (Table 6.19). This result was very satisfying as previous reports using $PyTriPdCl_2$ complexes as catalysts were only able to achieve poor conversion when heteroaryl halides were used and their compounds were not isolated for further characterization.⁶⁹



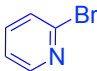
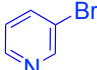
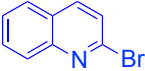
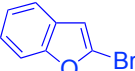
Het-Br	temp (°C)	time (h)	Yield (%)
	80	8	53 6v
	80	8	99 6w
	80	8	89 6x
	80	8	99 6y

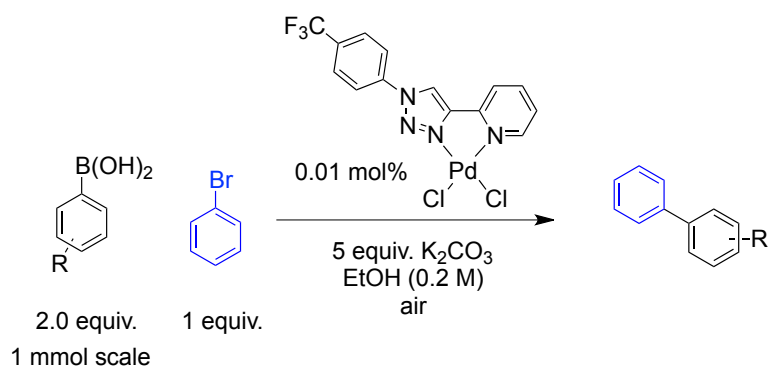
Table 6.19: CF₃PyTriPdCl₂ sets a new precedent and remains highly reactive with heteroaryl bromide substrates.

Initially, NMR characterization of these heteroaryl products was challenging. It was observed that these compounds degraded when the products were exposed to light or heat during concentration after column chromatography. This was surprising as this degradation was not reported in the literature but was consistent across the series of products containing the heteroaryl groups. However, when the purification and subsequent concentration of these reactions were performed with minimal exposure to light and heat the products could be obtained in a pure state and characterization could be performed.

The final goal for this project was to assess if there were limitations to the types of arylboronic acids that could be used. To determine this, bromobenzene was used as the common aryl halide and aryl boronic acids bearing electron-rich to electron-poor substitution were tested. It was observed that electron rich boronic acids reacted rapidly and the diaryl products (**6q**, **6aa**) could be isolated in near quantitative yields. As the electron density of the boronic acid decreased, the cross coupling to give the diaryl products (**6r**, **6z**) became more sluggish. Further while the most electron-poor boronic acid did react, the desired product (**6s**) could only be isolated in a 60% yield (Table 6.20).

Additionally, use of the heteroaromatic boronic acid, 3-furanylboronic acid, failed to proceed at either 40 °C or 80 °C using this system and only starting materials were observed after 24 h in both cases.

Satisfyingly, all of the initial goals of this project were met. Optimization of the reaction conditions, as well as assessing the effect of the electronic nature of the PyTriPdCl_2 catalyst, resulted in environmentally friendly reaction conditions, decreased catalyst loading, increased substrate tolerability, and increased yields of the desired products.



R-Ar-B(OH) ₂	temp (°C)	time (h)	Yield (%)	
	40	8	73	6z
	40	8	98	6q
	40	8	99	6aa
	40	8	70	6r
	40	8	60	6s

Table 6.20: Substrate scope of substituted aryl boronic acids shows that electron-rich to electron-poor substrates react efficiently.

6.6 References:

- 1) Peterson, E. J.; Menon, V. R.; Gatti, L.; Kipping, R.; Dewasinghe, D.; Perego, P.; Povirk, L. F.; Farrel, N. P. *Mol. Pharm.* **2015**, *12*, 287.
- 2) Renfrew, A. K.; Bryce, N. S.; Hambley, T. *Chem. Eur. J.* **2015**, *21*, 15224.
- 3) Millett, A. J.; Habtemariam, A.; Romero-Canelon, I.; Clarkson, G. J.; Sadler, P. J. *Organometallics*. **2015**, *34*, 2683.
- 4) Nardon, C.; Chiara, F.; Brustolin, L.; Gambalunga, A.; Ciscato, F.; Rasola, A.; Trevisan, A.; Fregona, D. *ChemistryOpen*. **2015**, *4*, 183.
- 5) Liu, F.; Suryadi, J.; Bierbach, U. *Chem. Res. Toxicol.* **2015**, *28*, 2170.
- 6) Donnelly, P. S. *Dalton Trans.* **2011**, *40*, 999.
- 7) Hartinger, C. G.; Dyson, P. J. *Chem. Soc. Rev.* **2009**, *38*, 391.
- 8) Hannon, M. J. *Pure Appl. Chem.* **2007**, *79*, 2243.
- 9) Che, C. M.; Siu, F. M. *Curr. Opin. Chem. Biol.* **2010**, *14*, 255.
- 10) Sun, R. W. Y.; Che, C. M. *Coord. Chem. Rev.* **2009**, *253*, 1682.
- 11) Sun, R. W. Y.; Ma, D. L.; Wong, E. L. M.; Che, C. M. *Dalton Trans.* **2007**, 4884.
- 12) Mewis, R. E.; Archibald, S. J. *Coord. Chem. Rev.* **2010**, *254*, 1686.
- 13) Metzler-Nolte, N. *Top. Organomet. Chem.* **2010**, *32*, 195.
- 14) Ducani, C.; Leczkowska, A.; Hodges, N. J.; Hannon, M. J. *Angew. Chem., Int. Ed.* **2010**, *49*, 8942.
- 15) Sanchez-Cano, C.; Hannon, M. J. *Dalton Trans.* **2009**, 10702.
- 16) Rach, S. F.; Kuehn, F. E. *Chem. Rev.* **2009**, *109*, 2061.
- 17) Diez-Gonzalez, S.; Marion, N.; Nolan, S. P. *Chem. Rev.* **2009**, *109*, 3612.
- 18) Daugulis, O.; Do, H. Q.; Shabashov, D. *Acc. Chem. Res.* **2009**, *42*, 1074.

- 19) Gruetzmacher, H. *Angew. Chem., Int. Ed.* **2008**, *47*, 1814.
- 20) Correa, A.; Garcia Mancheno, O.; Bolm, C. *Chem. Soc. Rev.* **2008**, *37*, 1108.
- 21) Kempe, R. *Chem. Eur. J.* **2007**, *13*, 2764.
- 22) Sandee, A. J.; Reek, J. N. H. *Dalton Trans.* **2006**, 3385.
- 23) Wilkinson, M. J.; van Leeuwen, P. W. N. M.; Reek, J. N. H. *Org. Biomol. Chem.* **2005**, *3*, 2371.
- 24) Kilpin, K. J.; Gavey, E. L.; McAdam, C. J.; Anderson, C. B.; Lind, S. J.; Keep, C. C.; Gordon, K. C.; Crowley, J. D. *Inorg. Chem.* **2011**, *50*, 6334.
- 25) Hein, J. E.; Fokin, V. V. *Chem. Soc. Rev.* **2010**, *39*, 1302.
- 26) Meldal, M.; Tornøe, C. W. *Chem. Rev.* **2008**, *108*, 2952.
- 27) Wu, P.; Fokin, V. V. *Aldrichim. Acta* **2007**, *40*, 7.
- 28) Struthers, H.; Mindt, T. L.; Schibli, R. *Dalton Trans.* **2010**, *39*, 675.
- 29) Bolje, A.; Kosmrij, J. *Org. Lett.* **2013**, *15*, 5084.
- 30) Nakamura, T.; Terashima, T.; Ogata, K.; Fukuzawa, S. I. *Org. Lett.* **2011**, *13*, 620.
- 31) Poulain, A.; Canseco-Gonzalez, D.; Hynes-Roche, R.; Muller-Bunz, H.; Schuster, O.; Stoeckli-Evans, H.; Neels, A.; Albrecht, M. *Organometallics* **2011**, *30*, 1021.
- 32) Nakamura, T.; Ogata, K.; Fukuzawa, S. I. *Chem. Lett.* **2010**, *39*, 920.
- 33) Partyka, D. V.; Gao, L.; Teets, T. S.; Updegraff, J. B.; Deligonul, N.; Gray, T. G. *Organometallics* **2009**, *28*, 6171.
- 34) Partyka, D. V.; Updegraff, J. B., III; Zeller, M.; Hunter, A. D.; Gray, T. G. *Organometallics* **2007**, *26*, 183.
- 35) Mathew, P.; Neels, A.; Albrecht, M. *J. Am. Chem. Soc.* **2008**, *130*, 13534.
- 36) Manbeck, G. F.; Brennessel, W. W.; Eisenberg, R. *Inorg. Chem.* **2011**, *50*, 3431.

- 37) Fleischel, O.; Wu, N.; Petitjean, A. *Chem. Commun.* **2010**, *46*, 8454.
- 38) Manbeck, G. F.; Brennessel, W. W.; Evans, C. M.; Eisenberg, R. *Inorg. Chem.* **2010**, *49*, 2834.
- 39) Chevy, A.; Teyssot, M. L.; Maisonial, A.; Lemoine, P.; Viossat, B.; Traikia, M.; Aitken, D. J.; Alves, G.; Morel, L.; Nauton, L.; Gautier, A. *Eur. J. Inorg. Chem.* **2010**, 3513.
- 40) Warsink, S.; Drost, R. M.; Lutz, M.; Spek, A. L.; Elsevier, C. J. *Organometallics* **2010**, *29*, 3109.
- 41) Kuang, G. C.; Michaels, H. A.; Simmons, J. T.; Clark, R. J.; Zhu, L. *J. Org. Chem.* **2010**, *75*, 6540.
- 42) Brotherton, W. S.; Michaels, H. A.; Simmons, J. T.; Clark, R. J.; Dalal, N. S.; Zhu, L. *Org. Lett.* **2009**, *11*, 4954.
- 43) Felici, M.; Contreras-Carballada, P.; Vida, Y.; Smits, J. M. M.; Nolte, R. J. M.; De Cola, L.; Williams, R. M.; Feiters, M. C. *Chem. Eur. J.* **2009**, *15*, 13124.
- 44) Beyer, B.; Ulbricht, C.; Escudero, D.; Friebe, C.; Winter, A.; Gonzalez, L.; Schubert, U. S. *Organometallics* **2009**, *28*, 5478.
- 45) Happ, B.; Escudero, D.; Hager, M. D.; Friebe, C.; Winter, A.; Gorls, H.; Altuntas, E.; Gonzalez, L.; Schubert, U. S. *J. Org. Chem.* **2010**, *75*, 4025.
- 46) Maisonial, A.; Serafin, P.; Traikia, M.; Debiton, E.; They, V.; Aitken, D. J.; Lemoine, P.; Viossat, B.; Gautier, A. *Eur. J. Inorg. Chem.* **2008**, 298.
- 47) Richardson, C.; Fitchett, C. M.; Keene, F. R.; Steel, P. J. *Dalton Trans.* **2008**, 2534.
- 48) Fletcher, J. T.; Bumgarner, B. J.; Engels, N. D.; Skoglund, D. A. *Organometallics* **2008**, *27*, 5430.
- 49) Yang, W. W.; Wang, L.; Zhong, Y. W.; Yao, J. *Organometallics* **2011**, *30*, 2236.
- 50) Brotherton, W. S.; Guha, P. M.; Phan, H.; Clark, R. J.; Shatruk, M.; Zhu, L. *Dalton Trans.* **2011**, *40*, 3655.

- 51) Zhang, C.; Shen, X.; Sakai, R.; Gottschaldt, M.; Schubert, U. S.; Hirohara, S.; Tanihara, M.; Yano, S.; Obata, M.; Xiao, N.; Satoh, T.; Kakuchi, T. *J. Polym. Sci., Part A: Polym. Chem.* **2011**, *49*, 746.
- 52) Ostermeier, M.; Berlin, M. A.; Meudtner, R. M.; Demeshko, S.; Meyer, F.; Limberg, C.; Hecht, S. *Chem. Eur. J.* **2010**, *16*, 10202.
- 53) Meudtner, R. M.; Ostermeier, M.; Goddard, R.; Limberg, C.; Hecht, S. *Chem. Eur. J.* **2007**, *13*, 9834.
- 54) Schulze, B.; Friebe, C.; Hager, M. D.; Winter, A.; Hoogenboom, R.; Goerls, H.; Schubert, U. S. *Dalton Trans.* **2009**, 787.
- 55) Schuster, E. M.; Botoshansky, M.; Gandelman, M. *Angew. Chem., Int. Ed.* **2008**, *47*, 4555.
- 56) Li, Y.; Huffman, J. C.; Flood, A. H. *Chem. Commun.* **2007**, 2692.
- 57) Schuster, E. M.; Nisnevich, G.; Botoshansky, M.; Gandelman, M. *Organometallics* **2009**, *28*, 5025.
- 58) Schuster, E. M.; Botoshansky, M.; Gandelman, M. *Organometallics* **2009**, *28*, 7001.
- 59) Garcia, L.; Maisonneuve, S. P.; Xie, J.; Guillot, R. G.; Dorlet, P.; Riviere, E.; Desmadril, M.; Lambert, F. O.; Policar, C. *Inorg. Chem.* **2010**, *49*, 7282.
- 60) Hao, E.; Wang, Z.; Jiao, L.; Wang, S. *Dalton Trans.* **2010**, 39, 2660.
- 61) Tamanini, E.; Flavin, K.; Motevalli, M.; Piperno, S.; Gheber, L. A.; Todd, M. H.; Watkinson, M. *Inorg. Chem.* **2010**, *49*, 3789.
- 62) Chandrasekhar, N.; Chandrasekar, R. *J. Org. Chem.* **2010**, *75*, 4852.
- 63) Bai, S. Q.; Kwang, J. Y.; Koh, L. L.; Young, D. J.; Hor, T. S. A. *Dalton Trans.* **2010**, 39, 2631.
- 64) Crowley, J. D.; Bandeen, P. H.; Hanton, L. R. *Polyhedron* **2010**, *29*, 70.
- 65) Crowley, J. D.; Bandeen, P. H. *Dalton Trans.* **2010**, 39, 612.
- 66) Kumar, S. V.; Scottwell, S. O.; Waugh, E.; McAdam, C. J.; Hanton, L. R.; Brooks, H. J. L.; Crowley, J. D. *Inorg. Chem.* **2016**, *55*, 9767.

- 67) Kim, T. Y.; Elliot, A. B. S.; Shaffer, K. J.; McAdam, C. J.; Gordon, K. C.; Crowley, J. D. *Polyhedron* **2013**, *52*, 1391.
- 68) Zakharchenko, B. V.; Khomenko, D. M.; Doroschuk, R. O.; Lampeka, R. D. *Fr.-Ukr. J. Chem.* **2015**, *3*, 1.
- 69) Jindabot, S.; Teerachanan, K.; Thonkam, P.; Kiatisevi, S.; Khamnaen, T.; Phiriyawirut, P.; Charoenchaidet, S.; Sooksimuang, T.; Kongsaree, P.; Sangtrirutnugul, P. *J. Organomet. Chem.* **2014**, *750*, 35.
- 70) Lo, W. K. C.; Huff, G. S.; Cubanski, J. R.; Kennedy, A. D. W.; McAdam, C. J.; McMorran, D. A.; Gordon, K. C.; Crowley, J. D. *Inorg. Chem.* **2015**, *54*, 1572.
- 71) Schweinfurth, D.; Pattacini, R.; Strobel, S.; Sarkar, B. *Dalton Trans.* **2009**, 9291.
- 72) Schweinfurth, D.; Strobel, S.; Sarkar, B. *Inorganica Chim. Acta* **2011**, *374*, 253.
- 73) Pages, B. J.; Sakoff, J.; Gilbert, J.; Zhang, Y.; Li, F.; Preston, D.; Crowley, J. D.; Aldrich-Wright, J. R. *J. Inorg. Biochem.* **2016**, *165*, 92.
- 74) Felici, M.; Contreras-Carballada, P.; Vida, Y.; Smits, J. M. M.; Nolte, R. J. M.; De Cola, L.; Williams, R. M.; Feiters, M. C. *Chem. Eur. J.* **2009**, *15*, 13124.
- 75) Kong, P. C.; Rochon, F. D. *Can. J. Chem.* **1978**, *56*, 441.
- 76) Deepthi, S. B.; Trivedi, R.; Sujitha, P.; Kumar, C. G.; Sridhar, B.; Bhargava, S. K. *J. Chem. Sci.* **2012**, *124*, 1405.
- 77) Nicolaou, K.C.; Bulger, P.G.; Sarlah, D. *Angew. Chem. Int. Ed.* **2005**, *44*, 4442.
- 78) Billingsley, K. L.; Anderson, K. W.; Buchwald, S. L.; *Angew. Chem. Int. Ed.* **2006**, *45*, 3484.
- 79) Fleckenstein, C.A.; Plenio, H. *Chem. Eur. J.* **2007**, *13*, 2701.
- 80) Fleckenstein, C.A.; Plenio, H. *J. Org. Chem.* **2008**, *73*, 3236.
- 81) Hoshi, T.; Nakazawa, T.; Saitoh, I.; Mori, A.; Suzuki, T.; Sakai, J.; Hagiwara, H. *Org. Lett.* **2008**, *10*, 2063.
- 82) Martin, R.; Buchwald, S. L. *Acc. Chem. Res.* **2008**, *41*, 1461.

- 83) Altenhoff, G.; Goddard, R.; Lehmann, C. W.; Glorius, F. *Angew. Chem. Int. Ed.* **2003**, *42*, 3690.
- 84) Diebolt, O.; Braunstein, P.; Nolan, S. P.; Cazin, C. S. J. *Chem. Commun.* **2008**, 3190.
- 85) Kantchev, E. A. B.; O'Brien, C. J.; Organ, M. G. *Angew. Chem. Int. Ed.* **2007**, *46*, 2768.
- 86) Marion, N.; Navarro, O.; Mei, J.; Stevens, E. D.; Scott, N. M.; Nolan, S. P. *J. Am. Chem. Soc.* **2006**, *128*, 4101.
- 87) Micksch, M.; Strassner, T. *Eur. J. Inorg. Chem.* **2012**, 5872.
- 88) O'Brien, C. J.; Kantchev, E. A. B.; Valente, C.; Hadei, N.; Chass, G. A.; Lough, A.; Hopkinson, A. C.; Organ, M. G. *Chem. Eur. J.* **2006**, *12*, 4743.
- 89) Organ, M. G.; Calimsiz, S.; Sayah, M.; Hoi, K. H.; Lough, A. J. *Angew. Chem. Int. Ed.* **2009**, *48*, 2383.
- 90) Kostas, I. D.; Coutsolelos, A. G.; Charalambidis, G.; Skondra, A. *Tetrahedron Lett.* **2007**, *48*, 6688.
- 91) Lee, D. H.; Jin, M. J. *Org. Lett.* **2011**, *13*, 252.
- 92) Amadio, E.; Bertoldini, M.; Scrivanti, A.; Chessa, G.; Beghetto, V.; Matteoli, U.; Bertani, R.; Dolmella, A. *Inorg. Chim. Acta* **2011**, *370*, 388.
- 93) Amadio, E.; Scrivanti, A.; Chessa, G.; Matteoli, U.; Beghetto, V.; Bertoldini, M.; Rancan, M.; Dolmella, A.; Venzo, A.; Bertani, R. *J. Organomet. Chem.* **2012**, *716*, 193.
- 94) Liu, P.; Yan, M.; He, R. *Appl. Organomet. Chem.* **2010**, *24*, 131.
- 95) Shen, L.; Huang, S.; Nie, Y.; Lei, F. *Molecules* **2013**, *18*, 1602.
- 96) Shahnaz, N.; Banik, B.; Das, P. *Tetrahedron Lett.* **2013**, *54*, 2886.
- 97) Zhou, C.; Wang, J.; Li, L.; Wang, R.; Hong, M.; *Green. Chem.* **2011**, *13*, 2100.

6.7 Supporting Information:

General Reagent Information

All reactions were set up on the benchtop in oven-dried glassware or dried scintillation vials. Flash column chromatography was performed using silica purchased from Silicycle. Solvents for chromatography were purchased from Fisher Chemicals and used as obtained. HPLC grade Acetonitrile (MeCN), Dichloromethane (DCM), and N,N-Dimethylformamide (DMF) was purchased from Fisher Chemicals and dried via passage through activated alumina in a commercial solvent purification system (Pure Process Technologies, Inc.). All other organic solvents were obtained from Fisher Chemicals or Acros Organics and dried over either sodium sulfate or molecular sieves (4Å). NMR solvents were purchased from Acros Organics or Cambridge Isotope Laboratories and used as obtained. The platinum precursors were stored in a glove box under nitrogen. Potassium tetrachloroplatinate (K_2PtCl_4), was purchased from Alfa Aesar and was used as obtained. Platinum dichloride ($PtCl_2$) was purchased from Ark Pharm Inc. and was used as obtained. Platinum *cis*-dichlorobis(dimethyl sulfoxide) ($PtCl_2(DMSO)_2$) was purchased from Sigma Aldrich and was used as obtained. Bis(acetonitrile)dichloropalladium(II) ($PdCl_2(MeCN)_2$) was purchased from Chem Impex Int'l Inc and was used as obtained. Tetrakis(acetonitrile)palladium(II) tetrafluoroborate ($Pd(MeCN)_4(BF_4)_2$) was

purchased from Sigma Aldrich was used as obtained. Silver tetrafluoroborate was purchased from Matrix Scientific and was used as obtained. Potassium carbonate (K_2CO_3), and other bases were purchased from Fisher Chemicals or Alfa Aesar and were used as obtained.

General analytical information

1H and ^{13}C NMR spectra were measured on a Varian Inova 500 (500 MHz) spectrometer using $DMSO-d_6$, $MeCN-d_3$, $acetone-d_6$, or $CDCl_3$ as solvents and tetramethylsilane as an internal standard. The following abbreviations are used singularly or in combination to indicate the multiplicity of signals: s - singlet, d - doublet, t - triplet, q - quartet, qn - quintet, sx - sextet, sp - septet, m - multiplet and br - broad. NMR spectra were acquired at 300 K. Gas chromatography (GC) was carried out on an Agilent Technologies 6850 Network GC System, and dodecane was used as the internal standard. ATR-IR spectra were taken on a Bruker:ALPHA FTIR Spectrometer. Attenuated total reflection infrared (ATR-IR) was used and the spectra was analyzed using the OPUS software with selected absorption maxima reported in wavenumbers (cm^{-1}). X-ray diffraction data was obtained using a suitable crystal on a 'Bruker APEX-II CCD' diffractometer. The crystal was kept at 100.0 K during data collection. Using Olex2, the structure was solved with the ShelXT structure solution program using Intrinsic Phasing and refined with the XL refinement package using Least Squares minimization. Elemental analysis was performed by Midwest Microlab on samples that were recrystallized 3 times and extensively dried under vacuum with heat.

General procedure for the production of (PyTri)₂Pt(BF₄)₂ complexes:

To an 8 mL scintillation vial equipped with a magnetic stir bar and Teflon-seal screw cap was added PtCl₂. MeCN was added as solvent followed by the PyTri ligand bearing the desired substitution dissolved in minimal MeCN. The reaction was heated to 65 °C and allowed to run for 30 min. The reaction was removed from heat and AgBF₄, dissolved in minimal MeCN was added dropwise. The reaction was placed back on the heating block at 65 °C and allowed to proceed for 18 h. During this time, precipitation of the bis-complex occurred. This solid was collected using a centrifuge and washed 3 times with cold MeCN to remove impurities. The bis-complex was obtained as a tan solid and was recrystallized out of boiling MeCN.

Synthesis of (MeOPyTri)₂Pt(BF₄)₂ (6a):

PtCl₂ (26 mg, 0.1 mmol) was added to an 8 mL scintillation vial equipped with a magnetic stir bar and Teflon-seal screw cap. MeCN (5 mL) was added as solvent. MeOPyTri ligand (62 mg, 0.25 mmol) was dissolved in minimal MeCN and added dropwise. The reaction was placed on a heating block at 65 °C and allowed to stir for 30 min. The reaction was removed from heat and AgBF₄ (38 mg, 0.2 mmol) dissolved in minimal MeCN was added dropwise. The reaction was placed back on the heating block and stirred for 18 h at 65 °C during which time the desired complex precipitated out of solution. The title compound was

obtained as a tan solid in 95% yield (83 mg, 0.095 mmol). ATR-IR: 3101, 1599, 1515, 1259, 1051, 1017, 834, 514, 451 cm^{-1} . ^1H NMR (500 MHz, $\text{DMSO-}d_6$) δ 10.13 (s, 1H), 9.89 (d, $J = 5$ Hz, 1H), 8.68 (t, $J = 7.5$ Hz, 1H), 8.46 (d, $J = 7.5$ Hz, 1H), 8.15 (d, $J = 9$ Hz, 2H), 8.10 (t, $J = 6.5$ Hz, 1H), 7.35 (d, $J = 8.5$ Hz, 2H), 3.93 (s, 3H). ^{13}C NMR (125 MHz, $\text{DMSO-}d_6$) δ 161.3, 152.4, 149.8, 147.9, 143.8, 128.7, 127.9, 125.8, 123.2, 122.9, 115.5, 56.0.

Synthesis of $(\text{MePyTri})_2\text{Pt}(\text{BF}_4)_2$ (6b):

PtCl_2 (26 mg, 0.1 mmol) was added to an 8 mL scintillation vial equipped with a magnetic stir bar and Teflon-seal screw cap. MeCN (5 mL) was added as solvent. MePyTri ligand (59 mg, 0.25 mmol) was dissolved in minimal MeCN and added dropwise. The reaction was placed on a heating block at 65 °C and allowed to stir for 30 min. The reaction was removed from heat and AgBF_4 (38 mg, 0.2 mmol) dissolved in minimal MeCN was added dropwise. The reaction was placed back on the heating block and stirred for 18 h at 65 °C during which time the desired complex precipitated out of solution. The title compound was obtained as a tan solid in 83% yield (70 mg, 0.083 mmol). ATR-IR: 3129, 1637, 1517, 1465, 1029, 821, 775, 500, 450 cm^{-1} . ^1H NMR (500 MHz, $\text{MeCN-}d_3$) δ 9.95 (d, $J = 6$ Hz, 1H), 9.29 (s, 1H), 8.50 (td, $J = 1$ Hz, $J = 7$ Hz, 1H), 8.32 (d, $J = 7.5$ Hz, 1H), 7.95 (m, 3H), 7.59 (d, $J = 8.5$ Hz, 2H), 2.53 (s, 3H). ^{13}C NMR (125 MHz, $\text{DMSO-}d_6$) δ 152.3, 149.8, 147.6, 143.9, 141.7, 133.1, 130.8, 128.0, 125.7, 123.0, 121.1, 20.8. Elemental analysis for $(\text{MePyTri})_2\text{Pt}(\text{BF}_4)_2 \cdot 4 \text{ MeCN}$ ($\text{C}_{36}\text{H}_{36}\text{B}_2\text{F}_8\text{N}_{12}\text{Pt}$): *Calculated* – C: 43.00, H: 3.61, N: 16.72. *Found* – C: 43.77,

H: 3.59, N: 16.66.

Synthesis of (PyTri)₂Pt(BF₄)₂ (6c):

PtCl₂ (26 mg, 0.1 mmol) was added to an 8 mL scintillation vial equipped with a magnetic stir bar and Teflon-seal screw cap. MeCN (5 mL) was added as solvent. PyTri ligand (56 mg, 0.25 mmol) was dissolved in minimal MeCN and added dropwise. The reaction was placed on a heating block at 65 °C and allowed to stir for 30 min. The reaction was removed from heat and AgBF₄ (38 mg, 0.2 mmol) dissolved in minimal MeCN was added dropwise. The reaction was placed back on the heating block and stirred for 18 h at 65 °C during which time the desired complex precipitated out of solution. The title compound was obtained as a tan solid in 91% yield (74 mg, 0.091 mmol). ATR-IR: 3132, 1604, 1499, 1470, 1022, 786, 768, 684, 521, 493, 448 cm⁻¹. ¹H NMR (500 MHz, DMSO-*d*₆) δ 10.24 (s, 1H), 9.92 (d, J = 6 Hz, 1H), 8.70 (td, J = 1 Hz, J = 7 Hz, 1H), 8.49 (d, J = 7.5 Hz, 1H), 8.24 (d, J = 7.5 Hz, 2H), 8.14 (td, J = 1 Hz, J = 6.5 Hz, 1H), 7.85 (t, J = 6.5 Hz, 2H), 7.79 (t, J = 7 Hz, 1H). ¹³C NMR (125 MHz, DMSO-*d*₆) δ 152.4, 150.0, 147.8, 143.9, 135.5, 131.5, 130.6, 128.0, 126.0, 123.0, 121.5.

Synthesis of (BrPyTri)₂Pt(BF₄)₂ (6d):

PtCl₂ (26 mg, 0.1 mmol) was added to an 8 mL scintillation vial equipped with a magnetic stir bar and Teflon-seal screw cap. MeCN (5 mL) was added as solvent. BrPyTri ligand (75 mg, 0.25 mmol) was dissolved in minimal MeCN and

added dropwise. The reaction was placed on a heating block at 65 °C and allowed to stir for 30 min. The reaction was removed from heat and AgBF₄ (38 mg, 0.2 mmol) dissolved in minimal MeCN was added dropwise. The reaction was placed back on the heating block and stirred for 18 h at 65 °C during which time the desired complex precipitated out of solution. The title compound was obtained as a tan solid in 88% yield (85 mg, 0.088 mmol). ATR-IR: 3156, 1637, 1604, 1478, 1047, 824, 784, 499, 452 cm⁻¹. ¹H NMR (500 MHz, DMSO-*d*₆) δ 10.24 (s, 1H), 9.88 (d, J = 5.5 Hz, 1H), 8.69 (t, J = 8 Hz, 1H), 8.47 (d, J = 7.5 Hz, 1H), 8.20 (d, J = 8.5 Hz, 2H), 8.10 (t, J = 6.5 Hz, 1H), 8.06 (d, J = 8.5 Hz, 2H). ¹³C NMR (125 MHz, DMSO-*d*₆) δ 152.5, 150.0, 147.6, 143.9, 134.8, 133.4, 128.1, 126.2, 124.6, 123.6, 123.0.

Synthesis of (CF₃PyTri)₂Pt(BF₄)₂ (6e):

PtCl₂ (26 mg, 0.1 mmol) was added to an 8 mL scintillation vial equipped with a magnetic stir bar and Teflon-seal screw cap. MeCN (5 mL) was added as solvent. CF₃PyTri ligand (72 mg, 0.25 mmol) was dissolved in minimal MeCN and added dropwise. The reaction was placed on a heating block at 65 °C and allowed to stir for 30 min. The reaction was removed from heat and AgBF₄ (38 mg, 0.2 mmol) dissolved in minimal MeCN was added dropwise. The reaction was placed back on the heating block and stirred for 18 h at 65 °C during which time the desired complex precipitated out of solution. The title compound was obtained as a tan solid in 92% yield (87 mg, 0.092 mmol). ATR-IR: 3111, 1608, 1326, 1061, 846, 781, 518, 452 cm⁻¹. ¹H NMR (500 MHz, DMSO-*d*₆) δ 10.36 (s,

1H), 9.94 (d, J = 6 Hz, 1H), 8.72 (td, J = 1 Hz, J = 7 Hz, 1H), 8.51 (m, 3H), 8.26 (d, J = 8.5 Hz, 2H), 8.13 (td, J = 1 Hz, J = 6.5 Hz, 2H). ¹³C NMR (125 MHz, DMSO-*d*₆) δ 152.5, 150.1, 147.6, 144.0, 138.4, 128.1, 127.8, 126.6, 124.9, 123.1, 122.6, 118.1.

General procedure for the production of PyTriPtCl₂ complexes:

To an 8 mL scintillation vial equipped with a magnetic stir bar and Teflon-seal screw cap was added PtCl₂(DMSO)₂. MeCN was added as solvent followed by the PyTri ligand bearing the desired substitution dissolved in minimal MeCN. The reaction was stirred at ambient temperature for 18 h. Once completed, the reaction solution was passed through a plug of celite and concentrated until a saturated solution was obtained. Upon standing, the PyTriPtCl₂ complex precipitated as a microcrystalline powder. Recrystallization of these complexes occurred in MeNO₂.

Synthesis of MeOPyTriPtCl₂ (6f):

PtCl₂(DMSO)₂ (46 mg, 0.11 mmol) was added to an 8 mL scintillation vial equipped with a magnetic stir bar and Teflon-seal screw cap. MeCN (5 mL) was added as solvent. MeOPyTri ligand (25 mg, 0.1 mmol) was dissolved in minimal MeCN and added dropwise. The reaction was stirred at ambient temperature for 18 h. During this time the desired complex precipitated out of solution. The title compound was obtained as a tan solid in 94% yield (49 mg, 0.094 mmol). ATR-IR: 3108, 2925, 1726, 1511, 1464, 1249, 1013, 828, 770, 512, 433 cm⁻¹. ¹H NMR (500 MHz, DMSO-*d*₆) δ 9.79 (s, 1H), 9.36 (d, J = 5.5 Hz, 1H), 8.41 (t, J = 7.5 Hz,

1H), 8.17 (d, J = 7.5 Hz, 1H), 7.85 (d, J = 9 Hz, 2H), 7.76 (t, J = 6.5 Hz, 1H), 7.24 (d, J = 9 Hz, 2H), 3.87 (s, 3H). ¹³C NMR (125 MHz, DMSO-*d*₆) δ 160.6, 149.1, 148.8, 148.6, 141.0, 129.3, 126.1, 124.8, 122.9, 122.1, 115.2, 55.8.

Synthesis of MePyTriPtCl₂ (6g):

PtCl₂(DMSO)₂ (46 mg, 0.11 mmol) was added to an 8 mL scintillation vial equipped with a magnetic stir bar and Teflon-seal screw cap. MeCN (5 mL) was added as solvent. MePyTri ligand (24 mg, 0.1 mmol) was dissolved in minimal MeCN and added dropwise. The reaction was stirred at ambient temperature for 18 h. During this time the desired complex precipitated out of solution. The title compound was obtained as a tan solid in 84% yield (42 mg, 0.084 mmol). ATR-IR: 2925, 1725, 1511, 1461, 1276, 1111, 832, 772, 503, 430 cm⁻¹. ¹H NMR (500 MHz, DMSO-*d*₆) δ 9.86 (s, 1H), 9.38 (d, J = 6 Hz, 1H), 8.42 (t, J = 8 Hz, 1H), 8.18 (d, J = 8 Hz, 1H), 7.82 (d, J = 8.5 Hz, 2H), 7.77 (t, J = 6.5 Hz, 1H), 7.52 (d, J = 8.5 Hz, 2H), 2.43 (s, 3H). ¹³C NMR (125 MHz, DMSO-*d*₆) δ 149.0, 148.9, 148.6, 141.0, 140.5, 133.8, 130.6, 126.2, 124.7, 122.1, 120.9, 20.7.

Synthesis of PyTriPtCl₂ (6h):

PtCl₂(DMSO)₂ (46 mg, 0.11 mmol) was added to an 8 mL scintillation vial equipped with a magnetic stir bar and Teflon-seal screw cap. MeCN (5 mL) was added as solvent. PyTri ligand (22 mg, 0.1 mmol) was dissolved in minimal MeCN and added dropwise. The reaction was stirred at ambient temperature for 18 h. During this time the desired complex precipitated out of solution. The title compound was obtained as a tan solid in 90% yield (44 mg, 0.09 mmol). ATR-IR:

3147, 3057, 1628, 1594, 1500, 1464, 1285, 1074, 768, 695, 497, 431 cm^{-1} . ^1H NMR (500 MHz, $\text{DMSO-}d_6$) δ 9.91 (s, 1H), 9.35 (d, $J = 6.5$ Hz, 1H), 8.41 (td, $J = 1.5$ Hz, $J = 6.5$ Hz, 1H), 8.19 (d, $J = 8$ Hz, 1H), 7.93 (d, $J = 7.5$ Hz, 2H), 7.76 (td, $J = 1$ Hz, $J = 4.5$ Hz, 1H), 7.72 (t, $J = 8$ Hz, 2H), 7.67 (tt, $J = 2$ Hz, $J = 7$ Hz, 1H). ^{13}C NMR (125 MHz, $\text{DMSO-}d_6$) δ 149.0, 148.9, 148.6, 141.0, 136.1, 130.6, 130.3, 126.2, 124.9, 122.2, 121.1. Elemental analysis for PyTriPtCl_2 ($\text{C}_{13}\text{H}_{10}\text{Cl}_2\text{N}_4\text{Pt}$): *Calculated* – C: 31.98, H: 2.06, N: 11.48. *Found* – C: 31.57, H: 1.98, N: 11.26.

Synthesis of BrPyTriPtCl_2 (6i):

$\text{PtCl}_2(\text{DMSO})_2$ (46 mg, 0.11 mmol) was added to an 8 mL scintillation vial equipped with a magnetic stir bar and Teflon-seal screw cap. MeCN (5 mL) was added as solvent. BrPyTri ligand (30 mg, 0.1 mmol) was dissolved in minimal MeCN and added dropwise. The reaction was stirred at ambient temperature for 18 h. During this time the desired complex precipitated out of solution. The title compound was obtained as a tan solid in 85% yield (48 mg, 0.085 mmol). ATR-IR: 3078, 1626, 1493, 1468, 1065, 1009, 827, 767, 519, 488, 428 cm^{-1} . ^1H NMR (500 MHz, $\text{DMSO-}d_6$) δ 9.93 (s, 1H), 9.38 (d, $J = 5.5$ Hz, 1H), 8.43 (t, $J = 7.5$ Hz, 1H), 8.18 (d, $J = 8$ Hz, 1H), 7.95 (d, $J = 9$ Hz, 2H), 7.91 (d, $J = 9$ Hz, 2H), 7.78 (t, $J = 7$ Hz, 1H). ^{13}C NMR (125 MHz, $\text{DMSO-}d_6$) δ 149.0, 148.8, 148.6, 141.0, 135.3, 133.2, 126.3, 124.9, 123.4, 123.0, 122.2.

Synthesis of $\text{CF}_3\text{PyTriPtCl}_2$ (6j):

PtCl₂(DMSO)₂ (46 mg, 0.11 mmol) was added to an 8 mL scintillation vial equipped with a magnetic stir bar and Teflon-seal screw cap. MeCN (5 mL) was added as solvent. CF₃PyTri ligand (29 mg, 0.1 mmol) was dissolved in minimal MeCN and added dropwise. The reaction was stirred at ambient temperature for 18 h. During this time the desired complex precipitated out of solution. The title compound was obtained as a tan solid in 88% yield (49 mg, 0.088 mmol). ATR-IR: 3080, 1615, 1327, 1162, 1124, 1057, 843, 769, 602, 520, 494, 433 cm⁻¹. ¹H NMR (500 MHz, DMSO-*d*₆) δ 10.06 (s, 1H), 9.36 (d, J = 6 Hz, 1H), 8.43 (td, J = 1 Hz, J = 6.5 Hz, 1H), 8.19 (m, 3H), 8.13 (d, J = 8.5 Hz, 2H), 7.78 (t, J = 6 Hz, 1H). ¹³C NMR (125 MHz, DMSO-*d*₆) δ 149.2, 148.7, 148.6, 141.1, 138.9, 130.2, 127.6, 126.4, 125.1, 122.3, 121.7, 120.7.

General procedure for the production of PyTriPdCl₂ complexes:

To an 8 mL scintillation vial equipped with a magnetic stir bar and Teflon-seal screw cap was added PdCl₂(MeCN)₂. DCM was added as solvent followed by the PyTri ligand bearing the desired substitution dissolved in minimal DCM. The reaction was stirred at ambient temperature for 18 h during which, precipitation of the complex occurred. The solid was collected via a centrifuge and washed 5 times with DCM to remove impurities. Recrystallization of these complexes occurred in DMF or MeNO₂.

Synthesis of MeOPyTriPdCl₂ (6k):

PdCl₂(MeCN)₂ (39 mg, 0.15 mmol) was added to an 8 mL scintillation vial equipped with a magnetic stir bar and Teflon-seal screw cap. DCM (5 mL) was

added as solvent. MeOPyTri ligand (25 mg, 0.1 mmol) was dissolved in minimal DCM and added dropwise. The reaction was stirred at ambient temperature for 18 h. During this time the desired complex precipitated out of solution. The solid was collected in a centrifuge tube and washed 5 times with DCM. The title compound was obtained as an orange solid in 93% yield (40 mg, 0.093 mmol). ATR-IR: 3110, 1602, 1511, 1463, 1255, 1014, 830, 773, 631, 510, 425 cm^{-1} . ^1H NMR (500 MHz, $\text{DMSO-}d_6$) δ 9.76 (s, 1H), 9.01 (d, $J = 5.5$ Hz, 1H), 8.36 (t, $J = 7.5$ Hz, 1H), 8.16 (d, $J = 8$ Hz, 1H), 7.84 (d, $J = 8.5$ Hz, 2H), 7.74 (t, $J = 6.5$ Hz, 1H), 7.24 (d, $J = 8.5$ Hz, 2H), 3.87 (s, 3H). ^{13}C NMR (125 MHz, $\text{DMSO-}d_6$) δ 160.6, 149.6, 148.2, 148.1, 141.6, 129.0, 125.8, 124.2, 122.9, 122.0, 115.2, 55.8.

Synthesis of MePyTriPdCl₂ (6I):

$\text{PdCl}_2(\text{MeCN})_2$ (39 mg, 0.15 mmol) was added to an 8 mL scintillation vial equipped with a magnetic stir bar and Teflon-seal screw cap. DCM (5 mL) was added as solvent. MePyTri ligand (23 mg, 0.1 mmol) was dissolved in minimal DCM and added dropwise. The reaction was stirred at ambient temperature for 18 h. During this time the desired complex precipitated out of solution. The solid was collected in a centrifuge tube and washed 5 times with DCM. The title compound was obtained as an orange solid in 83% yield (34 mg, 0.083 mmol). ATR-IR: 3095, 1623, 1514, 1462, 1283, 813, 774, 499, 419 cm^{-1} . ^1H NMR (500 MHz, $\text{DMSO-}d_6$) δ 9.83 (s, 1H), 9.01 (d, $J = 5.5$ Hz, 1H), 8.37 (t, $J = 7.5$ Hz, 1H), 8.16 (d, $J = 7.5$ Hz, 1H), 7.80 (d, $J = 8$ Hz, 2H), 7.75 (t, $J = 6.5$ Hz, 1H), 7.51 (d, $J = 8$ Hz, 2H), 2.43 (s, 3H). ^{13}C NMR (125 MHz, $\text{DMSO-}d_6$) δ 149.6, 148.2, 148.1,

141.6, 140.6, 133.6, 130.6, 125.8, 124.1, 122.0, 120.9 20.7.

Synthesis of PyTriPdCl₂ (6m):

PdCl₂(MeCN)₂ (39 mg, 0.15 mmol) was added to an 8 mL scintillation vial equipped with a magnetic stir bar and Teflon-seal screw cap. DCM (5 mL) was added as solvent. PyTri ligand (22 mg, 0.1 mmol) was dissolved in minimal DCM and added dropwise. The reaction was stirred at ambient temperature for 18 h. During this time the desired complex precipitated out of solution. The solid was collected in a centrifuge tube and washed 5 times with DCM. The title compound was obtained as an orange solid in 91% yield (36 mg, 0.091 mmol). ATR-IR: 3145, 1584, 1461, 1284, 1072, 768, 684, 494, 426 cm⁻¹. ¹H NMR (500 MHz, DMSO-*d*₆) δ 9.88 (s, 1H), 9.02 (d, J = 5.5 Hz, 1H), 8.37 (t, J = 7.5 Hz, 1H), 8.18 (d, J = 7.5 Hz, 1H), 7.92 (d, J = 7.5 Hz, 2H), 7.70 (m, 5H). ¹³C NMR (125 MHz, DMSO-*d*₆) δ 149.6, 148.1, 141.6, 140.1, 133.6, 130.6, 130.2, 125.9, 124.3, 122.0, 121.2.

Synthesis of BrPyTriPdCl₂ (6n):

PdCl₂(MeCN)₂ (39 mg, 0.15 mmol) was added to an 8 mL scintillation vial equipped with a magnetic stir bar and Teflon-seal screw cap. DCM (5 mL) was added as solvent. BrPyTri ligand (30 mg, 0.1 mmol) was dissolved in minimal DCM and added dropwise. The reaction was stirred at ambient temperature for 18 h. During this time the desired complex precipitated out of solution. The solid was collected in a centrifuge tube and washed 5 times with DCM. The title compound was obtained as a yellow solid in 99% yield (47 mg, 0.099 mmol).

ATR-IR: 3099, 1595, 1493, 1460, 1284, 1066, 830, 775, 498, 425 cm^{-1} . ^1H NMR (500 MHz, $\text{DMSO-}d_6$) δ 9.91 (s, 1H), 9.02 (d, $J = 5.5$ Hz, 1H), 8.37 (t, $J = 7.5$ Hz, 1H), 8.16 (d, $J = 8$ Hz, 1H), 7.95 (d, $J = 8.5$ Hz, 2H), 7.89 (d, $J = 8.5$ Hz, 2H), 7.76 (t, $J = 6.5$ Hz). ^{13}C NMR (125 MHz, $\text{DMSO-}d_6$) δ 149.6, 148.3, 147.9, 141.6, 135.1, 133.2, 125.9, 124.3, 123.5, 123.1, 122.1. Elemental analysis for BrPyTriPdCl_2 ($\text{C}_{13}\text{H}_9\text{BrCl}_2\text{N}_4\text{Pd}$) : *Calculated* – C: 32.63, H: 1.90, N: 11.71. *Found* – C: 32.68, H: 1.90, N: 11.54.

Synthesis of $\text{CF}_3\text{PyTriPdCl}_2$ (6o):

$\text{PdCl}_2(\text{MeCN})_2$ (39 mg, 0.15 mmol) was added to an 8 mL scintillation vial equipped with a magnetic stir bar and Teflon-seal screw cap. DCM (5 mL) was added as solvent. CF_3PyTri ligand (28 mg, 0.1 mmol) was dissolved in minimal DCM and added dropwise. The reaction was stirred at ambient temperature for 18 h. During this time the desired complex precipitated out of solution. The solid was collected in a centrifuge tube and washed 5 times with DCM. The title compound was obtained as a yellow solid in 98% yield (46 mg, 0.098 mmol). ATR-IR: 3074, 1615, 1327, 1161, 1124, 1064, 844, 771, 602, 489, 421 cm^{-1} . ^1H NMR (500 MHz, $\text{DMSO-}d_6$) δ 10.03 (s, 1H), 9.01 (d, $J = 5$ Hz, 1H), 8.38 (t, $J = 8$ Hz, 1H), 8.16 (m, 5H), 7.76 (d, $J = 6.5$ Hz, 1H). ^{13}C NMR (125 MHz, $\text{DMSO-}d_6$) δ 149.7, 148.5, 147.8, 141.7, 138.6, 130.4, 127.6, 126.0, 124.7, 124.6, 122.2, 121.8.

General procedure for the production of $(\text{PyTri})_2\text{Pd}(\text{BF}_4)_2$ complexes:

To an 8 mL scintillation vial equipped with a magnetic stir bar and Teflon-seal screw cap was added $\text{Pd}(\text{BF}_4)_2(\text{MeCN})_4$. MeCN was added as solvent followed by the PyTri ligand dissolved in minimal MeCN. The reaction was stirred at ambient temperature for 18 h during which, precipitation of the complex occurred. The solid was collected via a centrifuge and washed 3 times with MeCN to remove impurities.

Synthesis of $(\text{PyTri})_2\text{Pd}(\text{BF}_4)_2$ (6p):

$\text{Pd}(\text{MeCN})_4(\text{BF}_4)_2$ (44 mg, 0.1 mmol) was added to an 8 mL scintillation vial equipped with a magnetic stir bar and Teflon-seal screw cap. MeCN (5 mL) was added as solvent. PyTri ligand (52 mg, 0.22 mmol) was dissolved in minimal MeCN and added dropwise. The reaction was stirred at ambient temperature for 18 h during which time the desired complex precipitated out of solution. The solid was collected via a centrifuge and washed 3 times with MeCN to remove impurities. The title compound was obtained as a white solid in 96% yield (69 mg, 0.096 mmol).

or

PyTriPdCl_2 (40 mg, 0.1 mmol) was added to an 8 mL scintillation vial equipped with a magnetic stir bar and Teflon-seal screw cap. MeCN (5 mL) was added as solvent.

PyTri ligand (22 mg, 0.1 mmol) was dissolved in minimal MeCN and added dropwise. AgBF_4 (48 mg, 0.25 mmol) was dissolved in minimal MeCN and added dropwise. The reaction was heated to 65 °C and stirred for 18 h during which

time the desired complex precipitated out of solution. The solid was collected via a centrifuge and washed 3 times with MeCN to remove impurities. The title compound was obtained as a white solid in 90% yield (65 mg, 0.09 mmol). Characterization of this complex matches that published by: Kilpin, K. J.; Gavey, E. L.; McAdam, C. J.; Anderson, C. B.; Lind, S. J.; Keep, C. C.; Gordon, K. C.; Crowley, J. D. *Inorg. Chem.* **2011**, *50*, 6334.

General procedure for the preparation of stock solutions of RPyTriPdCl₂ complexes:

0.01 M (1 mol%) RPyTriPdCl₂ in DMF: To an 8 mL scintillation vial equipped with a Teflon-seal screw cap was added PyTriPdCl₂ (7.98 mg, 0.02 mmol) or MeOPyTriPdCl₂ (8.60 mg, 0.02 mmol) or CF₃PyTriPdCl₂ (9.35 mg, 0.02 mmol). Dry DMF (2 mL) was added and the solution was mixed until the catalyst was completely dissolved. The solution was a pale yellow color. 1 mL of solution contained 1 mol% of the PyTriPdCl₂ catalyst (3.99 mg) or MeOPyTriPdCl₂ catalyst (4.30 mg) or CF₃PyTriPdCl₂ catalyst (4.68 mg). 0.1 mL of solution contained 0.1 mol% of the PyTriPdCl₂ catalyst (0.39 mg) or MeOPyTriPdCl₂ catalyst (0.43 mg) or CF₃PyTriPdCl₂ catalyst (0.47 mg).

0.001 M (0.1 mol%) RPyTriPdCl₂ in DMF: To an 8 mL scintillation vial equipped with a Teflon-seal screw cap was added 0.1 mL of the 0.01M PyTriPdCl₂ solution. Dry DMF (0.9 mL) was added and the solution was stirred for 5 min. The solution was a very pale yellow color and 0.1 mL of solution contained 0.01 mol% of the

PyTriPdCl₂ catalyst (0.039 mg) or MeOPyTriPdCl₂ catalyst (0.043 mg) or CF₃PyTriPdCl₂ catalyst (0.047 mg).

General procedure for the optimization of RPyTriPdCl₂ complexes for Suzuki-Miyaura Cross-Coupling:

To a 20 mL scintillation vial equipped with a magnetic stir bar and PTFE coated screw cap was added phenylboronic acid followed by base, typically K₂CO₃. Solvent was added followed by 4-iodoanisole. The desired amount of PyTriPdCl₂ complex was added via a stock solution in DMF. The reaction was stirred at the desired temperature and the reaction was monitored using gas chromatography (GC) with dodecane as an internal standard to measure product formation.

Synthesis of 4-Methoxy-biphenyl (6q):

To a 20 mL scintillation vial equipped with a magnetic stir bar and PTFE coated screw cap was added phenylboronic acid (244 mg, 2 mmol) followed by K₂CO₃ (690 mg, 5 mmol). EtOH (5 mL) was added followed by 4-iodoanisole (234 mg, 1 mmol). CF₃PyTriPdCl₂ complex (0.047 mg, 0.0001 mmol) was added via 0.1 mL of a 0.001 M stock solution in DMF. The reaction was stirred at 40 °C for 8 h. The title compound was obtained as a white solid in 98% yield (180 mg, 0.98 mmol) after column chromatography on silica gel using 100% hexanes as the eluent.

or

To a 20 mL scintillation vial equipped with a magnetic stir bar and PTFE coated screw cap was added phenylboronic acid (244 mg, 2 mmol) followed by K₂CO₃ (690 mg, 5 mmol). EtOH (5 mL) was added followed by 4-bromoanisole (125 μL,

1 mmol). $\text{CF}_3\text{PyTriPdCl}_2$ complex (0.047 mg, 0.0001 mmol) was added via a 0.1 mL of a 0.001 M stock solution in DMF. The reaction was stirred at 40 °C for 8 h. The title compound was obtained as a white solid in 80% yield (148 mg, 0.80 mmol) after column chromatography on silica gel using 100% hexanes as the eluent.

or

To a 20 mL scintillation vial equipped with a magnetic stir bar and PTFE coated screw cap was added 4-methoxybenzeneboronic acid (304 mg, 2 mmol) followed by K_2CO_3 (690 mg, 5 mmol). EtOH (5 mL) was added followed by bromobenzene (107 μL , 1 mmol). $\text{CF}_3\text{PyTriPdCl}_2$ complex (0.047 mg, 0.0001 mmol) was added via a 0.1 mL of a 0.001 M stock solution in DMF. The reaction was stirred at 40 °C for 8 h. The title compound was obtained in 98% yield (181 mg, 0.98 mmol) after column chromatography on silica gel using 100% hexanes as the eluent.

Characterization of these samples of 4-Methoxy-biphenyl matches that published by: Wang, S. M.; Wang, X. Y.; Qin, H. L.; Zhang, C. P. *Chem. Eur. J.* **2016**, *22*, 6542.

Synthesis of 4-Methyl-biphenyl (6r):

To a 20 mL scintillation vial equipped with a magnetic stir bar and PTFE coated screw cap was added phenylboronic acid (244 mg, 2 mmol) followed by K_2CO_3 (690 mg, 5 mmol). EtOH (5 mL) was added followed by 4-bromotoluene (171 mg, 1 mmol). $\text{CF}_3\text{PyTriPdCl}_2$ complex (0.047 mg, 0.0001 mmol) was added via a 0.1 mL of a 0.001 M stock solution in DMF. The reaction was stirred at 40 °C for 8 h.

The title compound was obtained as a white solid in 68% yield (114 mg, 0.68 mmol) after column chromatography on silica gel using 100% hexanes as the eluent.

or

To a 20 mL scintillation vial equipped with a magnetic stir bar and PTFE coated screw cap was added 4-methylbenzeneboronic acid (272 mg, 2 mmol) followed by K_2CO_3 (690 mg, 5 mmol). EtOH (5 mL) was added followed by bromobenzene (107 μ L, 1 mmol). $CF_3PyTriPdCl_2$ complex (0.047 mg, 0.0001 mmol) was added via a 0.1 mL of a 0.001 M stock solution in DMF. The reaction was stirred at 40 °C for 8 h. The title compound was obtained in 70% yield (118 mg, 0.70 mmol) after column chromatography on silica gel using 100% hexanes as the eluent.

Characterization of these samples of 4-Methyl-biphenyl matches that published by: Wang, S. M.; Wang, X. Y.; Qin, H. L.; Zhang, C. P. *Chem. Eur. J.* **2016**, *22*, 6542.

Synthesis of 4-(Trifluoromethyl)-biphenyl (6s):

To a 20 mL scintillation vial equipped with a magnetic stir bar and PTFE coated screw cap was added phenylboronic acid (244 mg, 2 mmol) followed by K_2CO_3 (690 mg, 5 mmol). EtOH (5 mL) was added followed by 4-bromobenzotrifluoride (140 μ L, 1 mmol). $CF_3PyTriPdCl_2$ complex (0.047 mg, 0.0001 mmol) was added via a 0.1 mL of a 0.001 M stock solution in DMF. The reaction was stirred at 40 °C for 8 h. The title compound was obtained as a white solid in 98% yield (218

mg, 0.98 mmol) after column chromatography on silica gel using 100% pentane as the eluent.

or

To a 20 mL scintillation vial equipped with a magnetic stir bar and PTFE coated screw cap was added 4-(trifluoromethyl)benzeneboronic acid (380 mg, 2 mmol) followed by K_2CO_3 (690 mg, 5 mmol). EtOH (5 mL) was added followed by bromobenzene (107 μ L, 1 mmol). $CF_3PyTriPdCl_2$ complex (0.047 mg, 0.0001 mmol) was added via a 0.1 mL of a 0.001 M stock solution in DMF. The reaction was stirred at 40 °C for 8 h. The title compound was obtained in 60% yield (133 mg, 0.60 mmol) after column chromatography on silica gel using 100% pentanes as the eluent.

Characterization of these samples of 4-(Trifluoromethyl)-biphenyl matches that published by: Asghar, S.; Tailor, S. B.; Elorriaga, D.; Bedford, R. B. *Angew. Chem. Int. Ed.* **2017**, *56*, 16367.

Synthesis of 4-chloro-biphenyl (6t):

To a 20 mL scintillation vial equipped with a magnetic stir bar and PTFE coated screw cap was added phenylboronic acid (244 mg, 2 mmol) followed by K_2CO_3 (690 mg, 5 mmol). EtOH (5 mL) was added followed by 1-bromo-4-chlorobenzene (191 mg, 1 mmol). $CF_3PyTriPdCl_2$ complex (0.047 mg, 0.0001 mmol) was added via a 0.1 mL of a 0.001 M stock solution in DMF. The reaction was stirred at 40 °C for 8 h. The title compound was obtained as a white solid in

90% yield (170 mg, 0.90 mmol) after column chromatography on silica gel using 100% hexanes as the eluent.

Characterization of this sample of 4-chloro-biphenyl matches that published by: Wang, S. M.; Wang, X. Y.; Qin, H. L.; Zhang, C. P. *Chem. Eur. J.* **2016**, *22*, 6542.

Synthesis of 3-Methoxy-biphenyl (6u):

To a 20 mL scintillation vial equipped with a magnetic stir bar and PTFE coated screw cap was added phenylboronic acid (244 mg, 2 mmol) followed by K_2CO_3 (690 mg, 5 mmol). EtOH (5 mL) was added followed by 3-bromoanisole (127 μ L, 1 mmol). $CF_3PyTriPdCl_2$ complex (0.047 mg, 0.0001 mmol) was added via a 0.1 mL of a 0.001 M stock solution in DMF. The reaction was stirred at 40 °C for 8 h. The title compound was obtained as a white solid in 60% yield (111 mg, 0.60 mmol) after column chromatography on silica gel using 100% hexanes as the eluent.

Characterization of this sample of 3-methoxy-biphenyl matches that published by: Wang, S. M.; Wang, X. Y.; Qin, H. L.; Zhang, C. P. *Chem. Eur. J.* **2016**, *22*, 6542.

Synthesis of 2-(4-Methoxyphenyl)pyridine (6v):

To a 20 mL scintillation vial equipped with a magnetic stir bar and PTFE coated screw cap was added 4-methoxybenzeneboronic acid (302 mg, 2 mmol) followed by K_2CO_3 (690 mg, 5 mmol). *t*-BuOH (5 mL) was added followed by 2-bromopyridine (95 μ L, 1 mmol). $CF_3PyTriPdCl_2$ complex (0.094 mg, 0.0002 mmol) was added via a 0.2 mL of a 0.001 M stock solution in DMF. The reaction

was stirred at 80 °C for 8 h. The title compound was obtained as a white solid in 53% yield (98 mg, 0.53 mmol) after column chromatography on silica gel using a 5% diethyl/hexanes solution as the eluent. ATR-IR: 2961, 1579, 1512, 1430, 1243, 1018, 776 cm^{-1} . ^1H NMR (500 MHz, acetone- d_6) δ 8.61 (d, J = 4 Hz, 1H), 8.08 (d, J = 9 Hz, 2H), 7.85 (d, J = 8 Hz, 1H), 7.80 (td, J = 1.5 Hz, J = 6 Hz, 1H), 7.23 (t, J = 6 Hz, 1H), 7.03 (d, J = 8.5 Hz, 2H), 3.86 (s, 3H). ^{13}C NMR (125 MHz, acetone- d_6) δ 161.6, 157.4, 150.3, 137.6, 132.7, 128.8, 122.4, 120.0, 114.8, 55.7. HRMS calculated requires $[\text{M}+\text{H}]^+$: 186.0913. Found m/z : 186.0815.

Synthesis of 3-(4-Methoxyphenyl)pyridine (6w):

To a 20 mL scintillation vial equipped with a magnetic stir bar and PTFE coated screw cap was added 4-methoxybenzeneboronic acid (302 mg, 2 mmol) followed by K_2CO_3 (690 mg, 5 mmol). t -BuOH (5 mL) was added followed by 3-bromopyridine (95 μL , 1 mmol). $\text{CF}_3\text{PyTriPdCl}_2$ complex (0.094 mg, 0.0002 mmol) was added via a 0.2 mL of a 0.001 M stock solution in DMF. The reaction was stirred at 80 °C for 8 h. The title compound was obtained as a white solid in 99% yield (183 mg, 0.99 mmol) after gradient column chromatography on silica gel using (5% Et_2O /Hexanes up to 20% Et_2O /Hexanes) as the eluent. ATR-IR: 2918, 1605, 1517, 1281, 1250, 1021, 801, 705 cm^{-1} . ^1H NMR (500 MHz, acetone- d_6) δ 8.83 (t, J = 1.5 Hz, 1H), 8.51 (dt, J = 1 Hz, J = 4.5 Hz, 1H), 7.97 (dq, J = 1.5 Hz, J = 8 Hz, 1H), 7.64 (dd, J = 1 Hz, J = 7.5 Hz, 2H), 7.40 (ddt, J = 1 Hz, J = 3 Hz, J = 5 Hz, 1H), 7.07 (dd, J = 1 Hz, J = 8 Hz, 2H), 3.86 (s, 3H). ^{13}C NMR (125 MHz, acetone- d_6) δ 160.9, 148.8, 148.6, 136.8, 134.2, 131.0, 129.0,

124.4, 115.4, 55.7. HRMS calculated requires $[M+H]^+$: 186.0913. Found m/z : 186.0795.

Synthesis of 2-(4-Methoxyphenyl)quinoline (6x):

To a 20 mL scintillation vial equipped with a magnetic stir bar and PTFE coated screw cap was added 4-methoxybenzeneboronic acid (302 mg, 2 mmol) followed by K_2CO_3 (690 mg, 5 mmol). *t*-BuOH (5 mL) was added followed by 2-bromoquinoline (208 mg, 1 mmol). $CF_3PyTriPdCl_2$ complex (0.094 mg, 0.0002 mmol) was added via a 0.2 mL of a 0.001 M stock solution in DMF. The reaction was stirred at 80 °C for 8 h. The title compound was obtained as a white solid in 89% yield (209 mg, 0.89 mmol) after column chromatography on silica gel using a 5% diethyl/hexanes solution as the eluent. ATR-IR: 2959, 1595, 1496, 1248, 1027, 816, 748 cm^{-1} . 1H NMR (500 MHz, acetone- d_6) δ 8.34 (d, J = 8.5 Hz, 1H), 8.29 (dt, J = 2 Hz, J = 9 Hz, 2H), 8.06 (dd, J = 7.5 Hz, J = 8.5 Hz, 2H), 7.92 (dd, J = 1 Hz, J = 7 Hz, 1H), 7.74 (td, J = 1.5 Hz, J = 5 Hz, 1H), 7.54 (td, J = 1 Hz, J = 6 Hz, 1H), 7.10 (dt, J = 2.5 Hz, J = 9 Hz, 2H), 3.89 (s, 3H). ^{13}C NMR (125 MHz, acetone- d_6) δ 162.0, 157.1, 149.2, 137.6, 132.7, 130.4, 130.2, 129.6, 128.5, 127.9, 126.8, 119.0, 115.0, 55.7. HRMS calculated requires $[M+H]^+$: 236.1070. Found m/z : 236.1074.

Synthesis of 2-(4-Methoxyphenyl)benzofuran (6y):

To a 20 mL scintillation vial equipped with a magnetic stir bar and PTFE coated screw cap was added 4-methoxybenzeneboronic acid (302 mg, 2 mmol) followed by K_2CO_3 (690 mg, 5 mmol). *t*-BuOH (5 mL) was added followed by 2-

bromobenzofuran (197 mg, 1 mmol). $\text{CF}_3\text{PyTriPdCl}_2$ complex (0.094 mg, 0.0002 mmol) was added via a 0.2 mL of a 0.001 M stock solution in DMF. The reaction was stirred at 80 °C for 8 h. The title compound was obtained as a white solid in 99% yield (223 mg, 0.99 mmol) after column chromatography on silica gel using 100% hexanes as the eluent. ATR-IR: 1608, 1503, 1439, 1247, 1022, 799, 742 cm^{-1} . ^1H NMR (500 MHz, acetone- d_6) δ 7.87 (dt, $J = 2$ Hz, $J = 9$ Hz, 2H), 7.60 (dq, $J = 1$ Hz, $J = 7$ Hz, 1H), 7.53 (dd, $J = 1$ Hz, $J = 7.5$ Hz, 1H), 7.28 (td, $J = 1.5$ Hz, $J = 6$ Hz, 1H), 7.22 (td, $J = 1$ Hz, $J = 6.5$ Hz, 1H), 7.13 (s, 1H), 7.06 (dt, $J = 2$ Hz, $J = 9$ Hz, 2H), 3.87 (s, 3H). ^{13}C NMR (125 MHz, acetone- d_6) δ 161.3, 156.9, 155.5, 130.5, 127.2, 124.8, 123.9, 123.9, 121.6, 115.3, 111.6, 100.7, 55.7. HRMS calculated requires $[\text{M}+\text{H}]^+$: 225.0910. Found m/z : 225.0721.

Synthesis of 1,1-biphenyl (6z):

To a 20 mL scintillation vial equipped with a magnetic stir bar and PTFE coated screw cap was added phenylboronic acid (244 mg, 2 mmol) followed by K_2CO_3 (690 mg, 5 mmol). EtOH (5 mL) was added followed by bromobenzene (107 μL , 1 mmol). $\text{CF}_3\text{PyTriPdCl}_2$ complex (0.047 mg, 0.0001 mmol) was added via a 0.1 mL of a 0.001 M stock solution in DMF. The reaction was stirred at 40 °C for 8 h. The title compound was obtained in 73% yield (113 mg, 0.73 mmol) after column chromatography on silica gel using 100% hexanes as the eluent.

Characterization of this sample of 1,1-biphenyl matches that published by: Wang, Q.; Jing, X.; Han, J.; Yu, L.; Xu, Q. *Mater. Lett.* **2018**, *215*, 65.

Synthesis of 4-(tert-Butyl)-biphenyl (6aa):

To a 20 mL scintillation vial equipped with a magnetic stir bar and PTFE coated screw cap was added 4-(*tert*-butyl)benzeneboronic acid (356 mg, 2 mmol) followed by K_2CO_3 (690 mg, 5 mmol). EtOH (5 mL) was added followed by bromobenzene (107 μ L, 1 mmol). $CF_3PyTriPdCl_2$ complex (0.047 mg, 0.0001 mmol) was added via a 0.1 mL of a 0.001 M stock solution in DMF. The reaction was stirred at 40 °C for 8 h. The title compound was obtained in 99% yield (208 mg, 0.99 mmol) after column chromatography on silica gel using 100% hexanes as the eluent.

Characterization of this sample of 4-(*tert*-Butyl)-biphenyl matches that published by: Wang, S. M.; Wang, X. Y.; Qin, H. L.; Zhang, C. P. *Chem. Eur. J.* **2016**, *22*, 6542.

X-ray crystallography for $(PyTri)_2Pt(BF_4)_2$ complexes:

To obtain a suitable crystal of $(CF_3PyTri)_2Pt(BF_4)_2$, a saturated solution of the complex was prepared in MeCN. This solution was left to stand in a vial equipped with a PTFE coated screw cap at ambient temperature for 14 days. Clear colorless crystals formed and were of high enough quality for analysis.

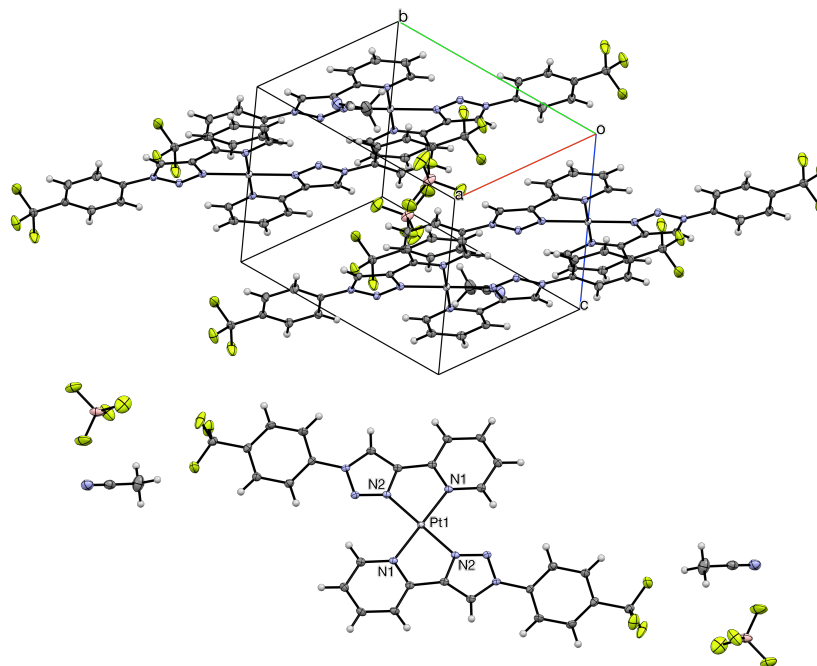


Table 1. Crystal data and structure refinement for **(CF₃PyTri)₂Pt(BF₄)₂**

Empirical formula	C ₃₂ H ₂₄ B ₂ F ₁₄ N ₁₀ Pt
Formula weight	1031.32
Temperature	100.0 K
Wavelength, Å	0.71073
Crystal system	Triclinic
space group	<i>P</i> -1
a, Å	7.2410(3)
b, Å	11.1823(5)
c, Å	11.4006(5)
α, °	81.682(2)
β, °	89.9830(10)
γ, °	74.1850(10)
Volume	878.09(7) Å ³
Z, Z'	1, 0.5
Calculated density, mg/m ³	1.950
Absorption coefficient, mm ⁻¹	4.113
F(000)	500
Crystal size, mm	0.26 x 0.24 x 0.22
Theta range for data collection, °	1.807 to 28.286
Index ranges	-9 ≤ h ≤ 9, -14 ≤ k ≤ 14, -15 ≤ l ≤ 14
Reflections collected / unique	15454 / 4368 [<i>R</i> _{int} = 0.0334]
Completeness to θ = 25.242°	100.0 %
Absorption correction	Semi-empirical from equivalents
Max. and min. transmission	0.5633 and 0.4870
Refinement method	Full-matrix least-squares on <i>F</i> ²
Data / restraints / parameters	4368 / 0 / 269

Goodness-of-fit on F^2	1.053
Final R indices [$I > 2\sigma(I)$]	$R1 = 0.0169$, $wR2 = 0.0410$
R indices (all data)	$R1 = 0.0169$, $wR2 = 0.0410$
Extinction coefficient	n/a
Largest diff. peak and hole, $e\text{\AA}^{-3}$	0.762 and -0.400

Table 2. Atomic coordinates ($\times 10^4$) and equivalent isotropic displacement parameters ($\text{\AA}^2 \times 10^3$) for $(\text{CF}_3\text{PyTri})_2\text{Pt}(\text{BF}_4)_2$. $U(\text{eq})$ is defined as one third of the trace of the orthogonalized U^{ij} tensor.

	x	y	z	$U(\text{eq})$
Pt(1)	10000	10000	5000	10(1)
F(2)	-488(2)	5837(1)	3452(1)	31(1)
F(4)	13697(2)	6156(1)	8226(1)	36(1)
F(6)	13015(2)	8258(1)	8228(1)	36(1)
F(1)	1253(2)	5642(2)	1942(1)	33(1)
F(3)	1862(2)	4199(1)	3462(2)	37(1)
F(5)	11803(3)	7052(2)	9627(1)	50(1)
N(1)	9192(2)	10259(2)	6687(1)	11(1)
N(3)	7288(2)	8445(2)	4506(1)	12(1)
F(7)	10707(2)	7384(2)	7702(2)	44(1)
C(2)	9283(3)	10997(2)	8546(2)	15(1)
N(4)	5918(2)	8076(2)	5128(1)	11(1)
C(10)	2420(3)	6267(2)	4832(2)	19(1)
C(11)	2615(3)	6088(2)	3655(2)	14(1)
C(12)	3960(3)	6514(2)	2968(2)	15(1)
N(2)	7981(2)	9080(1)	5194(1)	11(1)
C(1)	9957(3)	10854(2)	7421(2)	14(1)
N(5)	3176(3)	1851(2)	-959(2)	25(1)
C(4)	7008(3)	9886(2)	8200(2)	14(1)
C(3)	7787(3)	10516(2)	8941(2)	15(1)

C(00L)	1330(3)	5442(2)	3120(2)	16(1)
C(9)	3534(3)	6899(2)	5333(2)	18(1)
C(13)	5077(3)	7162(2)	3460(2)	14(1)
C(5)	7738(3)	9772(2)	7089(2)	12(1)
C(8)	4834(3)	7355(2)	4631(2)	12(1)
C(15)	2881(3)	2683(2)	-454(2)	20(1)
C(7)	5734(3)	8471(2)	6204(2)	13(1)
C(6)	7079(3)	9120(2)	6241(2)	12(1)
C(14)	2489(4)	3737(2)	214(3)	34(1)
B(1)	12282(4)	7209(2)	8462(2)	24(1)

Table 3. Bond lengths [Å] and angles [°] for (CF₃PyTri)₂Pt(BF₄)₂.

Pt(1)-N(1)	2.0475(15)
Pt(1)-N(1)#1	2.0475(15)
Pt(1)-N(2)	2.0000(16)
Pt(1)-N(2)#1	2.0000(16)
F(2)-C(00L)	1.342(2)
F(4)-B(1)	1.393(3)
F(6)-B(1)	1.407(3)
F(1)-C(00L)	1.328(2)
F(3)-C(00L)	1.336(2)
F(5)-B(1)	1.372(3)
N(1)-C(1)	1.346(2)
N(1)-C(5)	1.363(2)
N(3)-N(4)	1.340(2)
N(3)-N(2)	1.313(2)
F(7)-B(1)	1.385(3)
C(2)-C(1)	1.387(3)
C(2)-C(3)	1.383(3)
N(4)-C(8)	1.438(2)
N(4)-C(7)	1.357(2)
C(10)-C(11)	1.386(3)
C(10)-C(9)	1.380(3)
C(11)-C(12)	1.391(3)
C(11)-C(00L)	1.501(3)
C(12)-C(13)	1.390(3)
N(2)-C(6)	1.362(2)
N(5)-C(15)	1.135(3)
C(4)-C(3)	1.385(3)
C(4)-C(5)	1.382(3)
C(9)-C(8)	1.389(3)
C(13)-C(8)	1.386(3)
C(5)-C(6)	1.444(3)
C(15)-C(14)	1.458(3)

C(7)-C(6)	1.367(3)
N(1)-Pt(1)-N(1)#1	180.00(2)
N(2)-Pt(1)-N(1)	79.41(6)
N(2)#1-Pt(1)-N(1)#1	79.41(6)
N(2)#1-Pt(1)-N(1)	100.59(6)
N(2)-Pt(1)-N(1)#1	100.59(6)
N(2)-Pt(1)-N(2)#1	180.0
C(1)-N(1)-Pt(1)	126.41(13)
C(1)-N(1)-C(5)	117.90(16)
C(5)-N(1)-Pt(1)	115.69(12)
N(2)-N(3)-N(4)	105.03(14)
C(3)-C(2)-C(1)	119.87(18)
N(3)-N(4)-C(8)	120.11(15)
N(3)-N(4)-C(7)	112.21(15)
C(7)-N(4)-C(8)	127.69(16)
C(9)-C(10)-C(11)	120.29(19)
C(10)-C(11)-C(12)	120.83(18)
C(10)-C(11)-C(00L)	119.09(18)
C(12)-C(11)-C(00L)	120.07(18)
C(13)-C(12)-C(11)	119.34(18)
N(3)-N(2)-Pt(1)	133.50(12)
N(3)-N(2)-C(6)	111.25(15)
C(6)-N(2)-Pt(1)	115.24(12)
N(1)-C(1)-C(2)	121.90(18)
C(5)-C(4)-C(3)	118.90(18)
C(2)-C(3)-C(4)	118.71(17)
F(2)-C(00L)-C(11)	111.69(17)
F(1)-C(00L)-F(2)	106.17(17)
F(1)-C(00L)-F(3)	107.32(17)
F(1)-C(00L)-C(11)	113.17(17)
F(3)-C(00L)-F(2)	105.53(17)
F(3)-C(00L)-C(11)	112.46(16)
C(10)-C(9)-C(8)	118.53(18)
C(8)-C(13)-C(12)	118.99(18)
N(1)-C(5)-C(4)	122.71(18)
N(1)-C(5)-C(6)	112.90(16)
C(4)-C(5)-C(6)	124.39(18)
C(9)-C(8)-N(4)	118.73(17)
C(13)-C(8)-N(4)	119.27(17)
C(13)-C(8)-C(9)	121.98(18)
N(5)-C(15)-C(14)	179.0(2)
N(4)-C(7)-C(6)	104.53(16)
N(2)-C(6)-C(5)	116.67(16)
N(2)-C(6)-C(7)	106.98(16)
C(7)-C(6)-C(5)	136.33(17)

F(4)-B(1)-F(6)	108.1(2)
F(5)-B(1)-F(4)	110.3(2)
F(5)-B(1)-F(6)	109.6(2)
F(5)-B(1)-F(7)	111.4(2)
F(7)-B(1)-F(4)	108.3(2)
F(7)-B(1)-F(6)	109.0(2)

Symmetry transformations used to generate equivalent atoms:
 #1 -x+2,-y+2,-z+1

Table 4. Anisotropic displacement parameters ($\text{\AA}^2 \times 10^3$) for $(\text{CF}_3\text{PyTri})_2\text{Pt}(\text{BF}_4)_2$. The anisotropic displacement factor exponent takes the form: $-2\pi^2 [h^2 a^{*2} U^{11} + \dots + 2 h k a^* b^* U^{12}]$

	U ¹¹	U ²²	U ³³	U ²³	U ¹³	U ¹²
Pt(1)	10(1)	10(1)	9(1)	-2(1)	2(1)	-3(1)
F(2)	14(1)	38(1)	44(1)	-17(1)	3(1)	-10(1)
F(4)	34(1)	35(1)	28(1)	-11(1)	-4(1)	12(1)
F(6)	37(1)	33(1)	38(1)	1(1)	17(1)	-14(1)
F(1)	41(1)	53(1)	18(1)	-7(1)	0(1)	-32(1)
F(3)	36(1)	12(1)	61(1)	2(1)	-23(1)	-8(1)
F(5)	91(1)	37(1)	30(1)	-13(1)	37(1)	-29(1)
N(1)	11(1)	11(1)	11(1)	-1(1)	2(1)	-2(1)
N(3)	12(1)	12(1)	12(1)	-1(1)	1(1)	-4(1)
F(7)	25(1)	38(1)	62(1)	-2(1)	-6(1)	0(1)
C(2)	16(1)	15(1)	13(1)	-3(1)	1(1)	-3(1)
N(4)	10(1)	11(1)	12(1)	-1(1)	2(1)	-3(1)
C(10)	19(1)	22(1)	17(1)	1(1)	4(1)	-12(1)
C(11)	13(1)	12(1)	18(1)	-1(1)	-1(1)	-4(1)
C(12)	16(1)	17(1)	14(1)	-3(1)	2(1)	-6(1)
N(2)	11(1)	11(1)	11(1)	-1(1)	2(1)	-2(1)
C(1)	13(1)	14(1)	14(1)	-2(1)	1(1)	-3(1)
N(5)	22(1)	32(1)	23(1)	-4(1)	6(1)	-10(1)
C(4)	13(1)	16(1)	13(1)	-1(1)	2(1)	-3(1)
C(3)	16(1)	18(1)	11(1)	-3(1)	3(1)	-2(1)
C(00L)	15(1)	16(1)	19(1)	0(1)	-1(1)	-5(1)

C(9)	21(1)	23(1)	13(1)	-2(1)	4(1)	-10(1)
C(13)	13(1)	15(1)	15(1)	-2(1)	3(1)	-4(1)
C(5)	11(1)	11(1)	12(1)	0(1)	0(1)	-1(1)
C(8)	11(1)	10(1)	14(1)	-1(1)	0(1)	-3(1)
C(15)	14(1)	26(1)	19(1)	2(1)	1(1)	-6(1)
C(7)	14(1)	12(1)	12(1)	-1(1)	2(1)	-3(1)
C(6)	11(1)	10(1)	12(1)	0(1)	2(1)	-1(1)
C(14)	26(1)	30(1)	49(2)	-16(1)	0(1)	-6(1)
B(1)	26(1)	21(1)	21(1)	-1(1)	11(1)	-2(1)

Table 5. Hydrogen coordinates ($\times 10^4$) and isotropic displacement parameters ($\text{\AA}^2 \times 10^{-3}$) for $(\text{CF}_3\text{PyTri})_2\text{Pt}(\text{BF}_4)_2$.

	x	y	z	U(eq)
H(2)	9848	11424	9044	18
H(10)	1516	5953	5295	23
H(12)	4114	6364	2169	18
H(1)	10989	11186	7161	16
H(4)	5988	9538	8450	17
H(3)	7304	10615	9706	18
H(9)	3414	7020	6140	22
H(13)	5992	7469	3001	17
H(7)	4866	8329	6798	16
H(14A)	2199	4528	-339	51
H(14B)	3618	3670	719	51
H(14C)	1387	3723	709	51

X-ray crystallography for PyTriPtCl_2 complexes:

To obtain a suitable crystal of PyTriPtCl_2 , a saturated solution of the complex was prepared in MeNO_2 . This solution was left to stand in a vial equipped with a

screw cap that had been made to contain a small hole. The top of the vial was covered with a kim-wipe to prevent unwanted particles from entering the vial. The solution was allowed to slowly evaporate at ambient temperature for 14 days. Clear yellow crystals formed and were of high enough quality for analysis.

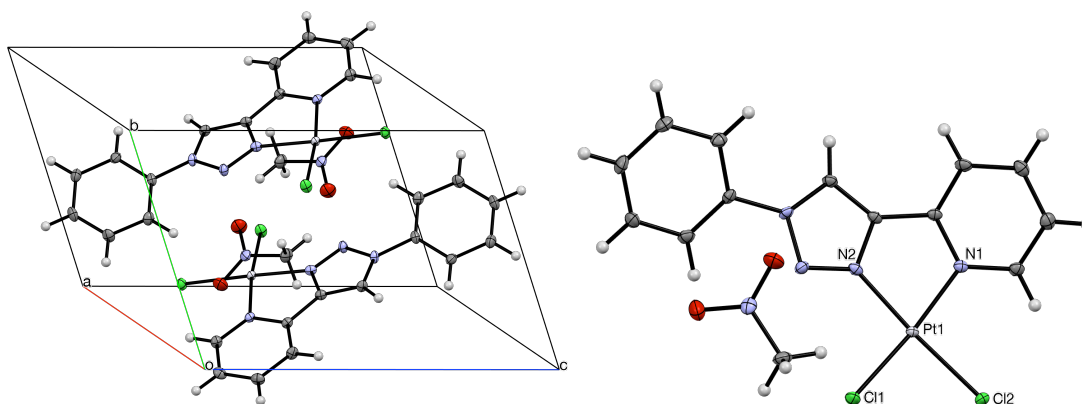


Table 1. Crystal data and structure refinement for **PyTriPtCl₂**.

Empirical formula	C ₁₄ H ₁₃ Cl ₂ N ₅ O ₂ Pt
Formula weight	549.28
Temperature	100.0 K
Wavelength, Å	0.71073
Crystal system	Triclinic
Space group	<i>P</i> -1
<i>a</i> , Å	8.5992(5)
<i>b</i> , Å	9.9079(6)
<i>c</i> , Å	11.2482(7)
α , °	108.356(2)
β , °	109.596(2)
γ , °	99.715(2)
Volume	815.56(9) Å ³
<i>Z</i>	2
Calculated density, mg/m ³	2.237
Absorption coefficient, mm ⁻¹	8.948
<i>F</i> (000)	520
Crystal size, mm	0.26 x 0.24 x 0.2
Theta range for data collection, °	2.097 to 28.380
Index ranges	-11 ≤ <i>h</i> ≤ 11, -13 ≤ <i>k</i> ≤ 11, -14 ≤ <i>l</i> ≤ 15
Reflections collected / unique	12634 / 4066 [<i>R</i> _{int} = 0.0442]
Completeness to θ = 25.242°	100.0 %
Absorption correction	Semi-empirical from equivalents
Max. and min. transmission	0.4920 and 0.3611
Refinement method	Full-matrix least-squares on <i>F</i> ²
Data / restraints / parameters	4066 / 0 / 212
Goodness-of-fit on <i>F</i> ²	1.026

Final R indices [$I > 2\sigma(I)$]	$R1 = 0.0269$, $wR2 = 0.0615$
R indices (all data)	$R1 = 0.0290$, $wR2 = 0.0624$
Extinction coefficient	n/a
Largest diff. peak and hole, $e\text{\AA}^{-3}$	1.827 and -1.412

Table 2. Atomic coordinates ($\times 10^4$) and equivalent isotropic displacement parameters ($\text{\AA}^2 \times 10^3$) for **PyTriPtCl₂**. $U(\text{eq})$ is defined as one third of the trace of the orthogonalized U^{ij} tensor.

	x	y	z	$U(\text{eq})$
Pt(1)	3158(1)	8452(1)	6002(1)	9(1)
Cl(2)	2478(1)	9050(1)	7861(1)	14(1)
Cl(1)	269(1)	7582(1)	4555(1)	16(1)
O(2)	4269(3)	4499(3)	3387(3)	24(1)
N(2)	3961(4)	7945(3)	4498(3)	10(1)
O(1)	1896(4)	2904(3)	1707(3)	26(1)
N(1)	5771(4)	9291(3)	7126(3)	10(1)
N(3)	3128(4)	7259(3)	3152(3)	12(1)
N(4)	4396(4)	7239(3)	2698(3)	11(1)
N(5)	2716(4)	3826(3)	2898(3)	15(1)
C(5)	6744(4)	9182(4)	6381(4)	10(1)
C(7)	5990(4)	7907(4)	3741(4)	12(1)
C(12)	1840(5)	4958(4)	-1029(4)	16(1)
C(1)	6578(5)	10043(4)	8503(4)	13(1)
C(6)	5708(4)	8372(4)	4905(4)	10(1)
C(10)	4529(5)	6535(4)	-688(4)	16(1)
C(3)	9338(5)	10639(4)	8412(4)	16(1)
C(8)	3901(5)	6585(4)	1238(4)	11(1)
C(4)	8527(5)	9831(4)	6994(4)	13(1)
C(2)	8343(5)	10739(4)	9164(4)	16(1)
C(13)	2314(5)	5510(4)	377(4)	14(1)

C(9)	5034(5)	7104(4)	724(4)	14(1)
C(11)	2937(5)	5467(4)	-1554(4)	16(1)
C(14)	1775(5)	4153(4)	3788(4)	19(1)

Table 3. Bond lengths [Å] and angles [°] for **PyTriPtCl₂**.

Pt(1)-Cl(2)	2.2854(9)
Pt(1)-Cl(1)	2.2900(9)
Pt(1)-N(2)	1.989(3)
Pt(1)-N(1)	2.035(3)
O(2)-N(5)	1.227(4)
N(2)-N(3)	1.314(4)
N(2)-C(6)	1.359(4)
O(1)-N(5)	1.227(4)
N(1)-C(5)	1.363(4)
N(1)-C(1)	1.347(5)
N(3)-N(4)	1.351(4)
N(4)-C(7)	1.349(4)
N(4)-C(8)	1.437(4)
N(5)-C(14)	1.480(5)
C(5)-C(6)	1.456(5)
C(5)-C(4)	1.385(5)
C(7)-H(7)	0.9500
C(7)-C(6)	1.363(5)
C(12)-H(12)	0.9500
C(12)-C(13)	1.384(5)
C(12)-C(11)	1.376(5)
C(1)-H(1)	0.9500
C(1)-C(2)	1.378(5)
C(10)-H(10)	0.9500
C(10)-C(9)	1.385(5)
C(10)-C(11)	1.382(5)
C(3)-H(3)	0.9500
C(3)-C(4)	1.390(5)
C(3)-C(2)	1.385(5)
C(8)-C(13)	1.381(5)
C(8)-C(9)	1.394(5)
C(4)-H(4)	0.9500
C(2)-H(2)	0.9500
C(13)-H(13)	0.9500
C(9)-H(9)	0.9500
C(11)-H(11)	0.9500
C(14)-H(14A)	0.9800
C(14)-H(14B)	0.9800
C(14)-H(14C)	0.9800

Cl(2)-Pt(1)-Cl(1)	90.06(3)
N(2)-Pt(1)-Cl(2)	174.82(8)
N(2)-Pt(1)-Cl(1)	94.90(9)
N(2)-Pt(1)-N(1)	79.84(12)
N(1)-Pt(1)-Cl(2)	95.30(9)
N(1)-Pt(1)-Cl(1)	173.67(8)
N(3)-N(2)-Pt(1)	132.6(2)
N(3)-N(2)-C(6)	111.7(3)
C(6)-N(2)-Pt(1)	115.7(2)
C(5)-N(1)-Pt(1)	115.5(2)
C(1)-N(1)-Pt(1)	125.5(2)
C(1)-N(1)-C(5)	118.7(3)
N(2)-N(3)-N(4)	104.3(3)
N(3)-N(4)-C(8)	118.2(3)
C(7)-N(4)-N(3)	112.1(3)
C(7)-N(4)-C(8)	129.7(3)
O(2)-N(5)-C(14)	118.3(3)
O(1)-N(5)-O(2)	123.6(3)
O(1)-N(5)-C(14)	118.1(3)
N(1)-C(5)-C(6)	113.0(3)
N(1)-C(5)-C(4)	122.1(3)
C(4)-C(5)-C(6)	124.8(3)
N(4)-C(7)-H(7)	127.4
N(4)-C(7)-C(6)	105.1(3)
C(6)-C(7)-H(7)	127.4
C(13)-C(12)-H(12)	119.8
C(11)-C(12)-H(12)	119.8
C(11)-C(12)-C(13)	120.4(4)
N(1)-C(1)-H(1)	119.2
N(1)-C(1)-C(2)	121.7(3)
C(2)-C(1)-H(1)	119.2
N(2)-C(6)-C(5)	115.8(3)
N(2)-C(6)-C(7)	106.7(3)
C(7)-C(6)-C(5)	137.5(3)
C(9)-C(10)-H(10)	120.0
C(11)-C(10)-H(10)	120.0
C(11)-C(10)-C(9)	120.0(4)
C(4)-C(3)-H(3)	120.5
C(2)-C(3)-H(3)	120.5
C(2)-C(3)-C(4)	118.9(3)
C(13)-C(8)-N(4)	120.1(3)
C(13)-C(8)-C(9)	121.6(3)
C(9)-C(8)-N(4)	118.2(3)
C(5)-C(4)-C(3)	118.6(3)
C(5)-C(4)-H(4)	120.7

C(3)-C(4)-H(4)	120.7
C(1)-C(2)-C(3)	119.9(4)
C(1)-C(2)-H(2)	120.0
C(3)-C(2)-H(2)	120.0
C(12)-C(13)-H(13)	120.6
C(8)-C(13)-C(12)	118.7(3)
C(8)-C(13)-H(13)	120.6
C(10)-C(9)-C(8)	118.6(4)
C(10)-C(9)-H(9)	120.7
C(8)-C(9)-H(9)	120.7
C(12)-C(11)-C(10)	120.7(4)
C(12)-C(11)-H(11)	119.7
C(10)-C(11)-H(11)	119.7
N(5)-C(14)-H(14A)	109.5
N(5)-C(14)-H(14B)	109.5
N(5)-C(14)-H(14C)	109.5
H(14A)-C(14)-H(14B)	109.5
H(14A)-C(14)-H(14C)	109.5
H(14B)-C(14)-H(14C)	109.5

Table 4. Anisotropic displacement parameters ($\text{\AA}^2 \times 10^3$) for **PyTriPtCl₂**. The anisotropic displacement factor exponent takes the form: $-2\pi^2 [h^2 a^{*2} U^{11} + \dots + 2 h k a^* b^* U^{12}]$

	U ¹¹	U ²²	U ³³	U ²³	U ¹³	U ¹²
Pt(1)	6(1)	11(1)	9(1)	3(1)	4(1)	3(1)
Cl(2)	11(1)	18(1)	11(1)	3(1)	6(1)	3(1)
Cl(1)	8(1)	23(1)	13(1)	4(1)	4(1)	4(1)
O(2)	14(1)	28(2)	25(2)	8(1)	7(1)	3(1)
N(2)	7(1)	11(1)	13(1)	5(1)	3(1)	4(1)
O(1)	24(2)	24(2)	17(2)	2(1)	5(1)	-2(1)
N(1)	9(1)	11(1)	12(2)	5(1)	5(1)	3(1)
N(3)	11(1)	16(2)	10(2)	5(1)	6(1)	5(1)
N(4)	10(1)	15(2)	11(2)	6(1)	7(1)	7(1)
N(5)	19(2)	13(2)	14(2)	7(1)	7(1)	5(1)
C(5)	8(2)	12(2)	13(2)	6(1)	5(1)	5(1)
C(7)	8(2)	15(2)	13(2)	6(2)	4(1)	4(1)
C(12)	10(2)	20(2)	13(2)	5(2)	2(2)	4(1)
C(1)	10(2)	16(2)	14(2)	6(2)	5(2)	6(1)
C(6)	7(1)	11(1)	13(1)	5(1)	3(1)	4(1)
C(10)	19(2)	19(2)	16(2)	9(2)	11(2)	7(2)
C(3)	11(2)	17(2)	16(2)	6(2)	2(2)	4(1)
C(8)	12(2)	15(2)	9(2)	5(1)	5(1)	8(1)
C(4)	7(2)	19(2)	15(2)	9(2)	4(2)	5(1)
C(2)	15(2)	14(2)	16(2)	4(2)	6(2)	7(1)
C(13)	12(2)	19(2)	16(2)	8(2)	8(2)	7(1)

C(9)	16(2)	13(2)	16(2)	7(2)	8(2)	4(1)
C(11)	20(2)	21(2)	9(2)	5(2)	6(2)	9(2)
C(14)	17(2)	21(2)	24(2)	8(2)	14(2)	6(2)

Table 5. Hydrogen coordinates ($\times 10^4$) and isotropic displacement parameters ($\text{\AA}^2 \times 10^{-3}$) for **PyTriPtCl₂**.

	x	y	z	U(eq)
H(7)	7075	8028	3677	14
H(12)	750	4222	-1636	19
H(1)	5913	10094	9033	15
H(10)	5276	6879	-1061	19
H(3)	10556	11114	8859	19
H(4)	9182	9725	6457	16
H(2)	8876	11288	10134	19
H(13)	1564	5156	744	17
H(9)	6130	7831	1330	17
H(11)	2596	5080	-2521	20
H(14A)	2603	4589	4757	29
H(14B)	936	3226	3599	29
H(14C)	1162	4862	3596	29

X-ray crystallography for PyTriPdCl₂ complexes:

To obtain a suitable crystal of MePyTriPdCl₂, a saturated solution of the complex was prepared in MeNO₂. This solution was left to stand in a vial equipped with a

screw cap that had been made to contain a small hole. The top of the vial was covered with a kim-wipe to prevent unwanted particles from entering the vial. The solution was allowed to slowly evaporate at ambient temperature for 14 days. Clear red crystals formed and were of high enough quality for analysis.

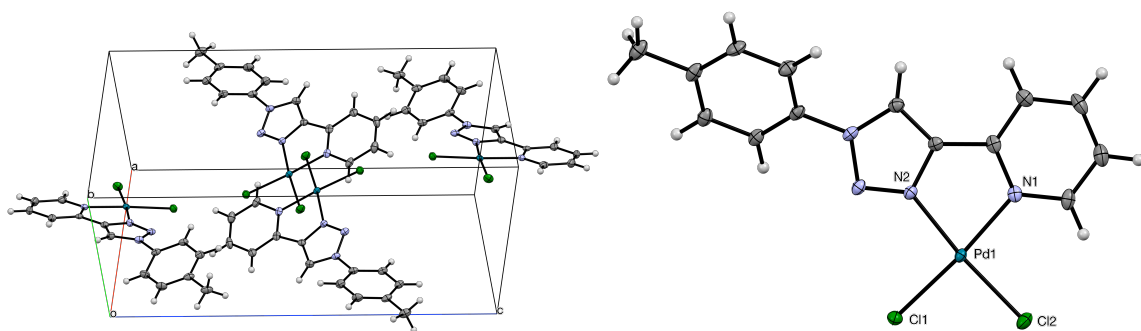


Table 1. Crystal data and structure refinement for **MePyTriPdCl₂**.

Empirical formula	C ₁₄ H ₁₂ Cl ₂ N ₄ Pd
Formula weight	417.58
Temperature	100.0 K
Wavelength, Å	0.71073
Crystal system	Monoclinic
Space group	<i>P</i> 21/ <i>c</i>
<i>a</i> , Å	11.0752(4)
<i>b</i> , Å	7.1960(3)
<i>c</i> , Å	18.7616(7)
α , °	90
β , °	94.668(2)
γ , °	90
Volume	1490.29(10) Å ³
<i>Z</i>	4
Calculated density, mg/m ³	1.861
Absorption coefficient, mm ⁻¹	1.603
<i>F</i> (000)	824
Crystal size, mm	0.3 x 0.28 x 0.24
Theta range for data collection, °	1.845 to 28.277
Index ranges	-14 ≤ <i>h</i> ≤ 14, -9 ≤ <i>k</i> ≤ 5, -25 ≤ <i>l</i> ≤ 25
Reflections collected / unique	17077 / 3697 [<i>R</i> _{int} = 0.0674]
Completeness to $\theta = 25.242^\circ$	99.9 %
Absorption correction	Semi-empirical from equivalents
Max. and min. transmission	0.2541 and 0.2102
Refinement method	Full-matrix least-squares on <i>F</i> ²
Data / restraints / parameters	3697 / 0 / 191
Goodness-of-fit on <i>F</i> ²	1.103
Final <i>R</i> indices [<i>I</i> > 2 σ (<i>I</i>)]	<i>R</i> 1 = 0.0451, <i>wR</i> 2 = 0.1166

<i>R</i> indices (all data)	<i>R</i> 1 = 0.0487, <i>wR</i> 2 = 0.1194
Extinction coefficient	n/a
Largest diff. peak and hole, eÅ ⁻³	2.671 and -0.758

Table 2. Atomic coordinates (× 10⁴) and equivalent isotropic displacement parameters (Å² × 10³) for **MePyTriPdCl₂**. *U*(eq) is defined as one third of the trace of the orthogonalized *U^{ij}* tensor.

	x	y	z	<i>U</i> (eq)
Pd(1)	5970(1)	3108(1)	5195(1)	11(1)
Cl(1)	6572(1)	4033(1)	6328(1)	15(1)
Cl(2)	7857(1)	3718(1)	4833(1)	19(1)
N(1)	5272(3)	2246(4)	4201(2)	13(1)
N(2)	4289(3)	2394(4)	5426(2)	12(1)
N(3)	3702(3)	2436(4)	6004(2)	14(1)
N(4)	2596(3)	1740(4)	5795(2)	14(1)
C(1)	5839(3)	2336(6)	3594(2)	18(1)
C(2)	5273(4)	1765(6)	2947(2)	22(1)
C(3)	4104(4)	1067(6)	2918(2)	21(1)
C(4)	3512(3)	987(5)	3539(2)	17(1)
C(5)	4121(3)	1610(5)	4172(2)	14(1)
C(6)	3589(3)	1686(5)	4855(2)	13(1)
C(7)	2481(3)	1260(5)	5097(2)	15(1)
C(8)	1676(3)	1650(5)	6293(2)	15(1)
C(9)	480(3)	2036(5)	6048(2)	19(1)
C(10)	-408(3)	1955(5)	6530(2)	20(1)
C(11)	-116(3)	1531(5)	7249(2)	18(1)
C(12)	1097(3)	1188(5)	7483(2)	18(1)
C(13)	1992(3)	1229(5)	7008(2)	16(1)
C(14)	-1089(4)	1452(6)	7771(2)	23(1)

Table 3. Bond lengths [Å] and angles [°] for **MePyTriPdCl₂**.

Pd(1)-Cl(1)	2.2744(8)
Pd(1)-Cl(2)	2.2921(8)
Pd(1)-N(1)	2.055(3)
Pd(1)-N(2)	2.012(3)
N(1)-C(1)	1.347(5)
N(1)-C(5)	1.352(5)
N(2)-N(3)	1.310(4)
N(2)-C(6)	1.368(4)
N(3)-N(4)	1.351(4)
N(4)-C(7)	1.351(5)
N(4)-C(8)	1.438(5)
C(1)-H(1)	0.9500
C(1)-C(2)	1.383(6)
C(2)-H(2)	0.9500
C(2)-C(3)	1.385(6)
C(3)-H(3)	0.9500
C(3)-C(4)	1.383(5)
C(4)-H(4)	0.9500
C(4)-C(5)	1.392(5)
C(5)-C(6)	1.454(5)
C(6)-C(7)	1.376(5)
C(7)-H(7)	0.9500
C(8)-C(9)	1.395(5)
C(8)-C(13)	1.392(5)
C(9)-H(9)	0.9500
C(9)-C(10)	1.390(6)
C(10)-H(10)	0.9500
C(10)-C(11)	1.395(6)
C(11)-C(12)	1.401(5)
C(11)-C(14)	1.514(5)
C(12)-H(12)	0.9500
C(12)-C(13)	1.386(5)
C(13)-H(13)	0.9500
C(14)-H(14A)	0.9800
C(14)-H(14B)	0.9800
C(14)-H(14C)	0.9800
Cl(1)-Pd(1)-Cl(2)	90.88(3)
N(1)-Pd(1)-Cl(1)	174.85(9)
N(1)-Pd(1)-Cl(2)	94.25(9)
N(2)-Pd(1)-Cl(1)	94.57(9)
N(2)-Pd(1)-Cl(2)	174.10(9)
N(2)-Pd(1)-N(1)	80.33(12)

C(1)-N(1)-Pd(1)	125.9(3)
C(1)-N(1)-C(5)	119.0(3)
C(5)-N(1)-Pd(1)	115.0(2)
N(3)-N(2)-Pd(1)	134.6(2)
N(3)-N(2)-C(6)	111.6(3)
C(6)-N(2)-Pd(1)	113.7(2)
N(2)-N(3)-N(4)	104.5(3)
N(3)-N(4)-C(8)	120.1(3)
C(7)-N(4)-N(3)	112.8(3)
C(7)-N(4)-C(8)	127.0(3)
N(1)-C(1)-H(1)	119.4
N(1)-C(1)-C(2)	121.3(4)
C(2)-C(1)-H(1)	119.4
C(1)-C(2)-H(2)	120.1
C(1)-C(2)-C(3)	119.8(4)
C(3)-C(2)-H(2)	120.1
C(2)-C(3)-H(3)	120.4
C(2)-C(3)-C(4)	119.2(3)
C(4)-C(3)-H(3)	120.4
C(3)-C(4)-H(4)	120.8
C(3)-C(4)-C(5)	118.4(4)
C(5)-C(4)-H(4)	120.8
N(1)-C(5)-C(4)	122.2(3)
N(1)-C(5)-C(6)	113.6(3)
C(4)-C(5)-C(6)	124.2(3)
N(2)-C(6)-C(5)	117.3(3)
N(2)-C(6)-C(7)	106.8(3)
C(7)-C(6)-C(5)	135.9(3)
N(4)-C(7)-C(6)	104.3(3)
N(4)-C(7)-H(7)	127.9
C(6)-C(7)-H(7)	127.9
C(9)-C(8)-N(4)	118.8(3)
C(9)-C(8)-C(13)	121.2(3)
C(13)-C(8)-N(4)	120.0(3)
C(8)-C(9)-H(9)	120.7
C(8)-C(9)-C(10)	118.7(4)
C(10)-C(9)-H(9)	120.7
C(9)-C(10)-H(10)	119.4
C(9)-C(10)-C(11)	121.2(4)
C(11)-C(10)-H(10)	119.4
C(10)-C(11)-C(12)	118.8(3)
C(10)-C(11)-C(14)	120.8(3)
C(12)-C(11)-C(14)	120.4(3)
C(11)-C(12)-H(12)	119.6
C(13)-C(12)-C(11)	120.9(3)
C(13)-C(12)-H(12)	119.6

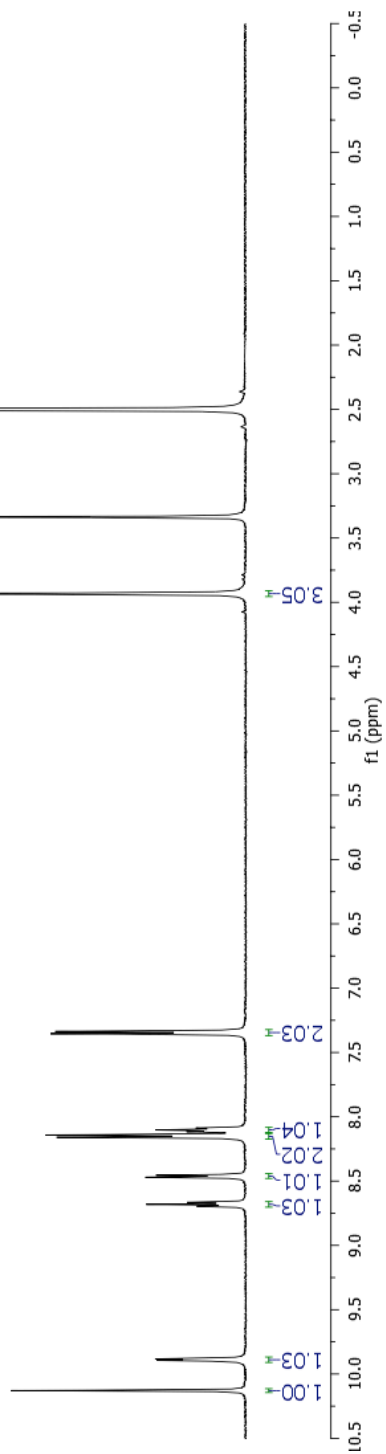
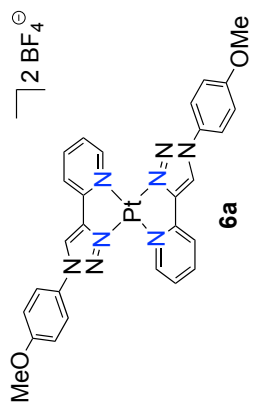
C(8)-C(13)-H(13)	120.4
C(12)-C(13)-C(8)	119.2(3)
C(12)-C(13)-H(13)	120.4
C(11)-C(14)-H(14A)	109.5
C(11)-C(14)-H(14B)	109.5
C(11)-C(14)-H(14C)	109.5
H(14A)-C(14)-H(14B)	109.5
H(14A)-C(14)-H(14C)	109.5
H(14B)-C(14)-H(14C)	109.5

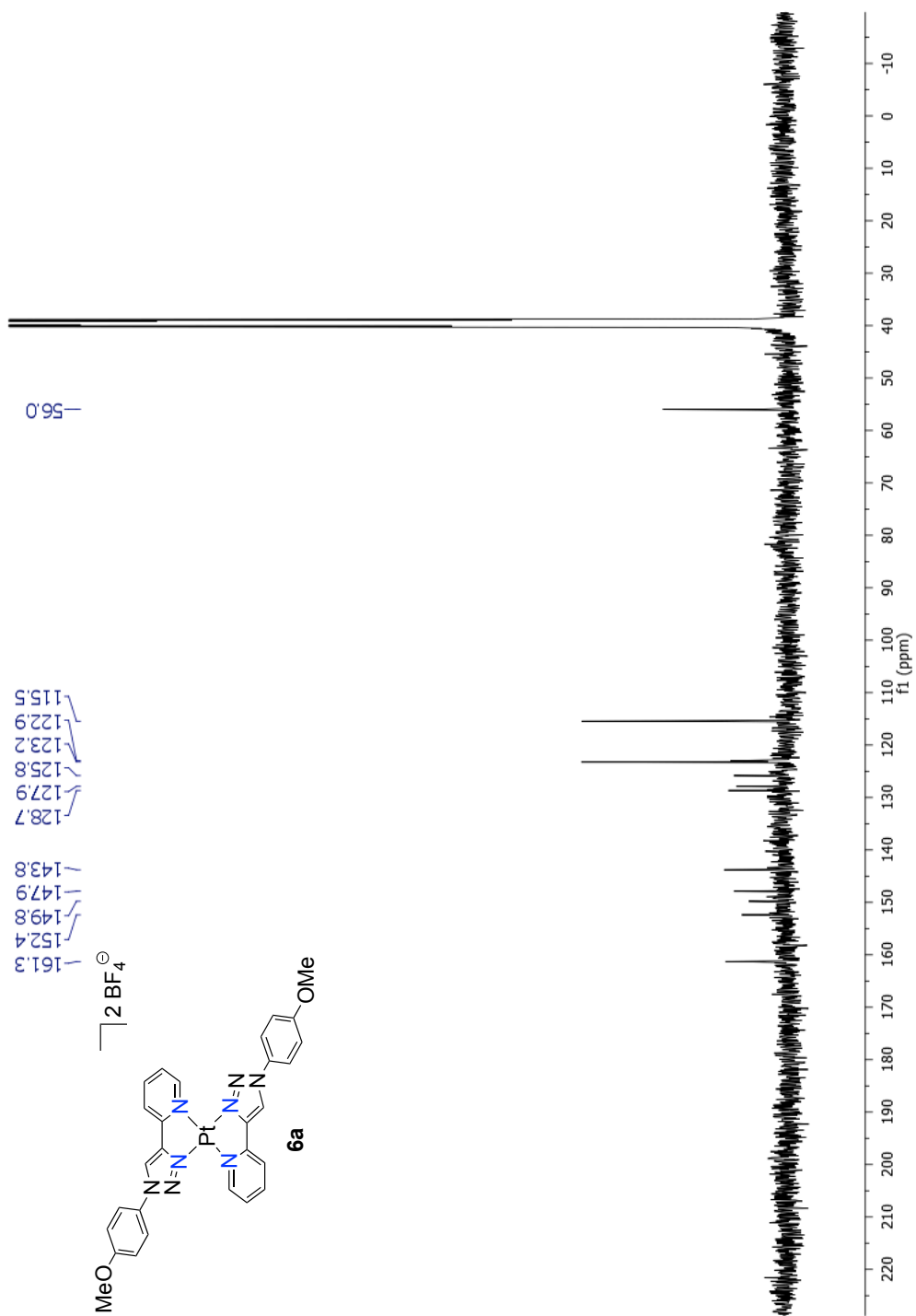
Table 4. Anisotropic displacement parameters ($\text{\AA}^2 \times 10^3$) for **MePyTriPdCl₂**. The anisotropic displacement factor exponent takes the form: $-2\pi^2 [h^2 a^{*2} U^{11} + \dots + 2 h k a^* b^* U^{12}]$

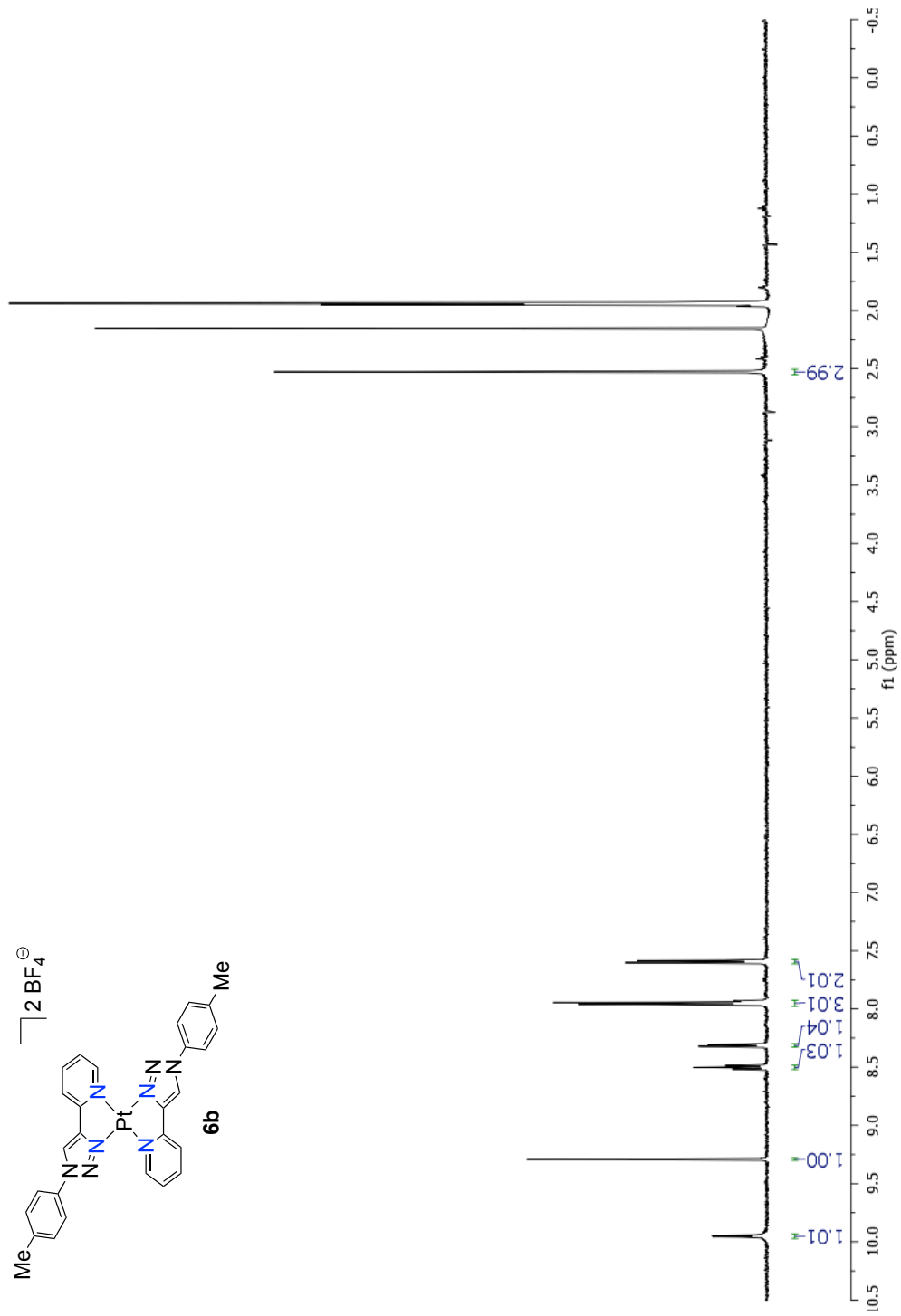
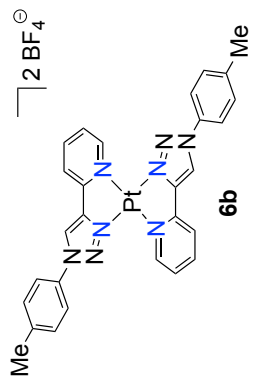
	U ¹¹	U ²²	U ³³	U ²³	U ¹³	U ¹²
Pd(1)	10(1)	11(1)	12(1)	2(1)	2(1)	1(1)
Cl(1)	14(1)	18(1)	14(1)	0(1)	0(1)	0(1)
Cl(2)	12(1)	24(1)	21(1)	4(1)	4(1)	0(1)
N(1)	14(1)	12(2)	13(1)	2(1)	1(1)	5(1)
N(2)	12(1)	12(2)	13(1)	1(1)	2(1)	0(1)
N(3)	13(1)	12(1)	17(1)	2(1)	4(1)	1(1)
N(4)	10(1)	14(2)	18(2)	1(1)	3(1)	-1(1)
C(1)	22(2)	16(2)	17(2)	5(2)	7(1)	6(1)
C(2)	28(2)	23(2)	15(2)	1(1)	5(2)	8(2)
C(3)	29(2)	20(2)	12(2)	-3(1)	-3(1)	8(2)
C(4)	21(2)	14(2)	16(2)	0(1)	-1(1)	2(1)
C(5)	18(2)	10(2)	15(2)	0(1)	2(1)	6(1)
C(6)	13(2)	10(2)	16(2)	-1(1)	1(1)	1(1)
C(7)	14(2)	14(2)	18(2)	-1(1)	1(1)	-1(1)
C(8)	13(2)	11(2)	21(2)	-1(1)	6(1)	-1(1)
C(9)	15(2)	19(2)	24(2)	4(1)	1(1)	1(1)
C(10)	11(2)	21(2)	29(2)	2(2)	2(1)	1(1)
C(11)	18(2)	12(2)	26(2)	2(2)	8(1)	1(1)
C(12)	19(2)	14(2)	20(2)	2(1)	6(1)	0(1)
C(13)	14(2)	12(2)	21(2)	1(1)	5(1)	2(1)
C(14)	19(2)	17(2)	33(2)	4(2)	10(2)	3(2)

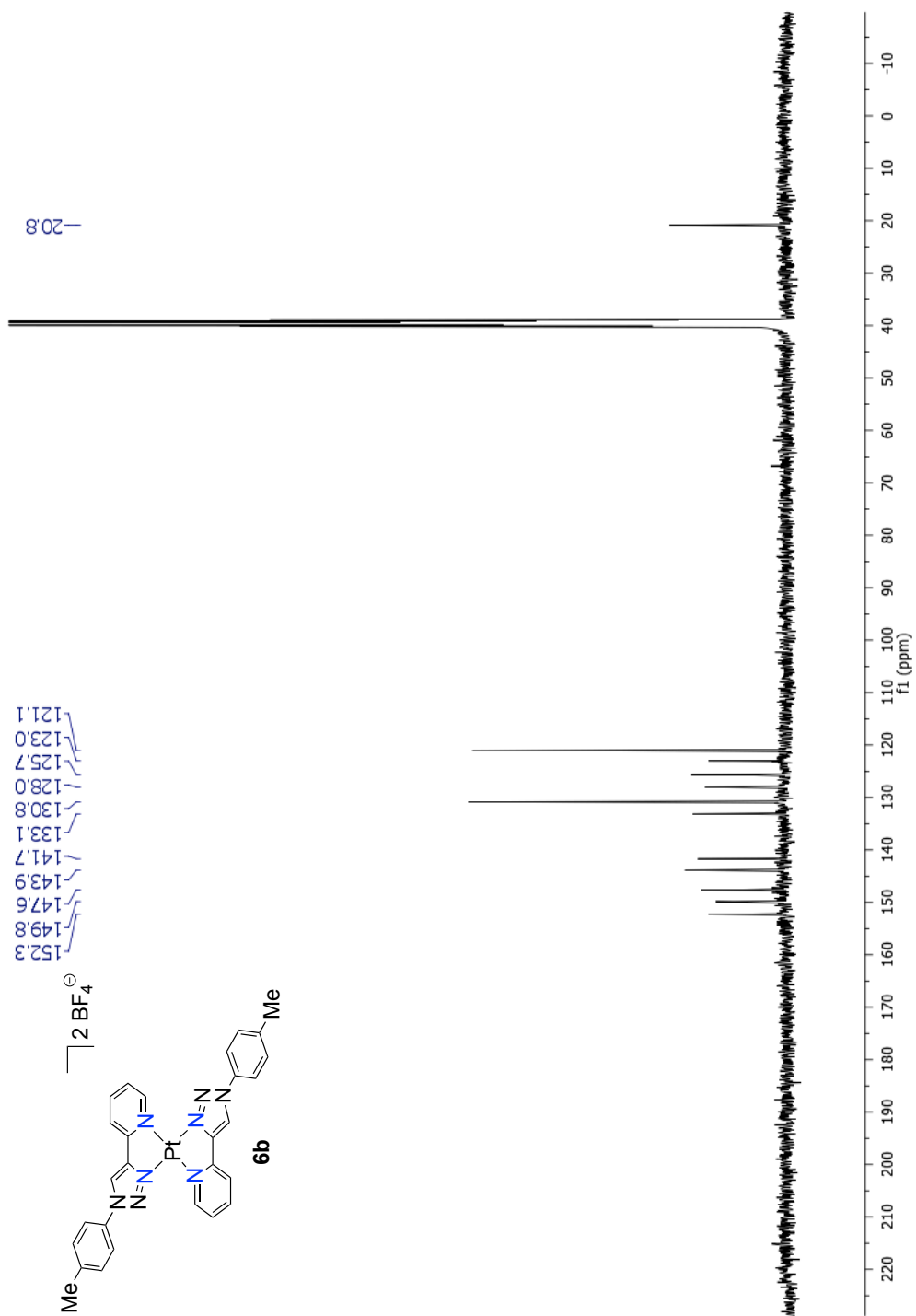
Table 5. Hydrogen coordinates ($\times 10^4$) and isotropic displacement parameters ($\text{\AA}^2 \times 10^{-3}$) for **MePyTriPdCl₂**.

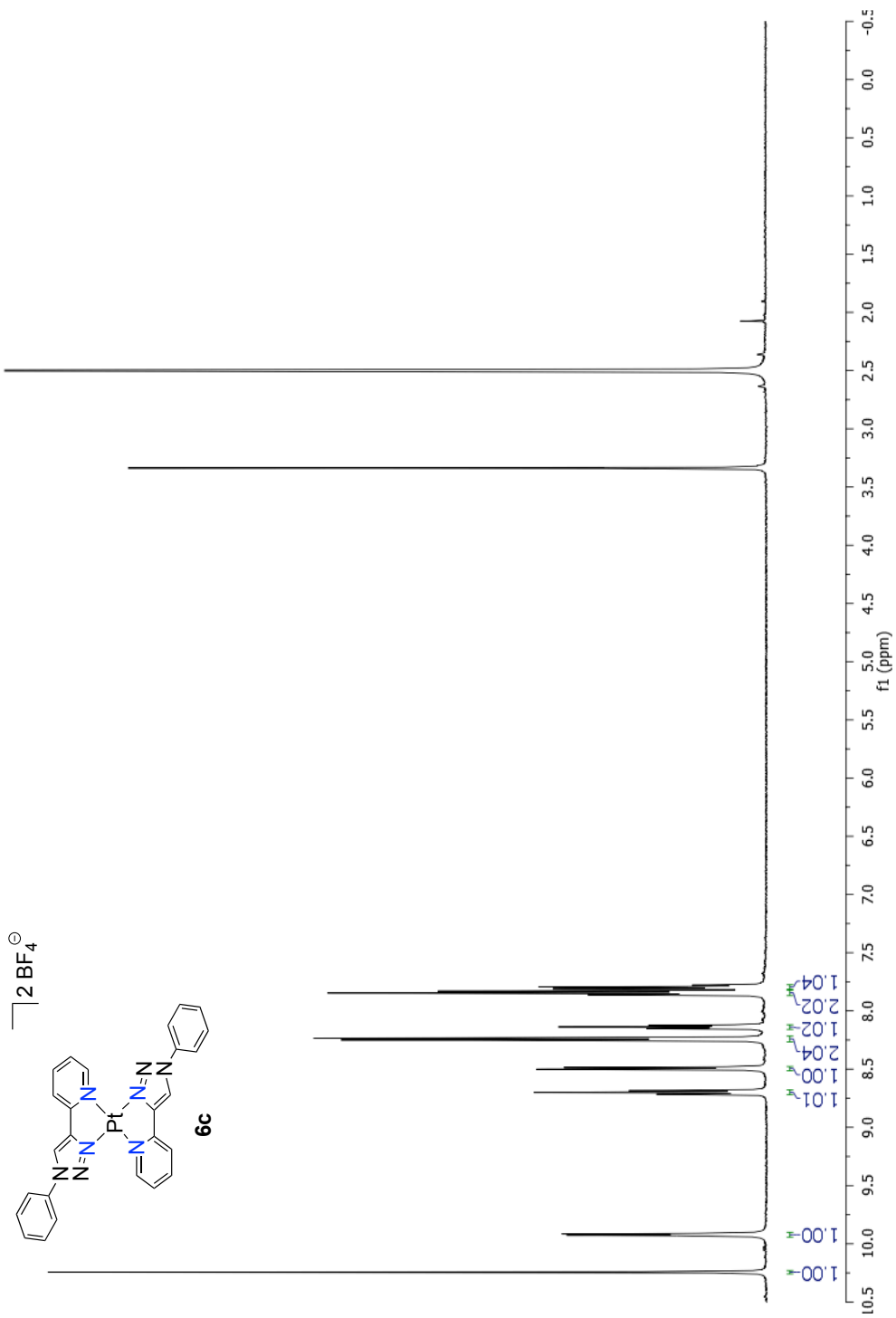
	x	y	z	U(eq)
H(1)	6644	2800	3610	22
H(2)	5684	1852	2523	26
H(3)	3714	648	2478	25
H(4)	2710	519	3533	21
H(7)	1793	747	4832	18
H(9)	275	2348	5561	23
H(10)	-1228	2193	6367	24
H(12)	1309	924	7973	21
H(13)	2811	972	7169	19
H(14A)	-1188	166	7928	34
H(14B)	-1856	1902	7536	34
H(14C)	-853	2237	8186	34

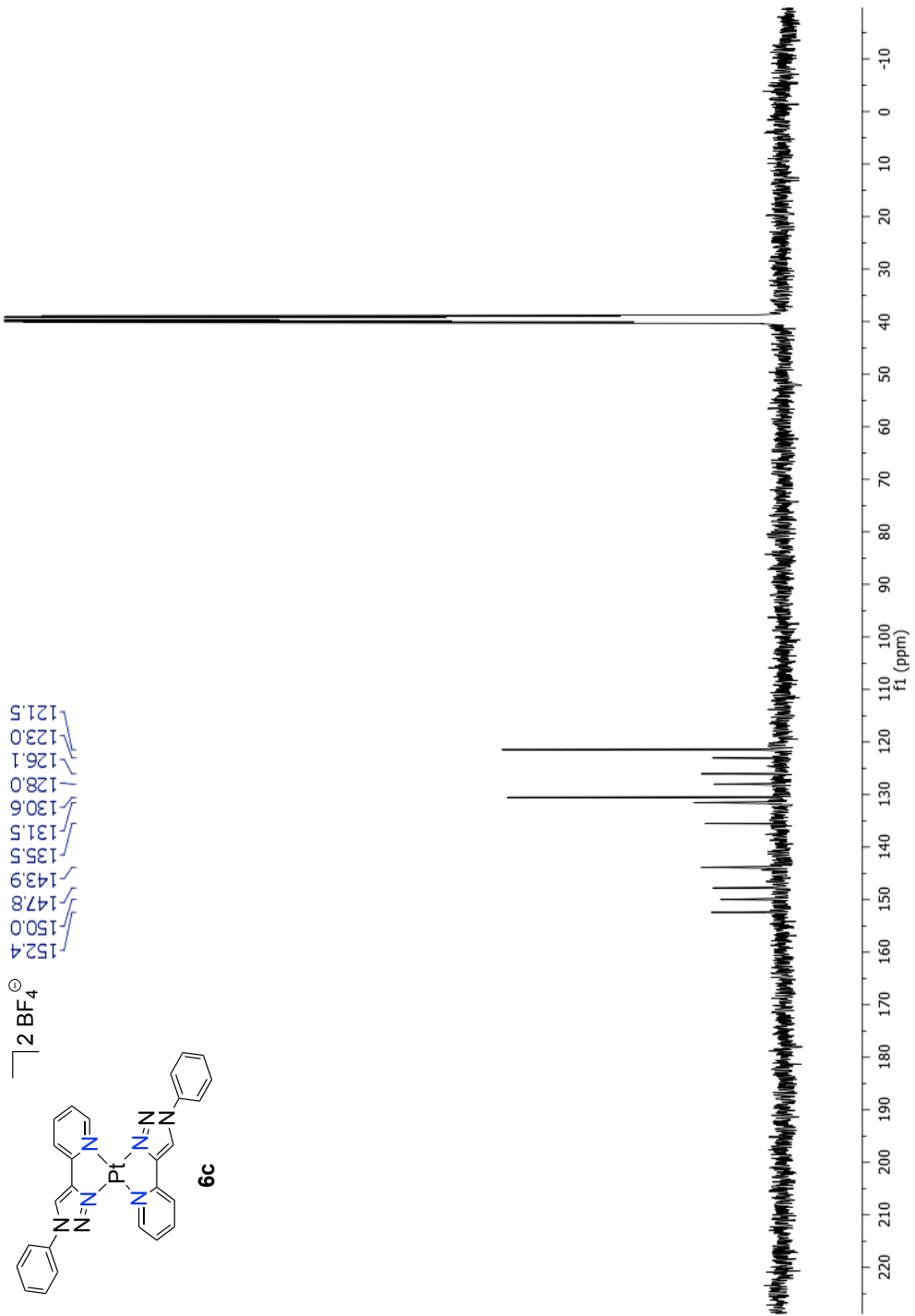


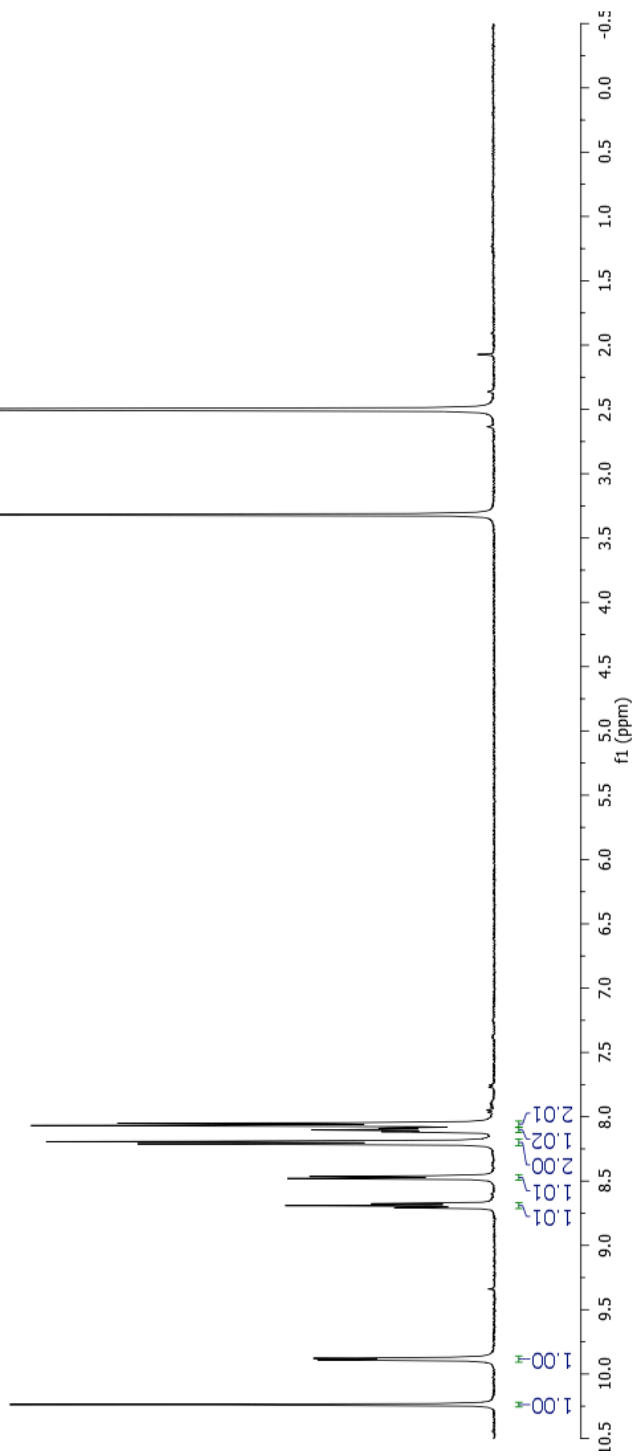
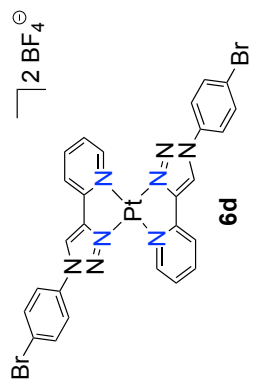


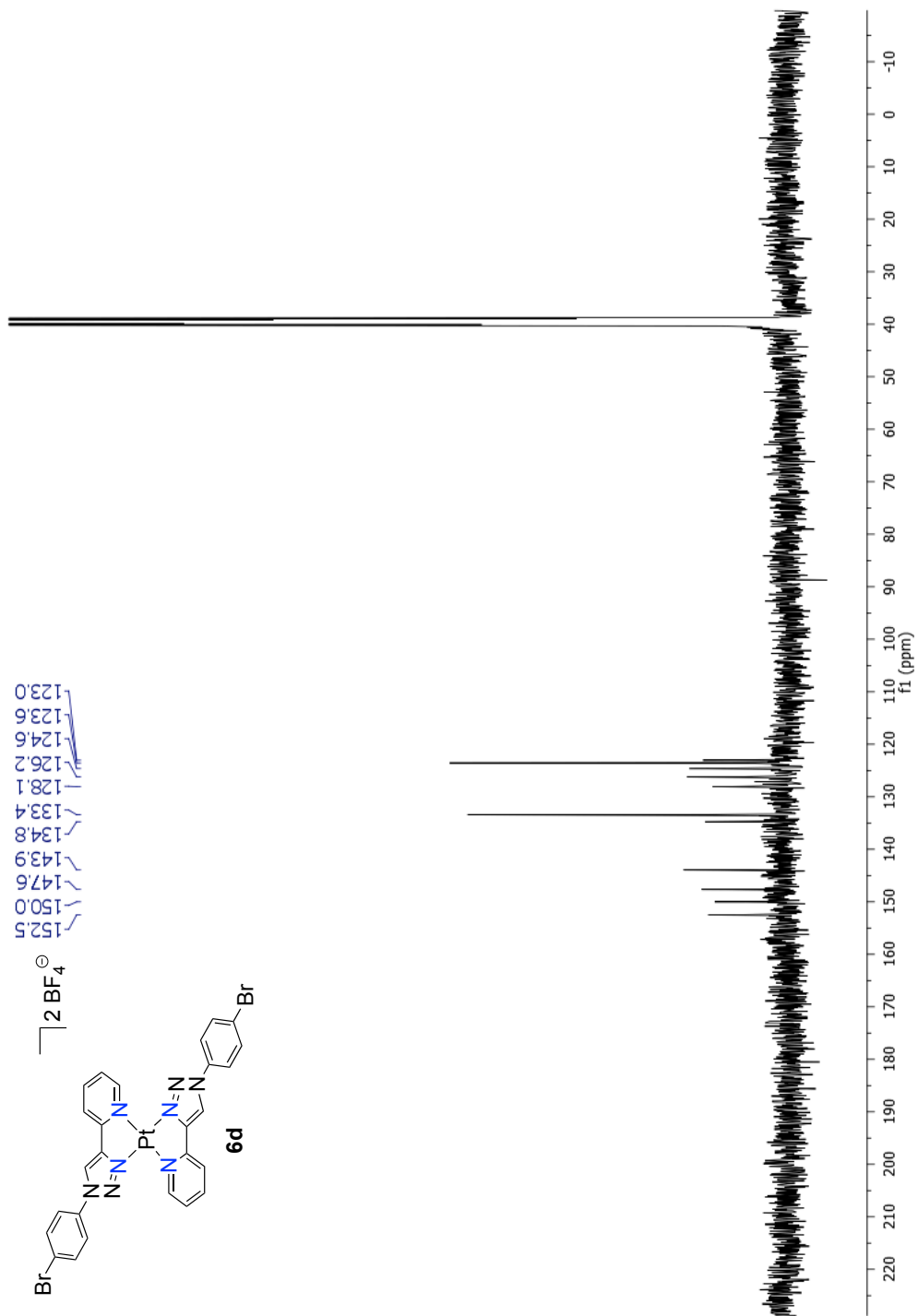


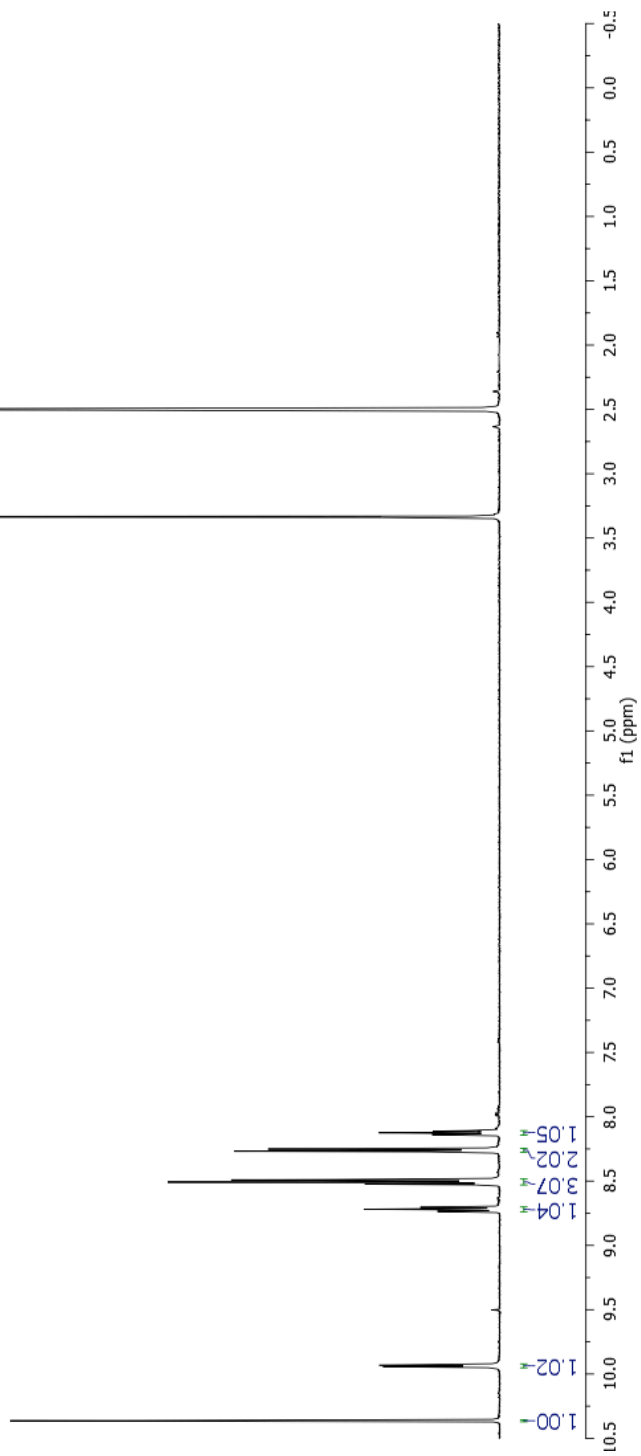
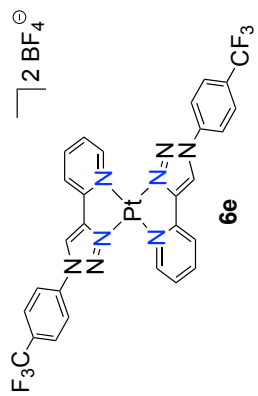


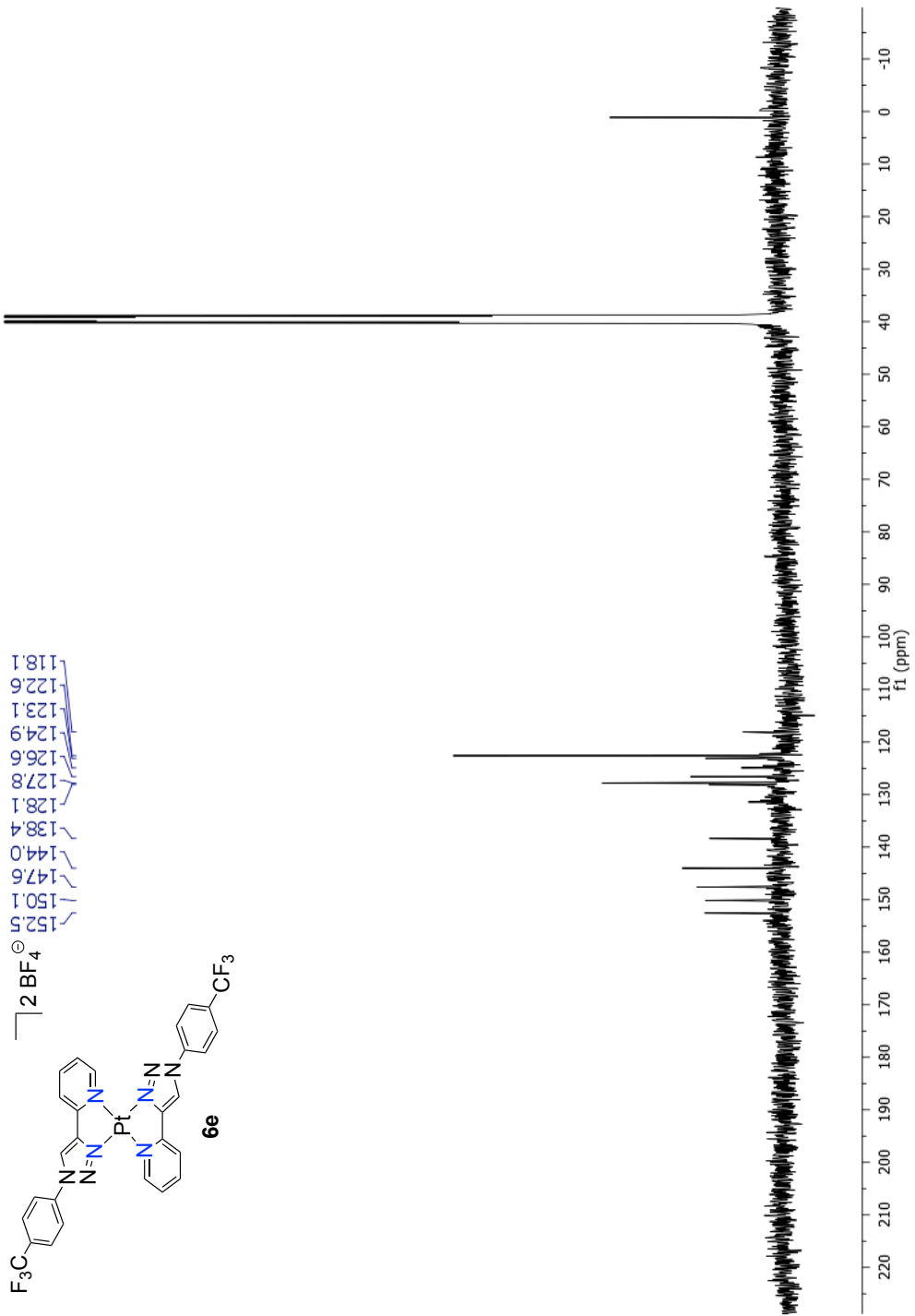


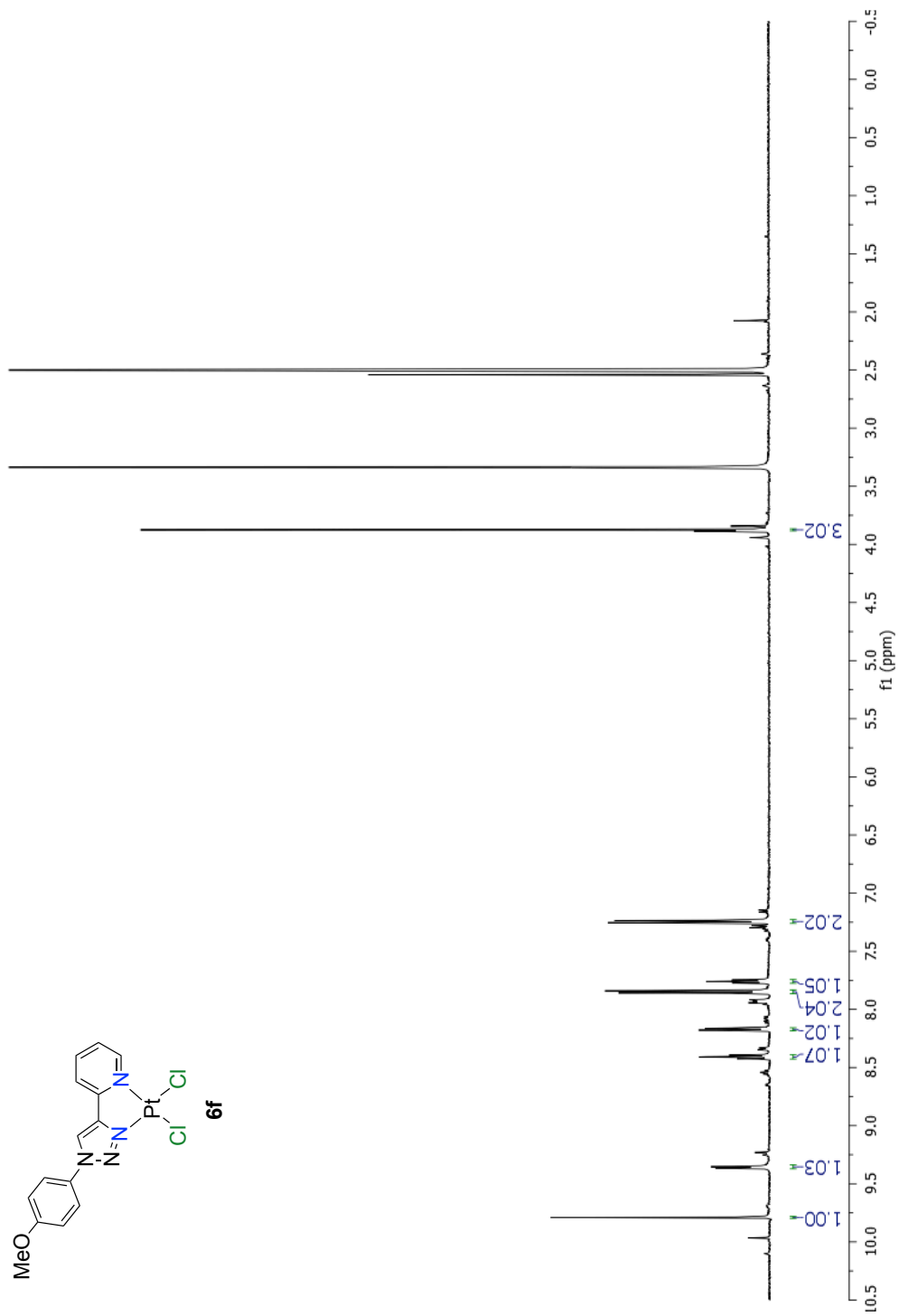
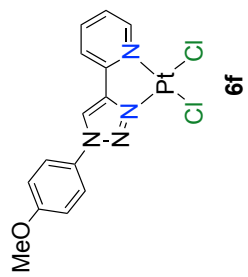


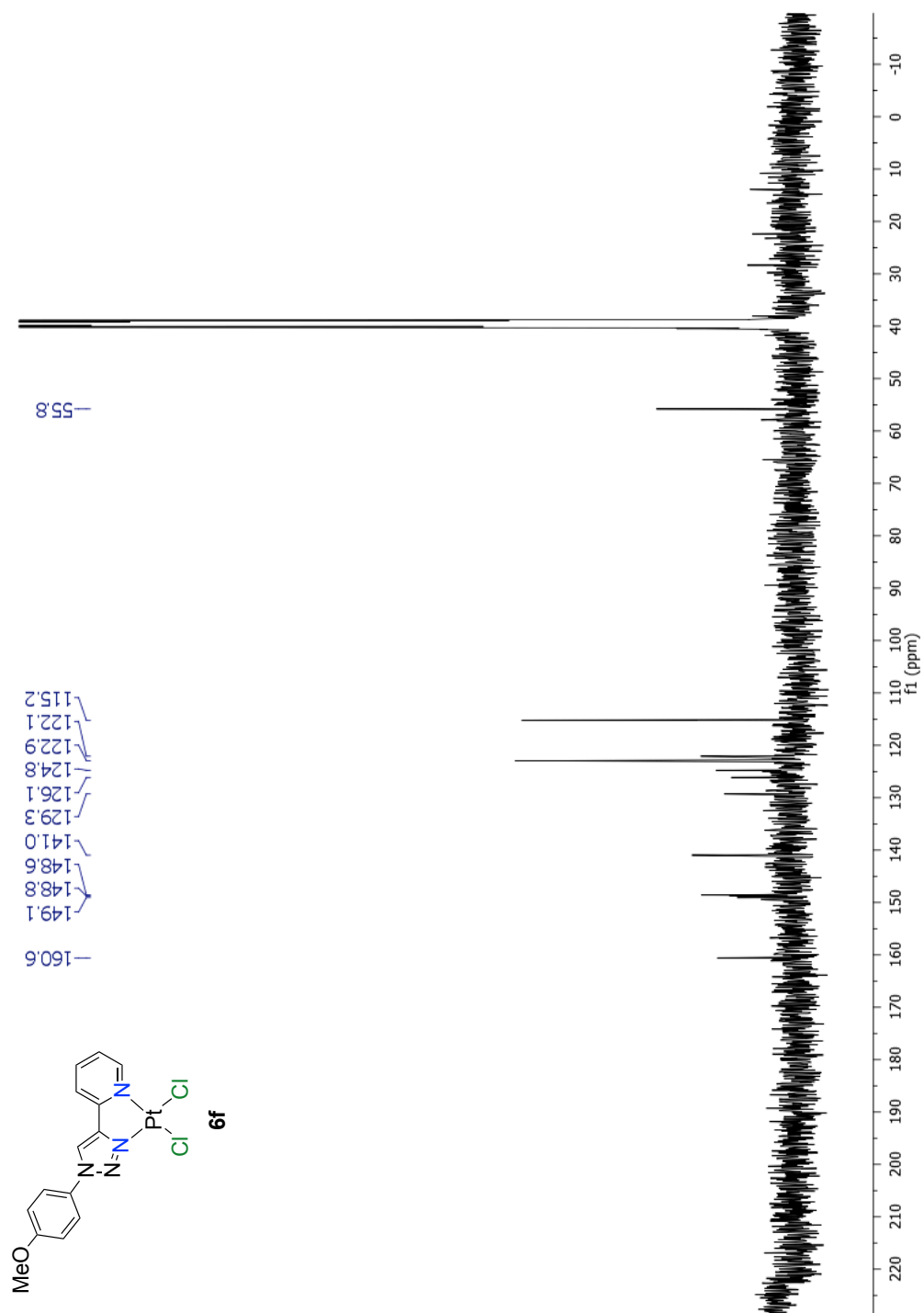


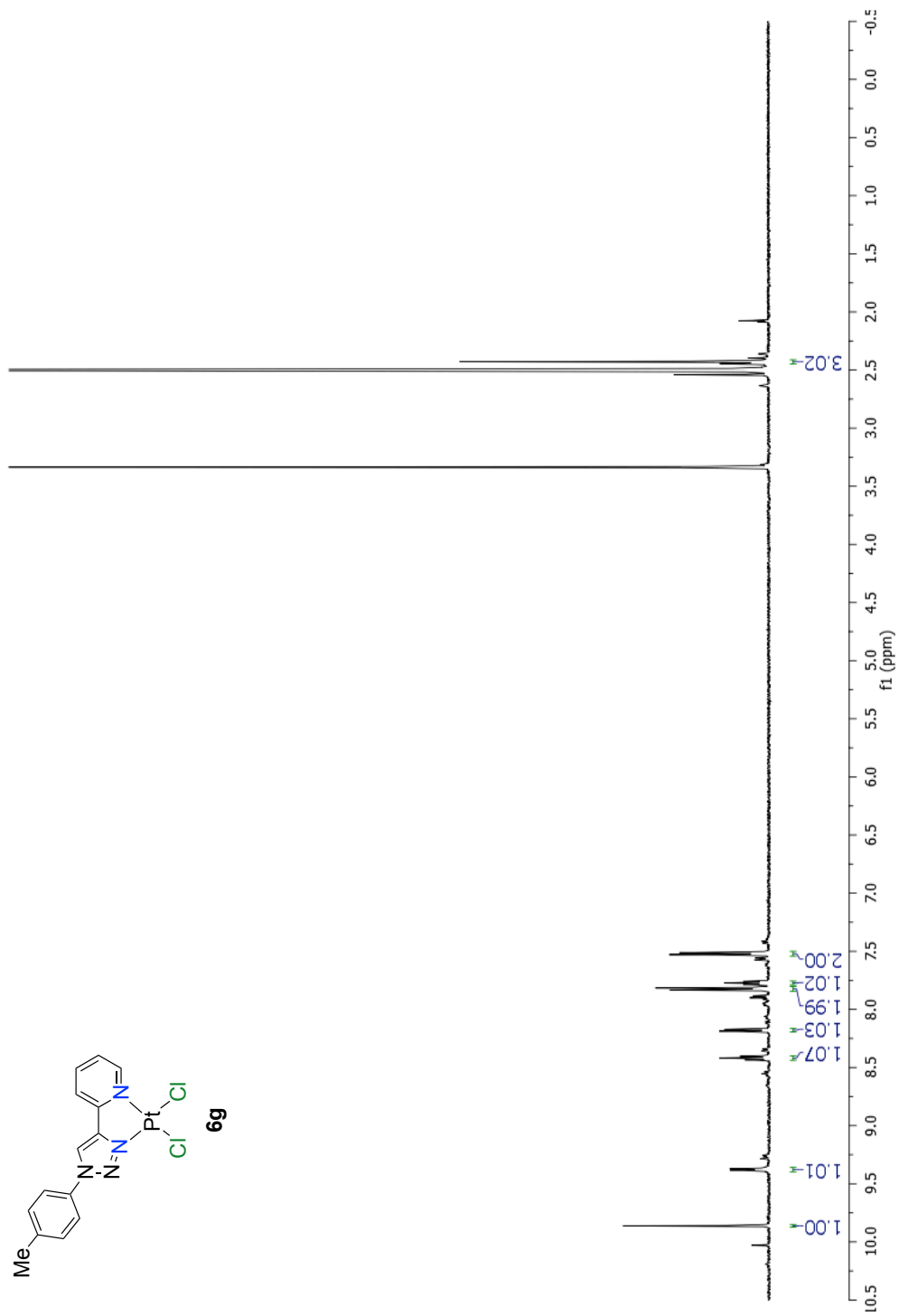
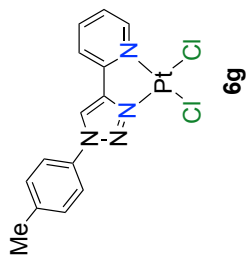


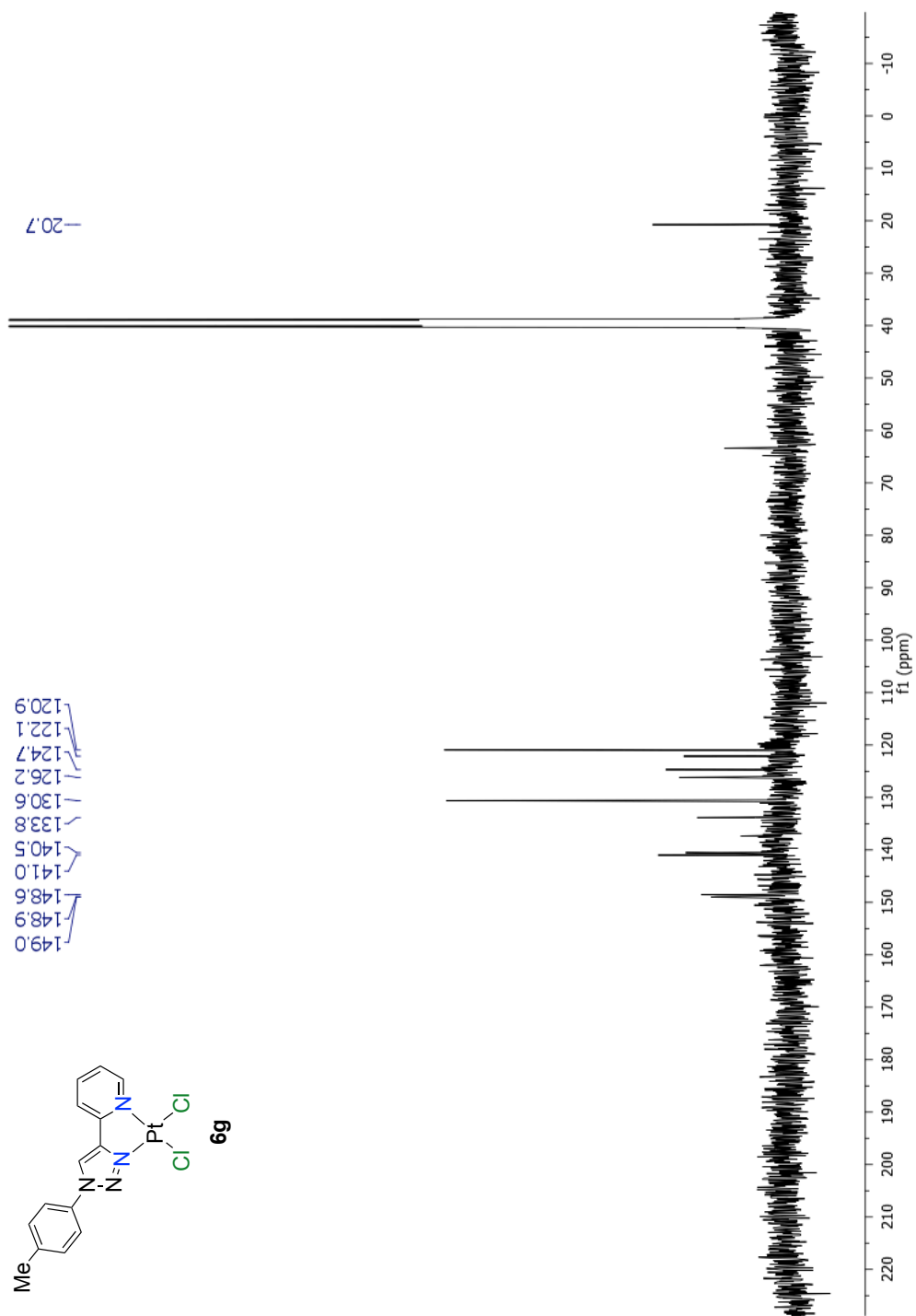


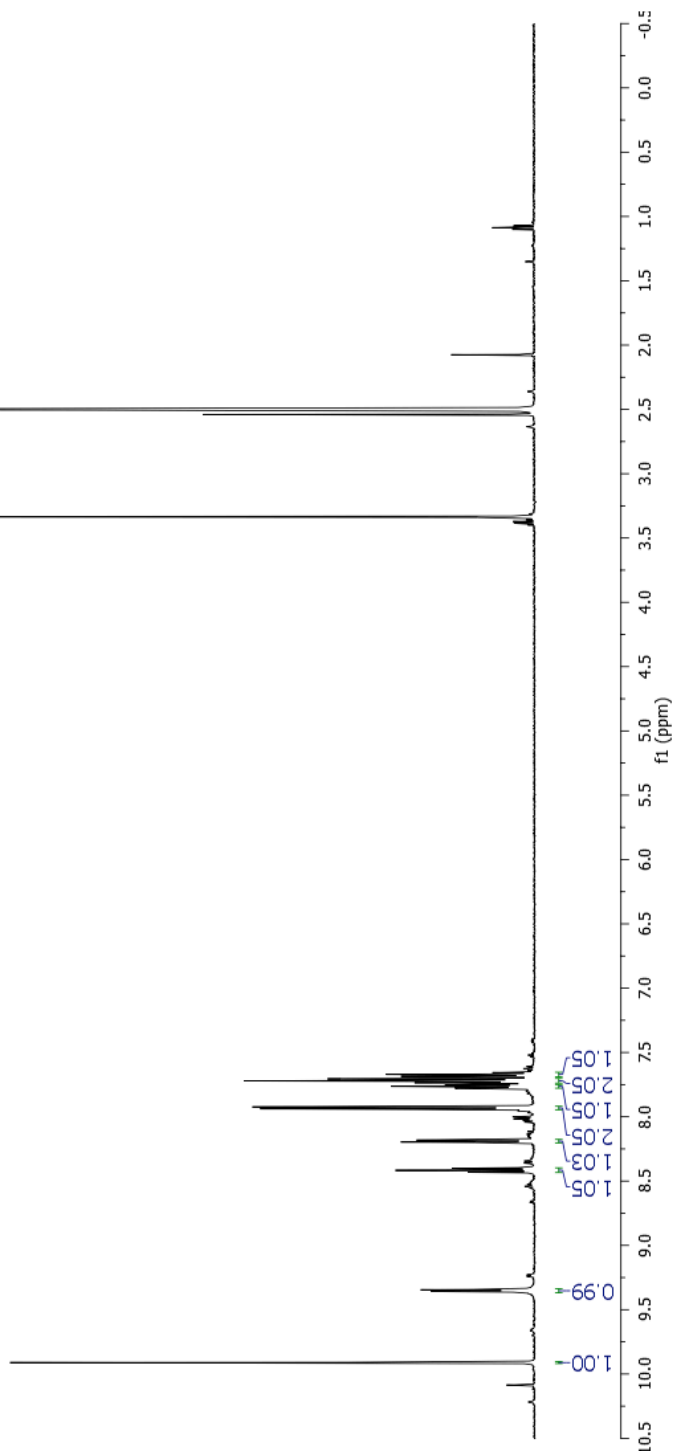
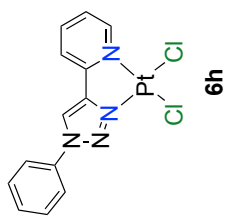


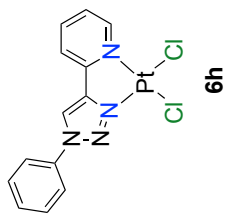
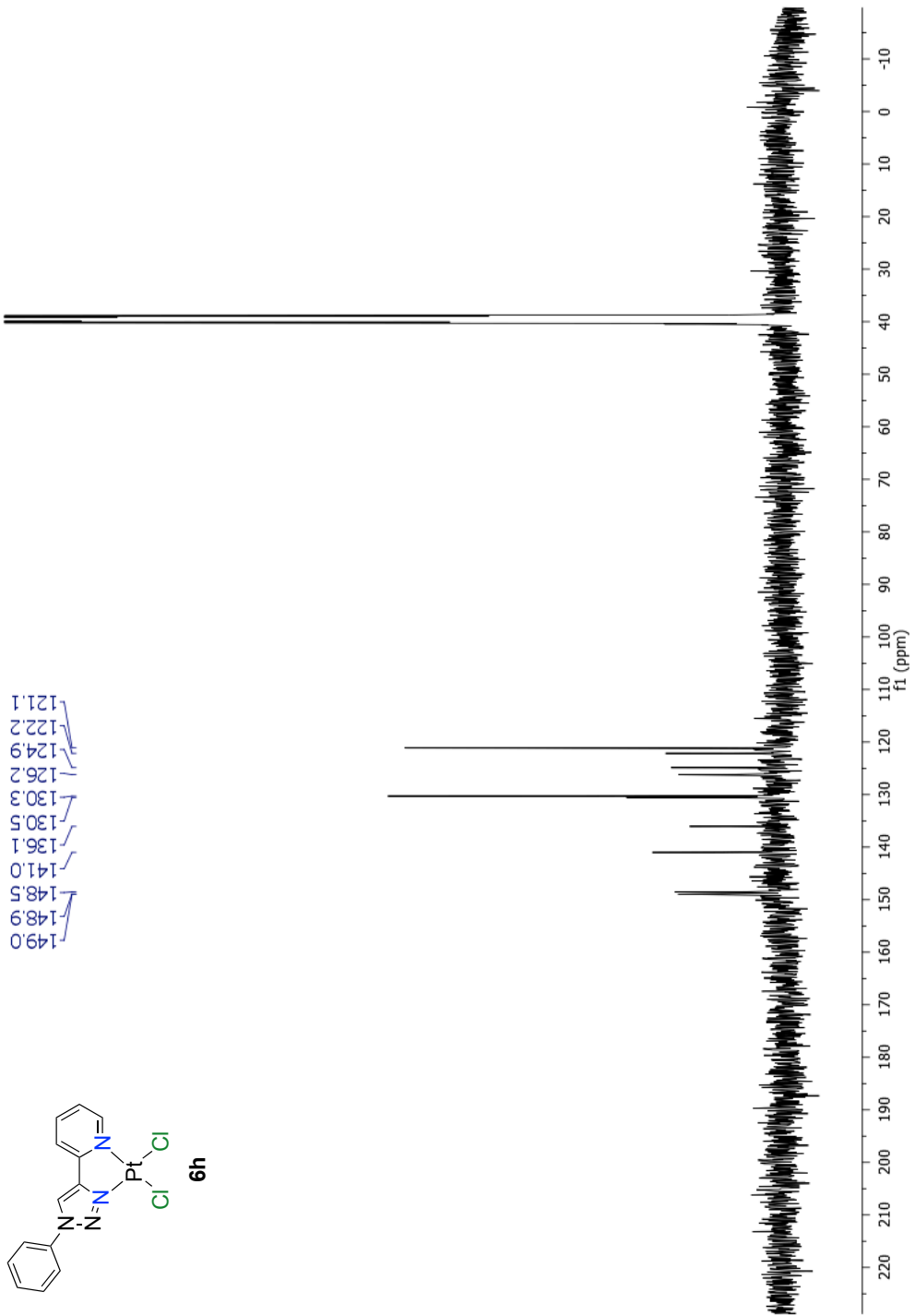


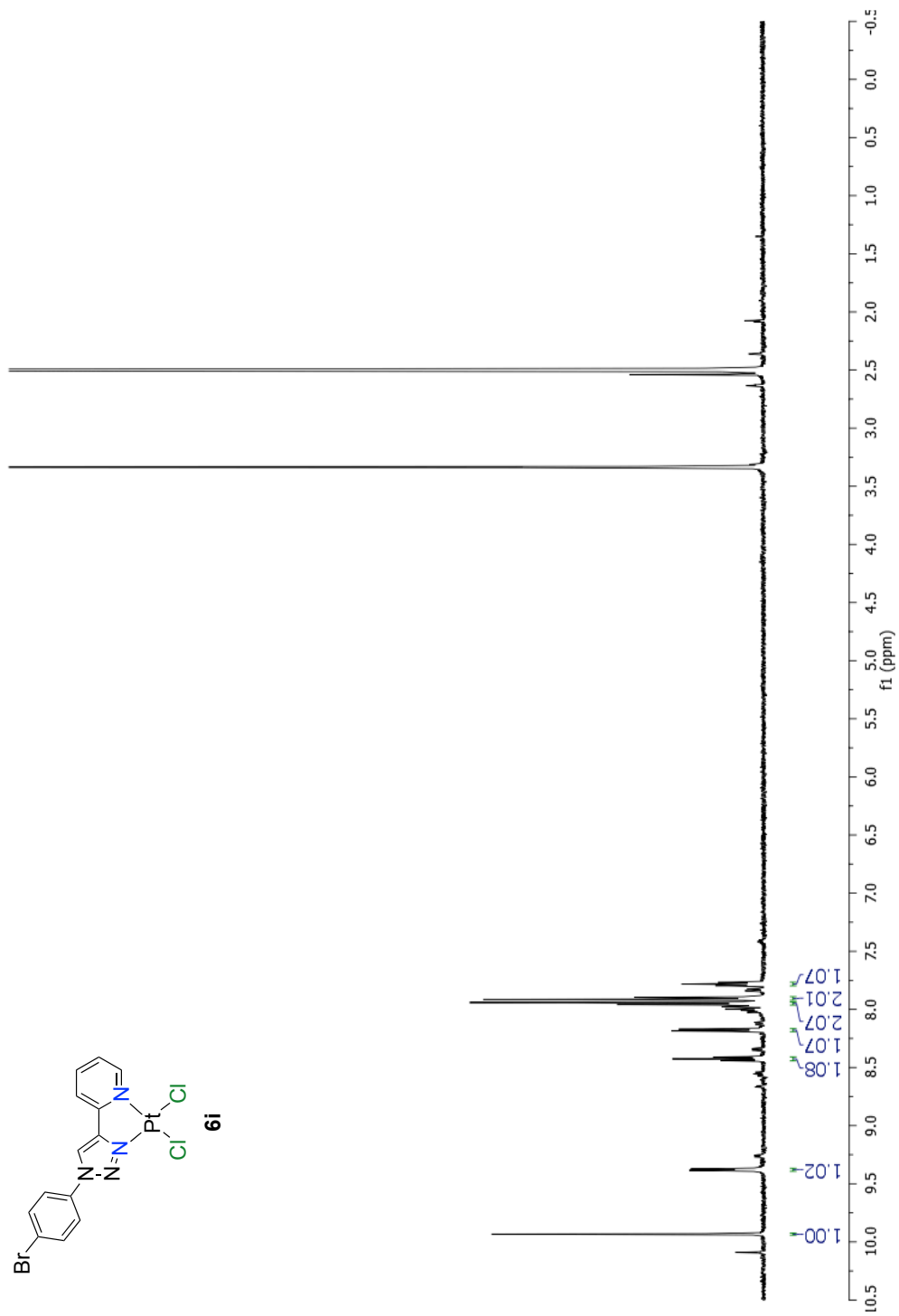
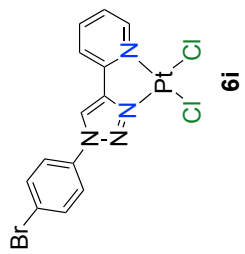


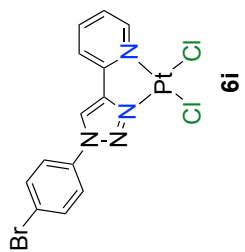




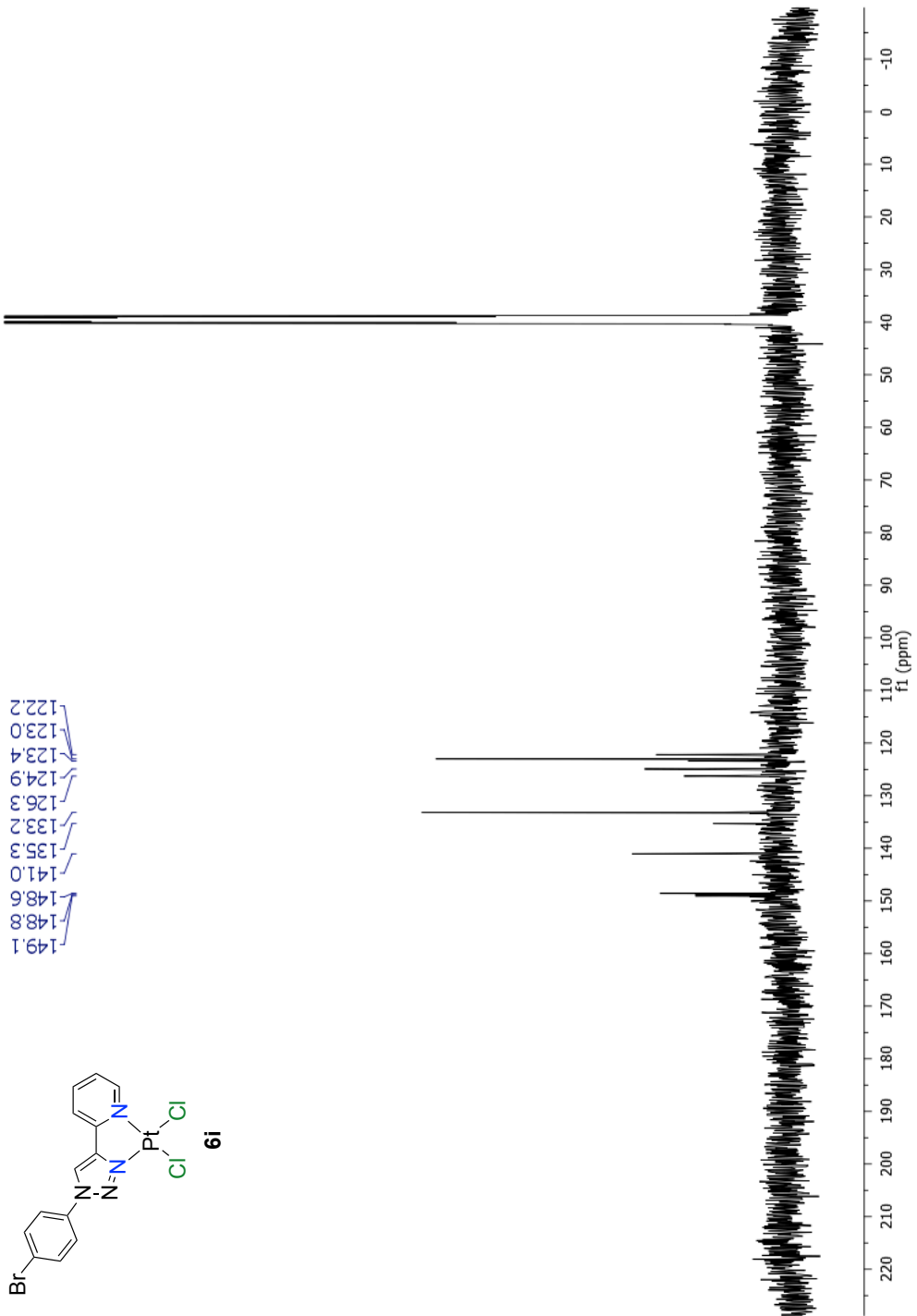


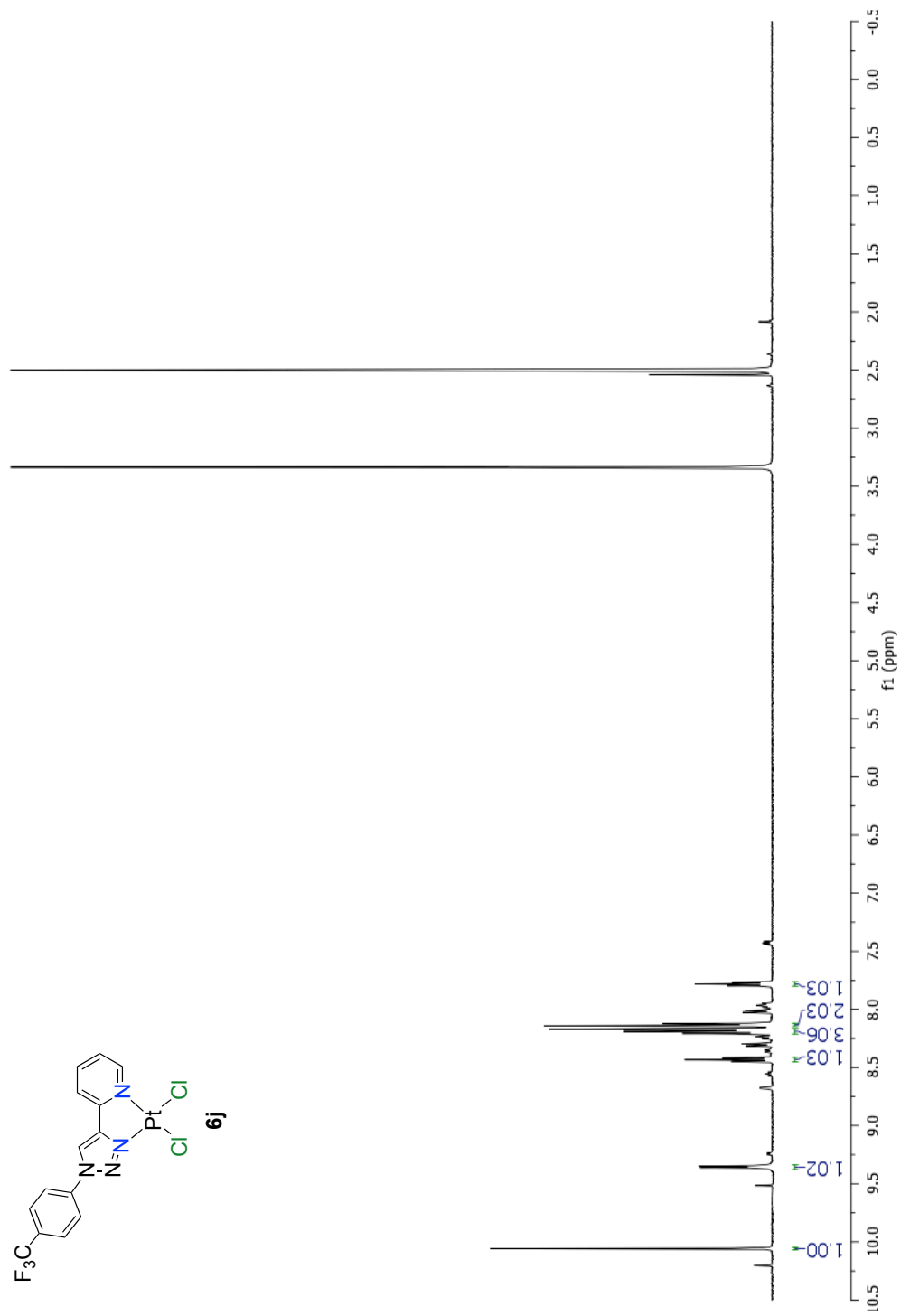
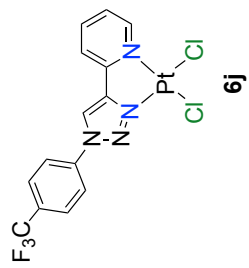


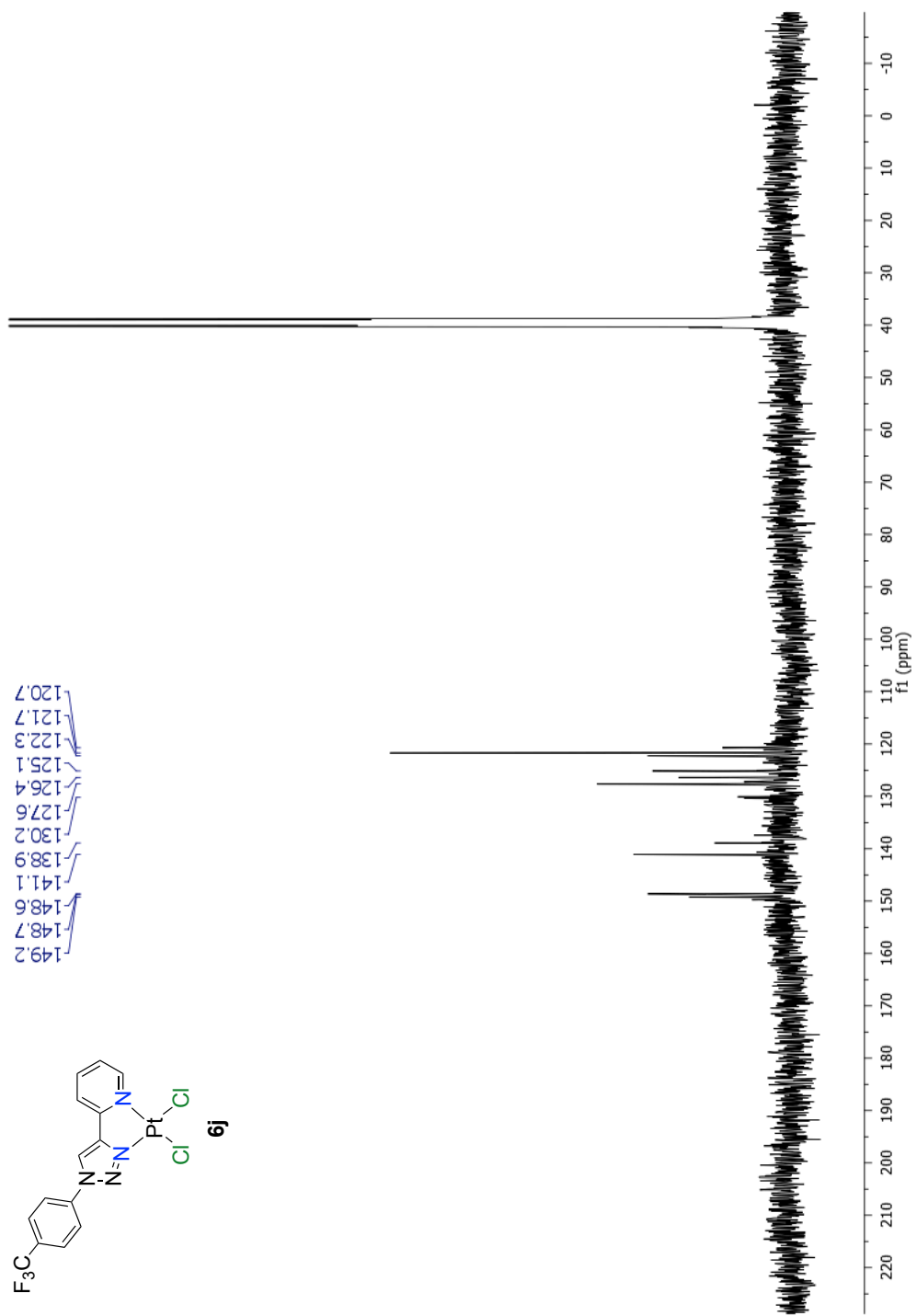


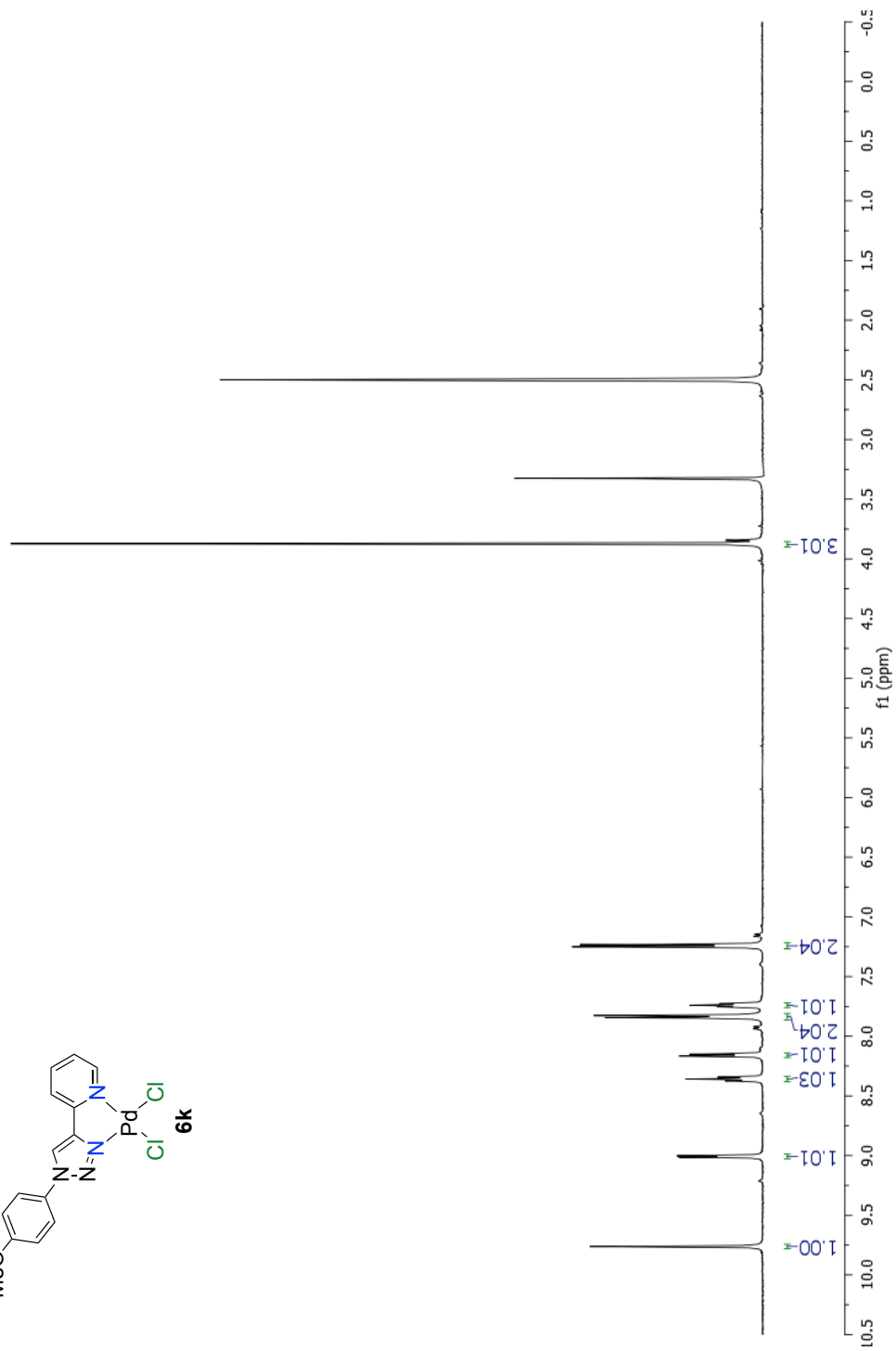
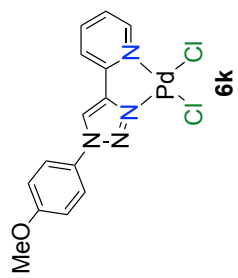


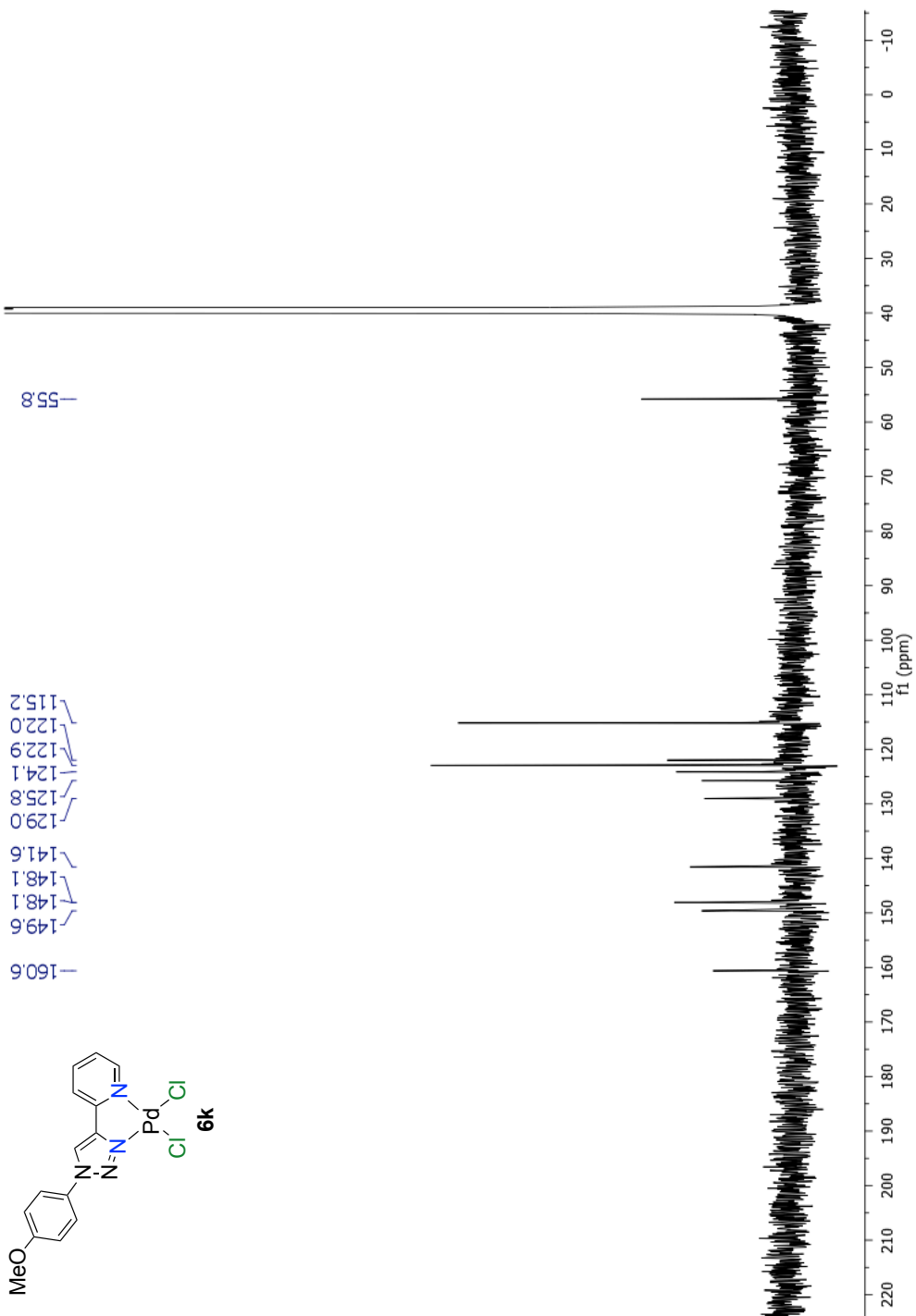
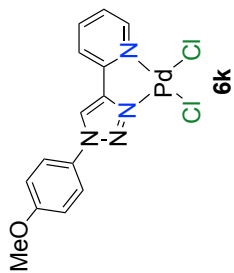
149.1
 148.8
 148.6
 141.0
 135.3
 133.2
 126.3
 124.9
 123.4
 123.0
 122.2

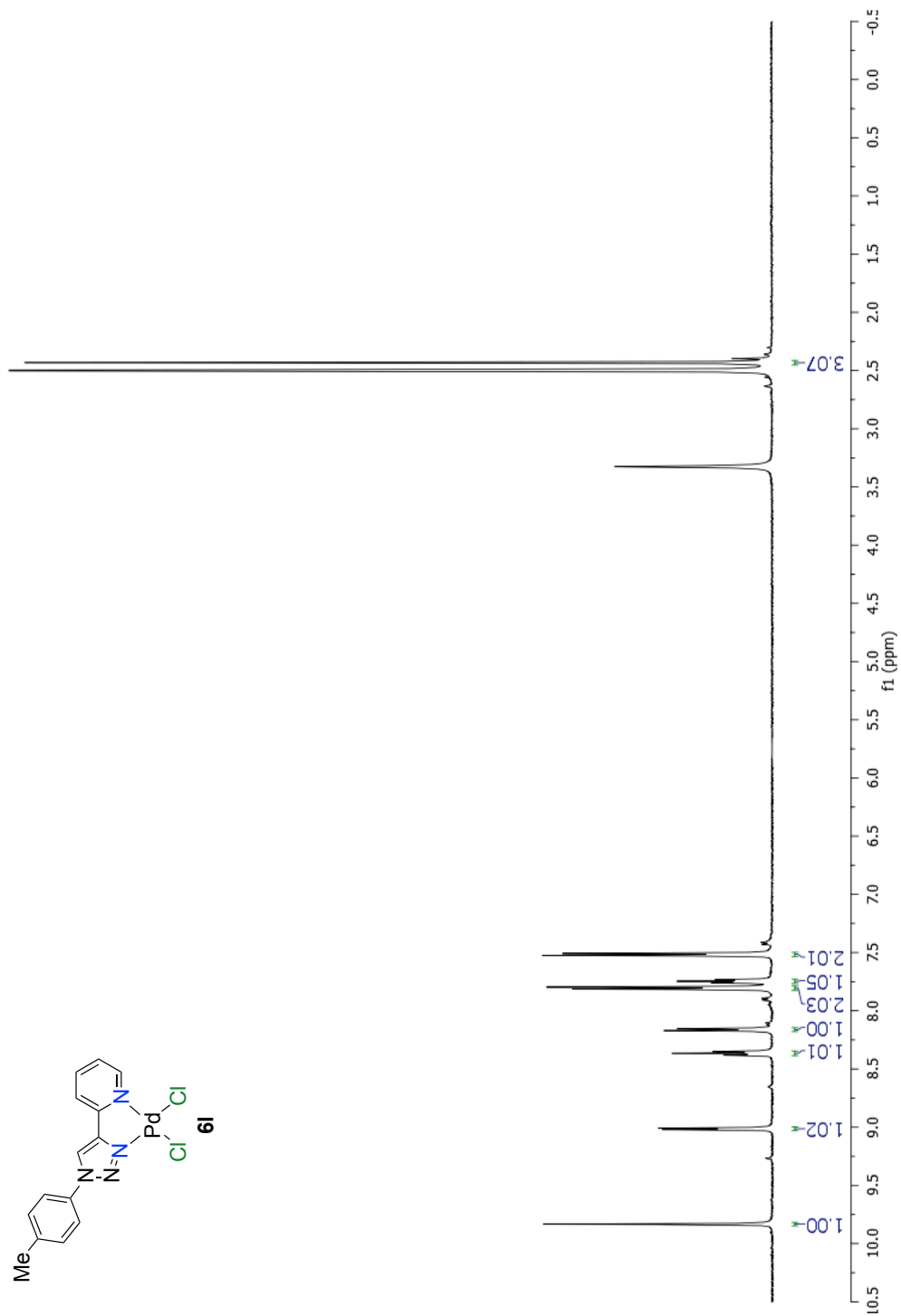
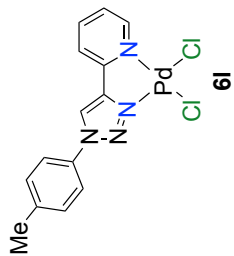


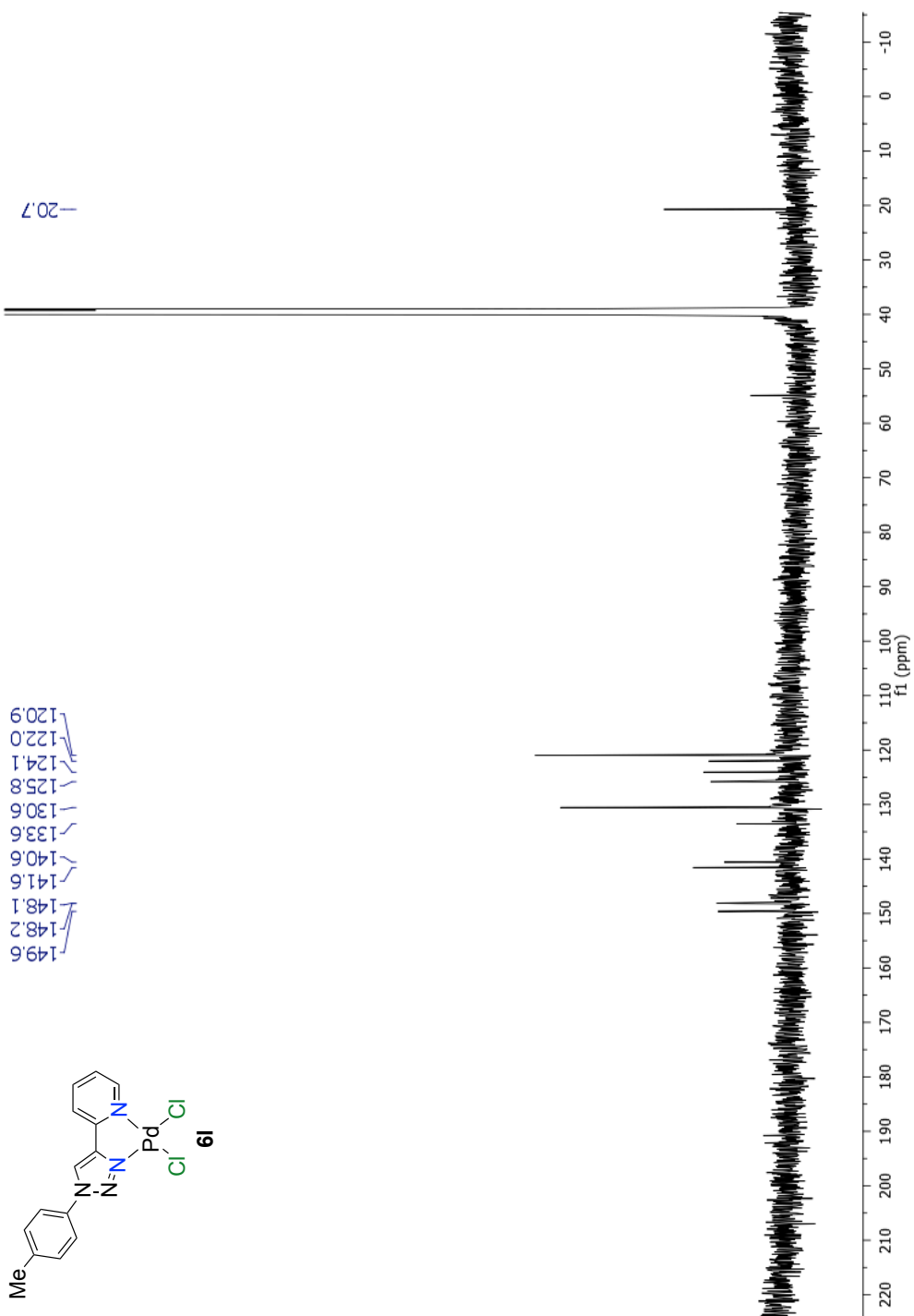


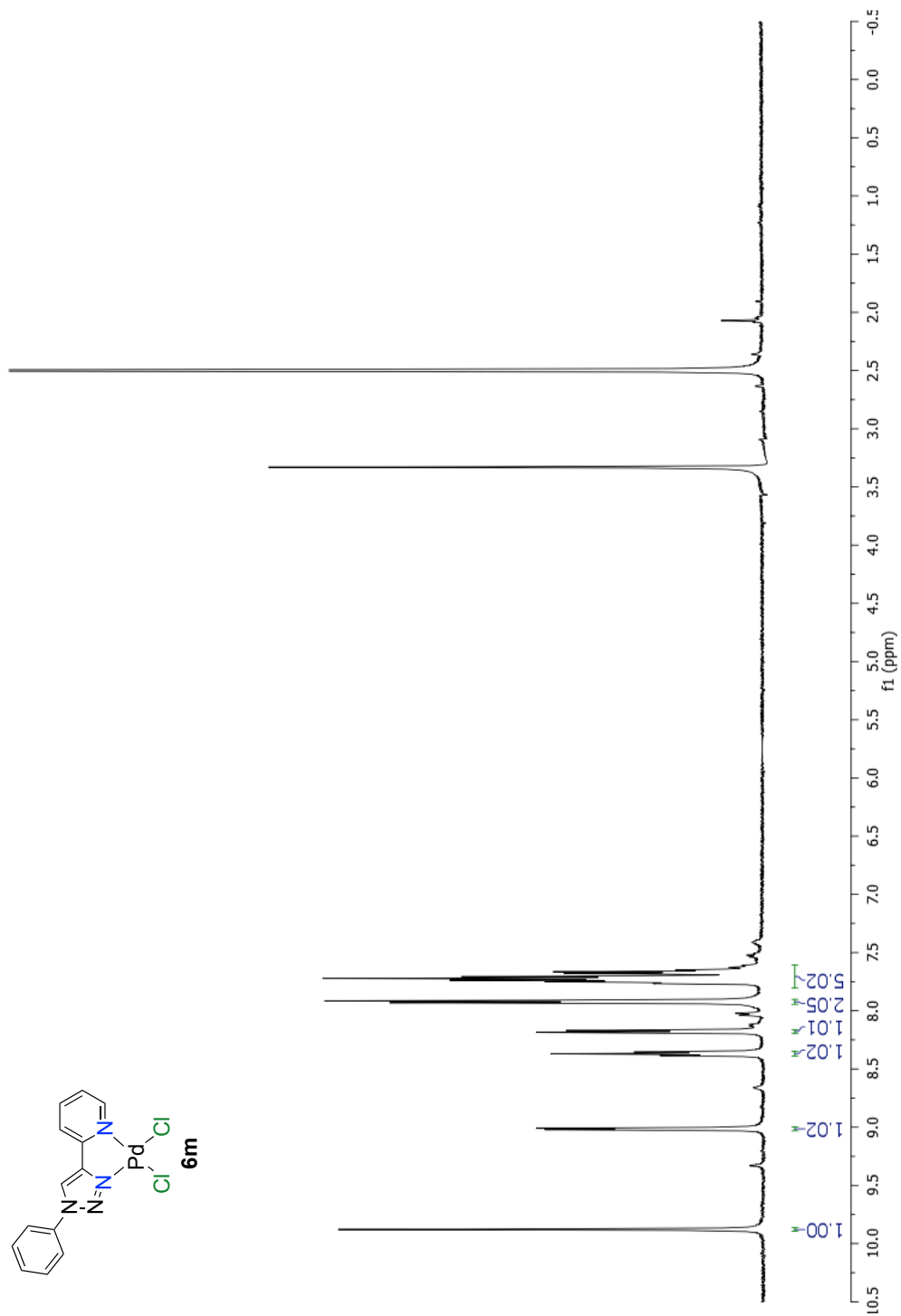
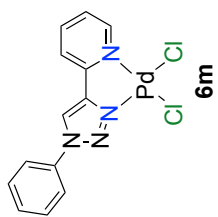


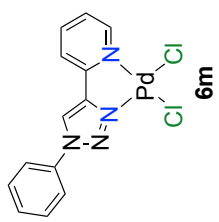
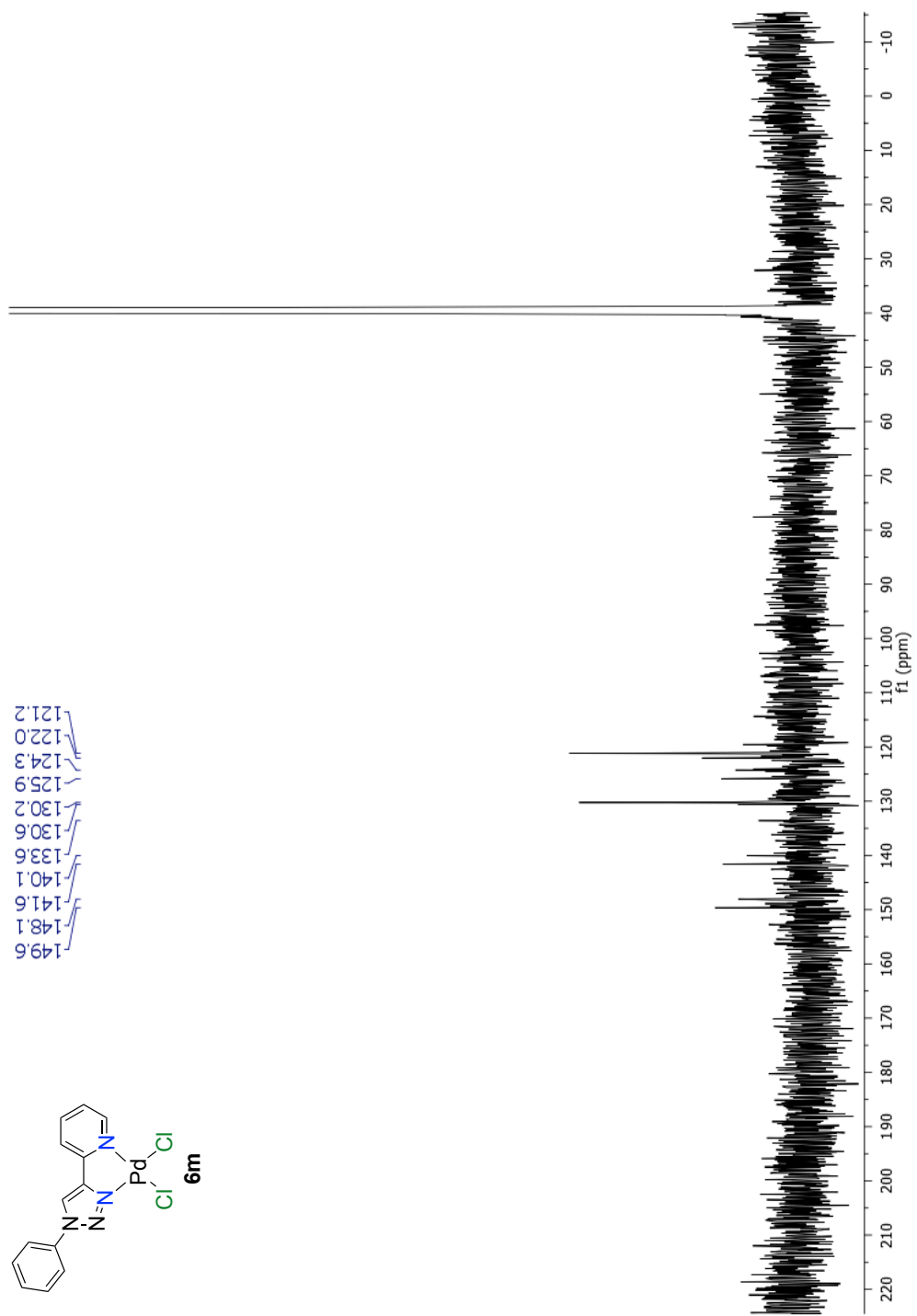


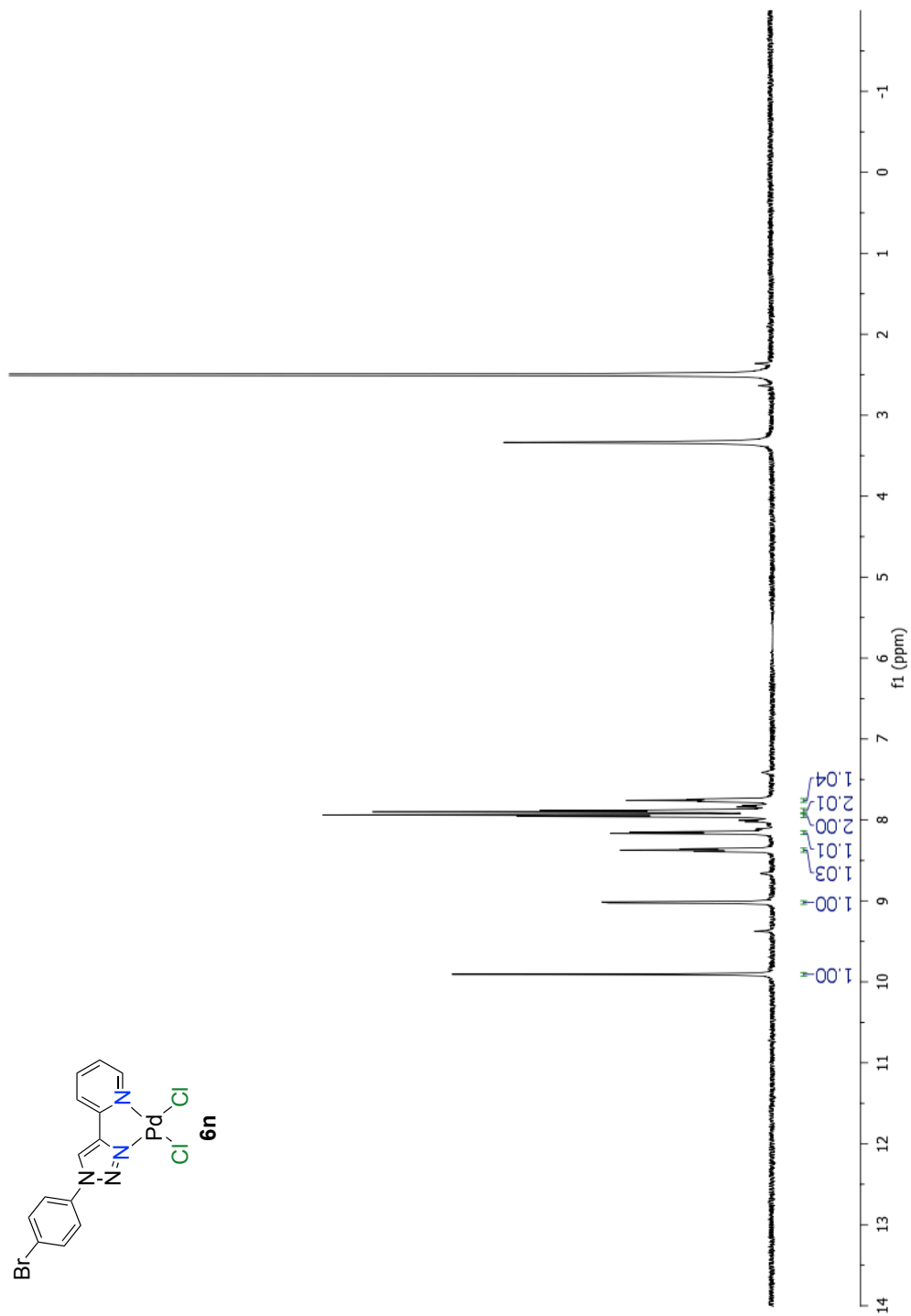
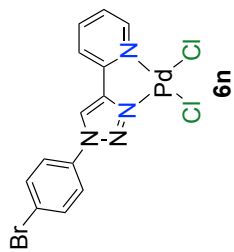


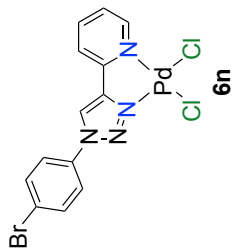




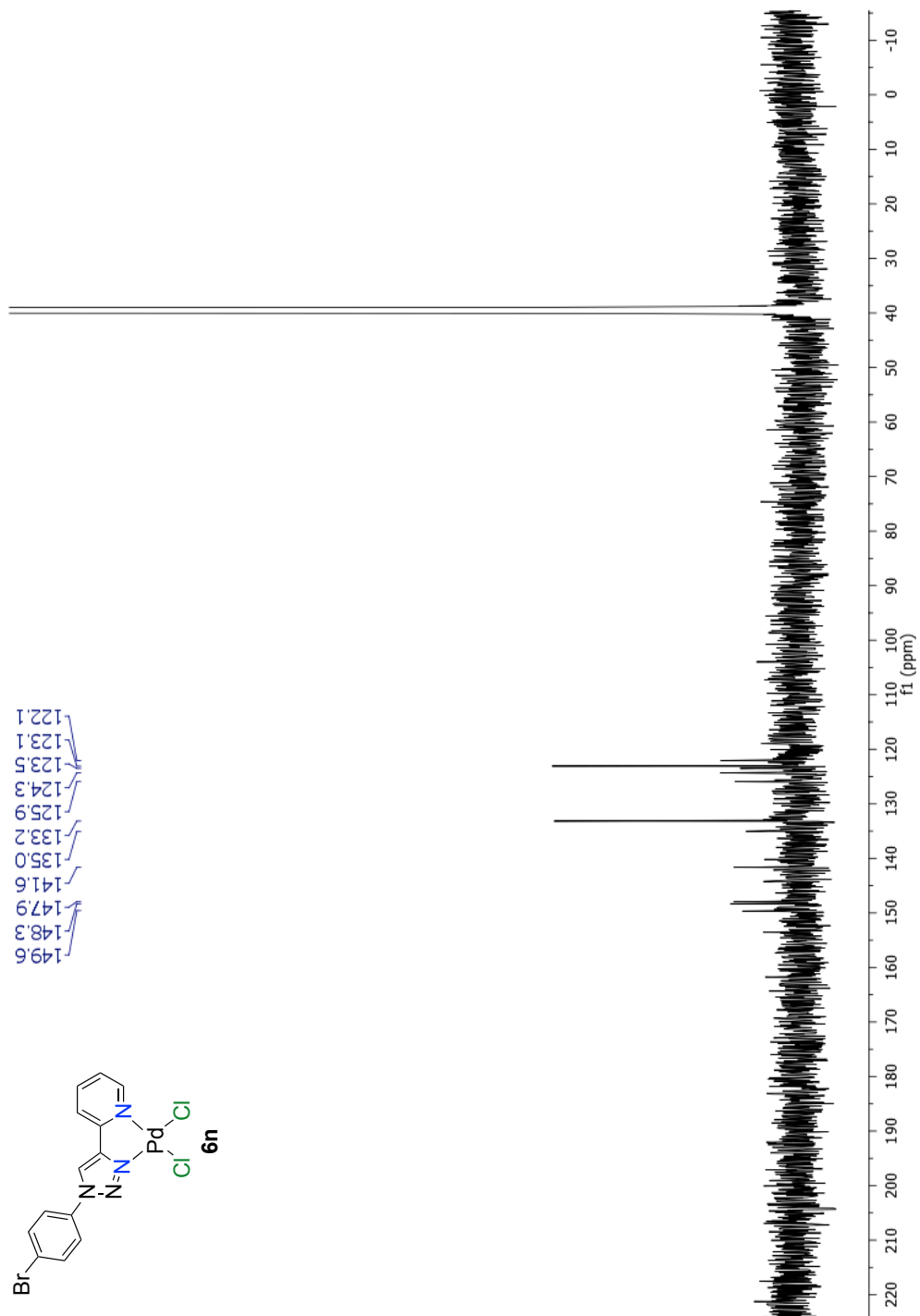


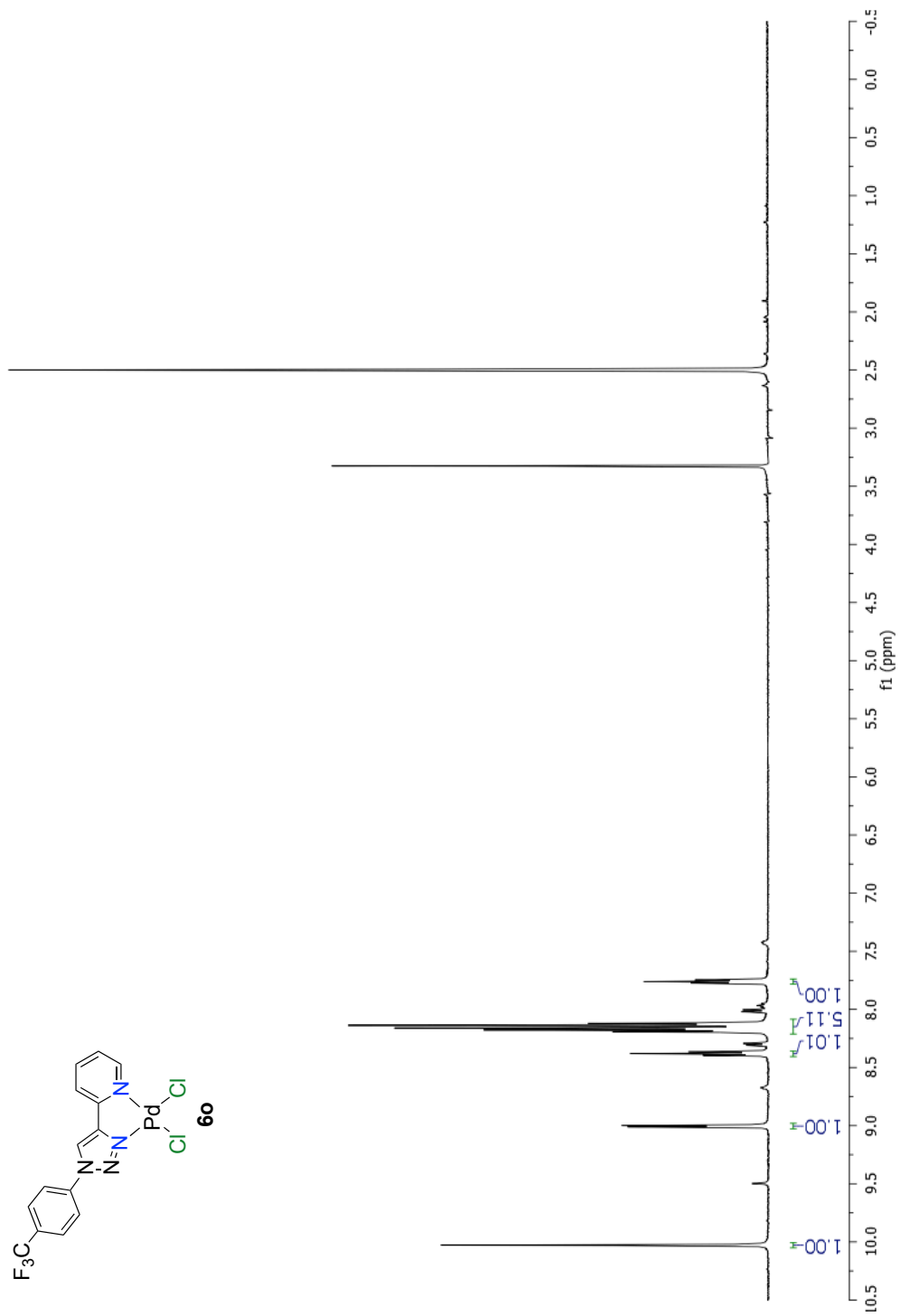
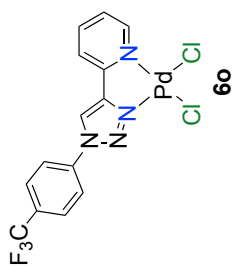


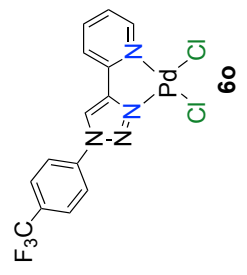
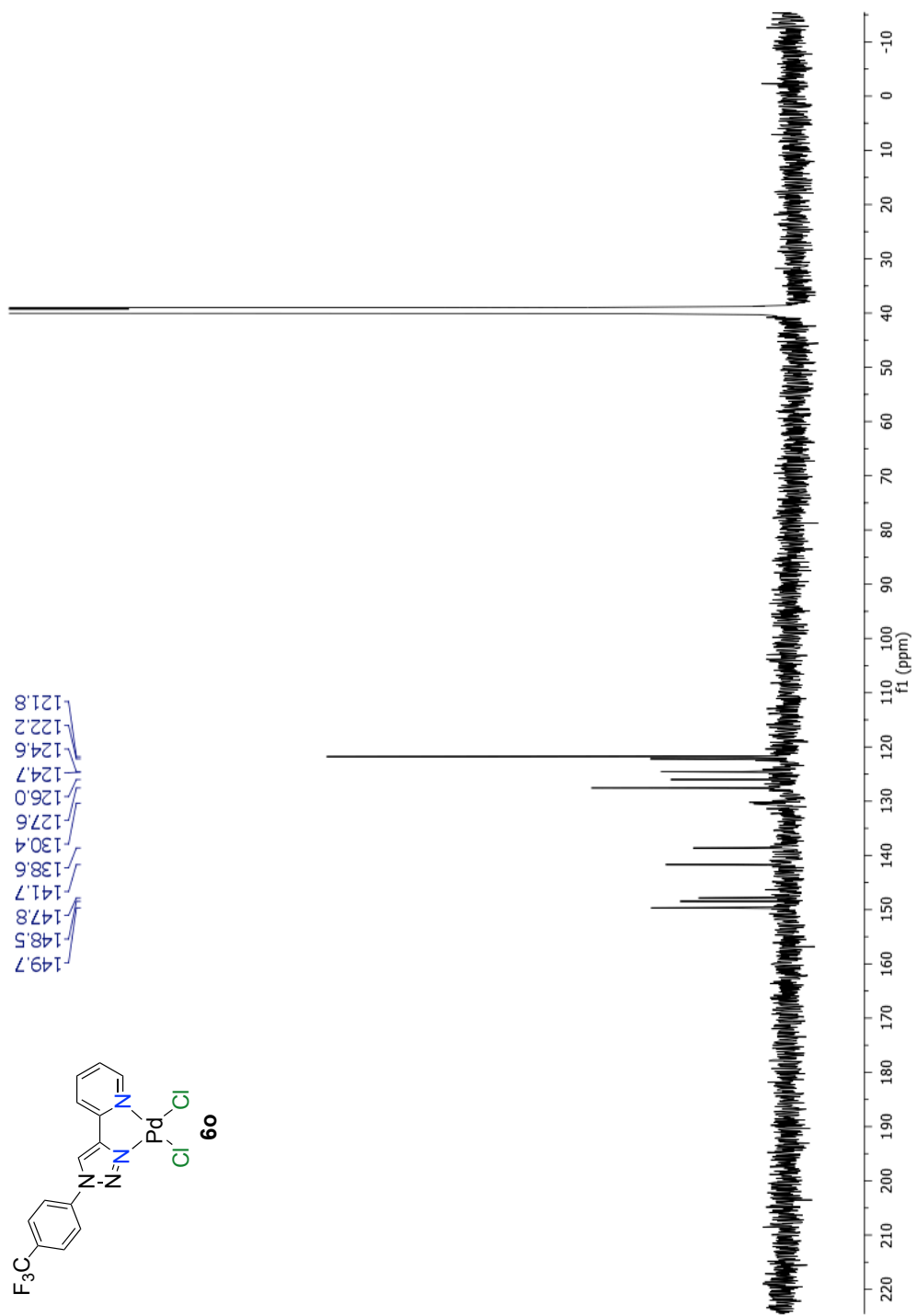


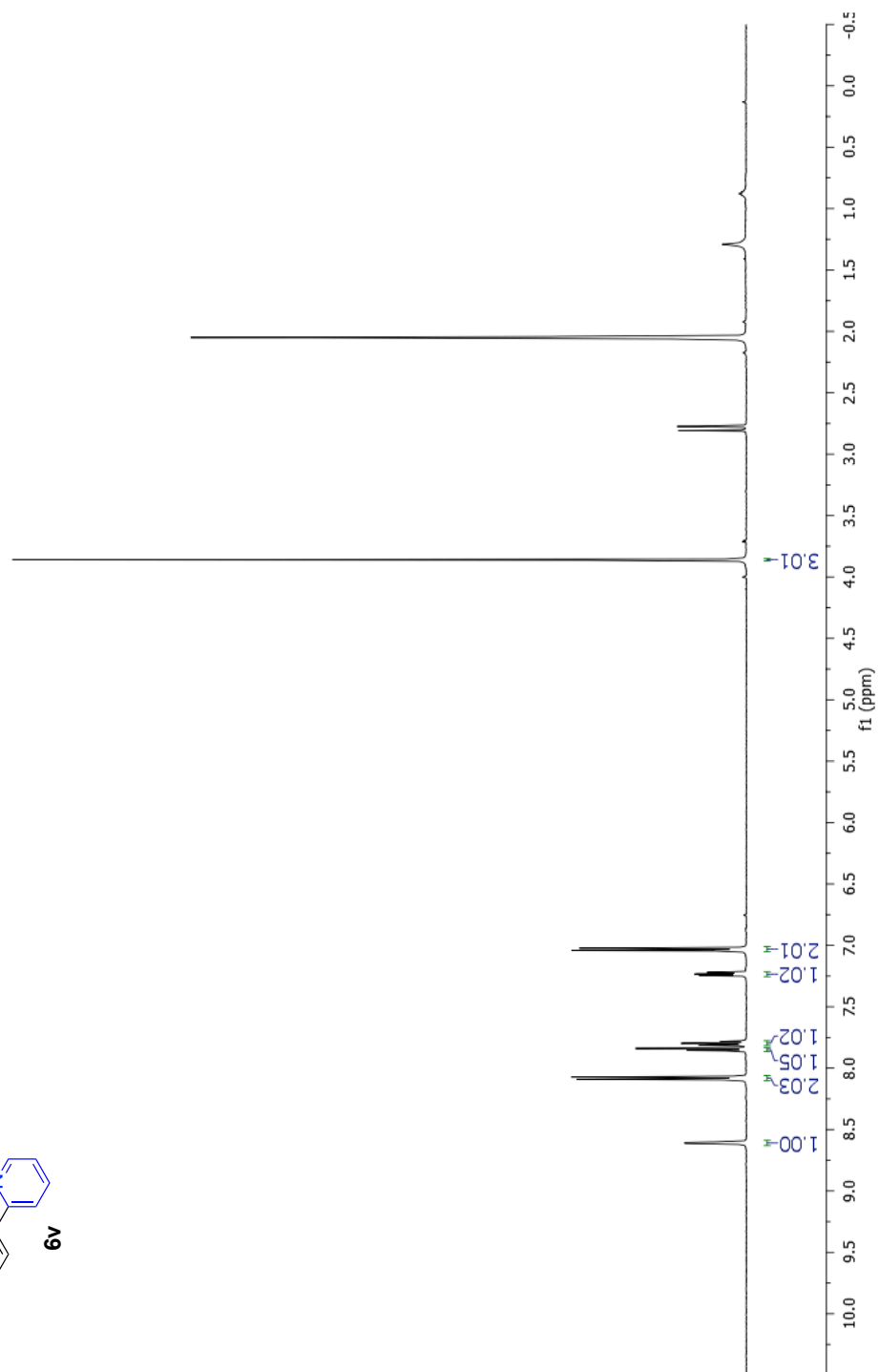
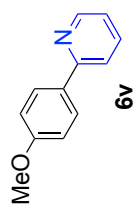


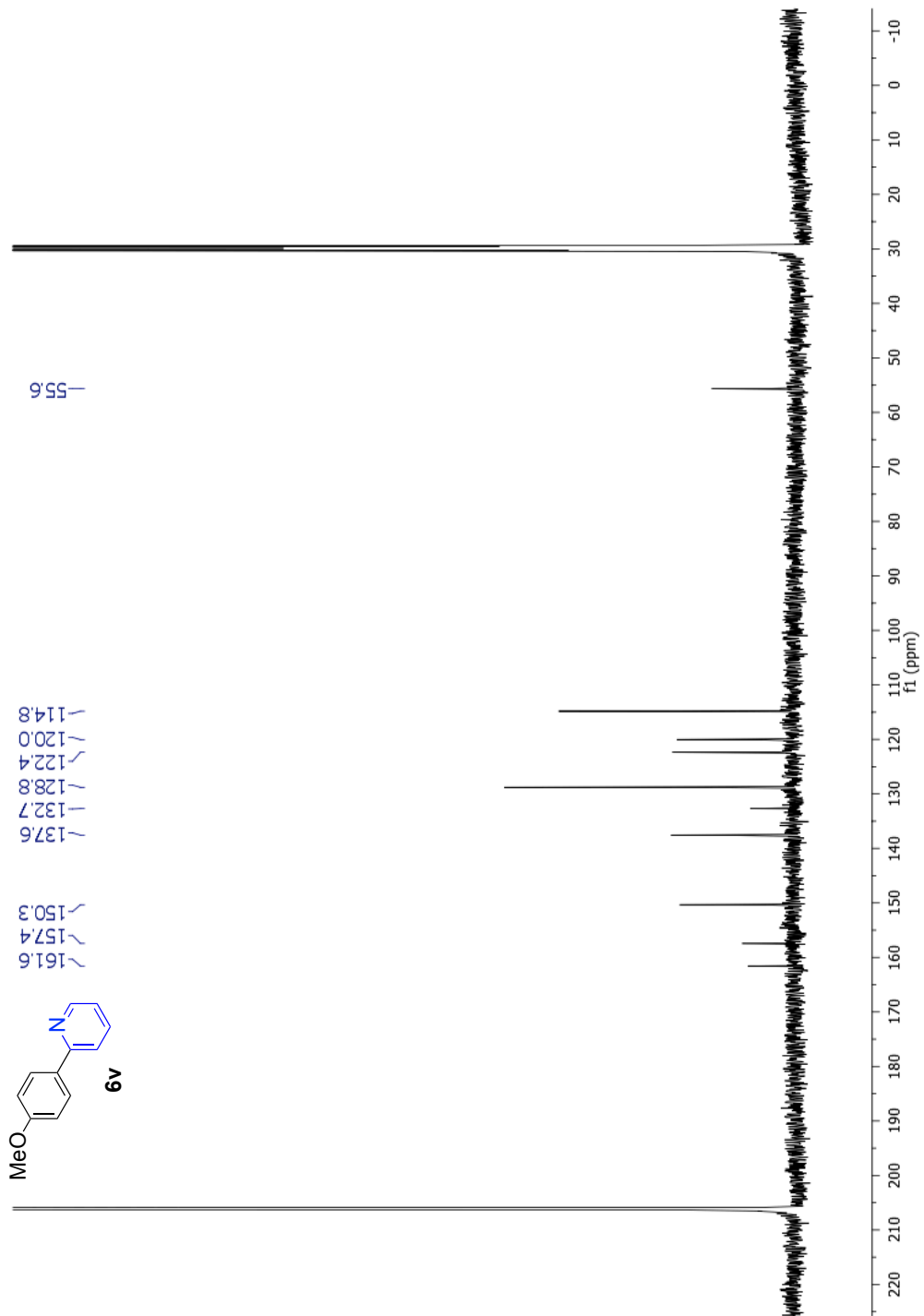
149.6
148.3
147.9
141.6
135.0
133.2
125.9
124.3
123.5
123.1
122.1

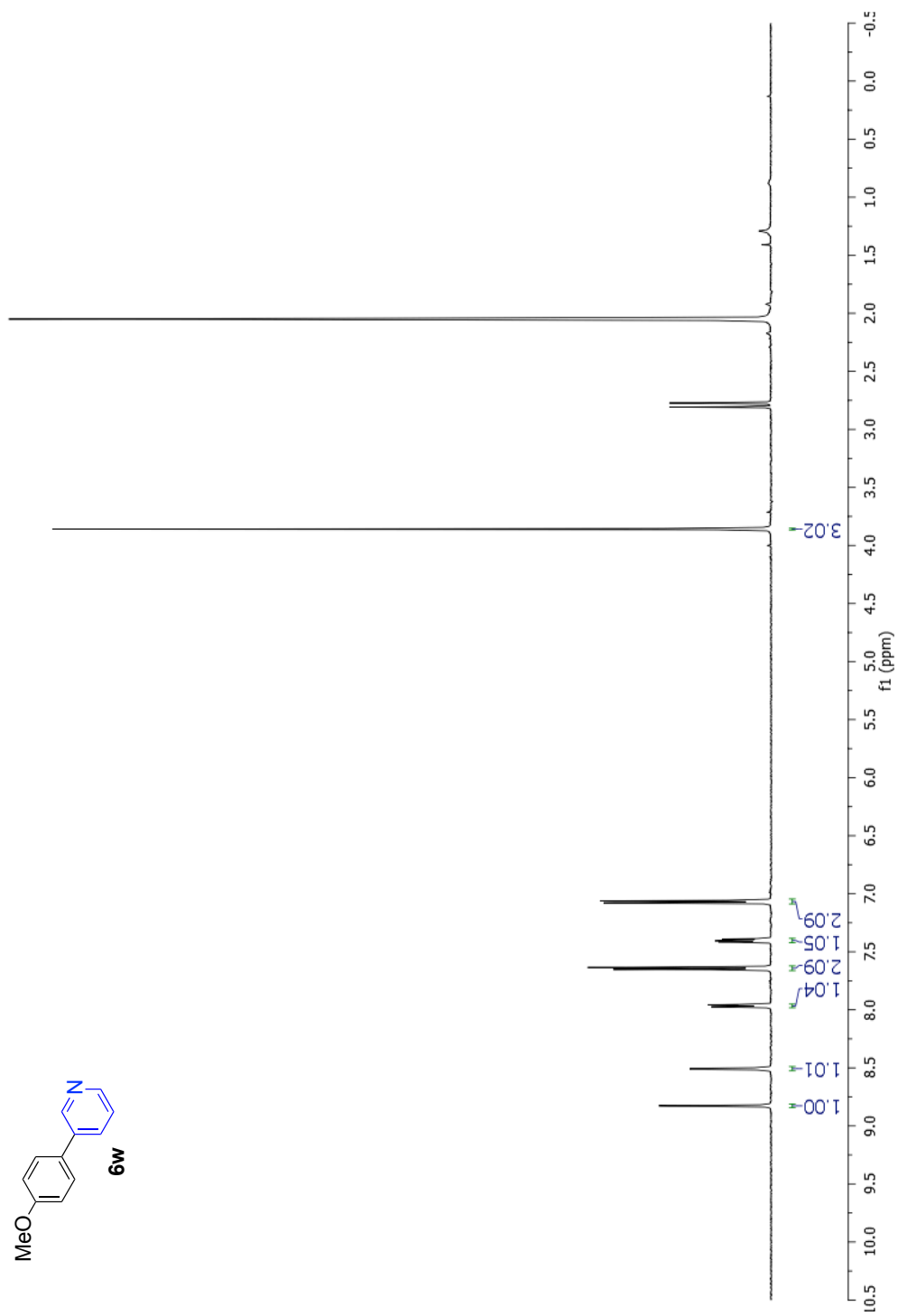
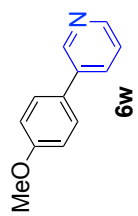


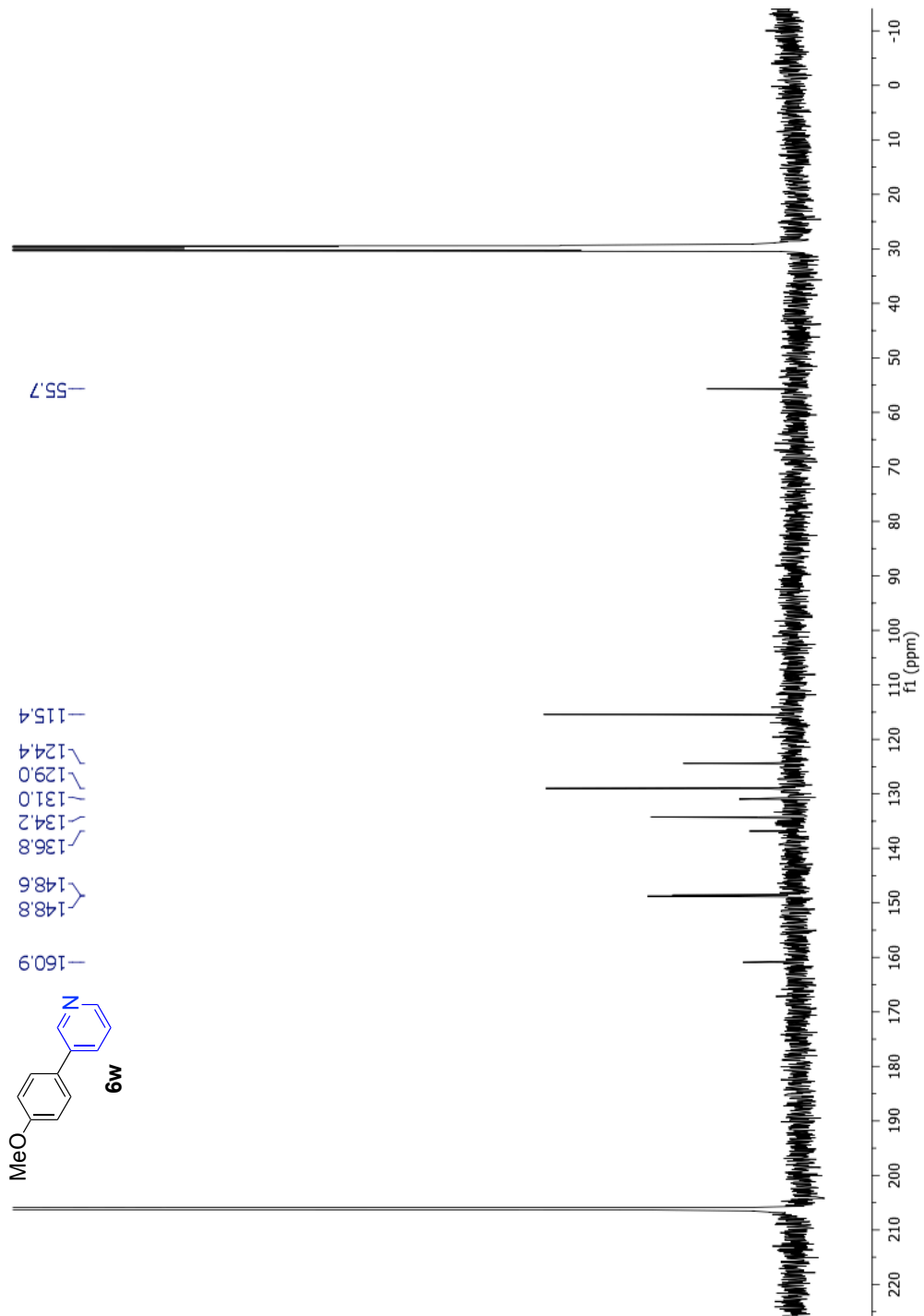


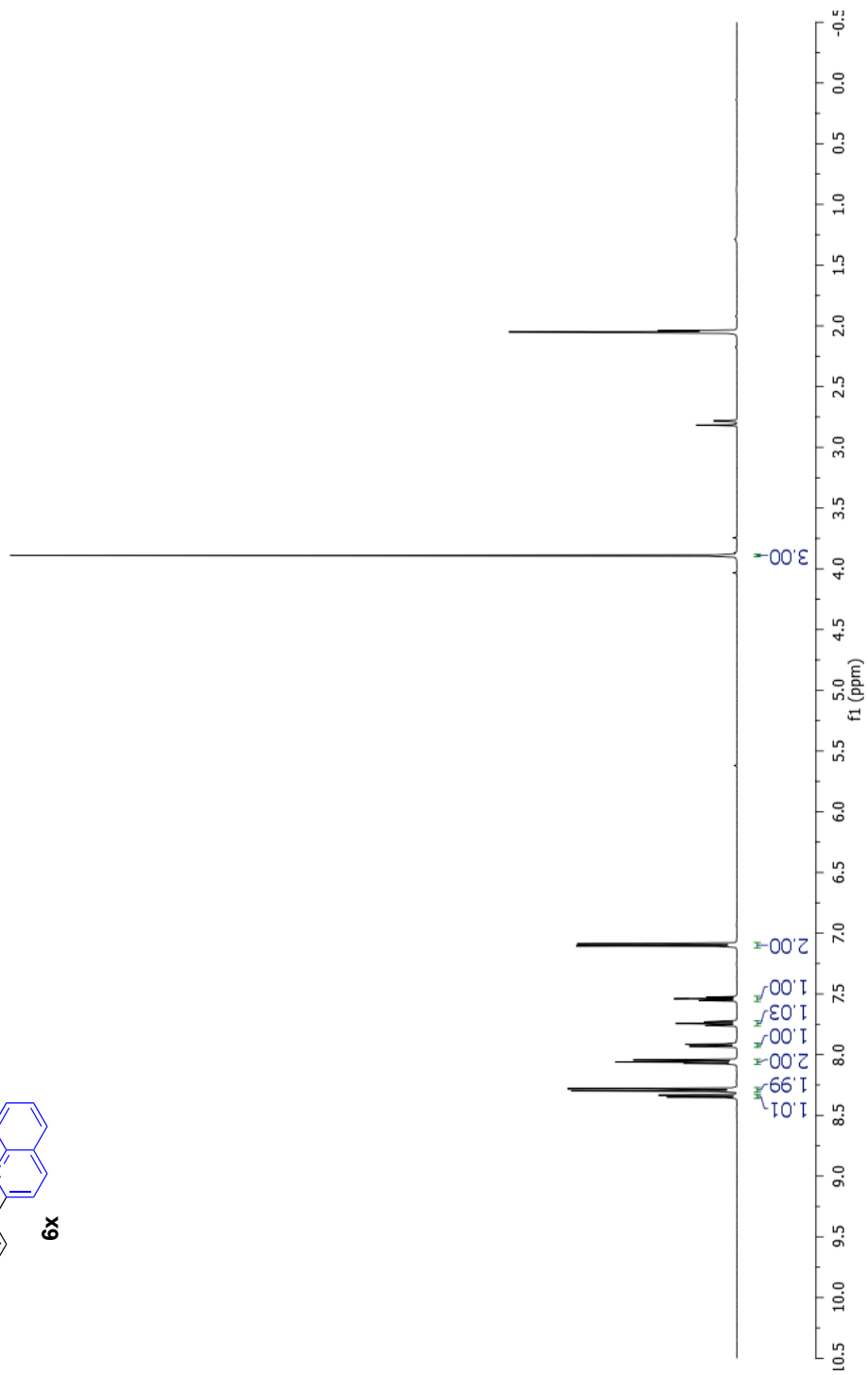
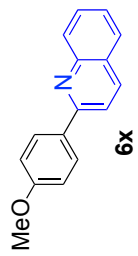


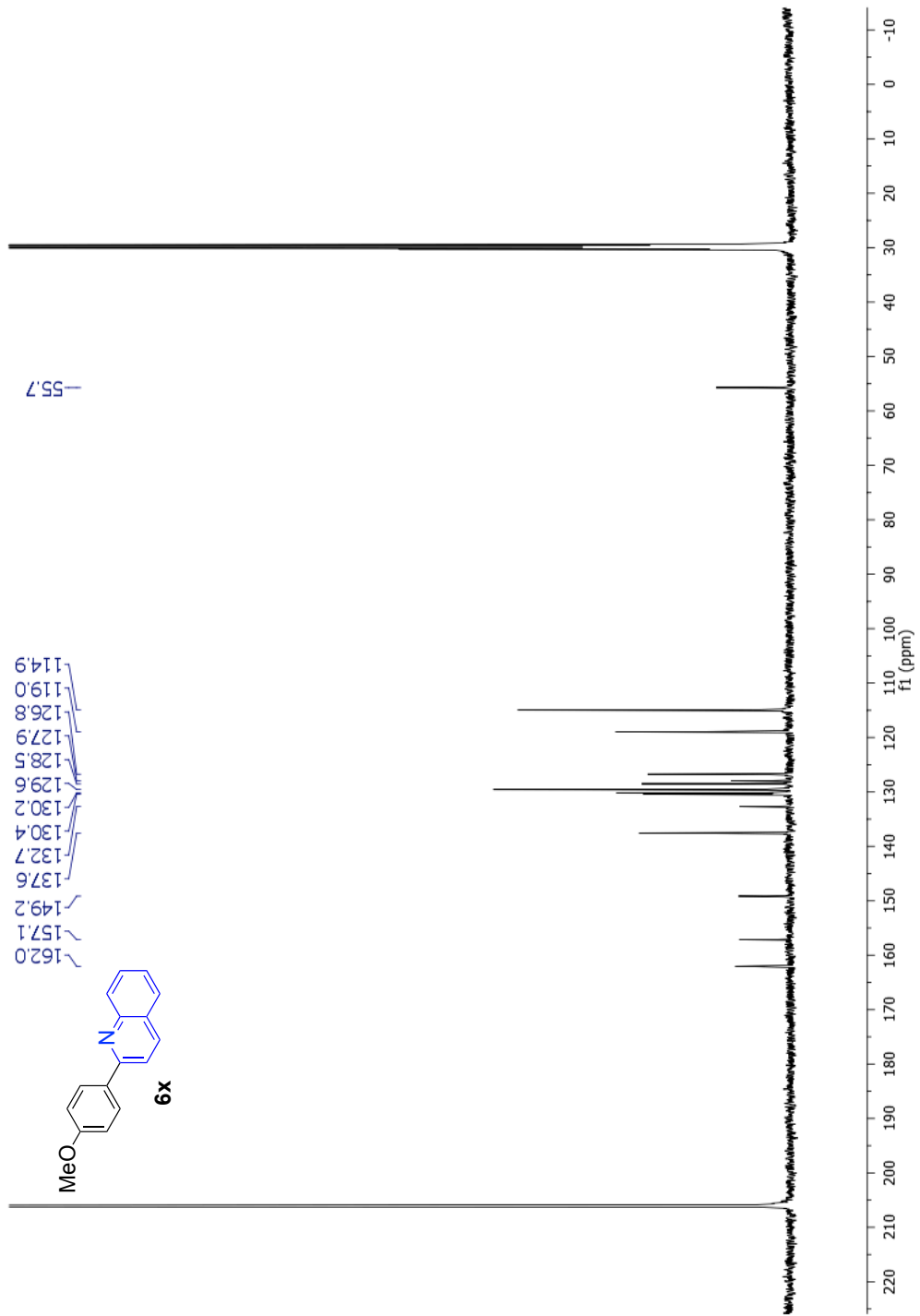


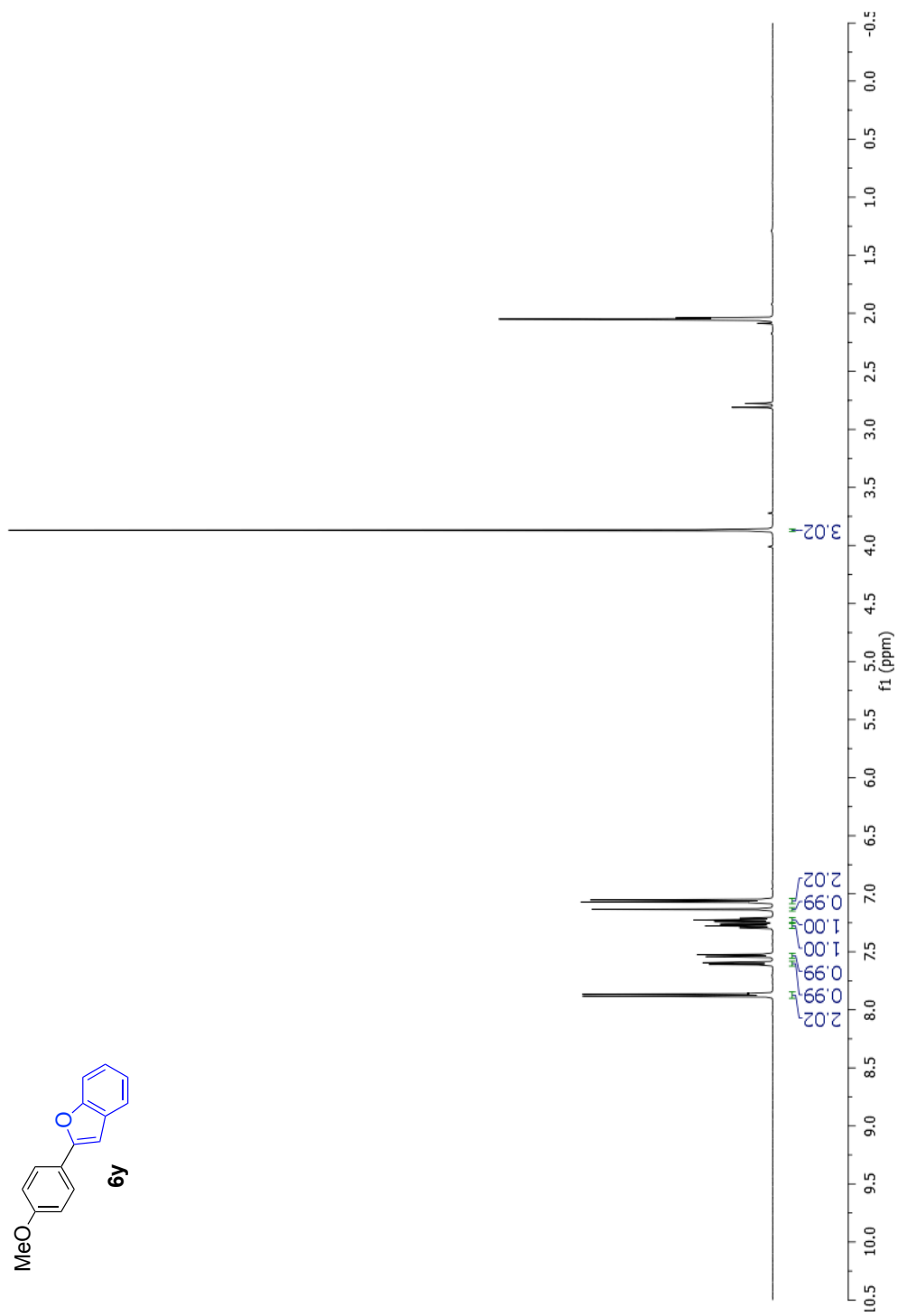
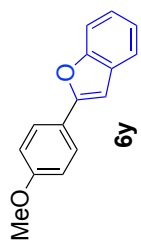


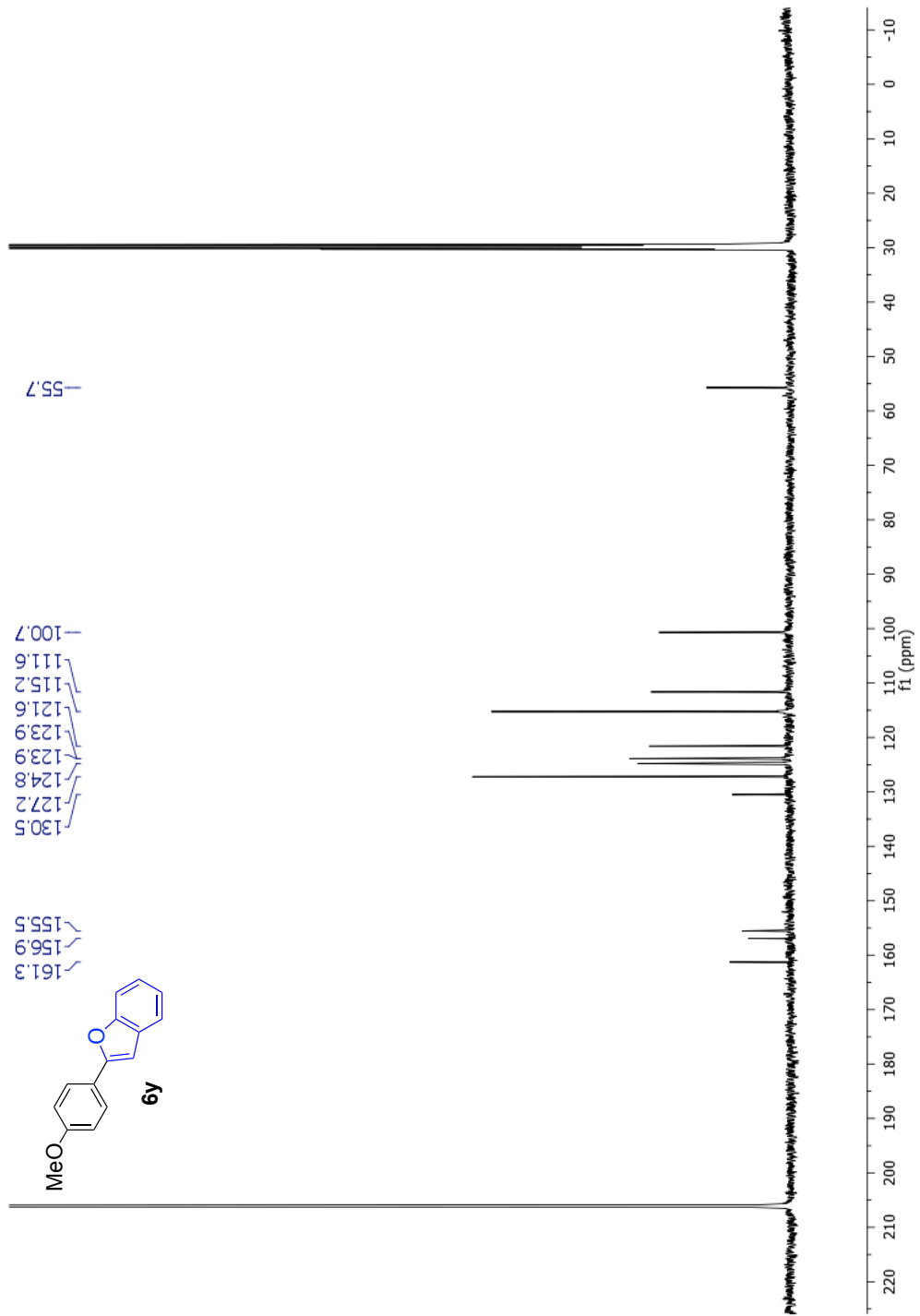












Chapter Seven: Pyridine Pyrazoles as Ligands and Complexation with Palladium

7.1 Introduction:

Pyrazoles and subsequent derivatives are a class of nitrogen-containing heterocycles, of which many possess biological and pharmaceutical activity.¹⁻³ Additionally, there are many examples of these compounds as synthetic building blocks and as ligands for important metal complexes.⁴⁻¹¹ As such, there has recently been increased efforts on the synthesis of pyrazoles and their use to form functionalized materials.

Of the methods that have been developed for the preparation of pyrazoles, the most widely used involves the reaction of hydrazines with 1,3-difunctional ketones or similar derivatives.¹²⁻¹⁵ Unfortunately, this condensation reaction also leads to the formation of undesired isomers as side products. Another method to access these compounds is through the reaction of chalcones with hydrazine hydrate.¹⁶ However, due to the structural limitations of chalcones, this method cannot be widely used to produce highly derivatized pyrazoles in an efficient manner. One method that is amenable to the synthesis of diverse pyrazoles is the 1,3-dipolar cycloaddition reaction between diazo compounds onto triple bonds.¹⁷ While these nitrile imines are known to be highly versatile building blocks, they have been shown to be highly toxic and potentially explosive.¹⁸⁻²⁰ Additionally, this cycloaddition reaction has been shown to typically afford mixtures of 4- and 5- substituted pyrazoles.²¹⁻²³ Synthesis of 3,5-

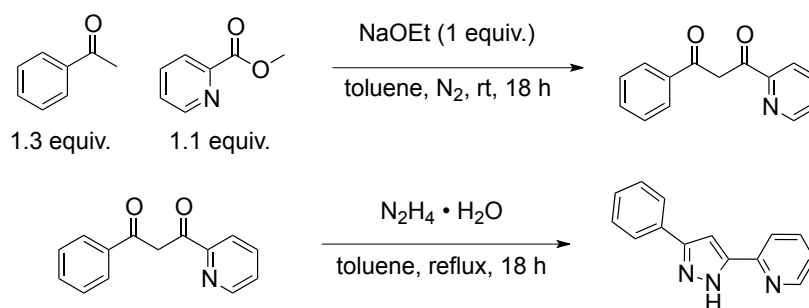
disubstituted pyrazoles using a one pot methodology employing cheap and readily available starting materials represents a more simple and highly efficient method.

A new procedure for generating aryl diazomethanes in situ from stabilized tosylhydrazone derivatives was reported in 2003.²⁴ The authors of this report showed that this approach could be utilized in the facile, one-pot synthesis of pyrazoles and excellent regioselectivity for the 3,5-disubstituted pyrazole was observed. Additionally, as the diazo compound is generated in situ, this method is a significantly safer alternative to handling purified aryl diazomethanes.²⁵ While this system has been proved to be highly useful and optimization of reaction parameters have been reported, only a select handful of substrates have been studied.²⁶ Adaptation of this system for the preparation of pyridyl pyrazoles (PyPyr) is of high importance as this class of compounds have been shown to be highly useful in the synthesis of complexes with varying metal centers. Utilization of this method, if controlled, should allow for the direct synthesis and isolation of the 3-substituted pyrazole pyridine isomer. Complexes with this isomer are a notable vacancy in the analysis of these types of complexes and a direct route to their synthesis is of high value.

7.2 Synthesis of Electronically Diverse Pyridine Pyrazoles:

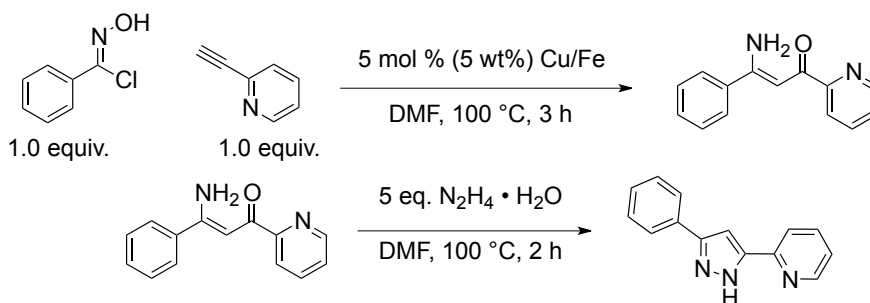
Methods for the preparation of PyPyr have traditionally used the aforementioned strategy of reacting a 1,3-diketone with hydrazine hydrate to afford the desired heterocycle (Scheme 7.1).²⁷⁻³⁰ While this has been effective at

preparing these compounds in high yield, the purchase of the diketone precursor is costly and its synthesis requires additional time and materials. Additionally as there is no stereocontrol to this reaction formation of both isomers, the 3-substituted and 5-substituted pyrazole can occur.



Scheme 7.1: Synthesis of pyridyl pyrazoles from 1,3 diketones and hydrazine hydrate.

A similar method for preparation of these pyrazoles, that is much more stereoselective, requires reacting a preformed amino-enone with hydrazine hydrate (Scheme 7.2).³¹ The amino-enones required for this method were obtained by reacting N-hydroxy-benzenecarboximidoyl chloride with 2-ethynylpyridine and 5 mol% of a copper-iron bimetallic catalyst. While this was effective at providing both isomers of the pyridyl pyrazole stereoselectively, it did so in moderately low yields (~46%). Further the fact that this method requires previous synthesis and isolation of the copper-iron catalyst as well as the amino-enones renders this not ideal for the preparation of further derivatized compounds.



Scheme 7.2: Synthesis of pyridyl pyrazoles from amino-enones and hydrazine hydrate.

Synthesis of pyridyl pyrazoles through the in situ generated aryl diazomethane and subsequent 1,3 cyclization with 2-ethynylpyridine is an attractive methodology. Here, the aryl diazomethane can be easily derivatized through use of substituted benzaldehydes, which are of low cost through commercially available sources. This will allow for the preparation of diverse PyPyrs where the electronic conditions can be varied.

Through the reaction of a benzaldehyde with tosylhydrazine the aryl tosylhydrazone bearing the desired substitution can be prepared. Reaction of this hydrazone with sufficient base allows for the formation of the substituted aryl diazomethane in situ. Upon treatment with 2-ethynylpyridine the desired pyridyl pyrazoles (**7a-7e**) can be generated and after recrystallization in MeCN can be isolated for further study (Table 7.1). While these compounds are currently isolated in low yield this method allows for the direct synthesis of a series of electronically diverse compounds in one pot from cheap, commercially available starting materials.

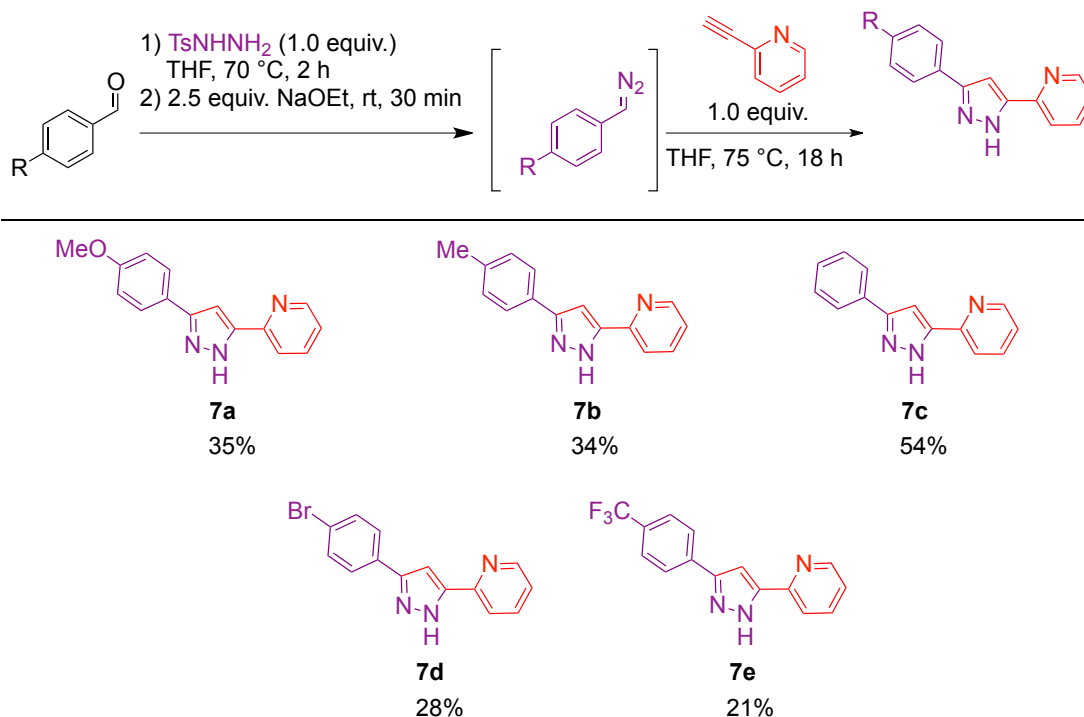
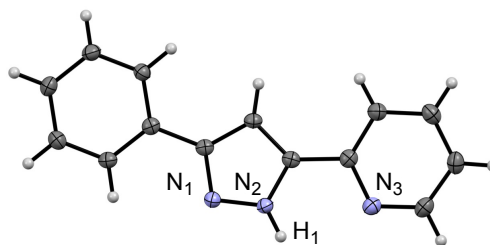
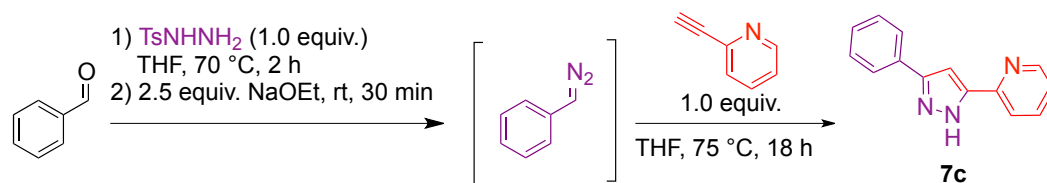


Table 7.1: Synthesis of electronically diverse pyridyl pyrazoles (PyPyrs) in one pot through 1,3-cyclization with ethynyl pyridine.

Characterization of these compounds with ¹HNMR was challenging. When the compounds were dissolved in deuterated solvents that contained trace amounts of H₂O, intermediate states of protonation were observed. As a result significant broadening of the proton resonances associated with the pyrazole and pyridine rings occurred. Many deuterated organic solvents were tried and significant broadening was observed in most all of them. To overcome this challenge a deuterated solvent was needed that would allow for adequate characterization of the entire series of PyPyr compounds. It was proposed that using a highly acidic solvent would allow for full protonation and this should lock the system in one orientation. This hypothesis was proved correct when the NMR

characterization was taken using deuterated trifluoroacetic acid as solvent. Here no broadening of the peaks were observed and comparison of the NMR spectra across the series of electronically diverse PyPyr ligands could be performed.



$\text{N}_1\text{-H}_1 = 20\%$
 $\text{N}_2\text{-H}_1 = 80\%$
 $\text{N}_2\text{-H}_1: 0.880 \text{ \AA}$
 $\text{N}_3\text{-H}_1: 2.454 \text{ \AA}$
 $\text{N}_2\text{-H}_1\text{-N}_3: 98.59^\circ$

Table 7.2: X-ray crystal structure of the PyPyr ligand.

In order to confirm the absolute configuration of these ligands, X-ray quality crystals were grown from a dilute sample of ligand in MeCN. Upon standing for 3 days at decreased temperature ($\sim 4^\circ\text{C}$) colorless crystals of very high quality were obtained for the phenyl substituted PyPyr ligand (**7c**). X-ray crystallography was performed and the predicted structure of the compound as the 3-substituted pyrazole pyridine was confirmed (Table 7.2).

7.3 Pyridine Pyrazoles as Ligands for Metal Complexes:

Since work first began on the formation of complexes with pyrazole ligands the study of their coordination chemistry has developed substantially over the last

four decades.³²⁻³⁶ It has been suggested that the nucleophilicity of the sp^2 hybridized nitrogen of the pyrazole and the acidity of the NH may be utilized when there is appropriate substitution at the 3, 4, or 5 position on the pyrazole ring.^{37,38} When the ring is substituted at the 3, or 5 position with pyridine there is the ability for the pyrazole to act as either an anionic, X-type donor ligand (3 position) or as a neutral L-type donor (5 position). Previous reports have traditionally made use of PyPyr in their neutral form as the resulting complexes are more stable and their preparation is facile. Additionally, these ligands are amenable to complexation with a wide range of metal centers. These include Ni,³⁹⁻⁴¹ Fe,⁴¹ Co,^{39,42} Cu,^{39,43-45} Ag,⁴⁵ Ir,^{46,47} Pb,⁴⁶ Rh,⁴⁷ Os,⁴⁷ Mo,⁴⁸ Pd,⁴⁹⁻⁵² Pt,⁴⁹ Ru,^{47,53-56} B,⁵⁷ and small metal ions including Li, Mg, Ca, and Zn.^{58,59} While the precedent for the use of these pyridyl pyrazoles in complex formation is substantial the analysis of the electronic conditions of the complexes when subtle changes are made to the ligands has not been studied. Thus, it was desirable to analyze whether complexes could be formed with the series of electronically diverse PyPyr ligands and what effect the electronics of the free ligand would have on the resulting complex.

7.4 Palladium Complexes with Diverse Pyridine Pyrazole Ligands:

Development of methodology for the formation of complexes with these derivatized PyPyr ligands began with the preparation of palladium complexes using $PdCl_2(MeCN)_2$. This allows for direct comparison of the reactivity of these

complexes with the previously discussed PyTriPdCl₂ complexes in Suzuki-Miyaura cross coupling reactions.

Formation of these complexes beings by dissolving the palladium precursor PdCl₂(MeCN)₂, in dry DCM at ambient temperature. The PyPyr ligands are measured out and placed in DCM, and typically required modest heating at 40-60 °C for 10 min to fully dissolve. Once dissolved, the ligand solution is added to the solution of metal and the complexation is stirred at ambient temperature for 18 h. When the complex is formed, precipitation of the complex occurs from the solution and the solid is isolated using a centrifuge. Satisfyingly, this method allows for the formation of PyPyrPdCl₂ complexes (**7f-fj**) with the entire series of electronically diverse PyPyr ligands (Table 7.3). Analysis of the series of substituted PyPyrPdCl₂ complexes by ¹H NMR showed a similar trend to previous complexes where the diagnostic pyrazole singlet could be tracked as it moved downfield in a stepwise fashion (Figure 7.1). In order to confirm the absolute orientation of the complexes, X-ray quality crystals were grown of the PyPyrPdCl₂ complex (**7h**). These crystals were obtained from slow evaporation of a dilute MeNO₂ solution of the complex and appeared orange in color. X-ray crystallography confirmed the predicted structure of the complex (Table 7.4).

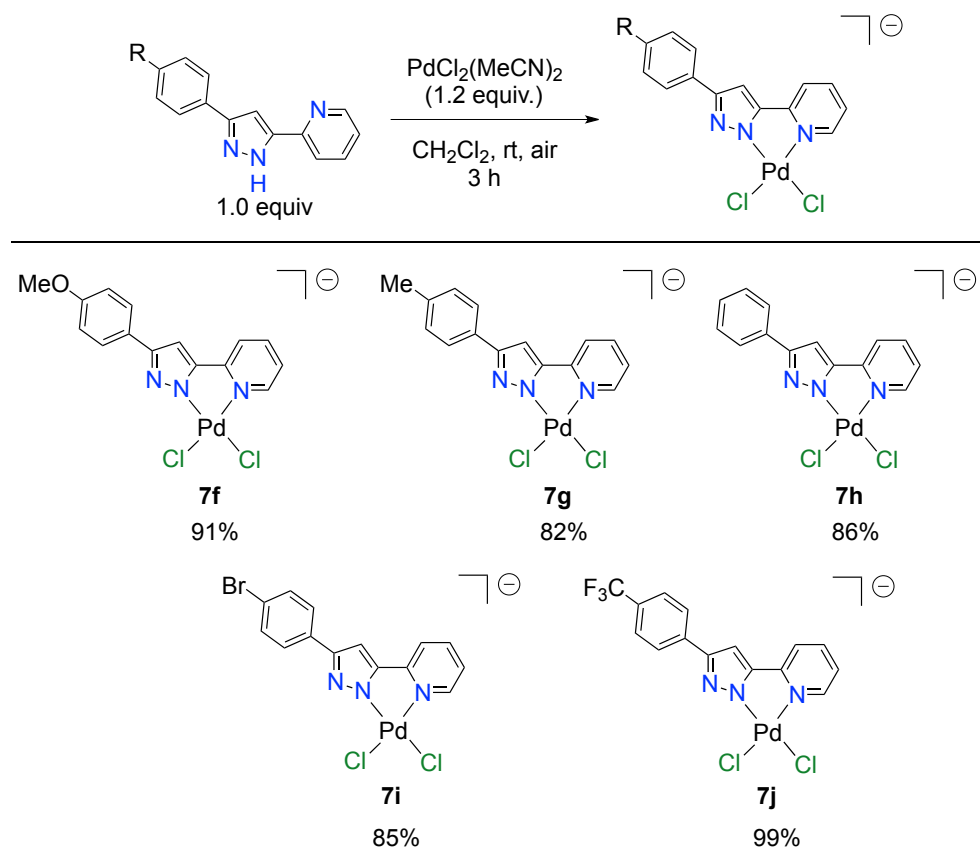


Table 7.3: Unique anionic PyPyrPdCl₂ complexes as potential catalysts for palladium catalyzed reactions.

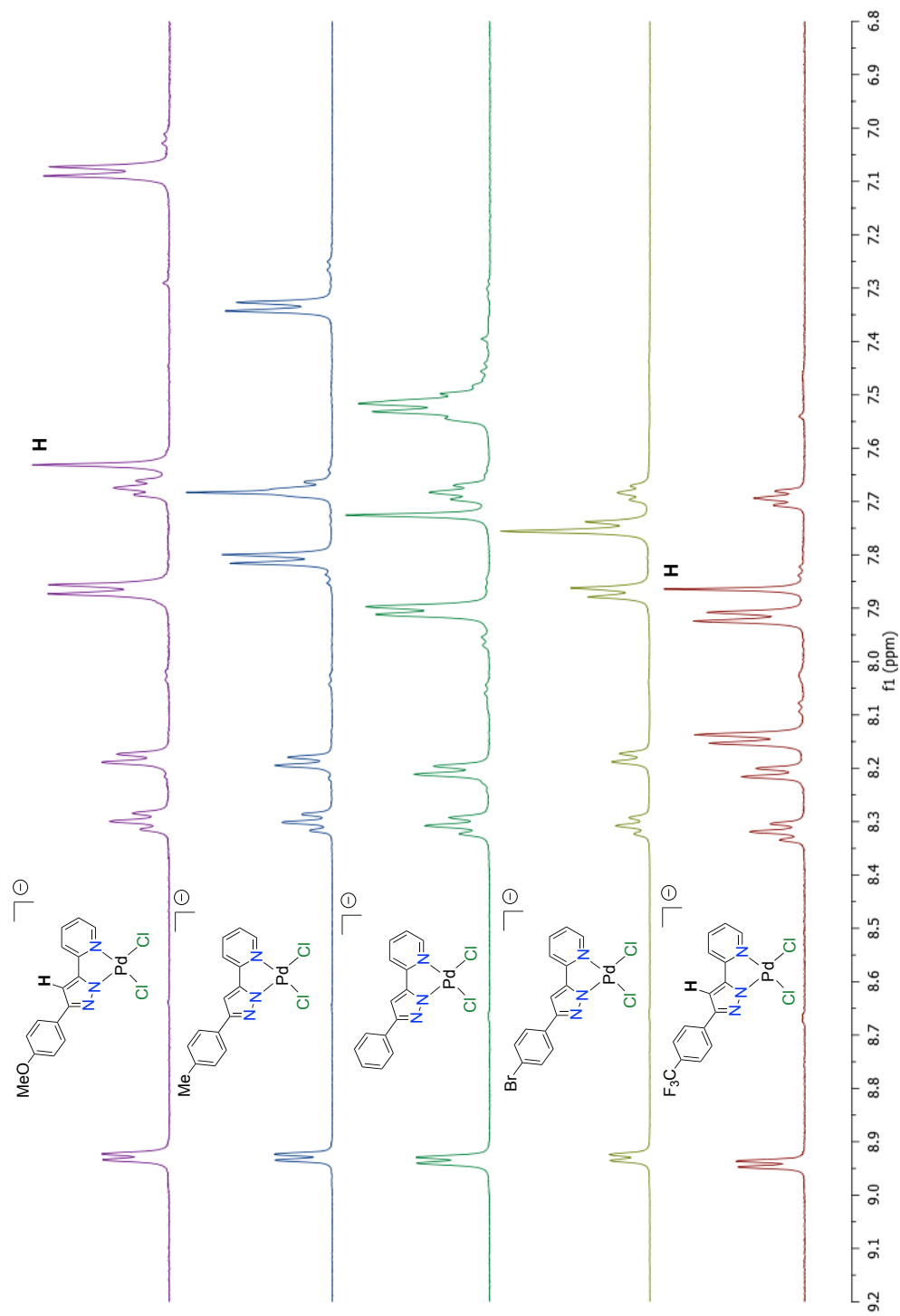
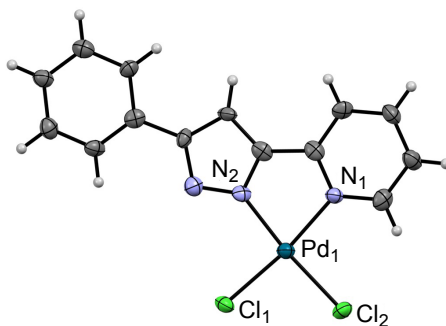
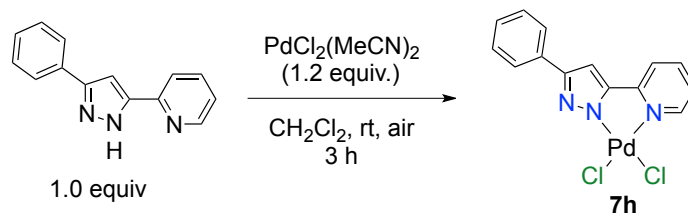


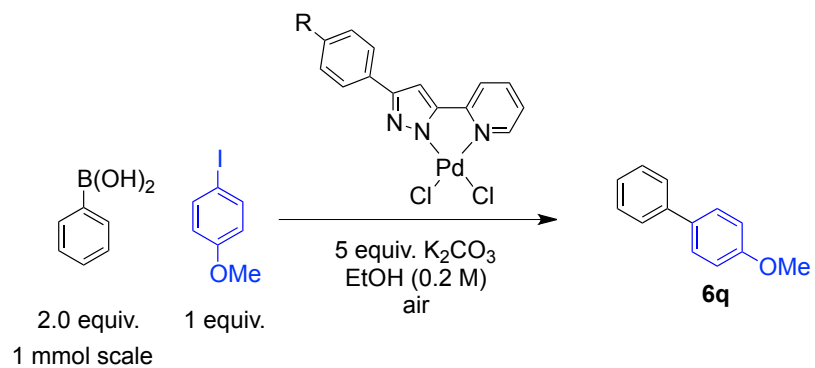
Figure 7.1: ¹H NMR analysis of the electronic diversity of PyPyrPdCl₂ complexes.



$\text{Pd}_1\text{-Cl}_1$: 2.288 Å
 $\text{Pd}_1\text{-N}_1$: 2.053 Å
 $\text{Pd}_1\text{-N}_2$: 2.014 Å
 $\text{N}_1\text{-Pd}_1\text{-N}_2$: 79.1°

Table 7.4: X-ray crystal structure of the PyPyrPdCl₂ complex.

Analysis of the reactivity of these PyPyrPdCl₂ complexes in Suzuki cross-coupling reactions was performed using the conditions that were previously optimized for the PyTriPdCl₂ complexes. When the electron-rich (**7f**), neutral (**7h**), and electron-poor (**7j**) complexes were tested under these conditions they all demonstrated significantly decreased reactivity compared to the PyTri complexes (Table 7.5). Future work on this project will determine whether a re-optimization of reaction conditions will allow for increased reactivity of these complexes. Additionally, it may be that while these complexes are not highly activity towards Suzuki cross-coupling, it should be explored whether they may be active in other types of palladium-catalyzed reactions.



R	Catalyst Loading	temp (°C)	time (h)	GC Yield (%)
OMe	0.01 mol%	40	18	5
H	0.01 mol%	40	18	8
CF ₃	0.01 mol%	40	18	10

^a All uncorrected GC yields.

Table 7.5: Screen of diverse PyPyrPdCl₂ catalysts shows decreased activity compared to PyTriPdCl₂.

7.5 References:

- 1) Qiao, J. X.; Cheng, X. H.; Smallheer, J. M.; Galemmo, R. A.; Drummond, S.; Pinto, D.; Cheney, D. L.; He, K.; Wong, P. C.; Luetzgen, J. M.; Knabb, R. M.; Wexler, R. R.; Lam, P. *Bioorg. Med. Chem. Lett.* **2007**, *17*, 1432.
- 2) Singh, P.; Paul, K.; Holzer, W. *Bioorg. Med. Chem.* **2006**, *14*, 5061.
- 3) Ache, H. J. *Angew. Chem. Int. Ed.* **1989**, *28*, 1.
- 4) Zhu, L. B.; Cheng, L.; Zhang, Y. X.; Xie, R. G.; You, J. S. *J. Org. Chem.* **2007**, *72*, 2737.
- 5) Kufelnicki, A.; Wozniczka, M.; Checinska, L.; Miernicka, M.; Budzisz, E. *Polyhedron* **2007**, *26*, 2589.
- 6) Ovejero, P.; Mayoral, M. J.; Cano, M.; Lagunas, M. C. *J. Organomet. Chem.* **2007**, *692*, 1690.
- 7) Burling, S.; Field, L. D.; Messerle, B. A.; Rumble, S. L. *Organometallics* **2007**, *26*, 4335.
- 8) Kealey, S.; Long, N. J.; Miller, P. W.; White, A.; Hitchcock, P. B.; Gee, A. *Dalton Trans.* **2007**, 2823.
- 9) Kawatsura, M.; Aburatani, S.; Uenishi, J. *Tetrahedron* **2007**, *63*, 4172.
- 10) Attanasi, O. A.; Berretta, S.; Crescentini, L. D.; Favi, G.; Filippone, P.; Giorgi, G.; Lillini, S.; Mantellini, F. *Tetrahedron Lett.* **2007**, *48*, 2449.
- 11) Cottineau, B.; Chenault, J. *Synlett* **2002**, 769.
- 12) Heller, S. T.; Natarajan, S. R. *Org. Lett.* **2006**, *8*, 2675.
- 13) Xie, F. C.; Cheng, G.; Hu, Y. H. *J. Comb. Chem.* **2006**, *8*, 286.
- 14) Armstrong, A.; Jones, L. H.; Knight, J. D.; Kelsey, R. D. *Org. Lett.* **2005**, *7*, 713.
- 15) Wang, Z. X.; Qin, H. L. *Green Chem.* **2004**, *6*, 90.
- 16) Outirite, M.; Lebrini, M.; Lagrenee, M.; Bentiss, F. *J. Heterocycl. Chem.* **2008**, *45*, 503.

- 17) Tufariello, J. J. In *1,3-Dipolar Cycloaddition Chemistry*, Vol. 2; Padwa, A., Ed.; John Wiley & Sons: New York, **1984**, 83.
- 18) Jiang, N.; Li, C. *Chem. Commun.* **2004**, 394.
- 19) Qi, X.; Ready, J. M. *Angew. Chem. Int. Ed.* **2007**, *46*, 3242.
- 20) Vuluga, D.; Legros, J.; Crousse, B.; Bonnet-Delpon, D. *Green Chem.* **2009**, *11*, 156.
- 21) Chandanshive, J. Z.; Bonini, F.; Gentili, D.; Fochi, M.; Bernardi, L.; Franchini, M. C. *Eur. J. Org. Chem.* **2010**, 6440.
- 22) Fuchi, N.; Doi, T.; Takahasi, T. *Chem. Lett.* **2005**, *34*, 438.
- 23) Bonini, B. F.; Franchini, M. C.; Gentili, D.; Locatelli, E.; Ricci, A. *Synlett* **2009**, *14*, 2328.
- 24) Aggarwal, V. K.; de Vicente, J.; Bonnert, R. V. *J. Org. Chem.* **2003**, *68*, 5381.
- 25) Creary, X. *Org. Synth.* **1986**, *64*, 207.
- 26) Wu, L.; Ge, Y.; He, T.; Zhang, L.; Fu, X.; Fu, H.; Chen, H.; Li, R. *Synthesis* **2012**, *44*, 1577.
- 27) Montoya, V.; Pons, J.; Branchadell, V.; Ros, J. *Tetrahedron* **2005**, *61*, 12377.
- 28) Ferles, M.; Liboska, R.; Trska, P. *Coll. Czech. Chem. Commun.* **1990**, *55*, 1228.
- 29) Nuriev, V.; Zyk, N.; Vatsadze, S. *Arkivoc* **2005**, *4*, 208.
- 30) Lin, T.; Tang, K.; Yang, S.; Shen, J.; Cheng, Y.; Pan, H.; Chi, Y.; Chou, P. *J. Phys. Chem. A* **2012**, *116*, 4438.
- 31) Kovacs, S.; Novak, Z. *Tetrahedron* **2013**, *69*, 8987.
- 32) Trofimenko, S. *Chem. Rev.* **1972**, *72*, 497.
- 33) Trofimenko, S. *Prog. Inorg. Chem.* **1986**, *34*, 115.
- 34) Trofimenko, S. *Chem. Rev.* **1993**, *93*, 943.
- 35) La Monica, G.; Ardizzoia, G.A. *Prog. Inorg. Chem.* **1997**, *46*, 151.

- 36) Mukherjee, R. *Coord. Chem. Rev.* **2000**, 203, 151.
- 37) Vos, J. G.; Groeneveld, W. C. *Inorg. Chim. Acta* **1978**, 26, 71.
- 38) Catalan, J.; Abboud, J. L. M.; Elguero, J. *Adv. Heterocycl. Chem.* **1987**, 41, 187.
- 39) Pons, J.; Chadghan, A.; Alvarex-Larena, A.; Piniella, J. F.; Ros, J. *Inorg. Chim. Acta* **2001**, 324, 342.
- 40) Pons, J.; Chadghan, A.; Casabo, J.; Alvarex-Larena, A.; Piniella, J. F.; Solans, X.; Font-Bardia, M.; Ros, J. *Polyhedron* **2001**, 20, 1029.
- 41) Nfor, E. N.; Asobo, P. F.; Nenwa, J.; Nfor, O. N.; Njapba, J. N.; Njong, R. N.; Offiong, O. E. *Int. J. Inorg. Chem.* **2013**, 987574.
- 42) Chadghan, A.; Pons, J.; Caubet, A.; Casabo, J.; Ros, J.; Alvarex-Larena, A.; Piniella, J. F. *Polyhedron* **2000**, 19, 855.
- 43) Pons, J.; Chadghan, A.; Casabo, J.; Alvarex-Larena, A.; Piniella, J. F. Ros, J. *Polyhedron* **2001**, 20, 2531.
- 44) Pons, J.; Lopez, X.; Casabo, J.; Teixidor, F.; Caubet, A.; Ruis, J.; Miravittles, C. *Inorg. Chim. Acta* **1992**, 195, 61.
- 45) Munakata, M.; Wu, L. P.; Yamamoto, M.; Kuroda-Sowa, T.; Maekawa, M.; Kawata, S.; Kitagawa, S. *J. Chem. Soc. Dalton. Trans.* **1995**, 1, 4099.
- 46) Ho, M.; Cheng, Y.; Wu, L.; Chou, P.; Lee, G.; Hsu, F.; Chi, Y. *Polyhedron* **2007**, 26, 4886.
- 47) Gupta, G.; Zheng, C.; Wang, P.; Rao, K. M. Z. *Anorg. Allg. Chem.* **2010**, 636, 758.
- 48) Thiel, W. R.; Eppinger, J. *Chem. Eur. J.* **1997**, 3, 696.
- 49) Pons, J.; Chadghan, A.; Casabo, J.; Alvarex-Larena, A.; Piniella, J. F.; Ros, J. *Inorg. Chem. Commun.* **2000**, 3, 296.
- 50) Perez, J. A.; Pons, J.; Solans, X.; Font-Bardia, M.; Ros, J. *Inorg. Chim. Acta* **2005**, 358, 617.
- 51) Montoya, V.; Pons, J.; Garcia-Anton, J.; Solans, X.; Font-Bardia, M.; Ros, J. *Organometallics* **2007**, 26, 3183.

- 52) Montoya, V.; Pons, J.; Branchadell, V.; Garcia-Anton, J.; Solans, X.; Font-Bardia, M.; Ros, J. *Organometallics* **2008**, *27*, 1084.
- 53) Benet-Buchholz, J.; Comba, P.; Llobet, A.; Roeser, S.; Vadivelu, P.; Wiesner, S. *Dalton Trans.* **2010**, *39*, 3315.
- 54) Roeser, S.; Maji, S.; Benet-Buchholz, J.; Pons, J.; Llobet, A. *Eur. J. Inorg. Chem.* **2013**, *2*, 232.
- 55) Kashiwame, Y.; Watanabe, M.; Araki, K.; Kuwata, S.; Ikariya, T. *Bull. Chem. Soc. Jpn.* **2011**, *84*, 251.
- 56) Muller, K.; Sun, Y.; Heimermann, A.; Menges, F.; Niedner-Schatteburg, G.; van Wullen, C.; Thiel, W. R. *Chem. Eur. J.* **2013**, *19*, 7825.
- 57) Cheng, C.; Yu, W.; Chou, P.; Peng, S.; Lee, G.; Wu, P.; Song, Y.; Chi, Y. *Chem. Commun.* **2003**, 2628.
- 58) Pons, J.; Lopez, X.; Benet, E.; Casabo, J.; Teixidor, F.; Sanchez, F. J. *Polyhedron* **1990**, *9*, 2839.
- 59) Kloubert, T.; Gorls, H.; Westerhausen, M. *Z. Naturforsch.* **2012**, *67b*, 519

7.6 Supporting Information:

General Reagent Information

All reactions were set up on the benchtop in oven-dried glassware or dried scintillation vials. HPLC grade Acetonitrile (MeCN), Dichloromethane (DCM), and Tetrahydrofuran (THF) was purchased from Fisher Chemicals and dried via passage through activated alumina in a commercial solvent purification system (Pure Process Technologies, Inc.). All other organic solvents were obtained from Fisher Chemicals or Acros Organics and dried over either sodium sulfate or molecular sieves (4Å). NMR solvents were purchased from Acros Organics or Cambridge Isotope Laboratories and used as obtained. The palladium precursors were stored in a glove box under nitrogen. Bis(acetonitrile)dichloropalladium(II) ($\text{PdCl}_2(\text{MeCN})_2$) was purchased from Chem Impex Int'l Inc and was used as obtained.

General analytical information

^1H and ^{13}C NMR spectra were measured on a Varian Inova 500 (500 MHz) or a Bruker Avance NEO 400 (400 MHz) spectrometer using CF_3COOD or $\text{DMSO}-d_6$ as solvents and tetramethylsilane as an internal standard. The following abbreviations are used singularly or in combination to indicate the multiplicity of signals: s - singlet, d - doublet, t - triplet, q - quartet, qn - quintet, sx - sextet, sp - septet, m - multiplet and br - broad. NMR spectra were acquired at 300 K. Gas chromatography (GC) was carried out on an Agilent Technologies 6850 Network GC System, and dodecane was used as the internal standard. ATR-IR spectra

were taken on a Bruker:ALPHA FTIR Spectrometer. Attenuated total reflection infrared (ATR-IR) was used and the spectra was analyzed using the OPUS software with selected absorption maxima reported in wavenumbers (cm^{-1}). X-ray diffraction data was obtained using a suitable crystal on a 'Bruker APEX-II CCD' diffractometer. The crystal was kept at 100.0 K during data collection. Using Olex2, the structure was solved with the ShelXT structure solution program using Intrinsic Phasing and refined with the XL refinement package using Least Squares minimization.

General procedure for the production of pyridine pyrazole (PyPyr) ligands.

To an oven dried 250 mL round bottom flask equipped with a magnetic stir bar and reflux condenser was added tosyl hydrazine followed by THF. The solution was stirred at ambient temperature until the hydrazine dissolves. Benzaldehyde bearing the desired substitution was added drop wise and the reaction was heated to 70 °C and stirred for 2 h. The reaction was then cooled to ambient temperature and 2.5 equivalents of sodium ethoxide (NaOEt) were added. The solution was stirred for 30 min during which the generation of the diazo intermediate occurred. The solution was then diluted with additional THF and 2-ethynylpyridine was added dropwise. The reaction was heated to reflux for 18 h. Upon completion, the reaction was quenched with DI- H_2O and the product was extracted with diethyl ether. After the organic extracts are combined and dried over sodium sulfate the solvent was removed to yield a crude oil. This oil was taken up in MeCN and the solution was placed in a beaker located in the freezer.

The desired substituted PyPyr ligand crystallized out of solution over the course of 48 h. Subsequent recrystallizations in MeCN yield pure PyPyr ligand as white / off-white crystalline solids.

2-(3-(4-methoxyphenyl)-1H-pyrazol-5-yl)pyridine (7a):

To an oven dried 250 mL round bottom flask equipped with a magnetic stir bar and reflux condenser was added tosyl hydrazine (930 mg, 5 mmol) followed by THF (60 mL). After all solids are dissolved, *p*-anisaldehyde (607 μ L, 5 mmol) was added dropwise. The solution was heated to 70 °C and stirred for 2 h. The reaction was then cooled to ambient temperature and NaOEt (850 mg, 12.5 mmol) was added. After 30 min of stirring the solution was diluted with additional THF (40 mL), and 2-ethynylpyridine (507 μ L, 5 mmol) was added dropwise. The reaction was then heated to reflux and stirred for 18 h. Upon completion the reaction was quenched with DI-H₂O (100 mL) and extracted with diethyl ether. After drying the organic extract was concentrated to yield an orange oil that was taken up in MeCN and the solution was left standing in the freezer for 48 h. After additional recrystallizations in MeCN the title compound was obtained as a white solid in 35% yield (443 mg, 1.75 mmol). ATR-IR: 3257, 2959, 2837, 1313, 1247, 1153, 1031, 776, 526, 479 cm⁻¹. ¹H NMR (400 MHz, CF₃COOD) δ 8.71 (d, J = 5.5 Hz, 1H), 8.59 (t, J = 8.5 Hz, 1H), 8.37 (d, J = 8 Hz, 1H), 7.96 (t, J = 7 Hz, 1H), 7.59 (d, J = 8.5 Hz, 2H), 7.32 (s, 1H), 7.00 (d, J = 8.5 Hz, 2H), 3.83 (s, 3H). ¹³C NMR (100 MHz, CF₃COOD) δ 144.44, 143.94, 137.62, 137.30, 136.44, 123.48,

122.84, 121.51, 114.27, 110.82, 107.96, 99.60, 50.66. HRMS calculated requires $[M+H]^+$: 252.1131. Found m/z : 252.1236.

2-(3-(4-methylphenyl)-1H-pyrazol-5-yl)pyridine (7b):

To an oven dried 250 mL round bottom flask equipped with a magnetic stir bar and reflux condenser was added tosyl hydrazine (930 mg, 5 mmol) followed by THF (60 mL). After all solids are dissolved, *p*-tolualdehyde (589 μ L, 5 mmol) was added dropwise. The solution was heated to 70 °C and stirred for 2 h. The reaction was then cooled to ambient temperature and NaOEt (850 mg, 12.5 mmol) was added). After 30 min of stirring the solution was diluted with additional THF (40 mL), and 2-ethynylpyridine (507 μ L, 5 mmol) was added dropwise. The reaction was then heated to reflux and stirred for 18 h. Upon completion the reaction was quenched with DI-H₂O (100 mL) and extracted with diethyl ether. After drying the organic extract was concentrated to yield an orange oil that was taken up in MeCN and the solution was left standing in the freezer for 48 h. After additional recrystallizations in MeCN the title compound was obtained as a white solid in 34% yield (405 mg, 1.7 mmol). ATR-IR: 3029, 2916, 1596, 1563, 1452, 1152, 771, 493 cm^{-1} . ¹H NMR (400 MHz, CF₃COOD) δ 8.70 (d, *J* = 5.5 Hz, 1H), 8.58 (t, *J* = 7.5 Hz, 1H), 8.36 (d, *J* = 8 Hz, 1H), 7.95 (t, *J* = 7 Hz, 1H), 7.45 (d, *J* = 8.5 Hz, 2H), 7.33 (s, 1H), 7.17 (d, *J* = 8 Hz, 2H), 2.22 (s, 3H). ¹³C NMR (100 MHz, CF₃COOD) δ 145.24, 143.94, 138.86, 137.35, 136.18, 125.66, 122.91, 121.59, 121.40, 117.19, 108.68, 99.81, 15.09. HRMS calculated requires $[M+H]^+$: 236.1182. Found m/z : 236.1467.

2-(3-phenyl-1H-pyrazol-5-yl)pyridine (7c):

To an oven dried 250 mL round bottom flask equipped with a magnetic stir bar and reflux condenser was added tosyl hydrazine (930 mg, 5 mmol) followed by THF (60 mL). After all solids are dissolved, benzaldehyde (508 μ L, 5 mmol) was added dropwise. The solution was heated to 70 °C and stirred for 2 h. The reaction was then cooled to ambient temperature and NaOEt (850 mg, 12.5 mmol) was added). After 30 min of stirring the solution was diluted with additional THF (40 mL), and 2-ethynylpyridine (507 μ L, 5 mmol) was added dropwise. The reaction was then heated to reflux and stirred for 18 h. Upon completion the reaction was quenched with DI-H₂O (100 mL) and extracted with diethyl ether. After drying the organic extract was concentrated to yield an orange oil that was taken up in MeCN and the solution was left standing in the freezer for 48 h. After additional recrystallizations in MeCN the title compound was obtained as a white solid in 54% yield (598 mg, 2.7 mmol). ATR-IR: 3235, 3059, 1596, 1468, 756, 657, 484, 419 cm^{-1} . ¹H NMR (400 MHz, CF₃COOD) δ 8.65 (d, J = 5.5 Hz, 1H), 8.55 (t, J = 6.8 Hz, 1H), 8.33 (d, J = 8 Hz, 1H), 7.91 (t, J = 6.8 Hz, 1H), 7.53 (m, 2H), 7.33 (m, 4H). ¹³C NMR (100 MHz, CF₃COOD) δ 144.81, 143.87, 138.08, 137.10, 136.77, 126.90, 124.91, 122.59, 121.37, 121.29, 120.49, 99.80. HRMS calculated requires [M+H]⁺: 222.1026. Found *m/z*: 222.1548.

2-(3-(4-bromophenyl)-1H-pyrazol-5-yl)pyridine (7d):

To an oven dried 250 mL round bottom flask equipped with a magnetic stir bar and reflux condenser was added tosyl hydrazine (930 mg, 5 mmol) followed by

THF (60 mL). After all solids are dissolved, 4-bromobenzaldehyde (925 mg, 5 mmol) was added dropwise. The solution was heated to 70 °C and stirred for 2 h. The reaction was then cooled to ambient temperature and NaOEt (850 mg, 12.5 mmol) was added). After 30 min of stirring the solution was diluted with additional THF (40 mL), and 2-ethynylpyridine (507 μ L, 5 mmol) was added dropwise. The reaction was then heated to reflux and stirred for 18 h. Upon completion the reaction was quenched with DI-H₂O (100 mL) and extracted with diethyl ether. After drying the organic extract was concentrated to yield an orange oil that was taken up in MeCN and the solution was left standing in the freezer for 48 h. After additional recrystallizations in MeCN the title compound was obtained as a white solid in 28% yield (415 mg, 1.4 mmol). ATR-IR: 3206, 1593, 1560, 1372, 1006, 954, 774, 511, 490, 468 cm⁻¹. ¹H NMR (400 MHz, CF₃COOD) δ 8.70 (d, J = 6 Hz, 1H), 8.60 (t, J = 8 Hz, 1H), 8.36 (d, J = 8 Hz, 1H), 7.95 (t, J = 7.2 Hz, 1H), 7.53 (d, J = 8.5 Hz, 2H), 7.46 (d, J = 8.5 Hz, 2H), 7.32 (s, 1H). ¹³C NMR (100 MHz, CF₃COOD) δ 143.86, 143.47, 138.85, 137.53, 136.93, 128.30, 122.71, 122.33, 121.22, 120.99, 119.95, 99.59. HRMS calculated requires [M+H]⁺: 300.0131. Found *m/z*: 300.0230.

2-(3-(4-(trifluoromethyl)phenyl)-1H-pyrazol-5-yl)pyridine (7e):

To an oven dried 250 mL round bottom flask equipped with a magnetic stir bar and reflux condenser was added tosyl hydrazine (930 mg, 5 mmol) followed by THF (60 mL). After all solids are dissolved, 4-trifluoromethylbenzaldehyde (670 μ L, 5 mmol) was added dropwise. The solution was heated to 70 °C and stirred

for 2 h. The reaction was then cooled to ambient temperature and NaOEt (850 mg, 12.5 mmol) was added). After 30 min of stirring the solution was diluted with additional THF (40 mL), and 2-ethynylpyridine (507 μ L, 5 mmol) was added dropwise. The reaction was then heated to reflux and stirred for 18 h. Upon completion the reaction was quenched with DI-H₂O (100 mL) and extracted with diethyl ether. After drying the organic extract was concentrated to yield an orange oil that was taken up in MeCN and the solution was left standing in the freezer for 48 h. After additional recrystallizations in MeCN the title compound was obtained as a white solid in 21% yield (297 mg, 1.05 mmol). ATR-IR: 3232, 1616, 1566, 1454, 1301, 1104, 776, 595, 474, 408 cm^{-1} . ¹H NMR (400 MHz, CF₃COOD) δ 8.62 (d, J = 6 Hz, 1H), 8.53 (t, J = 8 Hz, 1H), 8.29 (d, J = 8 Hz, 1H), 7.88 (t, J = 6.8 Hz, 1H), 7.67 (d, J = 8.5 Hz, 2H), 7.59 (d, J = 8.5 Hz, 2H), 7.31 (s, 1H). ¹³C NMR (100 MHz, CF₃COOD) δ 143.80, 142.64, 139.27, 137.95, 136.70, 128.50, 124.75, 122.06, 121.70, 120.70, 120.37, 117.67, 99.89. HRMS calculated requires [M+H]⁺: 290.0900. Found *m/z*: 290.1012.

General procedure for the production of pyridine pyrazole palladium

dichloride complexes:

In an oven dried 8 mL scintillation vial equipped with a magnetic stir bar was added palladium dichloride bisacetonitrile. The vial was purged with argon for 5 min. Dry dichloromethane (DCM) was added and the solution was stirred for 5 min to allow the initial palladium complex to dissolve. The pyridine pyrazole (PyPyr) ligand bearing the desired substitution was dissolved in minimal DCM

and added to the reaction dropwise. The complexation was allowed to proceed at ambient temperature for 18 h. During this time precipitation of the PyPyr palladium dichloride complex occurred. This solid was isolated via centrifuge and washed 5 times with additional DCM. The complex was isolated as a solid and was recrystallized via slow evaporation in MeNO₂.

2-(3-(4-methoxyphenyl)-pyrazol-5-yl)pyridine palladium dichloride (7f):

PdCl₂(MeCN)₂ (26 mg, 0.1 mmol) was added to an 8 mL scintillation vial and flushed with argon for 5 min. Dry DCM (5 mL) was added and the solution was stirred until all solids are dissolved. The solution takes on a dark orange color. MeOPyPyr ligand (25 mg, 0.1 mmol) dissolved in DCM (~1 mL) was added dropwise. Complexation occurred at ambient temperature over 18 h. The title compound was isolated as a yellow solid in 91% yield (39 mg, 0.091 mmol). ATR-IR: 3283, 3136, 3118, 3091, 2842, 1610, 1582, 1501, 1466, 606, 427 cm⁻¹. ¹H NMR (500 MHz, DMSO-*d*₆) δ 8.93 (d, J = 5.5 Hz, 1H), 8.30 (t, J = 7.5 Hz, 1H), 8.18 (d, J = 8 Hz, 1H), 7.86 (d, J = 8.5 Hz, 2H), 7.68 (t, J = 6 Hz, 1H), 7.63 (s, 1H), 7.08 (d, J = 8.5 Hz, 2H), 3.83 (s, 3H). ¹³C NMR (100 MHz, DMSO-*d*₆) δ 160.5, 152.3, 150.8, 149.4, 147.0, 141.3, 128.8, 125.3, 122.4, 119.5, 114.3, 102.2, 55.4.

2-(3-(4-methylphenyl)-pyrazol-5-yl)pyridine palladium dichloride (7g):

PdCl₂(MeCN)₂ (26 mg, 0.1 mmol) was added to an 8 mL scintillation vial and flushed with argon for 5 min. Dry DCM (5 mL) was added and the solution was stirred until all solids are dissolved. The solution takes on a dark orange color.

MePyPyr ligand (24 mg, 0.1 mmol) dissolved in DCM (~1 mL) was added dropwise. Complexation occurred at ambient temperature over 18 h. The title compound was isolated as a yellow solid in 82% yield (34 mg, 0.082 mmol). ATR-IR: 3247, 3141, 1617, 1565, 1501, 1466, 1370, 742, 496, 428 cm^{-1} . ^1H NMR (500 MHz, $\text{DMSO-}d_6$) δ 8.93 (d, $J = 6$ Hz, 1H), 8.30 (t, $J = 7$ Hz, 1H), 8.19 (d, $J = 8$ Hz, 1H), 7.81 (d, $J = 8$ Hz, 2H), 7.68 (m, 2H), 7.34 (d, $J = 8$ Hz, 2H), 2.37 (s, 3H). ^{13}C NMR (125 MHz, $\text{DMSO-}d_6$) δ 152.7, 151.1, 149.8, 147.5, 141.7, 140.2, 129.8, 127.6, 125.7, 124.7, 122.8, 103.1, 21.4.

2-(3-phenyl-pyrazol-5-yl)pyridine palladium dichloride (7h):

$\text{PdCl}_2(\text{MeCN})_2$ (26 mg, 0.1 mmol) was added to an 8 mL scintillation vial and flushed with argon for 5 min. Dry DCM (5 mL) was added and the solution was stirred until all solids are dissolved. The solution takes on a dark orange color. PyPyr ligand (22 mg, 0.1 mmol) dissolved in DCM (~1 mL) was added dropwise. Complexation occurred at ambient temperature over 18 h. The title compound was isolated as a yellow solid in 86% yield (34 mg, 0.086 mmol). ATR-IR: 3236, 3136, 1617, 1561, 1492, 1466, 1444, 812, 764, 487, 424 cm^{-1} . ^1H NMR (500 MHz, $\text{DMSO-}d_6$) δ 8.93 (d, $J = 5.5$ Hz, 1H), 8.31 (t, $J = 8$ Hz, 1H), 8.20 (d, $J = 7.5$ Hz, 1H), 7.90 (d, $J = 7$ Hz, 2H), 7.72 (s, 1H), 7.68 (t, $J = 6.5$ Hz, 1H), 7.52 (m, 3H). ^{13}C NMR (100 MHz, $\text{DMSO-}d_6$) δ 152.9, 151.2, 149.9, 147.5, 141.8, 130.5, 129.3, 127.8, 127.6, 125.9, 122.9, 103.6.

2-(3-(4-bromophenyl)-pyrazol-5-yl)pyridine palladium dichloride (7i):

$\text{PdCl}_2(\text{MeCN})_2$ (26 mg, 0.1 mmol) was added to an 8 mL scintillation vial and flushed with argon for 5 min. Dry DCM (5 mL) was added and the solution was stirred until all solids are dissolved. The solution takes on a dark orange color. BrPyPyr ligand (30 mg, 0.1 mmol) dissolved in DCM (~1 mL) was added dropwise. Complexation occurred at ambient temperature over 18 h. The title compound was isolated as a yellow solid in 85% yield (40 mg, 0.085 mmol). ATR-IR: 3311, 3119, 3080, 3024, 1600, 1458, 813, 778, 582, 424 cm^{-1} . ^1H NMR (500 MHz, $\text{DMSO-}d_6$) δ 8.93 (d, $J = 5.5$ Hz, 1H), 8.31 (t, $J = 7.5$ Hz, 1H), 8.18 (d, $J = 8$ Hz, 1H), 7.87 (d, $J = 8.5$ Hz, 2H), 7.75 (m, 3H), 7.68 (t, $J = 6.5$ Hz, 1H), ^{13}C NMR (100 MHz, $\text{DMSO-}d_6$) δ 152.4, 150.6, 149.5, 145.9, 141.4, 131.9, 129.3, 126.3, 125.5, 123.5, 122.5, 103.4.

2-(3-(4-(trifluoromethyl)phenyl)-pyrazol-5-yl)pyridine palladium dichloride

(7j):

$\text{PdCl}_2(\text{MeCN})_2$ (26 mg, 0.1 mmol) was added to an 8 mL scintillation vial and flushed with argon for 5 min. Dry DCM (5 mL) was added and the solution was stirred until all solids are dissolved. The solution takes on a dark orange color. CF_3PyPyr ligand (29 mg, 0.1 mmol) dissolved in DCM (~1 mL) was added dropwise. Complexation occurred at ambient temperature over 18 h. The title compound was isolated as a yellow solid in 99% yield (46 mg, 0.099 mmol). ATR-IR: 3209, 3090, 1617, 1464, 1444, 1325, 1122, 775, 623, 439 cm^{-1} . ^1H NMR (500 MHz, $\text{DMSO-}d_6$) δ 8.94 (d, $J = 5$ Hz, 1H), 8.32 (t, $J = 7.5$ Hz, 1H), 8.21 (d, J

= 7.5 Hz, 1H), 8.14 (d, $J = 8$ Hz, 2H), 7.91 (d, $J = 8$ Hz, 1H), 7.86 (s, 1H), 7.69 (t, $J = 6.5$ Hz, 1H), ^{13}C NMR (100 MHz, $\text{DMSO-}d_6$) δ 152.9, 150.9, 149.9, 145.8, 141.8, 131.4, 130.2, 128.5, 126.2, 126.0, 124.5, 123.0, 104.6.

X-ray crystallography for PyPyr ligands:

To obtain a suitable crystal of PyPyr ligand, a dilute solution of the ligand was prepared in MeCN. This solution was left to stand in a vial equipped with a screw cap at decreased temperature (~ 4 °C) for 48 h. Clear colorless crystals formed and were of high enough quality for analysis.

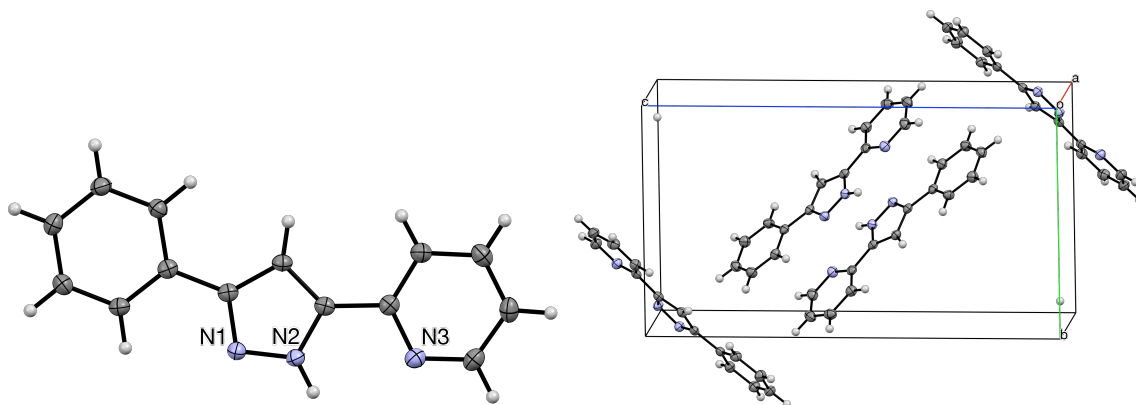


Table 1. Crystal data and structure refinement for **PyPyr** ligand.

Empirical formula	C ₁₄ H ₁₁ N ₃
Formula weight	221.26
Temperature	100.0 K
Wavelength, Å	1.54178
Crystal system	Monoclinic
Space group	<i>P</i> 2 ₁ / <i>n</i>
<i>a</i> , Å	5.6346(5)
<i>b</i> , Å	10.3767(13)
<i>c</i> , Å	18.5130(15)
α , °	90
β , °	90.897(4)
γ , °	90
Volume	1082.30(19) Å ³
<i>Z</i>	4
Calculated density, mg/m ³	1.358
Absorption coefficient, mm ⁻¹	0.660
<i>F</i> (000)	464
Crystal size, mm	0.29 x 0.27 x 0.22
Theta range for data collection, °	4.778 to 68.366
Index ranges	-6 ≤ <i>h</i> ≤ 6, -10 ≤ <i>k</i> ≤ 12, -19 ≤ <i>l</i> ≤ 22
Reflections collected / unique	6666 / 1967 [<i>R</i> _{int} = 0.0299]
Completeness to $\theta = 67.679^\circ$	99.1 %
Absorption correction	Semi-empirical from equivalents
Max. and min. transmission	0.7531 and 0.6645
Refinement method	Full-matrix least-squares on <i>F</i> ²
Data / restraints / parameters	1967 / 0 / 154
Goodness-of-fit on <i>F</i> ²	1.074
Final <i>R</i> indices [<i>I</i> > 2 σ (<i>I</i>)]	<i>R</i> 1 = 0.0361, <i>wR</i> 2 = 0.0928
<i>R</i> indices (all data)	<i>R</i> 1 = 0.0384, <i>wR</i> 2 = 0.0953
Extinction coefficient	n/a
Largest diff. peak and hole, eÅ ⁻³	0.260 and -0.144

Table 2. Atomic coordinates ($\times 10^4$) and equivalent isotropic displacement parameters ($\text{\AA}^2 \times 10^3$) for **PyPyr** ligand. $U(\text{eq})$ is defined as one third of the trace of the orthogonalized U^{ij} tensor.

	x	y	z	U(eq)
N(1)	1723(2)	4940(1)	5698(1)	19(1)
N(2)	2042(2)	3999(1)	5205(1)	19(1)
N(3)	3183(2)	2064(1)	4275(1)	23(1)
C(8)	5220(2)	3917(1)	5899(1)	19(1)
C(6)	3878(2)	5767(1)	6758(1)	18(1)
C(9)	4124(2)	3367(1)	5299(1)	18(1)
C(7)	3659(2)	4890(1)	6131(1)	18(1)
C(10)	4796(2)	2328(1)	4800(1)	19(1)
C(4)	6071(2)	6559(1)	7800(1)	24(1)
C(1)	2061(2)	6642(1)	6911(1)	21(1)
C(3)	4257(2)	7418(1)	7953(1)	23(1)
C(11)	6954(2)	1676(1)	4864(1)	22(1)
C(5)	5886(2)	5738(1)	7208(1)	21(1)
C(12)	7463(2)	716(1)	4368(1)	26(1)
C(14)	3727(2)	1140(1)	3800(1)	25(1)
C(13)	5826(2)	440(1)	3823(1)	26(1)
C(2)	2258(2)	7459(1)	7503(1)	23(1)

Table 3. Bond lengths [\AA] and angles [$^\circ$] for **PyPyr** ligand.

N(1)-H(001)	0.8800
N(1)-N(2)	1.3516(13)
N(1)-C(7)	1.3438(15)
N(2)-H(2)	0.8800
N(2)-C(9)	1.3526(15)
N(3)-C(10)	1.3484(16)
N(3)-C(14)	1.3389(16)
C(8)-H(8)	0.9500
C(8)-C(9)	1.3857(16)
C(8)-C(7)	1.4107(16)
C(6)-C(7)	1.4781(16)
C(6)-C(1)	1.4011(17)
C(6)-C(5)	1.3955(16)
C(9)-C(10)	1.4726(16)
C(10)-C(11)	1.3949(17)
C(4)-H(4)	0.9500
C(4)-C(3)	1.3880(18)
C(4)-C(5)	1.3912(17)
C(1)-H(1)	0.9500

C(1)-C(2)	1.3881(17)
C(3)-H(3)	0.9500
C(3)-C(2)	1.3913(18)
C(11)-H(11)	0.9500
C(11)-C(12)	1.3882(18)
C(5)-H(5)	0.9500
C(12)-H(12)	0.9500
C(12)-C(13)	1.3858(19)
C(14)-H(14)	0.9500
C(14)-C(13)	1.3883(19)
C(13)-H(13)	0.9500
C(2)-H(2A)	0.9500

N(2)-N(1)-H(001)	127.5
C(7)-N(1)-H(001)	127.5
C(7)-N(1)-N(2)	105.05(9)
N(1)-N(2)-H(2)	123.6
N(1)-N(2)-C(9)	112.82(9)
C(9)-N(2)-H(2)	123.6
C(14)-N(3)-C(10)	117.35(11)
C(9)-C(8)-H(8)	127.3
C(9)-C(8)-C(7)	105.48(10)
C(7)-C(8)-H(8)	127.3
C(1)-C(6)-C(7)	120.40(10)
C(5)-C(6)-C(7)	120.85(11)
C(5)-C(6)-C(1)	118.75(11)
N(2)-C(9)-C(8)	106.14(10)
N(2)-C(9)-C(10)	120.35(10)
C(8)-C(9)-C(10)	133.51(11)
N(1)-C(7)-C(8)	110.50(10)
N(1)-C(7)-C(6)	120.07(10)
C(8)-C(7)-C(6)	129.41(10)
N(3)-C(10)-C(9)	115.06(11)
N(3)-C(10)-C(11)	122.68(11)
C(11)-C(10)-C(9)	122.26(11)
C(3)-C(4)-H(4)	119.8
C(3)-C(4)-C(5)	120.48(11)
C(5)-C(4)-H(4)	119.8
C(6)-C(1)-H(1)	119.8
C(2)-C(1)-C(6)	120.44(11)
C(2)-C(1)-H(1)	119.8
C(4)-C(3)-H(3)	120.3
C(4)-C(3)-C(2)	119.35(11)
C(2)-C(3)-H(3)	120.3
C(10)-C(11)-H(11)	120.6
C(12)-C(11)-C(10)	118.70(11)

C(12)-C(11)-H(11)	120.6
C(6)-C(5)-H(5)	119.7
C(4)-C(5)-C(6)	120.50(11)
C(4)-C(5)-H(5)	119.7
C(11)-C(12)-H(12)	120.4
C(13)-C(12)-C(11)	119.21(12)
C(13)-C(12)-H(12)	120.4
N(3)-C(14)-H(14)	118.0
N(3)-C(14)-C(13)	123.97(12)
C(13)-C(14)-H(14)	118.0
C(12)-C(13)-C(14)	118.08(12)
C(12)-C(13)-H(13)	121.0
C(14)-C(13)-H(13)	121.0
C(1)-C(2)-C(3)	120.48(11)
C(1)-C(2)-H(2A)	119.8
C(3)-C(2)-H(2A)	119.8

Symmetry transformations used to generate equivalent atoms:

Table 4. Anisotropic displacement parameters ($\text{\AA}^2 \times 10^3$) for **PyPyr** ligand. The anisotropic displacement factor exponent takes the form: $-2\pi^2 [h^2 a^{*2} U^{11} + \dots + 2 h k a^* b^* U^{12}]$

	U ¹¹	U ²²	U ³³	U ²³	U ¹³	U ¹²
N(1)	19(1)	19(1)	19(1)	-1(1)	-1(1)	1(1)
N(2)	19(1)	20(1)	18(1)	-1(1)	-3(1)	0(1)
N(3)	23(1)	22(1)	22(1)	-1(1)	-1(1)	-2(1)
C(8)	18(1)	20(1)	19(1)	2(1)	-2(1)	0(1)
C(6)	19(1)	17(1)	18(1)	3(1)	1(1)	-3(1)
C(9)	18(1)	18(1)	19(1)	4(1)	1(1)	-1(1)
C(7)	18(1)	18(1)	18(1)	4(1)	0(1)	-2(1)
C(10)	21(1)	17(1)	19(1)	3(1)	2(1)	-3(1)
C(4)	22(1)	25(1)	24(1)	-1(1)	-6(1)	0(1)
C(1)	19(1)	23(1)	20(1)	1(1)	-2(1)	0(1)
C(3)	26(1)	22(1)	22(1)	-4(1)	0(1)	-2(1)
C(11)	21(1)	23(1)	24(1)	1(1)	-1(1)	0(1)
C(5)	20(1)	20(1)	24(1)	0(1)	-2(1)	2(1)
C(12)	23(1)	23(1)	32(1)	1(1)	5(1)	2(1)
C(14)	28(1)	26(1)	23(1)	-3(1)	-2(1)	-4(1)
C(13)	30(1)	22(1)	27(1)	-5(1)	6(1)	-3(1)
C(2)	22(1)	23(1)	25(1)	-1(1)	2(1)	3(1)

Table 5. Hydrogen coordinates ($\times 10^4$) and isotropic displacement parameters ($\text{\AA}^2 \times 10^{-3}$) for **PyPyr** ligand.

	x	y	z	U(eq)
H(001)	510	5470	5730	23
H(2)	1006	3816	4859	23
H(8)	6709	3687	6109	22
H(4)	7448	6532	8103	29
H(1)	684	6676	6609	25
H(3)	4381	7972	8360	28
H(11)	8054	1886	5240	27
H(5)	7137	5153	7109	26
H(12)	8916	254	4401	31
H(14)	2609	953	3426	30
H(13)	6131	-211	3476	32
H(2A)	1018	8052	7601	28

X-ray crystallography for PyPyrPdCl₂:

To obtain a suitable crystal of PyPyrPdCl₂ complex, a dilute solution of the complex was prepared in MeNO₂. This solution was left to stand in a vial equipped with a screw cap that had been made to contain a small hole. The top of the vial was covered with a kim-wipe to prevent unwanted particles from entering the vial. The solution was allowed to slowly evaporate at ambient temperature for 14 days. Clear red-orange crystals formed and were of high enough quality for analysis.

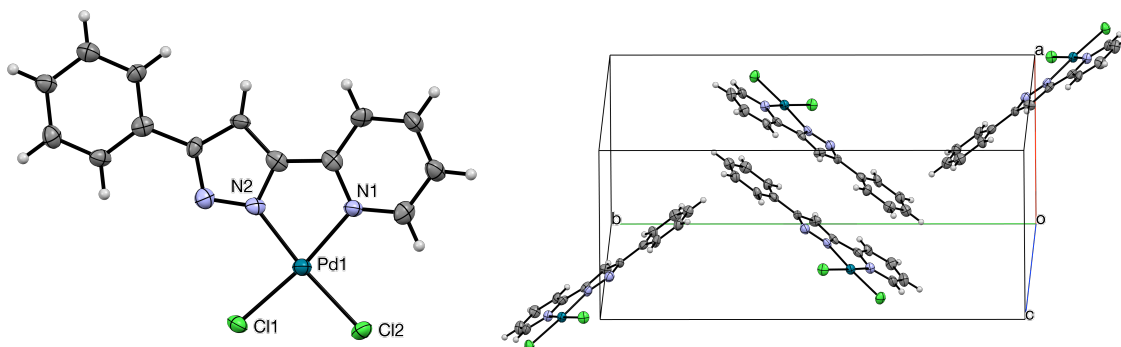


Table 1. Crystal data and structure refinement for **PyPyrPdCl₂**.

Empirical formula	C ₁₄ H ₁₀ Cl ₂ N ₃ Pd
Formula weight	397.55
Temperature	100.0 K
Wavelength, Å	1.54178
Crystal system	Monoclinic
Space group	<i>P</i> 2 ₁ / <i>c</i>
<i>a</i> , Å	8.448(2)
<i>b</i> , Å	21.242(5)
<i>c</i> , Å	8.7304(17)
α , °	90
β , °	117.669(15)
γ , °	90
Volume	1387.5(6) Å ³
<i>Z</i>	4
Calculated density, mg/m ³	1.903
Absorption coefficient, mm ⁻¹	14.260
<i>F</i> (000)	780
Crystal size, mm	0.16 x 0.09 x 0.04
Theta range for data collection, °	4.162 to 58.964
Index ranges	-9 ≤ <i>h</i> ≤ 8, -23 ≤ <i>k</i> ≤ 23, 0 ≤ <i>l</i> ≤ 9
Reflections collected / unique	6364 / 6364 [<i>R</i> _{int} = 0.077]
Completeness to $\theta = 58.964^\circ$	99.8 %
Absorption correction	Semi-empirical from equivalents
Max. and min. transmission	0.1665 and 0.0488
Refinement method	Full-matrix least-squares on <i>F</i> ²
Data / restraints / parameters	6364 / 0 / 170
Goodness-of-fit on <i>F</i> ²	1.059
Final <i>R</i> indices [<i>I</i> > 2 σ (<i>I</i>)]	<i>R</i> 1 = 0.0857, <i>wR</i> 2 = 0.2151
<i>R</i> indices (all data)	<i>R</i> 1 = 0.1075, <i>wR</i> 2 = 0.2305
Extinction coefficient	n/a
Largest diff. peak and hole, eÅ ⁻³	1.299 and -1.066

Table 2. Atomic coordinates ($\times 10^4$) and equivalent isotropic displacement parameters ($\text{\AA}^2 \times 10^3$) for **PyPyrPdCl₂**. U(eq) is defined as one third of the trace of the orthogonalized U^{ij} tensor.

	x	y	z	U(eq)
Pd(1)	1543(2)	4168(1)	7482(2)	25(1)
Cl(1)	2931(5)	4746(2)	9970(5)	31(1)
Cl(2)	566(5)	3435(2)	8769(6)	32(1)
N(1)	242(17)	3776(7)	5060(19)	25(3)
N(2)	2311(17)	4752(7)	6134(19)	24(3)
N(3)	3373(18)	5264(8)	6480(20)	29(3)
C(1)	-790(20)	3254(9)	4610(30)	33(4)
C(2)	-1650(20)	3045(9)	2930(20)	33(4)
C(3)	-1420(20)	3371(10)	1660(20)	34(4)
C(4)	-360(20)	3896(9)	2120(20)	28(4)
C(5)	460(20)	4095(9)	3810(20)	28(4)
C(6)	1630(20)	4642(9)	4470(20)	26(4)
C(7)	2220(20)	5095(9)	3660(20)	27(4)
C(8)	3350(20)	5476(8)	5000(20)	25(4)
C(9)	4386(13)	6033(4)	4956(13)	27(4)
C(10)	4260(13)	6214(5)	3372(11)	28(4)
C(11)	5191(14)	6738(5)	3271(11)	34(4)
C(12)	6249(14)	7082(5)	4752(14)	31(4)
C(13)	6375(13)	6901(5)	6336(11)	33(4)
C(14)	5444(14)	6377(5)	6438(11)	29(4)

Table 3. Bond lengths [\AA] and angles [$^\circ$] for **PyPyrPdCl₂**.

Pd(1)-Cl(1)	2.288(5)
Pd(1)-Cl(2)	2.286(4)
Pd(1)-N(1)	2.053(15)
Pd(1)-N(2)	2.014(14)
N(1)-C(1)	1.35(2)
N(1)-C(5)	1.37(2)
N(2)-N(3)	1.35(2)
N(2)-C(6)	1.31(2)
N(3)-C(8)	1.36(2)
C(1)-H(1)	0.9500
C(1)-C(2)	1.37(3)
C(2)-H(2)	0.9500

C(2)-C(3)	1.39(3)
C(3)-H(3)	0.9500
C(3)-C(4)	1.37(3)
C(4)-H(4)	0.9500
C(4)-C(5)	1.37(3)
C(5)-C(6)	1.46(3)
C(6)-C(7)	1.41(3)
C(7)-H(7)	0.9500
C(7)-C(8)	1.38(3)
C(8)-C(9)	1.482(18)
C(9)-C(10)	1.3900
C(9)-C(14)	1.3900
C(10)-H(10)	0.9500
C(10)-C(11)	1.3900
C(11)-H(11)	0.9500
C(11)-C(12)	1.3900
C(12)-H(12)	0.9500
C(12)-C(13)	1.3900
C(13)-H(13)	0.9500
C(13)-C(14)	1.3900
C(14)-H(14)	0.9500
Cl(2)-Pd(1)-Cl(1)	92.38(17)
N(1)-Pd(1)-Cl(1)	171.4(4)
N(1)-Pd(1)-Cl(2)	95.0(4)
N(2)-Pd(1)-Cl(1)	93.6(4)
N(2)-Pd(1)-Cl(2)	174.0(4)
N(2)-Pd(1)-N(1)	79.1(6)
C(1)-N(1)-Pd(1)	126.7(13)
C(1)-N(1)-C(5)	118.7(16)
C(5)-N(1)-Pd(1)	114.6(12)
N(3)-N(2)-Pd(1)	136.4(12)
C(6)-N(2)-Pd(1)	116.2(12)
C(6)-N(2)-N(3)	107.3(14)

N(2)-N(3)-C(8)	109.8(15)
N(1)-C(1)-H(1)	119.1
N(1)-C(1)-C(2)	121.8(18)
C(2)-C(1)-H(1)	119.1
C(1)-C(2)-H(2)	120.3
C(1)-C(2)-C(3)	119.3(18)
C(3)-C(2)-H(2)	120.3
C(2)-C(3)-H(3)	120.5
C(4)-C(3)-C(2)	119.0(18)
C(4)-C(3)-H(3)	120.5
C(3)-C(4)-H(4)	120.0
C(3)-C(4)-C(5)	120.0(17)
C(5)-C(4)-H(4)	120.0
N(1)-C(5)-C(4)	121.2(17)
N(1)-C(5)-C(6)	113.3(15)
C(4)-C(5)-C(6)	125.5(17)
N(2)-C(6)-C(5)	116.6(16)
N(2)-C(6)-C(7)	110.6(16)
C(7)-C(6)-C(5)	132.7(16)
C(6)-C(7)-H(7)	127.9
C(8)-C(7)-C(6)	104.3(15)
C(8)-C(7)-H(7)	127.9
N(3)-C(8)-C(7)	107.9(15)
N(3)-C(8)-C(9)	122.9(15)
C(7)-C(8)-C(9)	129.2(15)
C(10)-C(9)-C(8)	118.2(10)
C(10)-C(9)-C(14)	120.0
C(14)-C(9)-C(8)	121.7(10)
C(9)-C(10)-H(10)	120.0
C(9)-C(10)-C(11)	120.0
C(11)-C(10)-H(10)	120.0
C(10)-C(11)-H(11)	120.0
C(12)-C(11)-C(10)	120.0
C(12)-C(11)-H(11)	120.0

C(11)-C(12)-H(12)	120.0
C(13)-C(12)-C(11)	120.0
C(13)-C(12)-H(12)	120.0
C(12)-C(13)-H(13)	120.0
C(14)-C(13)-C(12)	120.0
C(14)-C(13)-H(13)	120.0
C(9)-C(14)-H(14)	120.0
C(13)-C(14)-C(9)	120.0
C(13)-C(14)-H(14)	120.0

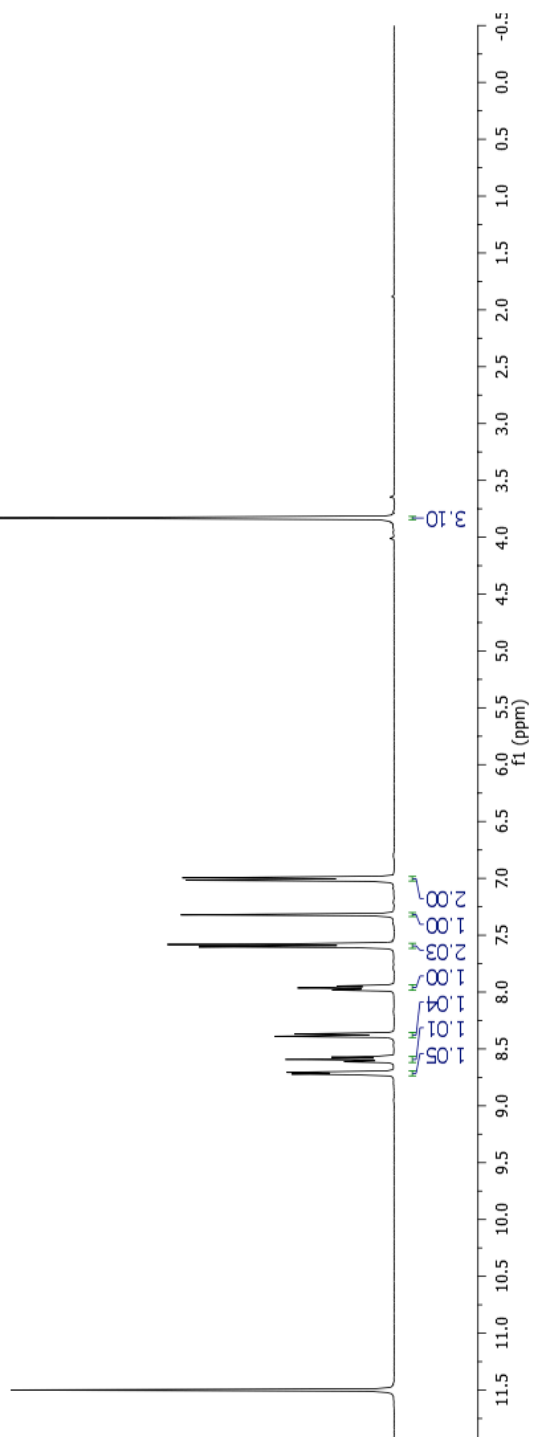
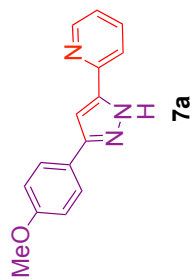
Symmetry transformations used to generate equivalent atoms:

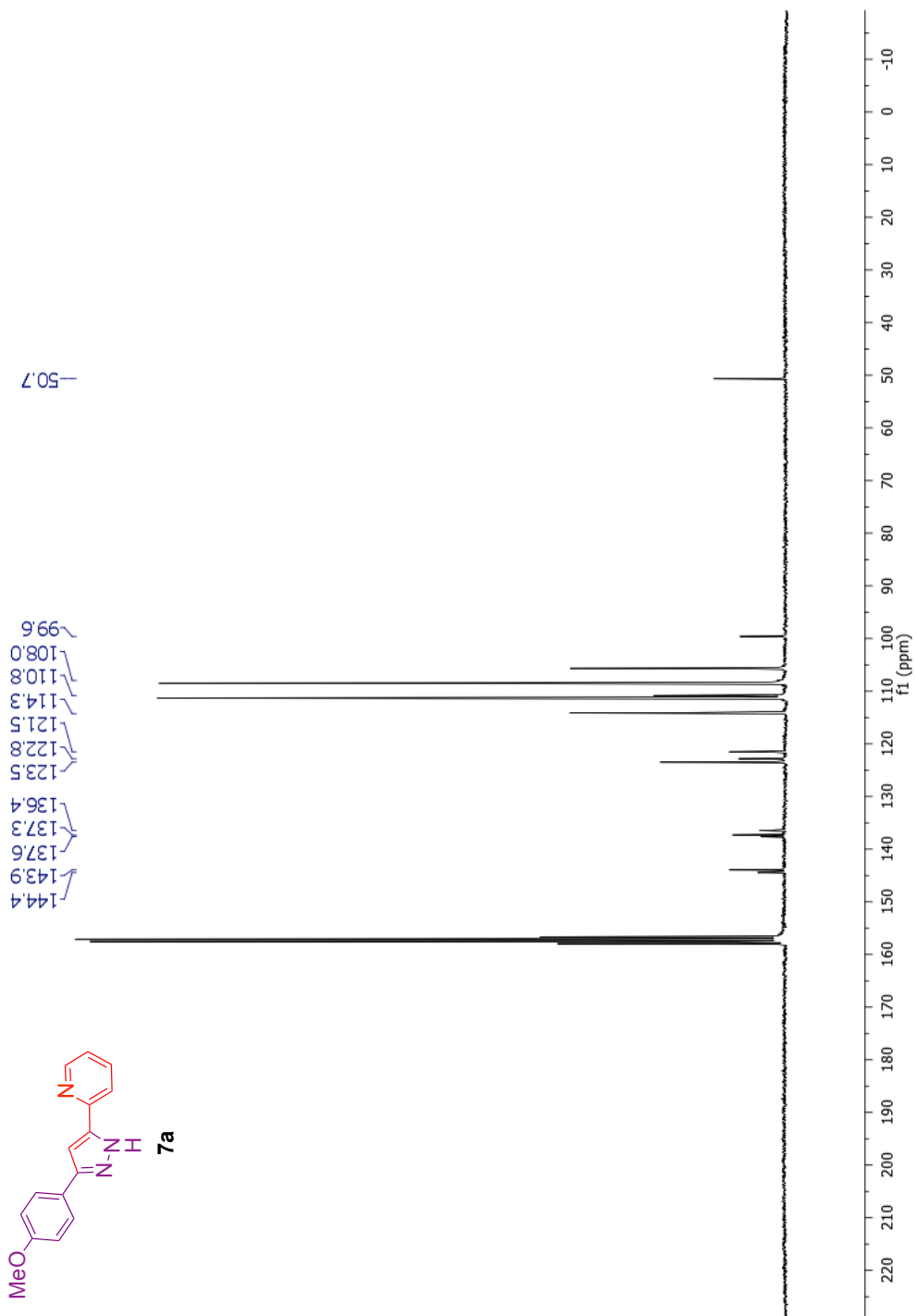
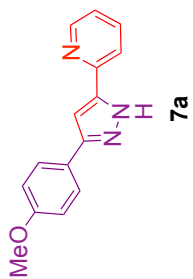
Table 4. Anisotropic displacement parameters ($\text{\AA}^2 \times 10^3$) for **PyPyrPdCl₂**. The anisotropic displacement factor exponent takes the form: $-2\pi^2 [h^2 a^{*2} U^{11} + \dots + 2 h k a^* b^* U^{12}]$

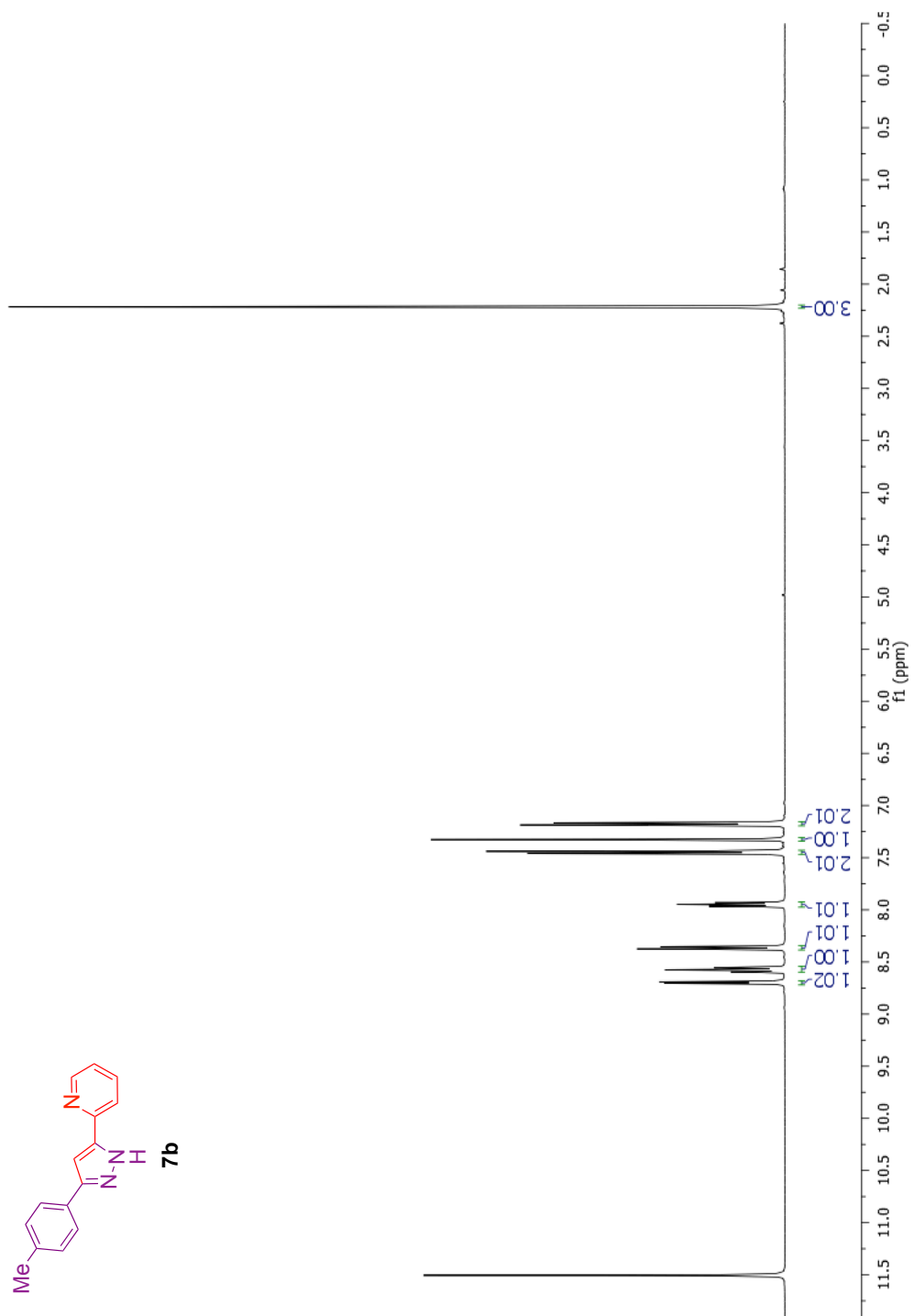
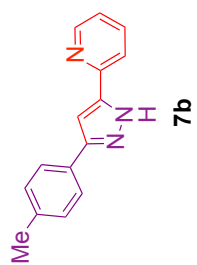
	U ¹¹	U ²²	U ³³	U ²³	U ¹³	U ¹²
Pd(1)	30(1)	24(1)	21(1)	1(1)	12(1)	2(1)
Cl(1)	36(2)	33(3)	19(2)	-4(2)	10(2)	-2(2)
Cl(2)	42(2)	27(3)	28(2)	7(2)	18(2)	-1(2)
N(1)	31(7)	23(9)	19(8)	1(6)	11(6)	2(6)
N(2)	32(7)	20(8)	23(9)	-1(7)	16(6)	6(6)
N(3)	34(7)	25(9)	32(9)	-2(7)	17(6)	2(6)
C(1)	41(9)	21(11)	42(13)	1(9)	24(9)	6(8)
C(2)	39(9)	25(11)	27(11)	-1(9)	8(8)	3(8)
C(3)	34(9)	35(12)	25(10)	-8(9)	8(8)	-4(8)
C(4)	35(8)	20(10)	28(11)	8(8)	14(8)	11(7)
C(5)	26(8)	27(11)	30(10)	-4(9)	14(7)	7(7)
C(6)	24(7)	25(10)	26(11)	-1(8)	9(7)	12(7)
C(7)	27(8)	37(11)	15(9)	2(8)	9(7)	-1(7)
C(8)	30(8)	17(10)	34(11)	-3(8)	20(8)	-2(7)
C(9)	27(8)	26(11)	31(10)	4(8)	15(7)	9(7)
C(10)	32(8)	24(11)	28(10)	5(8)	13(7)	0(7)
C(11)	34(9)	39(13)	27(10)	1(9)	12(8)	2(8)
C(12)	35(9)	30(11)	24(11)	2(8)	12(8)	4(8)
C(13)	36(9)	25(11)	36(12)	-5(9)	15(8)	0(8)
C(14)	43(9)	20(10)	23(10)	3(8)	15(8)	8(8)

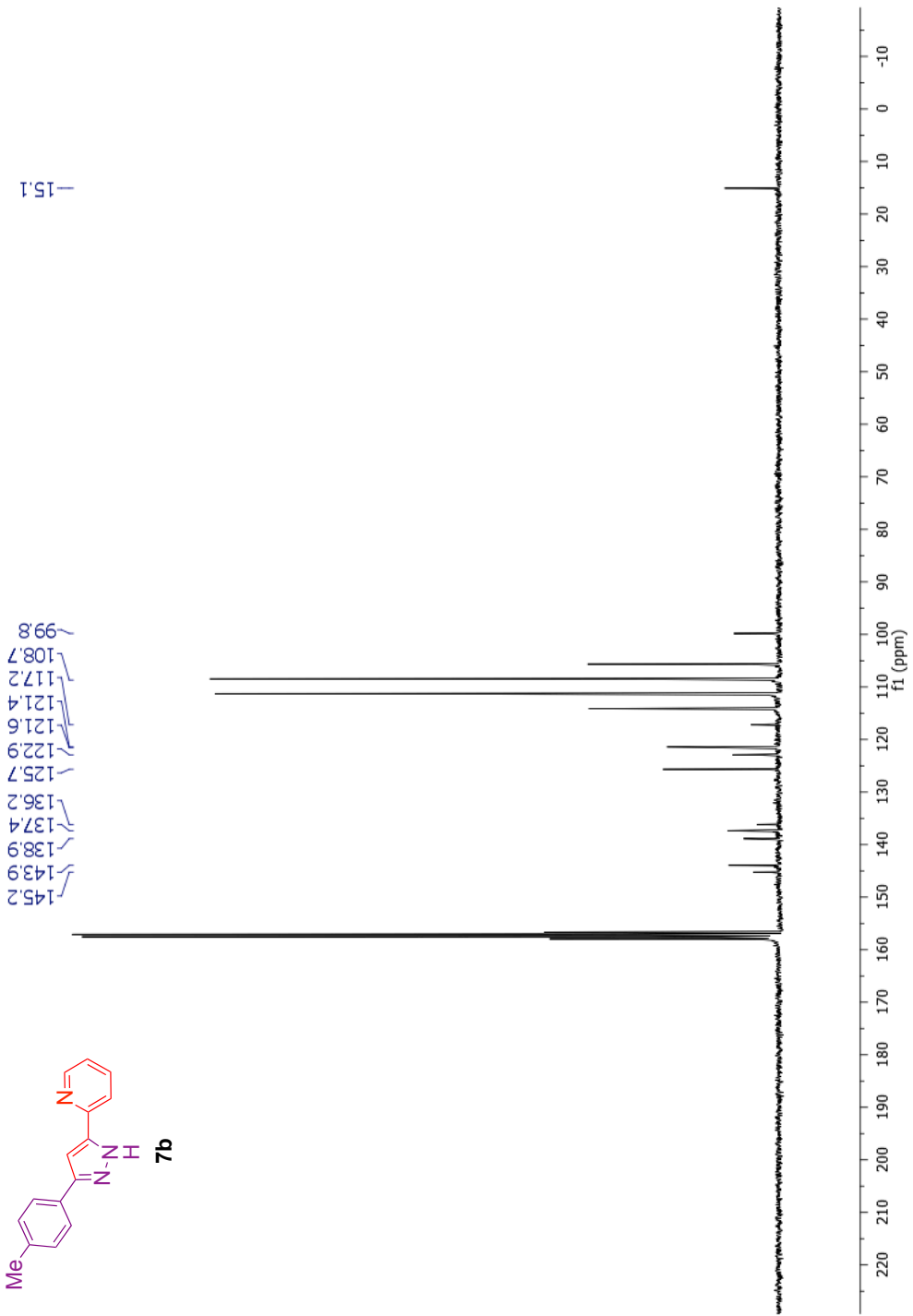
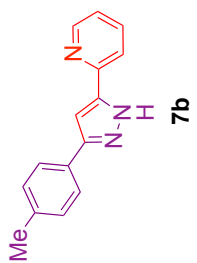
Table 5. Hydrogen coordinates ($\times 10^4$) and isotropic displacement parameters ($\text{\AA}^2 \times 10^{-3}$) for **PyPyrPdCl₂**.

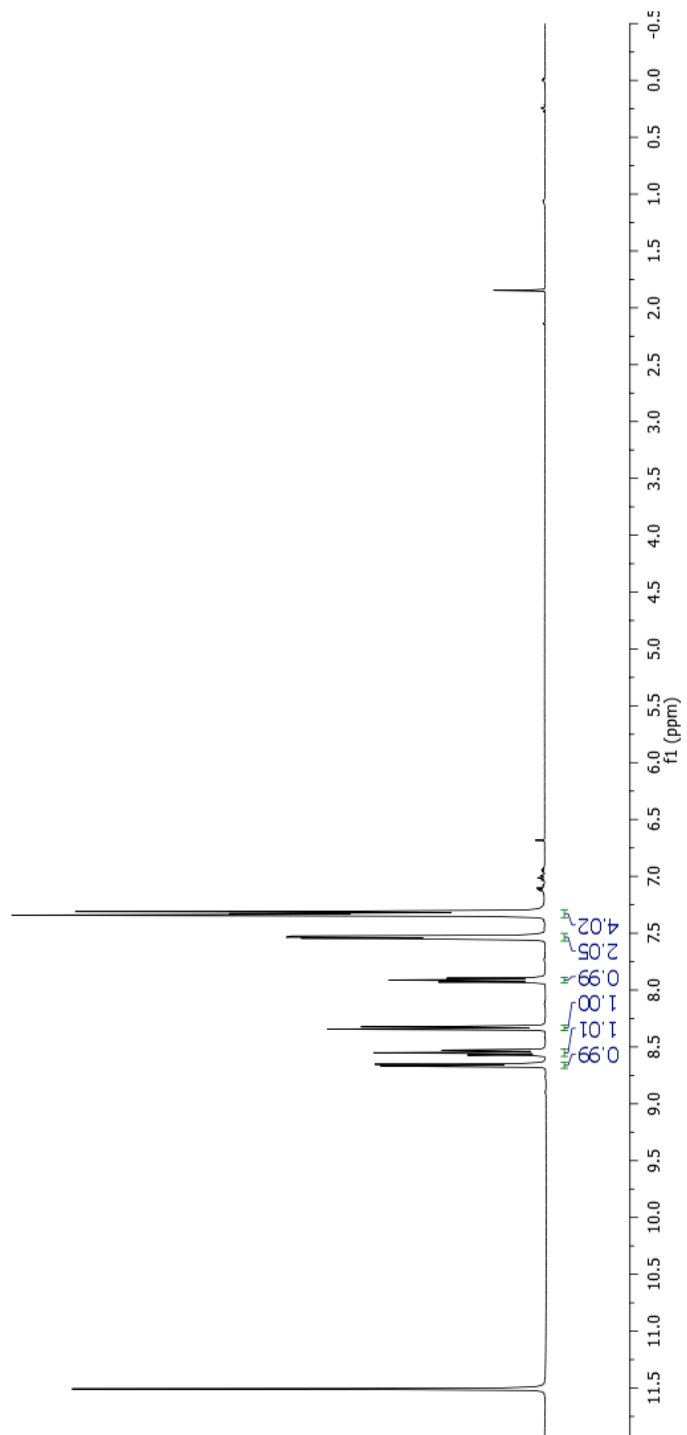
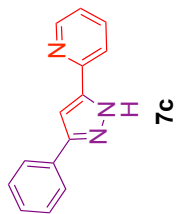
	x	y	z	U(eq)
H(1)	-925	3026	5475	39
H(2)	-2389	2682	2637	39
H(3)	-1997	3231	493	40
H(4)	-198	4123	1266	34
H(7)	1910	5129	2473	32
H(10)	3537	5979	2360	34
H(11)	5105	6861	2188	41
H(12)	6886	7440	4683	37
H(13)	7098	7136	7349	40
H(14)	5530	6254	7520	34

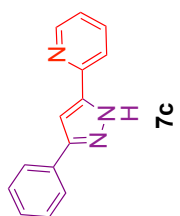












144.8
143.9
138.1
137.1
136.8
126.9
124.9
122.6
121.4
121.3
120.5
99.8

